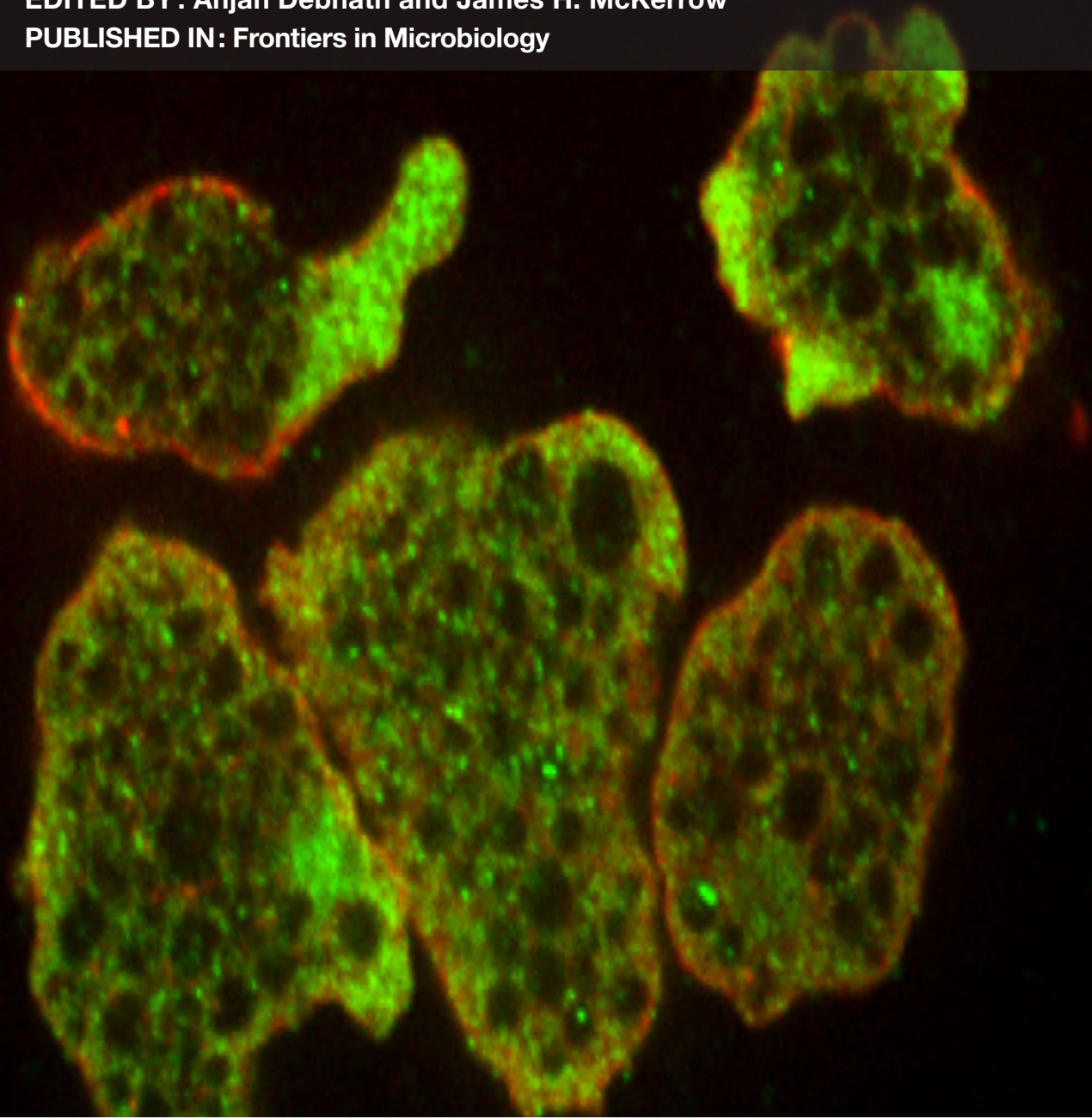


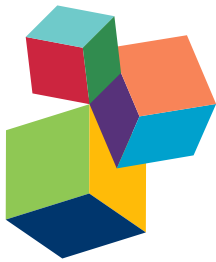
DRUG DEVELOPMENT FOR PARASITE-INDUCED DIARRHEAL DISEASES

EDITED BY: Anjan Debnath and James H. McKerrow

PUBLISHED IN: *Frontiers in Microbiology*



frontiers Research Topics



Frontiers Copyright Statement

© Copyright 2007-2017 Frontiers Media SA. All rights reserved.

All content included on this site, such as text, graphics, logos, button icons, images, video/audio clips, downloads, data compilations and software, is the property of or is licensed to Frontiers Media SA ("Frontiers") or its licensees and/or subcontractors. The copyright in the text of individual articles is the property of their respective authors, subject to a license granted to Frontiers.

The compilation of articles constituting this e-book, wherever published, as well as the compilation of all other content on this site, is the exclusive property of Frontiers. For the conditions for downloading and copying of e-books from Frontiers' website, please see the Terms for Website Use. If purchasing Frontiers e-books from other websites or sources, the conditions of the website concerned apply.

Images and graphics not forming part of user-contributed materials may not be downloaded or copied without permission.

Individual articles may be downloaded and reproduced in accordance with the principles of the CC-BY licence subject to any copyright or other notices. They may not be re-sold as an e-book.

As author or other contributor you grant a CC-BY licence to others to reproduce your articles, including any graphics and third-party materials supplied by you, in accordance with the Conditions for Website Use and subject to any copyright notices which you include in connection with your articles and materials.

All copyright, and all rights therein, are protected by national and international copyright laws.

The above represents a summary only. For the full conditions see the Conditions for Authors and the Conditions for Website Use.

ISSN 1664-8714

ISBN 978-2-88945-248-4

DOI 10.3389/978-2-88945-248-4

About Frontiers

Frontiers is more than just an open-access publisher of scholarly articles: it is a pioneering approach to the world of academia, radically improving the way scholarly research is managed. The grand vision of Frontiers is a world where all people have an equal opportunity to seek, share and generate knowledge. Frontiers provides immediate and permanent online open access to all its publications, but this alone is not enough to realize our grand goals.

Frontiers Journal Series

The Frontiers Journal Series is a multi-tier and interdisciplinary set of open-access, online journals, promising a paradigm shift from the current review, selection and dissemination processes in academic publishing. All Frontiers journals are driven by researchers for researchers; therefore, they constitute a service to the scholarly community. At the same time, the Frontiers Journal Series operates on a revolutionary invention, the tiered publishing system, initially addressing specific communities of scholars, and gradually climbing up to broader public understanding, thus serving the interests of the lay society, too.

Dedication to Quality

Each Frontiers article is a landmark of the highest quality, thanks to genuinely collaborative interactions between authors and review editors, who include some of the world's best academicians. Research must be certified by peers before entering a stream of knowledge that may eventually reach the public - and shape society; therefore, Frontiers only applies the most rigorous and unbiased reviews.

Frontiers revolutionizes research publishing by freely delivering the most outstanding research, evaluated with no bias from both the academic and social point of view.

By applying the most advanced information technologies, Frontiers is catapulting scholarly publishing into a new generation.

What are Frontiers Research Topics?

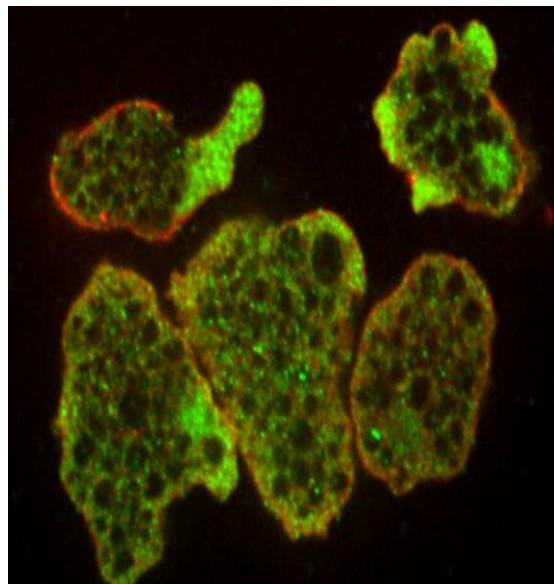
Frontiers Research Topics are very popular trademarks of the Frontiers Journals Series: they are collections of at least ten articles, all centered on a particular subject. With their unique mix of varied contributions from Original Research to Review Articles, Frontiers Research Topics unify the most influential researchers, the latest key findings and historical advances in a hot research area! Find out more on how to host your own Frontiers Research Topic or contribute to one as an author by contacting the Frontiers Editorial Office: researchtopics@frontiersin.org

DRUG DEVELOPMENT FOR PARASITE-INDUCED DIARRHEAL DISEASES

Topic Editors:

Anjan Debnath, University of California San Diego, United States

James H. McKerrow, University of California San Diego, United States



Hsp90 regulates phagocytosis in *Entamoeba histolytica*

Figure taken from: Singh M, Sharma S, Bhattacharya A and Tatu U (2015) Heat Shock Protein 90 regulates encystation in *Entamoeba*. Front. Microbiol. 6:1125. doi: 10.3389/fmicb.2015.01125

One of the top four contributors to the global burden of disease is diarrheal infections. Intestinal parasites are major causes of morbidity and mortality associated with diarrheal diseases in both the developed and developing world. Amebiasis is responsible for 50 million cases of invasive disease and 70,000 deaths annually in the world. Giardiasis has an estimated worldwide prevalence of 280 million cases annually. In developed countries, *Giardia lamblia* infects about 2% of adults and 6-8% of children. The prevalence of *G. lamblia* infection is generally higher in developing countries, ranging from 3% to 90%. Furthermore, giardial infections contribute substantially to the 2.5 million annual deaths from diarrheal disease. In Asia, Africa, and Latin America, about 500,000 new giardiasis cases are reported each year. *Cryptosporidium* accounts for 20% and 9% of diarrheal episodes in children in developing and developed countries, respectively. Infection with *Cryptosporidium* can be chronic and especially debilitating in immunosuppressed individuals and malnourished children.

A recent study to measure disease burden, based on disability-adjusted life years (DALYs), found that cryptosporidiosis and amebiasis produce about 10.6 million DALYs. This exceeds the DALYs of any helminth infection currently being targeted by the World Health Organization for preventive chemotherapy. Because of its link with poverty, *Giardia* and *Cryptosporidium* were included in the WHO Neglected Diseases Initiative in 2004. *E. histolytica*, *G. lamblia*, and *C. parvum* have been listed by the National Institutes of Health (NIH) as category B priority biodefense pathogens due to low infectious dose and potential for dissemination through compromised food and water supplies in the United States.

Despite the prevalence of amebiasis, giardiasis, and cryptosporidiosis there are no vaccines or prophylactic drugs. The first-line drugs for invasive amebiasis and giardiasis chemotherapy are nitroimidazoles, with the prototype, metronidazole, being the most common drug used worldwide. Metronidazole has been shown to be both mutagenic in a microbiological system and carcinogenic to rodents, and frequently causes gastrointestinal side effects. In spite of the efficacy of nitroimidazole drugs, treatment failures in giardiasis occur in up to 20% of cases. Clinical resistance of *G. lamblia* to metronidazole is proven and cross resistance is a concern with all commonly used anti-giardial drugs. Nitazoxanide, the only FDA-approved drug for the treatment of cryptosporidiosis, is effective in the treatment of immunocompetent patients and partially effective for immunosuppressed patients. Therefore, it is critical to search for more effective drugs to treat amebiasis, giardiasis, and cryptosporidiosis.

This Research Topic for Frontiers in Microbiology will explore the recent progress in drug development for parasitic diarrheal diseases. This includes an understanding of drug resistance mechanisms. We would also welcome submissions on the drug development for other diarrheal parasites. We hope that this research topic will include a comprehensive survey of various attempts by the parasitology research community to create effective drugs for these diseases.

Citation: Debnath, A., McKerrow, J. H., eds. (2017). Drug Development for Parasite-Induced Diarrheal Diseases. Lausanne: Frontiers Media. doi: 10.3389/978-2-88945-248-4

Table of Contents

06 Editorial: Drug Development for Parasite-Induced Diarrheal Diseases

Anjan Debnath and James H. McKerrow

Section 1:

09 Parasitic diarrheal disease: drug development and targets

Amir Azam, Mudasir N. Peerzada and Kamal Ahmad

21 Drug Development Against the Major Diarrhea-Causing Parasites of the Small Intestine, Cryptosporidium and Giardia

Yukiko Miyamoto and Lars Eckmann

38 New drug target in protozoan parasites: the role of thioredoxin reductase

Rosa M. Andrade and Sharon L. Reed

Section 2:

45 Antigiardial activity of novel triazolyl-quinolone-based chalcone derivatives: when oxygen makes the difference

Vijay Bahadur, Daniela Mastronicola, Amit K. Singh, Hemendra K. Tiwari, Leopoldo P. Pucillo, Paolo Sarti, Brajendra K. Singh and Alessandro Giuffrè

55 An antioxidant response is involved in resistance of Giardia duodenalis to albendazole

Raúl Argüello-García, Maricela Cruz-Soto, Rolando González-Trejo, Luz María T. Paz-Maldonado, M. Luisa Bazán-Tejeda, Guillermo Mendoza-Hernández and Guadalupe Ortega-Pierres

68 Albendazole induces oxidative stress and DNA damage in the parasitic protozoan Giardia duodenalis

Rodrigo Martínez-Espinosa, Raúl Argüello-García, Emma Saavedra and Guadalupe Ortega-Pierres

82 The FAD-dependent glycerol-3-phosphate dehydrogenase of Giardia duodenalis: an unconventional enzyme that interacts with the g14-3-3 and it is a target of the antitumoral compound NBDHEX

Marco Lalle, Serena Camerini, Serena Cecchetti, Renata Finelli, Gabriella Sferra, Joachim Müller, Giorgio Ricci and Edoardo Pozio

101 Giardia fatty acyl-CoA synthetases as potential drug targets

Fengguang Guo, Guadalupe Ortega-Pierres, Raúl Argüello-García, Haili Zhang and Guan Zhu

Section 3:

111 Identification of natural inhibitors of Entamoeba histolytica cysteine synthase from microbial secondary metabolites

Mihoko Mori, Ghulam Jeelani, Yui Masuda, Kazunari Sakai, Kumiko Tsukui, Danang Waluyo, Tarwadi, Yoshio Watanabe, Kenichi Nonaka, Atsuko Matsumoto, Satoshi Ōmura, Tomoyoshi Nozaki and Kazuro Shiomi

- 121 Heat Shock Protein 90 regulates encystation in Entamoeba**
Meetali Singh, Shalini Sharma, Alok Bhattacharya and Utpal Tatu
- 129 Heat shock protein 90 inhibitors repurposed against Entamoeba histolytica**
Dea Shahinas, Anjan Debnath, Christian Benedict, James H. McKerrow and Dylan R. Pillai
- 138 Phenotypic and transcriptional profiling in Entamoeba histolytica reveal costs to fitness and adaptive responses associated with metronidazole resistance**
Gil M. Penuliar, Kumiko Nakada-Tsukui and Tomoyoshi Nozaki

Section 4:

- 155 Quantitative RT-PCR assay for high-throughput screening (HTS) of drugs against the growth of Cryptosporidium parvum in vitro**
Haili Zhang and Guan Zhu
- 164 Oleylphosphocholine (OIPC) arrests Cryptosporidium parvum growth in vitro and prevents lethal infection in interferon gamma receptor knock-out mice**
Karine Sonzogni-Desautels, Axel E. Renteria, Fabio V. Camargo, Thomas Z. Di Lenardo, Alexandre Mikhail, Michael J. Arrowood, Anny Fortin and Momar Ndao



Editorial: Drug Development for Parasite-Induced Diarrheal Diseases

Anjan Debnath * and James H. McKerrow

Center for Discovery and Innovation in Parasitic Diseases, Skaggs School of Pharmacy and Pharmaceutical Sciences, University of California, San Diego, La Jolla, CA, USA

Keywords: parasite, diarrhea, drug, *Entamoeba*, *Giardia*, *Cryptosporidium*, chemotherapy, protozoa

Editorial on the Research Topic

Drug Development for Parasite-Induced Diarrheal Diseases

OPEN ACCESS

Edited by:

Ed Topp,

Agriculture and Agriculture-Food
Canada, Canada

Reviewed by:

Ed Topp,

Agriculture and Agriculture-Food
Canada, Canada

Claudio Silva,

Federal University of Uberlândia, Brazil
Elias Papadopoulos,

Aristotle University of Thessaloniki,
Greece

***Correspondence:**

Anjan Debnath

adebnath@ucsd.edu

Specialty section:

This article was submitted to
Antimicrobials, Resistance and
Chemotherapy,
a section of the journal
Frontiers in Microbiology

Received: 05 January 2017

Accepted: 21 March 2017

Published: 04 April 2017

Citation:

Debnath A and McKerrow JH (2017)

Editorial: Drug Development for
Parasite-Induced Diarrheal Diseases.

Front. Microbiol. 8:577.

doi: 10.3389/fmicb.2017.00577

Diarrhea continues to be a major contributing factor to morbidity and mortality worldwide. It is the second leading cause of death in children under 5 years old. Three enteroparasites, *Entamoeba histolytica*, *Giardia lamblia*, and *Cryptosporidium parvum* are common infectious agents causing persistent diarrhea. The Global Burden of Disease Study (GBDS) found that amebiasis was responsible for more than 55,000 deaths and 2.2 million disability-adjusted life years (DALYs), and cryptosporidiosis accounted for about 100,000 deaths and 8.4 million DALYs in 2010 (Hotez, 2014). According to the WHO Foodborne Disease Burden Epidemiology Reference Group (FERG), giardiasis produced 171,100 DALYs in 2010 (Torgerson et al., 2015). Though giardiasis did not result in deaths, the economic burden of acute giardiasis in the US continues to be substantial. The annual cost involving the hospital based treatment for giardiasis is approximately \$34 million (Collier et al., 2012). In addition, *E. histolytica*, *G. lamblia*, and *C. parvum* are considered to be bioterrorism threats by the National Institutes of Health (NIH) and Centers for Disease Control and Prevention (CDC).

In absence of vaccines to prevent these parasitic diseases, control relies on chemotherapy which is far from perfect and limited by adverse drug effects. For example, metronidazole is the most common drug used to treat invasive amebiasis and giardiasis, but treatment often leads to side effects, such as nausea, vomiting, diarrhea, or constipation. Moreover, potential resistance of *E. histolytica* to metronidazole is an increasing concern. Although millions of people are infected by *E. histolytica* each year, most individuals remain asymptomatic but may transmit amebiasis through fecal excretion of infective cysts. Therefore, an additional drug paromomycin is required following metronidazole treatment to eliminate cysts (Haque et al., 2003). However, treatment with two drugs for 20 days is long, burdensome, and reduces compliance. In spite of the reported efficacy of nitroimidazole drugs, treatment failures in giardiasis occur in up to 20% of cases and a recent report from the Hospital for Tropical Diseases, London found that the nitroimidazole therapy failure rate in giardiasis was 40.2% in 2013 (Nabarro et al., 2015). Nitazoxanide, the only treatment option for cryptosporidiosis, has an efficacy ranging from 56% in malnourished children to 80% in healthy adults and it is not effective for immunocompromised patients (Manjunatha et al., 2016). All these factors make the development of new antimicrobials to treat these infections a critical need to avert future outbreaks and deaths.

Recently, drug discovery efforts to treat parasite-induced diarrheal diseases are burgeoning. Researchers across the globe are working toward identifying better drug candidates for the treatment of these parasitic diseases. However, a comprehensive report of their endeavors encompassing these parasites is lacking. We launched this Research Topic to compile the recent

progress made by the parasitology research community to develop effective drugs for the treatment of parasitic diarrheal diseases. It may also provide a one-stop resource for drug development research targeting enteric protozoan parasites. Seventy-three authors enriched the Research Topic with their contributions leading to 14 articles. These articles have been organized in an e-book and can be categorized in four sections.

The first section opens with a review of different heterocyclic compounds for their activity against intestinal protozoan parasites, and current knowledge of the drug targets and mechanism of action of some of the compounds (Azam et al.). This review not only provides a survey of drug discovery research on *E. histolytica*, *G. lamblia*, and *C. parvum* but also includes an update on drug development for other intestinal parasites such as microsporidia, *Isospora* and *Cyclospora*. A review article by Miyamoto and Eckmann highlights different assays used for drug development and detailed the implementation of both the activity-centered and target-centered strategies to develop new drug leads for cryptosporidiosis and giardiasis. The third article of this section focused on repurposing of an FDA-approved drug auranofin for the treatment of amebiasis and giardiasis and the description of *E. histolytica* and *G. lamblia* thioredoxin reductase as an attractive drug target (Andrade and Reed). Auranofin showed promising activity against multiple parasites and identifying a broad-spectrum antiparasitic agent may be a useful drug discovery strategy for rare and neglected parasitic diseases instead of applying “one bug-one drug” approach.

The second section includes five original research articles on drug discovery for giardiasis. The articles range from medicinal chemistry to mechanism of resistance studies and new drug target identification. In the medicinal chemistry research article, the authors synthesized 45 novel chalcone analogs with triazolyl-quinolone scaffold and tested their activity against *G. lamblia* (Bahadur et al.). Four compounds were particularly selective for *G. lamblia* trophozoites with IC₅₀ better than metronidazole and less toxic against a human cell line. These new synthetic chalcone derivatives hold promise for future design of antigiardial compounds. Since resistance of *Giardia* to nitroimidazoles and albendazole is an emerging issue, it is imperative to understand the mechanisms involved in drug resistance in order to develop better treatment strategies. Arguello-Garcia et al. developed albendazole-resistant clones and compared the expression of different antioxidant enzymes in albendazole-sensitive and -resistant trophozoites. Albendazole was shown to induce the formation of reactive oxygen species causing DNA damage which led to apoptosis (Martinez-Espinosa et al.). In contrast, albendazole-resistant trophozoites over expressed antioxidant enzymes to detoxify reactive oxygen species. Two articles exploited *Giardia* metabolic enzymes for parasite specific drug development. An FAD-dependent glycerol-3-phosphate dehydrogenase of *G. lamblia* was characterized for activity and cellular localization (Lalle et al.). The authors validated the target by inhibiting *Giardia* glycerol-3-phosphate dehydrogenase activity chemically using an antitumor compound NBDHEX. Guo et al. considered *Giardia* acyl-CoA synthetase (GiACS) as potential drug target and recombinantly expressed GiACS1 and GiACS2. Chemical inhibition of GiACS1 and GiACS2 activity by

an ACS inhibitor triascin C led to growth inhibition of *G. lamblia* trophozoites at low micromolar concentration. These studies pave the way for future *in vivo* studies and also the development of more potent inhibitors targeting these metabolic enzymes.

The year 2015 was particularly exciting for the parasitology community because 2015 Nobel Prize in Physiology or Medicine was awarded to three scientists who developed therapies against parasitic infections. These drugs had their origin in microbial and plant natural products. Our third section consists of four articles on drug discovery for amebiasis. One article (Mori et al.) was contributed by researchers of Kitasato University and National Institute of Infectious Diseases, Japan and included Satoshi Omura as a co-author. Dr. Omura was awarded the 2015 Nobel Prize in Physiology or Medicine. This team screened the Kitasato Natural Products Library and extracts of 9,173 fungal and actinomycete broths against two recombinant *E. histolytica* cysteine synthases. Identification of deacetylkinamycin C and nanomycin A as potent amebicides may serve as a starting point for natural product based drug discovery for amebiasis. Identification of a protein that is involved in the virulence and regulation of different stages of life cycle of a parasite can aid in the development of new therapeutics. Singh et al. showed the involvement of *E. histolytica* heat shock protein 90 (Hsp90) in regulation of phagocytosis and encystation. This study together with a previous transcriptomic data of an increased expression of Hsp90 during excystation indicate that *E. histolytica* Hsp90 can be a promising therapeutic target. Shahinas et al. further validated the importance of parasite Hsp90 as a drug target by identifying five compounds that targeted *E. histolytica* Hsp90 and inhibited the growth of *E. histolytica* trophozoites. Though no *E. histolytica* clinical isolates with high levels of metronidazole resistance have been detected, reliance on a single drug for more than 50 years puts them at increased risk to develop drug resistance. Even a low level of metronidazole resistance in the culture led to several cellular changes in *E. histolytica* such as lower rates in growth, adhesion, phagocytosis, cytopathogenicity, and glucose consumption (Penuliar et al.). Transcriptional profiling identified genes related to oxidative stress, nucleotide binding, metabolism, and signal transduction that were differentially expressed in the resistant parasite (Penuliar et al.). This study should serve as a cautionary advice on the importance of continuing the search for an alternative drug.

The final section deals with an assay development for a *C. parvum* drug screen and identification of a new lead for the treatment of cryptosporidiosis. An improved and simplified qRT-PCR based assay was developed and made amenable to high-throughput screen for *C. parvum* (Zhang and Zhu). The assay was validated by screening a small set of compounds. Sonzogni-Desautels et al. identified oleylphosphocholine as a new drug lead for *C. parvum* infection. Oral treatment with 40 mg/kg/day of oleylphosphocholine cured the infection in immunocompromised mice and provided protection up to 30 days. It remains to be seen if similar protection can be achieved in immunocompetent mice. Still this is an encouraging finding for the development of future treatment in immunocompromised patients.

Together, this Research Topic provided the current status of drug discovery research in parasitic diarrheal diseases and covered a wide-spectrum of topics from traditional drug discovery method to target identification and mechanism of resistance.

AUTHOR CONTRIBUTIONS

AD wrote the article and JM edited the article.

REFERENCES

- Collier, S. A., Stockman, L. J., Hicks, L. A., Garrison, L. E., Zhou, F. J., and Beach, M. J. (2012). Direct healthcare costs of selected diseases primarily or partially transmitted by water. *Epidemiol. Infect.* 140, 2003–2013. doi: 10.1017/S0950268811002858
- Haque, R., Huston, C. D., Hughes, M., Houpt, E., and Petri, W. A. Jr. (2003). Amebiasis. *N. Engl. J. Med.* 348, 1565–1573. doi: 10.1056/NEJMra022710
- Hotez, P. J. (2014). Could nitazoxanide be added to other essential medicines for integrated neglected tropical disease control and elimination? *PLoS Negl. Trop. Dis.* 8:e2758. doi: 10.1371/journal.pntd.0002758
- Manjunatha, U. H., Chao, A. T., Leong, F. J., and Diagana, T. T. (2016). Cryptosporidiosis drug discovery: opportunities and challenges. *ACS Infect. Dis.* 2, 530–537. doi: 10.1021/acsinfecdis.6b00094
- Nabarro, L. E., Lever, R. A., Armstrong, M., and Chiodini, P. L. (2015). Increased incidence of nitroimidazole-refractory giardiasis at the Hospital for

ACKNOWLEDGMENTS

This Research Topic came to fruition because of the valuable contributions of all the authors. We are also grateful to the reviewers for their time, effort, and insightful suggestions. AD is supported by the National Institutes of Health, Grant #1KL2TR001444. The content is solely the responsibility of the authors and does not necessarily represent the official views of the NIH.

Tropical Diseases, London: 2008–2013. *Clin. Microbiol. Infect.* 21, 791–796. doi: 10.1016/j.cmi.2015.04.019

Torgerson, P. R., Devleesschauwer, B., Praet, N., Speybroeck, N., Willingham, A. L., Kasuga, F., et al. (2015). World Health Organization estimates of the global and regional disease burden of 11 foodborne parasitic diseases, 2010: a data synthesis. *PLoS Med.* 12:e1001920. doi: 10.1371/journal.pmed.1001920

Conflict of Interest Statement: The authors declare that the research was conducted in the absence of any commercial or financial relationships that could be construed as a potential conflict of interest.

Copyright © 2017 Debnath and McKerrow. This is an open-access article distributed under the terms of the Creative Commons Attribution License (CC BY). The use, distribution or reproduction in other forums is permitted, provided the original author(s) or licensor are credited and that the original publication in this journal is cited, in accordance with accepted academic practice. No use, distribution or reproduction is permitted which does not comply with these terms.



Parasitic diarrheal disease: drug development and targets

Amir Azam^{1*}, Mudasir N. Peerzada¹ and Kamal Ahmad²

¹ Medicinal Chemistry Laboratory, Department of Chemistry, Jamia Millia Islamia, New Delhi, India, ² Centre for Interdisciplinary Research in Basic Sciences, Jamia Millia Islamia, New Delhi, India

Diarrhea is the manifestation of gastrointestinal infection and is one of the major causes of mortality and morbidity specifically among the children of less than 5 years age worldwide. Moreover, in recent years there has been a rise in the number of reports of intestinal infections continuously in the industrialized world. These are largely related to waterborne and food borne outbreaks. These occur by the pathogenesis of both prokaryotic and eukaryotic organisms like bacteria and parasites. The parasitic intestinal infection has remained mostly unexplored and under assessed in terms of therapeutic development. The lack of new drugs and the risk of resistance have led us to carry out this review on drug development for parasitic diarrheal diseases. The major focus has been depicted on commercially available drugs, currently synthesized active heterocyclic compounds and unique drug targets, that are vital for the existence and growth of the parasites and can be further exploited for the search of therapeutically active anti-parasitic agents.

OPEN ACCESS

Edited by:

Anjan Debnath,
University of California, San Diego,
USA

Reviewed by:

Ximin Zeng,

University of Tennessee, USA

Sharon Lee Reed,

UC San Diego Health Sciences, USA

*Correspondence:

Amir Azam
amir_sumbul@yahoo.co.in

Specialty section:

This article was submitted to
Antimicrobials, Resistance and
Chemotherapy,
a section of the journal
Frontiers in Microbiology

Received: 10 June 2015

Accepted: 12 October 2015

Published: 27 October 2015

Citation:

Azam A, Peerzada MN and Ahmad K
(2015) Parasitic diarrheal disease:
drug development and targets.
Front. Microbiol. 6:1183.
doi: 10.3389/fmicb.2015.01183

INTRODUCTION

Diarrhea is a symptom of an infection in the intestinal tract, which can be caused by variety of bacterial, viral, and parasitic organisms. Infection spreads through contaminated food or drinking water or from person to person as a result of poor hygiene. Diarrheal diseases is the second leading cause of death in children under 5 years and is responsible for killing around 760,000 children every year (World Health Organization, 2013). The common symptoms include the frequent bowel movements, loose watery stool, incontinence, lower abdominal pain, or cramping and in severe cases it causes blood or flecks of mucus in the stool. The dreadful infection leads to the loss of appetite and patient is more likely to suffer from loss of weight. There are a number of non-infectious medical conditions that may cause diarrhea too. The inability in digesting dairy products which includes lactose intolerance, coeliac disease which is an intolerance of gluten in wheat and some other grains and pancreatic problems (cystic fibrosis) which interfere with production of important digestive substances (Haque et al., 2003). Several agents that cause diarrhea include viruses (rotavirus or Norwalk virus, enterovirus, or a hepatitis virus), bacteria (*Shigella* species, *Escherichia coli*, and *Campylobacter jejuni*) and parasites (*Giardia lamblia*, *Entamoeba histolytica*, and *Cryptosporidium* species; Shah et al., 2009). Diarrhea caused by parasites is unlike that of either bacterial or viral infections. For instance, *Giardia* has a slow onset of diarrhea and can be present for months, while most bacterial and viral infections are limited to 1–2 weeks (Petri, 2003). In addition, parasites are eukaryotic, which makes them larger and more complex than either viruses or bacteria and also more difficult to eradicate due to their similarity to the host. Though the infection is caused by a number of parasites which mainly include *G. lamblia*, *E. histolytica*, *Cryptosporidium parvum*,

Cyclospora cayetanensis, *Isospora belli*, *Blastocystis hominis* but the enzyme immunoassays are only available for the testing of three parasites *G. lamblia*, *E. histolytica*, and *C. parvum* (Slack, 2012).

Many of the new drug targets are being discovered with much more ease as the genomic sequences of many parasitic organisms are becoming available. This advancement has enabled researchers not only to identify new biochemical pathways and gene families that can be short-listed as potential drug targets but also has significantly increased their basic understanding of parasites that cause some of the most severe diseases. Moreover, biochemical analysis and genome sequencing both have helped in identifying potential targets, enzymes, transporters, and metabolites that are distinct in parasites and their mammalian host (Loftus et al., 2005). As a consequence one can design even better and safer effective drugs that can be used in future to combat the disease caused by the organism. The heterocyclic compounds with different modifications have been synthesized and their biological evaluation have identified them to fight the diarrhea causing parasites. In the following discussion some of the most important parasites causing diarrhea, their drugs, important traced targets and the active heterocyclic compounds synthesized against them have been summarized.

MICROSPORIDIA

Enterocytozoon bieneusi, *Encephalitozoon cuniculi*, and *Encephalitozoon intestinalis* are the reported species of microsporidia which are the causative agents of chronic diarrhea predominantly in immunocompromised individuals such as AIDS patients (Blanshard et al., 1992; Chokephaibulkit et al., 2001; Goodgame, 2003). The diarrheal disease caused by microsporidia spp. is treated by drugs fumagillin (1) and albendazole (2) (Goodgame, 2003; Agholi et al., 2013). The polyamine analogs, fumagillin-related compounds and analogs, nikkomycins (3), fluoroquinolones (4–9) and benzimidazole-related compounds are the active sources of new compounds against microsporidiosis. Fumagillin, a natural product (1) is an antibiotic and anti-angiogenic compound produced by *Aspergillus fumigatus* and has been found potent against *Encephalitozoon* spp. and *E. bieneusi* *in vitro* (Bacchi and Weiss, 2004). The antimicrosporidial activity of various fluoroquinolones derivatives such as norfloxacin (4) and ofloxacin (5) is more than gatifloxacin (6), lomefloxacin (7), moxifloxacin (8), and nalidixic acid (9) and can be the effective option of chemotherapy (Didier et al., 2005). It was observed that TNP-470 (10), ovalicin (11) and its derivatives inhibited *E. intestinalis* replication by more than 70% *in vitro* which indicates that these compounds can be used as medication for this infection (Didier et al., 2006). It has been also reported that the use of chlorine and ozone as disinfectants kills the *E. intestinalis* in water (John et al., 2005).

The albendazole, a benzimidazole derivative inhibits the microtubule assembly in *E. intestinalis* but not in *E. bieneusi* infections because benzimidazoles bind to the colchicine-binding site of β -tubulin monomer prior to dimerization with α -tubulin which blocks subsequent microtubule formation (Macdonald

et al., 2004). The β -tubulin subunit is the primary target of benzimidazole, where its predictive sensitive residues are Cys 165, Phe 167, Glu 198, Phe 200, Arg 242, and Val 268 (Macdonald et al., 2004; Tremoulet et al., 2004). It has been also reported that microtubule assembly gets inhibited due to the presence of hydrogen atom at the 1-position and a methoxycarbonylamino group at the 2-position of the benzimidazole ring (Friedman and Platzer, 1980). Fumagillin along with its analogs act on the methionine aminopeptidase type 2(MetAP2) by non-competitive inhibition, i.e., by irreversibly blocking the active site in *E. cuniculi* and it seems to be the potent inhibitor (Molina et al., 2002). Analysis of EcMetAP2 demonstrated conservation of the key residues associated with the active site of this class of enzymes including Asp251, Asp262, His331, Glu364, and Glu459 (involved in coordination of metal binding); His231 (to which fumagillin covalently binds); and Phe219, Leu328, Ile338, His339, Asp378, Tyr444, Leu447 (involved in binding substrates into the active site; Upadhyay et al., 2006). The aspartic proteases are a family of protease enzymes that use two highly conserved aspartic acid residues in the active site for catalytic cleavage of their peptide substrates (Pozio and Morales, 2005). Ritonavir (12) and indinavir (13) drugs are inhibitors of aspartyl protease, used in the highly-active antiretroviral therapy cocktail, inhibited the growth of *E. intestinalis* in tissue culture due to intermolecular hydrogen bonding between -NH group of these drugs with aspartic acid residue (Menotti et al., 2005; Pozio and Morales, 2005). The polyamine analogs are important as they act by causing depletion of polyamines, due to excessive acetylation and excretion of intracellular amines, followed by cytostasis, apoptosis and cell death (Bacchi et al., 2001). In sporoblasts of *E. cuniculi*, the chitin deacetylase activity (EcCDA) is present in the inner part of the cell wall tightly associated with the plasma membrane. This location was analyzed by biochemical and sequence data, and suggests a role in cell-wall formation. Late sporogony was characterized by the thickening of the chitin-containing endospore, but the mechanism of chitin deposition is unknown. Since the EcCDA enzyme is regularly distributed at the plasma membrane throughout sporogony, chitin may be produced all around the cell (Brosson et al., 2005). The chitin is potent target of nikkomycins due to their deacetylation activity (Bacchi et al., 2001). The fluoroquinolones interact with *E. cuniculi* targets significantly with DNA topoisomerases, which are the enzymes that have evolved to solve the topological problems associated with DNA metabolism such as transcription, replication, packing and unpacking of DNA in the cell (Hooper, 2000). So, present research studies are concentrating on compounds that target microsporidian polyamines (e.g., polyamine analogs), Chitin (e.g., nikkomycins), and DNA topoisomerases (e.g., fluoroquinolones; Bacchi et al., 2001; Zhang et al., 2005; Didier and Weiss, 2006).

ENTAMOEBA HISTOLYTICA

E. histolytica is the causative agent of amoebiasis, a contagious disease of the human gastrointestinal tract (Tengku and Norhayati, 2011; Watanabe et al., 2011). It is an organism

implicated in both diarrheal disease and invasive disease such as liver abscesses. Metronidazole (**14**) is the first line medication used against the infection but long-term uses produce several side effects in patients (Ordaz-Pichardo et al., 2005). It is potentially carcinogenic to humans because it is genotoxic to human cells (Bendesky et al., 2002). Furthermore, resistance of *E. histolytica* to standard drug metronidazole and relapses of intestinal and hepatic amoebiasis have been reported (Becker et al., 2011; Hwang et al., 2011). The authors have earlier reported diverse functionalized organic compounds synthesized and screened against *E. histolytica* (Azam and Agarwal, 2007, 2015). Nitroimidazole compounds have been used to treat a number of anaerobic bacteria and pathogenic protozoan infections, including *Trichomonas vaginalis*, *E. histolytica*, and *G. lamblia* since decades (Müller, 1983; Upcroft et al., 1999). Presently, metronidazole, tinidazole (**15**) and ornidazole (**16**) are highly recommended drugs for the treatment of protozoal infections (Azam and Agarwal, 2007). The interesting fact about the metronidazole analogs as an alternative to the treatment of parasitic infections is facilitated by the fact that not only the metronidazole is an effective drug but it also has a side chain which provides an opportunity to carry out various modifications whose significant activity has been reported (Kucik et al., 2004).

Chalcones are the important class of antiamoebic drugs and their analogs have been synthesized having better activity. A series of chalcones were synthesized bearing N-substituted ethanamine by aldol condensation reaction and the compound (**17**) was found to be very potent amoebicidal indicating that such compounds can be the effective therapeutic candidates (Zaidi et al., 2015). Metronidazole hydrazone conjugates were synthesized and screened *in vitro* for antiamoebic activity, the compound (**18**) was found more active (Ansari et al., 2015). A series of chloroquinoline-acetamide hybrids were synthesized and the compound (**19**) inhibit the growth of *E. histolytica* (Inam et al., 2015). The *N*-acylhydrazones derived from 7-chloro-4-piperazin-1-yl-quinoline were evaluated against *E. histolytica* and the compound (**20**) was more potent than metronidazole (Inam et al., 2014). Metronidazole-triazole hybrids (**21**) showed amoebicidal activity (Negi et al., 2014). Coordination complexes do exhibit the anti-amoebic activity and the efficacy depends on the selection of both central metal atom and ligands. The terpyridine ligand complexed with divalent metals viz Cu, Co, Mn, Ni, and Zn yield the coordination complexes of general formula [Metal(Fcpty)₂][PF₆]₂. The complex Ni(Fcpty)₂][PF₆]₂ (**22**) has been found to be having most promising activity against *E. histolytica* and therefore, can be used as significant drug candidates for amoebiasis (Juneja et al., 2014). Hydrazone and oxadiazoline derivatives of 2-methyl-5-nitro-1H-imidazole were being synthesized and evaluated *in vitro* against HM1:IMSS strain of *E. histolytica* and it was observed that compounds (**23**, **24**) were more potent against amoebiasis (Wani et al., 2013). A series of pyrazoline derivatives were synthesized and their *in vitro* screening against HM1: IMSS strain of *E. histolytica*, results showed the compounds (2E)-1,3-bis(4-methylphenyl)prop-2-en-1-one (**25**) and 1-(4,5-dihydro-5-(4-methoxyphenyl)-3-phenylpyrazol-1-yl)-2-(5-(4-methoxyphenyl)-1H-tetrazol-1-yl)ethanone (**26**)

exhibited the excellent antiamoebic activity and were having the IC₅₀-values of 4.19 and 1.16 μM, respectively (Wani et al., 2012b). Compounds bearing a tetrazole and triazine ring motifs in conjugation with a sulphonamide group were synthesized and N, N'-6-(1,3-benzodioxol-5-yl)-(1,3,5-triazine-2,4-diyl)-bis-4-nitrobenzene sulphonamide (**27**) was found to be more potent antiamoebic in nature and was having IC₅₀-value of 1.02 μM (Wani et al., 2012a). The *in vitro* antiamoebic activity of 4,6 aminopyrimidines and their sulphonamide derivatives was investigated against *E. histolytica* and it was found that the compound N-[4-(2-chlorophenyl)-6-phenylpyrimidin-2-yl]-benzenesulphonamide (**28**) having IC₅₀-value 0.44 μM was most active (Siddiqui and Azam, 2014). Various derivatives of dioxazoles were synthesized and *in vitro* analysis showed that the compound 5-(4-methoxy-phenyl)-3-(5-nitro-2-thienyl)-1,4,2-dioxazole (**29**) was having IC₅₀-value 1.60 μM and inhibited the growth of *E. histolytica* significantly (Irfan et al., 2010). Thiosemicarbazides are the focused moieties for antiamoebic drug synthesis and the attempt was made to synthesize a novel series of 4-substituted 1-{[4-(10,15,20-triphenylporphyrin-5-yl)phenyl]methylidene}thiosemicarbazide and their antiamoebic activity was investigated. The 4-(3-methylphenyl)-1-{[4-(10,15,20-triphenylporphyrin-5-yl)phenyl]methylidene}thiosemicarbazide (**30**) with an electron-withdrawing group attached to N(4) exhibited the best antiamoebic activity and was having IC₅₀-value 0.538 μM (Bhat et al., 2008). A new series of thiosemicarbazones of 7-hydroxy-8-acetylcoumarin with different thiosemicarbazides were synthesized and were tested against *E. histolytica*. The 7-hydroxy-8-acetylcoumarin-N(4,4)methylbenzyl thiosemicarbazone (**31**) was having IC₅₀-value 1.06 μM and found to be antiamoebic (Iqbal et al., 2009). Thiocarbamoyl bis-pyrazoline derivatives were synthesized by cyclization of chalcones with N-4 substituted thiosemicarbazides under basic conditions and the evaluation showed that the compound(4-nitrophenylamino)[5-(4-{1-[(4-nitrophenylamino)thioxomethyl]-3-phenyl(2-pyrazoline-5-yl-phenyl)}-3-phenyl(2-pyrazolinyl)]methane-1-thione (**32**) was having IC₅₀-value 0.42 μM and predominantly active as an amoebicidal candidate (Bhat et al., 2009a). An attempt was made to synthesize the amino-5-substituted-(3-phenyl(2-pyrazolinyl))methane-1-thione derivatives, 2-(5-substituted-3-phenyl-2-pyrazolinyl)-1,3-thiazolino[5,4-b]quinoxaline derivatives, and various chalcones derivatives for evaluation against HM1:IMSS strain of *E. histolytica*. The quinoxaline2-{5-[2-(methylethyl)phenyl]-3-phenyl-2-pyrazolinyl}-1,3-thiazolino[5,4-b]quinoxaline (**33**) showed most promising antiamoebic activity with IC₅₀-value of 0.17 μM. The results suggested that the further modification of such compounds can enhance their efficacy (Budakoti et al., 2009). The synthesis of bis-ferrocenyl-substituted core-modified porphyrins derivatives were synthesized under acidic conditions and their *in vitro* screening was performed against HM1:IMSS strain of *E. histolytica*. The promising results showed the 1,1'-(10,15-diphenyl-21,23-dithiaporphine-5,20-diyl)bis[2-{{methyl(phenylmethyl)amino}methyl}-ferrocene] (**34**) having IC₅₀-value of 0.59 μM was extremely potent (Bhat et al., 2009b). A library of isothiourea derivatives was synthesized and the

maximum activity was shown by compound (35) with IC₅₀-value 2.48 μM. These are the amphiphilic compounds and exist in cationic form which makes them active in biological systems (Kazimierczuk et al., 2010). Benzimidazoles proved to be having antiparasitic activity and 5(6)-chloro-1H-benzimidazole-2-(3H)-thione (36) was having IC₅₀-value of 0.005 μM for *E. histolytica* which indicates that these derivatives are having higher activity than metronidazole (Valdez et al., 2002). A series of ethyl and methyl quinoxaline-7-carboxylate 1,4-di-N-oxide derivatives were synthesized by Beirut reaction and evaluated against HM1:IMSS strain of *E. histolytica*. The methyl 2-acetyl-3-methyl-quinoxaline-7-carboxylate 1,4-di-N-oxide (37) and ethyl 2-amide-3-methylquinoxaline-7-carboxylate 1,4-di-N-oxide (38) were having IC₅₀-value 1.41 and 1.47 μM, respectively and showed higher potency toward amoebicidal activity (Duque-Montaña et al., 2013). The benzologue derivative of nitazoxanide 2-{{(6-Nitro-1,3-benzothiazol-2-yl)amino}carbonyl}phenyl acetate(39) having IC₅₀-value 0.297 μM showed better antiamoebic activity as compared to metronidazole and indicated that such derivatives can be explored for the search of effective chemotherapy (Navarrete-Vazquez et al., 2011). The amide derivatives of trifluoromethionine (TFM) have been observed to have excellent activity against *E. histolytica*. Using the TFM as lead 3,4-dimethoxyanilide trifluoromethionine (40) with methoxy group at meta and para positions was having IC₅₀-value 1.19 μM and was observed most active *in vitro* evaluation (Sato et al., 2010). The compound 1,5-bis[4-(5-methoxy-1H-benzimidazole-2-yl) phenoxy]pentane (41) was evaluated *in vitro* against *E. histolytica* showed remarkable IC₅₀-value 0.109 μM for amoebicidal potency due to methoxy group attached to benzimidazole ring (Torres-Gomez et al., 2008b). Acetamide and sulfonamide derivatives of imidazole viz N-benzyl-2-(2-methyl-4-nitro-1H-imidazol-1-yl)acetamide (42) and 2-methyl-1-[(4-methylphenyl)sulfonyl]-4-nitro-1H-imidazole (43) are important class of antiparasitic agents and were having IC₅₀-value 3.96 and 3.55 μM, respectively (Hernández-Nunez et al., 2009). Phenyl hydrazine derivatives were synthesized and it was observed that (E)-1-(3-nitrobenzylidene)-2-phenylhydrazine (44) was most potent against HM1:IMSS strain of *E. histolytica* *in vitro* having IC₅₀-value 0.84 μM. This indicated that hydrazine derivatives can be explored for the search of effective chemotherapeutic agent for amoebiasis and their mechanism of action needs to be elucidated (Toledano-Magana et al., 2015).

Emphasizing the elucidated drug targets and mechanism, the mode of action of metronidazole lies in that it gets reduced to nitroradical anion or nitrosoimidazole by thioredoxin reductase (TrxR) inside *E. histolytica* cell (Leitsch et al., 2007). The nitroradical anion formed reduces O₂ and thereby generates reactive oxygen species, which are highly noxious to the cells of microaerophilic *E. histolytica*. However, the nitroso imidazole reacts with non-protein thiols or proteins to forms adduct. The adduct causes depletion of non-protein thiols and the modification of thioredoxin reductase (TrxR), thioredoxin (Trx), superoxide dismutase (SOD), metronidazole target protein 1 (Mtp1), and purine nucleoside phosphorylase (PNP). The combination of proteins with activated metronidazole makes the

cells more vulnerable to oxidative stress and thereby kills *E. histolytica* (**Figure 1**; Samarawickrema et al., 1997; Leitsch et al., 2007). 5-Nitroimidazoles have been the mainstay of treatment, but resistance is a concern and new drug targets are needed. One potential target is the biosynthetic pathway for cysteine which is crucial for growth and various cellular activities (Diamond et al., 1978; Gilin and Diamond, 1980). Besides being precursor for protein biosynthesis, cysteine may compensate for the lack of glutathione, a major component of oxidative stress resistance in many organisms (Fahey et al., 1984; Loftus et al., 2005). It is also needed in the attachment to matrix, elongation and mobility of *E. histolytica* cells (Gillin and Diamond, 1980). In this organism, the condensation of O- acetylserine with sulfide is the major route of cysteine biosynthesis, which involves two key enzymes: O-acetyl-L-serine sulfhydrylase (OASS) and serine acetyltransferase (SATase; Nozaki et al., 1998). In general, in plants and most known organisms, the cysteine biosynthesis pathway is regulated both by the interaction of SAT and OASS to form the cysteine synthase complex (CSC) under sulfur sufficient condition but this type of regulation is absent in *E. histolytica*. These enzymes have been demonstrated to play a central role in controlling the intracellular cysteine concentration in *E. Histolytica* (Nozaki et al., 1999) and block of cysteine biosynthesis is therefore a possible strategy for inhibiting growth of *E. histolytica* (Ali and Nozaki, 2007). *E. histolytica* along with a number of other parasitic protists utilizes an unusual form of phosphofructo-1-kinase (PFK; EC 2.7.1.90) in a central step in carbohydrate metabolism. A homology model of *E. histolytica* PPI-PFK was constructed and screened with various bisphosphonates, which are analogs of pyrophosphate with a carbon instead of oxygen atom and synthetic pyrophosphate. It was found that the Compounds BA49280E (45) and CGP42446A (46) were good inhibitors of PFK in *E. histolytica*. Based on this study it has been suggested that PFK is attractive target for antiamoebic drugs (Reeves et al., 1974, 1976). Triosephosphate isomerase is another relatively well-studied glycolytic enzyme with both its sequence and structure known in a large number of organisms including *E. histolytica* (Rodriguez-Romero et al., 2002). It has been proposed to be a target for drug design due to presence of a cysteine residue (Cys 14) at the dimer interface in *E. histolytica* (Gómez-Puyou et al., 1995). Alcohol dehydrogenase 2 (EhADH2) is a bifunctional 97 kDa polypeptide having the alcohol and aldehyde (ALDH) dehydrogenase activities utilize NAD and Fe²⁺ as cofactor (Bruchhaus and Tannich, 1994). This enzyme does not have a homolog in man. However, *E. histolytica* possesses other NADP dependent ADH and ALDH enzymes that could serve a similar function i.e., EhADH1, EhADH3 and EhALDH1. EhADH1 enzyme does not utilize acetyl CoA as substrate thereby suggesting that EhADH2 is solely responsible for the conversion of acetyl CoA to acetaldehyde (Zhang et al., 1994). Based on this data it has been suggested that EhADH2 could also serve as a target for antiamoebic drugs. Calcium is an important secondary messenger in many signal transduction pathways, is thought to be involved in the pathogenesis of amoebiasis and the prevention of the influx of Ca²⁺ can be the potent target (Meza, 2000). In *E. histolytica*, a number of calcium binding proteins have been identified. More importantly

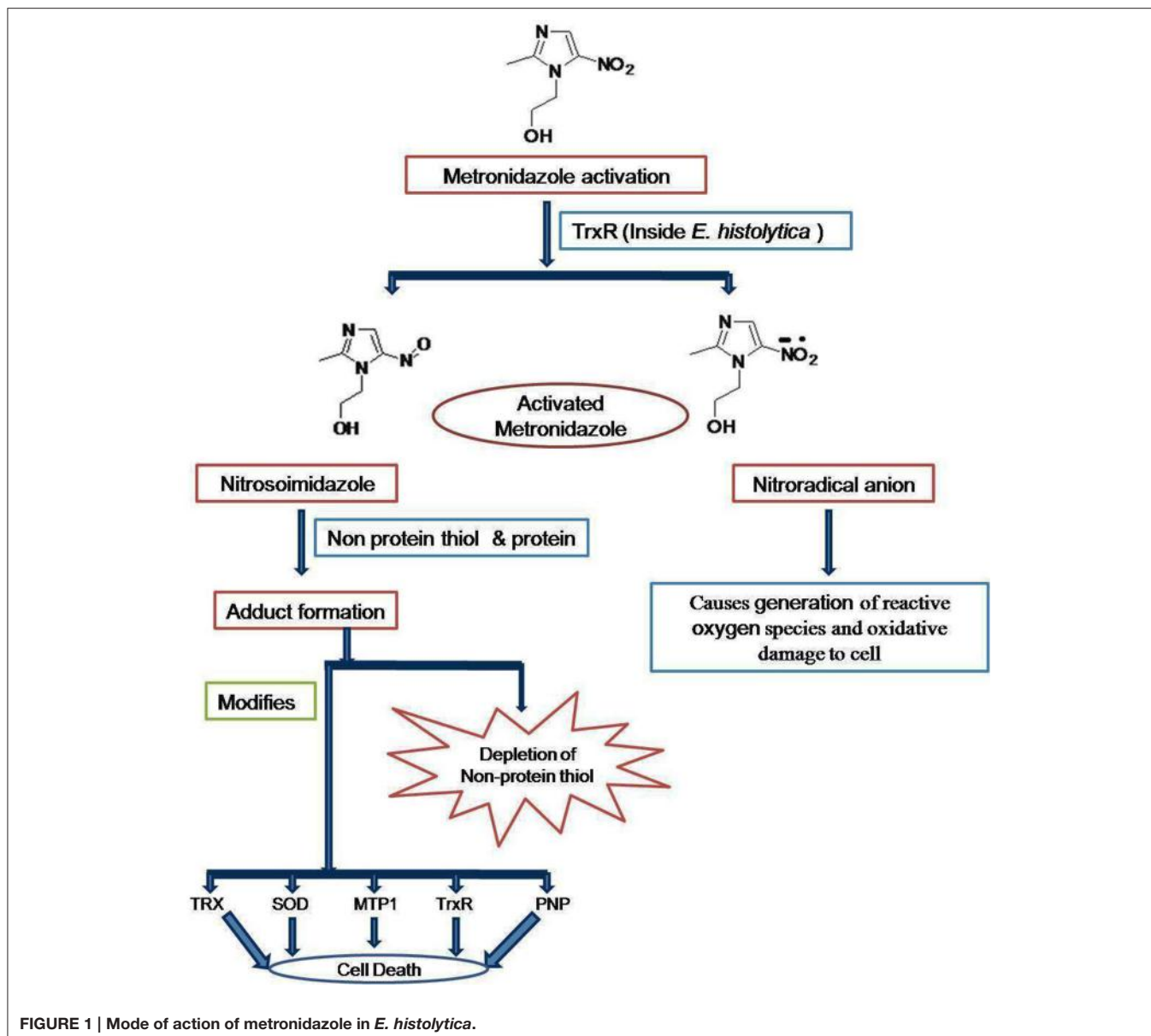


FIGURE 1 | Mode of action of metronidazole in *E. histolytica*.

two distinct calcium binding proteins EhCaBP1 and EhCaBP2, have been characterized and their role has been simultaneously approached (Sahoo et al., 2003). It has been characterized that cyclosporine A inhibits calcineurin and P-glycoprotein activity and thereby inhibits proliferation of *E. histolytica* (Carrero et al., 2004). Recently it has been shown that when expression of EhCaBP1(a calmodulin containing 134 amino acid long proteins demonstrated to be essential for *Entamoeba*) is blocked, the cellular proliferation in *E. histolytica* gets inhibited (Sahoo et al., 2004).

GIARDIA LAMBLIA

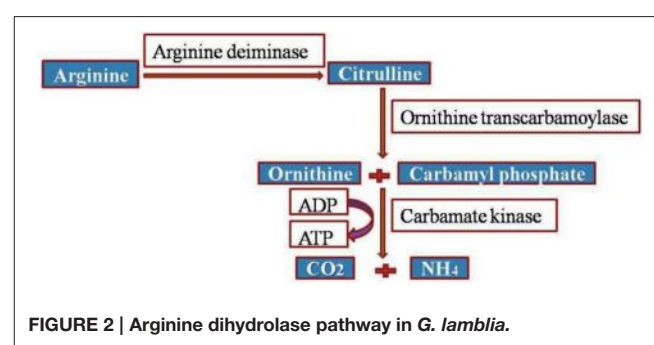
G. lamblia, an amitochondriate parasite is the major causative agent of human diarrheal disease, infecting an estimated 10%

of the world's population both endemically and epidemically (Huang and White, 2006). For the treatment of the intestinal infections caused by *G. lamblia* at least six different classes of drugs are used, but the drugs containing 5-nitroimidazole moiety are most often prescribed due to their significant efficacy. However, the other classes are used when the former fails in treatment. Metronidazole (14), tinidazole (15), ornidazole (16) and secnidazole (47) are the 5-nitroimidazole moiety containing drugs. Furazolidone (48) a nitrofuran derivative, albendazole (2) and mebendazole (49) the benzimidazole derivatives, quinacrine (50) an acridine derivative, paromomycin (51) an aminoglycoside derivative and nitazoxanide (52) a 5-nitrothiazolyl derivative are also used for the treatment of *G. lamblia* diarrheal disease depending on the age of patient. But these drugs have various side effects (Reynoldson et al., 1992;

Escobedo and Cimerman, 2007). The *in vivo* effects of benzyl and cyclohexyl derivatives like, 2-(1*H*-1-imidazolyl)-1-phenyl-1-ethanol, 2-(2-methyl-1 *H*-1-imidazolyl)-1-phenyl-1-ethanol, 2-(2-methyl-4-nitro-1*H*-1-imidazolyl)-1-phenyl-1-ethanol, 2-(1*H*-1-imidazolyl)-1-cyclohexanol and 1[bis-4-methoxyphenyl-phenylmethyl]-2-methyl-4-nitroimidazole (53–57) were studied on the *G. lamblia* trophozoite in the white Syrian mice model and were found to be active (Motazedian et al., 2014). The thieno[2,3-b]pyridine derivatives were synthesized and the 4-(4-methoxyphenylamino)thieno[2,3-b]pyridine-5-carbonitrile having the -OCH₃ group at para position (58) showed the excellent giardicidal effect possibly due to the higher electron density concentrated over phenyl ring (Bernardino et al., 2006). A series of novel hybrids of benzimidazole-pentamidine were prepared and 1,5-bis[2-methoxy-4-(5-methyl-1*H*-benzimidazole-2-yl)phenoxy] pentane (59) was found 3- and 9-folds more potent against *G. lamblia* infection than metronidazole and pentamidine, respectively and was having IC₅₀-value of 0.372 μM (Torres-Gomez et al., 2008a). The 2-(trifluoromethyl)benzimidazole derivatives like 5-chloro-1-methyl-2-(trifluoromethyl)benzimidazole (60), differently substituted at the 1-, 5-, and 6-positions proved to be active against *G. lamblia* in their *in vitro* analysis and IC₅₀-value of 0.042 μM was observed for compound (60) (Gabriel Navarrete-Vaa Zquez et al., 2001). A library of chalcones was prepared by condensing substituted acetophenones with benzaldehydes using the Claisen-Schmidt base-catalyzed aldol condensation reaction. Among these chalcones, substituted with -OCH₃, -H, -Cl, -F at different positions (E)-3-(6-fluorophenyl)-1-(4-methoxyphenyl)prop-2-en-1-one (61) with IC₅₀-value of 12.72 μM showed the excellent results toward the giardial infection (Montes-Avila et al., 2009). The benzimidazole derivative 5(6)-chloro-1*H*-benzimidazole-2-(3*H*)-thione (62) was reported active *in vitro* against *G. lamblia* with IC₅₀-value of 0.005 μM and inhibits tubulin polymerization (Valdez et al., 2002). The albendazole analogs 1-methyl-6-(propylthio)-2-(trifluoromethyl)-1*H*-benzimidazole (63) and 5(6)-(propylthio)-2-(trifluoromethyl)-1*H*-benzimidazole (64) were having IC₅₀-values 1.403 and 1.515 μM, respectively are active toward giardiasis. The mebendazole analogs 5-benzoyl-1-methyl-2-(trifluoromethyl)-1*H*-benzimidazole (65) and 6-benzoyl-1-methyl-2-(trifluoromethyl)-1*H*-benzimidazole (66) have also been found to be active against *G. lamblia* and these were having IC₅₀-values 1.098 μM 1.285 μM, respectively (Navarrete-Vazquez et al., 2003). Among the series of 3-tetrazolylmethyl-4*H*-chromen-4-ones the compound 3-((1-cyclohexyl-1*H*-tetrazol-5-yl)(3,4,5-trimethoxyphenyl)amino)methyl)-4*H*-chromen-4-one (67) having IC₅₀-value of 171.4 μM can represent the suitable alternatives against resistant *G. lamblia* parasites(Cano et al., 2014). Thiazole derivatives were synthesized and screened against *G. intestinalis*, two novel methyl 5-nitro-1,3-thiazol-2-ylcarbamate (68) and ethyl [(5-nitro-1,3-thiazol-2-yl)amino](oxo)acetate (69) proved to be potent giardicidal and were having IC₅₀-value of 0.010 and 6.410 μM, respectively(Nava-Zuazo et al., 2014). By using the Ugi-azide multicomponent reaction, novel

3-tetrazolylmethyl-4*H*-chromen-4-ones were synthesized and evaluated against *G. lamblia*. The *in vivo* investigation demonstrated that these compounds like (70) could be specifically considered drug candidates for giardial infection (Cano et al., 2014). A series of novel hybrids from benzimidazole and pentamidine were prepared and tested *in vitro* against the protozoa and it was observed that the compound 1,5-bis[2-methoxy-4-(5-methyl-1*H*-benzimidazole-2-yl)phenoxy] pentane (71) with IC₅₀-value 0.372 μM showed 3- and 9-fold more activity against *G. lamblia* than metronidazole and pentamidine, respectively (Torres-Gomez et al., 2008b). Benzologues of nitazoxanide and tizoxanide were synthesized and tested *in vitro* against *G. intestinalis*. The 2-[(6-nitro-1,3-benzothiazol-2-yl)amino]carbonylphenyl acetate (39) was having IC₅₀-value 3.515 μM and was 18-times more potent than metronidazole (Navarrete-Vazquez et al., 2011). Acetamide derivatives of imidazole like N-(4-cyanophenyl)-2-(2-methyl-4-nitro-1*H*-imidazol-1-yl) acetamide (72) and 2-methyl-4-nitro-1-[(4-nitrophenyl)sulfonyl]-1*H*-imidazole (73) were screened *in vitro* and were found active against *G. lamblia* with IC₅₀-value 11.25 and 7.50 μM, respectively. These can be further modified to enhance their activity (Hernández-Nunez et al., 2009).

Accentuating the targets, *G. lamblia* utilizes the arginine dihydrolase pathway to produce ATP from ADP and L-arginine (Schofield et al., 1990), a pathway which is lacking in higher eukaryotes including humans. The arginine dihydrolase pathway employs three enzymes, arginine deiminase, ornithine transcarbamoylase, and carbamate kinase (CK; EC 2.7.2.2). CK catalyzes the last step of the pathway, converting carbamoyl phosphate and ADP into carbamate and ATP (Figure 2; Lim et al., 2013). Carbamate kinase is essential enzyme of *Giardia lamblia*, and the antialcoholism drug disulfiram (74) kills the trophozoites and inhibits this enzyme. Disulfiram and their analogs act by modifying Cys242 adjacent to the active site and cure of giardiasis in mice has also been reported (Galkin et al., 2014). Nitazoxanide, nitroimidazoles, metronidazole and tinidazole use nitroreductases such as pyruvate ferredoxin oxidoreductase (PFOR) as their target sites in Giardial infection (Hoffman et al., 2007; Müller et al., 2007). The 5-nitroimidazoles like metronidazole act in *G. lamblia* by two distinct mechanisms. In one mechanism metronidazole gets reduced to toxic nitro-radical anion via pyruvate ferredoxin oxidoreductase/ferredoxin (PFOR/Fd) couple in presence of pyruvate and the cofactor



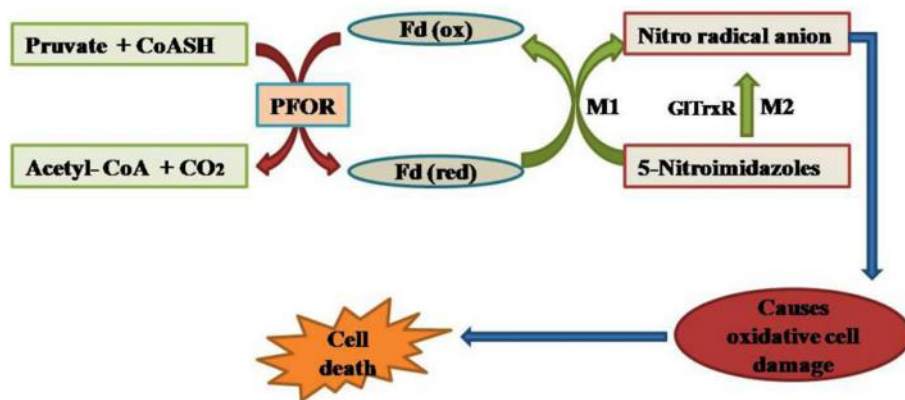


FIGURE 3 | Mode of action of nitroimidazoles in *G. lamblia*.

CoASH during the electron transport pathway in *G. lamblia*. In the second mechanism metronidazole reduction occurs due to the activity of *G. lamblia* thioredoxin reductase (GITrxR). The radicals formed cause oxidative damage to *G. lamblia* cell and thereby kills parasite (Figure 3).

Protein disulfide isomerases, specifically PDI2 and PDI4 have recently been reported as promising targets for new drugs effective against giardiasis (Müller et al., 2007). Furazolidone gets reduced by NADH oxidase when the reduced products obtained disrupt the action of DNA in Giardial infection (Brown et al., 1996; Upcroft and Upcroft, 1998). Recently, Hsp90 inhibitors as potential leads for antiparasitic chemotherapy have been reported. Hsp90 inhibitor prodrug (SNX-5422) was evaluated in animal models to proof the principle that an oral drug could be effective (Debnath et al., 2014). Metronidazole analogs were more active than metronidazole in changing significantly the morphology and ultrastructure of the parasite *G. lamblia*. The analogs affected parasite cell vesicle trafficking, autophagy, and triggered differentiation into cysts of *G. lamblia* (Busatti et al., 2013). The novel nitroreductase target sites viz GINR1 and GINR2 have been identified to be the potent targets for nitroimidazole, metronidazole, nitrothiazolide and nitazoxanide in *G. lamblia* (Muller et al., 2015).

CRYPTOSPORIDIUM PARVUM

The protozoan *C. parvum* causes cryptosporidiosis which is associated with watery diarrhea that may sometimes be profuse and prolonged in children (Current and Garcia, 1991; Bouzid et al., 2013). It is the second most common protozoan pathogen responsible for severe diarrhea and was also associated with death in young children under 12–23 months of age (Kotloff et al., 2013). Currently nitazoxanide (52), paromomycin (51), and azithromycin are the most commonly used for the treatment of cryptosporidiosis. However, nitazoxanide (52) is effective in the immunocompetent and ineffective in the immunocompromised patients (Mead, 2002; Gargala, 2008). The available medication is not effective in all the patients besides having side effects of headache, nausea, stomach pain,

severe or persistent dizziness, shortness of breath and unusual tiredness. Progress in the development of anti-cryptosporidial drugs has been very slow due to the difficulty in the *in vitro* culture of *Cryptosporidium* (Abrahamsen et al., 2004; Andrews et al., 2014). Many drug targets are not present in this parasite because it has completely lost the plastid derived apicoplast. Its mitochondrion lacks the citrate cycle and cytochrome based respiratory chain which directs the novel target identification for drug development. Recently a research group synthesized 11 derivatives of benzimidazole, out of which three compounds (75–77) showed anti-cryptosporidic effect equivalent to paromomycin (Graczyk et al., 2011). The dicationic carbazole compounds are active against *C. parvum* and compound (78) was elucidated to be potent against cryptosporidiosis (Blagburn et al., 1998). The macrolide antibiotics like spiramycin (79), roxithromycin (80), and clarithromycin (81) were thought to be promising drugs against cryptosporidiosis but the final clinical trials have not yet been completed. There is the intense need for the development of effective chemotherapy for cryptosporidiosis in immunodeficient patients (Saez-Llorens, 1989; Uip et al., 1998). The nitrogen-containing bisphosphonates (N-BPs) exhibit anticryptosporidium activities in low micromolar concentrations. It has been observed that NBPs act on the novel non-specific polyprenyl pyrophosphate synthase that can synthesize isoprenoids from C20->C45 in *Cryptosporidium spp* (Artz et al., 2008).

In *C. parvum*, phosphofructokinase enzyme is pyrophosphate specific (PPi-PFK; Denton et al., 1996). The accepted dogma is that PPi-PFK is advantageous to anaerobic organisms because its economic effect on the cell's consumption of ATP means that the net production from glycolysis is three ATP molecules per glucose molecule rather than the more usual two ATP molecules (Coombs and Müller, 1995). The critical role played by PPi-PFK in energy metabolism together with difference from the human host PFK, make it an attractive target for drug. A mannitol cycle is an important part of energy metabolism for *C. parvum*. A key feature of the cycle is that the enzyme initiates mannitol biosynthesis, mannitol-1-phosphate dehydrogenase, is regulated by the binding of a specific inhibitor, a protein that

has been found to belong to the 14-3-3 group of proteins. Inhibition of mannitol synthesis would be likely to have a severe impact upon the oocyst stage of the parasite and so reduces transmission (Schmatz, 1997). The inosine-5'-monophosphate dehydrogenase (IMPDH) and proteases are also proposed to be the target sites in cryptosporidial infection (Mandapati et al., 2014). It has a bacterial-type inosine-5'-monophosphate dehydrogenase (IMPDH) as the only means to convert AMP to GMP (Umejiego et al., 2008). The target site of the paromomycin is the A site of ribosome where upon action it disrupts the protein biosynthesis in *C. parvum* (Müller et al., 2007). Acyl-coenzyme-A synthetases have been observed to be inhibited by triacsin C in cryptosporidial infection in mice (Guo et al., 2014). The dicationic-substituted aromatic molecules act by binding to the minor groove of DNA in the *Cryptosporidium* and thereby affects DNA-associated enzymes such as topoisomerases, endo and exonucleases or other processes, such as DNA replication, recombination, and repair (Hildebrandt et al., 1998). Mebendazole or albendazole acts by interacting with the colchicine site of tubulin in the microtubules of *Cryptosporidium* spp (Brown et al., 1996).

BLASTOCYSTIS HOMINIS

Blastocystis hominis is a unicellular anaerobic protozoon and infects the human gastrointestinal tract. It gets transmitted via animal contact, water and food contaminated with excreted cysts of the organism (Eroglu and Koltas, 2010). The pathogenesis of *B. hominis* leads to symptoms such as diarrhea, flatulence, anorexia, abdominal pain, vomiting, perianal pruritis, and bloating (Sheehan et al., 1986; Chen et al., 2014). The currently used drugs against this infection are metronidazole (14) or tinidazole (15) (Sohail and Fischer, 2005; Tan, 2008). Metronidazole commonly used for the treatment of blastocystosis induces programmed cell death in the *B. hominis* (Nasirudeen et al., 2004). The reduction of the nitro group cytotoxic radicals in mitochondria causes the death of concerned pathogen (Kulda, 1999). Trimethoprim-sulfamethoxazole (TMP-SMX) (82, 83) is used as the second line medication when the first line treatment by metronidazole (14) does not work (Ok et al., 1999). Other compounds being occasionally used include pentamidine (84), iodochlorhydroxyquin (85), furazolidone (48), iodoquinol (86), tinidazole (15), nitazoxanide (52), and emetine (87) (Moghaddam et al., 2005; Sohail and Fischer, 2005). Paramomycin (51), a broad spectrum aminoglycoside antibiotic has exhibited superior performance in comparison to metronidazole (14). Therefore, it can act as the therapeutic agent for *B. hominis* infections (Van Hellemond et al., 2013).

The mechanism of action of several drugs, included metronidazole, have been studied and found linked to the induction of programmed cell death in the parasite, when treated with a surface reactive cytotoxic monoclonal antibody (MAb 1D5). The central vacuole of *B. hominis* grown in normal physiological conditions may contain lipid granules or electron-dense particles. This central vacuole is used for programmed cell death (PCD) process and it acts as a repository where apoptotic bodies are stored before being released into the extracellular

space. Central vacuole is potent target for apoptosis (Nasirudeen et al., 2001, 2004).

ISOSPORA BELLI

Isosporiasis is human intestinal disease caused by the parasite *I. belli*. It is most commonly observed in Africa, Asia and South America. The currently used drugs against this infection is combination of trimethoprim (82) and sulfamethoxazole (83) (Goodgame, 2003; Hunter et al., 2004). The pyrimethamine (88) and sulfadiazine (89) also cure the diarrheal disease caused by *I. belli* (Ferguson et al., 1980; Ebrahimzadeh and Bottone, 1996). Macrolide antibiotics like sirimamycin proved to be effective when pyrimethamine-sulfadoxine (88, 90) fails to cure the intestinal infection by *I. belli* specifically in AIDS patients (Ferguson et al., 1980). Similarly, roxithromycin (91) is also observed to be effective for chronic *I. belli* induced diarrhea when TMP-SMX (82, 83) or pyrimethamine (88) treatments become inadequate (Musey et al., 1988). It has been reported that metronidazole (14), tinidazole (15), quinacrine (50), and furazolidone (48) also cure the *I. belli* induced diarrhea but to lesser extent. However, the treatment with metronidazole is more efficient than tinidazole (15), quinacrine (50), and furazolidone (48) (Trier et al., 1974; Syrkis et al., 1975; Butler and De Boer, 1981; Weiss et al., 1988). The antimalarial compounds, primaquine phosphate (92) and chloroquine phosphate (93) may be helpful in immunocompetent patients with persistent *I. belli* infection (Trier et al., 1974). The synthesis of more potent drugs and tracing the valuable targets is the important area of research for *I. belli* intestinal infection.

CYCLOSPORA CAYETANENSIS

Cyclosporiasis is the gastrointestinal illness caused by the microscopic parasite *C. cayetanensis*. The extent of illness varies based on age, condition of the host and size of the infectious dose (Goodgame, 2003). Trimethoprim-sulfamethoxazole (82, 83) was at first used to treat cyclosporiasis in immunocompetent and immunocompromised patients (Madico et al., 1993; Guerrant et al., 2001). However, the patients who are allergic to sulpha drugs, the ciprofloxacin (94) or trimethoprim (82) is prescribed (Verdier et al., 2000). Nitazoxanide (52) had no severe side effects and was tolerated effectively and can be better option for intestinal infection caused by *C. cayetanensis* (Diaz et al., 2003). The development of effective drugs and the quest of essential targets are of prime importance to treat cyclosporiasis.

CONCLUSION

Drug development for parasite-induced diarrheal disease is in progress. There is a pressing need for the identification of compounds which are efficacious in *in vivo* animal studies and can be subjected to clinical trials. Drug development for *C. parvum* is particularly challenging because of the difficulty of *in vitro* screening. Maximum effort should be directed toward new compounds to treat cryptosporidiosis because of the limited availability of effective drugs. Resistance to the

current drugs, metronidazole, paromomycin, and nitazoxanide is a major concern. A major research focus on key biochemical pathways, identification of essential targets, better assay methods, and *in vivo* testing are urgently needed to identify new chemotherapeutic agents for parasite-induced diarrheal disease. As per our contemplated study, there is a need for the determination of mechanism of action of the synthesized compounds against *E. histolytica* and *G. lamblia*. The synthesized heterocyclic scaffolds bearing different substituents that have been found to be active *in vivo* studies against the parasites causing diarrhea, can be further explored as future drug candidates with higher efficacy, resistance effectiveness, and lesser side effects.

REFERENCES

- Abrahamsen, M. S., Templeton, T. J., Enomoto, S., Abrahante, J. E., Zhu, G., Lancet, C. A., et al. (2004). Complete genome sequence of the apicomplexan, *Cryptosporidium parvum*. *Science* 304, 441–445. doi: 10.1126/science.1094786
- Agholi, M., Hatam, G. R., and Motazedian, M. H. (2013). Microsporidia and coccidia as causes of persistence diarrhea among liver transplant children: incidence rate and species/genotypes. *Pediatr Infect Dis J* 32, 185–187. doi: 10.1097/INF.0b013e318273d95f
- Ali, V., and Nozaki, T. (2007). Current therapeutics, their problems, and sulfur-containing-amino-acid metabolism as a novel target against infections by amitochondriate protozoan parasites. *Clin. Microbiol. Rev.* 20, 164–187. doi: 10.1128/CMR.00019-06
- Andrews, K. T., Fisher, G., and Skinner-Adams, T. S. (2014). Drug repurposing and human parasitic protozoan diseases. *Int. J. Parasitol. Drugs Drug Resist.* 4, 95–111. doi: 10.1016/j.ijpddr.2014.02.002
- Ansari, M. F., Siddiqui, S. M., Agarwal, S. M., Vikramdeo, K. S., Mondal, N., and Azam, A. (2015). Metronidazole hydrazone conjugates: design, synthesis, antiamoebic and molecular docking studies. *Bioorg. Med. Chem. Lett.* 25, 3545–3549. doi: 10.1016/j.bmcl.2015.06.091
- Artz, J. D., Dunford, J. E., Arrowood, M. J., Dong, A., Chruszcz, M., Kavanagh, K. L., et al. (2008). Targeting a uniquely nonspecific prenyl synthase with bisphosphonates to combat cryptosporidiosis. *Chem. Biol.* 15, 1296–1306. doi: 10.1016/j.chembiol.2008.10.017
- Azam, A., and Agarwal, S. (2007). Targeting Amoebiasis: status and developments. *Curr. Bioact. Compd.* 3, 121–133. doi: 10.2174/157340707780809590
- Azam, A., and Agarwal, S. (2015). *Amoebiasis: Biology and Pathogenesis of Entamoeba*. New Delhi: Springer.
- Bacchi, C., and Weiss, L. (2004). “Chemotherapy of microsporidioses: Benzimidazoles, fumagillin and polyamine analogues,” in *Opportunistic Infections: Toxoplasma, Sarcocystis, and Microsporidia*, ed R. Decampo (New York, NY: Springer), 159–188.
- Bacchi, C. J., Lane, S., Weiss, L. M., Yarlett, N., Takvorian, P., and Wittner, M. (2001). Polyamine synthesis and interconversion by the microsporidian *Encephalitozoon cuniculi*. *J. Eukaryot. Microbiol.* 48, 374–381. doi: 10.1111/j.1550-7408.2001.tb00327.x
- Becker, S., Hoffman, P., and Houpt, E. R. (2011). Efficacy of antiamoebic drugs in a mouse model. *Am. J. Trop. Med. Hyg.* 84, 581–586. doi: 10.4269/ajtmh.2011.10-0580
- Bendesky, A. S., Menéndez, D., and Ostrosky-Wegman, P. (2002). Is metronidazole carcinogenic? *Mut. Res.* 511, 133–144. doi: 10.1016/S1383-5742(02)00007-8
- Bernardino, A. M. R., Da Silva Pinheiro, L. C., Rodrigues, C. R., Loureiro, N. I., Castro, H. C., Lanfredi-Rangel, A., et al. (2006). Design, synthesis, SAR, and biological evaluation of new 4-(phenylamino) thieno [2, 3-b] pyridine derivatives. *Bioorg. Med. Chem.* 14, 5765–5770. doi: 10.1016/j.bmc.2006.03.013
- Bhat, A. R., Athar, F., and Azam, A. (2009a). Bis-pyrazolines: synthesis, characterization and antiamoebic activity as inhibitors of growth of *Entamoeba histolytica*. *Eur. J. Med. Chem.* 44, 426–431. doi: 10.1016/j.ejmech.2007.11.005
- Bhat, A. R., Athar, F., Van Zyl, R. L., Chen, C. T., and Azam, A. (2008). Synthesis and biological evaluation of novel 4-substituted 1-[{4-(10,15,20-triphenylporphyrin-5-yl)phenyl}methylidene]thiosemicarbazides as new class of potential antiprotozoal agents. *Chem. Biodivers.* 5, 764–776. doi: 10.1002/cbdv.200890073
- Bhat, A. R., Bhat, A. I., Athar, F., and Azam, A. (2009b). Synthesis, characterization, and anti-amoebic screening of core-modified 5, 20-Bis {2-[(alkyl)(alkyl') amino] methyl} ferrocen-1-yl]-10, 15-diphenyl-21, 23-dithiaporphyrin (= 1, 1''-(10, 15-Diphenyl-21, 23-dithiaporphine-5, 20-diyl) bis [2-[(alkyl)(alkyl') amino] methyl] ferrocene) Derivatives. *Helv. Chim. Acta* 92, 1644–1656. doi: 10.1002/hlca.200800461
- Blagburn, B. L., Drain, K. L., Land, T. M., Kinard, R. G., Moore, P. H., Lindsay, D. S., et al. (1998). Comparative efficacy evaluation of dicationic carbazole compounds, nitazoxanide, and paromomycin against *Cryptosporidium parvum* infections in a neonatal mouse model. *Antimicrob. Agents Chemother.* 42, 2877–2882.
- Blanshard, C., Ellis, D. S., Tovey, D. G., Dowell, S., and Gazzard, B. G. (1992). Treatment of intestinal microsporidiosis with albendazole in patients with AIDS. *Aids* 6, 311–314. doi: 10.1097/00002030-199203000-00009
- Bouzid, M., Hunter, P. R., Chalmers, R. M., and Tyler, K. M. (2013). *Cryptosporidium* pathogenicity and virulence. *Clin. Microbiol. Rev.* 26, 115–134. doi: 10.1128/CMR.00076-12
- Brosson, D., Kuhn, L., Prensier, G. R., Vivaré S. C. P., and Texier, C. (2005). The putative chitin deacetylase of *Encephalitozoon cuniculi*: a surface protein implicated in microsporidian spore-wall formation. *FEMS Microbiol. Lett.* 247, 81–90. doi: 10.1016/j.femsle.2005.04.031
- Brown, D. M., Upcroft, J. A., and Upcroft, P. (1996). A H₂O-Producing NADH oxidase from the protozoan parasite *Giardia Duodenalis*. *Eur. J. Biochem.* 241, 155–161. doi: 10.1111/j.1432-1033.1996.0155t.x
- Bruchhaus, I., and Tannich, E. (1994). Purification and molecular characterization of the NAD(+) -dependent acetaldehyde/alcohol dehydrogenase from *Entamoeba histolytica*. *Biochem. J.* 303(Pt 3), 743–748. doi: 10.1042/bj3030743
- Budakoti, A., Bhat, A. R., and Azam, A. (2009). Synthesis of new 2-(5-substituted-3-phenyl-2-pyrazolinyl)-1,3-thiazolino[5,4-b]quinoxaline derivatives and evaluation of their antiamoebic activity. *Eur. J. Med. Chem.* 44, 1317–1325. doi: 10.1016/j.ejmech.2008.02.002
- Busatti, H. G., Alves, R. J., Santana-Anjos, K. G., Gil, F. F., Cury, M. C., Vannier-Santos, M. A., et al. (2013). Effects of metronidazole analogues on *Giardia lamblia*: experimental infection and cell organization. *Diagn. Microbiol. Infect. Dis.* 75, 160–164. doi: 10.1016/j.diagmicrobio.2012.11.001
- Butler, T., and De Boer, W. G. (1981). *Isospora belli* infection in Australia. *Pathology* 13, 593–595. doi: 10.3109/00313028109059077
- Cano, P. A., Islas-JáCome, A., Gonzalez-Marrero, J., Yepez-Mulia, L., Calzada, F., and Gamez-Montano, R. (2014). Synthesis of 3-tetrazolylmethyl-4H-chromen-4-ones via Ugi-azide and biological evaluation against *Entamoeba histolytica*, *Giardia lamblia* and *Trichomonas vaginalis*. *Bioorg. Med. Chem.* 22, 1370–1376. doi: 10.1016/j.bmc.2013.12.069
- Carrero, J. C., Lugo, H., Perez, D. G., Ortiz-Martinez, C., and Laclette, J. P. (2004). Cyclosporin A inhibits calcineurin (phosphatase 2B) and P-glycoprotein

The bold numbers in braces refer to the chemical structures of the respective compounds (see Supplementary Material).

ACKNOWLEDGMENTS

The research was carried out due to the mutual effort of the authors and no funding agency has assisted in this direction.

SUPPLEMENTARY MATERIAL

The Supplementary Material for this article can be found online at: <http://journal.frontiersin.org/article/10.3389/fmicb.2015.01183>

- activity in *Entamoeba histolytica*. *Int. J. Parasitol.* 34, 1091–1097. doi: 10.1016/j.ijpara.2004.05.004
- Chen, C.-H., Sun, H.-Y., Chien, H.-F., Lai, H.-S., and Chou, N.-K. (2014). *Blastocystis hominis* infection in a post-cardiotomy patient on extracorporeal membrane oxygenation support: a case report and literature review. *Inter. J. Surg. Case Rep.* 5, 637–639. doi: 10.1016/j.ijscr.2014.07.010
- Chokephabulkit, K., Wanachiwanawin, D., Tosasuk, K., Vanprapa, N., and Chearskul, S. (2001). A report case of Cyclospora and Cryptosporidium mixed infection in a HIV-negative child in Thailand. *J. Med. Assoc. Thai.* 84, 36–37. 589–592.
- Coombs, G. H., and Müller, M. (1995). 3 – Energy metabolism in Anaerobic protozoa. *Biochem. Mol. Biol. Parasites* 33–47. doi: 10.1016/B978-012473345-9/50004-0
- Current, W. L., and Garcia, L. S. (1991). Cryptosporidiosis. *Clin. Microbiol. Rev.* 4, 325.
- Debnath, A., Shahinas, D., Bryant, C., Hirata, K., Miyamoto, Y., Hwang, G., et al. (2014). Hsp90 inhibitors as new leads to target parasitic diarrheal diseases. *Antimicrob. Agents Chem.* 58, 4138–4144. doi: 10.1128/AAC.02576-14
- Denton, H., Brown, S. M., Roberts, C. W., Alexander, J., McDonald, V., Thong, K. W., et al. (1996). Comparison of the phosphofructokinase and pyruvate kinase activities of *Cryptosporidium parvum*, *Eimeria tenella* and *Toxoplasma gondii*. *Mol. Biochem. Parasitol.* 76, 23–29. doi: 10.1016/0166-6851(95)02527-8
- Diamond, L. S., Harlow, D. R., and Cunnick, C. C. (1978). A new medium for the axenic cultivation of *Entamoeba histolytica* and other Entamoeba. *Trans. R. Soc. Trop. Med. Hyg.* 72, 431–432. doi: 10.1016/0035-9203(78)90144-X
- Diaz, E., Mondragon, J., Ramirez, E., and Bernal, R. (2003). Epidemiology and control of intestinal parasites with nitazoxanide in children in Mexico. *Am. J. Trop. Med. Hyg.* 68, 384–385.
- Didier, E. S., and Weiss, L. M. (2006). Microsporidiosis: current status. *Curr. Opin. Infect. Dis.* 19, 485. doi: 10.1097/01.qco.0000244055.46382.23
- Didier, E. S., Bowers, L., Stovall, M. E., Kuebler, D., Mittleider, D., Brindley, P. J., et al. (2005). Antimicrosporidial activity of (fluoro)quinolones *in vitro* and *in vivo*. *Folia Parasitol.* 52, 173–181. doi: 10.14411/fp.2005.022
- Didier, P. J., Phillips, J. N., Kuebler, D. J., Nasr, M., Brindley, P. J., Stovall, M. E., et al. (2006). Antimicrosporidial activities of fumagillin, TNP-470, ovalicin, and ovalicin derivatives *in vitro* and *in vivo*. *Antimicrob. Agents Chemother.* 50, 2146–2155. doi: 10.1128/AAC.00020-06
- Duque-Montaña, B. E., Gómez-Caro, L. C., Sanchez-Sanchez, M., Monge, A., Hernandez-Baltazar, E., Rivera, G., et al. (2013). Synthesis and *in vitro* evaluation of new ethyl and methyl quinoxaline-7-carboxylate 1,4-di-N-oxide against *Entamoeba histolytica*. *Bioorg. Med. Chem.* 21, 4550–4558. doi: 10.1016/j.bmc.2013.05.036
- Ebrahimbadeh, A., and Bottone, E. J. (1996). Persistent diarrhea caused by *Isospora belli*: therapeutic response to pyrimethamine and sulfadiazine. *Diagn. Microb. Infect. Dis.* 26, 87–89. doi: 10.1016/S0732-8893(96)00175-7
- Eroglu, F., and Koltas, I. S. (2010). Evaluation of the transmission mode of *B. hominis* by using PCR method. *Parasitol. Res.* 107, 841–845. doi: 10.1007/s00436-010-1937-4
- Escobedo, A. A., and Cimerman, S. (2007). Giardiasis: a pharmacotherapy review. *Expert Opin. Pharmacother.* 8, 1885–1902. doi: 10.1517/14656566.8.12.1885
- Fahey, R. C., Newton, G. L., Arrick, B., Overdank-Bogart, T., and Aley, S. B. (1984). *Entamoeba histolytica*: a eukaryote without glutathione metabolism. *Science* 224, 70–72. doi: 10.1126/science.6322306
- Ferguson, D. J., Birch-Andersen, A., Hutchison, W. M., and Siim, J. C. (1980). Ultrastructural observations on microgametogenesis and the structure of the microgamete of *Isospora felis*. *Acta Pathol. Microbiol. Scand. B* 88, 151–159. doi: 10.1111/j.1699-0463.1980.tb02621.x
- Friedman, P. A., and Platzer, E. G. (1980). Interaction of anthelmintic benzimidazoles with *Ascaris suum* embryonic tubulin. *Biochim. Biophys. Acta* 630, 271–278. doi: 10.1016/0304-4165(80)90431-6
- Gabriel Navarrete-Vaa Zquez, A. R. C., Alicia Hernández-Campos, B., Liliaan, Y. B., Francisco Herna Ndez-Luis, A., Juan Valdez, A., Rau, L., et al. (2001). Synthesis and antiparasitic activity of 2-(Trichloromethyl)-benzimidazole derivatives. *Bioorg. Med. Chem. Lett.* 11, 187–190. doi: 10.1016/S0960-894X(00)00619-3
- Galkin, A., Kulakova, L., Lim, K., Chen, C. Z., Zheng, W., Turko, I. V., et al. (2014). Structural basis for inactivation of *Giardia lamblia* carbamate kinase by disulfiram. *J. Biolog. Chem.* 289, 10502–10509. doi: 10.1074/jbc.M114.553123
- Gargala, G. (2008). Drug treatment and novel drug target against *Cryptosporidium*. *Parasite* 15, 275–281. doi: 10.1051/parasite/2008153275
- Gilin, F. D., and Diamond, L. S. (1980). Attachment and short-term maintenance of motility and viability of *Entamoeba histolytica* in a defined medium. *J. Protozool.* 27, 220–225. doi: 10.1111/j.1550-7408.1980.tb04685.x
- Gómez-Puyou, A., Saavedra-Lira, E., Becker, I., Zubillaga, R. A., Rojo-Dominguez, A., and Perez-Montfort, R. (1995). Using evolutionary changes to achieve species-specific inhibition of enzyme action—studies with triosephosphate isomerase. *Chem. Biol.* 2, 847–855. doi: 10.1016/1074-5521(95)90091-8
- Goodgame, R. (2003). Emerging causes of travelers diarrhea: cryptosporidium, cyclospora, isospora, and microsporidia. *Curr. Infect. Dis. Rep.* 5, 66–73. doi: 10.1007/s11908-003-0067-x
- Graczyk, Z., Chomicz, L., Kozlowska, M., Kazimierczuk, Z., and Graczyk, T. K. (2011). Novel and promising compounds to treat *Cryptosporidium parvum* infections. *Parasitol. Res.* 109, 591–594. doi: 10.1007/s00436-011-2290-y
- Guerrant, R. L., Van Gilder, T., Steiner, T. S., Thielman, N. M., Slutsker, L., Tauxe, R. V., et al. (2001). Practice guidelines for the management of infectious diarrhea. *Clin. Infect. Dis.* 32, 331–351. doi: 10.1086/318514
- Guo, F., Zhang, H., Fritzler, J. M., Rider, S. D., Xiang, L., Mcnair, N. N., et al. (2014). Amelioration of *Cryptosporidium parvum* Infection *in vitro* and *in vivo* by targeting parasite fatty acyl-coenzyme a synthetases. *J. Infect. Dis.* 209, 1279–1287. doi: 10.1093/infdis/jit645
- Haque, R., Huston, C. D., Hughes, M., Houpt, E., and Petri, W. A. Jr. (2003). Amebiasis. *N. Engl. J. Med.* 348, 1565–1573. doi: 10.1056/NEJMra022710
- Hernández-Nunez, E., Tlahuext, H., Moo-Puc, R., Torres-Gomez, H., Reyes-Martinez, R., Cedillo-Rivera, R., et al. (2009). Synthesis and *in vitro* trichomoncidal, giardicidal and amebicidal activity of N-acetamide(sulfonamide)-2-methyl-4-nitro-1H-imidazoles. *Eur. J. Med. Chem.* 44, 2975–2984. doi: 10.1016/j.ejmech.2009.01.005
- Hildebrandt, E., Boykin, D. W., Kumar, A., Tidwell, R. R., and Dykstra, C. C. (1998). Identification and characterization of an endo/exonuclease in *Pneumocystis carinii* that is inhibited by dicationic diarylfurans with efficacy against Pneumocystis pneumonia. *J. Eukaryot. Microbiol.* 45, 112–121. doi: 10.1111/j.1550-7408.1998.tb05078.x
- Hoffman, P. S., Sisson, G., Croxen, M. A., Welch, K., Harman, W. D., Cremades, N., et al. (2007). Antiparasitic drug nitazoxanide inhibits the pyruvate oxidoreductases of *Helicobacter pylori*, selected anaerobic bacteria and parasites, and *Campylobacter jejuni*. *Antimicrob. Agents Chem.* 51, 868–876. doi: 10.1128/AAC.01159-06
- Hooper, D. C. (2000). Mechanisms of action and resistance of older and newer fluoroquinolones. *Clin. Infect. Dis.* 31, S24–S28. doi: 10.1086/314056
- Huang, D. B., and White, A. C. (2006). An updated review on cryptosporidium and giardia. *Gastroenterol. Clin. North Am.* 35, 291–314. doi: 10.1016/j.gtc.2006.03.006
- Hunter, P. R., Hughes, S., Woodhouse, S., Nicholas, R., Syed, Q., Chalmers, R. M., et al. (2004). Health sequelae of human cryptosporidiosis in immunocompetent patients. *Clin. Infect. Dis.* 39, 504–510. doi: 10.1086/422649
- Hwang, E. W., Cheung, L., Mojtahehd, A., and Cartwright, C. A. (2011). Relapse of intestinal and hepatic amebiasis after treatment. *Dig. Dis. Sci.* 56, 677–680. doi: 10.1007/s10620-010-1492-y
- Inam, A., Siddiqui, S. M., Macedo, T. S., Moreira, D. R., Leite, A. C., Soares, M. B., et al. (2014). Design, synthesis and biological evaluation of 3-[4-(7-chloroquinolin-4-yl)-piperazin-1-yl]-propionic acid hydrazones as antiprotozoal agents. *Eur. J. Med. Chem.* 75, 67–76. doi: 10.1016/j.ejmech.2014.01.023
- Inam, A., Van Zyl, R. L., Van Vuuren, N. J., Chen, C.-T., Avecilla, F., Agarwal, S. M., et al. (2015). Chloroquinoline-acetamide hybrids: a promising series of potential antiprotozoal agents. *RSC Adv.* 5, 48368–48381. doi: 10.1039/C5RA05472A
- Iqbal, P. F., Bhat, A. R., and Azam, A. (2009). Antiamoebic coumarins from the root bark of *Adina cordifolia* and their new thiosemicarbazone derivatives. *Eur. J. Med. Chem.* 44, 2252–2259. doi: 10.1016/j.ejmech.2008.06.003
- Irfan, I., Sawangjaroen, N., Bhat, A. R., and Azam, A. (2010). New dioxazole derivatives: synthesis and effects on the growth of *Entamoeba histolytica* and *Giardia intestinalis*. *Eur. J. Med. Chem.* 45, 1648–1653. doi: 10.1016/j.ejmech.2009.12.051
- John, D. E., Haas, C. N., Nwachukwu, N., and Gerba, C. P. (2005). Chlorine and ozone disinfection of *Encephalitozoon intestinalis* spores. *Water Res.* 39, 2369–2375. doi: 10.1016/j.watres.2005.04.013

- Juneja, A., Macedo, T. S., Magalhaes Moreira, D. R., Pereira Soares, M. B., Lima Leite, A. C., Kelle De Andrade Lemoine Neves, J., et al. (2014). Synthesis of 4'-(2-ferrocenyl)-2,2':6'2"-terpyridine: characterization and antiprotozoal activity of Mn(II), Co(II), Ni(II), Cu(II) and Zn(II) complexes. *Eur. J. Med. Chem.* 75, 203–210. doi: 10.1016/j.ejmech.2014.01.051
- Kazimierczuk, Z., Chalimoniu, M., Laudy, A. E., Moo-Puc, R., Cedillo-Rivera, R., Starosciak, B. J., et al. (2010). Synthesis and antimicrobial and nitric oxide synthase inhibitory activities of novel isothiourea derivatives. *Arch. Pharm. Res.* 33, 821–830. doi: 10.1007/s12272-010-0604-8
- Kotloff, K. L., Nataro, J. P., Blackwelder, W. C., Nasrin, D., Farag, T. H., Panchalingam, S., et al. (2013). Burden and aetiology of diarrhoeal disease in infants and young children in developing countries (the Global Enteric Multicenter Study, GEMS): a prospective, case-control study. *Lancet* 382, 209–222. doi: 10.1016/S0140-6736(13)60844-2
- Kucik, C. J., Martin, G. L., and Sortor, B. V. (2004). Common intestinal parasites. *Am. Fam. Phys.* 69, 1161–1168.
- Kulda, J. (1999). Trichomonads, hydrogenosomes and drug resistance. *Int. J. Parasitol.* 29, 199–212. doi: 10.1016/S0020-7519(98)00155-6
- Leitsch, D., Kolarich, D., Wilson, I., Altmann, F., and Duchêne, M. (2007). Nitroimidazole action in *Entamoeba histolytica*: a central role for thioredoxin reductase. *PLoS Biol.* 5:e211. doi: 10.1371/journal.pbio.0050211
- Lim, K., Kulakova, L., Galkin, A., and Herzberg, O. (2013). Crystal structures of carbamate kinase from *Giardia lamblia* bound with citric acid and AMP-PNP. *PLoS ONE* 8:e64004. doi: 10.1371/journal.pone.0064004
- Loftus, B., Anderson, I., Davies, R., Alsmark, U. C. M., Samuelson, J., Amedeo, P., et al. (2005). The genome of the protist parasite *Entamoeba histolytica*. *Nature* 433, 865–868. doi: 10.1038/nature03291
- Macdonald, L. M., Arsmom, A., Thompson, A. R., and Reynoldson, J. A. (2004). Characterisation of benzimidazole binding with recombinant tubulin from *Giardia duodenalis*, *Encephalitozoon intestinalis*, and *Cryptosporidium parvum*. *Mol. Biochem. Parasitol.* 138, 89–96. doi: 10.1016/j.molbiopara.2004.08.001
- Madico, G., Gilman, R., Miranda, E., Cabrera, L., and Sterling, C. (1993). Treatment of Cyclospora infections with co-trimoxazole. *Lancet* 342, 122–123. doi: 10.1016/0140-6736(93)91330-O
- Mandapati, K., Gorla, S. K., House, A. L., Mckenney, E. S., Zhang, M., Rao, S. N., et al. (2014). Repurposing Cryptosporidium inosine 5-monophosphate dehydrogenase inhibitors as potential antibacterial agents. *ACS Med. Chem. Lett.* 5, 846–850. doi: 10.1021/ml500203p
- Mead, J. R. (2002). Cryptosporidiosis and the challenges of chemotherapy. *Drug Resist. Updat.* 5, 47–57. doi: 10.1016/S1368-7646(02)00011-0
- Menotti, J., Santillana-Hayat, M., Cassinat, B., Sarfati, C., Derouin, F., and Molina, J.-M. (2005). Inhibitory activity of human immunodeficiency virus aspartyl protease inhibitors against *Encephalitozoon intestinalis* evaluated by cell culture-quantitative PCR assay. *Antimicrob. Agents Chem.* 49, 2362–2366. doi: 10.1128/AAC.49.6.2362-2366.2005
- Meza, I. (2000). Extracellular matrix-induced signaling in *Entamoeba histolytica*: its role in invasiveness. *Parasitol. Today* 16, 23–28. doi: 10.1016/S0169-4758(99)01586-0
- Moghaddam, D. D., Ghadirian, E., and Azami, M. (2005). *Blastocystis hominis* and the evaluation of efficacy of metronidazole and trimethoprim/sulfamethoxazole. *Parasitol. Res.* 96, 273–275. doi: 10.1007/s00436-005-1363-1
- Molina, J.-M., Tourneur, M., Sarfati, C., Chevret, S., De Gouvello, A., Gobert, J.-G., et al. (2002). Fumagillin treatment of intestinal microsporidioses. *N Engl. J. Med.* 346, 1963–1969. doi: 10.1056/NEJMoa12924
- Montes-Avila, J., Diaz-Camacho, S. P., Sicairos-Felix, J., Delgado-Vargas, F., and Rivero, I. (2009). Solution-phase parallel synthesis of substituted chalcones and their antiparasitic activity against *Giardia lamblia*. *Bioorg. Med. Chem.* 17, 6780–6785. doi: 10.1016/j.bmc.2009.02.052
- Motazedian, M. H., Mohammadpour, N., and Khabnadideh, S. (2014). “In vivo study of efficacy of some metronidazole derivatives on *Giardia lamblia*,” in 2nd International Conference on Innovation Challenges in Multidisciplinary Research and Practice (Shiraz: University of Medical Sciences).
- Muller, J., Rout, S., Leitsch, D., Vaithilingam, J., Hehl, A., and Muller, N. (2015). Comparative characterisation of two nitroreductases from *Giardia lamblia* as potential activators of nitro compounds. *Int. J. Parasitol. Drug. Drug Resist.* 5, 37–43. doi: 10.1016/j.ijpddr.2015.03.001
- Müller, J., Wastling, J., Sanderson, S., Müller, N., and Hemphill, A. (2007). A novel *Giardia lamblia* nitroreductase, GINR1, interacts with nitazoxanide and other thiazolides. *Antimicrob. Agents Chem.* 51, 1979–1986. doi: 10.1128/AAC.01548-06
- Müller, M. (1983). Mode of action of metronidazole on anaerobic bacteria and protozoa. *Surgery* 93, 165–171.
- Musey, K. L., Chidiac, C., Beaucaire, G., Houriez, S., and Fourrier, A. (1988). Effectiveness of roxithromycin for treating *Isospora belli* infection. *J. Infect. Dis.* 158, 646. doi: 10.1093/infdis/158.3.646
- Nasirudeen, A., Hian, Y. E., Singh, M., and Tan, K. S. (2004). Metronidazole induces programmed cell death in the protozoan parasite *Blastocystis hominis*. *Microbiol.* 150, 33–43. doi: 10.1099/mic.0.26496-0
- Nasirudeen, A., Singh, M., Yap, E., and Tan, K. (2001). *Blastocystis hominis*: evidence for caspase-3-like activity in cells undergoing programmed cell death. *Parasitol. Res.* 87, 559–565. doi: 10.1007/s004360100427
- Navarrete-Vazquez, G., Chávez-Silva, F., Argotte-Ramos, R., Rodríguez-Gutiérrez Mdel, C., Chan-Bacab, M. J., Cedillo-Rivera, R., et al. (2011). Synthesis of benzologues of Nitazoxanide and Tizoxanide: a comparative study of their *in vitro* broad-spectrum antiprotozoal activity. *Bioorg. Med. Chem. Lett.* 21, 3168–3171. doi: 10.1016/j.bmcl.2011.02.100
- Navarrete-Vazquez, G., Yepez, L., Hernandez-Campos, A., Tapia, A., Hernandez-Luis, F., Cedillo, R., et al. (2003). Synthesis and antiparasitic activity of albendazole and mebendazole analogues. *Bioorg. Med. Chem.* 11, 4615–4622. doi: 10.1016/S0968-0896(03)00497-8
- Nava-Zuazo, C., Chavez-Silva, F., Moo-Puc, R., Chan-Bacab, M. J., Ortega-Morales, B. O., Moreno-Diaz, H., et al. (2014). 2-acylamino-5-nitro-1,3-thiazoles: preparation and *in vitro* bioevaluation against four neglected protozoan parasites. *Bioorg. Med. Chem.* 22, 1626–1633. doi: 10.1016/j.bmcl.2014.01.029
- Negi, B., Raj, K. K., Siddiqui, S. M., Ramachandran, D., Azam, A., and Rawat, D. S. (2014). *In vitro* antiamoebic activity evaluation and docking studies of metronidazole-triazole hybrids. *Chem. Med. Chem.* 9, 2439–2444. doi: 10.1002/cmde.201402240
- Nozaki, T., Asai, T., Kobayashi, S., Ikegami, F., Noji, M., Saito, K., et al. (1998). Molecular cloning and characterization of the genes encoding two isoforms of cysteine synthase in the enteric protozoan parasite *Entamoeba histolytica*. *Mol. Biochem. Parasitol.* 97, 33–44. doi: 10.1016/S0166-6851(98)00129-7
- Nozaki, T., Asai, T., Sanchez, L. B., Kobayashi, S., Nakazawa, M., and Takeuchi, T. (1999). Characterization of the gene encoding serine acetyltransferase, a regulated enzyme of cysteine biosynthesis from the protist parasites *Entamoeba histolytica* and *Entamoeba dispar* regulation and possible function of the cysteine biosynthetic pathway in entamoeba. *J. Biol. Chem.* 274, 32445–32452. doi: 10.1074/jbc.274.45.32445
- Ok, U. Z., Girginkardeşler, N., Balcioglu, C., Ertan, P., Pirildar, T., and Kilimcioglu, A. A. (1999). Effect of trimethoprim-sulfamethaxazole in *Blastocystis hominis* infection. *Am. J. Gastroenterol.* 94, 3245–3247. doi: 10.1111/j.1527-0241.1999.01529.x
- Ordaz-Pichardo, C., Shibayama, M., Villa-Trevino, S., Arriaga-Alba, M., Angeles, E., and De La Garza, M. (2005). Antiamoebic and toxicity studies of a carbamic acid derivative and its therapeutic effect in a hamster model of hepatic amoebiasis. *Antimicrob. Agents Chemother.* 49, 1160–1168. doi: 10.1128/AAC.49.3.1160-1168.2005
- Petri, W. A. Jr. (2003). Therapy of intestinal protozoa. *Trends Parasitol.* 19, 523–526. doi: 10.1016/j.pt.2003.09.003
- Pozio, E., and Morales, M. A. G. (2005). The impact of HIV-protease inhibitors on opportunistic parasites. *Trends Parasitol.* 21, 58–63. doi: 10.1016/j.pt.2004.11.003
- Reeves, R. E., Serrano, R., and South, D. J. (1976). 6-phosphofructokinase (pyrophosphate). Properties of the enzyme from *Entamoeba histolytica* and its reaction mechanism. *J. Biol. Chem.* 251, 2958–2962.
- Reeves, R. E., South, D. J., Blytt, H. J., and Warren, L. G. (1974). Pyrophosphate: d-fructose 6-phosphate 1-phototransferase a new enzyme with the glycolytic function of 6-phosphofructokinase. *J. Biol. Chem.* 249, 7737–7741.
- Reynoldson, J., Thompson, R., and Horton, R. (1992). Albendazole as a future anti-giardial agent. *Parasitol. Today* 8, 412–414. doi: 10.1016/0169-4758(92)90193-6
- Rodriguez-Romero, A., Hernandez-Santoyo, A., Del Pozo Yauner, L., Kornhauser, A., and Fernandez-Velasco, D. A. (2002). Structure and inactivation of triosephosphate isomerase from *Entamoeba histolytica*. *J. Mol. Biol.* 322, 669–675. doi: 10.1016/S0022-2836(02)00809-4

- Saez-Llorens, X. (1989). Spiramycin for treatment of Cryptosporidium enteritis. *J. Infect. Dis.* 160, 342. doi: 10.1093/infdis/160.2.342
- Sahoo, N., Bhattacharya, S., and Bhattacharya, A. (2003). Blocking the expression of a calcium binding protein of the protozoan parasite *Entamoeba histolytica* by tetracycline regulatable antisense-RNA. *Mol. Biochem. Parasitol.* 126, 281–284. doi: 10.1016/S0166-6851(02)00284-0
- Sahoo, N., Labryure, E., Bhattacharya, S., Sen, P., Guillen, N., and Bhattacharya, A. (2004). Calcium binding protein 1 of the protozoan parasite *Entamoeba histolytica* interacts with actin and is involved in cytoskeleton dynamics. *J. Cell Sci.* 117, 3625–3634. doi: 10.1242/jcs.01198
- Samarawickrema, N., Brown, D., Upcroft, J., Thammapalerd, N., and Upcroft, P. (1997). Involvement of superoxide dismutase and pyruvate: ferredoxin oxidoreductase in mechanisms of metronidazole resistance in *Entamoeba histolytica*. *J. Antimicrob. Chemother.* 40, 833–840. doi: 10.1093/jac/40.6.833
- Sato, D., Kobayashi, S., Yasui, H., Shibata, N., Toru, T., Yamamoto, M., et al. (2010). Cytotoxic effect of amide derivatives of trifluoromethionine against the enteric protozoan parasite *Entamoeba histolytica*. *Int. J. Antimicrob. Agents* 35, 56–61. doi: 10.1016/j.ijantimicag.2009.08.016
- Schmatz, D. M. (1997). The mannitol cycle in Eimeria. *Parasitology* 114(Suppl.), S81–S89.
- Schofield, P., Costello, M., Edwards, M., and O'Sullivan, W. (1990). The arginine dihydrolase pathway is present in *Giardia intestinalis*. *Int. J. Parasitol.* 20, 697–699. doi: 10.1016/0020-7519(90)90133-8
- Shah, N., Dupont, H. L., and Ramsey, D. J. (2009). Global etiology of travelers diarrhea: systematic review from 1973 to the present. *Am. J. Med. Hyg.* 80, 609–614.
- Sheehan, D. J., Raucher, B., and McKittrick, J. C. (1986). Association of *Blastocystis hominis* with signs and symptoms of human disease. *J. Clin. Microbiol.* 24, 548–550.
- Siddiqui, S. M., and Azam, A. (2014). Synthesis, characterization of 4,6-disubstituted aminopyrimidines and their sulphonamide derivatives as anti-amoebic agents. *Med. Chem. Res.* 23, 2976–2984. doi: 10.1007/s00044-013-0877-9
- Slack, A. (2012). Parasitic causes of prolonged diarrhoea in travelers: diagnosis and management. *Aust. Fam. Physician.* 41, 782.
- Sohail, M. R., and Fischer, P. R. (2005). *Blastocystis hominis* and travelers. *Travel. Med. Infect. Dis.* 3, 33–38. doi: 10.1016/j.tmaid.2004.06.001
- Syrkis, I., Fried, M., Elian, I., Pietruska, D., and Lengy, J. (1975). A case of severe human coccidioides in Israel. *Isr. J. Med. Sci.* 11, 373–377.
- Tan, K. S. (2008). New insights on classification, identification, and clinical relevance of *Blastocystis* spp. *Clin. Microbiol. Rev.* 21, 639–665. doi: 10.1128/CMR.00022-08
- Tengku, S., and Norhayati, M. (2011). Review Paper Public health and clinical importance of amoebiasis in Malaysia: a review. *Trop. Biomed.* 28, 194–222.
- Toledano-Magana, Y., Garcia-Ramos, J. C., Navarro-Olivarria, M., Flores-Alamo, M., Manzanera-Estrada, M., Ortiz-Frade, L., et al. (2015). Potential amoebicidal activity of hydrazone derivatives: synthesis, characterization, electrochemical behavior, theoretical study and evaluation of the biological activity. *Molecules* 20, 9929–9948. doi: 10.3390/molecules20069929
- Torres-Gomez, H., Hernandez-Nunez, E., Leon-Rivera, I., Guerrero-Alvarez, J., Cedillo-Rivera, R., Moo-Puc, R., et al. (2008a). Design, synthesis and *in vitro* antiprotozoal activity of benzimidazole-pentamidine hybrids. *Bioorg. Med. Chem. Lett.* 18, 3147–3151. doi: 10.1016/j.bmcl.2008.05.009
- Torres-Gomez, H., Hernandez-Nunez, E., Leon-Rivera, I., Guerrero-Alvarez, J., Cedillo-Rivera, R., Moo-Puc, R., et al. (2008b). Design, synthesis and *in vitro* antiprotozoal activity of benzimidazole-pentamidine hybrids. *Bioorg. Med. Chem. Lett.* 18, 3147–3151. doi: 10.1016/j.bmcl.2008.05.009
- Tremoulet, A. H., Avila-Aguero, M. L., Paris, M. M., Canas-Coto, A., Ulloa-Gutierrez, R., and Faingezicht, I. (2004). Albendazole therapy for Microsporidium diarrhea in immunocompetent Costa Rican children. *Pediatr. Infect. Dis. J.* 23, 915–918. doi: 10.1097/01.inf.0000141724.06556.f9
- Trier, J. S., Moxey, P. C., Schimmel, E. M., and Robles, E. (1974). Chronic intestinal coccidioides in man: intestinal morphology and response to treatment. *Gastroenterology* 66, 923–935.
- Uip, D. E., Lima, A. L., Amato, V. S., Boulos, M., Neto, V. A., and Bem David, D. (1998). Roxithromycin treatment for diarrhoea caused by *Cryptosporidium* spp. in patients with AIDS. *J. Antimicrob. Chemother.* 41(Suppl. B), 93–97. doi: 10.1093/jac/41.suppl_2.93
- Umejiego, N. N., Gollapalli, D., Sharling, L., Volfsun, A., Lu, J., Benjamin, N. N., et al. (2008). Targeting a prokaryotic protein in a eukaryotic pathogen: identification of lead compounds against cryptosporidiosis. *Chem. Biol.* 15, 70–77. doi: 10.1016/j.chembiol.2007.12.010
- Upadhy, R., Zhang, H. S., and Weiss, L. M. (2006). System for expression of microsporidian methionine amino peptidase type 2 (MetAP2) in the yeast *Saccharomyces cerevisiae*. *Antimicrob. Agents Chemother.* 50, 3389–3395. doi: 10.1128/AAC.00726-06
- Upcroft, J., and Upcroft, P. (1998). My favorite cell: giardia. *Bioessays* 20, 256–263.
- Upcroft, J. A., Campbell, R. W., Benakli, K., Upcroft, P., and Vanelle, P. (1999). Efficacy of new 5-nitroimidazoles against metronidazole-susceptible and-resistant Giardia, Trichomonas, and Entamoeba spp. *Antimicrob. Agents Chemother.* 43, 73–76.
- Valdez, J., Cedillo, R., Hernandez-Campos, A., Yepez, L., Hernandez-Luis, F., Navarrete-Vazquez, G., et al. (2002). Synthesis and antiparasitic activity of 1H-benzimidazole derivatives. *Bioorg. Med. Chem. Lett.* 12, 2221–2224. doi: 10.1016/S0960-894X(02)00346-3
- Van Hellemond, J. J., Molhoek, N., Koelewijn, R., Wismans, P. J., and Van Genderen, P. J. (2013). Is paromomycin the drug of choice for eradication of Blastocystis in adults? *J. Infect. Chemother.* 19, 545–548. doi: 10.1007/s10156-012-0496-2
- Verdier, R.-I., Fitzgerald, D. W., Johnson, W. D., and Pape, J. W. (2000). Trimethoprim-sulfamethoxazole compared with ciprofloxacin for treatment and prophylaxis of *Isospora belli* and *Cyclospora cayetanensis* infection in HIV-infected patients: a randomized, controlled trial. *Ann. Intern. Med.* 132, 885–888. doi: 10.7326/0003-4819-132-11-200006060-00006
- Wani, M. Y., Bhat, A. R., Azam, A., and Athar, F. (2013). Nitroimidazolyl hydrazones are better amoebicides than their cyclized 1,3,4-oxadiazoline analogues: *in vitro* studies and Lipophilic efficiency analysis. *Eur. J. Med. Chem.* 64, 190–199. doi: 10.1016/j.ejmech.2013.03.034
- Wani, M. Y., Bhat, A. R., Azam, A., Choi, I., and Athar, F. (2012a). Probing the antiamoebic and cytotoxicity potency of novel tetrazole and triazine derivatives. *Eur. J. Med. Chem.* 48, 313–320. doi: 10.1016/j.ejmech.2011.12.033
- Wani, M. Y., Bhat, A. R., Azam, A., Lee, D. H., Choi, I., and Athar, F. (2012b). Synthesis and *in vitro* evaluation of novel tetrazole embedded 1,3,5-trisubstituted pyrazoline derivatives as *Entamoeba histolytica* growth inhibitors. *Eur. J. Med. Chem.* 54, 845–854. doi: 10.1016/j.ejmech.2012.03.049
- Watanabe, K., Gatanaga, H., Escueta-De Cadiz, A., Tanuma, J., Nozaki, T., and Oka, S. (2011). Amebiasis in HIV-1-infected Japanese men: clinical features and response to therapy. *PLoS. Negl. Trop. Dis.* 5:e1318. doi: 10.1371/journal.pntd.0001318
- Weiss, L. M., Perlman, D. C., Sherman, J., Tanowitz, H., and Wittner, M. (1988). *Isospora belli* infection: treatment with pyrimethamine. *Ann. Intern. Med.* 109, 474–475. doi: 10.7326/0003-4819-109-6-474
- World Health Organization (2013). *Diarrhoeal Disease*. Geneva: WHO.
- Zaidi, S. L., Mittal, S., Rajala, M. S., Avcilla, F., Husain, M., and Azam, A. (2015). Synthesis, characterization and antiamoebic activity of chalcones bearing N-substituted ethanamine tail. *Eur. J. Med. Chem.* 98, 179–189. doi: 10.1016/j.ejmech.2015.05.013
- Zhang, H., Huang, H., Cali, A., Takvorian, P. M., Feng, X., Zhou, G., et al. (2005). Investigations into microsporidian methionine aminopeptidase type 2: a therapeutic target for microsporidiosis. *Folia Parasitol.* 52, 182. doi: 10.14411/fp.2005.023
- Zhang, W. W., Shen, P. S., Descoteaux, S., and Samuelson, J. (1994). Cloning and expression of the gene for an NADP(+)-dependent aldehyde dehydrogenase of *Entamoeba histolytica*. *Mol. Biochem. Parasitol.* 63, 157–161. doi: 10.1016/0166-6851(94)90019-1
- Conflict of Interest Statement:** The authors declare that the research was conducted in the absence of any commercial or financial relationships that could be construed as a potential conflict of interest.
- Copyright © 2015 Azam, Peerzada and Ahmad. This is an open-access article distributed under the terms of the Creative Commons Attribution License (CC BY). The use, distribution or reproduction in other forums is permitted, provided the original author(s) or licensor are credited and that the original publication in this journal is cited, in accordance with accepted academic practice. No use, distribution or reproduction is permitted which does not comply with these terms.



Drug Development Against the Major Diarrhea-Causing Parasites of the Small Intestine, *Cryptosporidium* and *Giardia*

Yukiko Miyamoto and Lars Eckmann*

Department of Medicine, University of California at San Diego, La Jolla, CA, USA

Diarrheal diseases are among the leading causes of morbidity and mortality in the world, particularly among young children. A limited number of infectious agents account for most of these illnesses, raising the hope that advances in the treatment and prevention of these infections can have global health impact. The two most important parasitic causes of diarrheal disease are *Cryptosporidium* and *Giardia*. Both parasites infect predominantly the small intestine and colonize the lumen and epithelial surface, but do not invade deeper mucosal layers. This review discusses the therapeutic challenges, current treatment options, and drug development efforts against cryptosporidiosis and giardiasis. The goals of drug development against *Cryptosporidium* and *Giardia* are different. For *Cryptosporidium*, only one moderately effective drug (nitazoxanide) is available, so novel classes of more effective drugs are a high priority. Furthermore, new genetic technology to identify potential drug targets and better assays for functional evaluation of these targets throughout the parasite life cycle are needed for advancing anticryptosporidial drug design. By comparison, for *Giardia*, several classes of drugs with good efficacy exist, but dosing regimens are suboptimal and emerging resistance begins to threaten clinical utility. Consequently, improvements in potency and dosing, and the ability to overcome existing and prevent new forms of drug resistance are priorities in antigiardial drug development. Current work on new drugs against both infections has revealed promising strategies and new drug leads. However, the primary challenge for further drug development is the underlying economics, as both parasitic infections are considered Neglected Diseases with low funding priority and limited commercial interest. If a new urgency in medical progress against these infections can be raised at national funding agencies or philanthropic organizations, meaningful and timely progress is possible in treating and possibly preventing cryptosporidiosis and giardiasis.

OPEN ACCESS

Edited by:

Tzi Bun Ng,

The Chinese University of Hong Kong,
China

Reviewed by:

Atte Von Wright,

University of Eastern Finland, Finland
Guan Zhu,

University of Georgia, USA

*Correspondence:

Lars Eckmann

leckmann@ucsd.edu

Specialty section:

This article was submitted to
Antimicrobials, Resistance
and Chemotherapy,
a section of the journal
Frontiers in Microbiology

Received: 26 June 2015

Accepted: 16 October 2015

Published: 19 November 2015

Citation:

Miyamoto Y and Eckmann L (2015) Drug Development Against the Major Diarrhea-Causing Parasites of the Small Intestine, *Cryptosporidium* and *Giardia*. *Front. Microbiol.* 6:1208.
doi: 10.3389/fmicb.2015.01208

The two most frequent parasitic causes of diarrheal disease worldwide are *Cryptosporidium* and *Giardia*. Other parasites, such as *Entamoeba histolytica*, which is highly invasive and causes amebic colitis (as discussed in other chapters of this volume), and the coccidia, *Cystoisospora belli*, and *Cyclospora cayetanensis*, have clinical relevance but are less common causes of diarrheal illness. For instance, the two coccidian parasites are mostly associated with chronic diarrhea in HIV-positive

individuals (Dash et al., 2013; Mathur et al., 2013) and other forms of immunodeficiency, but are less important causes of diarrhea in immunocompetent individuals. This review focuses on the therapeutic challenges, current treatment options, and ongoing drug development efforts against cryptosporidiosis and giardiasis.

Cryptosporidium

Cryptosporidium is a major cause of diarrheal disease in humans and animals. It became clinically first known as a causative agent of profuse and persistent diarrhea and morbidity in immunocompromised patients, particularly those with acquired immunodeficiency syndrome, and as a major cause of waterborne diarrheal disease in outbreaks in otherwise healthy individuals. More recently, large population studies have shown that *Cryptosporidium* is among the five leading causes of diarrheal disease in young children worldwide (Checkley et al., 2015), underlining the urgency of addressing the medical needs posed by this parasite, particularly since current treatment options are severely limited.

Parasite

Cryptosporidium belongs to the phylum of apicomplexan protists, along with *Plasmodium* and *Toxoplasma*, although it displays significant differences to those parasites. Most notably, it has lost the phylum-defining apicomplexan plastid and lacks mitochondria. Genome comparisons suggest that *Cryptosporidium* is more closely related to gregarines, intestinal protozoa of invertebrates (Carreno et al., 1999; Ryan and Hijjawi, 2015). The parasite is an obligate endosymbiont, depending on invasion of host cells for numerous metabolic functions. Consistent with the exploitation of this metabolically rich biological niche, it has a relatively small eukaryotic genome of ~9 Mb with ~4,000 genes (Abrahamsen et al., 2004; Xu et al., 2004). *Cryptosporidium* represents a species complex comprising at least 27 individual species and over 40 genotypes with varying degrees of host specificity (Ryan and Hijjawi, 2015). Humans can be infected by nearly 20 of these species, but only two, *Cryptosporidium hominis* and *C. parvum*, cause the majority of clinically relevant infections. *C. hominis* is limited to humans, so the infectious cycle is strictly anthropotonic, while *C. parvum* has several subtypes of which some are human-specific and others have a broader host range and zoonotic transmission. Importantly, new drugs must be active against *C. parvum* and *C. hominis* as both species have worldwide distribution.

The entire *Cryptosporidium* life cycle occurs in a single host (monoxenous) and involves both asexual multiplication and sexual reproduction (Laurent et al., 1999) (**Figure 1**). Infectious oocysts are ingested by the host, and sporozoites emerge from the oocysts upon exposure to acidic conditions followed by neutralization and exposure to pancreatic enzymes and bile (Smith et al., 2005). Sporozoites attach to intestinal epithelial cells, are enveloped by the host cell apical cell membrane, and differentiate into spherical trophozoites, which occupy a location

that is commonly described as intracellular but extracytoplasmic (Smith et al., 2005). The parasites reside in a parasitophorous vacuole, which contains membrane components from the host and parasite, and allows acquisition of nutrients from the host cell (Tzipori and Griffiths, 1998). Importantly, the parasite is completely covered by host cell membrane during its epithelial growth phase, so drugs have to cross this membrane to be effective at that stage of the growth cycle.

During maturation of the *Cryptosporidium* trophozoite, asexual multiplication occurs and results in the formation of a type I schizont that contains six to eight merozoites. Rupture of the schizont results in the release of merozoites that, in turn, can invade adjacent host epithelial cells, where they develop subsequently into type I schizonts, leading to further rounds of asexual multiplication, or into type II schizonts, which initiate sexual reproduction by differentiating into male microgamonts or female macrogamonts (Current and Reese, 1986). Male microgamonts release microgametes that can fertilize the macrogametes inside the female macrogamont. After fertilization, two types of oocysts form, thin-walled oocysts, which are important in reinfection of the host and expansion of parasite numbers, and thick-walled oocysts, which exit the intestinal tract and are infectious for new hosts.

Pathogenesis and Disease

Transmission occurs by the fecal-oral spread of oocysts. In particular, fecal contamination of drinking water can serve as a vehicle for transmission of oocysts and is a substantial public health concern. Large-scale outbreaks have been associated with contamination of community drinking water (Widerstrom et al., 2014; Painter et al., 2015). *Cryptosporidium* invades and resides for major parts of its life cycles within epithelial cells, most commonly in the small intestine. The parasite can be viewed as a “minimally invasive” mucosal pathogen, because it does not usually penetrate into the deeper mucosal layers. This restricted epithelial localization has potential implications for drug design, as it raises the possibility that orally administered drugs might be effective locally in the intestine without extensive systemic absorption. Under conditions of immunodeficiency, *Cryptosporidium* infection can be more widespread and involve epithelial cells of the biliary tract, pancreatic duct, stomach, esophagus, and even respiratory tract (Chen et al., 2002). Under these conditions, systemic drug absorption is probably required, as a drug with limited intestinal activity would be unlikely to reach these other mucosal sites (Abubakar et al., 2007).

Clinical manifestations of *Cryptosporidium* infection, which occur after an incubation period of 2–14 days, include watery and often profuse diarrhea, as well as abdominal cramps, nausea, vomiting, weight loss, and a low-grade fever (Chen et al., 2002). In immunocompetent individuals, disease is usually self-limited lasting 1–3 weeks, whereas the illness is typically prolonged in immunocompromised hosts. In addition, in severe infections, malabsorption can be present due to decreased absorptive surface, which can contribute to the wasting syndrome in infected AIDS patients (Hunter and Nichols, 2002). Immunocompromised patients with bile duct infection may also

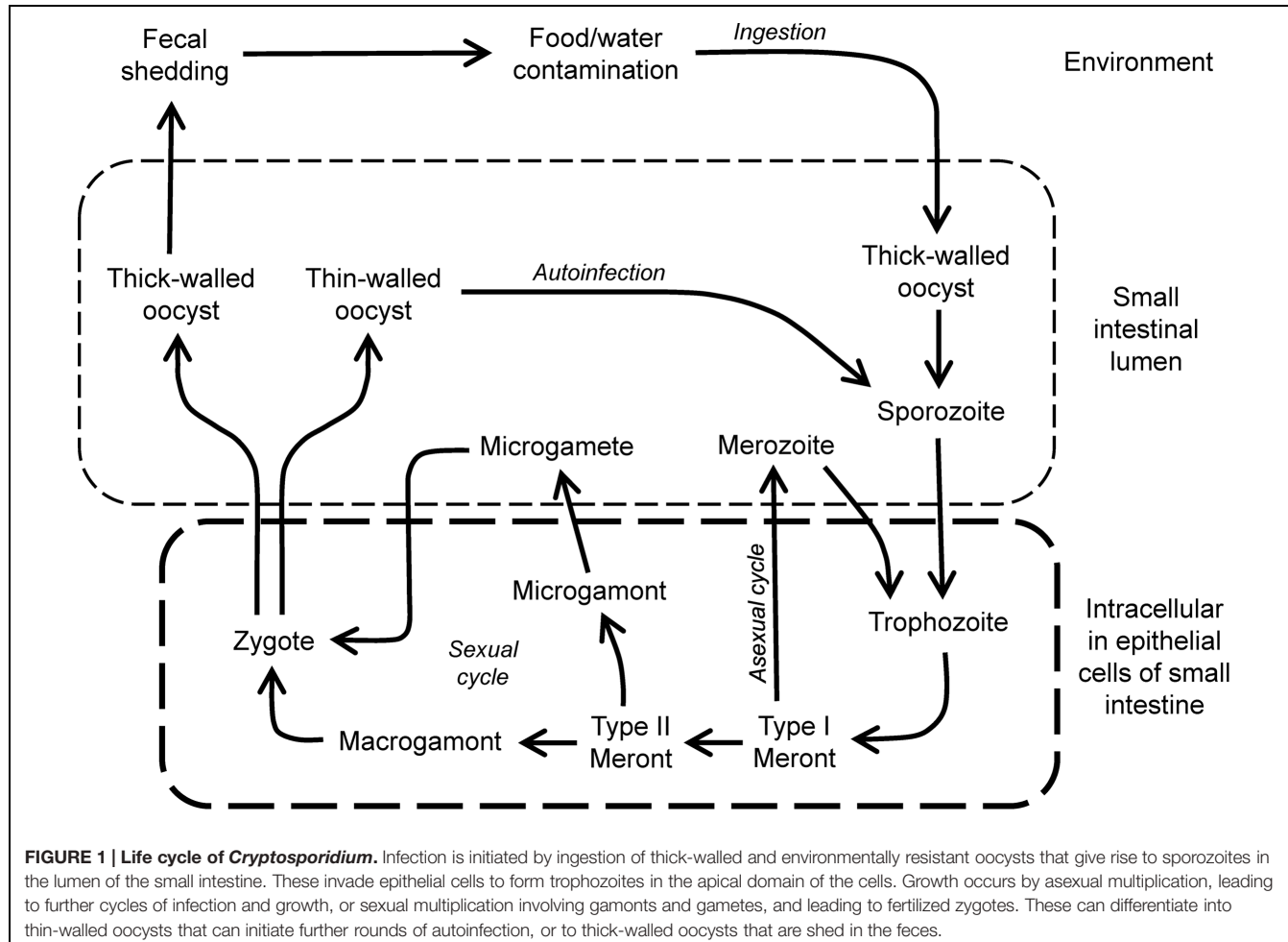


FIGURE 1 | Life cycle of *Cryptosporidium*. Infection is initiated by ingestion of thick-walled and environmentally resistant oocysts that give rise to sporozoites in the lumen of the small intestine. These invade epithelial cells to form trophozoites in the apical domain of the cells. Growth occurs by asexual multiplication, leading to further cycles of infection and growth, or sexual multiplication involving gamonts and gametes, and leading to fertilized zygotes. These can differentiate into thin-walled oocysts that can initiate further rounds of autoinfection, or to thick-walled oocysts that are shed in the feces.

present with jaundice secondary to biliary tract obstruction or with symptoms of pancreatitis. Furthermore, in young children, particularly if malnourished, the infectious diarrhea can be extensive and associated with significant mortality (Hunter and Nichols, 2002). In fact, cryptosporidiosis has recently been identified as the second leading cause (after rotavirus) of diarrheal disease in children <5 years in developing countries (Kotloff et al., 2013; Liu et al., 2014). With increasing use of the highly effective rotavirus vaccine it can be expected that *Cryptosporidium* will soon become the most important worldwide cause of childhood diarrhea.

Several mechanisms are thought to contribute to the pathogenesis of *Cryptosporidium*-induced diarrhea. In patients having large volume diarrhea, a secretory process appears to be important. An enterotoxic activity released by the parasite has been described (Guarino et al., 1995), but these findings remain controversial. In animal models of *C. parvum* infection, glucose-stimulated sodium absorption was inhibited and this paralleled the extent of villous and epithelial cell damage (Kapel et al., 1997). In addition, increased mucosal prostaglandin production (e.g., PGE₂ and PGI₂), which can inhibit neutral NaCl absorption and result in secretory diarrhea, has been demonstrated in the porcine model (Argenzi et al., 1990). Such effects may be due,

in part, to PGI₂ acting on components of the enteric nervous system (i.e., cholinergic and VIPergic neuronal pathways), and a direct action of PGE₂ on enterocytes (Argenzi et al., 1993, 1996). The mechanisms that lead to increased prostaglandin production and the cellular source of the prostaglandins are not known, although the latter may include mesenchymal and/or epithelial cells (Laurent et al., 1998). In addition, resident and recruited leukocytes in the mucosa (e.g., macrophages) have the potential to produce high levels of prostaglandins, and may also be a source of prostaglandin production during *C. parvum* infection. Alterations in intestinal permeability may also play a role in the diarrhea in *C. parvum*-infected individuals (Zhang et al., 2000).

Current Treatment Options

Current therapeutic options for cryptosporidiosis are limited and only one drug, nitazoxanide, has been approved by the Food and Drug Administration (FDA). Efficacy is variable, with resolution of diarrheal symptoms and parasitological cure in 50–90% of HIV-negative children and adults (Rossignol et al., 1998, 2001; Amadi et al., 2002; Hussien et al., 2013). Typical oral doses are 500-mg twice daily for adults and adolescents, 200-mg doses twice daily for children aged 4–11 years, and 100-mg doses twice

daily for children aged 1–3 years, with treatment duration of 3–14 days. The drug is generally well tolerated. Notably, placebo treatment resulted in symptom improvements in a significant fraction (30–40%) of patients (Rossignol et al., 2001; Amadi et al., 2002), underlining that the infection is usually self-limited in immunocompetent patients. In contrast, nitazoxanide is not effective in HIV-infected children (Amadi et al., 2002), and is not FDA approved for this indication.

Other pharmacological interventions have been used clinically against *Cryptosporidium*, but they are not FDA-approved for treating cryptosporidiosis and their efficacy is generally lower than nitazoxanide. For example, paromomycin (500 mg oral, four times daily for 2–3 weeks) led to symptom cessation and microbiological cure in 60–70% of immunocompetent patients (Vandenberg et al., 2012; Hussen et al., 2013). Results in HIV-infected adults have been variable, with some studies showing similar (60–70%) efficacy of paromomycin (Bissuel et al., 1994; Blanshard et al., 1997), while others reporting no effectiveness (Hewitt et al., 2000). Immunotherapy has shown some promise. Most notably, restoration of immune competence in immunocompromised hosts, particularly an increase toward normal in the CD4 T cell levels in patients with AIDS, is associated with clearance of *Cryptosporidium* (Flanigan et al., 1992). Passive immunotherapy by oral administration of colostrum-derived bovine immunoglobulins (which presumably contained anti-cryptosporidial antibodies as cows get commonly infected with *Cryptosporidium*) led to significant improvement of diarrheal symptoms, although microbiological cure was not evaluated (Greenberg and Cello, 1996). However, nitazoxanide remains the most effective current therapeutic agent available against cryptosporidiosis in immunocompetent individuals, while no consistently effective drugs exist against infection under conditions of immunodeficiency.

Assays for Drug Development

Antimicrobial drug development depends on suitable assays that recapitulate critical growth phases of the microbe in the host. This is not usually a problem for growth autonomous microorganisms, such as most bacterial pathogens, but can be a challenge for symbionts such as *Cryptosporidium* that rely partially or completely on host cells for growth and survival. Nonetheless, an array of cell culture and animal models is available for drug testing against the parasite.

Asexual and sexual development of *Cryptosporidium* can be achieved *in vitro* using several different cell lines, although the life cycle is incomplete and the number of oocysts produced is generally low. A widely used model is the human ileocecal adenocarcinoma cell line, HCT-8 (Upton et al., 1994; Alcantara Warren et al., 2008). Monolayers of the cells can be readily infected in culture (Figure 2), and infection can be optimized by adding nutritional supplements to the culture media (Upton et al., 1995). Other mammalian cell lines (e.g., MDCK and Vero) are also infectable, although parasite development tends to be less robust than in HCT-8 cells (Upton et al., 1994). Several of the epithelial cell lines, including human T84 and Caco-2 cells, can be grown as differentiated polarized monolayers on microporous filter supports, which permits studies of the

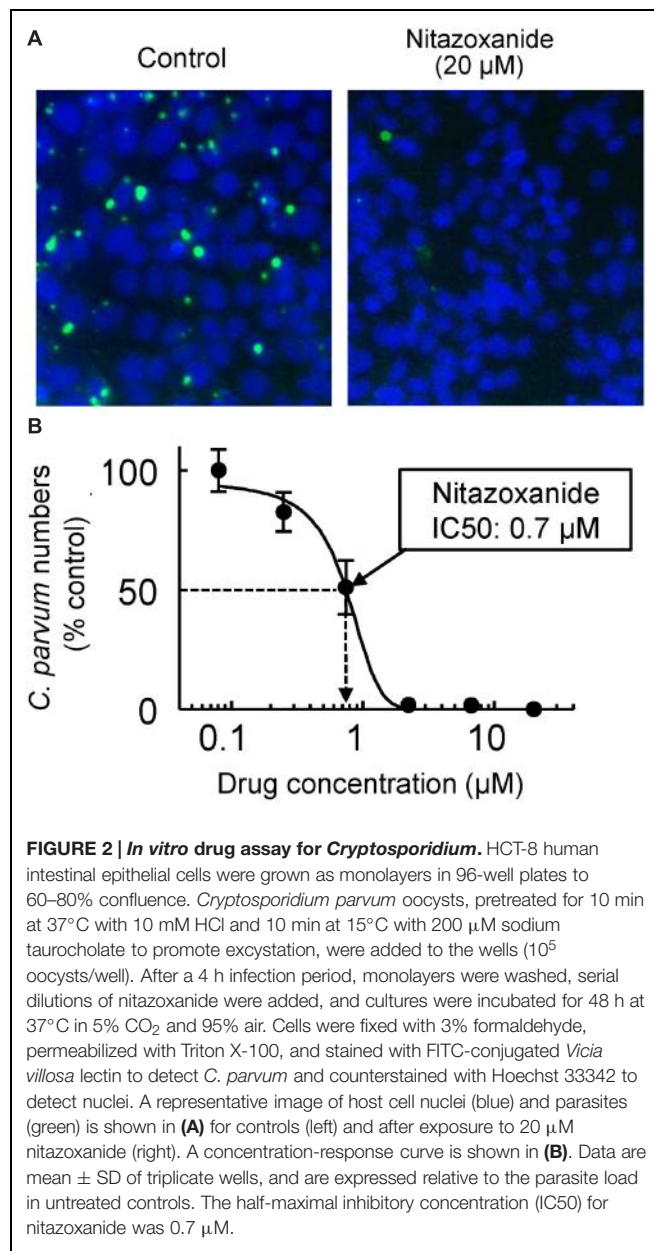


FIGURE 2 | *In vitro* drug assay for *Cryptosporidium*. HCT-8 human intestinal epithelial cells were grown as monolayers in 96-well plates to 60–80% confluence. *Cryptosporidium parvum* oocysts, pretreated for 10 min at 37°C with 10 mM HCl and 10 min at 15°C with 200 μM sodium taurocholate to promote excystation, were added to the wells (10⁵ oocysts/well). After a 4 h infection period, monolayers were washed, serial dilutions of nitazoxanide were added, and cultures were incubated for 48 h at 37°C in 5% CO₂ and 95% air. Cells were fixed with 3% formaldehyde, permeabilized with Triton X-100, and stained with FITC-conjugated *Vicia villosa* lectin to detect *C. parvum* and counterstained with Hoechst 33342 to detect nuclei. A representative image of host cell nuclei (blue) and parasites (green) is shown in (A) for controls (left) and after exposure to 20 μM nitazoxanide (right). A concentration-response curve is shown in (B). Data are mean ± SD of triplicate wells, and are expressed relative to the parasite load in untreated controls. The half-maximal inhibitory concentration (IC50) for nitazoxanide was 0.7 μM.

effects of *Cryptosporidium* infection on barrier functions, ion absorption and secretion, and cytokine responses (Griffiths et al., 1994; Laurent et al., 1997, 1998). A recent report has also used primary human intestinal epithelial cells, grown as self-sustaining organoids (enteroids), for *in vitro* infections with *Cryptosporidium* (Castellanos-Gonzalez et al., 2013a). These cultures, unlike epithelial cell lines, display the normal range of intestinal epithelial cell differentiation, which should allow more complete analysis of parasite–host interactions than possible in transformed cell lines, although establishment and maintenance of primary cultures are technically demanding at this time and may not yet be readily adaptable to high-throughput screens. Overall, epithelial cell cultures are poised to remain an indispensable tool for new drug development.

against *Cryptosporidium*. It must be borne in mind, however, that current culture systems probably do not capture all stages of the cryptosporidial life cycle with equal efficiency and physiological impact, so drug screening efforts may be skewed toward compounds that are particularly active in the intracellular life cycle stages, but not any extracellular stages (Hijjawi et al., 2002).

Antimicrobial activity *in vitro* is usually necessary for a new drug candidate, but it is not sufficient since many candidates that work *in vitro* fail to be active *in vivo*. Appropriate animal models are therefore critical for drug development. A number of mammals have been used for *Cryptosporidium* infections, including small (mice, rats) and large animals (pigs, cows), each with advantages and disadvantages. Most animal models reproduce the cryptosporidial growth cycle and lead to sustained infection and shedding of infectious oocysts, which is adequate for drug efficacy studies. Small animal models, particularly mice, are resource-effective, but are not associated with the characteristic infection-induced diarrhea seen in humans and can thus not be used for investigations of this clinical manifestation and its treatment. On the other hand, large animals such as piglets and calves develop marked diarrhea (Tzipori et al., 1981, 1983; Argenzio et al., 1993; Gookin et al., 2008; Adell et al., 2013; Operario et al., 2015), but require greater resources and are less amenable to genetic and pharmacological manipulations for mechanistic studies.

Mice are the most commonly used models for *in vivo* testing of drug candidates against *Cryptosporidium*. Newborn mice are susceptible to infection with *C. parvum* during the initial 3 weeks after birth, but subsequently become resistant to infection. Consequently, adult wild-type mice are generally not suitable for drug testing, which is presumably due to effective innate or acquired immune defenses. However, adult mice with selected immunodeficiencies can be readily infected with the parasite. For example, SCID mice (Kuhls et al., 1992) and mice deficient in IFN- γ or its receptor (Theodos et al., 1997; von Oettingen et al., 2008), major histocompatibility complex class II (Aguirre et al., 1994), CD40 or CD40 ligand (Cosyns et al., 1998; Hayward et al., 2001), or IL-12 p40 (Urban et al., 1996; Campbell et al., 2002) are all susceptible to intestinal *C. parvum* infection and have been used to varying degrees for drug testing. The observation that nitazoxanide has efficacy in immunocompetent patients, but less so or not at all in immunodeficient individuals suggests that intact host immunity contributes to drug effectiveness. It follows that the nature of an immune defect that renders adult mice susceptible to *Cryptosporidium* may impact the predictive value of *in vivo* drug testing. However, few if any comparative drug efficacy studies have been done between different murine models, so it is not clear whether any particular model is more representative of the human situation than others and thus potentially more predictive of clinical efficacy.

New Agents against *Cryptosporidium*

Antimicrobial drug development commonly proceeds along one of two pathways, focused either on whole-cell activity or on specific molecular targets. In an activity-centered approach, compound libraries are screened for activity against the live

parasite in a suitable *in vitro* assay. Upon identification of biologically active “hits”, the respective compounds are systematically optimized for *in vitro* and ultimately *in vivo* activity. In a target-centered approach, the focus is on exploiting molecular targets that are indispensable and, ideally, unique to the parasite. Target identification may come from genomic analyses or genetic screens, and is followed by pharmacological exploration of their “druggability” with suitable inhibitors. Both approaches have advantages and shortcomings. Activity-centered drug development can rapidly lead to strong hits and lead compounds, but if those fail in subsequent preclinical or clinical trials, development might run into a dead end because the molecular target is often not known can thus not be further exploited with alternative chemical scaffolds. Target-centered drug development is conceptually compelling, as it promises systematic exploitation of genome information without the uncertainty of large library screens. However, targets may not prove as physiologically critical as initially predicted, and development of specific inhibitors with adequate activity *in vitro* and *in vivo* may not be straightforward. Furthermore, tools for genetic manipulation of *Cryptosporidium* are not presently available, precluding genetic screens as a strategy for identifying critical target genes in this parasite. To date, activity-centered approaches have yielded most if not all clinically utilized antimicrobials, while target-centered approaches remain an intriguing but unfilled promise.

Both drug development strategies have been applied to *Cryptosporidium*. In particular, the obligate endosymbiotic growth phase has sparked great interest in the systematic exploitation of this apparent “Achilles’ heel” of the parasite. *Cryptosporidium* has degenerate mitosomes instead of mitochondria and has lost the mitochondrial genome and nuclear genes for many mitochondrial proteins, including those required for the tricarboxylic acid cycle, oxidative phosphorylation, and fatty acid oxidation (Abrahamsen et al., 2004; Xu et al., 2004). Also lacking are genes for *de novo* biosynthesis of amino acids, nucleotides, and sugars (Abrahamsen et al., 2004; Xu et al., 2004). Loss of genes from multiple metabolic pathways indicates that the parasite relies heavily on scavenging nutrients from the host, salvage rather than *de novo* biosynthesis, and glycolysis or substrate-level rather than oxidative phosphorylation for energy production (Ryan and Hijjawi, 2015). Consequently, the parasite must depend on these essential core metabolic pathways, which are absent in or highly divergent from those in humans and animals, making many of the enzymes in these pathways potential drug targets.

Perhaps the most extensively studied metabolic pathway for drug development is the salvage of purines for nucleic acid synthesis. *Cryptosporidium* cannot synthesize purine nucleotides *de novo*, but instead converts adenosine salvaged from the host into guanine nucleotides via a pathway involving inosine 5'-monophosphate dehydrogenase (IMPDH; Umejiego et al., 2004). This enzyme catalyzes the conversion of inosine-5'-monophosphate into xanthosine-5'-monophosphate as the rate-determining step in guanine nucleotide biosynthesis. Interestingly, the parasites appear to have obtained their IMPDH gene by lateral gene transfer from bacteria, making it structurally

distinct from mammalian IMPDH enzymes (Striepen et al., 2004). The exclusive reliance on this guanine salvage pathway makes IMPDH a potential drug target. Indeed, generic inhibitors of the enzyme have significant anticryptosporidial activity *in vitro* (Striepen et al., 2004). Subsequent studies have systematically advanced the development of more specific inhibitors. Based on high throughput screens, a number of structurally diverse IMPDH inhibitors were identified (Umejiego et al., 2008), and several of the most promising scaffolds were then explored for optimal activity *in vitro* and *in vivo*. For example, a number of derivatives of urea, benzoxazole, and benzopyrano[4,3-*c*]pyrazole are active against purified IMPDH in the low to mid nM range (Gorla et al., 2012, 2013; Sun et al., 2014), and several have activity against *C. parvum* in cell culture and in a mouse infection model *in vivo* (Gorla et al., 2014). As an alternative strategy to conventional hit identification and lead optimization of small “drug-like” molecules, peptides have been explored as IMPDH inhibitors. In particular, phylomer peptides, which represent naturally stable protein segments from phylogenetically diverse bacterial genomes with an evolutionarily optimized ability to bind protein surfaces (Watt, 2009), have been screened for inhibitory activity against *C. parvum* IMPDH (Jefferies et al., 2015). Peptides that interact with IMPDH were identified in a yeast two hybrid screen, and then tested for parasite inhibition *in vitro*. The best peptides suppressed *C. parvum* growth with 50% efficiency at 8–46 μM , but had only negligible cytotoxicity in human cells (Jefferies et al., 2015). Although the *in vivo* efficacy of these peptides remains to be established, the data underline that IMPDH is a valid pharmacological target for parasite inhibition. Taken together, the recent studies suggest that further preclinical development of IMPDH inhibitors, using either current scaffolds or perhaps yet to be discovered ones, holds great promise for a new class of anticryptosporidial agents.

Several other molecular targets have been explored against *Cryptosporidium*. For example, the *C. parvum* genome encodes three long chain fatty acyl-coenzyme A synthetases, which are essential in the fatty acid metabolism of the parasite (Guo et al., 2014). Their inhibition with triacsin C was highly effective against parasite growth *in vitro* and reduced oocyst production by 88% in infected IL-12 knockout mice (Guo et al., 2014). Another target, calcium-dependent protein kinase 1 (CDPK1), plays a role in calcium-mediated signaling of the parasite, which is important for regulating vital functions in *Cryptosporidium* and other apicomplexan parasites (Murphy et al., 2010; Ojo et al., 2010). Inhibition of CDPK1 with pyrazolopyrimidine derivatives blocked enzyme activity *in vitro* in the low nM range and parasite growth in epithelial cells in the low μM range (Murphy et al., 2010). Moreover, at least one of the derivatives exhibited significant efficacy after oral dosing in a mouse infection model (Castellanos-Gonzalez et al., 2013b). A third group of molecular targets are cysteine proteases, which have been associated with excystation and host cell invasion of *C. parvum* (Nesterenko et al., 1995; Perez-Cordon et al., 2011). Selective protease inhibitors have shown promising activity against the parasite *in vitro* and *in vivo* (Kang et al., 2012; Ndaø et al., 2013), although it remains to be established which out of the twenty or more members of the

papain-like family of cysteine proteases are responsible for these therapeutic effects.

Beyond target-centered drug development, several activity-centered drug screening approaches have been undertaken for *Cryptosporidium*. For example, a library of 727 FDA-approved drugs or drug-like compounds with a history of use in human clinical trials was tested for activity on parasite growth in HCT-8 epithelial cells (Bessoff et al., 2013). Approximately twenty compounds, representing a hit rate of ~3%, showed significant activity at <10 μM , with the best compounds displaying *in vitro* IC50s in the range of 0.2–5 μM (Bessoff et al., 2013). Mechanistic pursuit of one of these leads revealed that the drug target is 3-hydroxy-3-methyl-glutaryl-coenzyme A (HMG-CoA) reductase, which is required for the *de novo* synthesis of isoprenoids (Bessoff et al., 2013). Importantly, the parasite lacks all known enzymes required for the synthesis of isoprenoid precursors, so inhibition of the critical enzyme in the host blocks parasite growth because *Cryptosporidium* is dependent on the host cell for synthesis of isoprenoid precursors (Bessoff et al., 2013). This finding nicely supports the concept mentioned above that the obligate endosymbiosis of the parasite is a potential “Achilles’ heel” that may be exploited for drug development. It must be noted, however, that drugs that exclusively target host processes also have an increased risk for adverse effects, so it may be more difficult for such drugs compared to conventional microbe-targeted drugs to find an acceptable balance between parasite clearance and other drug effects.

In another screen, an existing library from the Medicines for Malaria Venture Open Access Malaria Box was tested for activity against *C. parvum* (Bessoff et al., 2014). The library represents a collection of 400 compounds selected from 19,000 structurally unique molecules with activity against the erythrocytic stage of *Plasmodium falciparum* in three large phenotypic high-throughput screening campaigns undertaken by large pharmaceutical companies. The screen yielded 19 compounds, representing a ~5% hit rate, with significant activity against *C. parvum* growth in HCT-8 cells at 6.6 μM (Bessoff et al., 2014), suggesting that the relatively high hit rate of the *Plasmodium*-active compounds against *Cryptosporidium* may be attributed to the general similarities between the two apicomplexan parasites. The most active compounds belonged to three chemical series, derived from the quinolin-8-ol, allopurinol-based, and 2,4-diaminoquinazoline, and several of the derivatives exhibited submicromolar potency *in vitro* (Bessoff et al., 2014). Further studies will have to explore their *in vivo* efficacy.

Outlook

Taken together, recent studies clearly demonstrate that new classes of antimicrobials against *Cryptosporidium* are biologically possible and pharmacologically feasible, either by advancing leads against already identified targets or by screening new and larger compound libraries for activity against the parasite. In addition, analyses of the genomes and metabolomes of different *Cryptosporidium* species and genotypes are likely to reveal more molecular drug targets. However, as scientifically promising as drug development against *Cryptosporidium* is at this time, the

major challenge for these efforts is the underlying economics (Striepen, 2013). As a disease that affects mostly developing countries and which had up to recently been significantly underestimated in its clinical prevalence and importance (Lal and Hales, 2015), cryptosporidiosis remains in the category of Neglected Diseases with low funding priority and limited commercial interest. If a new urgency in medical progress against the disease can be established at national funding agencies or philanthropic organizations, meaningful and timely progress could be made in treating and possibly preventing cryptosporidiosis.

Giardia

Giardiasis is a major cause of diarrheal illness worldwide with hundreds of millions annual cases. Compared to cryptosporidiosis, giardiasis is often associated with more prolonged, chronic diarrhea and disease even in immunocompetent individuals, which, particularly in children, can lead to long-term sequelae including intellectual deficits and failure to thrive. Furthermore, treatment options are currently broader than those for cryptosporidiosis, but resistance to existing antimicrobial drugs is becoming a clinical problem that has not yet been described for cryptosporidiosis.

Parasite

Giardiasis is caused by *Giardia lamblia* (syn. *G. duodenalis* or *G. intestinalis*), which was first discovered in the 1600s by van Leeuwenhoek in his own stool. *G. lamblia* is a flagellated, enteric parasite that belongs to the order of diplomonads in the phylum of metamonads, a large group of flagellate amitochondriate protozoa. The parasite has a comparatively simple life cycle (Figure 3), which occurs in a single host (monoxenous) and involves only two forms, the infectious cyst and the replicating trophozoite. Cysts are spread through contaminated drinking water or food, or person-to-person contact. *G. lamblia* is highly contagious, as evidenced by experimental human infection after oral ingestion of as few as 10 cysts (Nash et al., 1987). The low infectious dose, combined with the resistance of cysts to many common disinfectants (Betancourt and Rose, 2004; Erickson and Ortega, 2006), makes *G. lamblia* a constant threat to the safety of public water supplies. After passing through the stomach, trophozoites emerge from the cysts and colonize the upper small intestine. The sequence of exposure to an acidic environment, followed by neutral conditions and the presence of bile is sufficient to trigger excystation, as has been shown *in vitro* (Boucher and Gillin, 1990).

The haploid genome of *G. lamblia* comprises ~12 Mb of DNA encoding ~5,000 genes (Morrison et al., 2007; Franzen et al., 2009). The parasite is polyploid throughout its life cycle. Trophozoites have two nuclei, each carrying a diploid genome, so the overall genome is tetraploid (4N) in the trophozoite stage (Bernander et al., 2001). During encystation, the genome content acquires 16N ploidy through two successive rounds of chromosome replication without intervening cell division. Upon excystation, the cells have four nuclei, each with a

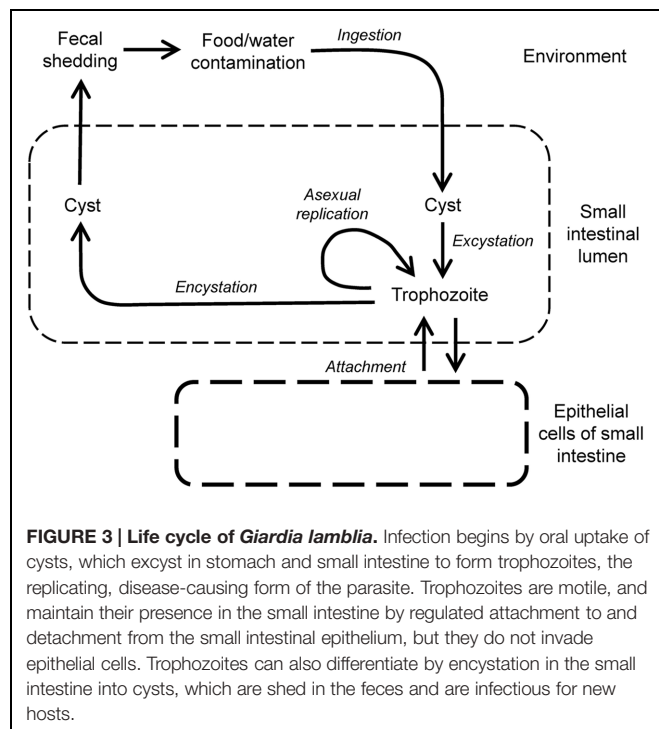


FIGURE 3 | Life cycle of *Giardia lamblia*. Infection begins by oral uptake of cysts, which excyst in stomach and small intestine to form trophozoites, the replicating, disease-causing form of the parasite. Trophozoites are motile, and maintain their presence in the small intestine by regulated attachment to and detachment from the small intestinal epithelium, but they do not invade epithelial cells. Trophozoites can also differentiate by encystation in the small intestine into cysts, which are shed in the feces and are infectious for new hosts.

ploidy of 4N, and divide twice to form four trophozoites containing two diploid nuclei each (Bernander et al., 2001). Besides the polyploidy, evidence exists for allelic sequence heterozygosity within single parasites (Ankarklev et al., 2012), further complicating the interpretation of genome information, as well as the use of genetic tools for identification of potential new drug targets. Moreover, *G. lamblia* displays considerable genetic diversity. Isolates are grouped into genetic Assemblages A–F, with all human pathogens belonging to groups A and B, while the others are pathogens in dogs, birds, and other species. Genome comparison of isolates from Assemblage A and B shows only 77% nucleotide and 78% amino acid identity in protein-coding regions (Franzen et al., 2009), indicating that these two assemblages truly represent different *Giardia* species, despite the historic convention of a single species name (Jarlstrom-Hultqvist et al., 2010). Importantly, Assemblage A and B strains infect humans throughout the world, making it critical that new drugs are active against divergent *G. lamblia* strains of both Assemblages.

Pathogenesis and Disease

Giardia lamblia causes hundreds of millions of annual cases of diarrheal disease in endemic and epidemic fashion worldwide (Karanis et al., 2007; Baldursson and Karanis, 2011). In the United States, the parasite is one of the two most common causes of outbreaks of parasitic disease, with prevalence rates of 1–7% depending on the population sampled (Furness et al., 2000; Barry et al., 2013). Infections are more frequent and severe in young children, particularly in day-care centers, and among travelers, hikers, and military personnel in the field (Overturf, 1994; Sharp et al., 1995). Following cyst ingestion, symptoms occur after

a 1–2 weeks incubation period, although only about half of all stool-positive *Giardia* infections are symptomatic. Frequent clinical manifestations of giardiasis include watery diarrhea, epigastric pain, nausea, and vomiting. The acute phase typically lasts 1–3 weeks, although some patients can have persistent symptoms for months. Most infections are self-limited but recurrences are common in endemic areas. Chronic infections can lead to weight loss and malabsorption and may be mistaken for inflammatory bowel disease or anorexia nervosa (Thomas Iv et al., 2014). Importantly, chronic giardiasis is associated with stunting (low height for age), wasting (low weight for height) and cognitive impairment in children in developing countries (Berkman et al., 2002; Nematian et al., 2008; Al-Mekhlafi et al., 2013), a finding that has been reproduced in murine models of infection (Bartelt et al., 2013). Furthermore, acute giardiasis may disable patients for extended periods and can elicit protracted post-infectious syndromes, including irritable bowel syndrome and chronic fatigue (Hanevik et al., 2014).

After emergence from cysts, the flagellated *G. lamblia* trophozoites colonize the upper small intestine, although colonization of the lower small intestine, as well as stomach and colon can occur. Trophozoites reside and replicate in the intestinal lumen and at the intestinal epithelial surface, but do not invade deeper layers of the mucosa. The parasite's ability to attach to the mucosal surface is critical for its persistence in the host (Lauwaet et al., 2010), yet the underlying mechanisms remain poorly defined. The ventral disk of the parasite can assume a domed conformation that is important for robust attachment (Woessner and Dawson, 2012), whereas flagellar motility is important for positioning and orienting trophozoites prior to attachment, but is not directly required for attachment (House et al., 2011). Despite its "off-shore" location outside the mucosa, the parasite actively engages mucosal immunity, although frank inflammation is typically absent in most cases (Oberhuber et al., 1997). However, villus and brush border microvillus atrophy are common, leading to digestive enzyme deficiencies (Solaymani-Mohammadi and Singer, 2011), and chronic giardiasis can lead to overt mucosal inflammation with pronounced villus loss (Hanevik et al., 2007).

Giardiasis is self-limiting in >85% of cases in non-endemic areas, indicating that effective immune defenses exist. Furthermore, symptoms of giardiasis are much less severe in endemic than non-endemic regions, suggesting gradual build-up of immunity (Faubert, 2000). Secretory IgA (Langford et al., 2002; Davids et al., 2006), intestinal hypermotility (Andersen et al., 2006; Li et al., 2006), and antimicrobial peptides and nitric oxide (Eckmann et al., 2000; Tako et al., 2013) have all been shown to have direct effector activity against the parasite, although their relative contributions to clearance of *Giardia* may be variable (Singer and Nash, 2000a; Langford et al., 2002). Beyond direct effectors, several immune cells and regulators are known to be involved in anti-giardial immune defense. Mast cells and CD4⁺ T cells, but not CD8⁺ T cells, are required for clearing *Giardia* infection (Singer and Nash, 2000a; Roxstrom-Lindquist et al., 2006; Solaymani-Mohammadi and Singer, 2010). CD4⁺ T cells may act in part by controlling anti-giardial IgA responses

(Heyworth, 1989), while their functions are not related to classical Th1 or Th2 subsets, since their signature cytokines, IFN-γ, or IL-4, play no role in immune defense (Singer and Nash, 2000a). In contrast, IL-6 and IL-17 are important in *Giardia* clearance (Bienz et al., 2003; Zhou et al., 2003; Dreesen et al., 2014; Dann et al., 2015). IL-6 appears to act by promoting dendritic cell functions during infection (Kamda et al., 2012), although it has many other activities, including activation of neutrophils and monocytes, enhancement of follicular helper T cell responses, and stimulation of B cell proliferation and antibody production.

A human vaccine against giardiasis is not available. A crude veterinary vaccine (GiardiaVax), composed of total cell lysates of a mixture of sheep, dog and human isolates, reduces symptoms and duration of cyst output in cats and dogs (Olson et al., 2000). Interestingly, the vaccine has also been used as an immunotherapeutic agent in dogs with chronic giardiasis that had failed standard drug treatment (Olson et al., 2001), raising the intriguing possibility that a vaccine may be effective post-exposure.

Current Treatment Options

Several classes of antimicrobial drugs are available for the treatment of giardiasis. The most commonly utilized worldwide are members of the 5-nitroimidazole (5-NI) family such as metronidazole and tinidazole. However, this first line therapy fails in up to 20% of cases and cross-resistance between different agents can occur (Gardner and Hill, 2001), and resistance to all major anti-giardial drugs has been reported (Ansell et al., 2015). Alternative agents exist for treatment failures and for special circumstances (e.g., pregnancy), but these are generally less effective than 5-NI drugs (Escobedo and Cimerman, 2007).

The oldest and most common 5-NI, metronidazole, is typically given in three divided daily 250 mg oral doses for 5–10 days, and has a reported efficacy of 80–95% (Gardner and Hill, 2001). More recently, tinidazole, first approved by the FDA in 2004, has become a good alternative for giardiasis because of its efficacy (85–90%), tolerability, and convenience (a single oral dose is recommended; Speelman, 1985). All 5-NI drugs are prodrugs whose microbial specificity is due to the requirement for reduction to toxic free radical intermediates by low redox potential reactions present only in the anaerobic target microbes (Upcroft and Upcroft, 2001). The metabolism of *G. lamblia* is fermentative, and electron transport proceeds in the absence of mitochondrial oxidative phosphorylation. However, the parasite is microaerotolerant and can reduce molecular oxygen and thus protect the highly oxygen-sensitive, central metabolic enzyme, pyruvate:ferredoxin oxidoreductase (PFOR), and iron-containing ferredoxins. PFOR decarboxylates pyruvate and donates electrons to ferredoxin, which in turn reduces other components in the electron transport chain and leads to ATP generation. Reduced ferredoxin can also reduce the critical nitro group of 5-NI prodrugs to toxic radicals which kill the parasite. Other reduction pathways, including nitroreductases and thioredoxin reductase, also activate 5-NI drugs in *Giardia* (Pal et al., 2009; Leitsch et al., 2011; Nillius et al., 2011), although their relative importance in reducing metronidazole and other nitro drugs remains to be established. The radicals that result

from nitro drug reduction form covalently bonded adducts on microbial target molecules, leading to their inactivation. The specific molecular targets of 5-NI drugs have not been defined in *G. lamblia*. In spite of the general efficacy of 5-NI drugs, treatment failures in giardiasis are common (up to 20%), clinical resistance is proven, and *in vitro* resistance can be induced so that parasites grow in clinically relevant levels of metronidazole (Wright et al., 2003; Tejman-Yarden et al., 2011).

Nitazoxanide is a nitrothiazole with broad-spectrum activity against intestinal parasites. Like 5-NI drugs, it is a prodrug that must be reduced to form toxic radicals, which inactivate various microbial target molecules including PFOR (Hoffman et al., 2007). It is usually given in two daily 500 mg doses for 3 days, which is more convenient dosing than metronidazole, but has slightly lower efficacy (70–80%) than 5-NI drugs (Gardner and Hill, 2001) and is also impacted by metronidazole resistance (Tejman-Yarden et al., 2011). In a clinical trial involving children with diarrheal illness, nitazoxanide reduced symptom duration in those afflicted with giardiasis as well as in those without a microbiological diagnosis (Rossignol et al., 2012), further underlining its utility as a broad-spectrum antimicrobial agent.

Benzimidazoles, such as albendazole and mebendazole, are generally used to treat intestinal helminth infections. Albendazole is also effective in giardiasis (Gardner and Hill, 2001; Solaymani-Mohammadi et al., 2010), although its efficacy varies markedly (25–90%) depending on the dosing regimen. Albendazole can be taken once daily for 5 days, making it more convenient than three-times-a-day metronidazole, and its anti-helminth activity makes it an attractive agent for dual use purposes (Granados et al., 2012). However, results from a Bolivian cohort study (a region with endemic *Giardia* and helminth infections) found that treatment with mebendazole reduced hookworm infections but paradoxically led to an increase in giardiasis (Blackwell et al., 2013), suggesting an antagonistic relationship between the two parasites and complicating the prospect of multi-target therapies.

Quinacrine, an old malaria drug, is an acridine derivative with excellent efficacy against giardiasis (90%). A recent report describes the experience of a family of four with giardiasis, three of whom failed therapy with tinidazole but were cured with quinacrine (Requena-Mendez et al., 2014). In a randomized trial in children with giardiasis, chloroquine was equally effective as tinidazole and superior to albendazole (Escobedo et al., 2003). Despite its good efficacy, quinacrine has potentially severe adverse effects, including a number of psychiatric and dermatologic manifestations, and is no longer commercially available in the United States or Canada.

Finally, paromomycin is an aminoglycoside with antigiardial activity *in vitro* (Edlind, 1989) and *in vivo* (Geurden et al., 2006). However, it less effective among adults with metronidazole-refractory disease than other therapies and is rarely used in clinical practice.

Therapeutic strategies for treatment-refractory giardiasis include longer duration and/or higher doses of the original agent, switching to a different class of drug, or combination therapy. In a case series of 10 patients who failed nitroimidazole therapy, all were cured with one of the following combinations: metronidazole or tinidazole + paromomycin + albendazole

in three cases, metronidazole + paromomycin in two cases, tinidazole + paromomycin in two cases, tinidazole + quinacrine in two cases, and metronidazole + quinacrine in one case (Morch et al., 2008). All the drugs were administered for 7 or 10 days except for tinidazole, which was given for 1–7 days. The combinations were well tolerated and had no serious adverse effects. In a case report, a HIV patient with giardiasis was unsuccessfully treated five times with metronidazole and albendazole, but was cured with nitazoxanide 500 mg b.i.d for 10 days and then 1 g b.i.d. for 15 days (Abboud et al., 2001). Susceptibility testing showed the strain to be resistant to metronidazole and albendazole, but susceptible to nitazoxanide (Abboud et al., 2001). Combination therapy generally decreases the risk of developing antimicrobial drug resistance, although it is presently not known how this concept applies to giardiasis.

Assays for Drug Development

Giardia lamblia trophozoites can be readily grown *in vitro* under axenic conditions, which greatly simplifies drug testing compared to the endosymbiont *Cryptosporidium*. Typical assays for *Giardia* involve serial drug dilutions in multi-well plates and parasite growth for 48 h under anaerobic conditions (Valdez et al., 2009; Miyamoto et al., 2013) (Figure 4). Cell numbers and viability can be assessed microscopically (Gut et al., 2011), or by determining ATP content in the cultures (Valdez et al., 2009) (Figure 2). A number of Assemblage A and B isolates are available, and resistant lines against all major antigiardial drugs have been generated in the laboratory (Upcroft et al., 1996a,b; Dunn et al., 2010; Tejman-Yarden et al., 2011). To date, drug-resistant axenic lines have not been generated from clinical isolates derived from patients who failed therapy, although short-term animal studies of such isolates have shown that resistance occurs *in vivo* (Lemee et al., 2000).

Appropriate animal infection models are a key requirement for antimicrobial drug development. A number of mammals, including different rodents, dogs and cats, can be experimentally infected with *G. lamblia*. In cats and dogs, giardiasis has veterinary relevance (Bouzid et al., 2015), so drug development has veterinary objectives in these species. For drug testing studies against human *G. lamblia*, the most common models are mice and Mongolian gerbils. Adult mice are not readily infectable with most human *G. lamblia* strains, with the sole exception of the Assemblage B strain, GS/M (Byrd et al., 1994). The strain was shown to cause diarrheal disease upon experimental inoculation in humans (Nash et al., 1987), so it is a clinically relevant, pathogenic strain, yet the reasons for its seemingly unique ability to colonize adult mice remain unclear. However, following the observation that resistance to infection could be conferred by co-housing of animals, it was shown that conditioning of mice with a cocktail of suitable antibiotics (typically vancomycin + gentamicin or neomycin + ampicillin or penicillin; none of these kill *G. lamblia*) in the drinking water sensitizes mice to infection with a range of different *G. lamblia* strains of both A and B assemblages (Singer and Nash, 2000b; Solaymani-Mohammadi and Singer, 2011). This conditioning regimen is now commonly used, although the impact on drug testing has not been explored. As an alternative, gerbils can be

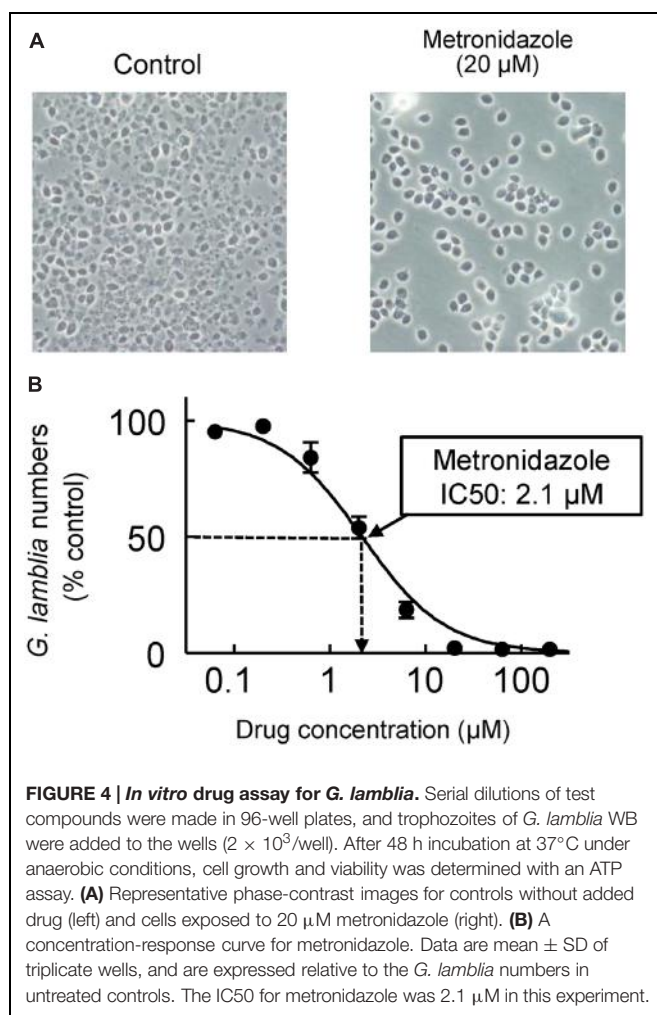


FIGURE 4 | *In vitro* drug assay for *G. lamblia*. Serial dilutions of test compounds were made in 96-well plates, and trophozoites of *G. lamblia* WB were added to the wells (2×10^3 /well). After 48 h incubation at 37°C under anaerobic conditions, cell growth and viability was determined with an ATP assay. **(A)** Representative phase-contrast images for controls without added drug (left) and cells exposed to 20 μ M metronidazole (right). **(B)** A concentration-response curve for metronidazole. Data are mean \pm SD of triplicate wells, and are expressed relative to the *G. lamblia* numbers in untreated controls. The IC₅₀ for metronidazole was 2.1 μ M in this experiment.

infected with a wide range of human *G. lamblia* strains without antibiotic conditioning (Tejman-Yarden et al., 2011, 2013; Benere et al., 2012). They have proven valuable for pathophysiologic and immunological studies, but have not been widely used for drug testing.

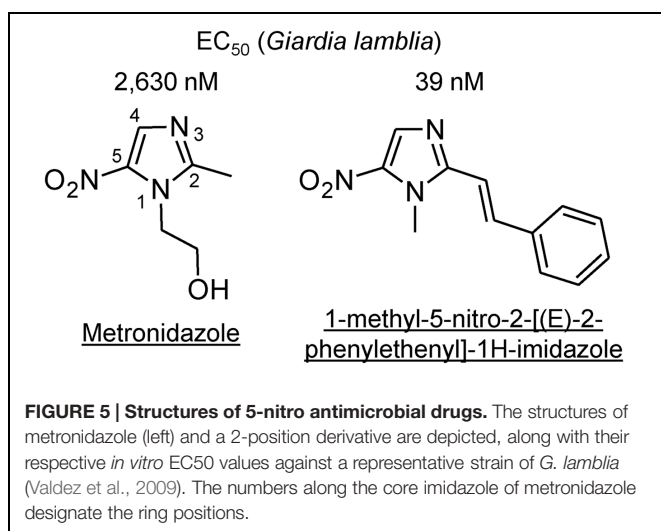
New Drugs

The discovery of antibiotics revolutionized medicine and represents a turning point in human history. Unfortunately, enthusiasm for these miracle drugs was soon tempered by the emergence of resistant strains. As in bacteria, protozoa like *Giardia* can develop resistance that make widely used agents ineffective. While still uncommon, antibiotic resistance (especially against 5-NI drugs) is increasing in *G. lamblia* and contributes to treatment failures (Lemee et al., 2000). Elucidating the complex resistance mechanisms is an active area of investigation and important insights have been gained over the last decade. Recent studies indicate that drug resistance in *G. lamblia* is caused by one of several different cellular adaptations. Of these, the best described mechanism is the loss of the parasite's ability to activate nitro prodrugs to toxic radicals by reduction, thus effectively allowing the parasite to

avoid suicidal drug activation. For example, suppression of PFOR leads to metronidazole resistance (Dan et al., 2000) and certain strains of metronidazole-resistant *G. lamblia* have reduced levels of this critical enzyme required for ferredoxin-dependent drug activation (Leitsch et al., 2011). Other drug activation pathways have been identified, and they can also be impacted in resistant cells (Pal et al., 2009; Leitsch et al., 2011; Nillius et al., 2011). Another mechanism of drug resistance to both metronidazole and nitazoxanide is altered expression of genes involved in stress responses, including heat-shock proteins and expression of nitazoxanide-binding proteins (Muller et al., 2008). Fortunately, metronidazole-resistant giardiasis is not yet common in clinical practice, perhaps because of the detrimental effects of metronidazole resistance on attachment and infectivity in a subset of organisms, although others with resistance can infect normally (Tejman-Yarden et al., 2011). Resistance to other anti-giardial drugs also exists. For example, resistance to benzimidazoles is thought to occur through mutations in the molecular target, β -tubulin (Aguayo-Ortiz et al., 2013). Overall, the studies on emerging drug resistance and the underlying mechanisms underline that the development of new anti-giardial agents to broaden the therapeutic armamentarium remains an important challenge.

The goals of new drug development against *G. lamblia* and *Cryptosporidium* are somewhat different. For *Cryptosporidium*, only one moderately effective drug (nitazoxanide) is available, so new classes of more effective drugs are a high priority. By comparison, for *G. lamblia*, several classes of drugs with good efficacy exist, but dosing regimens are suboptimal or emerging resistance begins to threaten clinical utility. Consequently, improvements in potency and dosing, and the ability to overcome existing and prevent new forms of drug resistance are priorities in anti-giardial drug development. A number of strategies have been employed for the development of new drugs against *G. lamblia*, which include, as for *Cryptosporidium*, both activity- and target-centered approaches. In addition, optimization within existing drug classes, analogous to the development of next-generation β -lactam antibiotics, has played a much more important role in drug development against *G. lamblia* compared to *Cryptosporidium*.

Prime examples for the potential of optimization within an existing drug class are the 5-NI compounds. The most common 5-NI, metronidazole, is composed of a 5-membered nitroimidazole core carrying simple hydroxyethyl and methyl side chains in the 1' and 2' position, respectively (Figure 5). Modifications of these side chains have been a productive strategy for developing new and improved agents. For example, substitution of side chains in the 1', 2', or 4' positions of the imidazole ring with larger and more complex functional groups has led to compounds with enhanced (up to 500-fold) anti-giardial activity (Upcroft et al., 2006; Valdez et al., 2009; Miyamoto et al., 2013) (Figure 5). Importantly, many of the new 5-NI compounds were able to overcome existing forms of metronidazole resistance (Miyamoto et al., 2013). The underlying mechanisms for improved activity remain to



be determined but may relate to differential drug activation by one or more reductases (Leitsch et al., 2011; Nillius et al., 2011). For other metronidazole derivatives it was shown that they were more active than the parent compound in altering the morphology and ultrastructure of *G. lamblia* by affecting vesicle trafficking and differentiation into cysts (Busatti et al., 2013). Similar advances have been demonstrated for the 5-nitrothiazole, nitazoxanide, where placement of a benzene ring between the nitro group and the thiazole ring was used to create new benzologues (Navarrete-Vazquez et al., 2011). The best compounds were five-times more active than nitazoxanide and 18-times more active than metronidazole against *G. lamblia* and showed minimal toxicity in mammalian cells (Navarrete-Vazquez et al., 2011). In another series of nitrothiazole derivatives, substitutions at 2' position with a range of acylamino side chains yielded compounds with >10-fold greater activity against *G. lamblia* than the reference compound nitazoxanide (Nava-Zuazo et al., 2014). Collectively, these studies demonstrate that systematic structural modifications of existing nitro drugs are likely to yield vastly improved antimicrobials that can serve as “next-generation” nitro drugs for the treatment of giardiasis and potentially other infections with clinically important anaerobic pathogens (Miyamoto et al., 2013).

Similar modification strategies have been applied to benzimidazoles, whose prototype compound, albendazole, has been used as an alternative to 5-NI drugs against giardiasis. A number of novel derivatives have been created, including an alkylthiol group at the 2' position and an ethoxy group at the 5' position of the benzimidazole ring, resulting in highly potent compounds with antigiardial activity in the 10–50 nM range (Perez-Villanueva et al., 2013). Using reverse-phase high performance liquid chromatography and permeability assays with cultured epithelial cells, it was observed that the antigiardial activity of a series of benzimidazole derivatives was influenced by their lipophilicity, hydrogen bond donors, and molecular volume, but not by their apparent permeability across epithelial cell monolayers (Hernandez-Covarrubias

et al., 2012). A computational analysis of the structure-activity relationships of multiple benzimidazoles showed complex activity landscapes for antigiardial activity, with substitution at position 2 on the benzimidazole moiety playing an important role in increasing potency and substitutions at positions 4–7 influencing selectivity against *G. lamblia* over other protozoan parasites (Perez-Villanueva et al., 2010). These findings offer hope that quantitative models may help to identify structural properties associated with enhanced antigiardial activity in future drug design, at least for compounds that have well-defined molecular targets such as β-tubulin for benzimidazoles (Aguayo-Ortiz et al., 2013). Similar structure activity analyses have been conducted for 5-NI derivatives (Miyamoto et al., 2013), although the current lack of understanding of the specific reductases involved in prodrug activation or the molecular targets of activated drugs confounds these analyses and complicates their exploitation in drug development.

Besides compound optimization within existing drug classes, activity-centered screens of drug libraries have also been applied to *G. lamblia*. For example, a screen of 1,520 compounds from the BIOMOL ICCB Known Bioactives 2 and NINDS Custom Collection 2 libraries for growth-inhibitory activity against *G. lamblia* yielded 48 initial hits, some of which, such as indirubin, were not known to kill *G. lamblia*, although many others had known antigiardial agents or were broad inhibitors of cellular functions (e.g., actinomycin D; Bonilla-Santiago et al., 2008). Such toxic compounds are not likely to be of clinical utility. By comparison, screening of libraries of FDA-approved drugs has the distinct advantage that preclinical safety testing has already been done, which can accelerate the progression to clinical trials of efficacy. For instance, screening of a library of 746 compounds available for human use found that auranofin, which is employed in the treatment of rheumatoid arthritis, inhibited the growth and survival of multiple different *G. lamblia* isolates (Tejman-Yarden et al., 2013). Importantly, auranofin completely overcame metronidazole resistance (Tejman-Yarden et al., 2013). The action mechanism involved inhibition of thioredoxin oxidoreductase, a critical enzyme involved in maintaining normal protein function and combating oxidative damage in *G. lamblia* and other parasites including *Entamoeba histolytica* and *Schistosoma mansoni* (Kuntz et al., 2007; Debnath et al., 2012; Tejman-Yarden et al., 2013). Given that its pharmacokinetic properties and toxicology are well established (Blocka et al., 1986), auranofin may be a promising new candidate for the treatment of drug-resistant giardiasis. In another screen, a total of 2,816 compounds from the Library of Pharmaceutical Active Compounds (LOPAC1280) and the NIH Chemical Genomics Center Pharmaceutical collection library (NPC) were tested for activity against *G. lamblia* (Chen et al., 2011). Detailed follow-up studies of 28 of the most active compounds identified three new drugs, fumagillin, carbadox, and tioxidazole, with strong activity against metronidazole-sensitive and -resistant *G. lamblia* isolates (Kulakova et al., 2014). Furthermore, fumagillin, a complex biomolecule derived from *Aspergillus fumigatus* with known antimicrobial activities against *Entamoeba* and microsporidia, was efficacious in a mouse giardiasis model (Kulakova et al., 2014).

An abbreviated form of activity-centered drug discovery is the retesting of compounds that have shown activity in related microbes. Screening of an NIH Chemical Genomics Center Pharmaceutical Collection containing >2,000 compounds identified 32 highly active compounds against *Plasmodium falciparum* (Yuan et al., 2011). One of these, tetrahydrolipstatin (orlistat), a lipase inhibitor approved for the treatment of obesity, was then tested for growth inhibition of *G. lamblia*, based on the general rationale that efficient lipid metabolism is important for a fast growing parasite such as *Giardia*. Orlistat showed a potent and dose-dependent inhibition of *G. lamblia* replication, with a half maximal inhibitory concentration significantly lower than that of metronidazole (Hahn et al., 2013). Notably, orlistat is poorly absorbed from the intestinal tract and remains highly active in the lumen until excreted in the stool, raising the possibility of essentially topical therapy of giardiasis. Disadvantages of orlistat are the potential malabsorption of lipids and other lipophilic drugs, as well as cost issues. Another example is miltefosine, a potent oral treatment for human visceral leishmaniasis due to *Leishmania donovani*. The drug had previously been shown to kill this parasite by inducing a cell death process with numerous cytoplasmic, nuclear, and membrane features of metazoan apoptosis (Paris et al., 2004). Subsequent testing of miltefosine against *G. lamblia* revealed good activity *in vitro* and efficacy in a mouse model *in vivo* (Eissa and Amer, 2012). As with orlistat, trials to ascertain the effectiveness of miltefosine in humans with giardiasis will be needed. More broadly, repurposing of existing human drugs can be a powerful and resource-efficient strategy for rapid progress in drug development, but the finite number of existing compounds (with only ~1,500 currently FDA-approved drugs) ultimately limits this discovery path in the ongoing struggle for new antimicrobial agents.

One way out of the closed loop of drug repurposing is the screening of unknown chemical entities. Plants and their extracts have historically been rich sources for new antimicrobial agents. One of these is the naturally occurring weed *Oxalis corniculata*, long used in India for treating dysentery and diarrhea. Systematic fractionation of extracts was used to isolate a novel galactoglycerolipid compound with anti-giardial activity comparable to metronidazole (Manna et al., 2010). The compound had no toxicity in human cells (Manna et al., 2010). Extracts of sandalwood, *Osiris alba*, have been used by traditional healers in Jordan to ameliorate diarrheal diseases. Phytochemical investigation identified a new pyrrolizidine alkaloid, osyrinine, which had significant activity against *Giardia* but was non-toxic to human cells (Al-Jaber et al., 2010). These examples demonstrate that crude plant extracts, or perhaps in the future other rich biological sources of structurally diverse compounds, can be the source of new anti-giardial compounds, although their medicinal characterization, synthesis, and optimization are likely to pose challenges not encountered with the exploration of libraries of chemically defined compounds with drug-like properties.

The third drug development strategy, exploitation of molecularly defined targets, has been less prominent for *Giardia* compared to *Cryptosporidium*. Nonetheless, a small number

of *G. lamblia* targets have been explored for druggability. The metabolic enzyme arginine deiminase (ADI) catalyzes the first step in a major pathway for generating ATP in the parasite (Knodler et al., 1998). Knock-down of ADI by RNA interference resulted in non-viable trophozoites, indicating that ADI is important for trophozoite survival (Li et al., 2009). Furthermore, ADI may also serve as a virulence factor by depleting arginine in the host, which may enable *Giardia* to evade the host immune response (Eckmann et al., 2000; Banik et al., 2013). Humans lack an analogous enzyme to ADI, making it an attractive target for drug development. Another enzyme target is carbamate kinase, which catalyzes the final step in the arginine dihydrolase pathway converting ADP and carbamoyl phosphate to ATP and carbamate. It is essential in *Giardia* metabolism, but has no equivalent in humans (Minotto et al., 1999). A luminescent enzyme activity assay was employed in a high throughput screen of over 4,000 compounds to identify 30 hits with activity in the low mM range (Chen et al., 2012). Although the detected activities are low at this point, the hits could be starting points for the development of more potent and selective inhibitors of carbamate kinase in *G. lamblia* and ultimately a novel class of anti-giardial drugs. A third attractive target enzyme in *Giardia* is fructose 1,6-bisphosphate aldolase (FBPA), which catalyzes the reversible cleavage of D-fructose-1,6-bisphosphate to dihydroxyacetone phosphate and glyceraldehyde 3-phosphate, a key step in the Embden–Meyerhof–Parnas glycolytic pathway used by amitochondriate protozoa as a main source of energy (Li et al., 2011). FBPA is critical for *Giardia* survival and had unique structural and functional features that distinguish it from human analogs (Galkin et al., 2007). Inhibitors of the enzyme have anti-giardial activity in the 100 nM range and very low mammalian cytotoxicity (Navarrete-Vazquez et al., 2015).

Outlook

Several treatment options currently exist for giardiasis, but important therapeutic challenges remain. One major objective is improvements in dosing, ideally in form of a single, highly effective oral dose, which is the ultimate goal for most if not all tropical infection diseases as it allows diagnosis and definitive treatment on a single clinic visit. Another objective is the ability to overcome and prevent drug resistance, which is not yet common for *G. lamblia*, but constitutes a continuous threat that should not be taken lightly. Current studies suggest that these objectives can be achieved within existing classes of drugs or with new classes of drugs and molecular targets. However, as for cryptosporidiosis, a major challenge are the economic incentives for new drug development against giardiasis, which is clinically important throughout the world but is typically considered a Neglected Disease with primary health impact in low-development countries (Escobedo et al., 2010).

FUNDING

This work was supported by NIH grant AI114671.

REFERENCES

- Abboud, P., Lemee, V., Gargala, G., Brasseur, P., Ballet, J. J., Borsig-Lebas, F., et al. (2001). Successful treatment of metronidazole- and albendazole-resistant giardiasis with nitazoxanide in a patient with acquired immunodeficiency syndrome. *Clin. Infect. Dis.* 32, 1792–1794. doi: 10.1086/320751
- Abrahamsen, M. S., Templeton, T. J., Enomoto, S., Abrahante, J. E., Zhu, G., Lancto, C. A., et al. (2004). Complete genome sequence of the apicomplexan, *Cryptosporidium parvum*. *Science* 304, 441–445. doi: 10.1126/science.1094786
- Abubakar, I., Aliyu, S. H., Arumugam, C., Hunter, P. R., and Usman, N. K. (2007). Prevention and treatment of cryptosporidiosis in immunocompromised patients. *Cochrane Database Syst. Rev.* 24:CD004932. doi: 10.1002/14651858.CD004932.pub2
- Adell, A. D., Miller, W. A., Harvey, D. J., Vanwermel, E., Wuertz, S., and Conrad, P. A. (2013). Individual subject meta-analysis of parameters for *Cryptosporidium parvum* shedding and diarrhoea in animal experimental models. *Epidemiol. Infect.* 141, 1662–1678. doi: 10.1017/S0950268812002294
- Aguayo-Ortiz, R., Mendez-Lucio, O., Romo-Mancillas, A., Castillo, R., Yepez-Mulia, L., Medina-Franco, J. L., et al. (2013). Molecular basis for benzimidazole resistance from a novel beta-tubulin binding site model. *J. Mol. Graph. Model.* 45, 26–37. doi: 10.1016/j.jmgm.2013.07.008
- Aguirre, S. A., Mason, P. H., and Perryman, L. E. (1994). Susceptibility of major histocompatibility complex (MHC) class I- and MHC class II-deficient mice to *Cryptosporidium parvum* infection. *Infect. Immun.* 62, 697–699.
- Alcantara Warren, C., Destura, R. V., Sevilleja, J. E., Barroso, L. F., Carvalho, H., Barrett, L. J., et al. (2008). Detection of epithelial-cell injury, and quantification of infection, in the HCT-8 organoid model of cryptosporidiosis. *J. Infect. Dis.* 198, 143–149. doi: 10.1086/588819
- Al-Jaber, H. I., Mosleh, I. M., Mallouh, A., Abu Salim, O. M., and Abu Zarga, M. H. (2010). Chemical constituents of *Osyris alba* and their antiparasitic activities. *J. Asian. Nat. Prod. Res.* 12, 814–820. doi: 10.1080/10286020.2010.502892
- Al-Mekhlafi, H. M., Al-Maktari, M. T., Jani, R., Ahmed, A., Anuar, T. S., Moktar, N., et al. (2013). Burden of Giardia duodenalis infection and its adverse effects on growth of schoolchildren in rural Malaysia. *PLoS Negl. Trop. Dis.* 7:e2516. doi: 10.1371/journal.pntd.0002516
- Amadi, B., Mwiya, M., Musuku, J., Watuka, A., Sianongo, S., Ayoub, A., et al. (2002). Effect of nitazoxanide on morbidity and mortality in Zambian children with cryptosporidiosis: a randomised controlled trial. *Lancet* 360, 1375–1380. doi: 10.1016/S0140-6736(02)11401-2
- Andersen, Y. S., Gillin, F. D., and Eckmann, L. (2006). Adaptive immunity-dependent intestinal hypermotility contributes to host defense against Giardia spp. *Infect. Immun.* 74, 2473–2476. doi: 10.1128/IAI.74.4.2473-2476.2006
- Ankarklev, J., Svärd, S. G., and Lebbad, M. (2012). Allelic sequence heterozygosity in single *Giardia* parasites. *BMC Microbiol.* 12:65. doi: 10.1186/1471-2180-12-65
- Anselli, B. R., McConvile, M. J., Ma'ayeh, S. Y., Dagley, M. J., Gasser, R. B., Svärd, S. G., et al. (2015). Drug resistance in *Giardia duodenalis*. *Biotechnol. Adv.* 33(Pt 1), 888–901. doi: 10.1016/j.biotechadv.2015.04.009
- Argenzio, R. A., Armstrong, M., and Rhoads, J. M. (1996). Role of the enteric nervous system in piglet cryptosporidiosis. *J. Pharmacol. Exp. Ther.* 279, 1109–1115.
- Argenzio, R. A., Lecce, J., and Powell, D. W. (1993). Prostanoids inhibit intestinal NaCl absorption in experimental porcine cryptosporidiosis. *Gastroenterology* 104, 440–447.
- Argenzio, R. A., Liacos, J. A., Levy, M. L., Meuten, D. J., Lecce, J. G., and Powell, D. W. (1990). Villous atrophy, crypt hyperplasia, cellular infiltration, and impaired glucose-Na absorption in enteric cryptosporidiosis of pigs. *Gastroenterology* 98, 1129–1140. doi: 10.1016/0016-5085(90)90325-U
- Baldursson, S., and Karanis, P. (2011). Waterborne transmission of protozoan parasites: review of worldwide outbreaks - an update 2004–2010. *Water Res.* 45, 6603–6614. doi: 10.1016/j.watres.2011.10.013
- Banik, S., Renner Viveros, P., Seeber, F., Klotz, C., Ignatius, R., and Aebscher, T. (2013). Giardia duodenalis arginine deiminase modulates the phenotype and cytokine secretion of human dendritic cells by depletion of arginine and formation of ammonia. *Infect. Immun.* 81, 2309–2317. doi: 10.1128/IAI.00004-13
- Barry, M. A., Weatherhead, J. E., Hotez, P. J., and Woc-Colburn, L. (2013). Childhood parasitic infections endemic to the United States. *Pediatr. Clin. North Am.* 60, 471–485. doi: 10.1016/j.pcl.2012.12.011
- Bartelt, L. A., Roche, J., Kolling, G., Bolick, D., Noronha, F., Naylor, C., et al. (2013). Persistent *G. lamblia* impairs growth in a murine malnutrition model. *J. Clin. Invest.* 123, 2672–2684. doi: 10.1172/JCI67294
- Benere, E., Van Assche, T., Van Ginneken, C., Peulen, O., Cos, P., and Maes, L. (2012). Intestinal growth and pathology of *Giardia duodenalis* assemblage subtype A(I), A(II), B and E in the gerbil model. *Parasitology* 139, 424–433. doi: 10.1017/S0031182011002137
- Berkman, D. S., Lescano, A. G., Gilman, R. H., Lopez, S. L., and Black, M. M. (2002). Effects of stunting, diarrhoeal disease, and parasitic infection during infancy on cognition in late childhood: a follow-up study. *Lancet* 359, 564–571. doi: 10.1016/S0140-6736(02)07744-9
- Bernander, R., Palm, J. E., and Svärd, S. G. (2001). Genome ploidy in different stages of the *Giardia lamblia* life cycle. *Cell Microbiol.* 3, 55–62. doi: 10.1046/j.1462-5822.2001.00094.x
- Bessoff, K., Sateriale, A., Lee, K. K., and Huston, C. D. (2013). Drug repurposing screen reveals FDA-approved inhibitors of human HMG-CoA reductase and isoprenoid synthesis that block *Cryptosporidium parvum* growth. *Antimicrob. Agents Chemother.* 57, 1804–1814. doi: 10.1128/AAC.02460-12
- Bessoff, K., Spangenberg, T., Foderaro, J. E., Juman, R. S., Ward, G. E., and Huston, C. D. (2014). Identification of *Cryptosporidium parvum* active chemical series by Repurposing the open access malaria box. *Antimicrob. Agents Chemother.* 58, 2731–2739. doi: 10.1128/AAC.02641-13
- Betancourt, W. Q., and Rose, J. B. (2004). Drinking water treatment processes for removal of *Cryptosporidium* and *Giardia*. *Vet. Parasitol.* 126, 219–234. doi: 10.1016/j.vetpar.2004.09.002
- Bienz, M., Dai, W. J., Welle, M., Gottstein, B., and Muller, N. (2003). Interleukin-6-deficient mice are highly susceptible to *Giardia lamblia* infection but exhibit normal intestinal immunoglobulin A responses against the parasite. *Infect. Immun.* 71, 1569–1573. doi: 10.1128/IAI.71.3.1569-1573.2003
- Bissuel, F., Cotte, L., Rabodonirina, M., Rougier, P., Piens, M. A., and Trepo, C. (1994). Paromomycin: an effective treatment for cryptosporidial diarrhea in patients with AIDS. *Clin. Infect. Dis.* 18, 447–449. doi: 10.1093/clinids/18.3.447
- Blackwell, A. D., Martin, M., Kaplan, H., and Gurven, M. (2013). Antagonism between two intestinal parasites in humans: the importance of co-infection for infection risk and recovery dynamics. *Proc. Biol. Sci.* 280, 20131671. doi: 10.1098/rspb.2013.1671
- Blanshard, C., Shanson, D. C., and Gazzard, B. G. (1997). Pilot studies of azithromycin, tetraazuril and paromomycin in the treatment of cryptosporidiosis. *Int. J. STD AIDS* 8, 124–129. doi: 10.1258/0956462971919543
- Blocka, K. L., Paulus, H. E., and Furst, D. E. (1986). Clinical pharmacokinetics of oral and injectable gold compounds. *Clin. Pharmacokinet.* 11, 133–143. doi: 10.2165/00003088-198611020-00003
- Bonilla-Santiago, R., Wu, Z., Zhang, L., and Widmer, G. (2008). Identification of growth inhibiting compounds in a *Giardia lamblia* high-throughput screen. *Mol. Biochem. Parasitol.* 162, 149–154. doi: 10.1016/j.molbiopara.2008.08.005
- Boucher, S. E., and Gillin, F. D. (1990). Excystation of in vitro-derived *Giardia lamblia* cysts. *Infect. Immun.* 58, 3516–3522.
- Bouzid, M., Halai, K., Jeffreys, D., and Hunter, P. R. (2015). The prevalence of *Giardia infection* in dogs and cats, a systematic review and meta-analysis of prevalence studies from stool samples. *Vet. Parasitol.* 207, 181–202. doi: 10.1016/j.vetpar.2014.12.011
- Busatti, H. G., Alves, R. J., Santana-Anjos, K. G., Gil, F. F., Cury, M. C., Vannier-Santos, M. A., et al. (2013). Effects of metronidazole analogues on *Giardia lamblia*: experimental infection and cell organization. *Diagn. Microbiol. Infect. Dis.* 75, 160–164. doi: 10.1016/j.diagmicrobio.2012.11.001
- Byrd, L. G., Conrad, J. T., and Nash, T. E. (1994). *Giardia lamblia* infections in adult mice. *Infect. Immun.* 62, 3583–3585.
- Campbell, L. D., Stewart, J. N., and Mead, J. R. (2002). Susceptibility to *Cryptosporidium parvum* infections in cytokine- and chemokine-receptor knockout mice. *J. Parasitol.* 88, 1014–1016. doi: 10.1645/0022-3395(2002)088[1014:STCPII]2.0.CO;2
- Carreno, R. A., Martin, D. S., and Barta, J. R. (1999). Cryptosporidium is more closely related to the gregarines than to coccidia as shown by phylogenetic analysis of apicomplexan parasites inferred using small-subunit ribosomal RNA gene sequences. *Parasitol. Res.* 85, 899–904. doi: 10.1007/s004360050655

- Castellanos-Gonzalez, A., Cabada, M. M., Nichols, J., Gomez, G., and White, A. C. Jr. (2013a). Human primary intestinal epithelial cells as an improved in vitro model for *Cryptosporidium parvum* infection. *Infect. Immun.* 81, 1996–2001. doi: 10.1128/IAI.01131-12
- Castellanos-Gonzalez, A., White, A. C. Jr., Ojo, K. K., Vidadala, R. S., Zhang, Z., Reid, M. C., et al. (2013b). A novel calcium-dependent protein kinase inhibitor as a lead compound for treating cryptosporidiosis. *J. Infect. Dis.* 208, 1342–1348. doi: 10.1093/infdis/jit327
- Checkley, W., White, A. C. Jr., Jaganath, D., Arrowood, M. J., Chalmers, R. M., Chen, X. M., et al. (2015). A review of the global burden, novel diagnostics, therapeutics, and vaccine targets for *Cryptosporidium*. *Lancet Infect. Dis.* 15, 85–94. doi: 10.1016/S1473-3099(14)70772-8
- Chen, C. Z., Kulakova, L., Southall, N., Marugan, J. J., Galkin, A., Austin, C. P., et al. (2011). High-throughput *Giardia lamblia* viability assay using bioluminescent ATP content measurements. *Antimicrob. Agents Chemother.* 55, 667–675. doi: 10.1128/AAC.00618-10
- Chen, C. Z., Southall, N., Galkin, A., Lim, K., Marugan, J. J., Kulakova, L., et al. (2012). A homogenous luminescence assay reveals novel inhibitors for *Giardia lamblia* carbamate kinase. *Curr. Chem. Genomics* 6, 93–102. doi: 10.2174/1875397301206010093
- Chen, X. M., Keithly, J. S., Paya, C. V., and LaRussa, N. F. (2002). Cryptosporidiosis. *N. Engl. J. Med.* 346, 1723–1731. doi: 10.1056/NEJMra013170
- Cosyns, M., Tsirkin, S., Jones, M., Flavell, R., Kikutani, H., and Hayward, A. R. (1998). Requirement of CD40-CD40 ligand interaction for elimination of *Cryptosporidium parvum* from mice. *Infect. Immun.* 66, 603–607.
- Current, W. L., and Reese, N. C. (1986). A comparison of endogenous development of three isolates of *Cryptosporidium* in suckling mice. *J. Protozool.* 33, 98–108. doi: 10.1111/j.1550-7408.1986.tb05567.x
- Dan, M., Wang, A. L., and Wang, C. C. (2000). Inhibition of pyruvate-ferredoxin oxidoreductase gene expression in *Giardia lamblia* by a virus-mediated hammerhead ribozyme. *Mol. Microbiol.* 36, 447–456. doi: 10.1046/j.1365-2958.2000.01863.x
- Dann, S. M., Manthey, C. F., Le, C., Miyamoto, Y., Gima, L., Abrahim, A., et al. (2015). IL-17A promotes protective IgA responses and expression of other potential effectors against the lumen-dwelling enteric parasite *Giardia*. *Exp. Parasitol.* 156, 68–78. doi: 10.1016/j.exppara.2015.06.003
- Dash, M., Padhi, S., Panda, P., and Parida, B. (2013). Intestinal protozoans in adults with diarrhea. *N. Am. J. Med. Sci.* 5, 707–712. doi: 10.4103/1947-2714.123261
- Davids, B. J., Palm, J. E., Housley, M. P., Smith, J. R., Andersen, Y. S., Martin, M. G., et al. (2006). Polymeric immunoglobulin receptor in intestinal immune defense against the lumen-dwelling protozoan parasite *Giardia*. *J. Immunol.* 177, 6281–6290. doi: 10.4049/jimmunol.177.9.6281
- Debnath, A., Parsonage, D., Andrade, R. M., He, C., Cobo, E. R., Hirata, K., et al. (2012). A high-throughput drug screen for *Entamoeba histolytica* identifies a new lead and target. *Nat. Med.* 18, 956–960. doi: 10.1038/nm.2758
- Dreesen, L., De Bosscher, K., Grit, G., Staels, B., Lubberts, E., Bauge, E., et al. (2014). *Giardia muris* infection in mice is associated with a protective interleukin 17A response and induction of peroxisome proliferator-activated receptor alpha. *Infect. Immun.* 82, 3333–3340. doi: 10.1128/IAI.01536-14
- Dunn, L. A., Burgess, A. G., Krauer, K. G., Eckmann, L., Vanelle, P., Crozet, M. D., et al. (2010). A new-generation 5-nitroimidazole can induce highly metronidazole-resistant *Giardia lamblia* in vitro. *Int. J. Antimicrob. Agents* 36, 37–42. doi: 10.1016/j.ijantimicag.2010.03.004
- Eckmann, L., Laurent, F., Langford, T. D., Hetsko, M. L., Smith, J. R., Kagnoff, M. F., et al. (2000). Nitric oxide production by human intestinal epithelial cells and competition for arginine as potential determinants of host defense against the lumen-dwelling pathogen *Giardia lamblia*. *J. Immunol.* 164, 1478–1487. doi: 10.4049/jimmunol.164.3.1478
- Edlind, T. D. (1989). Susceptibility of *Giardia lamblia* to aminoglycoside protein synthesis inhibitors: correlation with rRNA structure. *Antimicrob. Agents Chemother.* 33, 484–488. doi: 10.1128/AAC.33.4.484
- Eissa, M. M., and Amer, E. I. (2012). *Giardia lamblia*: a new target for miltefosine. *Int. J. Parasitol.* 42, 443–452. doi: 10.1016/j.ijpara.2012.02.015
- Erickson, M. C., and Ortega, Y. R. (2006). Inactivation of protozoan parasites in food, water, and environmental systems. *J. Food Prot.* 69, 2786–2808.
- Escobedo, A. A., Almirall, P., Robertson, L. J., Franco, R. M., Hanevik, K., Morsch, K., et al. (2010). Giardiasis: the ever-present threat of a neglected disease. *Infect. Disord. Drug Targets* 10, 329–348. doi: 10.2174/187152610793180821
- Escobedo, A. A., and Cimerman, S. (2007). Giardiasis: a pharmacotherapy review. *Expert Opin. Pharmacother.* 8, 1885–1902. doi: 10.1517/14656566.8.12.1885
- Escobedo, A. A., Nunez, F. A., Moreira, I., Vega, E., Pareja, A., and Almirall, P. (2003). Comparison of chloroquine, albendazole and tinidazole in the treatment of children with giardiasis. *Ann. Trop. Med. Parasitol.* 97, 367–371. doi: 10.1179/000349803235002290
- Faubert, G. (2000). Immune response to *Giardia duodenalis*. *Clin. Microbiol. Rev.* 13, 35–54. doi: 10.1128/CMR.13.1.35-54.2000
- Flanigan, T., Whalen, C., Turner, J., Soave, R., Toerner, J., Havlir, D., et al. (1992). Cryptosporidium infection and CD4 counts. *Ann. Intern. Med.* 116, 840–842. doi: 10.7326/0003-4819-116-10-840
- Franzen, O., Jerlstrom-Hultqvist, J., Castro, E., Sherwood, E., Ankarklev, J., Reiner, D. S., et al. (2009). Draft genome sequencing of *Giardia intestinalis* assemblage B isolate GS: is human giardiasis caused by two different species? *PLoS Pathog.* 5:e1000560. doi: 10.1371/journal.ppat.1000560
- Furness, B. W., Beach, M. J., and Roberts, J. M. (2000). Giardiasis surveillance—United States, 1992–1997. *MMWR CDC Surveill. Summ.* 49, 1–13.
- Galkin, A., Kulakova, L., Melamud, E., Li, L., Wu, C., Mariano, P., et al. (2007). Characterization, kinetics, and crystal structures of fructose-1,6-bisphosphate aldolase from the human parasite, *Giardia lamblia*. *J. Biol. Chem.* 282, 4859–4867. doi: 10.1074/jbc.M609534200
- Gardner, T. B., and Hill, D. R. (2001). Treatment of giardiasis. *Clin. Microbiol. Rev.* 14, 114–128. doi: 10.1128/CMR.14.1.114-128.2001
- Geurden, T., Claerebout, E., Dursin, L., Deflandre, A., Bernay, F., Kaltsatos, V., et al. (2006). The efficacy of an oral treatment with paromomycin against an experimental infection with *Giardia* in calves. *Vet. Parasitol.* 135, 241–247. doi: 10.1016/j.vetpar.2005.09.006
- Gookin, J. L., Foster, D. M., Coccaro, M. R., and Stauffer, S. H. (2008). Oral delivery of L-arginine stimulates prostaglandin-dependent secretory diarrhea in *Cryptosporidium parvum*-infected neonatal piglets. *J. Pediatr. Gastroenterol. Nutr.* 46, 139–146. doi: 10.1097/MGP.0b013e31815c0480
- Gorla, S. K., Kavitha, M., Zhang, M., Chin, J. E., Liu, X., Striepen, B., et al. (2013). Optimization of benzoxazole-based inhibitors of *Cryptosporidium parvum* inosine 5'-monophosphate dehydrogenase. *J. Med. Chem.* 56, 4028–4043. doi: 10.1021/jm400241j
- Gorla, S. K., Kavitha, M., Zhang, M., Liu, X., Sharling, L., Gollapalli, D. R., et al. (2012). Selective and potent urea inhibitors of *Cryptosporidium parvum* inosine 5'-monophosphate dehydrogenase. *J. Med. Chem.* 55, 7759–7771. doi: 10.1021/jm3007917
- Granados, C. E., Reveiz, L., Uribe, L. G., and Criollo, C. P. (2012). Drugs for treating giardiasis. *Cochrane Database Syst. Rev.* 12, CD007787. doi: 10.1002/14651858.CD007787.pub2
- Greenberg, P. D., and Cello, J. P. (1996). Treatment of severe diarrhea caused by *Cryptosporidium parvum* with oral bovine immunoglobulin concentrate in patients with AIDS. *J. Acquir. Immune. Defic. Syndr. Hum. Retrovir.* 13, 348–354. doi: 10.1097/00042560-19961201-00008
- Griffiths, J. K., Moore, R., Dooley, S., Keusch, G. T., and Tzipori, S. (1994). *Cryptosporidium parvum* infection of Caco-2 cell monolayers induces an apical monolayer defect, selectively increases transmonolayer permeability, and causes epithelial cell death. *Infect. Immun.* 62, 4506–4514.
- Guarino, A., Canani, R. B., Casola, A., Pozio, E., Russo, R., Bruzzese, E., et al. (1995). Human intestinal cryptosporidiosis: secretory diarrhea and enterotoxic activity in Caco-2 cells. *J. Infect. Dis.* 171, 976–983. doi: 10.1093/infdis/171.4.976
- Guo, F., Zhang, H., Fritzler, J. M., Rider, S. D. Jr., Xiang, L., McNair, N. N., et al. (2014). Amelioration of *Cryptosporidium parvum* infection in vitro and in vivo by targeting parasite fatty acyl-coenzyme A synthetases. *J. Infect. Dis.* 209, 1279–1287. doi: 10.1093/infdis/jit645
- Gut, J., Ang, K. K., Legac, J., Arkin, M. R., Rosenthal, P. J., and McKerrow, J. H. (2011). An image-based assay for high throughput screening of *Giardia lamblia*. *J. Microbiol. Methods* 84, 398–405. doi: 10.1016/j.mimet.2010.12.026

- Hahn, J., Seeber, F., Kolodziej, H., Ignatius, R., Laue, M., Aebsicher, T., et al. (2013). High sensitivity of *Giardia duodenalis* to tetrahydrolipstatin (orlistat) in vitro. *PLoS ONE* 8:e71597. doi: 10.1371/journal.pone.0071597
- Hanevik, K., Hausken, T., Morken, M. H., Strand, E. A., Mørch, K., Coll, P., et al. (2007). Persisting symptoms and duodenal inflammation related to *Giardia duodenalis* infection. *J. Infect.* 55, 524–530. doi: 10.1016/j.jinf.2007.09.004
- Hanevik, K., Wensaas, K. A., Rortveit, G., Eide, G. E., Mørch, K., and Langeland, N. (2014). Irritable bowel syndrome and chronic fatigue 6 years after *Giardia* infection: a controlled prospective cohort study. *Clin. Infect. Dis.* 59, 1394–1400. doi: 10.1093/cid/ciu629
- Hayward, A. R., Cosyns, M., Jones, M., and Ponnuraj, E. M. (2001). Marrow-derived CD40-positive cells are required for mice to clear *Cryptosporidium parvum* infection. *Infect. Immun.* 69, 1630–1634. doi: 10.1128/IAI.69.3.1630-1634.2001
- Hernandez-Covarrubias, C., Vilchis-Reyes, M. A., Yepez-Mulia, L., Sanchez-Diaz, R., Navarrete-Vazquez, G., Hernandez-Campos, A., et al. (2012). Exploring the interplay of physicochemical properties, membrane permeability and giardicidal activity of some benzimidazole derivatives. *Eur. J. Med. Chem.* 52, 193–204. doi: 10.1016/j.ejmech.2012.03.014
- Hewitt, R. G., Yiannoutsos, C. T., Higgs, E. S., Carey, J. T., Geiseler, P. J., Soave, R., et al. (2000). Paromomycin: no more effective than placebo for treatment of cryptosporidiosis in patients with advanced human immunodeficiency virus infection. *AIDS Clin. Trial. Group. Clin. Infect. Dis.* 31, 1084–1092. doi: 10.1086/318155
- Heyworth, M. F. (1989). Intestinal IgA responses to *Giardia muris* in mice depleted of helper T lymphocytes and in immunocompetent mice. *J. Parasitol.* 75, 246–251. doi: 10.2307/3282773
- Hijjawi, N. S., Meloni, B. P., Ryan, U. M., Olson, M. E., and Thompson, R. C. (2002). Successful in vitro cultivation of *Cryptosporidium andersoni*: evidence for the existence of novel extracellular stages in the life cycle and implications for the classification of *Cryptosporidium*. *Int. J. Parasitol.* 32, 1719–1726. doi: 10.1016/S0020-7519(02)00199-6
- Hoffman, P. S., Sisson, G., Croxen, M. A., Welch, K., Harman, W. D., Cremades, N., et al. (2007). Antiparasitic drug nitazoxanide inhibits the pyruvate oxidoreductases of *Helicobacter pylori*, selected anaerobic bacteria and parasites, and *Campylobacter jejuni*. *Antimicrob. Agents Chemother.* 51, 868–876. doi: 10.1128/AAC.01159-06
- House, S. A., Richter, D. J., Pham, J. K., and Dawson, S. C. (2011). *Giardia* flagellar motility is not directly required to maintain attachment to surfaces. *PLoS Pathog.* 7:e1002167. doi: 10.1371/journal.ppat.1002167
- Hunter, P. R., and Nichols, G. (2002). Epidemiology and clinical features of *Cryptosporidium* infection in immunocompromised patients. *Clin. Microbiol. Rev.* 15, 145–154. doi: 10.1128/CMR.15.1.145-154.2002
- Hussien, S. M., Abdella, O. H., Abu-Hashim, A. H., Aboshiesha, G. A., Taha, M. A., El-Shemy, A. S., et al. (2013). Comparative study between the effect of nitazoxanide and paromomycine in treatment of cryptosporidiosis in hospitalized children. *J. Egypt Soc. Parasitol.* 43, 463–470. doi: 10.12816/0006403
- Jefferies, R., Yang, R., Woh, C. K., Weldt, T., Milech, N., Estcourt, A., et al. (2015). Target validation of the inosine monophosphate dehydrogenase (IMPDH) gene in *Cryptosporidium* using Phylomer® peptides. *Exp. Parasitol.* 148, 40–48. doi: 10.1016/j.exppara.2014.11.003
- Jerlstrom-Hultqvist, J., Ankarklev, J., and Svärd, S. G. (2010). Is human giardiasis caused by two different *Giardia* species? *Gut. Microbes* 1, 379–382. doi: 10.4161/gmic.1.6.13608
- Kamda, J. D., Nash, T. E., and Singer, S. M. (2012). *Giardia duodenalis*: dendritic cell defects in IL-6 deficient mice contribute to susceptibility to intestinal infection. *Exp. Parasitol.* 130, 288–291. doi: 10.1016/j.exppara.2012.01.003
- Kang, J. M., Ju, H. L., Yu, J. R., Sohn, W. M., and Na, B. K. (2012). Cryptostatin, a chagasin-family cysteine protease inhibitor of *Cryptosporidium parvum*. *Parasitology* 139, 1029–1037. doi: 10.1017/S003118201200297
- Kapel, N., Huneau, J. F., Magne, D., Tome, D., and Gobert, J. G. (1997). Cryptosporidiosis-induced impairment of ion transport and Na⁺-glucose absorption in adult immunocompromised mice. *J. Infect. Dis.* 176, 834–837. doi: 10.1086/517316
- Karanis, P., Kourenti, C., and Smith, H. (2007). Waterborne transmission of protozoan parasites: a worldwide review of outbreaks and lessons learnt. *J. Water Health* 5, 1–38. doi: 10.2166/wh.2006.002
- Knodler, L. A., Sekyre, E. O., Stewart, T. S., Schofield, P. J., and Edwards, M. R. (1998). Cloning and expression of a prokaryotic enzyme, arginine deiminase, from a primitive eukaryote *Giardia intestinalis*. *J. Biol. Chem.* 273, 4470–4477. doi: 10.1074/jbc.273.8.4470
- Kotloff, K. L., Nataro, J. P., Blackwelder, W. C., Nasrin, D., Farag, T. H., Panchalingam, S., et al. (2013). Burden and aetiology of diarrhoeal disease in infants and young children in developing countries (the Global Enteric Multicenter Study, GEMS): a prospective, case-control study. *Lancet* 382, 209–222. doi: 10.1016/S0140-6736(13)60844-2
- Kuhls, T. L., Greenfield, R. A., Mosier, D. A., Crawford, D. L., and Joyce, W. A. (1992). Cryptosporidiosis in adult and neonatal mice with severe combined immunodeficiency. *J. Comp. Pathol.* 106, 399–410. doi: 10.1016/0021-9975(92)90024-O
- Kulakova, L., Galkin, A., Chen, C. Z., Southall, N., Marugan, J. J., Zheng, W., et al. (2014). Discovery of novel anti-giardiasis drug candidates. *Antimicrob. Agents Chemother.* 58, 7303–7311. doi: 10.1128/AAC.03834-14
- Kuntz, A. N., Davioud-Charvet, E., Sayed, A. A., Califf, L. L., Dessolin, J., Arner, E. S., et al. (2007). Thioredoxin glutathione reductase from *Schistosoma mansoni*: an essential parasite enzyme and a key drug target. *PLoS Med.* 4:e206. doi: 10.1371/journal.pmed.0040206
- Lal, A., and Hales, S. (2015). Heterogeneity in hotspots: spatio-temporal patterns in neglected parasitic diseases. *Epidemiol. Infect.* 143, 631–639. doi: 10.1017/S0950268814001101
- Langford, T. D., Housley, M. P., Boes, M., Chen, J., Kagnoff, M. F., Gillin, F. D., et al. (2002). Central importance of immunoglobulin A in host defense against *Giardia* spp. *Infect. Immun.* 70, 11–18. doi: 10.1128/IAI.70.1.11-18.2002
- Laurent, F., Eckmann, L., Savidge, T. C., Morgan, G., Theodos, C., Naciri, M., et al. (1997). *Cryptosporidium parvum* infection of human intestinal epithelial cells induces the polarized secretion of C-X-C chemokines. *Infect. Immun.* 65, 5067–5073.
- Laurent, F., Kagnoff, M. F., Savidge, T. C., Naciri, M., and Eckmann, L. (1998). Human intestinal epithelial cells respond to *Cryptosporidium parvum* infection with increased prostaglandin H synthase 2 expression and prostaglandin E2 and F2alpha production. *Infect. Immun.* 66, 1787–1790.
- Laurent, F., McCole, D., Eckmann, L., and Kagnoff, M. F. (1999). Pathogenesis of *Cryptosporidium parvum* infection. *Microbes Infect.* 1, 141–148. doi: 10.1016/S1286-4579(99)80005-7
- Lauwaet, T., Andersen, Y., Van de Ven, L., Eckmann, L., and Gillin, F. D. (2010). Rapid detachment of *Giardia lamblia* trophozoites as a mechanism of antimicrobial action of the isoflavone formononetin. *J. Antimicrob. Chemother.* 65, 531–534. doi: 10.1093/jac/dkp501
- Leitsch, D., Burgess, A. G., Dunn, L. A., Krauer, K. G., Tan, K., Duchene, M., et al. (2011). Pyruvate:ferredoxin oxidoreductase and thioredoxin reductase are involved in 5-nitroimidazole activation while flavin metabolism is linked to 5-nitroimidazole resistance in *Giardia lamblia*. *J. Antimicrob. Chemother.* 66, 1756–1765. doi: 10.1093/jac/dkr192
- Lemee, V., Zaharia, I., Nevez, G., Rabodonirina, M., Brasseur, P., Ballet, J. J., et al. (2000). Metronidazole and albendazole susceptibility of 11 clinical isolates of *Giardia duodenalis* from France. *J. Antimicrob. Chemother.* 46, 819–821. doi: 10.1093/jac/46.5.819
- Li, E., Zhou, P., and Singer, S. M. (2006). Neuronal nitric oxide synthase is necessary for elimination of *Giardia lamblia* infections in mice. *J. Immunol.* 176, 516–521. doi: 10.4049/jimmunol.176.1.516
- Li, Z., Kulakova, L., Li, L., Galkin, A., Zhao, Z., Nash, T. E., et al. (2009). Mechanisms of catalysis and inhibition operative in the arginine deiminase from the human pathogen *Giardia lamblia*. *Bioorg. Chem.* 37, 149–161. doi: 10.1016/j.bioorg.2009.06.001
- Li, Z., Liu, Z., Cho, D. W., Zou, J., Gong, M., Breece, R. M., et al. (2011). Rational design, synthesis and evaluation of first generation inhibitors of the *Giardia lamblia* fructose-1,6-biphosphate aldolase. *J. Inorg. Biochem.* 105, 509–517. doi: 10.1016/j.jinorgbio.2010.12.012
- Liu, J., Kabir, F., Manneh, J., Lertsethtakarn, P., Begum, S., Gratz, J., et al. (2014). Development and assessment of molecular diagnostic tests for 15 enteropathogens causing childhood diarrhoea: a multicentre study. *Lancet Infect. Dis.* 14, 716–724. doi: 10.1016/S1473-3099(14)70808-4

- Manna, D., Dutta, P. K., Achari, B., and Lohia, A. (2010). A novel galacto-glycerolipid from *Oxalis corniculata* kills *Entamoeba histolytica* and *Giardia lamblia*. *Antimicrob. Agents Chemother.* 54, 4825–4832. doi: 10.1128/AAC.00546-10
- Mathur, M. K., Verma, A. K., Makwana, G. E., and Sinha, M. (2013). Study of opportunistic intestinal parasitic infections in human immunodeficiency virus/acquired immunodeficiency syndrome patients. *J. Glob. Infect. Dis.* 5, 164–167. doi: 10.4103/0974-777X.122012
- Minotto, L., Tutticci, E. A., Bagnara, A. S., Schofield, P. J., and Edwards, M. R. (1999). Characterisation and expression of the carbamate kinase gene from *Giardia intestinalis*. *Mol. Biochem. Parasitol.* 98, 43–51. doi: 10.1016/S0166-6851(98)00141-8
- Miyamoto, Y., Kalisiak, J., Korthals, K., Lauwaet, T., Cheung, D. Y., Lozano, R., et al. (2013). Expanded therapeutic potential in activity space of next-generation 5-nitroimidazole antimicrobials with broad structural diversity. *Proc. Natl. Acad. Sci. U.S.A.* 110, 17564–17569. doi: 10.1073/pnas.1302664110
- Mørch, K., Hanevik, K., Robertson, L. J., Strand, E. A., and Langeland, N. (2008). Treatment-ladder and genetic characterisation of parasites in refractory giardiasis after an outbreak in Norway. *J. Infect.* 56, 268–273. doi: 10.1016/j.jinf.2008.01.013
- Morrison, H. G., McArthur, A. G., Gillin, F. D., Aley, S. B., Adam, R. D., Olsen, G. J., et al. (2007). Genomic minimalism in the early diverging intestinal parasite *Giardia lamblia*. *Science* 317, 1921–1926. doi: 10.1126/science.1143837
- Muller, J., Ley, S., Felger, I., Hemphill, A., and Muller, N. (2008). Identification of differentially expressed genes in a *Giardia lamblia* WB C6 clone resistant to nitazoxanide and metronidazole. *J. Antimicrob. Chemother.* 62, 72–82. doi: 10.1093/jac/dkn142
- Murphy, R. C., Ojo, K. K., Larson, E. T., Castellanos-Gonzalez, A., Perera, B. G., Keyloun, K. R., et al. (2010). Discovery of potent and selective inhibitors of calcium-dependent protein kinase 1 (CDPK1) from *C. parvum* and *T. gondii*. *ACS Med. Chem. Lett.* 1, 331–335. doi: 10.1021/ml100096t
- Nash, T. E., Herrington, D. A., Losonsky, G. A., and Levine, M. M. (1987). Experimental human infections with *Giardia lamblia*. *J. Infect. Dis.* 156, 974–984. doi: 10.1093/infdis/156.6.974
- Navarrete-Vazquez, G., Chavez-Silva, F., Argotte-Ramos, R., Rodriguez-Gutierrez Mdel, C., Chan-Bacab, M. J., Cedillo-Rivera, R., et al. (2011). Synthesis of benzologues of Nitazoxanide and Tizoxanide: a comparative study of their in vitro broad-spectrum antiprotozoal activity. *Bioorg. Med. Chem. Lett.* 21, 3168–3171. doi: 10.1016/j.bmcl.2011.02.100
- Navarrete-Vazquez, G., Chavez-Silva, F., Colin-Lozano, B., Estrada-Soto, S., Hidalgo-Figueroa, S., Guerrero-Alvarez, J., et al. (2015). Synthesis of nitro(benzo)thiazole acetamides and in vitro antiprotozoal effect against amitochondriate parasites *Giardia intestinalis* and *Trichomonas vaginalis*. *Bioorg. Med. Chem.* 23, 2204–2210. doi: 10.1016/j.bmc.2015.02.059
- Nava-Zuazo, C., Chavez-Silva, F., Moo-Puc, R., Chan-Bacab, M. J., Ortega-Morales, B. O., Moreno-Diaz, H., et al. (2014). 2-acylamino-5-nitro-1,3-thiazoles: preparation and in vitro bioevaluation against four neglected protozoan parasites. *Bioorg. Med. Chem.* 22, 1626–1633. doi: 10.1016/j.bmc.2014.01.029
- Nda, M., Nath-Chowdhury, M., Sajid, M., Marcus, V., Mashiyama, S. T., Sakanari, J., et al. (2013). A cysteine protease inhibitor rescues mice from a lethal *Cryptosporidium parvum* infection. *Antimicrob. Agents Chemother.* 57, 6063–6073. doi: 10.1128/AAC.00734-13
- Nematian, J., Gholamrezaeezad, A., and Nematian, E. (2008). Giardiasis and other intestinal parasitic infections in relation to anthropometric indicators of malnutrition: a large, population-based survey of schoolchildren in Tehran. *Ann. Trop. Med. Parasitol.* 102, 209–214. doi: 10.1179/136485908X267876
- Nesterenko, M. V., Tilley, M., and Upton, S. J. (1995). A metallo-dependent cysteine proteinase of *Cryptosporidium parvum* associated with the surface of sporozoites. *Microbios* 83, 77–88.
- Nullius, D., Muller, J., and Muller, N. (2011). Nitroreductase (GNR1) increases susceptibility of *Giardia lamblia* and *Escherichia coli* to nitro drugs. *J. Antimicrob. Chemother.* 66, 1029–1035. doi: 10.1093/jac/dkr029
- Oberhuber, G., Kastner, N., and Stolte, M. (1997). Giardiasis: a histologic analysis of 567 cases. *Scand. J. Gastroenterol.* 32, 48–51. doi: 10.3109/00365529709025062
- Ojo, K. K., Larson, E. T., Keyloun, K. R., Castaneda, L. J., Derocher, A. E., Inampudi, K. K., et al. (2010). *Toxoplasma gondii* calcium-dependent protein kinase 1 is a target for selective kinase inhibitors. *Nat. Struct. Mol. Biol.* 17, 602–607. doi: 10.1038/nsmb.1818
- Olson, M. E., Ceri, H., and Morck, D. W. (2000). Giardia vaccination. *Parasitol. Today* 16, 213–217. doi: 10.1016/S0169-4758(99)01623-3
- Olson, M. E., Hannigan, C. J., Gaviller, P. F., and Fulton, L. A. (2001). The use of a Giardia vaccine as an immunotherapeutic agent in dogs. *Can. Vet. J.* 42, 865–868.
- Operario, D. J., Bristol, L. S., Liotta, J., Nydam, D. V., and Houpt, E. R. (2015). Correlation between diarrhea severity and oocyst count via quantitative PCR or fluorescence microscopy in experimental cryptosporidiosis in calves. *Am. J. Trop. Med. Hyg.* 92, 45–49. doi: 10.4269/ajtmh.14-0488
- Overturf, G. D. (1994). Endemic giardiasis in the United States—role of the daycare center. *Clin. Infect. Dis.* 18, 764–765. doi: 10.1093/clinids/18.5.764
- Painter, J. E., Hlavsa, M. C., Collier, S. A., Xiao, L., and Yoder, J. S. (2015). Cryptosporidiosis surveillance - United States, 2011–2012. *MMWR Surveill. Summ.* 64(Suppl. 3), 1–14.
- Pal, D., Banerjee, S., Cui, J., Schwartz, A., Ghosh, S. K., and Samuelson, J. (2009). *Giardia*, *Entamoeba*, and *Trichomonas* enzymes activate metronidazole (nitroreductases) and inactivate metronidazole (nitroimidazole reductases). *Antimicrob. Agents Chemother.* 53, 458–464. doi: 10.1128/AAC.00909-08
- Paris, C., Loiseau, P. M., Bories, C., and Breard, J. (2004). Miltefosine induces apoptosis-like death in *Leishmania donovani* promastigotes. *Antimicrob. Agents Chemother.* 48, 852–859. doi: 10.1128/AAC.48.3.852-859.2004
- Perez-Cordon, G., Nie, W., Schmidt, D., Tzipori, S., and Feng, H. (2011). Involvement of host calpain in the invasion of *Cryptosporidium parvum*. *Microbes Infect.* 13, 103–107. doi: 10.1016/j.micinf.2010.10.007
- Perez-Villanueva, J., Hernandez-Campos, A., Yepez-Mulia, L., Mendez-Cuesta, C., Mendez-Lucio, O., Hernandez-Luis, F., et al. (2013). Synthesis and antiprotozoal activity of novel 2-[{2-(1H-imidazol-1-yl)ethyl}sulfanyl]-1H-benzimidazole derivatives. *Bioorg. Med. Chem. Lett.* 23, 4221–4224. doi: 10.1016/j.bmcl.2013.05.012
- Perez-Villanueva, J., Santos, R., Hernandez-Campos, A., Giulianotti, M. A., Castillo, R., and Medina-Franco, J. L. (2010). Towards a systematic characterization of the antiprotozoal activity landscape of benzimidazole derivatives. *Bioorg. Med. Chem.* 18, 7380–7391. doi: 10.1016/j.bmc.2010.09.019
- Requena-Mendez, A., Goni, P., Lobeza, S., Oliveira, I., Aldasoro, E., Valls, M. E., et al. (2014). A family cluster of giardiasis with variable treatment responses: refractory giardiasis in a family after a trip to India. *Clin. Microbiol. Infect.* 20, O135–O138. doi: 10.1111/1469-0951.12327
- Rossignol, J. F., Ayoub, A., and Ayers, M. S. (2001). Treatment of diarrhea caused by *Cryptosporidium parvum*: a prospective randomized, double-blind, placebo-controlled study of Nitazoxanide. *J. Infect. Dis.* 184, 103–106. doi: 10.1086/321008
- Rossignol, J. F., Hidalgo, H., Feregrino, M., Higuera, F., Gomez, W. H., Romero, J. L., et al. (1998). A double-blind placebo-controlled study of nitazoxanide in the treatment of cryptosporidial diarrhoea in AIDS patients in Mexico. *Trans. R. Soc. Trop. Med. Hyg.* 92, 663–666. doi: 10.1016/S0035-9203(98)90804-5
- Rossignol, J. F., Lopez-Chegne, N., Julcamoro, L. M., Carrion, M. E., and Bardin, M. C. (2012). Nitazoxanide for the empiric treatment of pediatric infectious diarrhea. *Trans. R. Soc. Trop. Med. Hyg.* 106, 167–173. doi: 10.1016/j.trstmh.2011.11.007
- Roxstrom-Lindquist, K., Palm, D., Reiner, D., Ringqvist, E., and Svart, S. G. (2006). Giardia immunity—an update. *Trends Parasitol.* 22, 26–31. doi: 10.1016/j.pt.2005.11.005
- Ryan, U., and Hijjawi, N. (2015). New developments in *Cryptosporidium* research. *Int. J. Parasitol.* 45, 367–373. doi: 10.1016/j.ijpara.2015.01.009
- Sharp, T. W., Thornton, S. A., Wallace, M. R., Defraites, R. F., Sanchez, J. L., Batchelor, R. A., et al. (1995). Diarrheal disease among military personnel during Operation Restore Hope, Somalia, 1992–1993. *Am. J. Trop. Med. Hyg.* 52, 188–193.
- Singer, S. M., and Nash, T. E. (2000a). T-cell-dependent control of acute *Giardia lamblia* infections in mice. *Infect. Immun.* 68, 170–175. doi: 10.1128/IAI.68.1.170-175.2000
- Singer, S. M., and Nash, T. E. (2000b). The role of normal flora in *Giardia lamblia* infections in mice. *J. Infect. Dis.* 181, 1510–1512. doi: 10.1086/315409
- Smith, H. V., Nichols, R. A., and Grimason, A. M. (2005). *Cryptosporidium* excystation and invasion: getting to the guts of the matter. *Trends Parasitol.* 21, 133–142. doi: 10.1016/j.pt.2005.01.007
- Soleymani-Mohammadi, S., Genkinger, J. M., Loffredo, C. A., and Singer, S. M. (2010). A meta-analysis of the effectiveness of albendazole

- compared with metronidazole as treatments for infections with *Giardia duodenalis*. *PLoS Negl. Trop. Dis.* 4:e682. doi: 10.1371/journal.pntd.000622
- Solaymani-Mohammadi, S., and Singer, S. M. (2010). *Giardia duodenalis*: the double-edged sword of immune responses in giardiasis. *Exp. Parasitol.* 126, 292–297. doi: 10.1016/j.exppara.2010.06.014
- Solaymani-Mohammadi, S., and Singer, S. M. (2011). Host immunity and pathogen strain contribute to intestinal disaccharidase impairment following gut infection. *J. Immunol.* 187, 3769–3775. doi: 10.4049/jimmunol.1100606
- Speelman, P. (1985). Single-dose tinidazole for the treatment of giardiasis. *Antimicrob. Agents Chemother.* 27, 227–229. doi: 10.1128/AAC.27.2.227
- Striepen, B. (2013). Parasitic infections: time to tackle cryptosporidiosis. *Nature* 503, 189–191. doi: 10.1038/503189a
- Striepen, B., Pruijssers, A. J., Huang, J., Li, C., Gubbels, M. J., Umezige, N. N., et al. (2004). Gene transfer in the evolution of parasite nucleotide biosynthesis. *Proc. Natl. Acad. Sci. U.S.A.* 101, 3154–3159. doi: 10.1073/pnas.0304686101
- Sun, Z., Khan, J., Makowska-Grzyska, M., Zhang, M., Cho, J. H., Suebsuwong, C., et al. (2014). Synthesis, in vitro evaluation and cocrystal structure of 4-oxo-[1]benzopyran[4,3-c]pyrazole *Cryptosporidium parvum* inosine 5'-monophosphate dehydrogenase (CpIMPDH) inhibitors. *J. Med. Chem.* 57, 10544–10550. doi: 10.1021/jm501527z
- Tako, E. A., Hassimi, M. F., Li, E., and Singer, S. M. (2013). Transcriptomic analysis of the host response to *Giardia duodenalis* infection reveals redundant mechanisms for parasite control. *MBio* 4:e00660. doi: 10.1128/mBio.00660-13
- Tejman-Yarden, N., Millman, M., Lauwaeet, T., Davids, B. J., Gillin, F. D., Dunn, L., et al. (2011). Impaired parasite attachment as fitness cost of metronidazole resistance in *Giardia lamblia*. *Antimicrob. Agents Chemother.* 55, 4643–4651. doi: 10.1128/AAC.00384-11
- Tejman-Yarden, N., Miyamoto, Y., Leitsch, D., Santini, J., Debnath, A., Gut, J., et al. (2013). A reproposed drug, auranofin, is effective against metronidazole-resistant *Giardia lamblia*. *Antimicrob. Agents Chemother.* 57, 2029–2035. doi: 10.1128/AAC.01675-12
- Theodos, C. M., Sullivan, K. L., Griffiths, J. K., and Tzipori, S. (1997). Profiles of healing and nonhealing *Cryptosporidium parvum* infection in C57BL/6 mice with functional B and T lymphocytes: the extent of gamma interferon modulation determines the outcome of infection. *Infect. Immun.* 65, 4761–4769.
- Thomas Iv, L. J., Zweig, A. P., and Tosh, A. K. (2014). An adolescent with chronic giardiasis mimicking anorexia nervosa. *Int. J. Adolesc. Med. Health* 26, 293–295. doi: 10.1515/ijamh-2013-0506
- Tzipori, S., and Griffiths, J. K. (1998). Natural history and biology of *Cryptosporidium parvum*. *Adv. Parasitol.* 40, 5–36. doi: 10.1016/S0065-308X(08)60116-5
- Tzipori, S., McCartney, E., Lawson, G. H., Rowland, A. C., and Campbell, I. (1981). Experimental infection of piglets with *Cryptosporidium*. *Res. Vet. Sci.* 31, 358–368.
- Tzipori, S., Smith, M., Halpin, C., Angus, K. W., Sherwood, D., and Campbell, I. (1983). Experimental cryptosporidiosis in calves: clinical manifestations and pathological findings. *Vet. Rec.* 112, 116–120. doi: 10.1136/vr.112.6116
- Umezige, N. N., Gollapalli, D., Sharling, L., Voltsun, A., Lu, J., Benjamin, N. N., et al. (2008). Targeting a prokaryotic protein in a eukaryotic pathogen: identification of lead compounds against cryptosporidiosis. *Chem. Biol.* 15, 70–77. doi: 10.1016/j.chembiol.2007.12.010
- Umezige, N. N., Li, C., Riera, T., Hedstrom, L., and Striepen, B. (2004). *Cryptosporidium parvum* IMP dehydrogenase: identification of functional, structural, and dynamic properties that can be exploited for drug design. *J. Biol. Chem.* 279, 40320–40327. doi: 10.1074/jbc.M407121200
- Upcroft, J. A., Campbell, R. W., and Upcroft, P. (1996a). Quinacrine-resistant *Giardia duodenalis*. *Parasitology* 112(Pt 3), 309–313. doi: 10.1017/S0031182000065823
- Upcroft, J., Mitchell, R., Chen, N., and Upcroft, P. (1996b). Albendazole resistance in *Giardia* is correlated with cytoskeletal changes but not with a mutation at amino acid 200 in beta-tubulin. *Microb. Drug Resist.* 2, 303–308. doi: 10.1089/mdr.1996.2.303
- Upcroft, J. A., Dunn, L. A., Wright, J. M., Benakli, K., Upcroft, P., and Vanelle, P. (2006). 5-Nitroimidazole drugs effective against metronidazole-resistant *Trichomonas vaginalis* and *Giardia duodenalis*. *Antimicrob. Agents Chemother.* 50, 344–347. doi: 10.1128/AAC.50.1.344-347.2006
- Upcroft, P., and Upcroft, J. A. (2001). Drug targets and mechanisms of resistance in the anaerobic protozoa. *Clin. Microbiol. Rev.* 14, 150–164. doi: 10.1128/CMR.14.1.150-164.2001
- Upton, S. J., Tilley, M., and Brillhart, D. B. (1994). Comparative development of *Cryptosporidium parvum* (Apicomplexa) in 11 continuous host cell lines. *FEMS Microbiol. Lett.* 118, 233–236. doi: 10.1111/j.1574-6968.1994.tb06833.x
- Upton, S. J., Tilley, M., and Brillhart, D. B. (1995). Effects of select medium supplements on in vitro development of *Cryptosporidium parvum* in HCT-8 cells. *J. Clin. Microbiol.* 33, 371–375.
- Urban, J. F. Jr., Fayer, R., Chen, S. J., Gause, W. C., Gately, M. K., Finkelman, F. D., et al. (1996). IL-12 protects immunocompetent and immunodeficient neonatal mice against infection with *Cryptosporidium parvum*. *J. Immunol.* 156, 263–268.
- Valdez, C. A., Tripp, J. C., Miyamoto, Y., Kalisiak, J., Hruz, P., Andersen, Y. S., et al. (2009). Synthesis and electrochemistry of 2-ethenyl and 2-ethanyl derivatives of 5-nitroimidazole and antimicrobial activity against *Giardia lamblia*. *J. Med. Chem.* 52, 4038–4053. doi: 10.1021/jm900356n
- Vandenberg, O., Robberecht, F., Dauby, N., Moens, C., Talabani, H., Dupont, E., et al. (2012). Management of a *Cryptosporidium hominis* outbreak in a day-care center. *Pediatr. Infect. Dis. J.* 31, 10–15. doi: 10.1097/INF.0b013e318235ab64
- von Oettingen, J., Nath-Chowdhury, M., Ward, B. J., Rodloff, A. C., Arrowood, M. J., and Ndaio, M. (2008). High-yield amplification of *Cryptosporidium parvum* in interferon gamma receptor knockout mice. *Parasitology* 135, 1151–1156. doi: 10.1017/S0031182008004757
- Watt, P. M. (2009). Phenotypic screening of phylomer peptide libraries derived from genome fragments to identify and validate new targets and therapeutics. *Future Med. Chem.* 1, 257–265. doi: 10.4155/fmc.09.28
- Widerstrom, M., Schonning, C., Lilja, M., Lebbad, M., Ljung, T., Allestam, G., et al. (2014). Large outbreak of *Cryptosporidium hominis* infection transmitted through the public water supply, Sweden. *Emerg. Infect. Dis.* 20, 581–589. doi: 10.3201/eid2004.121415
- Woessner, D. J., and Dawson, S. C. (2012). The Giardia median body protein is a ventral disc protein that is critical for maintaining a domed disc conformation during attachment. *Eukaryot. Cell* 11, 292–301. doi: 10.1128/EC.05262-11
- Wright, J. M., Dunn, L. A., Upcroft, P., and Upcroft, J. A. (2003). Efficacy of anti-giardial drugs. *Expert Opin. Drug Saf.* 2, 529–541. doi: 10.1517/14740338.2.6.529
- Xu, P., Widmer, G., Wang, Y., Ozaki, L. S., Alves, J. M., Serrano, M. G., et al. (2004). The genome of *Cryptosporidium hominis*. *Nature* 431, 1107–1112. doi: 10.1038/nature02977
- Yuan, J., Cheng, K. C., Johnson, R. L., Huang, R., Pattaradilokrat, S., Liu, A., et al. (2011). Chemical genomic profiling for antimalarial therapies, response signatures, and molecular targets. *Science* 333, 724–729. doi: 10.1126/science.1205216
- Zhang, Y., Lee, B., Thompson, M., Glass, R., Cama, R. I., Figueroa, D., et al. (2000). Lactulose-mannitol intestinal permeability test in children with diarrhea caused by rotavirus and *Cryptosporidium*. Diarrhea Working Group, Peru. *J. Pediatr. Gastroenterol. Nutr.* 31, 16–21. doi: 10.1097/00005176-200007000-00006
- Zhou, P., Li, E., Zhu, N., Robertson, J., Nash, T., and Singer, S. M. (2003). Role of interleukin-6 in the control of acute and chronic *Giardia lamblia* infections in mice. *Infect. Immun.* 71, 1566–1568. doi: 10.1128/IAI.71.3.1566-1568.2003

Conflict of Interest Statement: The authors declare that the research was conducted in the absence of any commercial or financial relationships that could be construed as a potential conflict of interest.

Copyright © 2015 Miyamoto and Eckmann. This is an open-access article distributed under the terms of the Creative Commons Attribution License (CC BY). The use, distribution or reproduction in other forums is permitted, provided the original author(s) or licensor are credited and that the original publication in this journal is cited, in accordance with accepted academic practice. No use, distribution or reproduction is permitted which does not comply with these terms.



New drug target in protozoan parasites: the role of thioredoxin reductase

Rosa M. Andrade^{1*†} and Sharon L. Reed^{2*†}

¹ Division of Infectious Diseases, Department of Medicine, University of California San Diego, La Jolla, CA, USA, ² Division of Infectious Diseases, Department of Pathology, School of Medicine, University of California San Diego, La Jolla, CA, USA

OPEN ACCESS

Edited by:

Yoji Morita,

Aichi Gakuin University, Japan

Reviewed by:

Sergio Adrian Guerrero,
CONICET-Universidad Nacional del
Litoral, Argentina
Diego Gustavo Arias,
CONICET-Universidad Nacional del
Litoral, Argentina
Michael Duchene,
Medical University of Vienna, Austria

*Correspondence:

Rosa M. Andrade and
Sharon L. Reed,

Division of Infectious Diseases,
Department of Medicine, University of
California San Diego, 9500 Gilman
Drive, MC 0612, La Jolla, CA
92093-0612, USA
randrade@ucsd.edu;
sreed@ucsd.edu

[†]These authors have contributed
equally to this work.

Specialty section:

This article was submitted to
Antimicrobials, Resistance and
Chemotherapy, a section of the journal
Frontiers in Microbiology

Received: 01 June 2015

Accepted: 02 September 2015

Published: 30 September 2015

Citation:

Andrade RM and Reed SL (2015)
New drug target in protozoan
parasites: the role of thioredoxin
reductase. *Front. Microbiol.* 6:975.
doi: 10.3389/fmicb.2015.00975

Amebiasis causes approximately 70,000 deaths annually and is the third cause of death due to parasites worldwide. It is treated primarily with metronidazole, which has adverse side effects, is mutagenic and carcinogenic, and emergence of resistance is an increasing concern. Unfortunately, better therapeutic alternatives are lacking. Re-purposing of older FDA approved drugs is advantageous to drug discovery since safety and pharmacokinetic effects in humans are already known. In high throughput screening studies, we recently demonstrated that auranofin, a gold containing compound originally approved to treat rheumatoid arthritis, has activity against trophozoites of *E. histolytica*, the causative agent of amebiasis. Auranofin's anti-parasitic activity is attributed to its monovalent gold molecule that readily inhibits *E. histolytica* thioredoxin reductase. This anti-oxidant enzyme is the only thiol-dependent flavo-reductase present in *E. histolytica*. Auranofin has also shown promising activity against other protozoans of significant public health importance. Altogether, this evidence suggests that auranofin has the potential to become a broad spectrum alternative therapeutic agent for diseases with a large global burden.

Keywords: amebiasis, thioredoxin reductase, auranofin, *Entamoeba histolytica*, protozoan, diarrhea

Introduction

The three major causes of protozoal diarrhea worldwide are *E. histolytica*, *G. lamblia*, and *Cryptosporidium* sp., which cause significant morbidity and mortality in developing and developed countries (Fletcher et al., 2012). In fact, it is estimated that *E. histolytica* infects approximately 500 million people worldwide, resulting in 50 million cases of invasive disease and about 70,000 deaths annually (Debnath et al., 2012). Meanwhile, *G. lamblia* infection prevalence is estimated at 280 million cases annually¹ while *Cryptosporidium* sp. accounts for about 20% and up to 9% of diarrheal episodes in children from developing (Simango and Mutikani, 2004; Cama et al., 2008) and developed² countries respectively. Although *Cryptosporidium* sp. infection can be self-limited in immunocompetent people, but it is chronic and debilitating in immunosuppressed and malnourished individuals (Cabada and White, 2010). Because of their link with poverty and association with poor cognitive function in early childhood (Berkman et al., 2002), *Giardia* and *Cryptosporidium* were included in the WHO Neglected Diseases Initiative in 2004

¹<http://www.cdc.gov/parasites/giardia/epi.html>. July 13, 2012

²<http://www.cdc.gov/mmwr/preview/mmwrhtml/ss6105a1.htm>

(Savioli et al., 2006). Also, the National Institutes of Health (NIH) has listed *G. lamblia*, *C. parvum*, and *E. histolytica* as category B priority biodefense pathogens because of their low infectious dose and potential for dissemination through compromised food and water supplies in the United States³.

Despite their global burden in public health, there are no vaccines or prophylactic medications to prevent amebiasis, giardiasis or cryptosporidiosis. Furthermore, first-line treatment for invasive amebiasis and giardiasis is metronidazole since 1966 (Powell et al., 1967) and 1963 (Lionetto et al., 1963) respectively. Metronidazole has been shown to be both mutagenic in a microbiological system and carcinogenic to rodents and frequently causes gastrointestinal side effects. *In vitro*, *E. histolytica* trophozoites can adapt to therapeutically relevant levels of metronidazole (Wassmann et al., 1999). Treatment failures in giardiasis occur in up to 20% of cases (Upcroft and Upcroft, 2001). Clinical resistance of *G. lamblia* to metronidazole has been documented along with cross resistance to the newer drugs, tinidazole and nitazoxanide, making drug resistance an increasing concern (Tejman-Yarden et al., 2013). Nitazoxanide, the only FDA-approved drug for the treatment of cryptosporidiosis, is effective in the treatment of immunocompetent patients but only partially effective for immunosuppressed patients. Therefore, it is critical to develop more effective drugs to treat amebiasis, giardiasis and cryptosporidiosis.

Reprofiling of FDA approved drugs is an advantageous approach to drug discovery since safety and pharmacokinetic effects in humans have already been confirmed clinically. These efforts led to the discovery that auranofin, a gold containing compound that is FDA approved for the treatment of rheumatoid arthritis, has anti-parasitic activity (Angelucci et al., 2009). Its anti-parasitic activity, likely stems from the gold molecule that readily dissociates and inhibits thiol-dependent flavoreductases (Saccoccia et al., 2012) such as thioredoxin-thioredoxin reductase and glutathione-glutathione reductase. These latter enzymes are the two main detoxifying systems that are independent of reactive oxygen species (ROS). These antioxidant systems are present in all protozoan parasites which are constantly exposed to ROS from their own metabolism and those from the host (Hirt et al., 2002).

Thioredoxin Reductase and its Diversity among Protozoan Parasites

Like all eukaryotes, protozoan parasites' defense mechanisms include anti-oxidant systems to handle ROS challenges. Among these anti-oxidant systems, free radicals and radical-free systems are pivotal to maintain the oxidation/reduction homeostasis and prevent oxidative stress.

Radical-free systems, that include thiol-oxidoreductases, are essential and abundant enzymatic systems that account for 0.5–1% of the cell proteome (Fomenko and Gladyshev, 2012). Many of these thiol-oxidoreductases form protein complexes where each thiol oxidoreductase frequently contains cysteine (Cys) as their conserved catalytic residue (Fomenko and Gladyshev, 2012). Thioredoxin-thioredoxin reductase (Trx/TrxR) and

glutathione-glutathione reductase (GSH/GR) are the two main detoxifying systems independent of ROS.

The Trx/TrxR system has drawn significant attention due to its broad substrate specificity, allowing it to play important roles in regulating DNA synthesis, gene transcription, cell growth and apoptosis (Nozaki et al., 1999; Becker et al., 2000). Thioredoxin reductases (TrxRs) are enzymes that belong to the flavoprotein family of pyridine nucleotide-disulphide oxidoreductases (Mustacich and Powis, 2000). These enzymes are homodimeric proteins where each monomer contains a FAD domain, a NADPH binding domain, and an active site containing a redox active disulfide (Mustacich and Powis, 2000). Cysteine is present in the catalytic redox active center, which is highly conserved in thiol-reductases. The majority of thiol-oxidoreductases have a single catalytic Cys, but some of these enzymes are composed of two or more thiol-oxidoreductase domains, each having the catalytic redox Cys (Fomenko and Gladyshev, 2012).

Two main types of TrxRs (McMillan et al., 2009) are recognized:

- High molecular weight (H-TrxR) enzymes that contain a redox active center (motif CXXXXC) in the FAD binding domain. H-TrxR is closely related to glutathione reductase (GR), trypanothione reductase (TryR), mercuric reductase (MerR) and lipoamide dehydrogenase (LipD) (Nozaki et al., 1999). There are two varieties of H-TrxR: (a) one that contains a selenocysteine at the penultimate position in the C-terminal interface domain: the mammalian form; (b) one where selenocysteine have been replaced by cysteine in the interface domain: the apicomplexan parasite form.
- Low molecular weight (L-TrxR) enzymes that contain a redox active disulfide (motif CXXC) in the NADPH domain. L-TrxRs are related to alkyl hydroperoxide reductase F52A (AhpF). It is present in bacteria, fungi, plants and some protozoan parasites including *Trichomonas vaginalis* (Nozaki et al., 1999; Williams et al., 2000; Coombs et al., 2004) and *Entamoeba histolytica* (Arias et al., 2007).

Despite only 20% primary sequence identity between H-TrxR and L-TrxR (Nozaki et al., 1999), they appear to have evolved from a common ancestor but developed independently. L-TrxR and H-TrxR are mutually exclusive, suggesting that they do not act synergistically (Nozaki et al., 1999).

Electrons are transferred from NADPH via FAD to the active-site disulphide of TrxR, which then reduces the substrate (thioredoxin). H-TrxR has 3 redox active centers, whereas the L-TrxR have 2 redox centers and the transfer of reducing equivalents requires a conformational change, in contrast to H-TrxR (Williams et al., 2000).

Trx/TrxR systems vary according to parasites subgroups. Among aerotolerant protozoans, the absence of GSH/GR makes Trx/TrxR a main member of their antioxidant systems. In fact, *E. histolytica*, *T. vaginalis* and *G. lamblia* possess a full thioredoxin system, consisting of thioredoxin (Trx), Trx peroxidase and a L-TrxR (Hughes et al., 2003; Coombs et al., 2004; Arias et al., 2007; Leitsch et al., 2009). In the Apicomplexan group, *Plasmodium* possesses both GSH/GR and Trx/TrxR redox systems. Its

³<http://www.niaid.nih.gov/topics/BiodefenseRelated/Biodefense/Pages/CatA.aspx>

complete thioredoxin system comprises thioredoxin reductase (TrxR), different thioredoxins, thioredoxin-like proteins, and thioredoxin-dependent peroxidases (TPx) (Kawazu et al., 2001; Nickel et al., 2006; Kehr et al., 2010).

Genome sequencing of *T. brucei* (Berriman et al., 2005), *T. cruzi* (El-Sayed et al., 2005), and *L. major* (Ivens et al., 2005) revealed that trypanosomatids lack genes for GSH/GR and Trx/TrxR. While in most eukaryotic organisms these latter systems maintain the intracellular thiol redox homeostasis, trypanosomatids depend exclusively on trypanothione [N1,N8-bis(glutathionyl)spermidine; T(SH)2] (Fairlamb et al., 1985; Fairlamb and Cerami, 1992) and trypanothione reductase (TryR) to keep dithiols in a reduced form (Fairlamb and Cerami, 1992; Krauth-Siegel and Comini, 2008). TryR is the only enzyme that connects the NADPH- and the thiol-based redox systems in these parasites, and it is related to H-TrxR. As such, it shares many physical and chemical properties with GR. TryR has been biochemically characterized in *T. cruzi* (Krauth-Siegel et al., 1987), *Leishmania* (Cunningham and Fairlamb, 1995), and *T. brucei* (Sullivan et al., 1989; Jones et al., 2010).

***Entamoeba histolytica* Thioredoxin Reductase**

E. histolytica trophozoites are considered aerotolerant organisms. They can survive in an anaerobic environment such as that of the human gut. During tissue invasion, they are exposed to high levels of ROS. Earlier studies showed that it can tolerate up to 5% oxygen in the gas phase (Bruchhaus et al., 1997; Choi et al., 2005; Loftus et al., 2005). Hence, the parasite must have means to minimize damage caused by ROS produced by the host immune system. In contrast to most organisms, *E. histolytica* lacks both glutathione reductase activity and glutathione synthetic enzymes; therefore, it relies on TrxR to prevent, regulate and repair the damage caused by oxidative stress.

The *E. histolytica* genome has a single TrxR-encoding gene (EHI_155440) (EhTrxR). EhTrxR belongs to the low molecular weight TrxR family (L-TrxR). It is 964 bp in length, lacks introns and encodes a 314-amino-acid protein with a molecular mass of 33.7 kDa and a pI of 6.34. EhTrxR size and domain topology resembles *E. coli* TrxR. Both proteins have an active site dithiol/disulfide center (Cys-Ala-Thr-Cys for EcTrxR, Cys-Ala-Ile-Cys for EhTrxR). In EhTrxR, the Cys residues in the catalytic center correspond to Cys 140 and Cys 143. Sequence homology to other TrxRs is 21% identity to *E. coli* TrxR (L-TrxR), *Trichomonas vaginalis* (23%), *Trypanosoma cruzi* (27%), and *Homo sapiens* (36%) (Arias et al., 2007).

The catalytic mechanism of L-TrxR has been extensively characterized in *E. coli*. Spatially, the NADPH and FAD domains of *E. coli* ThrxR do not make close contact with the isoalloxazine ring of FAD. Its NADPH domain rotates 66° while the FAD domain remains fixed. Then, the bound NADPH moves into close contact with the FAD isoalloxazine ring that allows electron transfer to FAD and the active-site disulphide (Waksman et al., 1994).

EhTrxR demonstrates an unusually high level of NADPH oxidase activity, which is protective against molecular oxygen required for the survival of these aerotolerant, anaerobic organisms (Bruchhaus et al., 1998). EhTrxR exhibited NADPH

oxidase activity with hyperbolic saturation kinetics for NADPH, and its estimated Km and Vmax values are 3.6 μM and 0.37 U/mg respectively (Arias et al., 2007). As described by Arias et al. (2007) EhTrxR is considered a true reductase of thioredoxin in that it is not able to transfer reducing equivalents directly to Ehp29 (peroxiredoxin). On the other hand, high intracellular levels of cysteine compensate for the lack of glutathione preventing auto-oxidation in highly reducing environments (Nozaki et al., 1999). Interestingly, despite the fact that neither thioredoxin nor thioredoxin reductase configurations include a transmembrane hydrophobic domain, *E. histolytica* thioredoxin-thioredoxin reductase system was primarily located in the plasma membrane (Arias et al., 2008) without evidence of intracytoplasmic presence.

Besides ROS, *E. histolytica* is exposed to high concentrations of reactive nitrogen species (RNS) such as nitric oxide (NO) or S-nitrosothiols (such as GSNO and CySNO) during tissue invasion. Although high levels of these RNS might inhibit *E. histolytica* growth *in vitro* (Arias et al., 2012), the parasite is able to survive and multiply during tissue invasion. This suggests that *E. histolytica* detoxification system is versatile enough to tolerate hostile environments. This versatility was recently demonstrated by *E. histolytica* Trx-TrxR system ability to reduce RNS and use an alternative electron donor such as NADH (Arias et al., 2012).

As *E. histolytica* lacks glutathione, Cys is its major intracellular low molecular mass thiol (Nozaki et al., 1999) that can also react with NO to generate CySNO. This metabolite is considered critical for S-nitrosylation (addition of NO to the thiol group in Cys) or S-thiolation (addition of Cys to another Cys thiol group) of cellular proteins (Arias et al., 2012). These metabolites can be reduced by EhTrxR as was demonstrated by *in vitro* assays where NADPH and EhTrxR were exposed to different concentrations of CySNO and GSNO. The rates of NADPH oxidation were increased proportionally, suggesting that these compounds (CySNO or GSNO) can be reduced in a reaction catalyzed by EhTrxR. The EhTrxR/Trx system reduces S-nitrosothiols (Arias et al., 2012) compounds and metronidazole (Leitsch et al., 2007) as well as interacts with downstream peroxidases that are critical for cellular redox homeostasis (Schlosser et al., 2013).

Unlike other thioredoxin reductases, EhTrxR does not exhibit high specificity for NADPH. Arias et al. (2012) evaluated the reduction of DTNB by EhTrxR using NADPH or NADH as electron donors. Although EhTrxR affinity for NADH is 10 times lower than that for NADPH, the enzyme activity with NADH is not negligible when compared to other thioredoxin reductases that exhibit high specificity toward NADPH (Arias et al., 2012). These results suggest that EhTrxR can use either NADPH or NADH as its reduced co-factor. This evidence strongly shows the versatility of EhTrx and its ability to protect the parasite from the ROS and RNI byproducts during host invasion. Altogether, EhTrxR properties make it an ideal drug target. In fact, metronidazole decreases EhTrxR reductase activity, by forming covalent adducts with this enzyme.

***Giardia lamblia* Thioredoxin Reductase**

Giardia lamblia (synonyms: *G. intestinalis* or *G. duodenalis*) is a flagellate whose trophozoites live in the small intestine, while the infectious cysts are shed in feces and survive outside the

host. Giardia cysts can infect or re-infect humans, and can be transmitted in food, water or fomites since they are resistant to environmental conditions and chemicals. Giardia is considered an aerotolerant organism as even its cyst is able to take up oxygen, although only at 10–20% of the level of trophozoites (Paget et al., 1993).

G. lamblia has a genome size of approximately 10–12 Mb divided among five chromosomes (Adam, 2001). Giardia isolates are divided into eight assemblages (genotypes) from A to H. Assemblages A and B are the only ones typically associated with human infections (Adam, 2001). Both human Giardia assemblages A and B possess a single TrxR-encoding gene (GL 50803_9827 and GL50581_832). This single gene is 945 bp in length, lacks introns and encodes a 314 amino acid protein (GLTrxR) with a molecular mass of approximately 33.8 kDa and a pI of 6.59.

Like most aerotolerant protozoans, *G. lamblia* lacks mitochondria, superoxide dismutase, catalase, glutathione-glutathione reductase system but possesses a thioredoxin-thioredoxin reductase system while cysteine is its major low molecular weight thiol (Brown et al., 1998). Given the lack of ROS-dependent anti-oxidant systems and glutathione, the thioredoxin-thioredoxin reductase system is thought to constitute a major part of the antioxidant defense in this organism. It consists of a soluble dimeric FAD containing NADPH-dependent disulfide reductase, which contains a two 35-kDa subunits and a partially purified 12-kDa protein; a putative thioredoxin, a low molecular weight thioredoxin reductase (TrxR), which has 75% identity to the *E. coli* thioredoxin reductase (Brown et al., 1998), and a thioredoxin-peroxidase. All genes are expressed in trophozoites and cysts, although transcripts of most genes are present at lower levels in cysts (Faghiri and Widmer, 2011). Since Giardia cysts can take up oxygen (Paget et al., 1993), the Giardia thioredoxin-thioredoxin reductase system must also be important to maintain oxidation/reduction homeostasis in its trophozoites and cyst forms, making it an attractive drug target. This target is even more important given that metronidazole, a drug used in the treatment of giardiasis, had no detectable effect on oxygen uptake or viability in cysts due to impermeability of the *Giardia* cysts to metronidazole (Paget et al., 1993).

Thioredoxin Reductase-gold Interactions: An Unexploited Drug Target

Despite the huge public health burden of parasites worldwide, the paucity of available anti-parasitic drugs is striking. Reprofiling of old FDA approved drugs has become an alternative expeditious approach to drug discovery. Its advantage relies on already known drug safety and pharmacokinetic effects in humans that make them readily available for off-label indications.

Auranofin, originally approved to treat rheumatoid arthritis, is now the leading compound for anti-parasitic treatment development. Indeed, we have recently demonstrated that auranofin has activity against trophozoites of *Entamoeba histolytica* (Debnath et al., 2012) and *Giardia lamblia* (Tejman-Yarden et al., 2013). Due to its activity shown in high throughput screening studies, *in vitro* and *in vivo* rodent models of

colitis and liver abscesses, auranofin was granted Orphan Drug Status. Auranofin has also shown promising activity against metronidazole-resistant *Giardia lamblia* (Tejman-Yarden et al., 2013), *Plasmodium falciparum* (Sannella et al., 2008), *Schistosoma mansoni* (Angelucci et al., 2009), *Leishmania infantum* (Ilari et al., 2012), *Brugia malayi* and *Onchocerca* (Bulman et al., 2015). Thus, auranofin has the potential to become an alternative broad spectrum anti-parasitic agent.

Auranofin as an Anti-parasitic Agent

Auranofin was the first oral gold salt approved by the FDA to treat rheumatoid arthritis over 25 years ago. Its pharmacokinetic characteristics are distinct from those of gold sodium thiomalate, a chrysotherapy agent of systemic administration. (Blodgett, 1983; Blodgett et al., 1984). Despite its clinical use, auranofin's mechanism of action is poorly understood.

Kuntz et al. (2007) were the first ones to describe the effect of auranofin in *S. mansoni*. In *in vitro* assays, they demonstrated

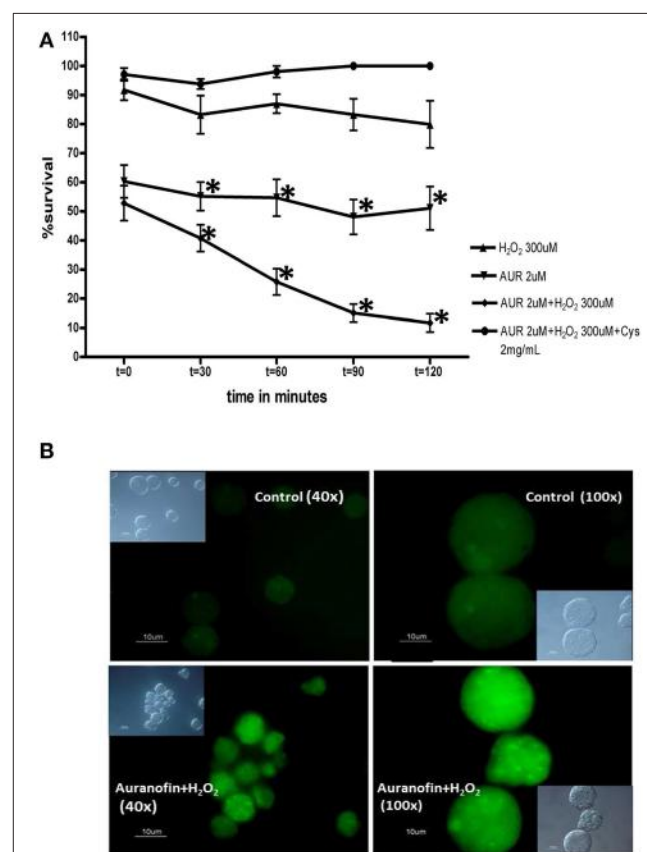
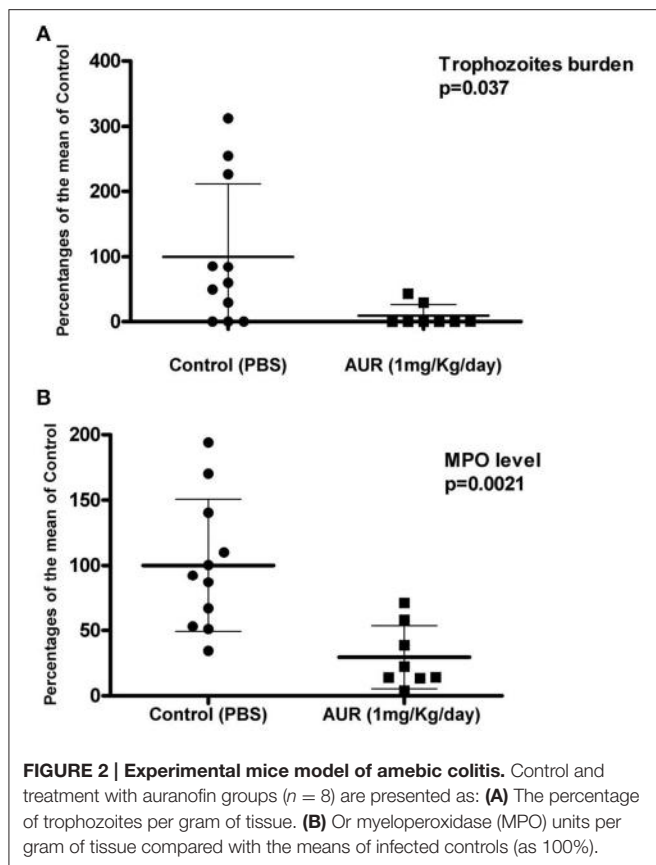


FIGURE 1 | (A) *In vitro* susceptibility of trophozoites (control and treated with auranofin) to reactive oxygen species (H_2O_2) and the effect of added cysteine. Time points with mean \pm SEM % survival. Experiments are shown in triplicates. * $p < 0.002$ by Student's *t*-test. **(B)** Immunofluorescence microscopy: Detection of reactive oxygen species within *E. histolytica* trophozoites following treatment with auranofin or auranofin plus H_2O_2 . Control trophozoites were treated with ethanol alone (auranofin carrier). Insets are differential interference contrast images. Scale bars, 10 μm . Figures were first published in Andrade and Reed (2015).



that auranofin rapidly killed juvenile and adult forms of *S. mansoni* (Kuntz et al., 2007). Their preliminary *in vivo* data correlated with their *in vitro* findings: mice infected with *S. mansoni* and treated with auranofin showed a 59 and 63% decrease in worm burden compared to control mice.

Additionally, auranofin strongly inhibits the growth of malarial parasite *Plasmodium falciparum* (Sannella et al., 2008), the pro-mastigote stage of *Leishmania infantum* (Ilari et al., 2012), the bloodstream and procyclic stages of *Trypanosoma brucei* (Lobanov et al., 2006) and the larval worms of *Echinococcus granulosus* (Bonilla et al., 2008). In all these studies, auranofin's anti-parasitic dose was in the nanomolar range, which is achievable in patients with rheumatoid arthritis (approximately 5 μ M serum blood levels) (Debnath et al., 2012).

Angelucci et al. further analyzed *S. mansoni* thioredoxin-glutathione reductase (TGR) crystal structure in the presence of auranofin (Angelucci et al., 2009). The structure revealed gold (I) rather than auranofin as an adduct between pairs of cysteines (Cys-Au-Cys) in two different sites and also bound to the proposed NADPH binding site of the reductase in a third location.

Similarly, the crystal structure of reduced *Leishmania infantum* trypanothione reductase complexed with NADPH and

auranofin also demonstrated that gold binds two active cysteine residues of trypanothione reductase (TryR) (Ilari et al., 2012), i.e., Cys52 and Cys57, while the thiol sugar moiety of auranofin binds to the trypanothione binding site; thus auranofin appears to inhibit TryR through a dual mechanism.

We recently demonstrated that auranofin has activity against *E. histolytica* trophozoites (Debnath et al., 2012). Our studies support the hypothesis that EhTrxR likely is the target for auranofin. Our qualitative *in vitro* assays showed that *E. histolytica* trophozoites treated with auranofin were more susceptible to oxidative stress in a time dependent manner (Figure 1A). Staining *E. histolytica* trophozoites with dichloro-dihydrofluorescein, which fluoresces green upon contact with ROS, showed that trophozoites treated with auranofin accumulated more ROS (Debnath et al., 2012) (Figure 1B). This effect was inhibited by cysteine, the major reductant in *E. histolytica*, which protected trophozoites that were treated with auranofin (Figure 1). Our *in vitro* findings were corroborated in animal models of colitis and liver abscesses where auranofin not only decreased the parasite tissue burden, but also the local inflammatory response as measured by activity of myeloperoxidase in cecal tissue (Debnath et al., 2012) (Figures 2A,B respectively). Besides its activity against trophozoites, auranofin seems to have activity against cysts of *E. invadens*, the only ameba to readily encyst *in vitro* (R. Andrade, manuscript in preparation).

G. lamblia assemblages A and B were also susceptible to auranofin, as demonstrated by Tejman-Yarden et al. (2013). Auranofin displayed a half-maximal effective concentrations (EC50s) of 4–6 μ M at 48-h. Most importantly, auranofin was able to overcome resistance to metronidazole. In fact, the EC50 for auranofin was not significantly different between metronidazole-sensitive parental *Giardia* isolates and several of their metronidazole-resistant isogenic derivative lines.

Similarly, to *E. histolytica* and *G. lamblia*, auranofin was found effective against *C. parvum* *in vitro* with EC50 about 2 μ M, which was comparable to nitazoxanide, the current drug of choice (Debnath et al., 2013).

Altogether, these findings suggest that auranofin may be a new promising broad spectrum antiparasitic agent with activity against ameba, giardia and cryptosporidium. Currently, clinical trials using auranofin to treat ameba and giardia infections are about to begin.

Funding

This publication was supported in part by a Harold Amos Minority Medical Faculty Development Program (RMA), UCSD Academic Senate Grant 70642 (RMA), NIH 2T32AI007036-31A1 (RMA), NIH grant 5U01AI077822-04, and U01 AI110435 (SLR). The funders had no role in study design, data collection and analysis, decision to publish, or preparation of the manuscript.

References

- Adam, R. D. (2001). Biology of *Giardia lamblia*. *Clin. Microbiol. Rev.* 14, 447–475. doi: 10.1128/CMR.14.3.447-475.2001
- Andrade, R. M., and Reed, S. L. (2015). “Thioredoxin reductase and its role as a new drug target,” in *Amebiasis: Biology and Pathogenesis of Entamoeba*, eds T. Nozaki and A. Bhattacharya (Tokyo: Springer), 543–552.
- Angelucci, F., Sayed, A. A., Williams, D. L., Boumis, G., Brunori, M., Dimastrogiovanni, D., et al. (2009). Inhibition of *Schistosoma mansoni* thioredoxin-glutathione reductase by auranofin: structural and kinetic aspects. *J. Biol. Chem.* 284, 28977–28985. doi: 10.1074/jbc.M109.020701
- Arias, D. G., Carranza, P. G., Lujan, H. D., Iglesias, A. A., and Guerrero, S. A. (2008). Immunolocalization and enzymatic functional characterization of the thioredoxin system in *Entamoeba histolytica*. *Free Radic. Biol. Med.* 45, 32–39. doi: 10.1016/j.freeradbiomed.2008.03.008
- Arias, D. G., Gutierrez, C. E., Iglesias, A. A., and Guerrero, S. A. (2007). Thioredoxin-linked metabolism in *Entamoeba histolytica*. *Free Radic. Biol. Med.* 42, 1496–1505. doi: 10.1016/j.freeradbiomed.2007.02.012
- Arias, D. G., Regner, E. L., Iglesias, A. A., and Guerrero, S. A. (2012). *Entamoeba histolytica* thioredoxin reductase: molecular and functional characterization of its atypical properties. *Biochim. Biophys. Acta* 1820, 1859–1866. doi: 10.1016/j.bbagen.2012.08.020
- Becker, K., Gromer, S., Schirmer, R. H., and Müller, S. (2000). Thioredoxin reductase as a pathophysiological factor and drug target. *Eur. J. Biochem.* 267, 6118–6125. doi: 10.1046/j.1432-1327.2000.01703.x
- Berkman, D. S., Lescano, A. G., Gilman, R. H., Lopez, S. L., and Black, M. M. (2002). Effects of stunting, diarrhoeal disease, and parasitic infection during infancy on cognition in late childhood: a follow-up study. *Lancet* 359, 564–571. doi: 10.1016/S0140-6736(02)07744-9
- Berriman, M., Ghedin, E., Hertz-Fowler, C., Blandin, G., Renauld, H., Bartholomew, D. C., et al. (2005). The genome of the African trypanosome *Trypanosoma brucei*. *Science* 309, 416–422. doi: 10.1126/science.1112642
- Blodgett, R. C. Jr. (1983). Auranofin: experience to date. *Am. J. Med.* 75, 86–89. doi: 10.1016/0002-9343(83)90480-1
- Blodgett, R. C. Jr., Heuer, M. A., and Pietrusko, R. G. (1984). Auranofin: a unique oral chrysotherapeutic agent. *Semin. Arthritis Rheum.* 13, 255–273. doi: 10.1016/0049-0172(84)90029-5
- Bonilla, M., Denicola, A., Novoselov, S. V., Turanov, A. A., Protasio, A., Izmendi, D., et al. (2008). Platyhelminth mitochondrial and cytosolic redox homeostasis is controlled by a single thioredoxin glutathione reductase and dependent on selenium and glutathione. *J. Biol. Chem.* 283, 17898–17907. doi: 10.1074/jbc.M710609200
- Brown, D. M., Upcroft, J. A., Edwards, M. R., and Upcroft, P. (1998). Anaerobic bacterial metabolism in the ancient eukaryote *Giardia duodenalis*. *Int. J. Parasitol.* 28, 149–164. doi: 10.1016/S0020-7519(97)00172-0
- Bruchhaus, I., Richter, S., and Tannich, E. (1997). Characterization of two *E. histolytica* proteins that inactivate reactive oxygen species. *Arch. Med. Res.* 28, Spec No:91-2.
- Bruchhaus, I., Richter, S., and Tannich, E. (1998). Recombinant expression and biochemical characterization of an NADPH:flavin oxidoreductase from *Entamoeba histolytica*. *Biochem. J.* 330(Pt 3), 1217–1221. doi: 10.1042/bj3301217
- Bulman, C. A., Bidlow, C. M., Lustigman, S., Cho-Ngwa, F., Williams, D., Rascón, A. A. Jr., et al. (2015). Repurposing auranofin as a lead candidate for treatment of lymphatic filariasis and onchocerciasis. *PLoS Negl. Trop. Dis.* 9:e0003534. doi: 10.1371/journal.pntd.0003534
- Cabada, M. M., and White, A. C. Jr. (2010). Treatment of cryptosporidiosis: do we know what we think we know? *Curr. Opin. Infect. Dis.* 23, 494–499. doi: 10.1097/QCO.0b013e32833de052
- Cama, V. A., Bern, C., Roberts, J., Cabrera, L., Sterling, C. R., Ortega, Y., et al. (2008). Cryptosporidium species and subtypes and clinical manifestations in children, Peru. *Emerg. Infect. Dis.* 14, 1567–1574. doi: 10.3201/eid1410.071273
- Choi, M. H., Sajed, D., Poole, L., Hirata, K., Herdman, S., Torian, B. E., et al. (2005). An unusual surface peroxiredoxin protects invasive *Entamoeba histolytica* from oxidant attack. *Mol. Biochem. Parasitol.* 143, 80–89. doi: 10.1016/j.molbiopara.2005.04.014
- Coombs, G. H., Westrop, G. D., Suchan, P., Puzova, G., Hirt, R. P., Embley, T. M., et al. (2004). The amitochondriate eukaryote *Trichomonas vaginalis* contains a divergent thioredoxin-linked peroxiredoxin antioxidant system. *J. Biol. Chem.* 279, 5249–5256. doi: 10.1074/jbc.M304359200
- Cunningham, M. L., and Fairlamb, A. H. (1995). Trypanothione reductase from *Leishmania donovani*. Purification, characterisation and inhibition by trivalent antimonials. *Eur. J. Biochem.* 230, 460–468. doi: 10.1111/j.1432-1033.1995.tb20583.x
- Debnath, A., Nda, M., and Reed, S. L. (2013). Reprofiling drug targets ancient protozoans: drug discovery for parasitic diarrheal diseases. *Gut Microbes* 4, 66–71. doi: 10.4161/gmic.22596
- Debnath, A., Parsonage, D., Andrade, R. M., He, C., Cobo, E. R., Hirata, K., et al. (2012). A high-throughput drug screen for *Entamoeba histolytica* identifies a new lead and target. *Nat. Med.* 18, 956–960. doi: 10.1038/nm.2758
- El-Sayed, N. M., Myler, P. J., Bartholomew, D. C., Nilsson, D., Aggarwal, G., Tran, A. N., et al. (2005). The genome sequence of *Trypanosoma cruzi*, etiologic agent of Chagas disease. *Science* 309, 409–415. doi: 10.1126/science.1112631
- Faghiri, Z., and Widmer, G. (2011). A comparison of the *Giardia lamblia* trophozoite and cyst transcriptome using microarrays. *BMC Microbiol.* 11:91. doi: 10.1186/1471-2180-11-91
- Fairlamb, A. H., Blackburn, P., Ulrich, P., Chait, B. T., and Cerami, A. (1985). Trypanothione: a novel bis(glutathionyl)spermidine cofactor for glutathione reductase in trypanosomatids. *Science* 227, 1485–1487. doi: 10.1126/science.3883489
- Fairlamb, A. H., and Cerami, A. (1992). Metabolism and functions of trypanothione in the Kinetoplastida. *Annu. Rev. Microbiol.* 46, 695–729. doi: 10.1146/annurev.mi.46.100192.003403
- Fletcher, S. M., Stark, D., Harkness, J., and Ellis, J. (2012). Enteric protozoa in the developed world: a public health perspective. *Clin. Microbiol. Rev.* 25, 420–449. doi: 10.1128/CMR.05038-11
- Fomenko, D. E., and Gladyshev, V. N. (2012). Comparative genomics of thiol oxidoreductases reveals widespread and essential functions of thiol-based redox control of cellular processes. *Antioxid. Redox Signal.* 16, 193–201. doi: 10.1089/ars.2011.3980
- Hirt, R. P., Müller, S., Embley, T. M., and Coombs, G. H. (2002). The diversity and evolution of thioredoxin reductase: new perspectives. *Trends Parasitol.* 18, 302–308. doi: 10.1016/S1471-4922(02)02293-6
- Hughes, M. A., Lee, C. W., Holm, C. F., Ghosh, S., Mills, A., Lockhart, L. A., et al. (2003). Identification of *Entamoeba histolytica* thiol-specific antioxidant as a GalNAC lectin-associated protein. *Mol. Biochem. Parasitol.* 127, 113–120. doi: 10.1016/S0166-6851(02)00326-2
- Ilari, A., Baiocco, P., Messori, L., Fiorillo, A., Boffi, A., Gramiccia, M., et al. (2012). A gold-containing drug against parasitic polyamine metabolism: the X-ray structure of trypanothione reductase from *Leishmania infantum* in complex with auranofin reveals a dual mechanism of enzyme inhibition. *Amino Acids* 42, 803–811. doi: 10.1007/s00726-011-0997-9
- Ivens, A. C., Peacock, C. S., Worthey, E. A., Murphy, L., Aggarwal, G., Berriman, M., et al. (2005). The genome of the kinetoplastid parasite, *Leishmania major*. *Science* 309, 436–442. doi: 10.1126/science.1112680
- Jones, D. C., Ariza, A., Chow, W. H., Oza, S. L., and Fairlamb, A. H. (2010). Comparative structural, kinetic and inhibitor studies of *Trypanosoma brucei* trypanothione reductase with *T. cruzi*. *Mol. Biochem. Parasitol.* 169, 12–19. doi: 10.1016/j.molbiopara.2009.09.002
- Kawazu, S., Komaki, K., Tsuji, N., Kawai, S., Ikenoue, N., Hatabu, T., et al. (2001). Molecular characterization of a 2-Cys peroxiredoxin from the human malaria parasite *Plasmodium falciparum*. *Mol. Biochem. Parasitol.* 116, 73–79. doi: 10.1016/S0166-6851(01)00308-5
- Kehr, S., Sturm, N., Rahlf, S., Przyborski, J. M., and Becker, K. (2010). Compartmentation of redox metabolism in malaria parasites. *PLoS Pathog.* 6:e1001242. doi: 10.1371/journal.ppat.1001242
- Krauth-Siegel, R. L., and Comini, M. A. (2008). Redox control in trypanosomatids, parasitic protozoa with trypanothione-based thiol metabolism. *Biochim. Biophys. Acta* 1780, 1236–1248. doi: 10.1016/j.bbagen.2008.03.006
- Krauth-Siegel, R. L., Enders, B., Henderson, G. B., Fairlamb, A. H., and Schirmer, R. H. (1987). Trypanothione reductase from *Trypanosoma cruzi*. Purification and characterization of the crystalline enzyme. *Eur. J. Biochem.* 164, 123–128. doi: 10.1111/j.1432-1033.1987.tb11002.x
- Kuntz, A. N., Davioud-Charvet, E., Sayed, A. A., Calif, L. L., Dessolin, J., Arnér, E. S., et al. (2007). Thioredoxin glutathione reductase from *Schistosoma mansoni*:

- an essential parasite enzyme and a key drug target. *PLoS Med.* 4:e206. doi: 10.1371/journal.pmed.0040206
- Leitsch, D., Kolarich, D., Binder, M., Stadlmann, J., Altmann, F., and Duchêne, M. (2009). *Trichomonas vaginalis*: metronidazole and other nitroimidazole drugs are reduced by the flavin enzyme thioredoxin reductase and disrupt the cellular redox system. Implications for nitroimidazole toxicity and resistance. *Mol. Microbiol.* 72, 518–536. doi: 10.1111/j.1365-2958.2009.06675.x
- Leitsch, D., Kolarich, D., Wilson, I. B., Altmann, F., and Duchêne, M. (2007). Nitroimidazole action in *Entamoeba histolytica*: a central role for thioredoxin reductase. *PLoS Biol.* 5:e211. doi: 10.1371/journal.pbio.0050211
- Lionetto, M. D., Manera, O. O., and Rocca, J. A. (1963). Treatment of *Giardia lamblia* Infection. *Dia Med.* 35, 1704–1705.
- lobanov, A. V., Gromer, S., Salinas, G., and Gladyshev, V. N. (2006). Selenium metabolism in Trypanosoma: characterization of selenoproteomes and identification of a Kinetoplastida-specific selenoprotein. *Nucleic Acids Res.* 34, 4012–4024. doi: 10.1093/nar/gkl541
- Loftus, B., Anderson, I., Davies, R., Alsmark, U. C., Samuelson, J., Amedeo, P., et al. (2005). The genome of the protist parasite *Entamoeba histolytica*. *Nature* 433, 865–868. doi: 10.1038/nature03291
- McMillan, P. J., Patzewitz, E. M., Young, S. E., Westrop, G. D., Coombs, G. H., Engman, L., et al. (2009). Differential inhibition of high and low Mr thioredoxin reductases of parasites by organotelluriums supports the concept that low Mr thioredoxin reductases are good drug targets. *Parasitology* 136, 27–33. doi: 10.1017/S0031182008005131
- Mustacich, D., and Powis, G. (2000). Thioredoxin reductase. *Biochem. J.* 346(Pt 1), 1–8. doi: 10.1042/bj3460001
- Nickel, C., Rahlf, S., Deponte, M., Koncarevic, S., and Becker, K. (2006). Thioredoxin networks in the malarial parasite *Plasmodium falciparum*. *Antioxid. Redox Signal.* 8, 1227–1239. doi: 10.1089/ars.2006.8.1227
- Nozaki, T., Asai, T., Sanchez, L. B., Kobayashi, S., Nakazawa, M., and Takeuchi, T. (1999). Characterization of the gene encoding serine acetyltransferase, a regulated enzyme of cysteine biosynthesis from the protist parasites *Entamoeba histolytica* and *Entamoeba dispar*. Regulation and possible function of the cysteine biosynthetic pathway in Entamoeba. *J. Biol. Chem.* 274, 32445–32452. doi: 10.1074/jbc.274.45.32445
- Paget, T. A., Manning, P., and Jarroll, E. L. (1993). Oxygen uptake in cysts and trophozoites of *Giardia lamblia*. *J. Eukaryot. Microbiol.* 40, 246–250. doi: 10.1111/j.1550-7408.1993.tb04911.x
- Powell, S. J., Wilmot, A. J., and Elsdon-Dew, R. (1967). Further trials of metronidazole in amoebic dysentery and amoebic liver abscess. *Ann. Trop. Med. Parasitol.* 61, 511–514.
- Saccoccia, F., Angelucci, F., Boumis, G., Brunori, M., Miele, A. E., Williams, D. L., et al. (2012). On the mechanism and rate of gold incorporation into thiol-dependent flavoreductases. *J. Inorg. Biochem.* 108, 105–111. doi: 10.1016/j.jinorgbio.2011.11.005
- Sannella, A. R., Casini, A., Gabbiani, C., Messori, L., Bilia, A. R., Vincieri, F. F., et al. (2008). New uses for old drugs. Auranofin, a clinically established antiarthritic metallodrug, exhibits potent antimalarial effects *in vitro*: mechanistic and pharmacological implications. *FEBS Lett.* 582, 844–847. doi: 10.1016/j.febslet.2008.02.028
- Savioli, L., Smith, H., and Thompson, A. (2006). Giardia and Cryptosporidium join the 'Neglected Diseases Initiative'. *Trends Parasitol.* 22, 203–208. doi: 10.1016/j.pt.2006.02.015
- Schlosser, S., Leitsch, D., and Duchêne, M. (2013). *Entamoeba histolytica*: identification of thioredoxin-targeted proteins and analysis of serine acetyltransferase-1 as a prototype example. *Biochem. J.* 451, 277–288. doi: 10.1042/BJ20121798
- Simango, C., and Mutikani, S. (2004). Cryptosporidiosis in Harare, Zimbabwe. *Cent. Afr. J. Med.* 50, 52–54.
- Sullivan, F. X., Shames, S. L., and Walsh, C. T. (1989). Expression of *Trypanosoma congoense* trypanothione reductase in *Escherichia coli*: overproduction, purification, and characterization. *Biochemistry* 28, 4986–4992. doi: 10.1021/bi00438a013
- Tejman-Yarden, N., Miyamoto, Y., Leitsch, D., Santini, J., Debnavi, A., Gut, J., et al. (2013). A reprofiled drug, auranofin, is effective against metronidazole-resistant *Giardia lamblia*. *Antimicrob. Agents Chemother.* 57, 2029–2035. doi: 10.1128/AAC.01675-12
- Upcroft, P., and Upcroft, J. A. (2001). Drug targets and mechanisms of resistance in the anaerobic protozoa. *Clin. Microbiol. Rev.* 14, 150–164. doi: 10.1128/CMR.14.1.150-164.2001
- Waksman, G., Krishna, T. S., Williams, C. H. Jr., and Kuriyan, J. (1994). Crystal structure of *Escherichia coli* thioredoxin reductase refined at 2 Å resolution. Implications for a large conformational change during catalysis. *J. Mol. Biol.* 236, 800–816. doi: 10.1006/jmbi.1994.1190
- Wassmann, C., Hellberg, A., Tannich, E., and Bruchhaus, I. (1999). Metronidazole resistance in the protozoan parasite *Entamoeba histolytica* is associated with increased expression of iron-containing superoxide dismutase and peroxiredoxin and decreased expression of ferredoxin 1 and flavin reductase. *J. Biol. Chem.* 274, 26051–26056. doi: 10.1074/jbc.274.37.26051
- Williams, C. H., Arscott, L. D., Müller, S., Lennon, B. W., Ludwig, M. L., Wang, P. F., et al. (2000). Thioredoxin reductase two modes of catalysis have evolved. *Eur. J. Biochem.* 267, 6110–6117. doi: 10.1046/j.1432-1327.2000.01702.x
- Conflict of Interest Statement:** The authors declare that the research was conducted in the absence of any commercial or financial relationships that could be construed as a potential conflict of interest.
- Copyright © 2015 Andrade and Reed. This is an open-access article distributed under the terms of the Creative Commons Attribution License (CC BY). The use, distribution or reproduction in other forums is permitted, provided the original author(s) or licensor are credited and that the original publication in this journal is cited, in accordance with accepted academic practice. No use, distribution or reproduction is permitted which does not comply with these terms.

Antigiardial activity of novel triazolyl-quinolone-based chalcone derivatives: when oxygen makes the difference

OPEN ACCESS

Edited by:

Anjan Debnath,
University of California, San Diego,
USA

Reviewed by:

David Lloyd,
Cardiff University, UK
Joachim Müller,
University of Bern, Switzerland

*Correspondence:

Alessandro Giuffrè,
CNR Institute of Molecular Biology
and Pathology, Piazzale Aldo Moro 5,
I-00185 Rome, Italy
alessandro.giuffre@uniroma1.it;

Brayendra K. Singh,
Bio-Organic Laboratory, Department
of Chemistry, University of Delhi, Delhi
110-007, India
singhbk@chemistry.du.ac.in

[†]These Authors have contributed
equally to this work.

Specialty section:

This article was submitted to
Antimicrobials, Resistance and
Chemotherapy, a section of the
journal Frontiers in Microbiology

Received: 13 February 2015

Paper pending published:

19 February 2015

Accepted: 16 March 2015

Published: 08 April 2015

Citation:

Bahadur V, Mastronicola D, Singh AK,
Tiwari HK, Pucillo LP, Sarti P,
Singh BK and Giuffrè A (2015)
Antigiardial activity of novel
triazolyl-quinolone-based chalcone
derivatives: when oxygen makes the
difference.
Front. Microbiol. 6:256.
doi: 10.3389/fmicb.2015.00256

Vijay Bahadur^{1†}, Daniela Mastronicola^{2,3†}, Amit K. Singh¹, Hemendra K. Tiwari¹,
Leopoldo P. Pucillo⁴, Paolo Sarti^{2,3}, Brajendra K. Singh^{1*} and Alessandro Giuffrè^{2*}

¹ Bio-Organic Laboratory, Department of Chemistry, University of Delhi, Delhi, India, ² CNR Institute of Molecular Biology and Pathology, Rome, Italy, ³ Department of Biochemical Sciences and Istituto Pasteur – Fondazione Cenci Bolognetti, Sapienza University of Rome, Rome, Italy, ⁴ L. Spallanzani National Institute for Infectious Diseases, Istituto di Ricovero e Cura a Carattere Scientifico, Rome, Italy

Giardiasis is a common diarrheal disease worldwide caused by the protozoan parasite *Giardia intestinalis*. It is urgent to develop novel drugs to treat giardiasis, due to increasing clinical resistance to the gold standard drug metronidazole (MTZ). New potential antiparasitic compounds are usually tested for their killing efficacy against *G. intestinalis* under anaerobic conditions, in which MTZ is maximally effective. On the other hand, though commonly regarded as an ‘anaerobic pathogen,’ *G. intestinalis* is exposed to relatively high O₂ levels *in vivo*, living attached to the mucosa of the proximal small intestine. It is thus important to test the effect of O₂ when searching for novel potential antigiardial agents, as outlined in a previous study [Bahadur et al. (2014) *Antimicrob. Agents Chemother.* 58, 543]. Here, 45 novel chalcone derivatives with triazolyl-quinolone scaffold were synthesized, purified, and characterized by high resolution mass spectrometry, ¹H and ¹³C nuclear magnetic resonance and infrared spectroscopy. Efficacy of the compounds against *G. intestinalis* trophozoites was tested under both anaerobic and microaerobic conditions, and selectivity was assessed in a counter-screen on human epithelial colorectal adenocarcinoma cells. MTZ was used as a positive control in the assays. All the tested compounds proved to be more effective against the parasite in the presence of O₂, with the exception of MTZ that was less effective. Under anaerobiosis eighteen compounds were found to be as effective as MTZ or more (up to three to fourfold); the same compounds proved to be up to >100-fold more effective than MTZ under microaerobic conditions. Four of them represent potential candidates for the design of novel antigiardial drugs, being highly selective against *Giardia* trophozoites. This study further underlines the importance of taking O₂ into account when testing novel potential antigiardial compounds.

Keywords: chemical synthesis, drug screening, anaerobic protozoa, intestinal disease, microaerobiosis

Introduction

The amitochondriate protozoon *Giardia intestinalis* is a human parasite, causing extensive morbidity worldwide (Ankarklev et al., 2010). Approximately 6–8% of children and 2%

of adults are estimated to be infected in urbanized countries around the world (Craun, 1996). In spite of its recognition as an important human pathogen for a long time, nearly 5,000 people are hospitalized with giardiasis annually in the United States (see (Lengerich et al., 1994; Gardner and Hill, 2001) and references therein). The disease spreads through fecal-oral transmission of the parasite cysts (Adam, 2001). The host is typically infected through ingestion of cyst-contaminated water or food. After exposure to the acidic environment of the stomach lumen, the cyst develops into the trophozoite, the vegetative form of the parasite, that in turn attaches to the mucosa of the proximal small intestine. This is the crucial step in establishing and maintaining the infection. In the small intestine, the trophozoite starts proliferating, causing symptoms like diarrhea, malabsorption, dehydration, weight loss, failure to thrive, and chronic fatigue. Following encystation, the parasite is ready to be expelled into the environment and infect a new host, thus completing the life cycle.

Giardiasis is commonly treated with several approved medications, that include metronidazole (MTZ), tinidazole, furazolidone, albendazole, paromomycin, or nitazoxanide (Ali and Nozaki, 2007; Tejman-Yarden and Eckmann, 2011). This notwithstanding, because of the limited efficacy, heavy side effects, and increasing resistance of the parasite to available treatments, it is mandatory to continue searching for novel anti-giardial drug candidates (Upcroft and Upcroft, 2001; Ali and Nozaki, 2007). The gold standard drug against giardiasis is MTZ, (Edwards, 1993), a pro-drug that needs to be activated intracellularly by reduction of the nitro moiety (Edwards, 1993). Relevant to this study, by reaction with O_2 the active form of MTZ is converted back to the inactive parent compound. Presence of O_2 in the epithelium of the proximal small intestine (Espey, 2013), where *Giardia* trophozoites adhere with their ventral disks, is therefore expected to significantly decrease the efficacy of MTZ *in vivo*. Given the fairly aerobic environment inhabited by *Giardia* in the host, it is important to consider possible effects of O_2 , when testing novel potential antigiardial drugs. Following this rationale, we have recently carried out a study (Bahadur et al., 2014) in which a set of synthetic compounds has been initially screened for its antigiardial activity under anaerobic condition, and then the compounds with the highest activity were assayed for their efficacy under microaerobic conditions too. This innovative approach allowed us to identify two chalcone derivatives that under microaerobic conditions proved to be selectively active against *Giardia* trophozoites and more effective than MTZ (Bahadur et al., 2014).

Nowadays, molecular hybridization is a coherent strategy that allows one to design new chemical entities of potential biomedical relevance by fusing two or more recognized active compounds and/or pharmacophoric units of known bioactive molecules (Viegas-Junior et al., 2007; Walsh and Bell, 2009). In this regard, chalcone derivatives linked to a triazolyl-quinolone moiety represent an attractive drug scaffold. Nitrogen containing heterocycles are indeed widely used for the synthesis of compounds of pharmaceutical interest (Syam et al., 2012) and chalcone analogs with their relatively

simple structure have a wide variety of pharmacological activities, largely attributed to their α,β unsaturated ketone moiety (Kumar et al., 2003). Moreover, quinoline (1-azanaphthalene) compounds are widely used as “parental” compounds to synthesize molecules with a broad range of biological activities including anti-inflammatory (el-Gazzar et al., 2009), antileishmanial (Palit et al., 2009), antifungal (Kategaonkar et al., 2010), and antituberculosis (Eswaran et al., 2010). Finally, triazoles represent another important class of heterocycles because of their varied biological activities and, accordingly, triazole-containing ring systems are found in numerous existing drugs, like fluconazole, itraconazole, and voriconazole, commonly used as anti-inflammatories, CNS-stimulants, sedatives, antianxiety, antimicrobials, and antimycotics (Shaker, 2006; Saadeh et al., 2010).

Here, we have synthesized, purified and thoroughly characterized a set of 45 novel chalcone analogs with triazolyl-quinolone scaffold, and comparatively evaluated their antigiardial activity both in anaerobiosis and microaerobiosis. This led to the identification of four compounds poorly toxic against human cells, yet able to affect *Giardia* trophozoites more effectively than MTZ under both anaerobic and microaerobic conditions.

Materials and Methods

Materials

All chemicals used in the synthesis of chalcones analogs were purchased from Sigma-Aldrich and Fluka and were used as such without any prior purification. MTZ, ATP, penicillin/streptomycin, bovine calf serum, bovine bile, and the chemicals for the Diamond's TYI-S-33 medium used for *Giardia* cell cultures were purchased from Sigma-Aldrich. Fetal bovine serum, glutamine, non-essential amino acids, trypsin-EDTA, and the Eagle's Minimum Essential Medium (EMEM) were purchased from GIBCO (Life technologies). Other chemicals and solvents purchased locally were of analytical grade. Caco-2 cells (ATCC® HTB-37™) were purchased from Sigma-Aldrich. Incubation bags for anaerobiosis (Anaerocult® A minisystem) and microaerobiosis (Anaerocult® C minisystem) were from Merck. Sterile 96-well white clear-bottom plates were purchased from Perkin Elmer. The ATP one-step luminescence assay systems for microbial (BacTiter-Glo™) and human (ATPlite™) cells were from Promega and Perkin Elmer, respectively.

Synthesis and Characterization of Chalcones

Chemical Methods

Homogeneity/purity of all the products was analyzed by thin-layer chromatography (TLC) on alumina coated plates (Merck). Product samples in MeOH were loaded on TLC plates and developed in $CHCl_3$ -MeOH (9.8:0.2, v/v). On detection of slight impurities by iodine vapor/UV light visualization, compounds were further purified by chromatography on silica gel columns (100–200 mesh size, CDH), using petroleum ether-ethyl acetate (3:2, v/v) as the eluent. Melting points were determined in open glass capillary tubes on a Buchi

M-560 instrument and are uncorrected. Infrared (IR) spectra were recorded in KBr medium using a Perkin-Elmer Fourier Transform-IR spectrometer, whereas ¹H and ¹³C nuclear magnetic resonance (NMR) spectra were recorded in CDCl₃ medium on a JNM ECX-400P (JEOL, USA) spectrometer with tetramethylsilane (TMS) as internal reference. IR and NMR spectra were recorded at the Department of Chemistry, University of Delhi, India. Absorption frequencies (ν) are expressed in cm⁻¹, chemical shifts in ppm (δ -scale) and coupling constants (J) in Hz. Splitting patterns are described as singlet (s), doublet (d), triplet (t), quartet (q), and multiplet (m). High resolution mass spectroscopy (HRMS) data were collected with a resolution of 10,000 on a KRATOS MS50TC spectrometer and a Kratos Mach III type at the University of Leuven (KU Leuven, Celestijnenlaan 200F, 3001 Leuven, Belgium).

General Procedure for the Synthesis of 2-chloroquinoline-3-carbaldehyde (Ramesh et al., 2008) (2)

2-chloroquinoline-3-carbaldehyde was synthesized from acetanilide (**1**) via a Vilsmeier-Haack reaction by traditional methods. To a well-stirred mixture of *N,N*-dimethylformamide (DMF, 3 equiv.) and acetanilide **1** (1 equiv.), POCl₃ (12 equiv.) was added dropwise slowly at 0°C. Afterward the reaction mixture was heated to 100°C for 16 h and the reaction progress was monitored by TLC. After completion of the reaction, the mixture was allowed to cool down to room temperature and poured into crushed ice under vigorous stirring. The obtained precipitate was filtered, washed with water and re-crystallized from dry EtOH to give the title compound **2** with 62% yield; mp 146–147°C (lit 148°C).

General Procedure for the Synthesis of 2-oxoquinoline-3-carbaldehyde (Ramesh et al., 2008) (3)

2-chloroquinoline-3-carbaldehyde **2** was refluxed in 70% acetic acid to obtain 2-oxoquinoline-3-carbaldehyde **3**. The reaction mixture was heated to 110°C for 12 h and the reaction progress was monitored by TLC. After completion of the reaction, the mixture was allowed to cool down to room temperature and poured into crushed ice under vigorous stirring. The obtained precipitate was filtered, washed with water and re-crystallized from dry EtOH to give the title compound **3** with 90% yield; mp 301–302°C (lit 304°C).

General Procedure for the Synthesis of 2-oxo-1-(prop-2-ynyl)-1,2-dihydroquinoline-3-carbaldehyde (Pal et al., 2011) (4)

To a solution of 2-oxo-1,2-dihydroquinoline-3-carbaldehyde **3** (1.0 equiv.) in K₂CO₃ (1.5 equiv.) and DMF, propargyl bromide (1.5 equiv) was added dropwise. The reaction mixture was stirred at room temperature for 12 h. After completion of the reaction, the mixture was poured into ice-cooled water. The solid separated was filtered, washed, dried, and re-crystallized from ethanol to give the title compound **4** with 75% yield; mp 195–197°C (lit 198°C).

General Procedure for the Synthesis of Azidobenzene and its Derivatives (Haridas et al., 2011) (5–9)

To a mixture of appropriate aniline (1 equiv.) in 17% HCl stirred at 0°C, aqueous sodium nitrite (1.2 equiv.) was added dropwise with continued stirring for 10 min at 0°C. Afterward, aqueous sodium azide (1.2 equiv.) was added dropwise to the reaction mixture at 0°C with continued stirring for additional 3 h at room temperature. The reaction progress was monitored by TLC [petroleum ether/ethyl acetate (5:1)]. After completion of the reaction, the mixture was subjected to extraction with ethyl acetate (2 × 25 mL). The combined organic layer was dried over Na₂SO₄ and concentrated under reduced pressure, to obtain an oily brown colored compound.

General Procedure for the Synthesis of 2-oxo-1-((1-phenyl-1H-1,2,3-triazol-4-yl)methyl)-1,2-dihydroquinoline-3-carbaldehyde (10–14)

The mixture of alkyne **4** (1 equiv.), appropriate azide (5–9; 1.5 equiv.), CuSO₄·5H₂O (0.2 equiv.), and sodium ascorbate (0.4 equiv.) was taken in a (3:1) mixture of tetrahydrofuran (THF) and water and stirred at room temperature for 12 h. The reaction progress was monitored by TLC using CHCl₃: MeOH (9.7:0.3, v/v) as the solvent system. After completion of the reaction, the mixture was subjected to extraction with ethyl acetate (3 × 30 mL). The combined ethyl acetate layer was dried over Na₂SO₄ concentrated under reduced pressure and finally purified by silica gel (100–200 mesh size) column chromatography using petroleum ether – ethyl acetate (3:2) as the eluent to yield the desired product.

General Procedure for the Synthesis of (E)-3-(3-oxo-3-phenylprop-1-en-1-yl)-1-((1-phenyl-1H-1,2,3-triazol-4-yl)methyl)quinolin-2(1H)-one (23–67).

To a solution of aryl ketone (15–22; 1 equiv.) and triazolyl-quininaldehyde (10–14; 1 equiv.) in dry MeOH, cat. sodium hydroxide was added. The resulting reaction mixture was stirred at room temperature for 24 h. The reaction progress was monitored by TLC using CHCl₃:MeOH (9.8:0.2, v/v) as the solvent system. After completion of the reaction, the mixture was poured into ice-cool water. The obtained colored precipitate was filtered and dried on vacuum. The compounds were finally purified by silica gel (100–200 mesh size) column chromatography using petroleum ether – ethyl acetate (3:2) as the eluent.

Assays on Cells

Cell Cultures

Trophozoites of *G. intestinalis* strain WB clone C6 (ATCC No. 50803TM) were cultured axenically at 37°C in 25-cm² flasks containing Diamond's TYI-S-33 medium supplemented with 10% bovine calf serum, 1 mg/mL bovine bile, 0.1 g/L streptomycin and 100 U/mL penicillin. Typically, 50 ml medium was inoculated with 25 × 10⁶ cells and after 2 days cells were harvested by chilling the flasks on ice for 30 min for drug susceptibility assays. Human epithelial colorectal adenocarcinoma (Caco-2) cells were grown in 25-cm² flasks in EMEM supplemented with 1% (v/v) non-essential amino acids, 2 mM glutamine, 5% (v/v)

fetal bovine serum, 0.1 g/L streptomycin, and 100 U/mL penicillin.

Assays on Giardia trophozoites

The assays were performed following the procedure described in Bahadur et al. (2014), using sterile 96-well white clear-bottom plates. In each well, 50 µL of *Giardia* trophozoites at a density of 1×10^5 cells/mL was added to 50 µL medium containing either the compound to be tested, serially diluted from a stock solution in dimethyl sulfoxide (DMSO), or the same amount of DMSO as a control; this yielded a final density of 5,000 cells/100 µL in each well. Each drug concentration was tested in at least six replicates. MTZ was used as an internal positive control in the assay. The microtiter plates were then incubated at 37°C under anaerobic or microaerobic conditions, ensured by the Anaerocult® A or the Anaerocult® C minisystem (Merck), respectively. According to the manufacturer instructions, the Anaerocult® A minisystem produces anaerobic conditions within ~1 h, whereas the Anaerocult® C minisystem generates microaerobic conditions (~5% O₂) within 24 h. Following 48 h incubation with the compound to be tested, 100 µL of the BacTiter-Glo™ Microbial Cell Viability Assay System reagent (Promega) was added to each well for one-step lysis and ATP level detection. Plates were then incubated at room temperature for 15 min and ATP levels finally detected by luminescence on a plate reader (Wallac Victor3 1420 Multilabel Counter, PerkinElmer).

Assays on Caco-2 Cells

Cells were detached with 0.5% trypsin-EDTA and seeded in sterile 96-well white clear-bottom plates at the same density of *Giardia* trophozoites and at increasing concentration of the compound to be tested, as described above. The assays were carried out exactly as reported for the *Giardia* trophozoites, except that the plates were incubated (still at 37°C) at atmospheric O₂ level, 5% CO₂, and 95% humidity. Each drug concentration was tested in at least seven replicates. MTZ was used as an internal negative control in the assay. Following 48 h incubation with each compound, according to the manufacturer instructions, 100 µL of the ATPlite™ luminescence assay system (Perkin Elmer) was added to each well for one-step lysis and ATP level detection by luminescence.

Determination of Half-Maximal Inhibitory Concentration (IC₅₀) and Selectivity Index (SI)

Luminometric data were calibrated using ATP standard curves and normalized to the ATP level measured in control DMSO-treated cells (taken as 100%). The measured ATP level percentage was plotted as a function of the compound concentration and the half-maximal inhibitory concentration (IC₅₀) was obtained by fitting the resulting titration profile to the Hill equation (Goutelle et al., 2008). The selectivity index (SI) of the compounds was then calculated as the ratio between the IC₅₀ value measured on human cells over the value determined on *Giardia* trophozoites (SI = IC_{50,Caco-2}/IC_{50, Giardia}).

Results

Synthesis of Novel Triazolyl-Quinolone Based Chalcones

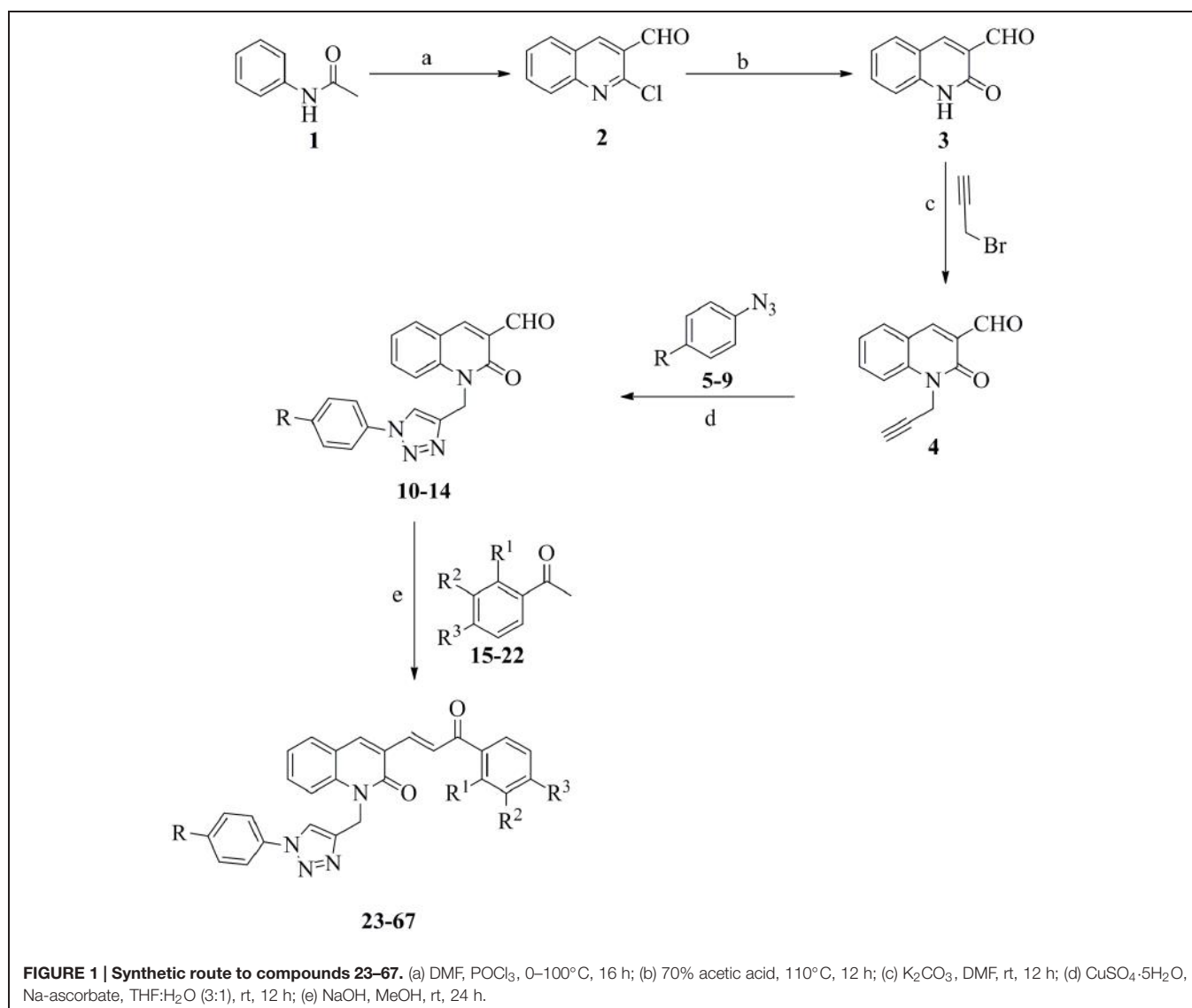
Forty-five novel triazolyl-quinolone-based chalcone derivatives were synthesized based on previously described Claisen-Schmidt condensation (Li et al., 1995), according to the synthetic route outlined in **Figure 1**. Intermediate triazolyl-quinolone compounds **10–14** were synthesized at room temperature in THF:water with 50–75% yield, by “click chemistry” (Barral et al., 2007) of the synthesized alkyne **4** with appropriate aromatic azides (**5–9**), using CuSO₄·5H₂O and sodium ascorbate as catalysts. As shown in **Figure 1**, compounds **23–67** were obtained at room temperature by reaction of the intermediate compounds **10–14** with commercially available aromatic acetophenones **15–22**, in the presence of NaOH in dry MeOH. After purification, the yield of products **23–67** ranged from 60 to 95%.

The newly synthesized triazolyl-quinolone-based chalcone derivatives were characterized by HRMS, ¹H and ¹³C NMR and IR spectroscopy, and relevant data are reported in Supplementary Material.

Antigiardial Activity of the Synthesized Chalcones

The antigiardial activity of the novel compounds **23–67** was tested under both anaerobic and microaerobic conditions. According to (Dunn et al., 2010; Bahadur et al., 2014), susceptibility of *Giardia* trophozoites to increasing concentrations of each compound was assessed based on ATP level determination by luminescence. Dose-response curves for each compound were obtained after 48 h-incubation and compared to the data collected under identical conditions with MTZ, the drug of choice for treatment of giardiasis. In these assays, the ATP level measured in control *Giardia* trophozoites grown under microaerobic conditions was found to be approximately 25% lower than in the same cells grown under anaerobic conditions, and DMSO at concentrations $\leq 2\%, v/v$ caused only marginal effects on cell ATP levels. Typical dose-response curves are shown in **Figure 2**, whereas the IC₅₀ values measured for the synthetic compounds and MTZ under anaerobic and microaerobic conditions are reported in **Table 1**. In agreement with the literature (Müller et al., 2006), under the experimental conditions of the assay, MTZ proved to be highly effective (IC₅₀ = 3.4 µM) against *Giardia* parasites in the absence of O₂, but remarkably less (IC₅₀ ≥ 25 µM) under microaerobic conditions. Under anaerobic conditions, 18 out of the 45 synthetic compounds were as effective as MTZ or more under identical conditions (see **Table 1**). Among them, compounds **41**, **43**, and **45** displayed the highest activity, being three to fourfold more efficient than MTZ.

Interestingly, at variance from MTZ, all the tested compounds displayed a higher efficacy against *Giardia* under microaerobic conditions than in the absence of O₂. Notably, apart from a few exceptions (namely, compounds **23** and **58**), due to their enhanced efficacy and the notably lower activity of MTZ, all the screened compounds were found to be more

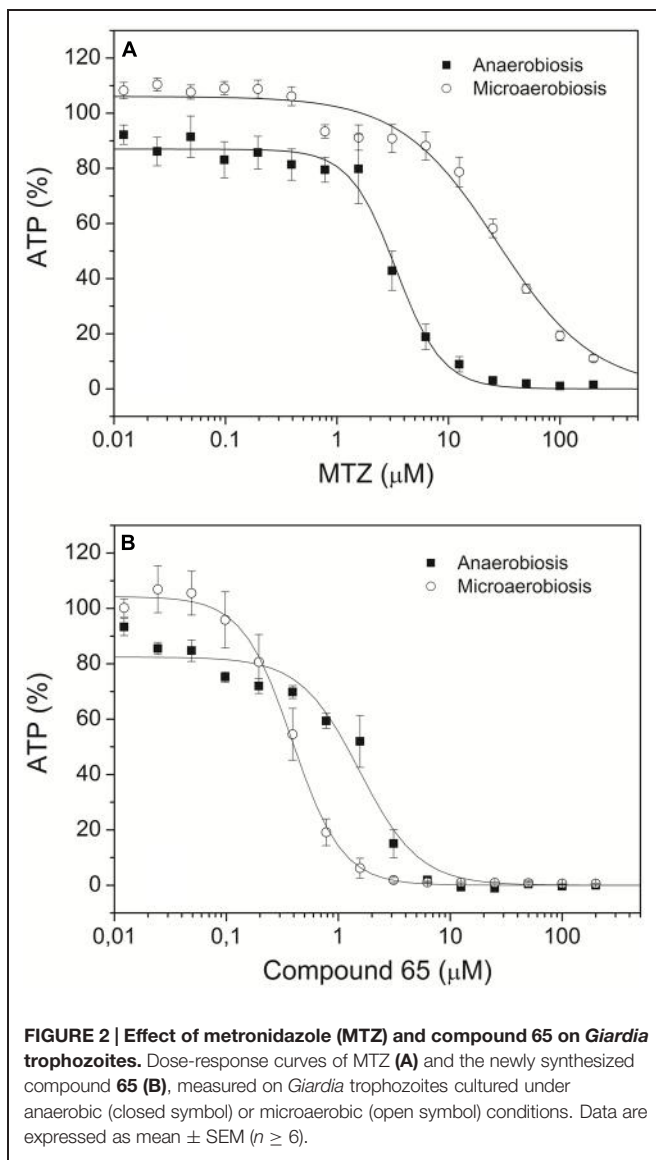


effective than MTZ under microaerobic conditions. In many cases, the effect of O_2 was remarkable, as it can be seen from the IC_{50} values reported in **Table 1**. Under microaerobic conditions approximately half of the tested compounds proved to be at least fivefold more active against *Giardia* than in the absence of O_2 . The effect of O_2 was particularly evident in the case of compounds 24, 31, 49, and 51, which displayed ≥ 10 -fold higher activities under microaerobic conditions than measured in anaerobiosis. Interestingly, up to 10 compounds displayed $IC_{50} \leq 0.5 \mu M$ under microaerobic conditions, thereby becoming > 50 -fold more active than MTZ under identical conditions.

Selectivity of the Synthetic Compounds

Selectivity of the newly synthesized compounds toward *Giardia* was assessed by running a counter-screen on human epithelial Caco-2 cells. Similarly to the screen carried out on *Giardia* trophozoites, dose-response curves and corresponding IC_{50}

values for each compound were obtained after 48 h-incubation, as reported above. This allowed us to calculate the compounds SI, defined as the ratio between the IC_{50} value measured on human cells over the value determined on *Giardia* trophozoites. In the assays on human cells, DMSO affected ATP cell levels only slightly (up to 10% at $\leq 2\%$ v/v, not shown) and, as expected, MTZ exhibited a high IC_{50} value ($> 100 \mu M$). Interestingly, under the same experimental conditions, 19 compounds were only poorly effective against human cells, being characterized by IC_{50} values $\geq 40 \mu M$ (**Table 1**). Among these, compounds 29, 39, 65, and 66 were particularly interesting in that they proved to be (i) more effective than MTZ against *Giardia* trophozoites both in anaerobiosis (IC_{50} ranging from 2.2 to $3.2 \mu M$) and microaerobiosis (IC_{50} ranging from 0.4 to $1.6 \mu M$), and (ii) much less effective on human cells ($IC_{50} \geq 40 \mu M$), thereby exhibiting a high selectivity toward *Giardia* trophozoites (with SI values exceeding 15 and 30 under anaerobiosis and microaerobiosis, respectively).



Discussion

Compared to other more distal tracts of the gut, the proximal small intestine is a fairly aerobic environment, where O₂ is supplied mostly by the submucosal vascular network and in part with swallowed air (Dawson et al., 1965; Levitt, 1970; Sheridan et al., 1990; He et al., 1999). In this tract of the gut, O₂ concentration is relatively high and subjected to sudden oscillations, particularly in the postprandial period when the metabolic demand increases upon transit of partly processed food (Espey, 2013). Relevant to the present study, O₂ concentration is particularly high at the level of the intestinal epithelium, where trophozoites of *G. intestinalis* adhere with their ventral disks. O₂ tension indeed decreases along a steep gradient from 80–100 to nearly 0 mm Hg, moving inward from the submucosa toward the luminal midpoint (Espey, 2013). Therefore, though commonly regarded as an anaerobic protozoan, *Giardia*

is likely exposed to fairly high and variable O₂ levels *in vivo*. The parasite is amitochondriate and thus unable to utilize O₂ to sustain energy metabolism. This notwithstanding, μM O₂ concentrations have been shown to produce profound changes in the metabolism of *Giardia* trophozoites, leading to stimulation of both ethanol and CO₂ production, elicited oxidation of the intracellular NAD(P)H pool and reduced alanine production (Paget et al., 1993). In addition to these adaptive metabolic changes, in order to survive oxidative stress conditions, *Giardia* needs to activate the antioxidant defense system (Brown et al., 1995; Mastronicola et al., 2011; Raj et al., 2014). In this regard, it has been established that, though lacking *bona fide* catalases or superoxide dismutases, *Giardia* is endowed with several alternative antioxidant enzymes that have been recently identified and partly characterized. These include: a NADH oxidase (Brown et al., 1996a) and a flavodiiron protein (Di Matteo et al., 2008; Vicente et al., 2009) detoxifying O₂ to H₂O, a flavohemoglobin converting nitric oxide into nitrate (Mastronicola et al., 2010, 2011; Rafferty et al., 2010), a superoxide reductase promptly degrading superoxide anion to H₂O₂ (Testa et al., 2011), a thioredoxin reductase (Brown et al., 1996b) and two peroxiredoxins (Mastronicola et al., 2014) implicated in peroxide detoxification and repair of oxidatively damaged molecules. Exposure to O₂ is therefore expected to cause notable changes in the metabolic and proteomic profile of *G. intestinalis*, an aspect that has not been studied in detail thus far.

Despite being physiologically exposed to O₂ *in vivo*, *Giardia* trophozoites are commonly assayed *in vitro* for their drug susceptibility under anaerobic conditions. This may bias the results of a screening. Leading to changes in cell metabolism, O₂ may indeed modify the susceptibility of the parasite to specific drugs, possibly up- or down-regulating molecular targets. Moreover, by directly reacting with the tested drugs, it may alter their mechanism of action, possibly leading to enhanced or reduced efficacy. This is the case of MTZ, the gold standard drug against giardiasis, whose efficacy is abolished upon reaction of its nitro-radical active form with O₂ (Edwards, 1993). When testing new potential antigiardial drugs, it is thus important to take O₂ into account also to attempt identifying antiparasitic compounds that could be fully effective under the more physiological microaerobic conditions in which MTZ efficacy is reduced due to O₂ presence. This issue has been highlighted in a recent study by our groups (Bahadur et al., 2014) in which O₂, while making MTZ expectedly less effective, was reported to enhance the efficacy of three piperidine/piperazine chalcone derivatives, pre-selected in a screen conducted under anaerobic conditions.

In the present study, 45 novel chalcone derivatives with triazolyl-quinolone scaffold were synthesized, purified, and characterized by HRMS, ¹H and ¹³C NMR and IR spectroscopy. As an innovative approach, all the compounds were comparatively tested for their efficacy against *G. intestinalis* trophozoites under both anaerobic and microaerobic conditions. Compared to anaerobic conditions, the presence of O₂ was found to increase the IC₅₀ of MTZ from 3.4 to ≥ 25 μM. This result agrees with

TABLE 1 | Chemical identity, IC₅₀ values and selectivity index (SI) of the novel synthetic compounds.

S. No	R	R ¹	R ²	R ³	Giardia (anaerobiosis)		Giardia (microaerobiosis)		Caco-2		Selectivity (IC _{50,Caco} /IC _{50,Giardia})	
					IC ₅₀	IC ₅₀	IC ₅₀	IC ₅₀	IC ₅₀	IC ₅₀	Anaerobiosis	Microaerobiosis
23	OMe	F	H	H	≥100	≥20	≥100	n.d.	n.d.	n.d.	n.d.	n.d.
24	OMe	H	F	H	≥100	8,4	≥50	n.d.	n.d.	≥6		
25	OMe	H	H	F	3,9	1,3	≥20	≥5	≥20	≥15		
26	OMe	H	H	Cl	5,0	2,6	≥20	≥4	≥20	≥7		
27	OMe	H	H	Br	9,6	2,0	≥20	≥2	≥20	≥10		
28	OMe	H	H	Me	5,4	1,5	≥80	≥14	≥80	≥53		
29	OMe	OMe	H	H	2,2	0,4	≥40	≥18	≥100			
30	OMe	H	OMe	H	5,9	1,3	≥200	≥33	≥200	≥153		
31	OMe	H	H	OMe	≥50	2,0	≥80	n.d.	≥80	≥40		
32	Me	F	H	H	3,2	0,6	17,6	5,5	≥100	29,3		
33	Me	H	F	H	4,0	0,7	13,4	3,4	13,4	19,1		
34	Me	H	H	F	3,8	1,2	9,4	2,5	9,4	7,8		
35	Me	H	H	Cl	2,4	0,8	7,0	2,9	≥100	8,8		
36	Me	H	H	Br	10,7	2,3	≥50	≥4	≥50	≥21		
37	Me	H	H	Me	6,3	1,6	≥50	≥7	≥50	≥31		
38	Me	OMe	H	H	2,0	0,4	13,7	6,9	≥100	34,3		
39	Me	H	OMe	H	2,9	1,3	≥34	≥34	≥100	≥76		
40	Me	H	H	OMe	≥15	2,4	≥60	n.d.	≥60	≥25		
41	F	F	H	H	0,9	0,2	5,2	5,8	≥100	26		
42	F	H	F	H	3,3	0,7	9,6	2,9	≥100	13,7		
43	F	H	H	F	1,2	0,3	7,0	5,8	≥100	23,3		
44	F	H	H	Cl	1,5	1,0	7,2	4,8	≥100	7,2		
45	F	H	H	Br	1,1	0,5	16,7	15,2	≥100	33,4		
46	F	H	H	Me	2,5	0,4	6,3	2,5	≥100	15,8		
47	F	OMe	H	H	2,7	0,3	≥20	≥7	≥20	≥66		
48	F	H	OMe	H	7,0	1,6	≥60	≥8	≥60	≥37		
49	F	H	H	OMe	13,0	1,3	≥50	≥3	≥50	≥38		
50	Cl	F	H	H	4,7	0,9	≥50	≥10	≥50	≥55		
51	Cl	H	F	H	10,0	0,9	≥100	≥10	≥100	≥111		
52	Cl	H	H	F	8,9	1,2	23,9	2,7	23,9	19,9		
53	Cl	H	H	Cl	9,0	1,1	≥30	≥3	≥30	≥27		
54	Cl	H	H	Br	9,2	1,9	≥20	≥2	≥20	≥10		
55	Cl	H	H	Me	8,7	1,1	20	2,3	20	18,2		
56	Cl	OMe	H	H	3,2	0,6	8,4	2,6	≥100	14,0		
57	Cl	H	OMe	H	6,6	1,1	14,7	2,2	14,7	11,3		
58	Cl	H	H	OMe	≥100	≥30	19,7	≤0,2	≥30	≤0,7		
59	H	F	H	H	1,9	0,4	11,2	5,9	≥100	28,0		
60	H	H	F	H	3,5	0,7	≥50	≥14	≥50	≥71		
61	H	H	H	F	5,3	0,8	18,2	3,4	18,2	22,8		
62	H	H	H	Cl	2,1	0,7	5,9	2,8	≥100	8,4		
63	H	H	H	Br	6,3	1,0	≥50	≥7	≥50	≥50		
64	H	H	H	Me	2,8	0,5	17,8	6,4	≥100	35,6		
65	H	OMe	H	H	1,6	0,4	≥50	≥31	≥50	≥125		
66	H	H	OMe	H	3,2	1,6	≥50	≥15	≥50	≥31		
67	H	H	H	OMe	5,9	0,8	≥100	≥16	≥100	≥125		
MTZ					3,4	≥25	≥100	≥29.0	≥100	n.d.		

Bold, IC₅₀ < IC_{50,MTZ} in anaerobiosis; Compounds **29**, **39**, **65** and **66** display IC₅₀ < IC_{50,MTZ} in both anaerobiosis and microaerobiosis, low toxicity against Caco-2 cells (IC₅₀ ≥ 40,0) and SI > 10.

the notion that O_2 interferes with MTZ, by converting its nitro-radical active form into the parental inactive form (Edwards, 1993). However, noteworthy, in spite of the reduced efficacy of MTZ, all the tested compounds proved to be more effective in the presence of O_2 , though to different extent. For most of the compounds the IC_{50} was four to sevenfold smaller than measured under anaerobic conditions, but in the case of four compounds (24, 31, 49, and 51) O_2 was particularly effective decreasing their IC_{50} by more than 10-fold. While under anaerobic conditions only 18 out of the 45 tested compounds proved to be as active as MTZ or more, in the presence of O_2 almost all the tested compounds (with the exception of compounds 23 and 58) were more effective than MTZ. Under microaerobic conditions, up to 10 compounds showed notably low IC_{50} values ($\leq 0.5 \mu M$), thereby becoming > 50 -fold more effective than MTZ under the same microaerobic conditions, yet less effective than the alternative antigiardial drug albendazole that under anaerobic conditions shows very low IC_{50} values ($< 0.1 \mu M$, Cedillo-Rivera and Munoz, 1992). Interestingly, 19 out of the 45 tested compounds displayed very poor toxicity against human Caco-2 cells ($IC_{50} \geq 40 \mu M$), and by comparing their efficacy on human and *Giardia* cells 10 out of these 19 compounds proved to be highly selective toward the parasite, being ≥ 10 -fold more effective against *Giardia* under both anaerobic and microaerobic conditions. Among these 10 compounds highly selective against *Giardia*, four can be considered as hits to develop potential antigiardial drugs, namely compounds 29, 39, 65, and 66, being more effective than MTZ under both anaerobic and aerobic conditions.

The compounds characterized here carry substitutions in two phenyl rings: ring A (attached to the triazole moiety) and ring B (attached to the α,β unsaturated moiety). By inspecting Table 1, it can be noted that on average the compounds with the highest antigiardial activity have either unsubstituted (compounds 59–67) or fluoro-substituted (compounds 41–49) ring A. Comparatively, less antigiardial activity is observed when the same ring is substituted with chloro (compounds 50–58), methoxy (compounds 23–31) or methyl (compounds 32–40) groups. Compared to other types of substitutions in ring A, the fluoro-substitution seems to result into higher toxicity of the compounds against human cells. The occurrence of substitutions at ring B and their position in the ring also appear to modulate the antigiardial activity. Comparison of compounds 29, 30, and 31 shows that the position of a methoxy substituent in ring B has great effects on the antiparasitic activity of the molecules. The *ortho* substituted compound 29 is more effective than the *meta* substituted compound 30, that in turn displays a higher antigiardial activity compared to the *para* substituted analog (compound 31). Interestingly, the same trend (*ortho* $>$ *meta* $>$ *para*) is invariably observed by comparing the compound triplets 38–40, 47–49, 56–58, and 65–67, all having methoxy-substituted ring B. Finally, it is worth noticing that the compounds optimally combining high antigiardial activity and low toxicity against human

cells (compounds 29, 39, 65, and 66) have ring B invariably methoxy-substituted at *ortho* or *meta* positions, and ring A either unsubstituted or substituted with methoxy or methyl groups.

To the best of our knowledge, this is the first study in which a complete set of new synthetic compounds has been screened for its ability to affect *Giardia* trophozoites under both anaerobic and microaerobic conditions, providing unequivocal evidence for an effect of O_2 . The results show that, as compared to anaerobic conditions, the presence of low, more physiological O_2 concentrations elicits the antiparasitic activity of the tested compounds, while having opposite effects on MTZ. The molecular mechanism underlying the observed effects of O_2 has yet to be established. A possibility is that O_2 , by directly affecting *Giardia* trophozoites, on the one hand impairs MTZ activation and on the other makes the cells more susceptible to the novel synthetic drugs here described. A more intriguing possibility is that, in response to O_2 exposure, the parasite activates specific metabolic pathways that are selectively targeted by the compounds tested in the present study, but not MTZ. To address this issue, it would be important in future studies to acquire more detailed information on the pathways that are activated in *Giardia* in the metabolic transition from anaerobic to microaerobic conditions.

Conclusion

In this study we have identified four new compounds that under both anaerobic and more physiological microaerobic conditions are highly effective against *Giardia* trophozoites, targeting the parasite selectively and more efficiently than MTZ. These four synthetic chalcone derivatives represent potential candidates for the design of novel antigiardial drugs. This work further highlights that it is important to take O_2 into account when screening new potential antigiardial drugs.

Acknowledgments

This work was partially supported by Ministero dell'Istruzione, dell'Università e della Ricerca of Italy (PNR-CNR Aging Program 2012–2014 AG, FIRB RBIN06E9Z8 and PRIN 20107Z8XBW_005 to PS), Ministry of Science and Technology, Department of Science and Technology (DST/INT/UKR/2012/P-10), India, Council of Scientific and Industrial Research and University of Delhi under the Strengthening R&D Doctoral Research Programme, Delhi, India.

Supplementary Material

The Supplementary Material for this article can be found online at: <http://www.frontiersin.org/journal/10.3389/fmicb.2015.00256/abstract>

References

- Adam, R. D. (2001). Biology of *Giardia lamblia*. *Clin. Microbiol. Rev.* 14, 447–475. doi: 10.1128/CMR.14.3.447-475.2001
- Ali, V., and Nozaki, T. (2007). Current therapeutics, their problems, and sulfur-containing-amino-acid metabolism as a novel target against infections by “amitochondriate” protozoan parasites. *Clin. Microbiol. Rev.* 20, 164–187. doi: 10.1128/CMR.00019-06
- Ankarklev, J., Jerlstrom-Hultqvist, J., Ringqvist, E., Troell, K., and Svärd, S. G. (2010). Behind the smile: cell biology and disease mechanisms of *Giardia* species. *Nat. Rev. Microbiol.* 8, 413–422. doi: 10.1038/nrmicro2317
- Bahadur, V., Mastronicola, D., Tiwari, H. K., Kumar, Y., Falabella, M., Pucillo, L. P., et al. (2014). O(2)-dependent efficacy of novel piperidine- and piperazine-based chalcones against the human parasite *Giardia intestinalis*. *Antimicrob. Agents Chemother.* 58, 543–549. doi: 10.1128/AAC.00990-913
- Barral, K., Moorhouse, A. D., and Moses, J. E. (2007). Efficient conversion of aromatic amines into azides: a one-pot synthesis of triazole linkages. *Org. Lett.* 9, 1809–1811. doi: 10.1021/o1070527h
- Brown, D. M., Upcroft, J. A., and Upcroft, P. (1995). Free radical detoxification in *Giardia duodenalis*. *Mol. Biochem. Parasitol.* 72, 47–56. doi: 10.1016/0166-6851(95)00065-9
- Brown, D. M., Upcroft, J. A., and Upcroft, P. (1996a). A H_2O -producing NADH oxidase from the protozoan parasite *Giardia duodenalis*. *Eur. J. Biochem.* 241, 155–161. doi: 10.1111/j.1432-1033.1996.0155t.x
- Brown, D. M., Upcroft, J. A., and Upcroft, P. (1996b). A thioredoxin reductase-class of disulphide reductase in the protozoan parasite *Giardia duodenalis*. *Mol. Biochem. Parasitol.* 83, 211–220. doi: 10.1016/S0166-6851(96)02776-4
- Cedillo-Rivera, R., and Munoz, O. (1992). In-vitro susceptibility of *Giardia lamblia* to albendazole, mebendazole and other chemotherapeutic agents. *J. Med. Microbiol.* 37, 221–224. doi: 10.1099/00222615-37-3-221
- Craun, G. F. (1996). “Waterborne outbreaks of giardiasis: current status,” in *Giardia and Giardiasis: Biology, Pathogenesis, and Epidemiology*, eds S. L. Erlandsen and E. A. Meyer (New York, NY: Plenum Press), 243–261.
- Dawson, A. M., Trenchard, D., and Guz, A. (1965). Small bowel tonometry: assessment of small gut mucosal oxygen tension in dog and man. *Nature* 206, 943–944. doi: 10.1038/206943b0
- Di Matteo, A., Scandurra, F. M., Testa, F., Forte, E., Sarti, P., Brunori, M., et al. (2008). The O_2 -scavenging flavodiiron protein in the human parasite *Giardia intestinalis*. *J. Biol. Chem.* 283, 4061–4068. doi: 10.1074/jbc.M705605200
- Dunn, L. A., Burgess, A. G., Krauer, K. G., Eckmann, L., Vanelle, P., Crozet, M. D., et al. (2010). A new-generation 5-nitroimidazole can induce highly metronidazole-resistant *Giardia lamblia* in vitro. *Int. J. Antimicrob. Agents Chemother.* 36, 37–42. doi: 10.1016/j.ijantimicag.2010.03.004
- Edwards, D. I. (1993). Nitroimidazole drugs—action and resistance mechanisms. I. mechanisms of action. *J. Antimicrob. Chemother.* 31, 9–20. doi: 10.1093/jac/31.1.9
- el-Gazzar, A. B., Hafez, H. N., and Nawwar, G. A. (2009). New acyclic nucleosides analogues as potential analgesic, anti-inflammatory, anti-oxidant and anti-microbial derived from pyrimido[4,5-b]quinolines. *Eur. J. Med. Chem.* 44, 1427–1436. doi: 10.1016/j.ejmech.2008.09.030
- Espey, M. G. (2013). Role of oxygen gradients in shaping redox relationships between the human intestine and its microbiota. *Free Radic. Biol. Med.* 55, 130–140. doi: 10.1016/j.freeradbiomed.2012.10.554
- Eswaran, S., Adhikari, A. V., and Ajay Kumar, R. (2010). New 1,3-oxazolo[4,5-c]quinoline derivatives: synthesis and evaluation of antibacterial and antituberculosis properties. *Eur. J. Med. Chem.* 45, 957–966. doi: 10.1016/j.ejmech.2009.11.036
- Gardner, T. B., and Hill, D. R. (2001). Treatment of giardiasis. *Clin. Microbiol. Rev.* 14, 114–128. doi: 10.1128/CMR.14.1.114-128.2001
- Goutelle, S., Maurin, M., Rougier, F., Barbaut, X., Bourguignon, L., Ducher, M., et al. (2008). The Hill equation: a review of its capabilities in pharmacological modelling. *Fundam. Clin. Pharmacol.* 22, 633–648. doi: 10.1111/j.1472-8206.2008.00633.x
- Haridas, V., Sahu, S., and Kumar, P. P. P. (2011). Triazole-based chromogenic and non-chromogenic receptors for halides. *Tetrahedron Lett.* 52, 6930–6934. doi: 10.1016/j.tetlet.2011.10.066
- He, G., Shankar, R. A., Chzhan, M., Samoilov, A., Kuppusamy, P., and Zweier, J. L. (1999). Noninvasive measurement of anatomic structure and intraluminal oxygenation in the gastrointestinal tract of living mice with spatial and spectral EPR imaging. *Proc. Natl. Acad. Sci. U.S.A.* 96, 4586–4591. doi: 10.1073/pnas.96.8.4586
- Kategaonkar, A. H., Pokalwar, R. U., Sonar, S. S., Gawali, V. U., Shingate, B. B., and Shingare, M. S. (2010). Synthesis, in vitro antibacterial and antifungal evaluations of new alpha-hydroxyphosphonate and new alpha-acetoxyphosphonate derivatives of tetrazolo [1, 5-a] quinoline. *Eur. J. Med. Chem.* 45, 1128–1132. doi: 10.1016/j.ejmech.2009.12.013
- Kumar, S. K., Hager, E., Pettit, C., Gurulingappa, H., Davidson, N. E., and Khan, S. R. (2003). Design, synthesis, and evaluation of novel boronic-chalcone derivatives as antitumor agents. *J. Med. Chem.* 46, 2813–2815. doi: 10.1021/jm030213+
- Lengerich, E. J., Addiss, D. G., and Juranek, D. D. (1994). Severe giardiasis in the United States. *Clin. Infect. Dis.* 18, 760–763. doi: 10.1093/clinids/18.5.760
- Levitt, M. D. (1970). Oxygen tension in the gut. *N. Engl. J. Med.* 282, 1039–1040. doi: 10.1056/NEJM197004302821814
- Li, R., Kenyon, G. L., Cohen, F. E., Chen, X., Gong, B., Dominguez, J. N., et al. (1995). In vitro antimalarial activity of chalcones and their derivatives. *J. Med. Chem.* 38, 5031–5037. doi: 10.1021/jm00026a010
- Mastronicola, D., Falabella, M., Testa, F., Pucillo, L. P., Teixeira, M., Sarti, P., et al. (2014). Functional characterization of peroxiredoxins from the human protozoan parasite *Giardia intestinalis*. *PLoS Negl. Trop. Dis.* 8:e2631. doi: 10.1371/journal.pntd.0002631
- Mastronicola, D., Giuffrè, A., Testa, F., Mura, A., Forte, E., Bordi, E., et al. (2011). *Giardia intestinalis* escapes oxidative stress by colonizing the small intestine: a molecular hypothesis. *IUBMB Life* 63, 21–25. doi: 10.1002/iub.409
- Mastronicola, D., Testa, F., Forte, E., Bordi, E., Pucillo, L. P., Sarti, P., et al. (2010). Flavohemoglobin and nitric oxide detoxification in the human protozoan parasite *Giardia intestinalis*. *Biochem. Biophys. Res. Commun.* 399, 654–658. doi: 10.1016/j.bbrc.2010.07.137
- Müller, J., Ruhle, G., Müller, N., Rossignol, J. F., and Hemphill, A. (2006). In vitro effects of thiazolidines on *Giardia lamblia* WB clone C6 cultured axenically and in coculture with Caco2 cells. *Antimicrob. Agents Chemother.* 50, 162–170. doi: 10.1128/AAC.50.1.162-170.2006
- Paget, T. A., Kelly, M. L., Jarroll, E. L., Lindmark, D. G., and Lloyd, D. (1993). The effects of oxygen on fermentation in *Giardia lamblia*. *Mol. Biochem. Parasitol.* 57, 65–71. doi: 0166-6851(93)90244-R
- Pal, S., Durgadas, S., Nallapati, S. B., Mukkanti, K., Kapavarapu, R., Meda, C. L., et al. (2011). Novel 1-alkynyl substituted 1,2-dihydroquinoline derivatives from nimesulide (and their 2-oxo analogues): a new strategy to identify inhibitors of PDE4B. *Bioorg. Med. Chem. Lett.* 21, 6573–6576. doi: 10.1016/j.bmcl.2011.08.033
- Palit, P., Paira, P., Hazra, A., Banerjee, S., Gupta, A. D., Dastidar, S. G., et al. (2009). Phase transfer catalyzed synthesis of bis-quinolines: antileishmanial activity in experimental visceral leishmaniasis and in vitro antibacterial evaluation. *Eur. J. Med. Chem.* 44, 845–853. doi: 10.1016/j.ejmech.2008.04.014
- Rafferty, S., Luu, B., March, R. E., and Yee, J. (2010). *Giardia lamblia* encodes a functional flavohemoglobin. *Biochem. Biophys. Res. Commun.* 399, 347–351. doi: 10.1016/j.bbrc.2010.07.073
- Raj, D., Ghosh, E., Mukherjee, A. K., Nozaki, T., and Ganguly, S. (2014). Differential gene expression in *Giardia lamblia* under oxidative stress: significance in eukaryotic evolution. *Gene* 535, 131–139. doi: 10.1016/j.gene.2013.11.048
- Ramesh, E., Sree Vidhya, T. K., and Raghunathan, R. (2008). Indium chloride/silica gel supported synthesis of pyrano/thiopyranoquinolines through intramolecular imino Diels–Alder reaction using microwave irradiation. *Tetrahedron Lett.* 49, 2810–2814. doi: 10.1016/j.tetlet.2008.02.128
- Saadeh, H. A., Mosleh, I. M., Al-Bakri, A. M., and Mubarak, M. S. (2010). Synthesis and antimicrobial activity of new 1,2,4-triazole-3-thiol metronidazole derivatives. *Monatsh. Chem.* 141, 471–478. doi: 10.1007/s00706-010-0281-289
- Shaker, R. M. (2006). The chemistry of mercapto- and thione- substituted 1,2,4-triazoles and their utility in heterocyclic synthesis. *ARKIVOC* 2006, 59–112. doi: 10.3998/ark.5550190.0007.904
- Sheridan, W. G., Lowndes, R. H., and Young, H. L. (1990). Intraoperative tissue oximetry in the human gastrointestinal tract. *Am. J. Surg.* 159, 314–319. doi: 10.1016/S0002-9610(05)81226-7

- Syam, S., Abdelwahab, S. I., Al-Mamary, M. A., and Mohan, S. (2012). Synthesis of chalcones with anticancer activities. *Molecules* 17, 6179–6195. doi: 10.3390/molecules17066179
- Tejman-Yarden, N., and Eckmann, L. (2011). New approaches to the treatment of giardiasis. *Curr. Opin. Infect. Dis.* 24, 451–456. doi: 10.1097/QCO.0b013e32834ad401
- Testa, F., Mastronicola, D., Cabelli, D. E., Bordi, E., Pucillo, L. P., Sarti, P., et al. (2011). The superoxide reductase from the early diverging eukaryote *Giardia intestinalis*. *Free Radic. Biol. Med.* 51, 1567–1574. doi: 10.1016/j.freeradbiomed.2011.07.017
- Upcroft, P., and Upcroft, J. A. (2001). Drug targets and mechanisms of resistance in the anaerobic protozoa. *Clin. Microbiol. Rev.* 14, 150–164. doi: 10.1128/CMR.14.1.150-164.2001
- Vicente, J. B., Testa, F., Mastronicola, D., Forte, E., Sarti, P., Teixeira, M., et al. (2009). Redox properties of the oxygen-detoxifying flavodiiron protein from the human parasite *Giardia intestinalis*. *Arch. Biochem. Biophys.* 488, 9–13. doi: 10.1016/j.abb.2009.06.011
- Viegas-Junior, C., Danuello, A., Da Silva Bolzani, V., Barreiro, E. J., and Fraga, C. A. (2007). Molecular hybridization: a useful tool in the design of new drug prototypes. *Curr. Med. Chem.* 14, 1829–1852. doi: 10.2174/092986707781058805
- Walsh, J. J., and Bell, A. (2009). Hybrid drugs for malaria. *Curr. Pharm. Des.* 15, 2970–2985. doi: 10.2174/138161209789058183

Conflict of Interest Statement: The authors declare that the research was conducted in the absence of any commercial or financial relationships that could be construed as a potential conflict of interest.

Copyright © 2015 Bahadur, Mastronicola, Singh, Tiwari, Pucillo, Sarti, Singh and Giuffrè. This is an open-access article distributed under the terms of the Creative Commons Attribution License (CC BY). The use, distribution or reproduction in other forums is permitted, provided the original author(s) or licensor are credited and that the original publication in this journal is cited, in accordance with accepted academic practice. No use, distribution or reproduction is permitted which does not comply with these terms.

An antioxidant response is involved in resistance of *Giardia duodenalis* to albendazole

Raúl Argüello-García¹, Maricela Cruz-Soto², Rolando González-Trejo¹,
Luz María T. Paz-Maldonado³, M. Luisa Bazán-Tejeda¹,
Guillermo Mendoza-Hernández⁴ and Guadalupe Ortega-Pierres^{1*}

¹ Departamento de Genética y Biología Molecular, Centro de Investigación y de Estudios Avanzados Instituto Politécnico Nacional, Mexico City, Mexico, ² Probiomed, Tenancingo, Mexico, ³ Ingeniería de Biorreactores, Facultad de Ciencias Químicas, Universidad Autónoma de San Luis Potosí, San Luis Potosí, Mexico, ⁴ Departamento de Bioquímica, Facultad de Medicina, Universidad Nacional Autónoma de México, Mexico City, Mexico

OPEN ACCESS

Edited by:

Anjan Debnath,
University of California, San Diego,
USA

Reviewed by:

Dmitri Debabov,
NovaBay Pharmaceuticals, USA
Yukiko Miyamoto,
University of California, San Diego,
USA

*Correspondence:

Guadalupe Ortega-Pierres,
Departamento de Genética y Biología Molecular, Centro de Investigación y de Estudios Avanzados Instituto Politécnico Nacional, Avenida Instituto Politécnico Nacional 2508, San Pedro Zacatenco, 07360 Mexico City,
Mexico
gortega@ciinvestav.mx

Specialty section:

This article was submitted to
Antimicrobials, Resistance and Chemotherapy, a section of the journal Frontiers in Microbiology

Received: 14 February 2015

Accepted: 23 March 2015

Published: 10 April 2015

Citation:

Argüello-García R, Cruz-Soto M, González-Trejo R, Paz-Maldonado LMT, Bazán-Tejeda ML, Mendoza-Hernández G and Ortega-Pierres G (2015) An antioxidant response is involved in resistance of *Giardia duodenalis* to albendazole.

Front. Microbiol. 6:286.

doi: 10.3389/fmicb.2015.00286

Albendazole (ABZ) is a therapeutic benzimidazole used to treat giardiasis that targets β -tubulin. However, the molecular bases of ABZ resistance in *Giardia duodenalis* are not understood because β -tubulin in ABZ-resistant clones lacks mutations explaining drug resistance. In previous work we compared ABZ-resistant (1.35, 8, and 250 μ M) and ABZ-susceptible clones by proteomic analysis and eight proteins involved in energy metabolism, cytoskeleton dynamics, and antioxidant response were found as differentially expressed among the clones. Since ABZ is converted into sulphoxide (ABZ-SO) and sulphone (ABZ-SOO) metabolites we measured the levels of these metabolites, the antioxidant enzymes and free thiols in the susceptible and resistant clones. Production of reactive oxygen species (ROS) and levels of ABZ-SO/ABZ-SOO induced by ABZ were determined by fluorescein diacetate-based fluorescence and liquid chromatography respectively. The mRNA and protein levels of antioxidant enzymes (NADH oxidase, peroxiredoxin 1a, superoxide dismutase and flavodiiiron protein) in these clones were determined by RT-PCR and proteomic analysis. The intracellular sulphhydryl (R-SH) pool was quantified using dinitrobenzoic acid. The results showed that ABZ induced ROS accumulation in the ABZ-susceptible *Giardia* cultures but not in the resistant ones whilst the accumulation of ABZ-SO and ABZ-SOO was lower in all ABZ-resistant cultures. Consistent with these findings, all the antioxidant enzymes detected and analyzed were upregulated in ABZ-resistant clones. Likewise the R-SH pool increased concomitantly to the degree of ABZ-resistance. These results indicate an association between accumulation of ABZ metabolites and a pro-oxidant effect of ABZ in *Giardia*-susceptible clones. Furthermore the antioxidant response involving ROS-metabolizing enzymes and intracellular free thiols in ABZ-resistant parasites suggest that this response may contribute to overcome the pro-oxidant cytotoxicity of ABZ.

Keywords: *Giardia duodenalis*, albendazole, drug resistance, antioxidant enzymes, sulphhydryl pool

Introduction

Giardia duodenalis (syn. *G. lamblia*, *G. intestinalis*) is the protozoan causing giardiasis that is a leading cause of parasitic diarrheal disease in humans and animals. According to estimations of the World Health Organization (WHO), giardiasis accounts for almost a billion cases worldwide with ~3 billion people living in areas in which the incidence of the infection is around 30% (Escobedo et al., 2010). The disease incidence may increase due to increasing migrations from and to highly endemic countries (Ekdahl and Andersson, 2005) and eventual climate changes (Parkison et al., 2014). The socioeconomic and clinical impact of giardiasis has prompted its inclusion within the WHO's Neglected Diseases Initiative (Savioli et al., 2006). The control of this infection requires both the inactivation of the infectious cysts disseminated in the environment and the elimination of pathogenic trophozoites that attach to small intestinal epithelium. Fatty to watery diarrhea is a hallmark of acute and chronic giardiasis that in children may result into malabsorption, failure to thrive and deficit in weight gain. Adult asymptomatic carriers are frequently observed (Adam, 2001; Escobedo and Cimerman, 2007).

To date, vaccines for giardiasis are only available for animals and the control of *Giardia* infections in humans relies on improvements in sanitation and hygiene (Olson et al., 2000). Currently available antigiardial drugs include 5-nitro derivatives of imidazole (metronidazole, tinidazole), furan (furazolidone) and thiazole (nitazoxanide) as well as alternative drugs such as acridines (quinacrine, chloroquine), aminoglycosides (paromomycin) and benzimidazoles [albendazole (ABZ), mebendazole]. Although 5-nitro derivatives of imidazole have a high overall efficiency according to non-randomized clinical trials (60–100%; Busatti et al., 2009), therapeutic failures occur in 20% of individuals in spite of the compliance of drug dosage and duration (Upcroft, 1998). The reasons for failures of drug treatment vary among patients and these include: reinfections, inadequate doses in drug treatment, immunosuppression, drug sequestration in the gallbladder or pancreatic ducts, and infections caused by drug resistant in *Giardia* (Nash et al., 2001).

Since 1990, ABZ (methyl [5-(propylthio)-1*H*-benzimidazole-2-yl] carbamate, ABZ), was used in combination with mebendazole to treat giardiasis. Although ABZ is as effective as metronidazole against giardiasis, the efficacy of ABZ may vary significantly (25–90%) depending on the duration of the treatment (1–5 days; Watkins and Eckmann, 2014). Failures of drug treatments for giardiasis have been reported when ABZ is used alone (Kollaritsch et al., 1993; Brasseur and Favenne, 1995; Nash et al., 2001) and when ABZ has been used in combination with metronidazole (Abboud et al., 2001; Mørch et al., 2008). Benzimidazoles are given at single dose to deworm children at 6 month-intervals (i.e., a suboptimal regime for giardiasis) in community- or cohort-based programs in endemic regions of Mexico, Bangladesh, and Bolivia. This results in poor elimination of *Giardia* trophozoites (Quihui-Cota and Morales-Figueroa, 2012) and an increase in *Giardia* burdens among the patients (Northrop-Clewes et al., 2001; Blackwell et al., 2013). In this context, *in vitro* studies suggest that ABZ-susceptible and

ABZ-resistant *G. duodenalis* trophozoites subpopulations may coexist in culture and continuous exposure to sublethal (e.g., IC₅₀) ABZ concentrations could render not only variant proportions of these subpopulations (Argüello-García et al., 2004) but variations in gene expression (Argüello-García et al., 2009). When ABZ concentration is continuously increased in cultures the surviving parasites may be derived from the selection of drug-resistant trophozoites or by the adaptation of drug-susceptible ones. Thus ABZ resistance in giardiasis is an issue of growing concern for public health. In order to identify and analyze the mechanism(s) involved in ABZ resistance in *G. duodenalis*, cultures able to grow in the presence of 1.35, 8 and 250 μM ABZ [minimal lethal concentration (MLC) of parent WB strain: 0.32 μM] were obtained by continuous exposure of trophozoite subculture under increasing sub-lethal drug concentrations (Argüello-García et al., 2009). Since specific mutations at hot-spot amino acid positions (50, 134, 165, 167, 198, and 200) in β-tubulin were associated with ABZ-resistant helminthic parasites (Venkatesan, 1998), these positions were initially analyzed in ABZ resistant *Giardia* clones; however, no mutations were found at these sites (Argüello-García et al., 2009). Further proteomic and RT-PCR analyses showed a subset of seven genes that were upregulated in the ABZ-resistant clones at the protein and mRNA levels. Some of these genes encoded proteins that are involved in cytoskeletal dynamics (alpha-2-giardin, ran-binding protein), energy metabolism (phosphoglycerate kinase and ornithine carbamoyltransferase) and antioxidant response (NADH oxidase; Paz-Maldonado et al., 2013). These data are consistent with the notion that ABZ not only affects parasite microtubules but also glucose uptake (Vinaud et al., 2008) and the induction of oxidative stress in the parasites (Docampo, 1990; Cvilink et al., 2009a). This stress is likely to play an important role in the drug-resistant phenotype since ABZ may be oxidized by phase I enzymes into sulphonide (ABZ-SO) and sulphone (ABZ-SOO) metabolites that in turn could play a role in the parasite susceptibility or resistance to this drug (Cvilink et al., 2008, 2009b).

In this work we analyzed the pro-oxidant activity of ABZ to assess the production of its metabolites, and to determine the presence and levels of antioxidant components in drug-susceptible and -resistant *G. duodenalis* clones in order to unravel the effector mechanisms involved in ABZ-resistance in this parasite.

Materials and Methods

Trophozoite Cultures

The ABZ-resistant clones able to grow under 1.35, 8, and 250 μM concentrations of this drug were obtained as previously described (Argüello-García et al., 2009). A control culture of an ABZ-susceptible clone grown in the presence of 0.5% v/v dimethylformamide (DMF: vehicle), were used throughout this study. Trophozoites were axenically sub-cultured in 4.5 ml screw-capped vials, tubes or bottles at 37°C in modified Diamond's TYI-S-33 medium (ATCC no. 1404; Keister, 1983). Parasites were harvested at late-log phase by chilling culture tubes on

ice for 30 min, washed three times in phosphate-buffered saline (PBS) pH 7.2, counted in a haemocytometer and adjusted to the required cell density.

Determination of ABZ and ABZ-Metabolite Levels

To assess the conversion of this drug into sulphoxide and sulphone metabolites in ABZ-susceptible and -resistant *G. duodenalis* trophozoites, the intracellular concentration of ABZ species was determined by high performance liquid chromatography (HPLC) in cell lysates obtained at different time periods (0–48 h) after exposure of parasites to ABZ. To standardize this technique, synthetic derivatives of ABZ (sulphoxide, sulphone and amino) and of MBZ were previously analyzed by thin layer chromatography and melting point after dissolving in water:methanol. Then these components were separated (loop: 200 µL) using a mixture of acetonitrile:water at different proportions containing 0.5% v/v acetic acid as mobile phase through a Nucleosil™ C18 column (5 µm particle size, 125 × 4.6 mm) coupled to a binary pump (Waters™ 1525) and a detector with photodiode array (Waters™ 996). In all assays, chromatographic running was carried out for 13-min to separate peaks of each ABZ species and MBZ either in cell-free samples or when added at different concentrations to lysates of non-treated trophozoites. All species were recovered from cell lysates by ethyl acetate extraction followed by solubilisation in methanol/water. The corresponding values of the area under curve (AUC) were analyzed to generate the concentration-AUC calibration curves in which the experimental values of AUCs in lysates from ABZ-treated trophozoites were interpolated. This procedure was used to quantify the intracellular ABZ species. In this assay trophozoites lysates were prepared after incubation of 50×10^6 parasites (ABZ-susceptible and -resistant, previously maintained 5 days in ABZ-free medium) in 15 mL culture tubes in TYI-S-33 medium containing 10 µM ABZ at 37°C for different time periods. Cells were harvested as described above and washed three times with PBS containing 0.2% w/v trichloroacetic acid and three times with PBS alone. After counting parasites cell pellets were resuspended in 180 µL deionized sterile water, frozen at -70°C for 5 min and thawed at 37°C for 5 min and this procedure was carried out five times. Lysates were extracted by adding ethyl acetate (700 µL) and incubating the lysates at 37°C for 45 min. Supernatants were recovered by centrifugation at 750 × g for 10 min and dried under vacuum (SpeedVac™ centrifuge). For HPLC analysis, all the test samples were resuspended in 50 µL ethanol, stirred and mixed with 150 µL of MBZ 10 µM in water as internal standard. Results were expressed as micro-molar concentration of each ABZ species per 1×10^6 trophozoites.

Production of Reactive Oxygen Species (ROS) by Trophozoites Exposed to ABZ

To monitor the induction of oxidative stress in ABZ-exposed *G. duodenalis* trophozoites, the Image-iT™ Live Green ROS detection kit (Molecular Probes™, USA) was used with some

modifications. This assay is based in the non-fluorescent 5-(and-6)-carboxy-2', 7'-dichlorodihydrofluorescein diacetate (carboxy-H₂DCFDA) that penetrates into the live cells, as deacetylated by non-specific intracellular esterases. This compound upon the presence of non-specific ROS generated in the cell (particularly during oxidative stress) is oxidized and it emits bright green fluorescence that is detected by UV light microscopy using standard fluorescein filters. In these assays, 1×10^6 trophozoites were exposed to ABZ for 24 h at 37°C, washed three times with warm PBS, transferred to 1.5 mL microcentrifuge tubes and labeled in suspension by the addition of 300 µL PBS containing 25 µM carboxy-H₂DCFDA for 45 min at 37°C in the darkness. Then cells were washed again with PBS, transferred to 10-mL capped polystyrene tubes and resuspended in 200 µL of this buffer prior to analysis by fluorescence microscopy (microscope Zeiss Axioskop 40) and flow cytometry (flow cytometer Beckman FACScalibur II).

Determination of the Expression and Levels of Antioxidant Elements in ABZ-Susceptible and -Resistant Trophozoites

Proteomic Analyses

Proteomic assays were carried out as previously reported (Paz-Maldonado et al., 2013). In brief, protein extraction was done on 1×10^7 trophozoites that were sonicated in the presence of protease inhibitors (Complete, Roche™, USA); proteins were extracted with acetone-trichloroacetic acid-β-mercaptoethanol and then were precipitated at -20°C overnight. Pellets were washed with ice-cold methanol or acetone, dried and resuspended in IEF buffer containing urea, thiourea, CHAPS, dithiothreitol (DTT), carrier ampholytes pH 3–10 (Amersham Biosciences™, USA) and bromophenol blue. Protein concentrations were quantified using the Lowry assay with bovine serum albumin as a standard. For two-dimensional electrophoresis, 250 µg of protein were loaded on each IPG dry gel strip (13 cm, pH 3–10; Amersham Biosciences™). After isoelectro-focusing, strips were reduced with DTT and alkylated with iodoacetamide. Following slab gel electrophoresis (12.5% acrylamide gels) protein spots were stained with silver nitrate. Three replicate gels were obtained for each clone analyzed. In this study specific protein spots corresponding to antioxidant enzymes namely NADH oxidase (NADHox), peroxiredoxin 1a (PXR1a), flavodiiron protein (FDP) and superoxide reductase (SOR) were analyzed. As a first approach spots corresponding to the expected molecular weight and isoelectric point of these proteins were defined in stained gels. To identify the selected spots, tandem mass spectrometry (MS/MS) was performed using a 3200 Q TRAP™ hybrid spectrometer (Applied Biosystems/MDS Sciex™, Canada) as described before (Paz-Maldonado et al., 2013). Database searching (NCBI-nr) and protein identification were carried out from the MS/MS spectra using the Mascot Software (<http://www.matrixscience.com>, Matrix Science™, UK). For image analysis, stained gels were scanned with LabScan software on Imagescanner and analyzed using the Image Master v 5.0 system (Amersham Biosciences™, USA) according to

manufacturer's protocols. The following criteria for differential protein expression were used: a % volume n-fold > 1.0 of spot was considered as increase of expression or a % volume n-fold < 1.0 of spot was considered as decrease of expression in ABZ-resistant clones as compared to sensitive ones.

mRNA Levels of Antioxidant Enzymes

In order to analyze the relative levels of mRNA expression of each of the aforementioned antioxidant enzymes in ABZ-resistant or -sensitive *G. duodenalis* clones, a standardized retrotranscription-PCR protocol (end point RT-PCR) was used. This technique has already provided data consistent with semi-quantitative proteomics results but with intrinsic higher sensitivity (Paz-Maldonado et al., 2013). RNA was extracted and purified from each culture using the TRIzol reagent (InvitrogenTM) and resulting material was used for cDNA synthesis with the SuperScriptTM III First-Strand Synthesis System (InvitrogenTM) following manufacturer's instructions. To standardize conditions, both RNA and cDNA were quantified by spectrophotometry (Nanodrop model 2000, Thermo ScientificTM, USA). In the PCR reactions, 50 ng cDNA from each clone was amplified using oligonucleotide primer pairs (0.4 μ M each primer) that were designed for test gene loci (*nadhox*, *pxr1a*, *fdp* and *sor*) and reference gene loci (protein disulfide isomerase-1 [*pdi1*] and ubiquitin [*ubiq1*]). Primer sequences and conditions used for primer annealing and amplification are listed in Table 1. In general, primer extension was performed at 72°C for 45 s, except for *nadhox* (1 min), with a final extension step at 72°C for 7 min. After electrophoresis in 2.0% agarose gels, the semi-quantification of amplicons was performed by densitometry using the Image JTM v 1.48 software. The ratio of band intensity (test locus/reference locus) for each ABZ-resistant culture was divided by the corresponding test/reference ratio of the DMF clone to calculate the fold decrease/increase level of expression of each tested gene.

Determination of Free Sulphydryl (R-SH) Pools

The concentration of free thiols in cell lysates from ABZ-resistant and -susceptible clones was determined using an adapted 5,5'-dithio-bis(2-nitrobenzoic acid) (DTNB, Elman's

reagent) method. In this, DTNB reacts with free R-SH groups and releases 2-nitro-5-benzoate which displays a yellowish color with absorbance at $\lambda = 412$ nm (Riddles et al., 1979). Assays were performed in 1 mL-reactions by suspending 1.2×10^7 PBS-washed trophozoites in 900 μ L of 45 mM NaH₂PO₄ at pH 7 and adding 100 μ L of 1.5 mM DTNB (SigmaTM, USA). The mixture was sonicated with six pulses at 12 microns (60% amplitude) with 30 s-intervals until suspension was clear. After incubation at 37°C for 10 min, absorbances were recorded at 412 nm in a SmartSpec 3000 spectrophotometer (BioRadTM, USA). To obtain a calibration curve, lysates were substituted for cysteine (stock = 15.5 mM) and experimental absorbances were interpolated to express results as the micromolar concentration of thiols per 1.2×10^7 trophozoites.

Protein Modeling

The tertiary structure of the antioxidant enzymes assessed in the previous experiments was obtained from amino acid sequences reported in GiardiaDB using the I-Tasser online server (Zhang, 2008; Roy et al., 2010). Sequences in FASTA format were input in I-Tasser which performs structural alignments between query sequences and known templates in the protein databank (PDB) library. This platform retrieves specific parameters for constructed models as the TM score (range: 0–1), an index reflecting the accuracy of alignment for two given structures and considering the root-mean-square-deviation (RMSD) score that indicates a measure of the differences between values predicted by retrieved models and the values observed in PDB templates. As recommended, significant structure alignments when TM > 0.5 were considered. The Cscore (range: -5 to 2) is an index that includes the TM and the RMSD scores and allows to rank the degrees of similarity between two given protein structures.

Statistical Analyses

In all experiments the data obtained in assays using ABZ-resistant and -susceptible clones were quantitatively compared with the least-square method to linearize calibration curves (Microsoft Excel 2010TM) and differences in mean \pm SD values were assessed by the *t*-student test at a significance of $P < 0.05$.

TABLE 1 | Loci used as test and housekeeping genes in reverse transcriptase-PCR assays.

Locus	Orf in GiardiaDB (GL50803)	Forward and reverse primer sequences (5'-3')	Tm (°C)	Product size (bp)	Cycle number
Peroxiredoxin 1a (<i>pxr1a</i>) ^a	16076	AGAACGACCATGGATGCCGTCCCCATCTCTCTCC ATGGTCTTCTGAACGTCT'	55	628	25
NADH Oxidase LTC (<i>nadhox</i>) ^a	33769	GTGACGGAGAGGTATGACAAGGTAGTGGGGCTGGAA GAAAAA	55	1020	20
Flavodiiron protein LTC (<i>fdp</i>) ^a	10358	AGGAATGGCTCTCGTATGACGGTGCTTGCAGTTCA	55	582	25
Superoxide reductase (<i>sor</i>) ^a	GLCHR01	CTTGGCATCACTAAGGAGCTAGAGCTCATGTTCTC	52	175	25
Ubiquitin (<i>ubiq</i>) ^b	7110	GAGCTCATGCAGATCTTCGTCAACCTCTGGATGGAGTAGT	58	190	25
Protein disulfide isomerase-1 (<i>pdi1</i>) ^b	29487	ACTCCTCTGCTCCCTGTGCTCCTCGCTGCTTCAC	55	456	25

^aTest gene; ^bHousekeeping gene; Primer annealing temperature (Tm); Lateral transfer candidate (LTC).

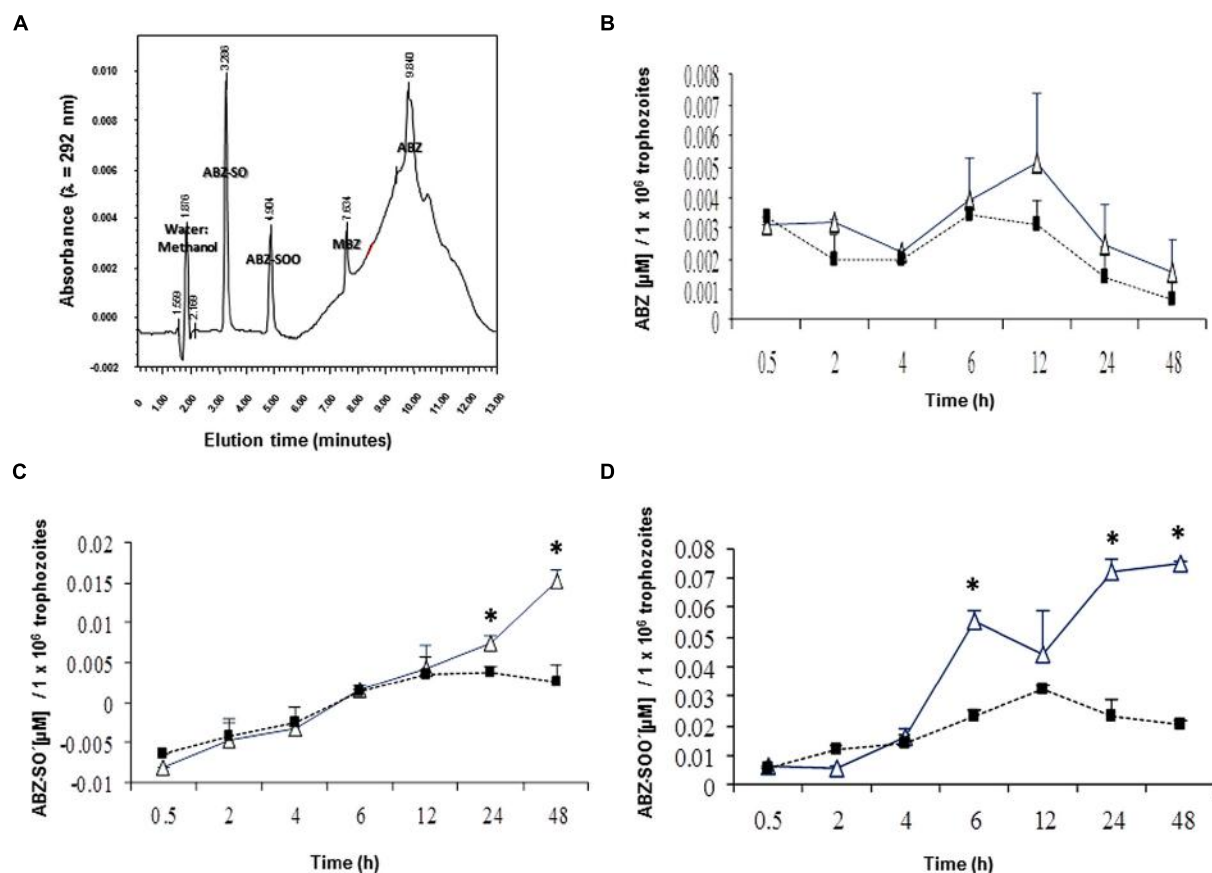


FIGURE 1 | Differential levels of accumulation of ABZ and ABZ metabolites in *Giardia duodenalis* clones susceptible and resistant to ABZ. Trophozoites from ABZ-susceptible clone (WBDMF, open triangles) and a representative ABZ-resistant clone (WBR250, filled squares) were exposed to 10 μ M ABZ for the times indicated in X-axis at 37°C and cell lysates were analyzed by HPLC using MBZ as internal standard. Chromatography assay was

standardized using cell-free mixtures, adjusted to 13-min lasting elutions and each ABZ species was separated at the retention time indicated in the corresponding peak (A). These conditions were used in samples of cell lysates and the AUCs were used to determine the levels of ABZ (B), ABZ-SO (C), and ABZ-SOO (D). Results are the mean \pm SD. of three independent experiments and asterisks indicate statistical difference at $P < 0.05$.

Results

ABZ Metabolites are Differentially Accumulated in *G. duodenalis* Clones Susceptible and Resistant to ABZ

In this study, we initially determined if ABZ is metabolized, i.e., oxidized by *G. duodenalis* trophozoites. The ABZ-SO and ABZ-SOO metabolites were identified using a HPLC protocol standardized to detect the three ABZ species and MBZ as the

internal standard. A discontinuous gradient, starting with 70% water:30% acetonitrile followed by changes in relative proportions of vehicles to 50:50% (at 5 min), 20:80% (at 8 min), 40:60% (at 10 min) and returning to 70:30% (at 11 min), produced an efficient separation of each ABZ species and MBZ (Figure 1A). Under these conditions ABZ species presented maximal emission peaks nearby to 221 and 292 nm (Table 2); of these, samples including cell lysates gave low backgrounds at 292 nm hence quantitative chromatograms were obtained at that λ . In addition, the increasing baseline starting at 6–10 min of elution, peaks at 10 min and drops to initial A_{292} values by 12 min (Figure 1A) was due to the changing proportions of acetonitrile in the mobile phase and not by artifacts from any of tested compounds, especially ABZ and MBZ for which AUCs were obtained considering these changes in baselines. Likewise controls of ABZ and MBZ-free cell lysates showed this changing baseline with the absence of absorbance peaks and the calibration curves rendered reliable quantifications of each drug species ($R^2 \geq 0.97$). Thus, the results showed that ABZ ($[I_0] = 10 \mu\text{M}$) accumulated at varying concentrations by either drug-susceptible (WBDMF) or

TABLE 2 | Experimental time periods of retention and wavelengths of emission of ABZ species and MBZ (internal standard) as determined by HPLC.

Species	Retention time (min)	λ of emission (nm)
ABZSO	3.668 \pm 0.3	221.1 \pm 3.5
ABZSOO	5.201 \pm 0.3	221.2 \pm 2.9
MBZ	7.593 \pm 0.1	221.1 \pm 1.8
ABZ	9.459 \pm 0.5	293.3 \pm 2.4

-resistant (WBRA250) parasites during the first 12 h of exposure and this concentration dropped by 24–48 h (**Figure 1B**). Although these concentrations were consistently higher in the ABZ-susceptible clone from 2 to 48 h, these differences were not statistically significant, which is likely due to the very short time in which ABZ remains unbound or unmodified. This could also explain the lower levels of ABZ detected in cell lysates as compared to ABZ-SO and ABZ-SOO (see scales in Y-axis). On the other hand, the oxidized species ABZ-SO and ABZ-SOO were progressively accumulated by the two clones. However, in the ABZ-resistant clone WBRA250, these species peaked at 12 h and were maintained at similar levels at 24 and 48 h when cells were still viable. At latter times in the WB-DMF clones, an increasing accumulation of ABZ-SO and ABZ-SOO (**Figures 1C,D**) was detected and this was concomitant with generalized cell death.

ABZ Elicits Higher ROS Levels in ABZ-Susceptible Trophozoites

Since ABZ was metabolized into oxidized species, it was of interest to assess if this pro-drug could induce a state of oxidative stress in *G. duodenalis* trophozoites. The use of carboxy-H₂DCF as a fluorescent ROS tracer allowed the detection of

these reactive species by fluorescence microscopy. We observed the distribution of these species in the cytoplasm in the ABZ-susceptible clone (WBDMF), with most cells displaying a punctate pattern (**Figure 2A**). In the cells with altered morphology (a typical effect of ABZ), bright and diffuse fluorescence was observed (**Figure 2A**, arrows). This latter pattern was also seen in some WBDMF trophozoites exposed to *tert*-butyl hydroperoxide (TBHP), which is another ROS-forming compound (arrows in **Figure 2A**) that was included as positive control because unlike ABZ, TBHP does not alter trophozoite morphology. Interestingly, not all the ABZ-resistant clones displayed significant ROS-associated fluorescence (**Figure 2A**) despite the exposure of these clones to ABZ concentrations (1.35, 8, and 250 μ M) that were higher than the one used with the WBDMF clone (0.18 μ M). These observations were corroborated by flow cytometry analyses in which the proportions of fluorescent cells were quantified (**Figure 2B**). In quadrant graphics and histograms, we observed the displacement of cell fluorescence (from R4 to R2 and from left to R1 respectively) in the WBDMF clone exposed to ABZ or TBHP, and the absence of such an effect in the representative clone WBR250. In general up to 30% of WBDMF cells displayed ROS fluorescence

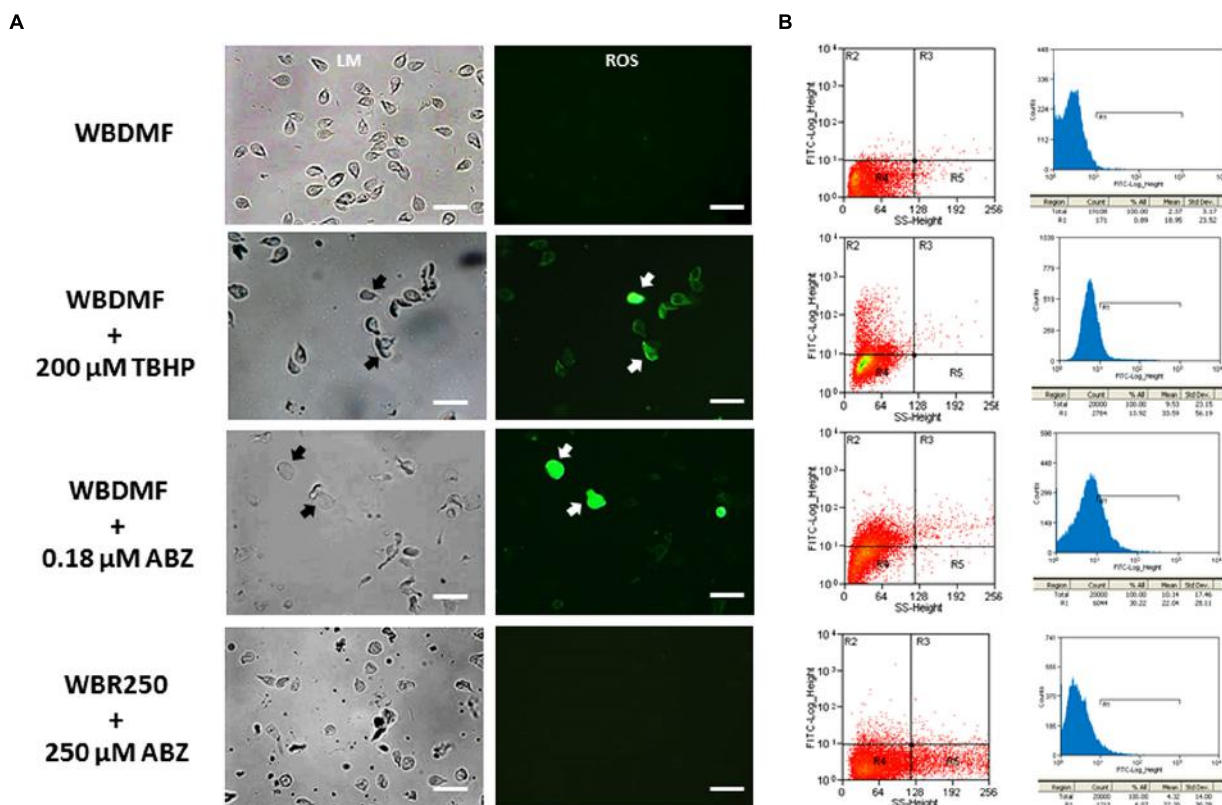


FIGURE 2 | Determination of ROS produced by ABZ exposure in ABZ-susceptible and ABZ-resistant clones. Trophozoites from the ABZ-susceptible clone WBDMF or the representative ABZ-resistant clone WBR250 were exposed to ABZ (test) or TBHP (positive control) at the concentrations indicated at the left for 24 h at 37°C and observed by light microscopy (LM) and cell fluorescence microscopy (ROS; **A**). The same samples

were processed for flow cytometry analysis (**B**) with a window calibrated with fluorescein filters and readings of 20,000 events per sample. Graphs at the left are quadrant-based distributions of cells by size/granularity (X-axis) and fluorescence intensity (Y-axis) and histograms at the right show the quantitative displacement of cell fluorescence. Arrows indicate cells displaying profuse ROS staining. Scale bars: 20 μ m.

while in ABZ-resistant clones this proportion was lower (6–9%).

The Antioxidant Enzymes NADHox and PXR1a are Overexpressed in ABZ-Resistant *G. duodenalis* Trophozoites

Since ABZ was able to induce oxidative stress in ABZ-susceptible *G. duodenalis* trophozoites, we examined the expression levels of some antioxidant enzymes in susceptible and resistant parasites. After two dimensional gel electrophoresis, the intensity of protein spots corresponding to antioxidant enzymes as NADHox, PXR1a, FDP and SOR were evaluated by image analysis, and these regions of the gel were also excised for tandem MS/MS analysis. FDP and SOR were elusive to detection because no reproducible spot was found in gel zones nearby to their expected size and isoelectric point (**Figure 3A**). However, NADHox and PXR1a were unequivocally identified as peptides covering 41% of NADHox and 5.7% of Pxr1a amino acid sequences were determined from MS/MS analysis (score > 50; **Table 2**). When the sequences of these two enzymes were submitted to the I-Tasser server, the retrieved protein models are good quality. For NADHox, the model exhibits high degree of structural alignment (75%) and a low structural difference (6.6 Å) with crystallized analogs contained in PDB. For Pxr1a these parameters were even more defined (90% and 2.8 Å respectively; **Figures 3B,C** respectively). In particular, these giardial molecules display maximal structural identity with bacterial and archaeal template homologs: gNADHox with *Lactobacillus sanfranciscensis* NADHox (PDB entry: 2cdub) and gPxr1a with *Aeropyrum pernix* Pxr (PDB entry: 3a2vA). When protein expression levels were determined, the two enzymes detected displayed spots with higher intensity in all ABZ-resistant clones and the WBR250 exhibited the highest increases. Thus NADHox was overexpressed in the fold range of 2.7–3.1 and for Pxr1a this range was of 1.4–3.2 (**Table 3**). These results suggest that at least two antioxidant enzymes are upregulated at the protein level in ABZ-resistant clones.

mRNAs of Several Antioxidant Enzymes are Upregulated in ABZ-resistant *G. duodenalis* Trophozoites

Although we did not observe protein spots on the 2-D gels corresponding to some antioxidant enzymes, this does not necessarily imply that these proteins are absent since they may be present at cellular levels too low for detection by this method. Thus RT-PCR was used to examine the mRNA levels of the genes encoding the antioxidant enzymes and two normalizer genes (*pdi1* and *ubiq*). As expected all the mRNAs from the aforementioned loci could be amplified under the conditions detailed in **Table 1**. The mRNAs for three out of four antioxidant enzymes analyzed were upregulated in ABZ-resistant clones (**Figure 4**). In the case of *pxr1a* mRNA, the clones WBR1.35 and WBR250 displayed increases (>2-fold) that were slightly higher than the one observed in clone WBR8. The increase for *nadhox* mRNA was more pronounced in the clone WBR1.35 (~6-fold) while the remainder ABZ-resistant clones did not show significant changes. The *fdp* mRNA exhibited an increase as follows: WBR1.35>WBR8>WBR250. In contrast, the *sor* mRNA

did not show significant changes among the clones. Among the ABZ-resistant clones displaying mRNA overexpression in the antioxidant enzymes, the WBR1.35 culture exhibited the highest increases of these mRNAs.

The Antioxidant R-SH Pool Increases in *G. duodenalis* Trophozoites Concomitantly with the Degree of ABZ Resistance

Since the antioxidant repertoire of a cell usually comprises enzymes and low MW thiols (R-SH), we were interested in analyzing the R-SH pool in the ABZ resistance model. The thiol groups are antioxidant moieties localized in monomeric (e.g., cysteine) or oligomeric (e.g., glutathione) amino acids or complex polypeptides that can react with the DTNB reagent. We were able to determine the total free thiol pool in trophozoite lysates using calibration curves with reliable accuracy ($R^2 > 0.95$, **Figure 5A**). Furthermore, it was possible to detect the interaction of DTNB reagent with free intracellular thiols with low backgrounds levels in these assays due to the use of sonication to lyse the cells. In **Figure 5B** are shown the micromolar concentrations of R-SH groups per 1.2×10^7 trophozoites, a cell amount useful to obtain detectable absorbance that could be interpolated in the calibration curves (0.05–0.80). In these assays there were statistically significant increases of R-SH levels in all ABZ-resistant clones as compared to the ABZ-susceptible counterpart. Interestingly, there was an increase in the steady-state R-SH pool levels with increasing ABZ concentrations to which ABZ-resistant cultures were adapted to grow. All together, these data were consistent with the notion that ABZ elicits an antioxidant response in ABZ-resistant trophozoites in which antioxidant enzymes were over-expressed and the increase on the R-SH pools might play an important role in the resistant phenotype.

DISCUSSION

The pathogenic period of giardiasis involves the establishment of trophozoites into the small intestine milieu of susceptible hosts and the attachment of parasites to the intestinal epithelium. To survive in a hostile microenvironment, trophozoites need to cope with potentially cytotoxic factors such as dietary microbicides, digestive enzymes, bile salts, fatty acids, mucus as well as the innate or adaptive elements of the host immune response. In this context, *G. duodenalis* is able to display complex responses including antigenic variation, encystation and secretion of metabolic enzymes and proteases (Ankarklev et al., 2010; Lujan, 2011). However, these processes are usually bypassed when effective antigiardial compounds are used (Harhay et al., 2010; Beech et al., 2011; Andrews et al., 2014) since drugs are preferentially directed against parasitic molecule(s) with crucial function in trophozoite survival.

Drug resistance in helminthic and protozoal species such as benzimidazole- or ABZ-resistance has been recognized as a matter of concern in humans and livestock species. To date, the β -tubulin locus in ABZ-resistant *Giardia* generated by *in vitro*

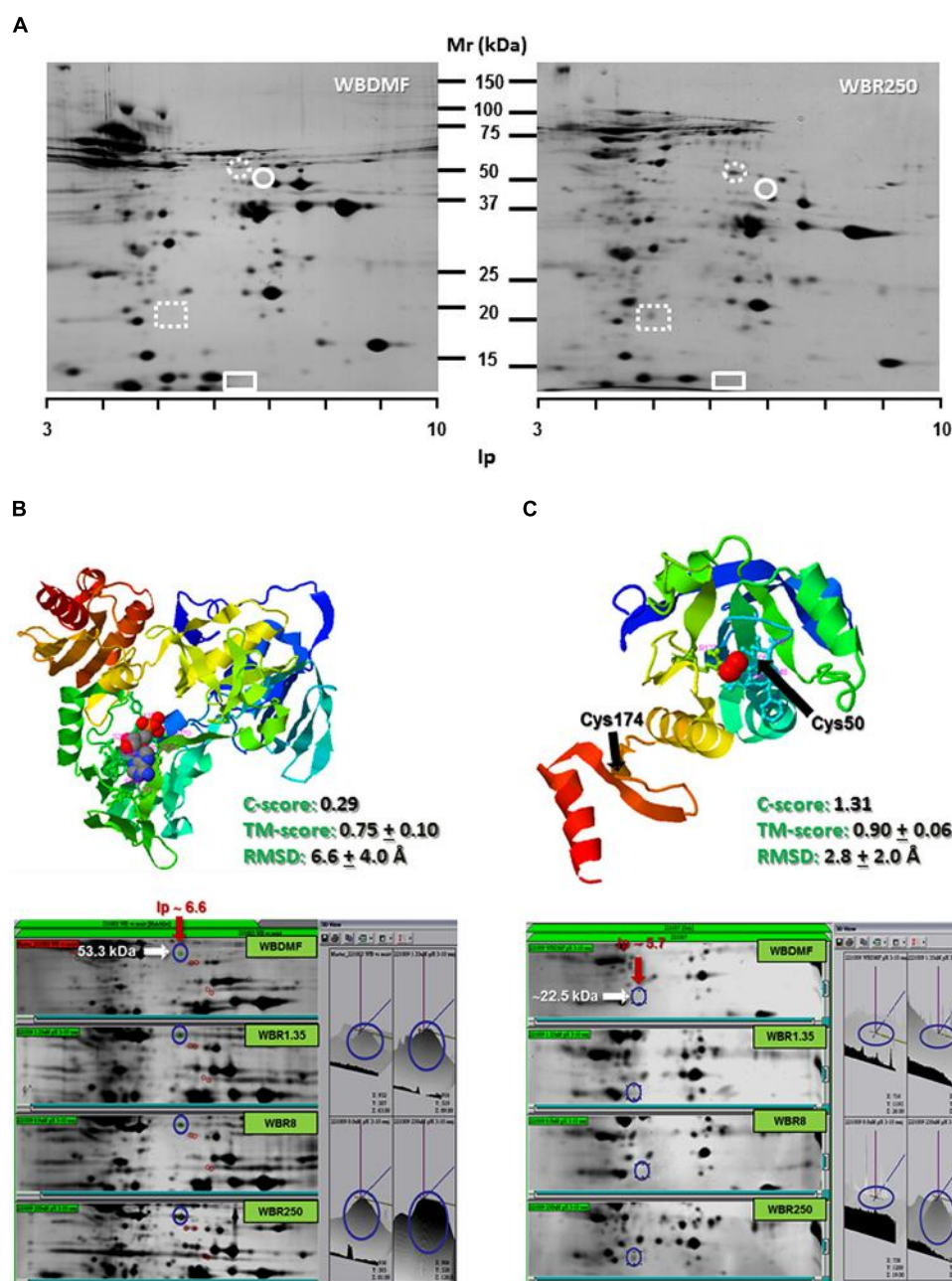


FIGURE 3 | Determination of NADHox and Pxr1a overexpression in ABZ-resistant *G. duodenalis* clones. Trophozoite lysates from clones susceptible (WBDMF) and resistant (WBR1.35, WBR8, and WBR250) to ABZ were separated by two dimensional gel electrophoresis (**A**) and the zones matching the expected molecular weight and isoelectric point of NADHox (dashed circle), FDP (circle), Pxr1a (dashed rectangle) and SOR (rectangle) were

cut and processed by LC-MS/MS. Proteins detected and identified were NADHox (**B**) and Pxr1a (**C**) and the protein model with the scores of quality parameters is shown in the upper panel. The image analyses of protein spots in representative gels of each clone displaying differential peak volumes are shown in the lower panels. Ligands in protein models (ADP for NADHox and peroxide ion for Pxr1a) are shown in ball conformation.

subculture is the most extensively model studied (Upcroft et al., 1996; Argüello-García et al., 2009). Since mutations reported in benzimidazole-resistant helminthes (F167Y, E198A, and F200Y) are absent in the giardial β -tubulin locus, it is likely that other mechanism(s) related to drug transport or metabolism are contributing to the resistant phenotype. ABC like efflux transporters

(e.g., P-glycoprotein, PgP) are unlikely to be involved in ABZ-resistant *Giardia* since this drug, along to MBZ, are not suitable substrates for PgP (Dupuy et al., 2010), and we observed similar kinetics of ABZ accumulation between ABZ-susceptible and -resistant trophozoites in this study (**Figure 1B**). Aside from the direct interaction of ABZ with *G. duodenalis* β -tubulin

TABLE 3 | Determination of protein expression levels of antioxidant enzymes in *G. duodenalis* clones susceptible and resistant to ABZ.

ID of protein spot	ORF in GiardiaDB (GL50803)	Sequence coverage (%)	MW (kDa)	Ip	R1.35/DMF	R8/DMF	R250/DMF	Expression
NADH oxidase	33769	41	51.0	6.68	3.01	2.71	3.10	Overexpressed
Peroxiredoxin 1a	16076	5.7	21.0	5.34	1.42	1.45	3.29	Overexpressed
Flavodiiron protein	10358	ND	46.6 ^a	6.90 ^a	ND	ND	ND	ND
Superoxide reductase	GLCHR01	ND	12.5 ^a	6.28 ^a	ND	ND	ND	ND

^a Theoretical molecular weight (kDa) and isoelectric point (Ip).

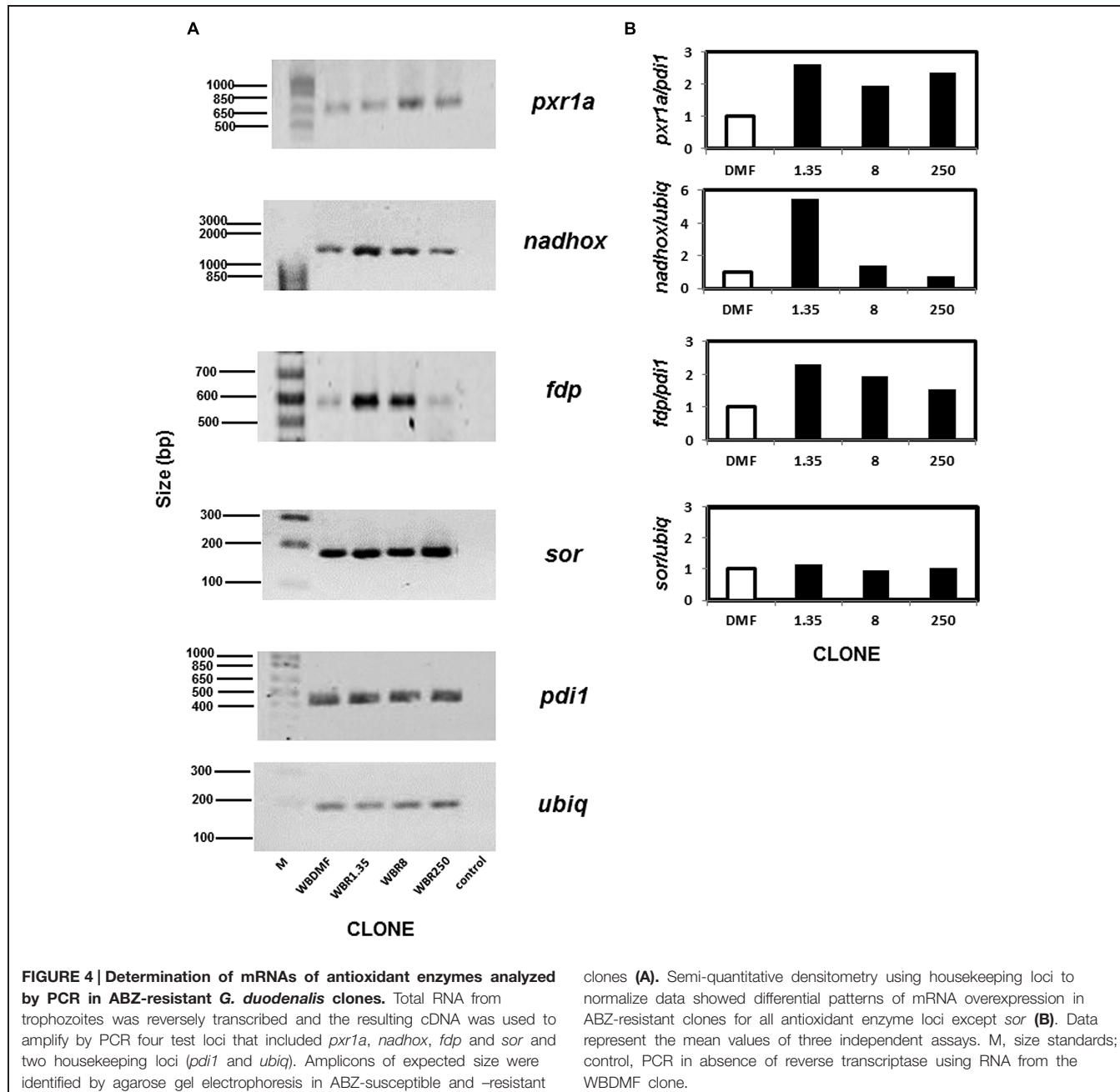
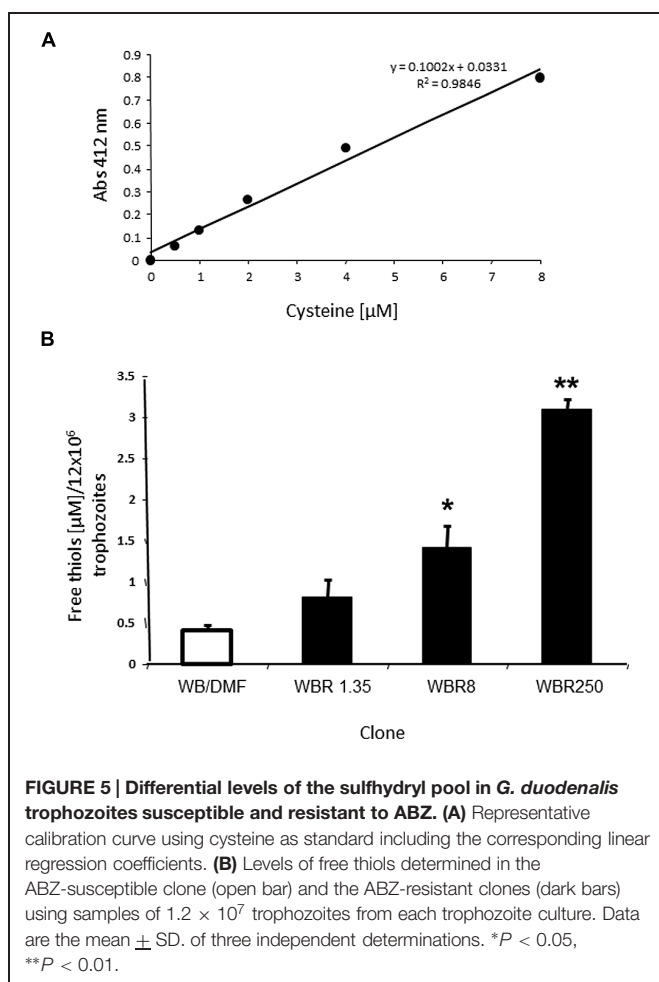


FIGURE 4 | Determination of mRNAs of antioxidant enzymes analyzed by PCR in ABZ-resistant *G. duodenalis* clones. Total RNA from trophozoites was reversely transcribed and the resulting cDNA was used to amplify by PCR four test loci that included *pxr1a*, *nadhox*, *fdp* and *sor* and two housekeeping loci (*pdi1* and *ubiq*). Amplicons of expected size were identified by agarose gel electrophoresis in ABZ-susceptible and -resistant

clones (A). Semi-quantitative densitometry using housekeeping loci to normalize data showed differential patterns of mRNA overexpression in ABZ-resistant clones for all antioxidant enzyme loci except *sor* (B). Data represent the mean values of three independent assays. M, size standards; control, PCR in absence of reverse transcriptase using RNA from the WBDFM clone.

(MacDonald et al., 2004; Aguayo-Ortiz et al., 2013), these observations suggest an additional cytotoxic role of ABZ as pro-drug against this parasite.

During ABZ metabolism, new cytotoxic species are generated that may induce the development of resistance in *Giardia* trophozoites to this drug. ABZ is a xenobiotic component that in living



cells is processed by phase I enzymes (most commonly flavin-containing mono-oxygenases or cytochrome P450-like,) which insert two oxygen atoms in the sulfur atom at the 5-propylthio group of ABZ in a two-step process (Souhaili-El Amri et al., 1988; Moroni et al., 1995; Cvilink et al., 2009a). Cytochrome P450-like gene families (e.g., CYP35) have been identified in helminthes such as *Caenorhabditis elegans* (Menzel et al., 2005), but there are no obvious CYP homologues from searching the GiardiaDB genome database. The resulting sulphoxide (ABZSO) and sulphone (ABZSOO) metabolites still have a parasitcidal effect albeit ABZSO may retain more potency than ABZSOO (Souhaili-El Amri et al., 1988; Bártilová et al., 2010; García-Rodríguez et al., 2012). These oxidized species, particularly ABZSO, have been reportedly detected in several helminthes (Cvilink et al., 2008, 2009a,b; García-Rodríguez et al., 2012; Vokrál et al., 2013). The present study is in agreement with a previous study in which ABZ metabolites were detected in trophozoites by antibody-based microscopy techniques (Oxberry et al., 2000) and confirms that *G. duodenalis* has oxygenases that metabolize both ABZ and ABZSO. Our results that show the greater accumulation of ABZSO and ABZSOO in ABZ-susceptible *Giardia* as compared to its ABZ resistant counterparts (Figures 1C,D), is in agreement with recent studies in *Haemonchus contortus* where the

S-oxidation of ABZ determined by LC-MS/MS was also lower in the resistant BR strain as compared to the susceptible ISE strain (Vokrál et al., 2013). In this context, it is likely that ABZ-resistant parasites have altered rates of drug metabolism aimed to avoid ABZSO/ABZSOO levels reaching the cytotoxic levels observed in ABZ-susceptible ones.

Albendazole could also be cytotoxic by the generation of oxidative stress in parasites. This phenomenon has been suggested to be induced by other anti-parasitic agents (Docampo, 1990). A hallmark of oxidative stress status is the excessive accumulation of ROS such as oxygen (O_2), superoxide anion ($\cdot O_2^-$), peroxide ($\cdot O_2^{2-}$), hydrogen peroxide (H_2O_2), hydroxyl radical ($\cdot OH$), hydroxyl ion (OH^-). These species are a result of endogenous reactions from mitochondrial [superoxide dismutase (SOD)] or membrane-associated (NADPH oxidase and 5-lipoxygenase) enzymes or from exogenous agents (e.g., pollution, radiation and xenobiotics including drugs). Cellular damage provoked by ROS includes oxidative transformation of DNA, protein aminoacids and lipid peroxidation associated to apoptotic or necrotic cell death. The precise pathway of ROS production by ABZ in mammals and parasites is yet unknown, hence a direct participation of ABZSO and ABZSOO cannot be ruled out as these are S-oxidized species. Moreover benzimidazoles are also able to induce or modify the oxidative stress status in the host (Locatelli et al., 2004; Dimitrijević et al., 2012). In *G. duodenalis*, a microaerophilic organism, oxidative stress may be induced using H_2O_2 , drugs (metronidazole) as well as cysteine- and ascorbic acid-depleted media. The damage observed varies according to the inducing agent and include cell cycle blockade, apoptotic-like processes (caspase-independent) and changes in gene expression profiles (Ghosh et al., 2009; Raj et al., 2014). In this study, ABZ induced ROS accumulation in susceptible trophozoites as did hydroperoxide, but ABZ had a more marked effect in cell morphology (Figure 2A). Therefore, the evidence of oxidative damage to DNA, lipids and proteins, as well as the cell death process elicited by ABZ have been addressed by our group (publication in process). Moreover, the production of ABZ metabolites warrants further studies since three of these metabolites have been detected at distinct locations within ABZ-exposed trophozoites (Oxberry et al., 2000). In contrast, oxidative stress was not observed in ABZ-resistant trophozoites (Figures 2A,B), which indicates that an antioxidant response that avoids accumulation of both ABZ metabolites and ROS is associated to the resistant phenotype.

Antioxidant responses are complex but well-orchestrated processes that are evolutionarily conserved from bacteria to higher eukaryotes. These usually involve enzyme systems and molecular antioxidants based on the tripeptide glutathione, single amino acids as cysteine or the R-SH pool that are used to scavenge toxic oxidants and radicals including ROS. *G. duodenalis* belongs to one of the earliest lines of eukaryotic descent and lacks the catalase, SOD, glutathione and glutathione-dependent reductases and peroxidases. However, *Giardia* contains alternative antioxidants such as (a) a NADH oxidase (NADHox) and a FDP (A-type flavoprotein), that can detoxify O_2^- from trophozoites to form water (Brown et al., 1996; Di Matteo et al., 2008); (b) a SOR that converts $\cdot O_2^-$ into H_2O_2 (Testa et al., 2011); (c) 2-cys

peroxiredoxins (Pxr1a and Pxr1b) with ability to detoxify H₂O₂ to form oxygen and water (Mastronicola et al., 2014); and (d) cysteine as the major molecular antioxidant. Based on a *reverse proteomics* (effect-to-cause) strategy to search for the expression of the aforementioned enzymes, two of these enzymes, namely NADHox and Pxr1a, could be detected and were found overexpressed in ABZ-resistant clones. Furthermore, the up-regulation of NADHox, Pxr1a and FDP mRNAs in ABZ-resistant clones suggest that FDP could be overexpressed at the protein level since proteomics and RT-PCR assays gave qualitatively similar results (**Figures 3 and 4**; Paz-Maldonado et al., 2013). The functional significance of changes of expression of antioxidant enzymes (at protein and mRNA levels) could reflect the levels of substrates that are processed by these enzymes, or alternatively, by differences in total catalytical activities between ABZ-susceptible and -resistant trophozoites. In the first scenario, the higher expression of NADHox, Pxr1a and FDP is likely related to a requirement to detoxify O₂ and H₂O₂ under *constitutive* conditions in resistant parasites while ·O₂⁻ levels are not increased under ABZ exposure because SOR mRNA levels were virtually unchanged (**Figure 4**). In the second scenario, the likely increased in the total activity of antioxidant enzymes in ABZ-resistant *Giardia* could be a process associated with resistance to ABZ and other drugs in protozoa and helminthes (Cvilink et al., 2009a; James et al., 2009; Vokál et al., 2013). Collectively, these observations support the notion that ABZ-resistance in *Giardia* is associated with increased (mRNA or protein) levels of antioxidant enzymes that could cope more efficiently with ROS levels generated during ABZ-induced oxidative stress.

The role of the increased R-SH pool in antioxidant responses and drug resistance has been scarcely studied albeit found in mammalian cell lines, fungal and bacterial models (Cantoni et al., 1994; Cánovas et al., 2004; Song et al., 2013). The requirement of *Giardia* for L-cysteine as a major constituent of its R-SH pool is largely known. In ABZ-resistant trophozoites, the increasing thiol pool observed with the increasing degree of ABZ resistance

(**Figure 5**) suggest that another mechanism to scavenge oxidant species generated by ABZ metabolism and/or ROS accumulation besides antioxidant enzymes is present. It is also possible that other drug resistance mechanisms are involved in this phenomenon, such as a higher expression or activity of transporters for antioxidant molecules as L-cysteine.

Taken together, the results from this work emphasize the presence of ABZ biotransforming systems in *G. duodenalis* and the association of increased levels of antioxidant elements (enzymes and R-SH pool) with an efficient antioxidant response in ABZ-resistant trophozoites to avoid accumulation of ABZ metabolites and ROS. This antioxidant response is carried out mostly by archaeal or bacterial-like molecules present in this parasite. Nevertheless it is not expected to be ABZ-specific since peroxiredoxins have been shown upregulated in trophozoites transfected with vectors for neomycin or puromycin selection (Su et al., 2007) and NADHox displayed higher activity in furazolidone-resistant cultures (Brown et al., 1998). Future studies on the regulation of the activity of antioxidant enzymes and the R-SH pool will provide additional insights on the molecular basis underlying ABZ resistance in this parasite and also for drug development in giardiasis.

Acknowledgments

Authors are grateful to Janet Yee for her help in reviewing the English language, Blanca E. Herrera-Ramírez and Isabel Torres for their helpful technical assistance, QFB Víctor Hugo Rosales-García (Unit of Flow Cytometry, CINVESTAV) for his valuable assistance in obtaining and analyzing flow cytometry data and Dr. Rafael Castillo (Facultad de Química-UNAM) for his support to carry out HPLC assays. We are also grateful to Arturo Pérez-Taylor for informatics assistance. LMTPZ was recipient of a post-doctoral fellowship from CINVESTAV-IPN. This work was partially supported by Conacyt Grant N° 49724-M.

References

- Abboud, P., Lemée, V., Gargala, G., Brasseur, P., Ballet, J. J., Borsig-Lebas, F., et al. (2001). Successful treatment of metronidazole- and albendazole-resistant giardiasis with nitazoxanide in a patient with acquired immunodeficiency syndrome. *Clin. Infect. Dis.* 15, 1792–1794. doi: 10.1086/320751
- Adam, R. D. (2001). Biology of *Giardia lamblia*. *Clin. Microbiol. Rev.* 14, 447–475. doi: 10.1128/CMR.14.3.447-475.2001
- Aguayo-Ortiz, R., Méndez-Lucio, O., Romo-Mancillas, A., Castillo, R., Yépez-Mulia, L., Medina-Franco, J. L., et al. (2013). Molecular basis for benzimidazole resistance from a novel β-tubulin binding site model. *J. Mol. Graph. Model.* 45, 26–37. doi: 10.1016/j.jmgm.2013.07.008
- Andrews, K. T., Fisher, G., and Skinner-Adams, T. S. (2014). Drug repurposing and human parasitic protozoan diseases. *Int. J. Parasitol. Drugs Drug Resist.* 24, 95–111. doi: 10.1016/j.ijpddr.2014.02.002
- Ankarklev, J., Jerlström-Hultqvist, J., Ringqvist, E., Troell, K., and Svärd, S. G. (2010). Behind the smile: cell biology and disease mechanisms of *Giardia* species. *Nat. Rev. Microbiol.* 8, 413–422. doi: 10.1038/nrmicro2317
- Argüello-García, R., Cruz-Soto, M., Romero-Montoya, L., and Ortega-Pierres, G. (2004). Variability and variation in drug susceptibility among *Giardia duodenalis* isolates and clones exposed to 5-nitroimidazoles and benzimidazoles in vitro. *J. Antimicrob. Chemother.* 54, 711–721. doi: 10.1093/jac/dkh388
- Argüello-García, R., Cruz-Soto, M., Romero-Montoya, L., and Ortega-Pierres, G. (2009). In vitro resistance to 5-nitroimidazoles and benzimidazoles in *Giardia duodenalis*: variability and variation in gene expression. *Infect. Genet. Evol.* 9, 1057–1064. doi: 10.1016/j.meegid.2009.05.015
- Bártiková, H., Vokál, I., Skálová, L., Lamka, J., and Szotáková, B. (2010). In vitro oxidative metabolism of xenobiotics in the lancet fluke (*Dicrocoelium dendriticum*) and the effects of albendazole and albendazole sulphoxide ex vivo. *Xenobiotica* 40, 593–601. doi: 10.3109/00498254.2010.497565
- Beech, R. N., Skuce, P., Bartley, D. J., Martin, R. J., Prichard, R. K., and Gillearde, J. S. (2011). Anthelmintic resistance: markers for resistance, or susceptibility? *Parasitology* 138, 160–174. doi: 10.1017/S0031182010001198
- Blackwell, A. D., Martin, M., Kaplan, H., and Gurven, M. (2013). Antagonism between two intestinal parasites in humans: the importance of coinfection for infection risk and recovery dynamics. *Proc. Biol. Sci.* 280, 20131671. doi: 10.1098/rspb.2013.1671
- Brasseur, P., and Favenne, L. (1995). Two cases of giardiasis unsuccessfully treated by albendazole. *Parasite* 2, 422.
- Brown, D. M., Upcroft, J. A., Edwards, M. R., and Upcroft, P. (1998). Anaerobic bacterial metabolism in the ancient eukaryote *Giardia duodenalis*. *Int. J. Parasitol.* 28, 149–164. doi: 10.1016/S0020-7519(97)00172-0
- Brown, D. M., Upcroft, J. A., and Upcroft, P. A. (1996). H₂O-producing NADH oxidase from the protozoan parasite *Giardia duodenalis*. *Eur. J. Biochem.* 241, 155–161. doi: 10.1111/j.1432-1033.1996.0155t.x

- Busatti, H. G., Santos, J. F., and Gomes, M. A. (2009). The old and new therapeutic approaches to the treatment of giardiasis: where are we? *Biologics* 3, 273–287.
- Cánovas, D., Vooijs, R., Schat, H., and de Lorenzo, V. (2004). The role of thiol species in the hypertolerance of *Aspergillus* sp. P37 to arsenic. *J. Biol. Chem.* 279, 51234–51240. doi: 10.1074/jbc.M408622200
- Canton, O., Sestili, P., Guidarelli, A., and Cattabeni, F. (1994). Development and characterization of hydrogen peroxide-resistant Chinese hamster ovary (CHO) cell variants—II. Relationships between non-protein sulphydryl levels and the induction/stability of the oxidant-resistant phenotype. *Biochem. Pharmacol.* 47, 1258–12561. doi: 10.1016/0006-2952(94)90398-0
- Cvilink, V., Lamka, J., and Skalova, L. (2009a). Xenobiotic metabolizing enzymes and metabolism of anthelmintics in helminths. *Drug Metab. Rev.* 41, 8–26. doi: 10.1080/03602530802602880
- Cvilink, V., Szotáková, B., Krizová, V., Lamka, J., and Skalová, L. (2009b). Phase I biotransformation of albendazole in lancet fluke (*Dicrocoelium dendriticum*). *Res. Vet. Sci.* 86, 49–55. doi: 10.1016/j.rvsc.2008.05.006
- Cvilink, V., Skalova, L., Szotakova, B., Lamka, J., Kostiainen, R., and Ketola, R. A. (2008). LC-MS-MS identification of albendazole and flubendazole metabolites formed ex vivo by *Haemonchus contortus*. *Anal. Bioanal. Chem.* 391, 337–343. doi: 10.1007/s00216-008-1863-9
- Di Matteo, A., Scandurra, F. M., Testa, F., Forte, E., Sarti, P., Brunori, M., et al. (2008). The O₂-scavenging flavodiron protein in the human parasite *Giardia intestinalis*. *J. Biol. Chem.* 283, 4061–4068. doi: 10.1074/jbc.M705605200
- Dimitrijević, B., Borozan, S., Katić-Radivojević, S., and Stojanović, S. (2012). Effects of infection intensity with *Strongyloides papilliferus* and albendazole treatment on development of oxidative/nitrosative stress in sheep. *Vet. Parasitol.* 186, 364–375. doi: 10.1016/j.vetpar.2011.11.017
- Docampo, R. (1990). Sensitivity of parasites to free radical damage by antiparasitic drugs. *Chem. Biol. Interact.* 73, 1–27. doi: 10.1016/0009-2797(90)90106-w
- Dupuy, J., Alvinerie, M., Ménez, C., and Lespine, A. (2010). Interaction of anthelmintic drugs with P-glycoprotein in recombinant LLC-PK1-mdrl1 cells. *Chem. Biol. Interact.* 186, 280–286. doi: 10.1016/j.cbi.2010.05.013
- Ekdahl, K., and Andersson, Y. (2005). Imported giardiasis: impact of international travel, immigration, and adoption. *Am. J. Trop. Med. Hyg.* 72, 825–830.
- Escobedo, A. A., Almirall, P., Robertson, L. J., Franco, R. M., Hanevik, K., Mørch, K., et al. (2010). Giardiasis: the ever-present threat of a neglected disease. *Infect. Disord. Drug Targets* 10, 329–348. doi: 10.2174/187152610793180821
- Escobedo, A. A., and Cimerman, S. (2007). Giardiasis: a pharmacotherapy review. *Expert Opin. Pharmacother.* 8, 1885–1902. doi: 10.1517/14656566.8.1.2185
- García-Rodríguez, J. J., Del Vegas-Sánchez, M. C., Torrado-Durán, J. J., and Bolás-Fernández, F. (2012). Enantiomeric pharmacokinetic prevalence of (+) albendazole sulphoxide in *Trichinella spiralis* muscle larvae. *Parasitol. Res.* 110, 993–999. doi: 10.1007/s00436-011-2586-y
- Ghosh, E., Ghosh, A., Ghosh, A. N., Nozaki, T., and Ganguly, S. (2009). Oxidative stress-induced cell cycle blockage and a protease-independent programmed cell death in microaerophilic *Giardia lamblia*. *Drug Des. Devel. Ther.* 21, 103–110. doi: 10.2147/DDDT.S5270
- Harhay, M. O., Horton, J., and Olliaro, P. L. (2010). Epidemiology and control of human gastrointestinal parasites in children. *Expert Rev. Anti-Infect. Ther.* 8, 219–234. doi: 10.1586/eri.09.119
- James, C. E., Hudson, A. L., and Davey, M. W. (2009). Drug resistance mechanisms in helminths: is it survival of the fittest? *Trends Parasitol.* 25, 328–335. doi: 10.1016/j.pt.2009.04.004
- Keister, D. B. (1983). Axicen culture of *Giardia lamblia* in TYI-S-33 medium supplemented with bile. *Trans. R. Soc. Trop. Med. Hyg.* 77, 487–488. doi: 10.1016/0035-9203(83)90120-7
- Kollaritsch, H., Jeschko, E., and Wiedermann, G. (1993). Albendazole is highly effective against cutaneous larva migrans but not against *Giardia* infection: results of an open pilot trial in travellers returning from the tropics. *Trans. R. Soc. Trop. Med. Hyg.* 87, 689. doi: 10.1016/0035-9203(93)90296-3
- Locatelli, C., Pedrosa, R. C., De Bem, A. F., Creczynski-Pasa, T. B., Cordova, C. A., and Wilhelm-Filho, D. (2004). A comparative study of albendazole and mebendazole-induced, time-dependent oxidative stress. *Redox Rep.* 9, 89–95. doi: 10.1179/135100004225004751
- Lujan, H. D. (2011). Mechanisms of adaptation in the intestinal parasite *Giardia lamblia*. *Essays Biochem.* 51, 177–191. doi: 10.1042/bse0510177
- MacDonald, L. M., Armon, A., Thompson, A. R., and Reynoldson, J. A. (2004). Characterisation of benzimidazole binding with recombinant tubulin from *Giardia duodenalis*, *Encephalitozoon intestinalis*, and *Cryptosporidium parvum*. *Mol. Biochem. Parasitol.* 138, 89–96. doi: 10.1016/j.molbiopara.2004.08.001
- Mastronicola, D., Falabella, M., Testa, F., Pucillo, L. P., Teixeira, M., Sarti, P., et al. (2014). Functional characterization of peroxiredoxins from the human protozoan parasite *Giardia intestinalis*. *PLoS Negl. Trop. Dis.* 8:e2631. doi: 10.1371/journal.pntd.0002631
- Menzel, R., Rodel, M., Kulas, J., and Steinberg, C. E. (2005). CYP35: xenobiotically induced gene expression in the nematode *Caenorhabditis elegans*. *Arch. Biochem. Biophys.* 438, 93–102. doi: 10.1016/j.abb.2005.03.020
- Mørch, K., Hanevik, K., Robertson, L. J., Strand, E. A., and Langeland, N. (2008). Treatment-ladder and genetic characterisation of parasites in refractory giardiasis after an outbreak in Norway. *J. Infect. Dis.* 56, 268–73. doi: 10.1016/j.jinf.2008.01.013
- Moroni, P., Buronfosse, T., Longin-Sauvageon, C., Delatour, P., and Benoit, E. (1995). Chiral sulfoxidation of albendazole by the flavin adenine dinucleotide-containing and cytochrome P450-dependent monooxygenases from rat liver microsomes. *Drug Metab. Dispos.* 23, 160–165.
- Nash, T. E., Ohl, C. A., Thomas, E., Subramanian, G., Keiser, P., and Moore, T. A. (2001). Treatment of patients with refractory giardiasis. *Clin. Infect. Dis.* 33, 22–28. doi: 10.1086/320886
- Northrop-Clewes, C. A., Rousham, E. K., Mascie-Taylor, C. N., and Lunn, P. G. (2001). Anthelmintic treatment of rural Bangladeshi children: effect on host physiology, growth, and biochemical status. *Am. J. Clin. Nutr.* 73, 53–60.
- Olson, M. E., Ceri, H., and Morck, D. W. (2000). *Giardia* vaccination. *Parasitol. Today* 16, 213–217. doi: 10.1016/S0169-4758(99)01623-3
- Oxberry, M. E., Reynoldson, J. A., and Thompson, R. C. (2000). The binding and distribution of albendazole and its principal metabolites in *Giardia duodenalis*. *J. Vet. Pharmacol. Ther.* 23, 113–120. doi: 10.1046/j.1365-2885.2000.00254.x
- Parkison, A. J., Evengard, B., Semenza, J. C., Ogden, N., Børresen, M. L., Berner, J., et al. (2014). Climate change and infectious diseases in the Arctic: establishment of a circumpolar working group. *Int. J. Circumpolar Health* 73:25163. doi: 10.3402/ijch.v73.25163
- Paz-Maldonado, L. M. T., Argüello-García, R., Cruz-Soto, M., Mendoza-Hernández, G., and Ortega-Pierres, G. (2013). Proteomic and transcriptional analyses of genes differentially expressed in *Giardia duodenalis* clones resistant to albendazole. *Infect. Genet. Evol.* 15, 10–17. doi: 10.1016/j.meegid.2012.08.021
- Quihui-Cota, L., and Morales-Figueroa, G. G. (2012). Persistence of intestinal parasitic infections during the national de-worming campaign in schoolchildren of northwestern Mexico: a cross-sectional study. *Ann. Gastroenterol.* 25, 57–60.
- Raj, D., Ghosh, E., Mukherjee, A. K., Nozaki, T., and Ganguly, S. (2014). Differential gene expression in *Giardia lamblia* under oxidative stress: significance in eukaryotic evolution. *Gene* 535, 131–139. doi: 10.1016/j.gene.2013.11.048
- Riddles, P. W., Blakeley, R. L., and Zerner, B. (1979). Ellman's reagent: 5,5'-dithiobis(2-nitrobenzoic acid)—a reexamination. *Anal. Biochem.* 94, 75–81. doi: 10.1016/0003-2697(79)90792-9
- Roy, A., Kucukural, A., and Zhang, Y. (2010). I-TASSER: a unified platform for automated protein structure and function prediction. *Nat. Protoc.* 5, 725–738. doi: 10.1038/nprot.2010.5
- Savioli, L., Smith, H., and Thompson, A. (2006). *Giardia* and *Cryptosporidium* join the “Neglected Diseases Initiative.” *Trends Parasitol.* 22, 203–208. doi: 10.1016/j.pt.2006.02.015
- Song, M., Husain, M., Jones-Carson, J., Liu, L., Henard, C. A., and Vázquez-Torres, A. (2013). Low-molecular-weight thiol-dependent antioxidant and antinitrosative defences in *Salmonella* pathogenesis. *Mol. Microbiol.* 87, 609–622. doi: 10.1111/mmi.12119
- Souhaili-El Amri, H., Mothe, O., Totis, M., Masson, C., Batt, A. M., Delatour, P., et al. (1988). Albendazole sulfonation by rat liver cytochrome P-450c. *J. Pharmacol. Exp. Ther.* 246, 758–764.
- Su, L. H., Lee, G. A., Huang, Y. C., Chen, Y. H., and Sun, C. H. (2007). Neomycin and puromycin affect gene expression in *Giardia lamblia* stable transfection. *Mol. Biochem. Parasitol.* 156, 124–135. doi: 10.1016/j.molbiopara.2007.07.015

- Testa, F., Mastronicola, D., Cabelli, D. E., Bordi, E., Pucillo, L. P., Sarti, P., et al. (2011). The superoxide reductase from the early diverging eukaryote *Giardia intestinalis*. *Free Radic. Biol. Med.* 51, 1567–1574. doi: 10.1016/j.freeradbiomed.2011.07.017
- Upcroft, J., Mitchell, R., Chen, N., and Upcroft, P. (1996). Albendazole resistance in *Giardia* is correlated with cytoskeletal changes but not with a mutation at amino acid 200 in beta-tubulin. *Microb. Drug Resist.* 2, 303–308. doi: 10.1089/mdr.1996.2.303
- Upcroft, P. (1998). Drug resistance in *Giardia*: clinical versus laboratory isolates. *Drug Resist. Updat.* 1, 166–168. doi: 10.1016/S1368-7646(98)80035-6
- Venkatesan, P. (1998). Albendazole. *J. Antimicrob. Chemother.* 41, 145–147. doi: 10.1093/jac/41.2.145
- Vinaud, M. C., Ferreira, C. S., Lino Rde, S. Jr., and Bezerra, J. C. (2008). *Taenia crassiceps*: energetic and respiratory metabolism from cysticerci exposed to praziquantel and albendazole in vitro. *Exp. Parasitol.* 120, 221–226. doi: 10.1016/j.exppara.2008.07.008
- Vokřál, I., Jirásko, R., Stuchlíková, L., Bártíková, H., Szotáková, B., Lamka, J., et al. (2013). Biotransformation of albendazole and activities of selected detoxification enzymes in *Haemonchus contortus* strains susceptible and resistant to anthelmintics. *Vet. Parasitol.* 196, 373–381. doi: 10.1016/j.biortech.2013.06.105
- Watkins, R. R., and Eckmann, L. (2014). Treatment of giardiasis: current status and future directions. *Curr. Infect. Dis. Rep.* 16, 396. doi: 10.1007/s11908-014-0396-y
- Zhang, Y. (2008). I-TASSER server for protein 3D structure prediction. *BMC Bioinformatics* 9:40. doi: 10.1186/1471-2105-9-40

Conflict of Interest Statement: The authors declare that the research was conducted in the absence of any commercial or financial relationships that could be construed as a potential conflict of interest.

Copyright © 2015 Argüello-García, Cruz-Soto, González-Trejo, Paz-Maldonado, Bazán-Tejeda, Mendoza-Hernández and Ortega-Pierres. This is an open-access article distributed under the terms of the Creative Commons Attribution License (CC BY). The use, distribution or reproduction in other forums is permitted, provided the original author(s) or licensor are credited and that the original publication in this journal is cited, in accordance with accepted academic practice. No use, distribution or reproduction is permitted which does not comply with these terms.

Albendazole induces oxidative stress and DNA damage in the parasitic protozoan *Giardia duodenalis*

Rodrigo Martínez-Espinosa¹, Raúl Argüello-García¹, Emma Saavedra² and Guadalupe Ortega-Pierres^{1*}

¹ Departamento de Genética y Biología Molecular, Centro de Investigación y de Estudios Avanzados del Instituto Politécnico Nacional, México City, Mexico, ² Department of Biochemistry, Instituto Nacional de Cardiología Ignacio Chávez, México City, Mexico

OPEN ACCESS

Edited by:

Anjan Debnath,
University of California, San Diego,
USA

Reviewed by:

Nigel Yarlett,
Pace University, USA
Tomoyoshi Nozaki,
National Institute of Infectious
Diseases, Japan

*Correspondence:

Guadalupe Ortega-Pierres,
Departamento de Genética y Biología
Molecular, Centro de Investigación y
de Estudios Avanzados del Instituto
Politécnico Nacional, Avenue Instituto
Politécnico Nacional 2508, San Pedro
Zacatenco, 07360 México City,
Mexico
gortega@cinvestav.mx

Specialty section:

This article was submitted to
Antimicrobials, Resistance
and Chemotherapy,
a section of the journal
Frontiers in Microbiology

Received: 13 March 2015

Accepted: 22 July 2015

Published: 06 August 2015

Citation:

Martínez-Espinosa R, Argüello-García R, Saavedra E and Ortega-Pierres G (2015) Albendazole induces oxidative stress and DNA damage in the parasitic protozoan *Giardia duodenalis*. *Front. Microbiol.* 6:800.
doi: 10.3389/fmicb.2015.00800

The control of *Giardia duodenalis* infections is carried out mainly by drugs, among these albendazole (ABZ) is commonly used. Although the cytotoxic effect of ABZ usually involves binding to β -tubulin, it has been suggested that oxidative stress may also play a role in its parasiticidal mechanism. In this work the effect of ABZ in *Giardia* clones that are susceptible or resistant to different concentrations (1.35, 8, and 250 μ M) of this drug was analyzed. Reactive oxygen species (ROS) were induced by ABZ in susceptible clones and this was associated with a decrease in growth that was alleviated by cysteine supplementation. Remarkably, ABZ-resistant clones exhibited partial cross-resistance to H_2O_2 , whereas a *Giardia* H_2O_2 -resistant strain can grow in the presence of ABZ. Lipid oxidation and protein carbonylation in ABZ-treated parasites did not show significant differences as compared to untreated parasites; however, ABZ induced the formation of 8OHdG adducts and DNA degradation, indicating nucleic acid oxidative damage. This was supported by observations of histone H2AX phosphorylation in ABZ-susceptible trophozoites treated with 250 μ M ABZ. Flow cytometry analysis showed that ABZ partially arrested cell cycle in drug-susceptible clones at G2/M phase at the expense of cells in G1 phase. Also, ABZ treatment resulted in phosphatidylserine exposure on the parasite surface, an event related to apoptosis. All together these data suggest that ROS induced by ABZ affect *Giardia* genetic material through oxidative stress mechanisms and subsequent induction of apoptotic-like events.

Keywords: *Giardia duodenalis*, albendazole, oxidative stress, DNA damage, apoptosis

Introduction

Giardia duodenalis is an intestinal parasitic protozoan that causes the infection known as giardiasis which affects about 280 million people around the world; 500,000 new cases are reported each year (Lane and Lloyd, 2002; Plutzer et al., 2010). This parasite is orally transmitted by the ingestion of infective cysts. Once in the host's stomach excystation occurs and trophozoites emerge. At the duodenum the parasites replicate and colonize this portion of the intestine. Subsequently trophozoites are transported by peristalsis to the jejunum and the ileum where encystation takes place and mature cysts are expelled in the stool (Ankarklev et al., 2010; Watkins and Eckmann, 2014). The infection can be asymptomatic or present several clinical manifestations ranging from mild to severe symptoms that include diarrhea, steatorrhea, post-prandial epigastric pain, anorexia,

bloating, and flatulence (Rossignol et al., 2012; Nash, 2013). Some infected patients may develop a chronic infection with recurrent diarrhea, steatorrhea, malabsorption, weight loss, and poor growth in children (Plutzer et al., 2010; Watkins and Eckmann, 2014).

The control of this infection is mainly carried out by treatment with chemotherapeutic agents. Among the drugs used are components that belong to 5-nitroimidazoles (e.g., metronidazole) and benzimidazoles (e.g., albendazole) derivatives. Other drugs prescribed against *Giardia* include nitazoxanide, furazolidone, paromomycin, and quinacrine (Tejman-Yarden and Eckmann, 2011; Watkins and Eckmann, 2014). Among these drugs albendazole (ABZ) is given in massive chemotherapy interventions against helminths based on its relative safety, high efficacy, broad spectrum against helminths, and low cost (Rossignol, 2010; Watkins and Eckmann, 2014). Further ABZ has been used against *Giardia*, particularly when metronidazole refractory cases occur (Lemée et al., 2000; Solaymani-Mohammadi et al., 2010). The side effects of this drug are rare but in some cases anorexia, constipation and neutropenia have been reported (Dayan, 2003). The use of ABZ is contraindicated during pregnancy due to possible teratogenic effects, although such effects have not been entirely confirmed (Gardner and Hill, 2001; Dayan, 2003).

In pharmacokinetic studies it has been determined that after its absorption, ABZ is oxidized to its metabolites, sulphoxide and sulphone, by cytochrome P450 and/or by flavin-dependent oxidases (Dayan, 2003). The production of these metabolites has been reported in *Giardia* after ABZ exposure (Oxberry et al., 2000; Argüello-García et al., 2015). It has also been reported that in helminths and fungi ABZ selectively binds to four β -tubulin sites, preventing its polymerization and affecting microtubule stability which in turn inhibits mobility and transport of molecules within the microorganism (Robinson et al., 2004; Diawara et al., 2013; Watkins and Eckmann, 2014). In helminths, ABZ-resistant parasites harbor *hot-spot* mutations in β -tubulin encoding different amino acids, particularly at glutamate 198 and phenylalanine 200 (Rossignol, 2010; Diawara et al., 2013; Hansen et al., 2013). In *Giardia*, it has been established that *hot-spot* amino acid mutations in β -tubulin are absent (Upcroft et al., 1996; Argüello-García et al., 2009) suggesting that the induction of ABZ-resistant phenotypes involves different mechanisms.

Regarding ABZ resistance in *Giardia*, it has been reported that resistant trophozoites display morphological changes, particularly in the median body, despite the conserved amino acid residues at positions 198 and 200 in β -tubulin (Chavez et al., 1992; Upcroft et al., 1996; Argüello-García et al., 2009). On the other hand, chromosomal rearrangements have been documented in ABZ-treated parasites, although there is no evidence of a gene or group of genes that may be affected during ABZ resistance in this parasite (Upcroft and Upcroft, 2001). Previous studies by our group suggest that diverse metabolic mechanisms may be involved in the ABZ resistance in *Giardia* that could include components of antioxidant and energy metabolism as well as cytoskeletal changes in the parasite (Paz-Maldonado et al., 2013).

In this context, recent reports have suggested a direct relationship between the use of ABZ and oxidative stress. In

a report in which ABZ was administered to rats in various doses and times, oxidative stress was elicited particularly in hepatocytes (Locatelli et al., 2004). Other studies have also shown the ability of ABZ to induce oxidative stress in sheep liver (Dimitrijević et al., 2012), and ABZ consumption may be correlated with liver damage in humans (Nandi and Sarkar, 2013). In *Dicrocoelium dendriticum*, a fluke of veterinary and human health importance, an increase in antioxidant enzyme activity after ABZ exposure was identified (Bártiková et al., 2010). However, no reports on oxidative damage due to ABZ in other parasites are available.

To determine in more detail the mode of action of ABZ in *Giardia*, in this work we have assessed the induction of oxidative stress by ABZ in *G. duodenalis* trophozoites by monitoring reactive oxygen species (ROS) formation. Results identified ABZ-induced oxidative stress in this protozoan. Oxidative damage to the parasite's DNA is associated with cell cycle arrest and apoptosis. The consequences of this stress and its possible relationship to ABZ resistance in *Giardia* are discussed.

Materials and Methods

Trophozoite Cultures, Growth of ABZ-Resistant Clones and Obtention of H₂O₂-Resistant Trophozoites

Giardia duodenalis trophozoites of the WB strain (ATCC#30957) and ABZ-resistant clones were maintained in TYI-S-33 medium supplemented with 10% adult bovine serum (HyClone) and antibiotic/antimycotic solution (Thermo, USA) at 37°C (Keister, 1983) in 4.5 mL screw-capped vials. ABZ-resistant trophozoites were selected by continuous subculture under increasing sub-lethal concentrations of ABZ (Sigma cat. A-4673). When parasites were adapted to each increase of drug concentration, cultures were cloned by limiting dilution using the corresponding ABZ concentration (Paz-Maldonado et al., 2013). Trophozoites were sub-cultured twice a week under the continuous presence of drug (for ABZ-resistant clones) and for the ABZ-sensitive clones only in the presence of the vehicle (N, N-dimethylformamide; DMF, Sigma). To obtain the H₂O₂-resistant parasites (ROX), trophozoites were selected by continuous subculture under increasing sub-lethal concentrations of H₂O₂ (Sigma, USA). Vials containing trophozoites were refilled to three-quarter capacity and H₂O₂-resistant parasites were cultured as described above for ABZ-resistant *Giardia*. Stock solutions (0.01–25 mM) of ABZ in DMF or DMF alone were used in all assays. Oxidative stress was induced by exposing the parasites to 100 μ M H₂O₂ and these cultures were used as positive controls (Raj et al., 2013).

Determination of Trophozoite Growth

Trophozoite growth was assessed by the fluorescent tracer SYTOX Green according to the manufacturer's instructions (Invitrogen, USA). Briefly, trophozoites were washed three times in phosphate buffered saline (PBS) then suspended in lysis buffer (6% SDS, 10 mM HEPES) using a Vortex shaker for 10 s. A stock solution of SYTOX Green (5 mM) was added in a 1:5 v/v ratio and incubated for 10 min in the dark. The standard

growth curve was obtained using variable numbers of lysed trophozoites and absorbance values of each sample from non-treated and treated trophozoites were determined in 96-well, black-bottomed microtiter plates using a FACSCalibur reader fitted with 504/525 nm excitation/emission filters (Gerphagnon et al., 2013). Negative control absorbance values were obtained from wells with no cells.

Detection of Reactive Oxygen Species (ROS) in Trophozoites Incubated with ABZ or H₂O₂

Albendazole-sensitive trophozoites were incubated with ABZ (1.35, 8, and 250 μ M), Dimethylformamide (DMF referred as vehicle) or H₂O₂ (100 μ M) as control for oxidative stress, for 16 h at 37°C. ROS formation was assessed by Image-IT LIVE Green Reactive Oxygen Species Detection Kit™ according to manufacturer's instructions (Life Technologies, USA). After incubation, trophozoites were washed in PBS and suspended in 25 μ M 6-carboxy-2',7'-dichlorodihydrofluorescein diacetate (carboxy-H₂DCFDA) at 37°C for 30 min. Then Hoechst 33342 was added at a final concentration of 1 μ M for 5 min. Cell fluorescence signals were detected at the end of the incubation period in a Beckman FACSCalibur Flow Cytometer or in an optical microscope using the BD FACSComp software.

Determination of Cross-Resistance to ABZ and H₂O₂ and Protection by Cysteine

The cross resistance between ABZ and H₂O₂ was evaluated using the ABZ-resistant and H₂O₂-resistant clones mentioned above. The ABZ-resistant clones (R1.35, R8, R250) were exposed to 0, 25, 50, 75, and 100 μ M H₂O₂ for 24 h at 37°C. Cell number was determined by SYTOX Green. Resistance to ABZ was determined in ROX (H₂O₂-resistant) parasites which were exposed to 0.05, 0.1, 0.2, 0.4, and 0.8 μ M of ABZ for 24 h at 37°C. In control cultures, ABZ or H₂O₂ were not added. Cell number was also determined using SYTOX Green. For cysteine protection assays, ABZ-sensitive trophozoites were grown in TYI-S-33 medium supplemented with different concentrations of cysteine (0.5, 1, 2, or 4 mM). Then, trophozoites were incubated in the presence of 0.2 μ M ABZ for 48 h at 37°C. Cell growth was determined by SYTOX Green as indicated above.

Detection of Protein Carbonylation and Lipid Peroxidation

Albendazole-sensitive trophozoites were incubated with DMF, ABZ (1.35, 8, and 250 μ M) or H₂O₂ (100 μ M) for 24 h at 37°C. Protein carbonylation was determined using a commercial kit (Protein Carbonyl Assay, Cayman Chemical, USA). Trophozoites were washed with PBS, suspended in lysis solution (50 mM MES, 1 mM EDTA at pH 7.4) and lysed by three cycles of freezing-thawing followed by centrifugation at 10,000 $\times g$ for 10 min. Subsequently the protein was derivatized with dinitrophenylhydrazine (DNPH) for 60 min in the dark, the reaction was stopped with 20% trichloroacetic acid and samples were centrifuged at 10,000 $\times g$ for 10 min. Then the samples were washed three times with ethanol/ethyl acetate solution. Finally, the proteins were suspended in guanidine hydrochloride and the absorbance was determined at 450 nm (Krisko and Radman,

2010). The concentration of protein in the soluble fraction was determined by absorbance at 280 nm.

For lipid peroxidation determination, after incubation with compounds or vehicle a solution of 1-methyl-2-phenylindole in a mixture of acetonitrile/methanol (3:1) was added to trophozoite homogenates. For malondialdehyde (MDA) determination, the reaction was initiated by adding HCl to a 37% v/v final concentration and for the 4-hydroxyneonal (HNE) assay methanesulfonic acid and FeCl₃ at 34 μ M (final concentration each) were used. The absorbance at 586 nm was measured upon incubation of the reaction mixture at 45°C for 40 min. For each series of assays, the absorbance of a control containing water instead of a sample was always subtracted. For each assay homogenate, a control sample in which the reagent was replaced by acetonitrile/methanol (3:1, v/v) was included. A standard curve of trimethoxypropane was used in all assays (Gérard-Monnier et al., 1998; Orozco-Ibarra et al., 2007).

Detection of DNA Fragmentation

Albendazole-sensitive trophozoites were incubated with different concentrations of ABZ (1.35, 8 and 250 μ M), DMF or H₂O₂ (100 μ M) for 24 h at 37°C, then washed twice in PBS 1X and incubated overnight at 42°C in a lysis solution (10 mM Tris-HCl, pH 7.4, 10 mM EDTA, 150 mM NaCl, 0.4% sodium dodecyl sulfate, and 200 μ g/mL proteinase K). RNA was removed by incubating samples with 20 mg/mL RNase A at 37°C for 30 min. The lysate was treated with phenol/chloroform (1:1) and nucleic acids were precipitated at -20°C with 0.3 M sodium acetate pH 7 and ethanol. After quantification, the extent of DNA fragmentation was analyzed by electrophoresis on 1% agarose/ethidium bromide gels (Ghosh et al., 2009).

Detection of Oxidative DNA Damage

DNA damage was assessed by immunofluorescence with an anti-8-hydroxydeoxyguanosine (8OHdG) monoclonal antibody (Santa Cruz Technologies, USA). ABZ-sensitive trophozoites treated with DMF, different concentrations of ABZ (1.35, 8, and 250 μ M) or H₂O₂ (100 μ M) for 16 h at 37°C were incubated for 1 h at 37°C on poly-L-lysine-coated (2 mg/ml) coverslips, rinsed twice with PBS and fixed with a solution of methanol:acetone (1:1 v/v) at -20°C. Fixed cells were treated with 0.05 N HCl for 5 min on ice, rinsed with PBS and washed with PBS containing 35, 50, and 75% ethanol consecutively for 3 min each time. DNA was denatured *in situ* with 0.15 N NaOH in 70% ethanol for 4 min. The precipitate was rinsed twice with PBS and incubated with 0.2 μ g/ml Hoechst dye for 10 min. Subsequently parasites were washed with PBS containing 75, 50, and 35% ethanol consecutively in the presence of 4% formaldehyde for 2 min each time. The samples were incubated in trypsin solution (49.5 mM Tris base, 1 mM EDTA, 150.7 mM Na₂HPO₄, 14.9 mM K₂HPO₄, 0.1% trypsin at pH 7.2) for 10 min at 37°C and washed three times with PBS. Trophozoites were then incubated for 30 min with 1% bovine serum albumin (BSA) to block nonspecific binding and incubated with mouse monoclonal anti- 8-OHdG for 1 h. After a wash with PBS, cells were incubated for 1 h at room temperature with goat anti-mouse IgG coupled to FITC (Santa Cruz Technologies, USA). Samples were analyzed using a

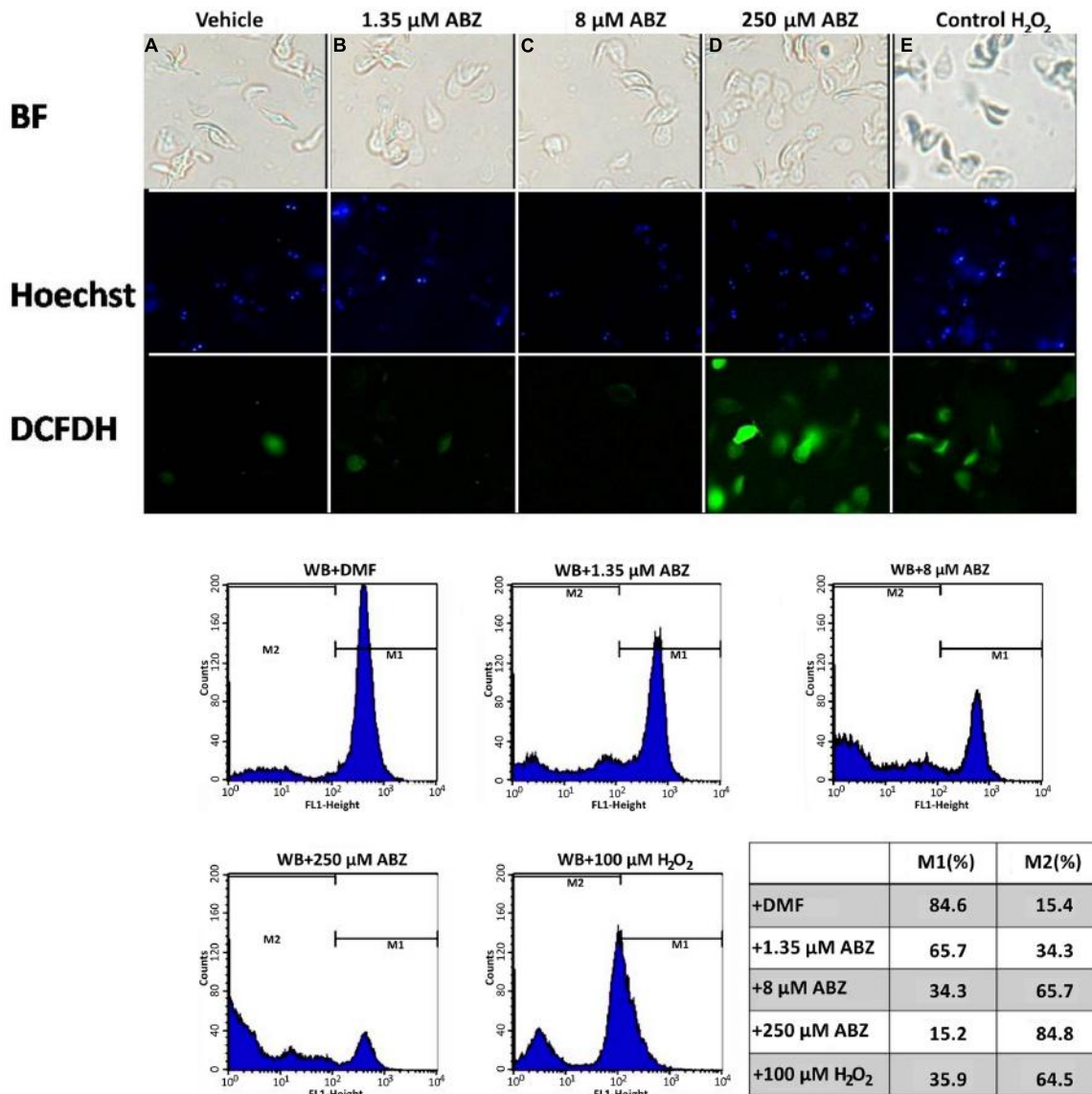


FIGURE 1 | Reactive oxygen species (ROS) are produced in *Giardia duodenalis* trophozoites exposed to Albendazole (ABZ). ABZ-sensitive *Giardia* strain (WB) was exposed to vehicle (DMF, **A**) and to 1.35 μ M (**B**), 8 μ M (**C**), or 250 μ M (**D**) of ABZ for 8 h at 37°C, then DCFDH was added to monitor ROS production. In these experiments a control of intracellular ROS production was included. In this WB trophozoites were incubated with 100 μ M H₂O₂ (**E**). Trophozoites micrographs are as follows: top panels bright field (BF), middle panel trophozoites' nuclei stained with Hoechst and lower panel trophozoites

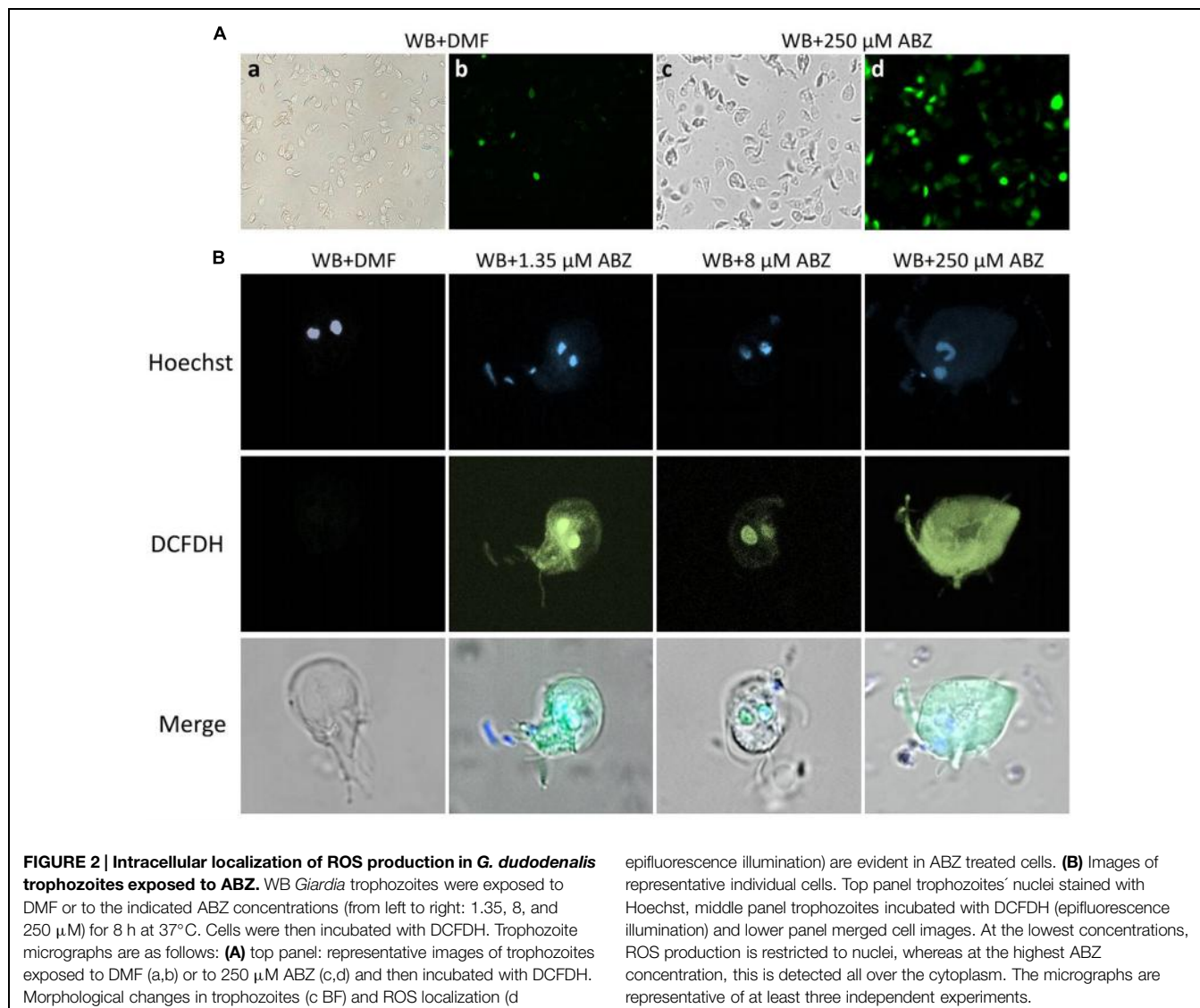
stained with DCFDH. The cells showed increased ROS production by ABZ treatment in comparison to control cells with no drug. Bottom panels are ROS production monitored by flow cytometry, the shift of fluorescence in X axis indicates ROS production by live trophozoites (determined by Trypan blue exclusion) at the highest ABZ concentration. The table shows population percent in M1 (negative to ROS) and M2 (positive to ROS) according to flow cytometry data. Micrographs are from representative results of at least three experiments performed with independent batch cultures.

Zeiss microscope equipped with epifluorescence illumination as previously described (Suzuki et al., 2006).

Detection of Protein-MDA Adducts and H2AX Phosphorylation by Western Blot

Both protein-MDA adducts and histone H2AX phosphorylation (at ser139) were evaluated by Western blot assays using specific antibodies. In these, ABZ-sensitive trophozoites were incubated with DMF, different concentrations of ABZ (1.35, 8, and 250 μ M)

or H₂O₂ (100 μ M) for 24 h at 37°C, washed with PBS three times and suspended in lysis buffer. Twenty microgram of protein were analyzed by SDS-PAGE in 12% acrylamide gels for the protein-MDA assay and in 15% acrylamide gels for detection of H2AX phosphorylation. After electrophoresis, gels were transferred to nitrocellulose membranes. Membranes were blocked with PBS containing 0.1% Tween-20 and 1% skim milk for 2 h at 37°C. After washing with Tris-buffered saline (TBS) membranes were incubated with rabbit anti-MDA (Abcam, USA)



and rabbit anti-H2AX (Millipore, USA) antibodies for 1 h at room temperature under constant shaking. Membranes were washed and incubated with horseradish peroxidase-conjugated mouse anti-rabbit IgG (Thermo, USA). Chemiluminescence detection was performed with the Amersham ECL detection kit according to manufacturer's instructions (Hofštetrová et al., 2010; Moore et al., 2013).

Identification and Quantification of Apoptotic and Necrotic Cells

The cells undergoing apoptotic or necrotic processes after ABZ- or H₂O₂ exposure were analyzed by flow cytometry in which fluorescence by annexin V binding (green) and propidium iodide (PI) uptake (red) were quantified. Positioning of quadrants on annexin V/PI dot plots was analyzed according to the following pattern: living cells (annexin V-/PI-), early apoptotic/primary apoptotic cells (annexin V+/PI-), late apoptotic/secondary apoptotic cells (annexin V+/PI+) and necrotic cells (annexin

V-/PI+). The assay was carried out using the Annexin V-FITC Apoptosis Detection Kit (BioVision, USA) following the manufacturer's instructions. Briefly, cells were incubated with DMF, different concentrations of ABZ (1.35, 8, and 250 μ M) or H₂O₂ (100 μ M) for 24 h. Then, trophozoites were centrifuged at 440 \times g at 4°C and suspended in 500 μ l of 1X binding buffer. Cells were then incubated with 5 μ l of annexin V-FITC and 5 μ l of PI (50 μ g/ml) for 5 min in the dark at room temperature. The FITC and PI fluorescence was measured with a FACS Calibur Flow Cytometer equipped with an FL-1 filter (530 nm) and an FL-2 filter (585 nm), respectively, in at least 10,000 events (Ghosh et al., 2009) in each experiment.

Determination of Cell Cycle Stages in *G. duodenalis* Trophozoites Exposed to ABZ

To determine the proportions of trophozoites at the different cycle stages, nuclear staining with PI was coupled to flow cytometry. In brief, ABZ-sensitive trophozoites were exposed to

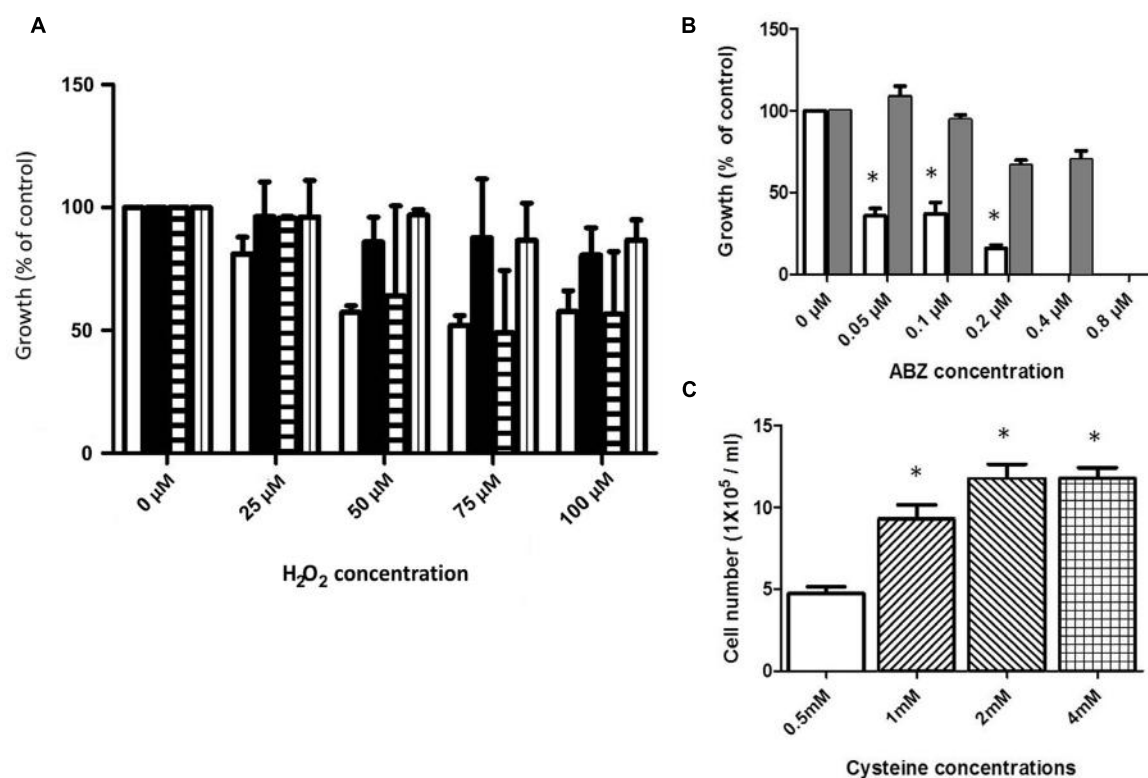


FIGURE 3 | Cross-resistance to ABZ and H₂O₂ and cysteine (Cys) protection in trophozoites exposed to ABZ. **(A)** Cross-resistance to H₂O₂ was evaluated in the ABZ-resistant clones R1.35 (black bars), R8 (horizontal lined bars), and R250 (vertical lined bars) previously obtained in our group (Paz-Maldonado et al., 2013). Parasites were exposed to the indicated H₂O₂ concentrations for 24 h and the cell number was determined by SYTOX Green. As control, wild type WB strain (white bars) was incubated with the indicated H₂O₂ concentration. **(B)** Cross-resistance to ABZ in a H₂O₂-resistant *G. duodenalis*. A H₂O₂-resistant Giardia strain (ROX) was obtained by sub-culturing the WB strain in increasing H₂O₂ concentration for 6 months. Control WB (white bars) and ROX (gray bars) trophozoites were exposed to the indicated increasing ABZ concentrations for 24 h and the cell number was determined using the

fluorescent tracer SYTOX Green. The ROX strain showed cross-resistance to ABZ. **(C)** Cysteine protection of *Giardia* trophozoites exposed to ABZ. WB trophozoites were incubated in growth medium with 0.5 mM (white bar), 1 mM (lined up to the right bar), 2 mM (lined up to the left bar), or 4 mM (boxed bar) of cysteine for 24 h and then trophozoites were further incubated with 0.2 μM ABZ for 48 h. In all graphs the results are the mean ± SD of at least three independent experiments. In graphs **(B,C)** * indicates $p \leq 0.05$ by ANOVA and Tukey's analysis in which values obtained with WB trophozoites were compared with values obtained in ROX trophozoites exposed to the different ABZ concentrations **(B)**. **(C)** Values obtained in WB trophozoites treated with 0.5 mM cysteine were compared to values obtained in WB trophozoites treated with different cysteine concentrations and then exposed to ABZ.

different concentrations of ABZ (1.35, 8, and 250 μM) for 4 h at 37°C, washed with PBS and fixed 30 min with 70% ethanol in PBS. Then cells were washed again and incubated in PBS containing 0.1 mg/mL RNAase overnight at 4°C. Finally cell pellets were washed, stained with PI (1 μM in PBS), washed and resuspended in small volume (200–300 μL) for analysis in a FACS Calibur Flow Cytometer in at least 10,000 events per sample. The histogram areas were identified as reported by Reaume et al. (2013).

Statistical Analyses

All the data were obtained from at least three experiments and where indicated the results are expressed as mean ± SD. Inter-group variation was assessed by one-way analysis of variance (ANOVA) followed by Tukey's multiple comparison test. Statistical significance was determined if $p \leq 0.05$.

Results

Intracellular ROS Formation

In some reports using animal models ABZ was shown to produce oxidative damage (Locatelli et al., 2004; Bártiková et al., 2010). In *G. duodenalis* oxidative stress damage has been induced using pro-oxidant compounds such as H₂O₂ (Ghosh et al., 2009; Raj et al., 2013) in which intracellular ROS formation hallmarks this phenomenon. ABZ-exposed parasites showed greater ROS signals than parasites not exposed to the drug (**Figure 1**, top panels). The effect was mainly detected at the highest ABZ concentration tested (250 μM), however, ROS formation could be determined by flow cytometry at lower concentrations (**Figure 1**, bottom panels).

To determine the localization of intracellular ROS formation within the trophozoites confocal microscopy was used. In these experiments the typical altered morphology caused by

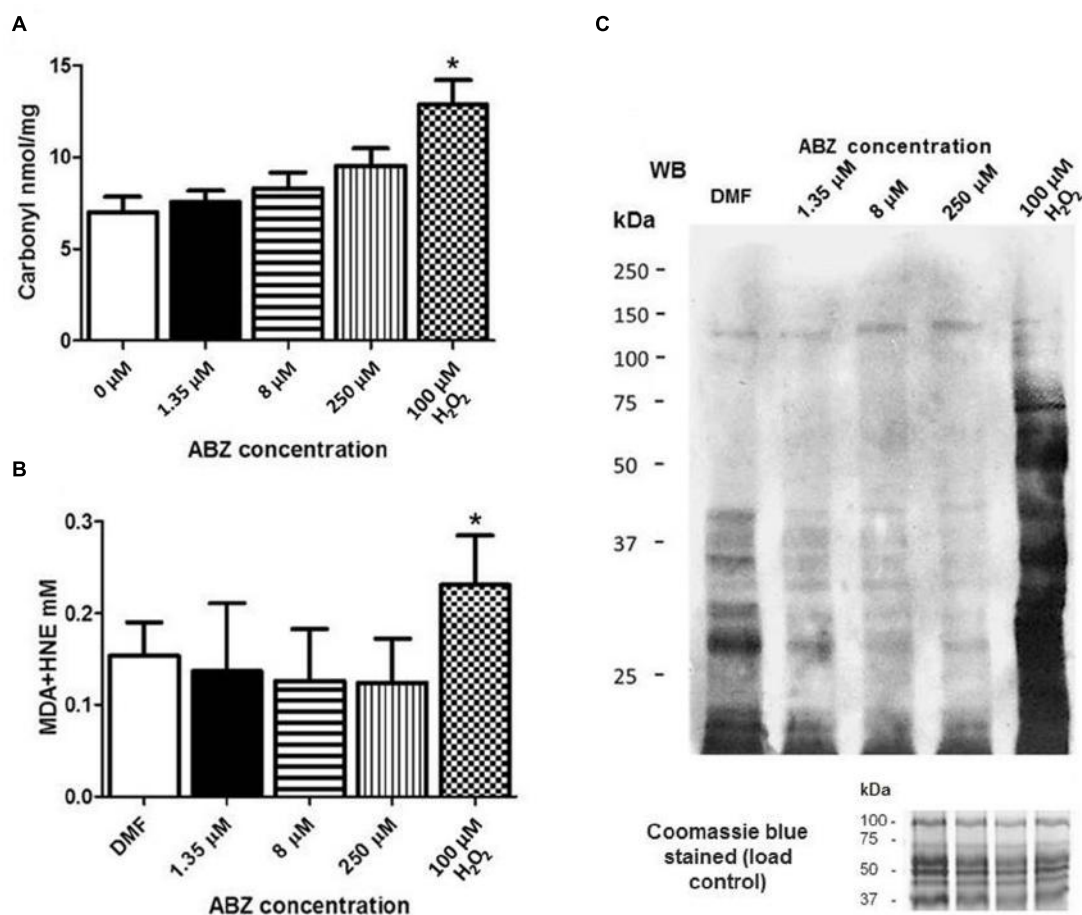


FIGURE 4 | Oxidative damage to proteins in *G. duodenalis* trophozoites exposed to ABZ. (A) Protein carbonylation in *G. duodenalis* ABZ-sensitive trophozoites (WB) exposed to ABZ. Parasites were exposed to vehicle (DMF white bars) or to different ABZ concentrations (1.35 μM black bars; 8 μM horizontal lined bars; 250 μM vertical lined bars) for 16 h at 37°C. Control WB trophozoites were exposed to direct ROS damage with 100 μM H₂O₂ (white and black boxes). Proteins from each sample were obtained and were derivatized with DNPH for protein carbonylation determination. DNP-protein adducts were detected by absorbance at 450 nm. **(B)** Lipoperoxidation in trophozoites exposed to ABZ. After

trophozoites were exposed to the different ABZ concentrations as indicated in **(A)**. HNE or MDA were determined by absorbance at 586 nm. The values in **(A,B)** are the mean ± SD. *p ≤ 0.05 by ANOVA and Tukey's analysis in which values obtained with trophozoites treated with the different ABZ concentrations were compared to values obtained with the DMF treated parasites. **(C)** MDA-protein adducts were detected by Western blot in the same trophozoite samples treated with the indicated ABZ concentrations using rabbit anti-MDA antibodies. At the bottom of panel **(C)** the Coomassie blue stained gel is included and shows that similar protein amounts of each sample were loaded.

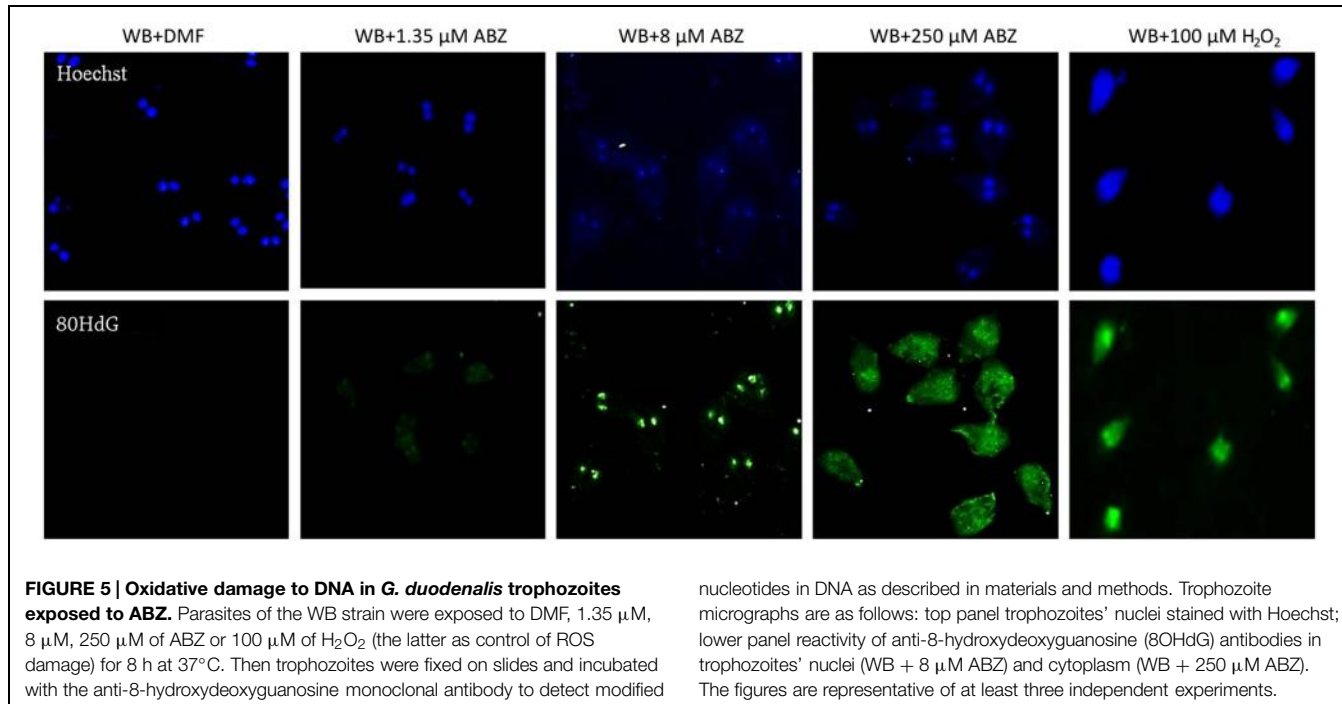
benzimidazoles (Paz-Maldonado et al., 2013) was observed in ABZ-treated trophozoites (**Figure 2A** top panel c). In these cells ROS formation was also evident in most cells as determined by fluorescent staining (**Figure 2A** top panel d). When individual cells were observed the trophozoites' nuclei were determined as the primary site of ROS formation (**Figure 2B**) as judged by fluorescent staining at low ABZ concentrations used (1.35 μM and 8 μM). At the highest drug concentration used (250 μM) there was a widespread distribution of ROS throughout the trophozoite cytoplasm (**Figure 2B** middle panel).

Cross Resistance to ABZ and H₂O₂ in *Giardia* Trophozoites

The ABZ-resistant clones, namely R1.35, R.8, and R.250 (Argüello-García et al., 2009; Paz-Maldonado et al., 2013)

were used to determine whether cross-resistance to classical oxidative stressor (H₂O₂) and ABZ was induced in the resistant trophozoites. For this purpose the ABZ-resistant clones were incubated under increasing concentrations of H₂O₂, and cell growth was determined. In general the resistant clones R1.35 and R.250 showed a tendency to increased resistance to H₂O₂-induced death in comparison to the ABZ-susceptible WB strain (**Figure 3A**). A special case is the R8 resistant strain which frequently behave, in this and other studies, as a "transition state" between low and high ABZ resistance depending on the parameter that is evaluated (see also **Figure 6A**; Argüello-García et al., 2009; Paz-Maldonado et al., 2013).

Resistance to H₂O₂ was achieved by using continuous trophozoite subcultures under increasing concentrations of H₂O₂. Following this procedure for approximately 6 months, a



strain displaying resistance to 75 μ M H_2O_2 was obtained (ROX). This strain was incubated in the presence of ABZ showing a significantly higher growth rate as compared with the H_2O_2 -susceptible WB strain (Figure 3B).

Cysteine Increases Tolerance to ABZ in the Drug Treated Trophozoites

Giardia duodenalis possesses a bacterial-like antioxidant metabolism in which cysteine is the major antioxidant thiol instead of glutathione. To test if increased levels of extracellular cysteine may confer increased tolerance to the drug in ABZ-susceptible trophozoites, these clones were incubated in culture media containing different cysteine concentrations and subsequently ABZ at 0.2 μ M was added and after 48 h-incubation trophozoite growth was measured. As a result, parasites incubated at cysteine concentrations higher than 1 mM showed higher growth after ABZ exposure than those incubated at lower concentrations of this amino acid (Figure 3C). These results suggest that cysteine may help to contend the ROS damage upon ABZ exposure.

Damage to Biomolecules after ABZ Exposure in *G. duodenalis* Trophozoites

The formation of intracellular ROS may trigger oxidative damage to various biomolecules such as proteins, lipids, and DNA. Protein carbonylation was determined in ABZ-sensitive trophozoites exposed to increasing ABZ concentrations. As can be seen in Figure 4A, a consistent but not statistically significant increase in protein carbonylation correlated with the increase in drug concentration, confirming the presence of oxidative damage by ABZ treatment in cellular proteins of *G. duodenalis*.

The levels of lipid peroxidation in healthy cells are maintained under controlled limits but these can be affected, i.e., increased, when cells are treated with pro-oxidant xenobiotics. This process leads to the formation of some intermediates such as MDA and HNE. The determination of such intermediates was carried out after ABZ exposure of drug-sensitive trophozoites. In both cases there was not a significant change in ABZ-treated parasites as compared with untreated cultures contrary to the drug susceptible clones exposed to H_2O_2 used as a control (Figure 4B). This observation was further corroborated using antibodies detecting MDA-protein adducts which displayed more intense staining only when drug susceptible trophozoites were exposed to H_2O_2 (Figure 4C).

Oxidative damage to DNA by ABZ treatment was determined by immunocytochemistry assays using antibodies against 8-OHdG. In these, a significant increase in intranuclear staining, denoting 8-OHdG-containing DNA in ABZ-treated cells was observed (Figure 5). At the highest drug concentrations used (250 μ M) the fluorescent signal was observed in nucleus and the entire cytosol displayed a diffuse pattern with a punctuated pattern in some regions within the trophozoites (Figure 5).

Characterization of DNA Damage in *G. duodenalis* Trophozoites Induced by ABZ

From the previous observations we concluded that ABZ caused a preferential oxidative damage at the DNA level over other biomolecules which could be severe as judged by the extra nuclear 8OHdG detection at higher ABZ concentrations. To assess damage to DNA integrity, genomic DNA was purified from control and ABZ-exposed trophozoites and analyzed in agarose gels to assess its integrity (presence of a high-sized band) or partial/total degradation. As shown in Figure 6A, genomic DNA

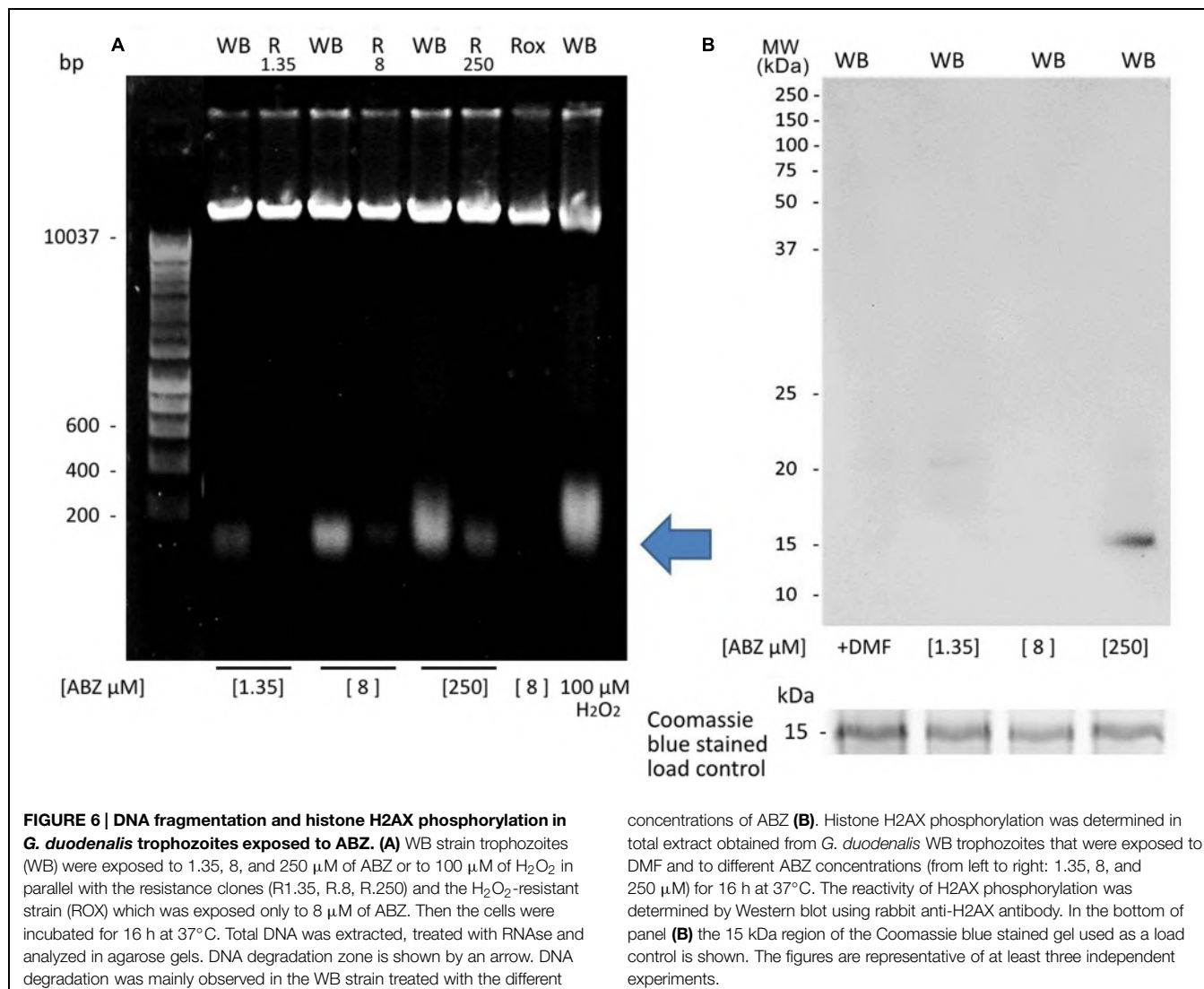


FIGURE 6 | DNA fragmentation and histone H2AX phosphorylation in *G. duodenalis* trophozoites exposed to ABZ. (A) WB strain trophozoites (WB) were exposed to 1.35, 8, and 250 μM of ABZ or to 100 μM of H₂O₂ in parallel with the resistance clones (R1.35, R.8, R.250) and the H₂O₂-resistant strain (ROX) which was exposed only to 8 μM of ABZ. Then the cells were incubated for 16 h at 37°C. Total DNA was extracted, treated with RNase and analyzed in agarose gels. DNA degradation zone is shown by an arrow. DNA degradation was mainly observed in the WB strain treated with the different

concentrations of ABZ (**B**). Histone H2AX phosphorylation was determined in total extract obtained from *G. duodenalis* WB trophozoites that were exposed to DMF and to different ABZ concentrations (from left to right: 1.35, 8, and 250 μM) for 16 h at 37°C. The reactivity of H2AX phosphorylation was determined by Western blot using rabbit anti-H2AX antibody. In the bottom of panel (**B**) the 15 kDa region of the Coomassie blue stained gel used as a load control is shown. The figures are representative of at least three independent experiments.

was broken down in ABZ-exposed trophozoites as determined by the presence of diffuse and low molecular weight bands. This DNA degradation was absent or present at a lesser extent in the ABZ- and ROX-resistant strains. To further confirm the damage to the double stranded DNA, anti-histone H2AX antibodies were used. This protein becomes phosphorylated upon DNA double-strand break. In **Figure 6B** it is shown that exposure of parasites to the highest ABZ concentration (250 μM) induced a H2A signal indicating damage to DNA. The level of phosphorylated *Giardia* H2A was proportional to the DNA damage, therefore the signal was better observed at the highest concentration of ABZ.

ABZ Induces Apoptosis-Like Death and Partial Cell Cycle Arrest in *G. duodenalis* Trophozoites

To determine if ABZ causes necrosis or an apoptotic-like phenomenon, the translocation of phosphatidylserine in ABZ treated trophozoites was detected using anti-annexin V antibodies as a specific marker of early apoptosis. Trophozoites exposed to ABZ displayed a significant increase in annexin V

staining. At higher drug concentration a significant number of cells positive to both markers indicated a process of cell death involving late apoptosis and necrosis (**Figure 7**). In further experiments the trophozoites nuclei were stained with PI to assess if ABZ exposure may alter the cell cycle progression between control and ABZ-exposed trophozoites. As can be observed in **Figure 8**, ABZ produced a noticeable and consistent decrease in the G1 subpopulation (yellow area, from 14.6% in vehicle-treated cells to 2.7% in 250 μM ABZ-treated cells), a slight decrease in the S-phase subpopulation in 1.35 μM ABZ-treated cells as compared to DMF-treated cells (stripped area, from 27 to 22.1%, respectively) and a moderated increase in G2 subpopulation between these same samples (blue area, from 61.0 to 69.9%, respectively). The cells treated with 8 μM ABZ displayed a similar distribution to the one observed in the population exposed to 250 μM ABZ. These data suggest that cytotoxic ABZ concentrations allow only a partial G1→S→G2 transit in cells in a pattern (G2 >> S > G1 > M) that indicates an arrested state at the G2/M phase boundary.

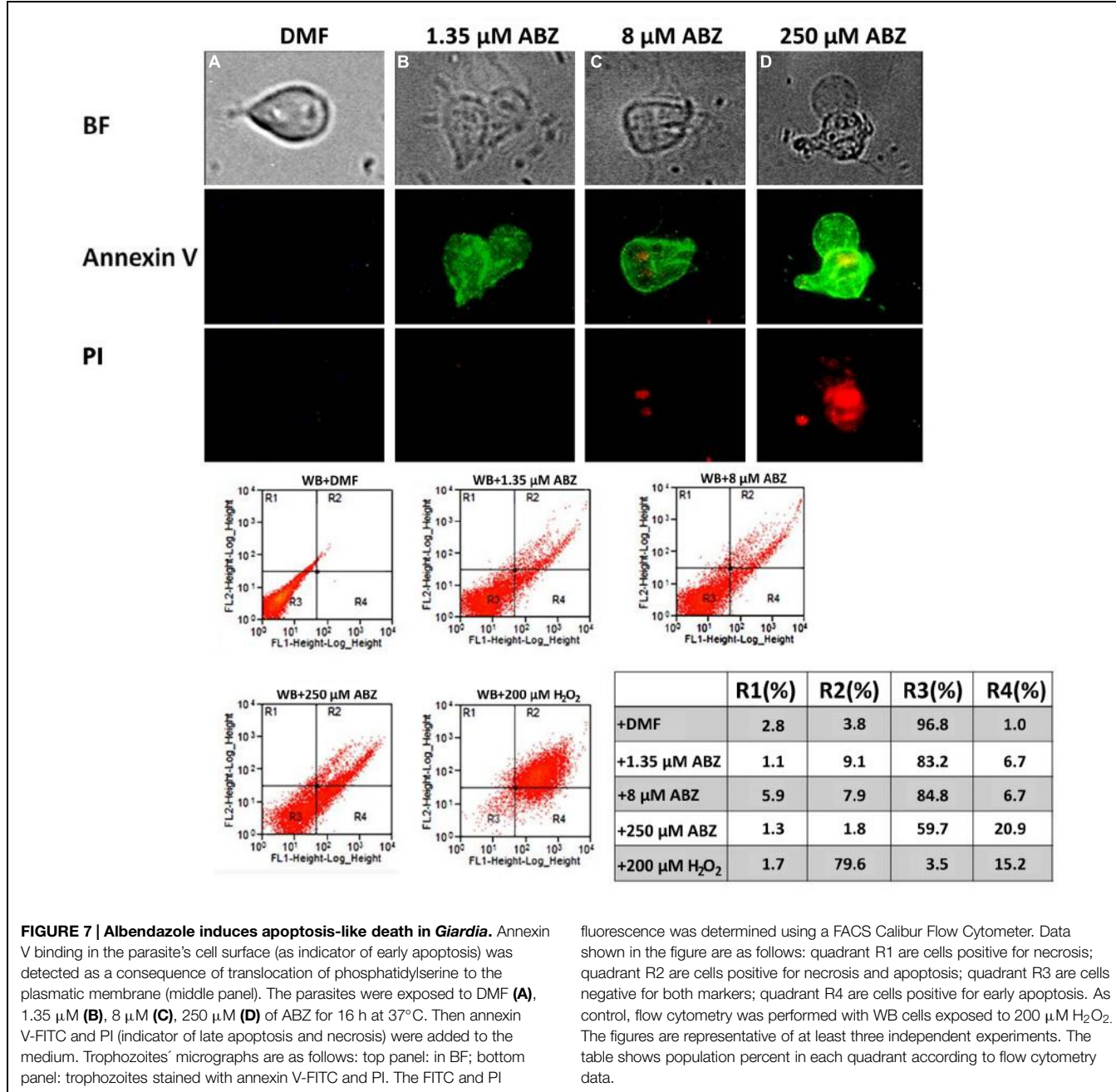


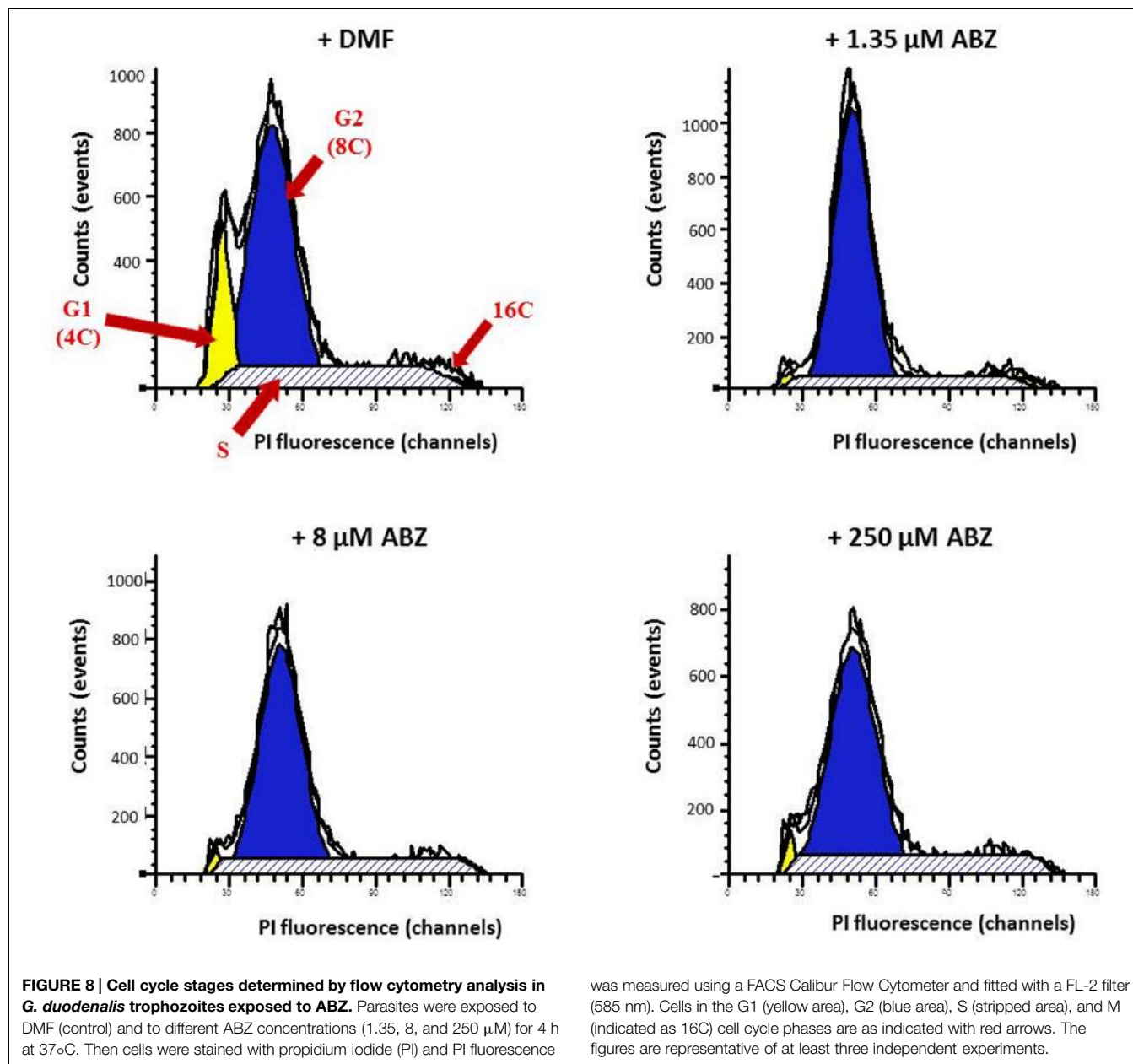
FIGURE 7 | Albendazole induces apoptosis-like death in *Giardia*. Annexin V binding in the parasite's cell surface (as indicator of early apoptosis) was detected as a consequence of translocation of phosphatidylserine to the plasmatic membrane (middle panel). The parasites were exposed to DMF (**A**), 1.35 μ M (**B**), 8 μ M (**C**), 250 μ M (**D**) of ABZ for 16 h at 37°C. Then annexin V-FITC and PI (indicator of late apoptosis and necrosis) were added to the medium. Trophozoites' micrographs are as follows: top panel: in BF; bottom panel: trophozoites stained with annexin V-FITC and PI. The FITC and PI

fluorescence was determined using a FACS Calibur Flow Cytometer. Data shown in the figure are as follows: quadrant R1 are cells positive for necrosis; quadrant R2 are cells positive for necrosis and apoptosis; quadrant R3 are cells negative for both markers; quadrant R4 are cells positive for early apoptosis. As control, flow cytometry was performed with WB cells exposed to 200 μ M H₂O₂. The figures are representative of at least three independent experiments. The table shows population percent in each quadrant according to flow cytometry data.

Discussion

Parasitic diseases by protozoa and helminths represent a serious health problem worldwide. The control of the infections caused by these parasites is carried out mainly by drug treatment. The drug ABZ is a broad spectrum benzimidazole with an anti-helminthic effect and its low cost makes this drug a suitable candidate for mass drug administration programs to deworm children in countries where giardiasis is endemic as well. However, up to five 400 mg doses are needed to clear infections by *G. duodenalis*, limiting the utility of these campaigns to diminish burdens of giardiasis. Also, the use of suboptimal

doses may engender and disseminate ABZ-resistant *Giardia* (Tian et al., 2010; Watkins and Eckmann, 2014). Likewise many parasites including *Giardia* exhibit cross-resistance to diverse drugs. Therefore, it is essential to understand the mechanisms involved in the toxicity of the drugs used; this understanding can help to devise high efficiency regimes and new and effective drugs against resistant strains (Watkins and Eckmann, 2014). Understanding the mechanisms of the effects of ABZ on *Giardia* will also help to define at least in part, the ABZ toxicity reported in some patients particularly in the liver, as well as other side effects such as possible teratogenesis (Dayan, 2003; Nandi and Sarkar, 2013).



In this context, the mechanisms of ABZ action have been studied mainly in helminthic parasites and information in protozoans is limited. The main mechanism of ABZ action involves binding to β -tubulin causing the destabilization of the cytoskeleton. In this regard, resistance to ABZ has been associated with point mutations in this protein and so far other effects of ABZ have received little attention. Some studies in mammalian cells have correlated the use of ABZ to the presence of oxidative stress. Since the susceptibility of many parasites to oxidative stress has been reported (Pal and Bandyopadhyay, 2012), in this study we have evaluated the capacity of ABZ to induce oxidative stress in the protozoan parasite *G. duodenalis*.

The results indicated that ABZ exposure induced intracellular ROS formation in drug susceptible trophozoites

and interestingly ROS were detected mainly in the nuclei. Therefore, oxidative-stress caused by ABZ can be part of the cytotoxic effect of this drug in *Giardia*. An important aspect to be addressed in future studies is to determine which ROS are involved as well as the mechanisms inducing their formation.

Since ABZ cytotoxicity was herein related to oxidative stress, another pro-oxidant molecule (H_2O_2) was evaluated. Of note, a partial degree of cross-resistance to this agent was detected in the ABZ-resistant clones suggesting that similar antioxidant responses may be induced by each compound. This correlation between drug resistance and antioxidant response has also been suggested in drug resistant *Leishmania* strains (Berg et al., 2015) and in other pathogens such as

Plasmodium and *Pseudomonas* (Lehane et al., 2012; Poole, 2014). The phenomenon of cross-resistance in *Giardia* to different drugs including metronidazole and ABZ has already been reported (Müller et al., 2007) although the causes of this have not yet been fully elucidated. The protection conferred by cysteine in ABZ-treated trophozoites further suggests that this drug induces some toxicity through oxidative stress thus cysteine may provide a reductive environment, however, the mechanisms involved in this protective effect remains to be elucidated. Interestingly in a recent study of our group, a set of antioxidant enzymes present in *Giardia* (e.g., NADH oxidase, flavoprotein-A, superoxide reductase, peroxiredoxins, Li and Wang, 2006; Mastronicola et al., 2014) have shown an increased expression along to increased intracellular cysteine concentrations in the ABZ-resistant clones used in this study (Argüello-García et al., 2015). Other processes as drug metabolism could also play a role in resistance because *Giardia* apparently has metronidazole-activating enzymes (nitro reductases; Pal et al., 2009) and ABZ metabolites (sulphoxide and sulphone) have been detected in this parasite (Oxberry et al., 2000). Interestingly these are accumulated in lower levels in the ABZ-resistant clones (Argüello-García et al., 2015).

Regarding the damage promoted by ABZ in trophozoites, two interesting findings were observed: (a), the lack of lipid peroxidation and protein carbonylation, and (b) the presence of DNA damage as a main mechanism of the cytotoxic effect of ABZ. The lack of lipid peroxidation may be due either to the fact that *Giardia* uptakes lipids and cholesterol from exogenous sources, to the unique lipid metabolism in this parasite, or to the nuclear localization of ROS that may limit damage to membrane-associated lipid metabolites (Gibson et al., 1999; Das et al., 2002). Moreover, protein carbonylation, an irreversible oxidative damage, showed only a tendency (not statistically significant) to increase when high ABZ concentrations were used, despite being easily detected when the parasites were treated with H₂O₂. Although carbonylation is an important marker for protein damage, it will also be important to analyze if other mechanisms of oxidative damage to proteins (Møller et al., 2011) may occur in the ABZ treated trophozoites.

The detection of 8OHdG adducts, together with DNA degradation in ABZ exposed trophozoites indicated that the DNA was the most affected molecule by the pro-oxidant action of ABZ. The *in vitro* damage of DNA by drugs such as metronidazole has been recently shown in *Giardia* (Uzlikova and Nohynkova, 2015). Other redox active drugs such as benznidazole and hydroxymethylnitrofuranzone have been reported to affect mainly DNA (Davies et al., 2014), a pattern commonly present in necrosis. Further evidence of DNA damage in ABZ-treated trophozoites included histone H2AX phosphorylation that indicates a repair signal after DNA double strand break. In particular, H2AX phosphorylation observed in parasites treated with 250 μM ABZ could be due to the cell damage induced by the drug. Thus, phosphorylation of histone H2AX will be activated upon damage of trophozoites by ABZ. As shown in **Figure 7**, a process of necrosis appears particularly significantly when the

parasites are exposed to 250 μM and in this condition H2AX phosphorylation occurs.

In other parasites such as *Toxoplasma gondii*, the phosphorylation of H2AX has been correlated with loss of pathological potential and reduced growth rates (Vonlaufen et al., 2010). It is worth mentioning that the typical ladder pattern of DNA degradation observed in *Giardia* exposed to ABZ was not entirely similar to the one associated with apoptosis in other organisms or as commonly present in necrosis (Bagchi et al., 2012). Thus the DNA degradation pattern correlates with an apoptotic-like phenomenon present in *G. duodenalis*. Indeed, the detection of phosphatidylserine translocation to the outer side of the cell membrane suggested an apoptotic-like event.

Our findings resemble studies reported by others regarding an apoptotic-like process in *Giardia* when it is exposed to classical inducers of oxidative stress and to metronidazole (Bagchi et al., 2012). Interestingly a partial arrest in S and G2 phases of the cell cycle was observed in ABZ-exposed trophozoites that correlate with the induction of oxidative stress and an apoptotic-like process. It is noteworthy that the cell cycle arrest is not complete and this allows a portion of the cell population to continue through the cell cycle. The effect of different drugs on the *Giardia* cell cycle has been reported to show different phenomena, including partial arrest in different cell cycle stages depending on the drug under study (Reaume et al., 2013). In our work, ABZ-treated trophozoites showed a pattern consistent with *Giardia* trophozoites displaying incomplete cytokinesis upon exposure to microtubule-acting compounds (Mariante et al., 2005).

In summary, this work demonstrated that ABZ induces the formation of intracellular of ROS in *G. duodenalis* leading to an oxidative stress status where the main affected biomolecule is DNA. This damage involves the formation of 8OHdG adducts and double-strand DNA break. This damage in turn leads to cell cycle dysregulation and eventually apoptotic-like cell death. These observations allow us to expand our understanding on the cytotoxic mechanism of ABZ in *Giardia* and opens future directions to a rational drug design for giardiasis, considering antioxidant responses as likely mechanisms of multidrug resistance. In this context, generating ROS or inhibiting endogenous antioxidant enzymes would be a rational approach to developing new anti-*Giardia* drugs as previously proposed for other parasites (Pal and Bandyopadhyay, 2012).

Acknowledgments

We would like to thank Dean Befus and Benjamin Rosenthal for critically reading the manuscript and for their help in reviewing the English language. Authors are grateful to José Pedraza Chaverri and Omar Medina Campos for their help in the assays for the detection of lipid peroxidation, to Blanca E. Herrera-Ramirez, Isabel Torres, Olga Garibay Cerdaneras, and Viridiana Olin-Sandoval for their helpful technical assistance and to Arturo Pérez-Taylor for informatics assistance. RM-E was recipient of a doctoral fellowship from CONACYT (Reference No. 215120). This work was partially supported by Conacyt Grant No 49724-M.

References

- Ankarklev, J., Jerlström-Hultqvist, J., Ringqvist, E., Troell, K., and Svärd, S. G. (2010). Behind the smile: cell biology and disease mechanisms of *Giardia* species. *Nat. Rev. Microbiol.* 8, 413–422. doi: 10.1038/nrmicro2317
- Argüello-García, R., Cruz-Soto, M., González-Trejo, R., Paz-Maldonado, L. M., Bazán-Tejeda, M. L., Mendoza-Hernández, G., et al. (2015). An antioxidant response is involved in resistance of *Giardia duodenalis* to albendazole. *Front. Microbiol.* 10:286. doi: 10.3389/fmicb.2015.00286
- Argüello-García, R., Cruz-Soto, M., Romero-Montoya, L., and Ortega-Pierres, G. (2009). In vitro resistance to 5-nitroimidazoles and benzimidazoles in *Giardia duodenalis*: variability and variation in gene expression. *Infect. Genet. Evol.* 9, 1057–1064. doi: 10.1016/j.meegid.2009.05.015
- Bagchi, S., Oniku, A. E., Topping, K., Mamhoud, Z. N., and Paget, T. A. (2012). Programmed cell death in *Giardia*. *Parasitology* 139, 894–903. doi: 10.1017/S003118201200011X
- Bártová, H., Vokřál, I., Skálová, L., Lamka, J., and Szotáková, B. (2010). In vitro oxidative metabolism of xenobiotics in the lancet fluke (*Dicrocoelium dendriticum*) and the effects of albendazole and albendazole sulphoxide ex vivo. *Xenobiotica* 40, 593–601. doi: 10.3109/00498254.2010.497565
- Berg, M., García-Hernández, R., Cuypers, B., Vanaerschot, M., Manzano, J. I., Poveda, J. A., et al. (2015). Experimental resistance to drug combinations in *Leishmania donovani*: metabolic and phenotypic adaptations. *Antimicrob. Agents Chemother.* 59, 2242–2255. doi: 10.1128/AAC.04231-14
- Chavez, B., Cedillo-Rivera, R., and Martínez-Palomo, A. (1992). *Giardia lamblia*: ultrastructural study of the in vitro effect of benzimidazoles. *J. Protozool.* 39, 510–515. doi: 10.1111/j.1550-7408.1992.tb04841.x
- Das, S., Stevens, T., Castillo, C., Villasenor, A., Arredondo, H., and Reddy, K. (2002). Lipid metabolism in mucous-dwelling amitochondriate protozoa. *Int. J. Parasitol.* 32, 655–675. doi: 10.1016/S0020-7519(02)00006-1
- Davies, C., Dey, N., Negrette, O. S., Parada, L. A., Basombrio, M. A., and Garg, N. J. (2014). Hepatotoxicity in mice of a novel anti-parasite drug candidate hydroxymethylnitrofurazone: a comparison with Benznidazole. *PLoS Negl. Trop. Dis.* 8:e3231. doi: 10.1371/journal.pntd.0003231
- Dayan, A. D. (2003). Albendazole, mebendazole and praziquantel. Review of non-clinical toxicity and pharmacokinetics. *Acta. Trop.* 86, 141–159. doi: 10.1016/S0001-706X(03)00031-7
- Diawara, A., Halpenny, C. M., Churcher, T. S., Mwandawiro, C., Kihara, J., Kaplan, R. M., et al. (2013). Association between response to albendazole treatment and β-tubulin genotype frequencies in soil-transmitted helminths. *PLoS Negl. Trop. Dis.* 7:e2247. doi: 10.1371/journal.pntd.0002247
- Dimitrijević, B., Borožan, S., Katić-Radivojević, S., and Stojanović, S. (2012). Effects of infection intensity with *Strongyloides papilliferus* and albendazole treatment on development of oxidative/nitrosative stress in sheep. *Vet. Parasitol.* 186, 364–375. doi: 10.1016/j.vetpar.2011.11.017
- Gardner, T. B., and Hill, D. R. (2001). Treatment of giardiasis. *Clin. Microbiol. Rev.* 14, 114–128. doi: 10.1128/CMR.14.1.114-128.2001
- Gérard-Monnier, D., Erdelmeier, I., Régnard, K., Moze-Henry, N., Yadan, J. C., and Chaudière, J. (1998). Reactions of 1-methyl-2-phenylindole with malondialdehyde and 4-hydroxyalkenals. Analytical applications to a colorimetric assay of lipid peroxidation. *Chem. Res. Toxicol.* 11, 1176–1183. doi: 10.1021/tx9701790
- Gerphagnon, M., Latour, D., Colombe, J., and Sime-Ngando, T. (2013). A double staining method using SYTOX green and calcofluor white for studying fungal parasites of phytoplankton. *Appl. Environ. Microbiol.* 79, 3943–3951. doi: 10.1128/AEM.00696-13
- Ghosh, E., Ghosh, A., Ghosh, A. N., Nozaki, T., and Ganguly, S. (2009). Oxidative stress-induced cell cycle blockage and a protease-independent programmed cell death in microaerophilic *Giardia lamblia*. *Drug. Des. Devel. Ther.* 3, 103–110.
- Gibson, G. R., Ramirez, D., Maier, J., Castillo, C., and Das, S. (1999). *Giardia lamblia*: incorporation of free and conjugated fatty acids into glycerol-based phospholipids. *Exp. Parasitol.* 92, 1–11. doi: 10.1006/expr.1999.4389
- Hansen, T. V., Thamsborg, S. M., Olsen, A., Prichard, R. K., and Nejsum, P. (2013). Genetic variations in the beta-tubulin gene and the internal transcribed spacer 2 region of *Trichuris* species from man and baboons. *Parasit Vectors.* 6:236. doi: 10.1186/1756-3305-6-236
- Hofstetrová, K., Uzlíková, M., Tůmová, P., Troell, K., Svärd, S. G., and Nohýnková, E. (2010). *Giardia intestinalis*: aphidicolin influence on the trophozoite cell cycle. *Exp. Parasitol.* 124, 159–166. doi: 10.1016/j.exppara.2009.09.004
- Keister, D. B. (1983). Axenic culture of *Giardia lamblia* in TYI-S-33 medium supplemented with bile. *Trans. R. Soc. Trop. Med. Hyg.* 77, 487–488. doi: 10.1016/0035-9203(83)90120-7
- Krisko, A., and Radman, M. (2010). Protein damage and death by radiation in *Escherichia coli* and *Deinococcus radiodurans*. *Proc. Natl. Acad. Sci. U.S.A.* 107, 14373–14377. doi: 10.1073/pnas.1009312107
- Lane, S., and Lloyd, D. (2002). Current trends in research into the waterborne parasite *Giardia*. *Crit. Rev. Microbiol.* 28, 123–147. doi: 10.1080/1040-840291046713
- Lehane, A. M., McDevitt, C. A., Kirk, K., and Fidock, D. A. (2012). Degrees of chloroquine resistance in *Plasmodium* – is the redox system involved? *Int. J. Parasitol. Drugs Drug Resist.* 2, 47–57. doi: 10.1016/j.ijpddr.2011.11.001
- Lemée, V., Zaharia, I., Nevez, G., Rabodonirina, M., Brasseur, P., Ballet, J. J., et al. (2000). Metronidazole and albendazole susceptibility of 11 clinical isolates of *Giardia duodenalis* from France. *J. Antimicrob. Chemother.* 46, 819–821. doi: 10.1093/jac/46.5.819
- Li, L., and Wang, C. C. (2006). A likely molecular basis of the susceptibility of *Giardia lamblia* towards oxygen. *Mol. Microbiol.* 59, 202–211. doi: 10.1111/j.1365-2958.2005.04896.x
- Locatelli, C., Pedrosa, R. C., De Bem, A. F., Creczynski-Pasa, T. B., Cordova, C. A., and Wilhelm-Filho, D. (2004). A comparative study of albendazole and mebendazole-induced, time-dependent oxidative stress. *Redox. Rep.* 9, 89–95. doi: 10.1179/135100004225004751
- Mariante, R. M., Vancini, R. G., Melo, A. L., and Benchimol, M. (2005). *Giardia lamblia*: evaluation of the in vitro effects of nocodazole and colchicine on trophozoites. *Exp. Parasitol.* 110, 62–72. doi: 10.1016/j.exppara.2005.01.007
- Mastronicola, D., Falabella, M., Testa, F., Pucillo, L. P., Teixeira, M., Sarti, P., et al. (2014). Functional characterization of peroxiredoxins from the human protozoan parasite *Giardia intestinalis*. *PLoS Negl. Trop. Dis.* 8:e2631. doi: 10.1371/journal.pntd.0002631
- Møller, I. M., Rogowska-Wrzesińska, A., and Rao, R. S. (2011). Protein carbonylation and metal-catalyzed protein oxidation in a cellular perspective. *J. Proteomics.* 74, 2228–2242. doi: 10.1016/j.jprot.2011.05.004
- Moore, C. J., Shao, C. H., Nagai, R., Kutty, S., Singh, J., and Bidasee, K. R. (2013). Malondialdehyde and 4-hydroxyxonenal adducts are not formed on cardiac ryanodine receptor (RyR2) and sarco(endo)plasmic reticulum Ca²⁺-ATPase (SERCA2) in diabetes. *Mol. Cell. Biochem.* 376, 121–135. doi: 10.1007/s11010-013-1558-1
- Müller, J., Sterk, M., Hemphill, A., and Müller, N. (2007). Characterization of *Giardia lamblia* WB C6 clones resistant to nitazoxanide and to metronidazole. *J. Antimicrob. Chemother.* 60, 280–287. doi: 10.1093/jac/dkm205
- Nandi, M., and Sarkar, S. (2013). Albendazole-induced recurrent hepatitis. *Indian Pediatr.* 50, 1064. doi: 10.1007/s13132-013-0285-8
- Nash, T. E. (2013). Unraveling how *Giardia* infections cause disease. *J. Clin. Invest.* 123, 2346–2347. doi: 10.1172/JCI69956
- Orozco-Ibarra, M., Medina-Campos, O. N., Sánchez-González, D. J., Martínez-Martínez, C. M., Floriano-Sánchez, E., Santamaría, A., et al. (2007). Evaluation of oxidative stress in D-serine induced nephrotoxicity. *Toxicology* 229, 123–135. doi: 10.1016/j.tox.2006.10.008
- Oxberry, M. E., Reynoldson, J. A., and Thompson, R. C. (2000). The binding and distribution of albendazole and its principal metabolites in *Giardia duodenalis*. *J. Vet. Pharmacol. Ther.* 23, 113–120. doi: 10.1046/j.1365-2885.2000.00254.x
- Pal, C., and Bandyopadhyay, U. (2012). Redox-active antiparasitic drugs. *Antioxid. Redox. Signal.* 17, 555–582. doi: 10.1089/ars.2011.4436
- Pal, D., Banerjee, S., Cui, J., Schwartz, A., Ghosh, S. K., and Samuelson, J. (2009). *Giardia*, *Entamoeba*, and *Trichomonas* enzymes activate metronidazole (nitroreductases) and inactivate metronidazole (nitroimidazole reductases). *Antimicrob. Agents Chemother.* 53, 458–464. doi: 10.1128/AAC.00909-08
- Paz-Maldonado, M. T., Argüello-García, R., Cruz-Soto, M., Mendoza-Hernández, G., and Ortega-Pierres, G. (2013). Proteomic and transcriptional analyses of genes differentially expressed in *Giardia duodenalis* clones resistant to albendazole. *Infect. Genet. Evol.* 15, 10–17. doi: 10.1016/j.meegid.2012.08.021
- Plutzer, J., Ongerth, J., and Karanis, P. (2010). *Giardia* taxonomy, phylogeny and epidemiology: facts and open questions. *Int. J. Hyg. Environ. Health.* 213, 321–333. doi: 10.1016/j.ijheh.2010.06.005

- Poole, K. (2014). Stress responses as determinants of antimicrobial resistance in *Pseudomonas aeruginosa*: multidrug efflux and more. *Can. J. Microbiol.* 60, 783–791. doi: 10.1139/cjm-2014-2666
- Raj, D., Ghosh, E., Mukherjee, A. K., Nozaki, T., and Ganguly, S. (2013). Differential gene expression in *Giardia lamblia* under oxidative stress: significance in eukaryotic evolution. *Gene.* 535, 131–139. doi: 10.1016/j.gene.2013.11.048
- Reaume, C., Moore, B., Hernández, P., Ruzzini, A., Chlebus, M., Wasserman, M., et al. (2013). Evaluation of drugs and stationary growth on the cell cycle of *Giardia intestinalis*. *Mol. Biochem. Parasitol.* 187, 72–76. doi: 10.1016/j.molbiopara.2012.11.005
- Robinson, M. W., McFerran, N., Trudgett, A., Hoey, L., and Fairweather, I. (2004). A possible model of benzimidazole binding to beta-tubulin disclosed by invoking an inter-domain movement. *J. Mol. Graph. Model.* 23, 275–284. doi: 10.1016/j.jmgm.2004.08.001
- Rossignol, J. F. (2010). Cryptosporidium and *Giardia*: treatment options and prospects for new drugs. *Exp. Parasitol.* 124, 45–53. doi: 10.1016/j.exppara.2009.07.005
- Rossignol, J. F., Lopez-Chegne, N., Julcamoro, L. M., Carrion, M. E., and Bardin, M. C. (2012). Nitazoxanide for the empiric treatment of pediatric infectious diarrhea. *Trans. R. Soc. Trop. Med. Hyg.* 106, 167–173. doi: 10.1016/j.trstmh.2011.11.007
- Solaymani-Mohammadi, S., Genkinger, J. M., Loffredo, C. A., and Singer, S. M. (2010). A meta-analysis of the effectiveness of albendazole compared with metronidazole as treatments for infections with *Giardia duodenalis*. *PLoS Negl. Trop. Dis.* 4:e682. doi: 10.1371/journal.pntd.0000682
- Suzuki, K., Ojima, M., Kodama, S., and Watanabe, M. (2006). Delayed activation of DNA damage checkpoint and radiation-induced genomic instability. *Mutat. Res.* 597, 73–77. doi: 10.1016/j.mrfmmm.2005.04.024
- Tejman-Yarden, N., and Eckmann, L. (2011). New approaches to the treatment of giardiasis. *Curr. Opin. Infect. Dis.* 24, 451–456. doi: 10.1097/QCO.0b013e32834ad401
- Tian, H. F., Chen, B., and Wen, J. F. (2010). Giardiasis, drug resistance, and new target discovery. *Infect. Disord. Drug Targets.* 10, 295–302. doi: 10.2174/187152610791591629
- Upcroft, J., Mitchell, R., Chen, N., and Upcroft, P. (1996). Albendazole resistance in *Giardia* is correlated with cytoskeletal changes but not with a mutation at amino acid 200 in beta-tubulin. *Microb. Drug Resist.* 2, 303–308. doi: 10.1089/mdr.1996.2.303
- Upcroft, P., and Upcroft, J. A. (2001). Drug targets and mechanisms of resistance in the anaerobic protozoa. *Clin. Microbiol. Rev.* 14, 150–164. doi: 10.1128/CMR.14.1.150-164.2001
- Uzlikova, M., and Nohynkova, E. (2015). The effect of metronidazole on the cell cycle and DNA inmetronidazole-susceptible and –resistant *Giardia* cell lines. *Mol. Biochem. Parasitol.* 198, 75–81. doi: 10.1016/j.molbiopara.2015.01.005
- Vonlaufen, N., Naguleswaran, A., Coppens, I., and Sullivan, W. J. Jr. (2010). MYST family lysine acetyltransferase facilitates ataxia telangiectasia mutated (ATM) kinase-mediated DNA damage response in *Toxoplasma gondii*. *J. Biol. Chem.* 285, 11154–11161. doi: 10.1074/jbc.M109.066134
- Watkins, R. R., and Eckmann, L. (2014). Treatment of giardiasis: current status and future directions. *Curr. Infect. Dis. Rep.* 16, 396. doi: 10.1007/s11908-014-0396-y

Conflict of Interest Statement: The authors declare that the research was conducted in the absence of any commercial or financial relationships that could be construed as a potential conflict of interest.

Copyright © 2015 Martínez-Espinosa, Argüello-García, Saavedra and Ortega-Pierres. This is an open-access article distributed under the terms of the Creative Commons Attribution License (CC BY). The use, distribution or reproduction in other forums is permitted, provided the original author(s) or licensor are credited and that the original publication in this journal is cited, in accordance with accepted academic practice. No use, distribution or reproduction is permitted which does not comply with these terms.

The FAD-dependent glycerol-3-phosphate dehydrogenase of *Giardia duodenalis*: an unconventional enzyme that interacts with the g14-3-3 and it is a target of the antitumoral compound NBDHEX

OPEN ACCESS

Edited by:

Anjan Debnath,
University of California, San Diego,
USA

Reviewed by:

Steven Singer,
Georgetown University, USA
Siddhartha Das,
University of Texas at El Paso, USA

*Correspondence:

Marco Lalle,
Department of Infectious, Parasitic
and Immunomediated Diseases,
Istituto Superiore di Sanità, Viale
Regina Elena 299, 00161 Rome, Italy
marco.lalle@iss.it

Specialty section:

This article was submitted to
Antimicrobials, Resistance
and Chemotherapy,
a section of the journal
Frontiers in Microbiology

Received: 04 March 2015

Accepted: 17 May 2015

Published: 01 June 2015

Citation:

Lalle M, Camerini S, Cecchetti S,
Finelli R, Sferra G, Müller J, Ricci G
and Pozio E (2015)
The FAD-dependent
glycerol-3-phosphate dehydrogenase
of *Giardia duodenalis*: an
unconventional enzyme that interacts
with the g14-3-3 and it is a target
of the antitumoral compound
NBDHEX.
Front. Microbiol. 6:544.
doi: 10.3389/fmicb.2015.00544

Marco Lalle^{1*}, Serena Camerini², Serena Cecchetti², Renata Finelli¹, Gabriella Sferra¹, Joachim Müller³, Giorgio Ricci⁴ and Edoardo Pozio¹

¹ Department of Infectious, Parasitic and Immunomediated Diseases, Istituto Superiore di Sanità, Rome, Italy, ² Department of Cell Biology and Neurosciences, Istituto Superiore di Sanità, Rome, Italy, ³ Institute of Parasitology, Vetsuisse Faculty, University of Bern, Bern, Switzerland, ⁴ Department of Sciences and Chemical Technologies, University of Rome "Tor Vergata", Rome, Italy

The flagellated protozoan *Giardia duodenalis* is a worldwide parasite causing giardiasis, an acute and chronic diarrheal disease. Metabolism in *G. duodenalis* has a limited complexity thus making metabolic enzymes ideal targets for drug development. However, only few metabolic pathways (i.e., carbohydrates) have been described so far. Recently, the parasite homolog of the mitochondrial-like glycerol-3-phosphate dehydrogenase (gG3PD) has been identified among the interactors of the g14-3-3 protein. G3PD is involved in glycolysis, electron transport, glycerophospholipids metabolism, and hyperosmotic stress response, and is emerging as promising target in tumor treatment. In this work, we demonstrate that gG3PD is a functional flavoenzyme able to convert glycerol-3-phosphate into dihydroxyacetone phosphate and that its activity and the intracellular glycerol level increase during encystation. Taking advantage of co-immunoprecipitation assays and deletion mutants, we provide evidence that gG3PD and g14-3-3 interact at the trophozoite stage, the intracellular localization of gG3PD is stage dependent and it partially co-localizes with mitosomes during cyst development. Finally, we demonstrate that the gG3PD activity is affected by the antitumoral compound 6-(7-nitro-2,1,3-benzoxadiazol-4-ylthio)hexanol, that results more effective *in vitro* at killing *G. duodenalis* trophozoites than the reference drug metronidazole. Overall, our results highlight the involvement of gG3PD in processes crucial for the parasite survival thus proposing this enzyme as target for novel antigiardial interventions.

Keywords: *Giardia duodenalis*, FAD-dependent glycerol-3-phosphate dehydrogenase, 14-3-3 protein, energy metabolism, mitosome, encystation, NBDHEX, nitroreduction

Introduction

The flagellated protozoan *Giardia duodenalis* (syn. *lamblia*, *intestinalis*) is a parasite of the upper part of small intestine of mammals, including humans. Infection with *G. duodenalis* causes giardiasis, one of the most common foodborne and waterborne gastroenteric diseases (Halliez and Buret, 2013; Ryan and Cacciò, 2013). The parasite has a simple two-stages life cycle consisting of the trophozoite, that replicates and colonizes the host intestine causing symptoms, and the cyst, the environmentally resistant stage that is spread with feces and is responsible for transmission of the infection. Generally, infection is acquired by ingestion of cysts in contaminated water and food or by the fecal-oral route (Ryan and Cacciò, 2013). Clinical symptoms of giardiasis can vary from asymptomatic infection to acute and chronic diarrhea, ultimately leading to chronic post-infectious gastrointestinal complications, including irritable bowel syndrome and chronic fatigue (Halliez and Buret, 2013). Up to date, no human vaccine for giardiasis is available and treatment relies only on a limited panel of effective approved drugs. Nitroheterocyclics, such as metronidazole (MTZ) and nitazoxanide (NTZ), are the anti-giardial drugs of choice. Unfortunately, treatment failure has been reported in 10–20% of cases and strains resistant to different compounds have been either clinically isolated or induced *in vitro* (Lalle, 2010; Watkins and Eckmann, 2014). In this scenario, alternative, safe, and effective therapies are required.

Giardia duodenalis has a peculiar energy metabolism. It is a microaerophilic organism that, instead of mitochondria, contains mitosomes, highly reduced mitochondria-derived organelles which sole function seems to be restricted to Fe-S cluster biosynthesis (Tovar et al., 2003; Jedelský et al., 2011). Energy is then generated by substrate level phosphorylation and fermentation occurring in the cytoplasm or at the inner side of the plasma membrane (Adam, 2001). In terms of sequence similarity, these metabolic pathways of *G. duodenalis* consist of a mixture of eukaryote-like and bacteria-like enzymes. Therefore, energy and intermediate metabolism of *G. duodenalis* have been shown to provide opportunities to identify novel and effective compounds, as well as potentially interesting targets by means of high-throughput drug screening and target-based drug design (Müller and Hemphill, 2013; Watkins and Eckmann, 2014).

We recently detected a putative glycerol-3-phosphate dehydrogenase/flavin-dependent oxidoreductase (gG3PD, GL50803_16125) of *G. duodenalis* among proteins interacting with the parasite 14-3-3 isoform, g14-3-3 (Lalle et al., 2012). The 14-3-3s are a family of highly conserved eukaryotic phosphoserine/phosphothreonine-binding proteins which participate to the regulation of key cellular processes by direct interaction with 100s of target proteins (Gardino and Yaffe, 2011; Kleppe et al., 2011). The characterized g14-3-3 interactome provides evidences that g14-3-3 can be involved in parasite energy metabolism, as supported by the identification and confirmation of components of both the glycolytic/gluconeogenetic pathway and pyruvate metabolism (Lalle et al., 2012).

Flavin adenine dinucleotide (FAD)-dependent glycerol-3-phosphate dehydrogenase (G3PD, EC 1.1.5.3) is a key enzyme at the crossroad of glycolysis, redox, and fatty acid metabolism, in both prokaryotes and eukaryotes. G3PD catalyzes the oxidation of glycerol-3-phosphate (G3P) to dihydroxyacetone phosphate (DHAP) with simultaneous reduction of FAD to FADH₂ and transfer of electrons to quinones (e.g., ubiquinone; Unden and Bongaerts, 1997; Mráček et al., 2013). In eukaryotes, a single subunit enzyme (mG3PD, 69–75 kDa) is strongly associated, as peripheral protein, with the outer face of the inner mitochondrial membrane (Janssen et al., 2002; Mráček et al., 2013). The mG3PD has multiple functions: (i) it forms the glycerophosphate shuttle in combination with the cytosolic NADH-dependent G3PD (cG3PD, EC 1.1.1.8) to re-oxidize the cytosolic NADH produced by glycolysis; (ii) it is part of the mitochondrial respiratory electron transport chain (ETC) channeling electron to quinone pool and bypassing Complex I; (iii) it regulates the cytosolic level of G3P (Bell and Coleman, 1980; Mráček et al., 2013). Prokaryotes harbor two distinct membrane-associated FAD-dependent G3PDs, both necessary for bacterial growth in presence of glycerol or G3P as sole carbon source, and represent key primary dehydrogenases transferring reducing equivalents to a short respiratory ETC with different terminal reductases and electron acceptor (O₂, nitrate, or fumarate; Unden and Bongaerts, 1997). The homodimeric GlpD is associated with the cytoplasmic side of plasma membrane, shows 30–33% homology with eukaryotic mG3PD, and is expressed under aerobic conditions when O₂ is the terminal acceptor (Walz et al., 2002; Yeh et al., 2008). The heterotrimeric GlpACB is induced under anaerobic conditions, with fumarate as terminal acceptor (Cole et al., 1988; Varga and Weiner, 1995): it forms a functional-associated complex with fumarate reductase and contributes to generate a proton gradient across the membrane via an associated ETC (Miki and Wilson, 1978). The GlpAC heterodimer (62 and 41 kDa, respectively) is the soluble catalytic subunit, containing the FAD and FMN binding sites (Cole et al., 1988). The GlpB (44 kDa) subunit, that contains a ferredoxin-type (4Fe-4S) cluster binding motif, anchors the GlpAC dimer to the inner cytoplasmic membrane and mediate the transfer of reducing equivalent to the menaquinone pool and finally to the fumarate reductase (Varga and Weiner, 1995).

The G3PDs are also involved in pathogenicity as a source of reactive oxygen species (ROS). The mG3PD has been implied in the establishment of a pro-oxidative environment that promotes the fast growth of undifferentiated tumors (Chowdhury et al., 2007; Mráček et al., 2013), whereas the oxidase activity of GlpD of *Mycoplasma* sp. seems to be crucial for the pathogenicity, leading to high levels of H₂O₂, and host cell damage (Großhennig et al., 2013).

In the present work, we investigated gG3PD expression, activity, and cellular localization in the *G. duodenalis* trophozoite stage and during the encystation process. Moreover, we demonstrated that the antitumoral compound [NBDHEX, 6-(7-nitro-2,1,3-benzoxadiazol-4-ylthio)hexanol] is an effective anti-giardial compound that negatively affected gG3PD activity. Overall, our results pointed out the role of gG3PD in biological processes crucial for the parasite survival, thus suggesting that

this enzyme could represent a good candidate for targeted anti-giardial interventions.

Materials and Methods

Chemicals

The NBDHEX was synthetized as previously described (Ricci et al., 2005). MTZ, FAD disodium salt, sn-g3p, phenazine methosulfate (PMS), 3-(4,5-dimethylthiazol-2-yl)-2,5-diphenyltetrazolium bromide (MTT) were from Sigma-Aldrich (St. Louis, MO, USA).

Parasite Cultivation, Differentiation, and Transfection

The *G. duodenalis* isolate WB clone C6 (WB-C6) was axenically grown in TYI-S-33 medium at 37°C and differentiation into cyst (encystation) was induced in TYI-S-33 medium containing 5 mg/ml of bovine bile at pH 7.8 for the indicated time (Schupp et al., 1988). Parasites were collected by chilling tubes on ice and centrifugation at 800 × g. Transgenic lines were generated by trophozoite electroporation with 15 µg of plasmid DNA and selected and maintained under constant selection with 100 µM puromycin (Invivogen, Toulouse, France).

Vector Construction

Escherichia coli BL21-DE3 competent cells were used. The full-length sequence of gG3PD (accession number GL50803_16125), the gG3PD N-terminal (nucleotide 3-1590; gG3PD_N), and the C-terminal half (nucleotide 1569-3333; gG3PD_C), were PCR amplified from the *G. duodenalis* WB-C6 genomic DNA, prepared as previously described (Lalle et al., 2012). The primers used and their combinations are reported in Table 1. Reactions were performed on a T-Personal Thermocycler (Biometra, Göttingen, Germany) using 100 ng of gDNA, 10 units of high fidelity Pfu turbo DNA polymerase (Agilent Technologies, Santa Clara, CA, USA), 50 µM dNTP, 20 pmols of each primer in 50 µl of reaction mixture. Amplification conditions were: 1 cycle at 95°C for 2 min; 30 cycles at 95°C for 30 s, 58°C for 30 s, and 72°C for 30 s; and 1 cycle at 72°C for 7 min. PCR fragments were cloned either in the *BamHI/PspOMI* digested pTUB-FLAG_HApac vector (Lalle et al., 2012) for expression in *G. duodenalis*, or in the *BamHI/NotI* digested pQ30 vector (Qiagen, Germany) for expression in bacteria as N-terminal 6xHIS-tagged fusion protein.

TABLE 1 | Primer list.

Target	Forward primer ^a	Reverse primer ^b
Full length glycerol-3-phosphate dehydrogenase (gG3PD)	gG3PDforw 5'- <u>GGATCC</u> ACCACCGCTCACCTTACC-3'	gG3PDrev 5'- <u>GCGGCCGC</u> TCACTTCATAGCCGAATGTTC-3'
N-terminal gG3PD	gG3PDforw	NTrev 5'- <u>GCGGCCGC</u> TCAGTATGCCCTGTCCATCGGGGTG-3'
C-terminal gG3PD	CTforw 5'- <u>GGATCC</u> ACCCCGATGGACAAGGCATAC-3'	gG3PDrev

^aThe *BamHI* site is underlined.

^bThe *NotI* site is underlined.

Expression and Purification of the Recombinant Proteins

Transformed *E. coli* were grown in SOB medium and recombinant proteins expression was induced at OD₆₀₀ = 0.6, with 0.5 mM isopropyl-thio-β-D-galactoside at 37°C for 4 h. All 6xHIS-fused proteins were purified under native condition by affinity chromatography on nickel resin (Qiagen) and eluted with 250 mM imidazole (pH 8.0). Proteins were dialyzed against PBS (140 mM NaCl, 2.7 mM KCl, 10 mM Na₂HPO₄, 1.8 mM KH₂PO₄, pH 7.4) using Slide-A-Lyzer dialysis cassettes (cut-off 3.5 kDa, Thermo Fisher Scientific, Rockford, IL, USA). The protein concentration was determined by Bradford assay (Thermo Fisher Scientific) and proteins were stored at -70°C until use.

Production of Polyclonal Antibodies

Purified HIS-gG3PD fusion protein was used to immunize intraperitoneally two BALB/c mice (Charles River Laboratories International, Inc., Wilmington, MA, USA) on days 0, 21, and 42 with 50 µg protein in 300 µl of emulsified 1:1 PBS/Freund's complete adjuvant (Sigma-Aldrich; at day 0) or 1:1 PBS/Freund's incomplete adjuvant (Sigma-Aldrich; at day 21) or without any adjuvant (at day 42). Blood was collected from the tail vein before initial immunization and after each boost. Sera fractions were assayed for specific antibody content.

Preparation of *G. duodenalis* Proteins

Total soluble proteins (S) and octyl β-D-glucopyranoside solubilized proteins from membranous material (M) were prepared as previously described (Lalle et al., 2012) starting from 2 × 10⁹ trophozoites or encysting parasites. The protein concentration was determined by Bradford methods (Thermo Fisher Scientific) and the protein lysates were stored at -70°C. Alternatively, to assess the G3PD enzymatic activity in *G. duodenalis*, 10⁶ parasites were collected, washed two times with cold PBS, suspended in 200 µl of PBS/1% TritonX100 and incubated 1 h on ice. After centrifugation at 13.000 × g for 15 min, supernatant was collected, protein concentration quantified by Bradford methods and the preparation was immediately used for the enzymatic assay as detailed below.

Western Blot Analysis

Proteins were separated on SDS-PAGE and transferred onto PVDF membrane with 39 mM glycine, 48 mM Tris, 0.1% SDS,

and 10% methanol, using a semidry apparatus (BioRad, Hercules, CA, USA). Membranes were blocked with 5% skin milk in TTBS (20 mM Tris-HCl, pH 7.5, 100 mM NaCl, 0.05% Tween 20) for 1 h and then incubated with the primary antibody (Ab) in 2.5% skin milk/TTBS buffer. After incubation with an appropriate HRP-conjugated secondary Ab (1:3000), the interaction was revealed by chemiluminescence (Millipore, France). Antibodies were used at the following dilution: mouse polyclonal anti-gG3PD antiserum 1:3000; mouse anti-HA mAb (Sigma-Aldrich) 1:3000; rabbit N14 (anti-g14-3-3) antiserum (Lalle et al., 2006) 1:5000; mouse anti- α Tubulin (Sigma-Aldrich) 1:10000; rabbit anti-gPGN (phosphoacetylglucosamine mutase, Lopez et al., 2003) 1:1000; mouse anti-HIS mAb (Qiagen) 1:2000.

Blue Native PAGE (BN-PAGE)

Three to twelve percentage of BN-PAGE (Invitrogen, Carlsbad, CA, USA) was carried out using 1 μ g of purified HIS-tagged recombinant proteins according to the manufacturer. This technique allows the separation of very high molecular weight multiprotein complexes. Gels were run in Running buffer (0.002% Coomassie G-250, 50 mM BisTris/50 mM Tricine, pH 6.8) at 150 V for approximately 2 h. Gels were incubated in Tris/glycine/SDS buffer for 30 min and either stained with a Silver Staining kit (Invitrogen) or processed for western blot as described.

Affinity Purification

FLAG-tagged proteins were purified by affinity chromatography on mouse anti-FLAG M2 mAb covalently bound to agarose beads (Sigma-Aldrich) as previously reported (Lalle et al., 2012) and directly eluted from the resin by incubation with 200 μ M FLAG-peptide at 4°C for 1 h. The eluted materials were stored at -70°C until use.

Confocal Laser Scanning Microscopy (CLSM)

Trophozoites or encysting parasites were fixed and permeabilized as previously described (Lalle et al., 2006). Antibodies were used at the following dilution: polyclonal rabbit N14 antiserum 1:50; mouse polyclonal anti-gG3PD antiserum 1:50; polyclonal rabbit anti-gTom40 antiserum (Dagley et al., 2009) 1:50; FITC-conjugated mouse anti-HA mAb (Miltenyi Biotec, Germany) 1:50; Cy5-conjugated anti-CWP mAb (Waterborne Inc., New Orleans, LA, USA) 1:30. Alexa-Fluor 647- and 488-conjugated anti-rabbit and anti-mouse secondary Ab (Invitrogen) were used at a 1:500 dilution. After parasite staining, coverslips were extensively rinsed and then mounted using Vectashield[®] mounting medium (Vector Laboratories Inc., Burlingame, CA, USA) containing 300 nM of 4',6-diamidino-2-phenylindole (DAPI). Confocal laser scanning microscopy (CLSM) observations were performed on a Leica TCS SP2 AOBS (Leica Microsystems, Germany) apparatus, using excitation spectral laser lines at 405, 488, and 647 nm and selecting emission wavelengths by a proper setting of the spectral detection system. Signals from different fluorescent probes were taken in sequential scan mode. Image acquisition and processing were conducted using the Leica Confocal Software (Leica Microsystems). Image deconvolution was performed using the

Huygens software (Scientific Volume Imaging BV, Hilversum, The Netherlands). Data were inferred from two independent experiments following the analysis of different fields of view (>200 cells) on the microscope for each labeling condition.

G3PD Enzymatic Assay, Spectrophotometric, and Fluorimetric Analysis

The dehydrogenase activity of gG3PD was assayed spectrophotometrically according to Kistler and Lin (1972) measuring the rate of PMS-mediated reduction of the tetrazolium dye, MTT, to its formazan by addition of g3p. Reactions were performed in 96 well plate using either 100 μ g of *G. duodenalis* Triton X-100 protein lysate or 16 pmol of purified recombinant HIS-tagged proteins in a final volume of 200 μ l containing 67 mM of potassium phosphate (pH 7.5), 0.2% Triton X100, 6.6 μ g of MTT, 20 μ g of PMS, and 17 mM of g3p with or without 10 μ M FAD. The g3p was omitted in the blank. Since crude extracts could contain substantial endogenous substrates, to ensure a linear rate of MTT reduction, reactions were pre-incubated at 25°C for 5 min prior to the addition of MTT and g3p. Plates were sealed with an air-tight adhesive tape (Greiner Bio One, Austria) to prevent evaporation. After blank subtraction, the enzyme activity was calculated and expressed as micromoles per minute per milligram of protein, considering that the extinction coefficient of reduced MTT is 17 mM⁻¹cm⁻¹ at 570 nm. UV-visible spectra of HIS-gG3PD (10 μ g/ μ l) in 67 mM of potassium phosphate (pH 7.5), were recorded at 25°C in 10 μ l quartz capillaries. UV-visible spectra of 100 μ M NBDHEX were recorded in 67 mM of potassium phosphate (pH 7.5), 17 mM of g3p, with or without HIS-gG3PD (42 pmol) in 0.5 ml quartz cuvette. All measures were done at 25°C in a Multiskan Spectrum (Thermo) spectrophotometer. Fluorescent spectra (excitation at 430 nm) were acquired in a Luminescence Spectrometer LS50B (Perkin-Elmer, Waltham, MA, USA).

Determination of Intracellular Glycerol

For the assay, 10⁶ parasites were collected as previously described, suspended in 100 μ l of PBS, incubated 10 min at 95°C and the supernatant collected after centrifugation at 12,000 \times g for 1 min. Protein concentration was measured by Bradford assay. Intracellular glycerol level was enzymatically determined using the Free Glycerol Reagent kit (Sigma-Aldrich) by measuring spectrophotometrically the production of a quinoneimine dye at 540 nm. Assay was performed on 96 well-plate according to the manufacturer's instruction, using 40 μ l of parasite lysate and 160 μ l of enzyme mixture per well. After 5 min of incubation at 37°C, absorbance was read by Multiskan Spectrum (Thermo Scientific) spectrophotometer. Intracellular glycerol concentration was calculated interpolating the obtained absorbance with a glycerol standard curve and expressed as pmol of glycerol/ μ g of total protein. Each condition was assayed in triplicate and the experiment was performed independently three times.

In Vitro Drug Susceptibility Assay

The *in vitro* assays were performed according to Bénéré et al. (2007) and Houkong et al. (2011) with modifications.

All compounds were dissolved and serially diluted in 1:1 vol ethanol/DMSO. *G. duodenalis* trophozoites (5×10^5 parasite/ml) were cultured in 96-well plates (Nunc Δ surface, Thermo Scientific) in TYIS-33 medium and 3 μl of 100X concentrated compound, or solvent, were added to reach the desired compound concentration. The plates were sealed with an airtight adhesive tape (Greiner Bio-One GmbH, Austria) and incubated for 48 h at 37°C. After the incubation period, culture medium was removed. Adherent trophozoites were immediately fixed with 300 μl of methanol for 2 min and then stained with a solution of 0.1% methylene blue in PBS for 10 min at RT. Wells were washed three times with PBS and incubated with 200 μl of ethanol and 0.1 M HCl [1:1 (v/v) in H₂O], to elute the dye. Absorbance was determined at 655 nm by Multiskan Spectrum (Thermo Scientific) microplate spectrophotometer. Growth inhibition was calculated as the percentage of treated parasite in comparison with untreated parasite. Three independent experiments were performed and each drug dilution was assayed in triplicate. Alternatively, for drug efficacy tests with resazurin (Bénéré et al., 2007), trophozoites were grown in the presence of serial dilutions of the drugs, or DMSO as control, in an anaerobic growth chamber (100% N₂, 37°C). After 72 h, the medium was removed, the wells were washed three times with pre-warmed PBS containing 1% of glucose (0.2 ml per well), and finally, 0.2 ml PBS with glucose containing 10 mg/l resazurin were added. Reduced resazurin was quantified by fluorimetry (excitation at 365 nm, emission at 455 nm) using a 96-well-multimode plate reader Enspire (Perkin-Elmer).

For immunolocalization and enzymatic assays, drug treatments were performed in 10 ml screw cap tubes using 1×10^5 parasite/ml of *G. duodenalis* trophozoites. Twenty five microliter of 20 mM NBDHEX in ethanol, or the equal volume of ethanol, was added to 10 ml of TYS-I-33 medium (final concentration 50 μM) and parasites were incubated at 37°C for the indicated time periods and cells were processed as described in previous paragraphs.

Mass Spectrometry Analysis

Proteins were separated on a 1D-gel NuPAGE 4–12% (Novex, Invitrogen) run in morpholinepropanesulfonic acid (MOPS) buffer and stained with the Colloidal Blue Staining kit (Invitrogen). Slices were excised and digested with modified sequencing-grade trypsin (Promega Corporation, France), as previously described (Shevchenko et al., 1996). Nanoflow reversed-phase liquid chromatography tandem mass spectrometry (RP-LC-MS/MS) analysis of peptide mixtures was performed using an HPLC Ultimate 3000 (DIONEX, Sunnyvale, CA, USA) coupled with a linear ion trap (LTQ, Thermo Electron, San Jose, CA, USA) mass spectrometer. Peptides were desalted in a trap column (Acclaim PepMap 100 C18, LC Packings, DIONEX) and separated in the analytical column, a 10 cm long fused silica capillary (Silica Tips FS 360-75-8, New Objective) in house slurry-packed with a 5 μm , 200 Å pore size C18 resin (Michrom BioResources, Auburn, CA, USA). Peptides were eluted using a 40 min linear gradient from 96% aqueous buffer containing 5% acetonitrile and 0.1%

formic acid to 60% organic buffer constituted by acetonitrile with 5% H₂O and 0.1% formic acid, at 300 nL/min flow rate. Analyses were performed in positive ion mode and the HV Potential was set up around 1.7–1.8 kV. Tandem mass spectra were matched against the *G. duodenalis* protein database (Giardia DB version 1.2) downloaded from the Web site <http://www.giardiadb.org/giardiadb> and through the SEQUEST algorithm incorporated in the Bioworks software (version 3.3, Thermo Electron). The following match parameters were considered: fully tryptic cleavage constraints (one miscleavage allowed), static cysteine carbamidomethylation, and variable methionine oxidation. Precursor and fragment ions were searched with 1.5 and 1 Da tolerance, respectively. Possible NBDHEX adducts on cysteine or lysine residues were searched. The mass increments considered were +296, +281, +265 Da, for the intact, partially or completely nitro-reduced NBDHEX adducts, respectively. Statistical parameters used for legitimate protein identification were described elsewhere (Lalle et al., 2012).

Chemical Reduction of NBDHEX

Sodium dithionite was prepared as a 1M solution in ddH₂O and was used 100 mM to chemically reduce 10 mM NBDHEX in 20 μl 0.5% NH₃. After 5 min, 2 μl reaction was diluted to 200 μl in 67 mM potassium phosphate buffer (pH 7.5). NBDHEX fluorescence quenching was verified at 25°C in a Luminescence Spectrometer LS50B (Perkin-Elmer) whereas the UV-visible spectra was acquired at 25°C in a Multiskan Spectrum (Thermo Scientific) spectrophotometer in 0.5 ml quartz cuvettes. For the mass spectrometry analysis, the reaction mixture was diluted in 50% ethanol and 1% ammonia and directly infused in the LTQ mass spectrometer through a glass tip. The nanospray ionization in positive ion mode was allowed applying 1.5–1.6 kV. HV Potential. Full MS in the 150–350 m/z range were acquired; then MS3 fragmentation of the ions 280 and 250, derived from MS2 of 298 and 268, respectively, was induced.

Sequence Analysis

Conserved functional domains and sites in the protein sequence were search using ELM (Dinkel et al., 2014) and BLASTP¹ algorithms. Transmembrane (TM) regions were search by TMHMM Server v.2.0². Mitochondrial targeting signal were search using Psort II³ and MitoProt II⁴. Genomic sequences of 1133 organisms were downloaded from EggNog database v.3.0 (Powell et al., 2012). If more than one strain was available, only the strain classified as “core” was retained. This selection resulted in 774 organisms, which were included in the reference set. The Smith-Waterman algorithm available in the FASTA package (Pearson and Lipman, 1988) was exploited using as query the gG3PD full-length sequence, or the protein portions encompassing: the first 500 residues (referred as N-terminal domain); or the residues 501–950 (referred as central domain); or

¹<http://blast.ncbi.nlm.nih.gov>

²<http://www.cbs.dtu.dk/services/TMHMM/>

³<http://psort.hgc.jp/form2.html>

⁴<http://ihg.gsf.de/ihg/mitoprot.html>

the residues 951–1111 (referred as the C-terminal domain); or the protein portion including the N- and central domains (residues 1–950). Sequences having a match result with *E*-value lower than 10^{-6} were selected, except for the C-terminal domain for which the *E*-value threshold was set at 10^{-3} . Sequence analysis, editing and phylogenetic analysis were performed using Bioedit (Hall, 1999), MEGA 5.0 (Tamura et al., 2013), and Jalview 2.8.2 (Waterhouse et al., 2009).

Statistics

Statistical analyses were performed with PRISM 6.0 software (GraphPad Software, Inc; La Jolla, CA, USA) and significance was calculated by Student unpaired *t*-test and one-way ANOVA. A *P*-value <0.05 was considered statistically relevant.

Results

Sequence Analysis of the Putative FAD-D glycerol-3-Phosphate Dehydrogenase (gG3PD) of *G. duodenalis* Reveals an Unusual Protein Organization

The GL50803_16125 entry encodes a protein of 1111 amino acids (~ 119 kDa) annotated as FAD-dependent oxidoreductase/glycerol-3-phosphate dehydrogenase, that we named gG3PD. A combined search for conserved regions in the gG3PD protein sequence retrieved three principal domains (Supplementary Figure S1A). The region encompassing residues 31–510 contains the multidomain TIGR03377 corresponding to the protein family of the subunit A (GlpA) of anaerobic GlpACB. A second domain, residues 587–910, corresponds to a small NADH binding domain within a larger FAD binding domain (Pyr_redox_2, PF07992) which is common to flavoproteins of the pyridine nucleotide-disulphide oxidoreductases family [e.g., thioredoxin reductases (TRxR), NADH oxidases, and peroxidases]. The last domain (DUF 1667), encompassing residues 1039–1103, was previously found in archaeal and bacterial hypothetical proteins, some of which are annotated as being potential metal-binding proteins. As for other G3PDs, no TM regions could be detected. Due to its unusual domain organization, the full-length or three portions (residues 1–510, 511–950, and 951–111) of the gG3PD protein sequence were used as query against a large non-redundant set of high quality reference genomes obtained from EggNog. Despite an homologous sequence present in the genome of the closely related diplomonad *Spironucleus salmonicida*, only protozoan parasites of the genus *Entamoeba* encode for a single sequence orthologous to the full length gG3PD and also annotated as glycerol-3-phosphate dehydrogenase. One orthologue of the first two portions of the gG3PD was found in the genomes of *Eggerthella* sp., a non-sporulating medically important anaerobic Gram-positive bacillus, and annotated as FAD-dependent oxidoreductase. On the contrary several hundred orthologues of the first portion of gG3PD (residues 1–510), all annotated as glycerol-3-phosphate-dehydrogenases, were found in the genome of human and animal pathogenic bacteria, such as *Treponema* sp. (Spirochaetes) and *Clostridium*

sp. (Firmicutes), or to halophilic archaea, e.g., *Halorhabdus utahensis*, (Supplementary Figure S1B). More than 100 orthologues of the second portion (residues 501–950) were found in human and animal pathogenic bacteria, but also in soil and plant bacteria (data not shown). Although several of these proteins were annotated as oxidoreductases it was not possible to define, in terms of substrate or biochemical pathway, any specific enzymatic function. Finally, only 33 orthologues were found respect to the third portion of gG3PD (residues 951–111), which putative function could be that of metal-binding proteins.

The Intracellular Localization and Stage Expression of gG3PD Protein

According to the data reported in GiardiaDB, the expression level of the *gg3pd* is downregulated during encystation. To investigate whether the gG3PD protein expression level was similarly regulated we used a mouse polyclonal antibody raised against a full-length HIS-tagged recombinant gG3PD expressed in bacteria. As shown in **Figure 1A**, a band of approximately 120 kDa was immunodecorated with comparable intensity by the anti-gG3PD Ab, both in cellular lysates from trophozoites and from parasites harvested at different time points after encystation induction (at 6, 12, and 24 h). Encystation progress was checked by immunostaining with anti-phosphoacetylglucosamine mutase (gPGN) Ab, a protein induced during cyst formation (Lopez et al., 2003). The anti-gG3PD Ab was also used to study the intracellular localization of the protein by CLSM. In the trophozoite (**Figure 1Ba**) the anti-gG3PD strongly stained the plasma membrane of the parasite ventral surface likely corresponding to the marginal groove and ventrolateral flanges (VLF), fingerlike projections of the plasma membrane involved in parasite attachment to the surface and to the host cell (Sousa et al., 2001). As previously reported, the g14-3-3 showed a spotty broad distribution in the parasite cell body, excluding the nuclei and the median body (smile-like microtubule aggregate in the middle of parasite body). The widespread g14-3-3 staining makes it difficult to claim for a discrete co-localization with the gG3PD, although a slight co-localization signal (pseudo color yellow) was visible at the posterior edge of the trophozoite (**Figure 1Ba**, merge). *G. duodenalis* encystation was monitored by the progressive appearance of specialized structures for the secretion of the cyst wall proteins (CWP), the encysting specific vesicles (ESVs), which were stained, together with the cyst wall, by the anti-CWP mAb. In encysting parasites, in addition to the ventral plasma membrane, the anti-gG3PD Ab (**Figures 1Bb,c**) labeled several structures, similar to aggregates/small vesicles, in the cytoplasm. These structures did not co-localize with the ESVs and no straightforward co-localization with g14-3-3 could be detected (**Figures 1Bb,c**). In cysts, the gG3PD was diffused in the cytoplasm, although a marked aggregation close to the plasma membrane, below the cyst wall was evident (**Figure 1Bd**). A faint co-localization with g14-3-3 (pseudo color yellow) was detected below the cyst wall.

Since the staining with the anti-gG3PD Ab observed in encysting parasites resembled that of mitosomes, additional co-localization experiments were performed using an antibody

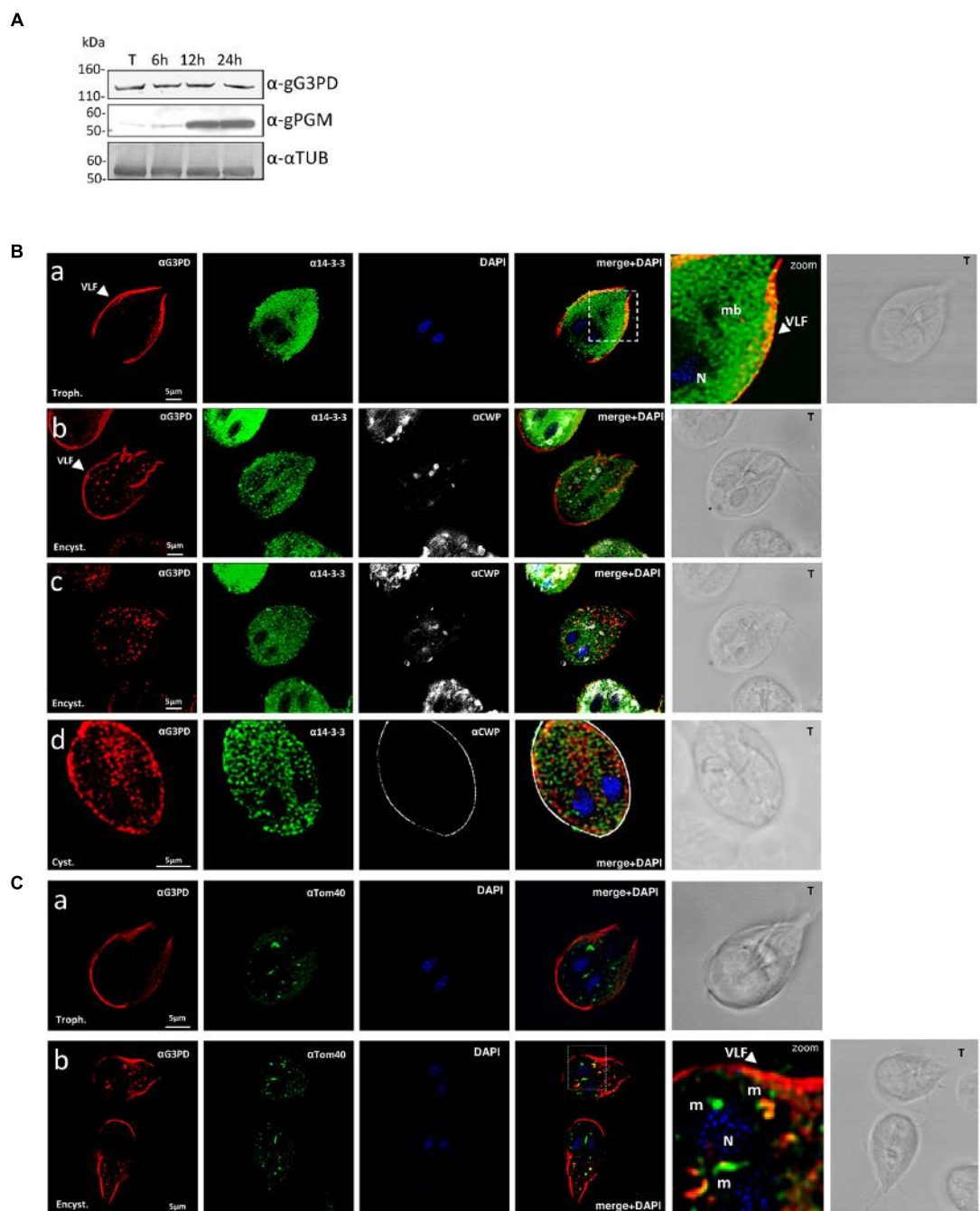


FIGURE 1 | Expression and localization of the glycerol-3-phosphate dehydrogenase (gG3PD) during the differentiation stages of *Giardia duodenalis*. **(A)** Western blot from three independent analysis of Triton lysates (20 µg) from *G. duodenalis* WB-C6 trophozoites (T) and parasites harvested at 6, 12, and 24 h after encystation induction. Immunoblotting was performed with: anti-gG3PD polyclonal serum (α -gG3PD); anti-phosphoacetylglucosamine mutase (α -PGM) (Lopez et al., 2003), to follow the progression of encystation; the anti- α -tubulin (α - α -TUB), as loading control. Molecular size markers (kDa) are reported on the left. The analysis is representative of three independent experiments. **(B)** Confocal laser scanning microscopy (CLSM) observations of fixed and permeabilized *G. duodenalis* WB-C6 parasites at different stages: trophozoite (panel a, Trophozoite), encysting parasite after 12 h of encystation (panel b and c, Encystation) and

cyst (panel d, Cyst) stained with the mouse polyclonal serum α -gG3PD (red) and the α -g14-3-3 rabbit polyclonal (green). Cyst wall and encystation specific vesicles (ESVs) were stained with Cy3-conjugated α -CWP mAb (gray). Nuclei (N) were stained with 4',6-diamidino-2-phenylindole (DAPI; blue). Displayed micrographs correspond to a single z-stack: a and b, ventral stacks; c and d, central stacks encompassing the nuclei. T, transmission light acquisition. Scale bars, 5 µm. Arrows indicate the ventrolateral flanges (VLF). A magnification (zoom) of the indicated area in the merged image is shown. **(C)** CLSM observation as in **(B)**. Parasites were stained with α -gG3PD (red) and α -Tom40 antiserum (green; Dagley et al., 2009). Nuclei (N) were stained with DAPI (blue). A magnification (zoom) of the indicated area in the merged image is shown. Mitosomes are indicated (m). Images in **(B)** and **(C)** are representative of >50 fields analyzed in two independent experiments.

directed against the mitosomal marker Tom40 (Dagley et al., 2009). As shown in **Figures 1Ca,b**, both in trophozoites and encysting parasites, the anti-Tom40 Ab stained the main central mitosome between the nuclei and several peripheral smaller mitosomes. In trophozoites no co-localization with anti-gG3PD could be detected (**Figure 1Ca**), whereas in encysting parasites superimposable signals (mean average $42 \pm 6\%$; **Figure 1Cb**, pseudo color yellow) were mainly evident in the peripheral mitosomes (mean average $27 \pm 5\%$), and to a lesser extent in the central one (mean average $2 \pm 0.5\%$), suggesting a partial re-localization of the protein to mitosomes.

Interaction between gG3PD and g14-3-3

To further characterize the gG3PD, a N-terminally FLAG-HA tagged gG3PD was expressed in *G. duodenalis* under the α -tubulin constitutive promoter. The FLAG-HA-gG3PD was expressed at the same level, and comparable to the endogenous protein, both in trophozoites and during the encystation stage (**Figure 2A**) and the intracellular localization largely resembled that of the endogenous gG3PD (Supplementary Figure S2). By following protein fractionation (soluble and membrane fractions), the endogenous and the FLAG-HA-gG3PD were mainly detected in the soluble fraction at both stages (**Figure 2B**). Whereas, a small protein amount could be detected in the membrane fraction only at the trophozoite stage (**Figure 2B**), partially in agreement with immunolocalization observations, suggesting that the gG3PD could form strong interactions with the membrane or with membrane proteins. To better investigate the previously suggested interaction between g14-3-3 and gG3PD (Lalle et al., 2012), immunoprecipitation experiments were performed. As shown by anti-HA immunoblotting (**Figure 2C**, upper), the

anti-FLAG mAb immunoprecipitated the FLAG-HA-gG3PD only from transfected parasite extracts. Despite FLAG-HA-gG3PD was comparably immunoprecipitated from both trophozoites and encysting parasites, g14-3-3 was mainly co-immunoprecipitated from trophozoites, whereas only a faint signal was observed in the immunoprecipitate from encysting parasites (**Figure 2C**, lower).

To shed light on the relevance of the two principal domains characterizing the gG3PD protein, two deletion mutants were constructed and independently expressed in *G. duodenalis* as FLAG-HA-tagged proteins. The FLAG-HA-gG3PD_N corresponds to N-terminal half of the protein (Supplementary Figure S1A) and contains the FAD-dependent anaerobic glycerol-3-phosphate dehydrogenase-like domain (residues 2–530); whereas the FLAG-HA-gG3PD_C corresponds to the C-terminal half and contains the FAD-dependent pyridine nucleotide-disulphide oxidoreductase-like domain (residues 524–1111). As shown by immunoblot (**Figure 3A**, upper and middle), the expression of both FLAG-HA-tagged proteins was detected at both stages. In all transfection experiments, the expression of deletion mutants was lower than that of the full-length FLAG-HA-gG3PD.

Intracellular localization of both mutants was performed with anti-HA antibody. CLSM analyses (**Figures 3Ba,b**) showed that, in trophozoites and encysting parasites, the FLAG-HA-gG3PD_N partially localized to the ventral plasma membrane and VLF, like the endogenous gG3PD. Although a spotty cytoplasmic and an intense nuclear/perinuclear staining were evident, in contrast with the endogenous and the full-length FLAG-HA-gG3PD, suggesting that a fraction of the deleted protein could be misfolded and/or mislocalized. In FLAG-HA-gG3PD_C transgenic parasites the protein was completely mislocalized and appeared widespread distributed, also inside

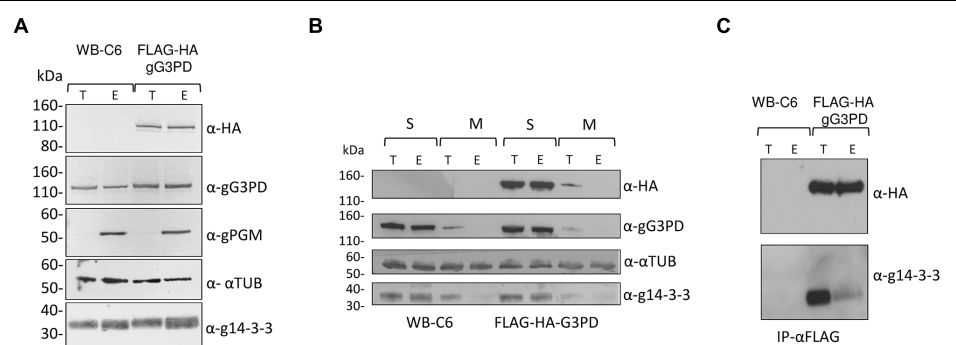


FIGURE 2 | Expression of the recombinant FLAG-HA-gG3PD in *G. duodenalis* and its interaction with g14-3-3. (A) Western blot analysis of Triton lysates from trophozoites (T) or parasites after 12 h of encystation (E) obtained from FLAG-HA-gG3PD transfected line or from the control WB6 strain. Twenty-microgram of protein extracts were loaded in each lane and separated on a 4–12% SDS-PAGE, then transferred on nitrocellulose membrane and finally probed with the indicated antibodies. Equal protein loading was monitored by anti-TUB Ab, whereas encystation induction was confirmed by anti-gPGM Ab. Molecular size markers (kDa) are reported in the left. **(B)** Subcellular distribution of gG3PD. Thirty-microgram of fractionated protein lysate, soluble (S) or octyl

β -D-glucopyranoside solubilized membrane proteins (M), from trophozoites (T) or 12 h encysting parasites (E) of FLAG-HA-gG3PD transfected parasites or control WB6, were treated as described in **(A)** and probed with the indicated antibodies. Molecular size markers are on the left. **(C)** Co-immunoprecipitation assay of endogenous g14-3-3 with FLAG-HA-gG3PD. An aliquot (1:5) of the FLAG peptide-eluted material from WB6 or FLAG-HA-gG3PD transgenic line, deriving from trophozoites (T) or encysting parasite (E), was separated on 4–12% SDS-PAGE and immunoblotted with anti-HA (α -HA) or anti-g14-3-3 polyclonal serum (α -g14-3-3). Molecular size markers are on the left. Immunoblots of **(A–C)** are representative of three independent experiments.

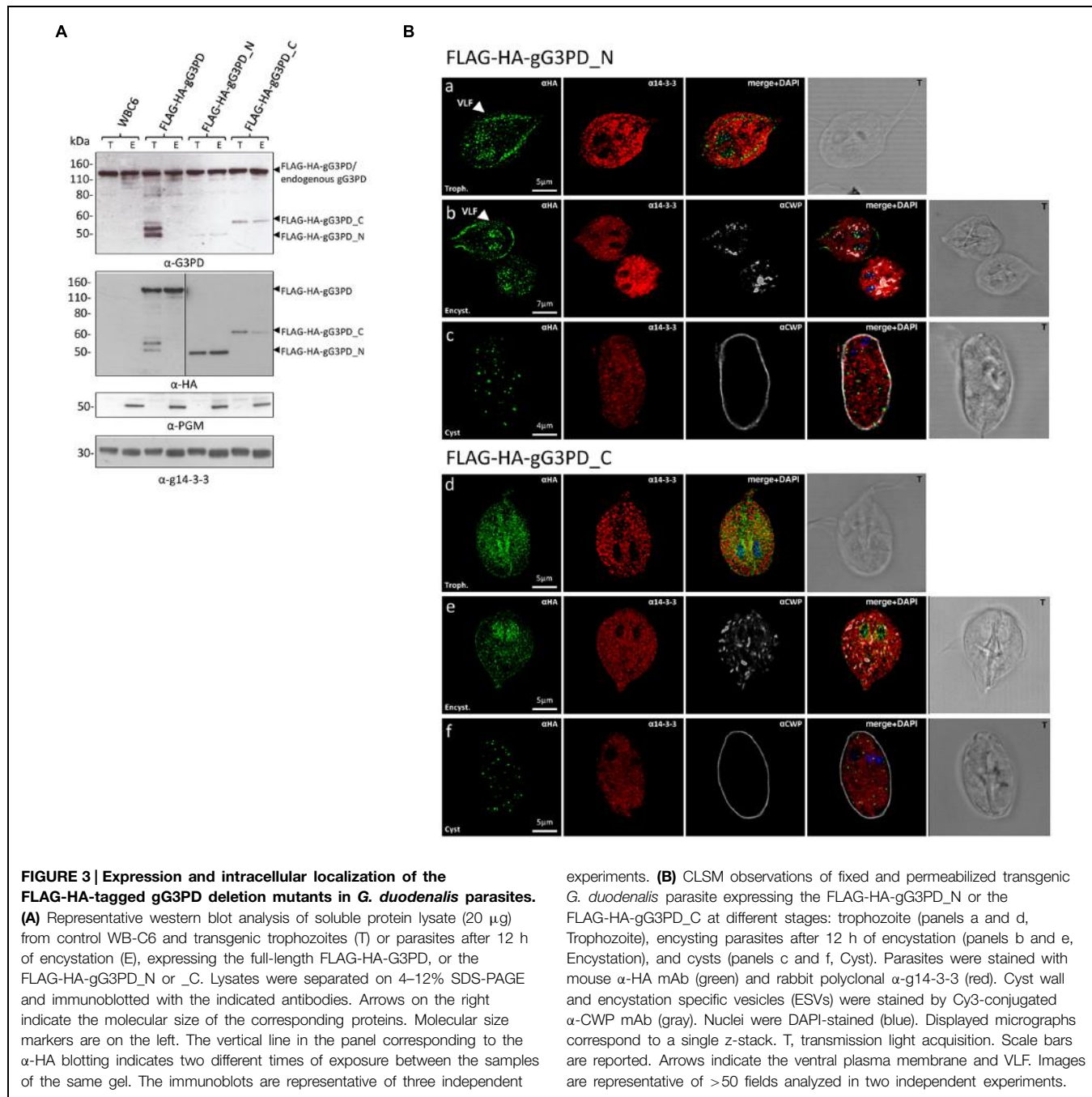


FIGURE 3 | Expression and intracellular localization of the FLAG-HA-tagged gG3PD deletion mutants in *G. duodenalis* parasites.

(A) Representative western blot analysis of soluble protein lysate (20 µg) from control WB-C6 and transgenic trophozoites (T) or parasites after 12 h of encystation (E), expressing the full-length FLAG-HA-gG3PD, or the FLAG-HA-gG3PD_N or _C. Lysates were separated on 4–12% SDS-PAGE and immunoblotted with the indicated antibodies. Arrows on the right indicate the molecular size of the corresponding proteins. Molecular size markers are on the left. The vertical line in the panel corresponding to the α-HA blotting indicates two different times of exposure between the samples of the same gel. The immunoblots are representative of three independent

experiments. (B) CLSM observations of fixed and permeabilized transgenic *G. duodenalis* parasites expressing the FLAG-HA-gG3PD_N or the FLAG-HA-gG3PD_C at different stages: trophozoite (panels a and d, Trophozoite), encysting parasites after 12 h of encystation (panels b and e, Encystation), and cysts (panels c and f, Cyst). Parasites were stained with mouse α-HA mAb (green) and rabbit polyclonal α-g14-3-3 (red). Cyst wall and encystation specific vesicles (ESVs) were stained by Cy3-conjugated α-CWP mAb (gray). Nuclei were DAPI-stained (blue). Displayed micrographs correspond to a single z-stack. T, transmission light acquisition. Scale bars are reported. Arrows indicate the ventral plasma membrane and VLF. Images are representative of >50 fields analyzed in two independent experiments.

nuclei, with the nuclear/perinuclear localization even more evident in encysting parasites (Figures 3Bd,e). No mitosome-like staining was observed in encysting parasites for any of the mutants (Figures 3Bb,e). Few cysts with a spotty cytoplasmic localization of the protein were observed in both transgenic strains (Figures 3Bc,f). These observations likely suggest, that the N-terminal half of the protein contains the structural/sequence determinants necessary to localize the gG3PD at the ventral plasma membrane and VLF. Looking for the domain(s) involved in the interaction with g14-3-3, co-immunoprecipitation with anti-FLAG was also performed using the FLAG-HA deletion

mutants. Despite several attempts no conclusive results were obtained (data not shown), likely due to the low expression of these proteins or to the presence of other factors that could affect the interaction (e.g., partial misfolding, incomplete phosphorylation).

Evaluation of gG3PD Enzymatic Activity

To better define the role of gG3PD during *G. duodenalis* differentiation, we first characterized the protein activity using N-terminally HIS-tagged versions of both full-length gG3PD and deletion mutants heterologously expressed in *E. coli*. All

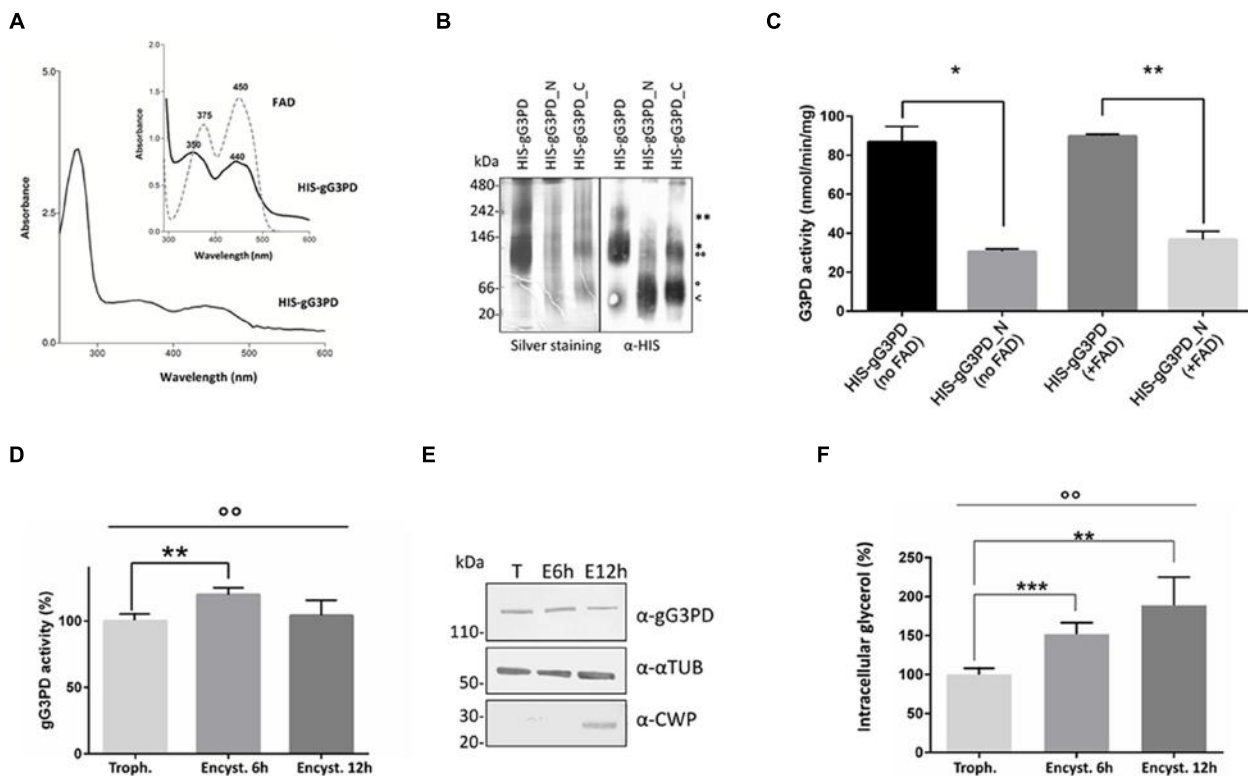


FIGURE 4 | Evaluation of the gG3PD enzymatic activity.

(A) Spectrophotometric analysis of purified HIS-gG3PD. The UV-visible spectrum of HIS-gG3PD (10 mg/ml) in 67 mM of potassium phosphate buffer, pH 7.5, was recorded at 25°C. The insert shows a magnification of the HIS-gG3PD spectrum (solid line) in comparison with the spectrum of authentic FAD (dotted line) recorded in the same buffer. Peak maxima are reported. Spectra are representative of three independent experiments.

(B) Assessment of HIS-gG3PD dimerization *in vitro*. Purified recombinant proteins (3 μmol) were separated on 3–12% Blue Native-PAGE and silver-stained or transferred on polyvinylidene difluoride (PVDF) membrane and probed with anti-HIS mAb. Native size markers (kDa) are indicated on the left. Asterisks indicate HIS-gG3PD monomer (*) or dimer (**). Empty dots indicate HIS-gG3PD_C monomer (°) or dimer (°°). The arrow indicates HIS-gG3PD_N monomer (<). Native-PAGE and immunoblot are representative of three independent experiments. **(C)** The enzymatic activities of both the purified HIS-gG3PD and the deletion mutant HIS-gG3PD_N were measured *in vitro*, by MTT assay, in the presence (+FAD) or absence (no FAD) of 10 μM FAD. The G3PD activity (mean ± SD) from three independent experiments is expressed as nmol of reduced MTT per min per mg of recombinant protein. Statistical analyses were performed using unpaired *t*-test between the full length and the deletion mutant: **P* < 0.05 and

P* < 0.01. **(D)** The FAD-glycerol-3-phosphate dehydrogenase activity was measured in protein extract (100 μg) from *G. duodenalis* trophozoites (Trophozoite) or in parasite after 6 or 12 h from encystation induction (Encystation). The relative enzymatic activity (mean ± SD) from three independent experiments is expressed as the percentage change respect to the value measured in trophozoites. Statistical analyses were performed using unpaired *t*-test [Trophozoite vs. Encystation 6 h (P* < 0.01) and Trophozoite vs. Encystation 12 h (ns)], and one-way ANOVA (°*P* < 0.001). **(E)** Western blot analysis of protein extracts (20 μg) used to assay the gG3PD enzymatic activity (as described in **D**), extracts were separated on 4–12% SDS-PAGE and immunoblotted with the indicated antibodies. Molecular size markers are indicated on the left. Immunoblot is representative of three independent experiments. **(F)** The intracellular glycerol content was measured in supernatant from *G. duodenalis* trophozoites (Trophozoite) and parasites after 6 or 12 h from encystation induction (Encystation). The relative glycerol amount of three independent experiments (mean ± SD) is expressed as the percentage change respect to the amount detected in trophozoites. Statistical analyses were performed using unpaired *t*-test between Trophozoite and Encystation 6 h (****P* < 0.001) and Trophozoite vs Encystation 12 h (***P* < 0.01). One-way ANOVA confirmed that differences among groups were statistically significant (°*P* < 0.001).

recombinants were expressed as soluble proteins and could be purified (up to 95%) under native conditions (Supplementary Figure S3). The purified full-length HIS-gG3PD, but not the deletion mutants, showed a distinctive yellow color (data not shown), compatible with the presence of a flavin cofactor. Indeed, the UV-visible spectra of the HIS-gG3PD showed two absorbance peaks with a maximum approximately at 350 and 440 nm (Figure 4A), very close to those of free flavin (either FAD or FMN or both), supporting that the gG3PD is a flavoprotein. No similar peaks could be observed in the spectra of any deletion

mutants (data not shown). Since mG3PD/glpD are homodimeric proteins (Mráček et al., 2013), the dimeric nature of gG3PD was assayed using native PAGE. As shown in Figure 4B, the HIS-gG3PD_N was exclusively monomeric (60 kDa); whereas the HIS-gG3PD migrated in the gel both as a 120 kDa monomer and as a 240 kDa dimer, as confirmed by immunoblot assay with anti-HIS. Similarly, the HIS-gG3PD_C migrated as a monomer around 60 kDa, and as a dimer of 120 kDa, thus suggesting that at least one function of the gG3PD C-terminal half is to mediate protein dimerization.

The FAD-glycerol-3-phosphate dehydrogenase activity of the HIS-gG3PD was then assayed by measuring the g3p-dependent reduction of MTT in presence of PMS, which mediates the transfer of reducing equivalent from the enzyme to the terminal dye (Kistler and Lin, 1972). As shown in **Figure 4C**, the HIS-gG3PD displayed a specific activity corresponding to 86.7 ± 5.6 nmol/min/mg in the absence of exogenous FAD, that did not significantly increase (89.8 ± 0.7 nmol/min/mg) even when $10 \mu\text{M}$ FAD was added. Moreover, no activity could be observed either in the absence of g3p or PMS (data not shown), thus proving that g3p is indeed the substrate of the enzyme and that an electron carrier molecule, such as PMS, is required to reduce MTT. This is in agreement with the role of quinone described for other FAD-dependent G3PDs (Unden and Bongaerts, 1997; Mráček et al., 2013). Intriguingly (**Figure 4C**), the HIS-gG3PD_N, containing the GlpA-like domain, also displayed a basal enzymatic activity (30.5 ± 1.0 nmol/min/mg), 2.8-fold lower in comparison with the full length protein, and it showed an increase of 17% in the activity (36.7 ± 3.0 nmol/min/mg) after stimulation with exogenous FAD. On the contrary, the HIS-gG3PD_C did not show any enzymatic activity in any condition (data not shown). These results support the homology data and confirm that the glycerol-3-phosphate dehydrogenase activity is localized to the N-terminal half of the gG3PD.

To study the possible correlation between encystation-dependent intracellular re-localization of gG3PD and its function, the enzyme activity was measured in trophozoites and encysting parasites extracts. Indeed, compared to trophozoites, the gG3PD activity showed a 20% increase at 6 h of encystation (**Figure 4D**), then it was reduced nearly down to the trophozoite level after 12 h of encystation. No variation in the expression level of the gG3PD protein could be observed at any time points (**Figure 4E**). The encystation process in *G. duodenalis* has been proposed as a primitive response to cellular stress (Argüello-García et al., 2009). In unicellular organisms, as response to stress signals, the intracellular level of glycerol increases, as consequence of a massive conversion of DAPH to g3p, due to the greater activity of the NADPH-dependent G3PDs and in some cases also to that of FAD-dependent G3PDs (Yang et al., 2007). To test this hypothesis we measured the intracellular content of glycerol during encystation. The amount of glycerol increased up to 60% already at 6 h post-encystation induction (**Figure 4F**) and then of an additional 15% in 12 h encysting parasites, thus suggesting a possible relationship between the enhanced gG3PD activity and the glycerol accumulation occurring during parasite differentiation.

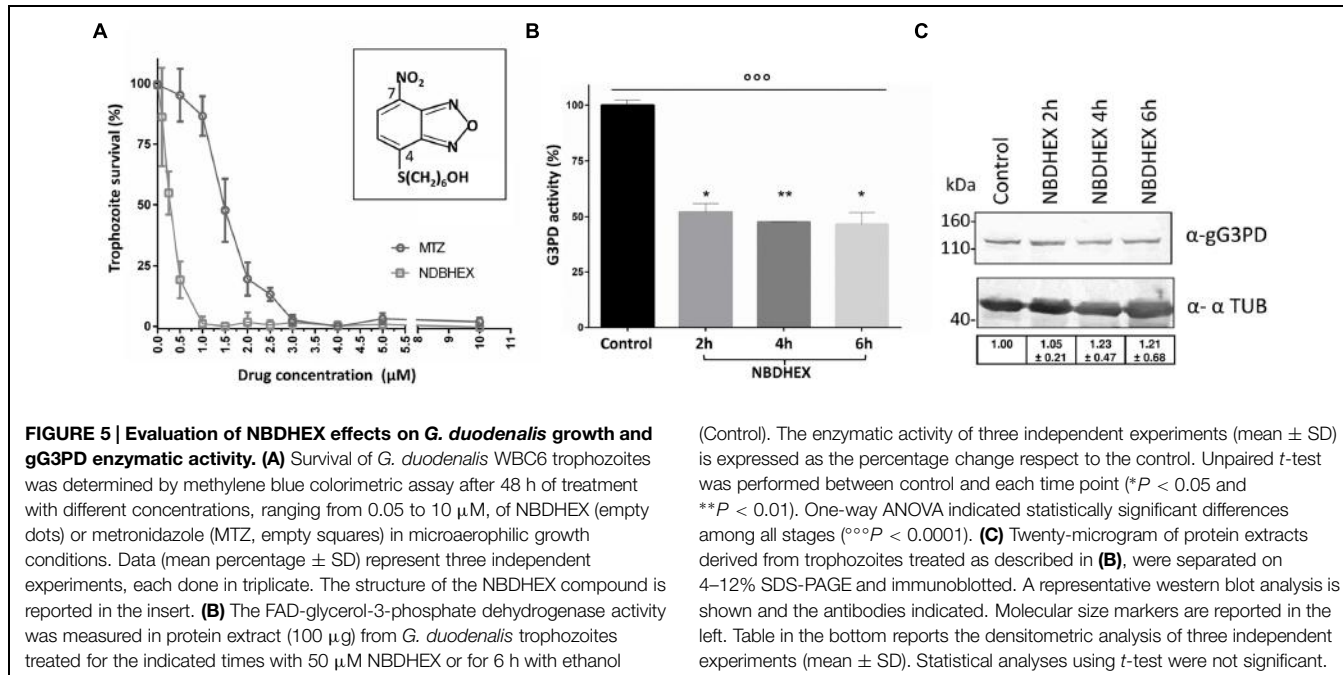
In Vivo Effects of NBDHEX on *G. duodenalis* Survival and gG3PD Activity

Recently, a 7-nitro benzoxadiazole (NBD) derivative has been shown to impair the growth of PC-3 adenocarcinoma cell line by a significant inhibition of the glycerol-3-phosphate oxidoreductase activity of mG3PD (Singh, 2014). We wondered whether this class of molecules could be effective against *G. duodenalis* trophozoites and the gG3PD. We selected the

NBDHEX, a promising antitumoral drug acting as a suicide inhibitor of human glutathione S-transferases (GSTs), that also shows a good tolerance in mouse models (Ricci et al., 2005; Turella et al., 2005; Pellizzari Tregno et al., 2009; Tentori et al., 2011). NBDHEX cytotoxicity against *G. duodenalis* trophozoites was evaluated *in vitro* after 48 h of treatment in microaerophilic growth conditions, using a colorimetric assay. As shown (**Figure 5A**), NBDHEX was effective against the parasite ($\text{IC}_{50}: 0.3 \pm 0.1 \mu\text{M}$) at a lower concentration (5.6-fold) than that of the reference drug MTZ ($\text{IC}_{50}: 1.5 \pm 0.1 \mu\text{M}$). Moreover, under anaerobic growth conditions NBDHEX was also more effective than MTZ ($\text{IC}_{50}: 0.6 \pm 0.4 \mu\text{M}$ for NBDHEX and $\text{IC}_{50}: 1.9 \pm 0.2 \mu\text{M}$ for MTZ; data not shown). To maximize in a short time period the possible NBDHEX effects, taking into account the parasite intracellular environment, trophozoites were treated *in vivo* with $50 \mu\text{M}$ NBDHEX and then the gG3PD enzymatic activity was assayed in parasite extracts. A 50% decrease of the gG3PD activity was already evident after 2 h of treatment (**Figure 5B**, $P < 0.01$), and a further 5% decrease was achieved after 4 and 6 h. This suggests that *in vivo* NBDHEX treatment reduces the gG3PD activity, without inducing any statistically relevant variation of the protein expression level (**Figure 5C**).

Interaction of NBDHEX with gG3PD

To ascertain if the effects on the gG3PD activity were due to a direct NBDHEX binding to the enzyme, co-localization experiments were performed by CLSM (**Figure 6A**), taking advantage of the fluorescent properties of the compound (maximum emission peak at 525 nm; Ricci et al., 2005). Only trophozoites treated with NBDHEX showed a spotted faint fluorescence in the cytoplasm. A more intense signal was observed around the nuclei, in the areas corresponding to the median body, in the intracellular portion of ventral flagella and, intriguingly, at the ventral plasma membrane. As shown, co-localization signal (pseudo color yellow) between gG3PD and NBDHEX was evident only at plasma membrane, without any relevant alteration in the intracellular localization of gG3PD (for comparison see **Figures 1B,Ca**). To further study the interaction between NBDHEX and gG3PD, *E. coli* expressing the HIS-gG3PD was incubated with NBDHEX, then the recombinant protein was purified and, finally, the enzymatic activity was assayed. Similar to the *in vivo* treatment of *G. duodenalis* with NBDHEX, incubation of bacteria with the compound resulted in a recombinant HIS-gG3PD having a 25% reduced enzymatic activity (**Figure 6B**). Next, we wondered whether NBDHEX could bind HIS-gG3PD. We take advantage of the property of NBD derivatives covalently bound to a protein to be visualized by fluorescence under ultraviolet (UV) light after SDS-PAGE (Bragg and Hou, 1999). Indeed, HIS-gG3PD, purified from NBDHEX treated bacteria, was fluorescent under UV-light (**Figure 6C**, right), even in the presence of a reducing agent (such as DTT). On the contrary, no fluorescence was associated with the HIS-gG3PD purified from untreated bacteria. These results suggest that NBDHEX strongly binds HIS-gG3PD. To confirm this hypothesis, purified HIS-gG3PD from bacteria, treated or not with NBDHEX, was subjected to mass spectrometry analysis.



MS/MS spectra were acquired matching two HIS-gG3PD peptides carrying NBDHEX derived adducts on cysteine residues: the detected mass shift was compatible with an NBDHEX form in which the nitro group was reduced to amine (Figure 6D). No adduct with the intact NBDHEX moiety could be found, probably because it was unstable or not detectable under the applied experimental conditions. The presence of nitro-reduced NBDHEX adducts was in favor of an electrochemical reduction of the drug, likely by gG3PD. Therefore, NBDHEX properties were evaluated by spectrophotometric and fluorimetric analyses after *in vitro* incubation with HIS-gG3PD. The UV-visible spectra of NBDHEX, incubated either with g3p or with HIS-gG3PD, showed the typical peak centered around 430 nm (Figure 7A), even after 80 min of incubation (data not shown). Incubation in the presence of both HIS-gG3PD and g3p led to the progressive decrease of the 430 nm absorption peak and to the appearance of a less intense new one around 450–455 nm (Figure 7A). The reaction was also associated with a change in color, from bright yellow to brown (Figure 7B, insert) and the disappearance of the 525 nm emission peak of NBDHEX in the fluorescence spectra (Figure 7B). Since the amount of NBDHEX was in large excess compared to HIS-gG3PD, the observed spectral alterations were not imputable to binding of NBDHEX to the enzyme, but they argued on NBDHEX modification by the glycerol-3-phosphate dehydrogenase activity of HIS-gG3PD. Such modifications could be ascribable to a partial or complete reduction of the nitro group to hydroxylamine or amine. Chemical reduction of the NBDHEX nitro group to amine by sodium dithionite, proved by mass spectrometry analysis (Supplementary Figure S4), resulted in the decrease of the NBDHEX absorption peak at 430 nm, although with the appearance of a new peak at 405 nm (Figure 7C), and loss of fluorescence too (Figure 7D). The observed differences between UV-visible spectra of HIS-gG3PD and sodium dithionite

(Control). The enzymatic activity of three independent experiments (mean \pm SD) is expressed as the percentage change respect to the control. Unpaired *t*-test was performed between control and each time point (* $P < 0.05$ and ** $P < 0.01$). One-way ANOVA indicated statistically significant differences among all stages (** $P < 0.0001$). (C) Twenty-microgram of protein extracts derived from trophozoites treated as described in (B), were separated on 4–12% SDS-PAGE and immunoblotted. A representative western blot analysis is shown and the antibodies indicated. Molecular size markers are reported in the left. Table in the bottom reports the densitometric analysis of three independent experiments (mean \pm SD). Statistical analyses using *t*-test were not significant.

treated NBDHEX suggest that the enzymatic activity produced an optical species, probably compatible with an incomplete reduced form of NBDHEX, carrying an hydroxylamine instead of an amine moiety. On the other side, looking to the NBDHEX-treated HIS-gG3PD, both in the presence or absence of g3p, the enzyme resulted fluorescent under UV light after SDS-PAGE (Figure 7E). This suggests that protein adducts with the unreduced NBDHEX occurred despite, enzyme activation. Products from *in vitro* reactions between HIS-gG3PD and NBDHEX were also analyzed by mass spectrometry. In the sample incubated in the presence of g3p, some HIS-gG3PD cysteine residues were modified by NBDHEX and MS/MS spectra analysis allowed to detect mass shifts compatible with NBDHEX adducts carrying the NO₂ moiety completely reduced to NH₂, but also the semi-reduced hydroxylamine group (Supplementary Figure S5). These adducts could not be detected when g3p was omitted.

Since toxicity of the nitrocompound MTZ over *G. duodenalis* has been related to its reduction to nitrosoimidazole or hydroxylamine intermediate by flavin enzymes (Leitsch et al., 2007, 2009, 2011), we asked whether the gG3PD could be able to nitroreduce MTZ. We then monitored variation in the MTZ absorbance at 320 nm (Leitsch et al., 2011). As shown, no decrease in MTZ absorbance occurred even after 80 min of incubation in the presence of HIS-gG3PD and g3p (Figure 7F), thus suggesting that in our experimental conditions MTZ is not nitroreduced by gG3PD.

Discussion

In this work we have characterized, for the first time, the FAD-dependent glycerol-3-phosphate dehydrogenase of *G. duodenalis*

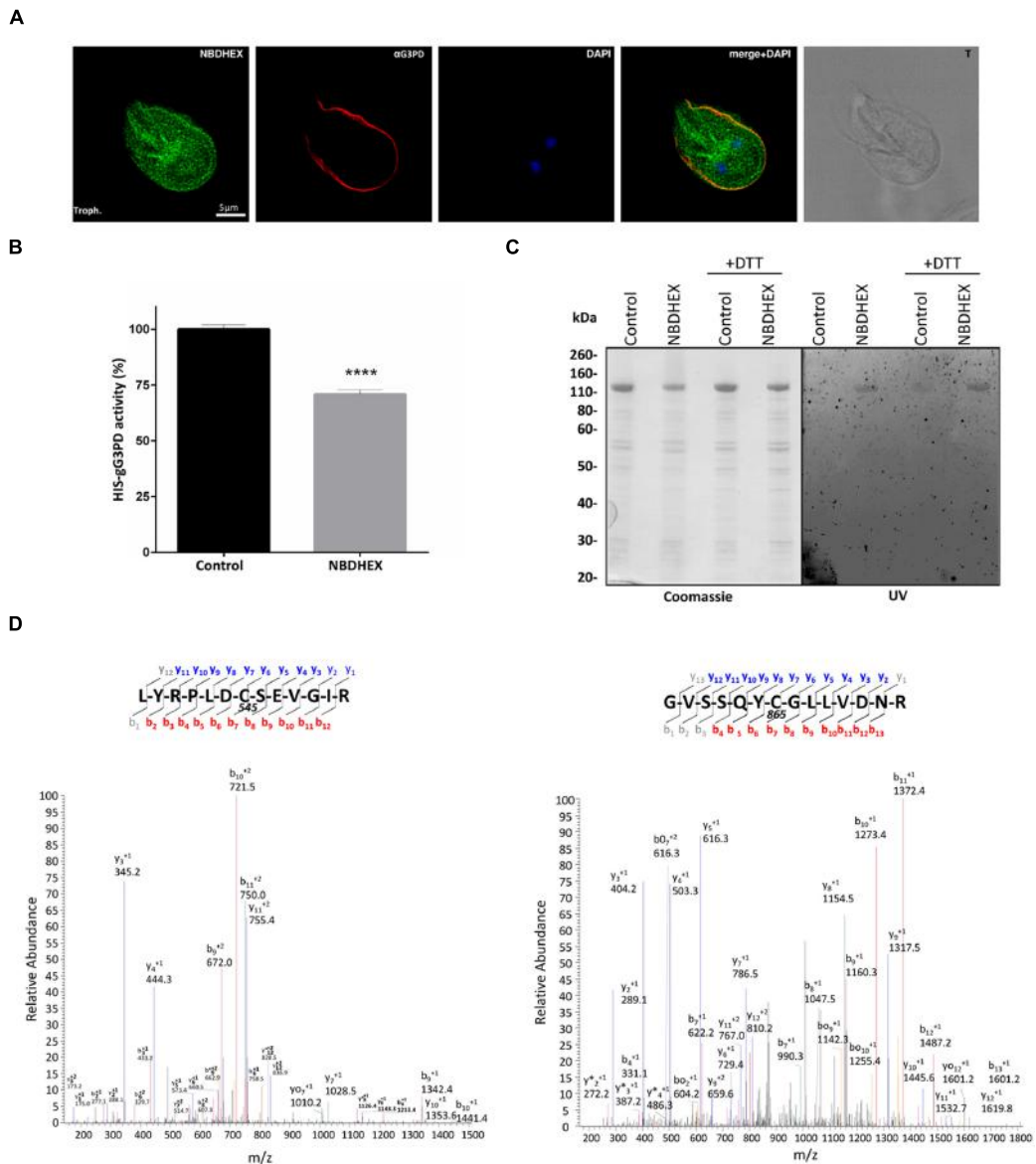


FIGURE 6 | Interaction of NBDHEX with gG3PD. (A) CLSM analysis of fixed and permeabilized *G. duodenalis* WBC6 trophozoites after 2 h incubation with 50 μ M NBDHEX. NBDHEX (green) was directly visualized using the laser light at 488 nm ex. Parasites were stained with rabbit polyclonal anti-g14-3-3 and AlexaFluor 647-conjugated anti-rabbit (red). Nuclei were stained with DAPI (blue). Displayed micrographs correspond to a single z-stack. T, transmission light acquisition. Scale bar is reported. Images are representative of >50 fields analyzed in two independent experiments. **(B)** Histograms represent the FAD-glycerol-3-phosphate dehydrogenase activity (mean percentage \pm SD) of recombinant HIS-gG3PD (16 pmol) purified from *HIS-gG3PD-overproducing E. coli* after 2 h incubation with 50 μ M NBDHEX (NBDHEX) or ethanol (Control). The relative change in the enzymatic activity is given as percentage in relation to the control. Statistical analyses were performed using unpaired *t*-test ($****P < 0.0001$) on three independent experiments. **(C)** SDS-PAGE (4–12%) of 2 μ g of purified NBDHEX-treated (NBDHEX) or ethanol-treated (Control) HIS-gG3PD, as described in **(B)**, under reducing (+DTT) or not reducing condition. On the left, gel stained with Coomassie blue; on the right, the same gel photographed under UV light prior to staining. Molecular size markers are indicated on the left. **(D)** MS/MS spectra matching the gG3PD peptides (residues 539–551, left, and residues 859–872, right) carrying a mass increase of 265 Da on the cysteine residues C545 and C865, respectively. The mass shift is compatible with an NBDHEX-derived adduct in which the nitro group was completely reduced to an amine. Data shown in **(C)** and **(D)** are representative of three independent experiments.

both at molecular and functional level, and we have shown that the antitumoral 7-NBD derivative NBDHEX displays a remarkable antigiardial activity, targets the gG3PD and, when *in vivo* administered to *G. duodenalis*, induces gG3PD activity reduction.

The full length gG3PD has no orthologues in other organisms, including humans, except for the diplomonad *S. salmonicida* and the amebidae *Entamoeba* sp. The presence in the gram-positive anaerobic actinobacteria *Eggerthella* sp. of an orthologue of the first 950 amino acids suggests that a first gene fusion

event between a GlpA-like gG3PD and a pyridine nucleotide-disulphide oxidoreductase occurred in this prokaryotic lineage. A lateral gene transfer (LGT) event could account for the presence of this multi-domain protein both in *G. duodenalis* and *Entamoeba* sp., that share with *Eggerthella* sp. the mammalian intestine as ecological niche. LGT events have been already well documented for genes of the anaerobic metabolism in eukaryotic protozoan parasites such as *Entamoeba histolytica*, *Trichomonas vaginalis*, and *G. duodenalis* (as well as in *S. salmonicida*; Andersson et al., 2007; Morrison et al., 2007; Alsmark et al., 2009).

We demonstrate that the gG3PD is an active flavoenzyme able to use g3p as source of reducing equivalents. In agreement with the domain topology and homology with bacterial GlpA subunit, the enzymatic activity, as proven by deletion mutants, resides in the N-terminal half of the protein. It is worth noting that the modest stimulatory effect exerted by additional FAD on the enzymatic activity of both the gG3PD and the gG3PD_N, could be explained by different reasons (i) the full length gG3PD is fully complexed with FAD; and/or (ii) the deletion mutant lacks the ability to properly bind FAD; and/or (iii) the enzyme needs FMN in addition to FAD. Indeed, the maximal activity of *E. coli* trimeric GlpACB *in vitro* requires both FMN and FAD (Cole et al., 1988), whereas glpD binds only FAD (Yeh et al., 2008). Furthermore, we show that gG3PD is able to dimerize and that the C-terminal half is required for the dimer formation. The dimerization properties of this gG3PD region, absent in bacterial GlpA, could be ascribable to its homology with members of the FAD-dependent pyridine nucleotide-disulphide oxidoreductases, a family of generally dimeric proteins (Argyrou and Blanchard, 2004).

Localization of the gG3PD to the ventral plasma membrane, likely in correspondence to the VLF, and the detection of the enzymatic activity in parasite extracts are in favor of the existence of functional glycerol biosynthetic pathway and of a role of the protein in *G. duodenalis* energy metabolism. Similar to bacteria (Unden and Bongaerts, 1997), metabolization of g3p by *G. duodenalis* could occur at plasma membrane via gG3PD thus providing an extra source of DHAP for glycolysis and reducing equivalents to putative ETCs. Experimental evidences indicate that *G. duodenalis* can proliferate *in vitro* even in absence of glucose, its main energy source (Adam, 2001), either in the presence of serum (Schofield et al., 1991) or of a defined mixture of bile salts, phosphatidylcholine (PC) and cholesterol (Gillin et al., 1986; Gault et al., 1987). Incorporation of free glycerol and g3p in trophozoites has been reported to be negligible (Jarroll et al., 1981). Nevertheless, mammalian bile and intestinal epithelium mucus are rich of PC, that is efficiently taken up by *G. duodenalis* trophozoites (Stevens et al., 1997). PC, in turns, can potentially be converted to g3p by the combined activity of a phospholipase PLB and a putative GPC-PDE, both encoded by *G. duodenalis* genome (Morrison et al., 2007; Yichoy et al., 2011).

We show that the gG3PD activity increases early at encystation, without up-regulation of protein expression. In this phase of encystation, energy metabolism and galactosamine synthesis require extra carbon sources as consequence of the highly reduced glucose uptake and decrease in oxygen

consumption (Paget et al., 1998). We may speculate that gG3PD could provide extra carbon to glycolysis, via an improved metabolization of g3p to DHAP. In parallel, we also observed an increase in intracellular glycerol levels. In response to stress conditions, including hyperosmotic stress, several microorganisms synthesized glycerol as stress protector via an increased DHAP to g3p conversion mediated by the NAD(P)H-dependent G3PD (Albertyn et al., 1994; Yang et al., 2007; Chen et al., 2012; Suescún-Bolívar and Thomé, 2015). The increase in the bile salt, together with a slight alkaline pH, is a key encystation signal eventually perceived by *G. duodenalis* as hyperosmotic stress. It is worth to note that, in *E. histolytica*, intracellular accumulation of both g3p and glycerol occurs in response to oxidative stress despite only the gG3PD orthologue is present and no NAD(P)H-dependent G3PD activity has been detected (Husain et al., 2012). The unusual domain architecture of FAD-dependent G3PDs from both *G. duodenalis* and *E. histolytica* may explained for a bi-directional activity of this enzymes. A further characterization of the gG3PD and a detailed metabolomics analysis of the trophozoite and encystation stage of *G. duodenalis* will be necessary to unravel any metabolic re-arrangement occurring during the parasite differentiation and its link with gG3PD activity.

The subcellular localization of gG3PD requires also other considerations. The presence, only in trophozoites but not in encysting parasites, of a fraction of the enzyme in the membrane preparation is in agreement with the immunolocalization data and suggests that gG3PD can associate with membranes in a stage dependent-manner. The structural/sequence determinant(s) responsible for the localization of the protein may reside in the N-terminal half of gG3PD, as supported by the partial localization of the gG3PD_N deletion mutant to the ventrolateral side of the trophozoite. In addition, we confirm that gG3PD and g14-3-3 co-precipitate (this work; Lalle et al., 2012) mainly at the trophozoite stage implying a role of the g14-3-3 in gG3PD localization to ventral plasma membrane. The presence of several putative mode-1 and mode-2 binding sites along the sequence of gG3PD (Supplementary Figure S1; Lalle et al., 2012) can allow for a direct interaction between the two proteins. Nevertheless, we cannot exclude that the interaction between gG3PD and g14-3-3 is indirect and that both proteins are present in a multiprotein complex, and further studies with different deletion and point mutants will clarify this issue. However, beyond the exact interaction mechanism, a clear relationship between g14-3-3 and gG3PD localization and, possibly, its enzymatic activity, is indicated by the strongly reduced co-precipitation of g14-3-3 with gG3PD during encystation and the partial re-localization of gG3PD to mitosomes.

The re-localization of gG3PD to mitosomes, despite the absence of any predictable mitochondrial targeting sequence or cleavage site in the N-terminus, has been proved at least for another *G. duodenalis* protein, namely GiiscS (Dolezal et al., 2005). In our case, the lost of mitosomal localization in both gG3PD deletion mutants suggests that targeting to these organelles at least requires the full-length protein. Although *G. duodenalis* mitosomes clearly miss the TCA cycle and the typical ATP-generating mitochondrial respiratory

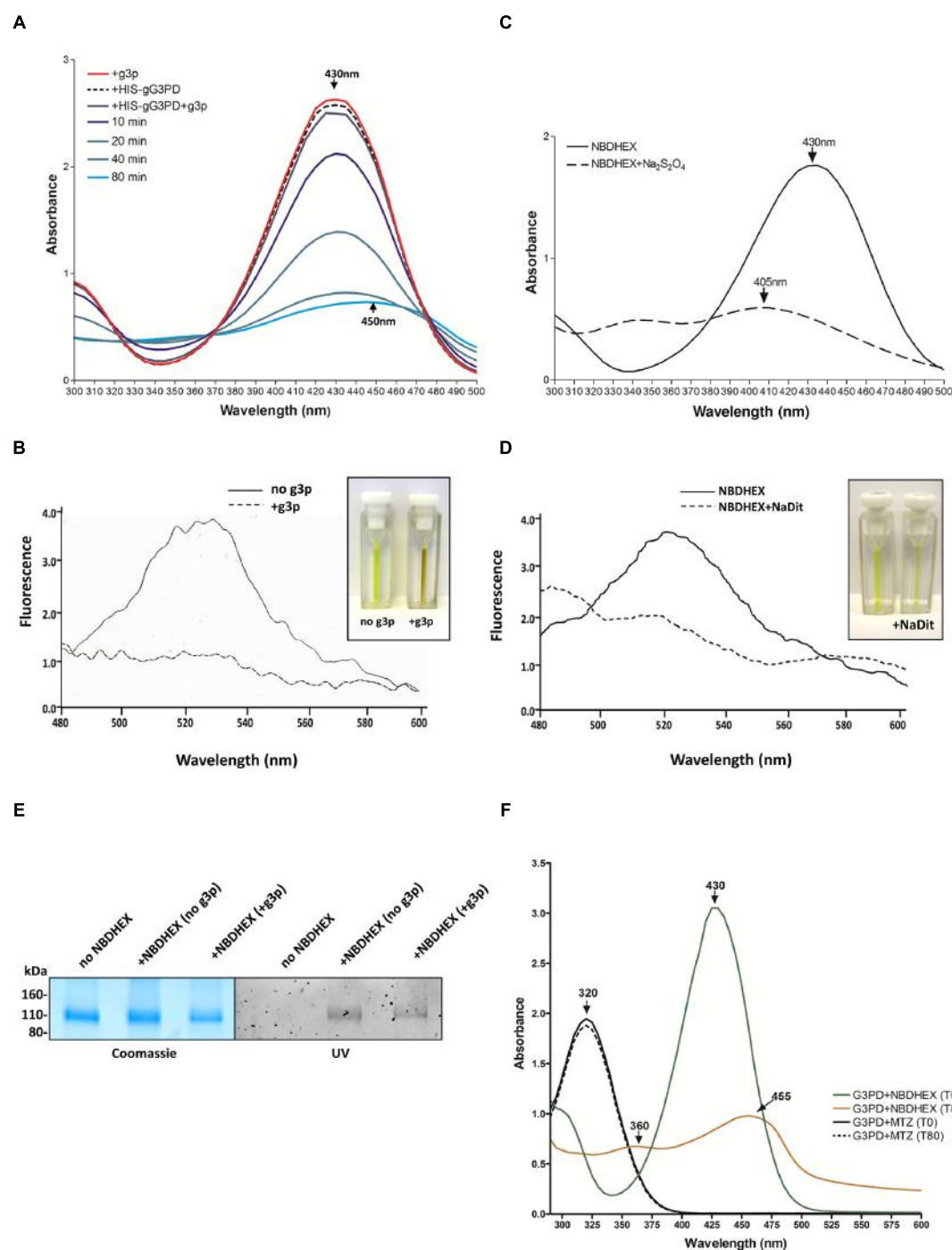


FIGURE 7 | NBDHEX is substrate of HIS-gG3PD. **(A)** Spectrophotometric analysis of the reaction between NBDHEX and gG3PD. The UV-visible spectrum of NBDHEX (100 μ M) in 67 mM potassium phosphate buffer (pH 7.5) was recorded at 25°C either in the presence of 17 mM g3p (red line, +g3p) or 80 nM HIS-gG3PD (dashed black line, +HIS-gG3PD). The NBDHEX (100 μ M) UV-visible spectrum was also recorded at different time points (0, 10, 20, 40, and 80 min) in the presence of both 17 mM g3p and 80 nM HIS-gG3PD (+HIS-gG3PD+g3p). Arrows indicate the wavelength (nm) of the maximal absorption. **(B)** Fluorescence spectra of 100 μ M NBDHEX (excitation at 430 nm) after 80 min of incubation with 80 nM HIS-gG3PD, either in the presence (solid line) or absence (dashed line) of 17 mM g3p. Fluorimetric

analyses were recorded at 25°C in 67 mM potassium phosphate buffer (pH 7.5). NBDHEX fluorescence emission has a maximum peak wavelength at 525 nm. Fluorescence intensity (y axis) is arbitrary. The change in color of the two reactions is shown in the insert. **(C)** The UV-visible spectrum of NBDHEX (100 μ M) in 67 mM potassium phosphate buffer (pH 7.5) was recorded at 25°C before (solid line) and after (dashed line) treatment with sodium dithionite ($\text{Na}_2\text{S}_2\text{O}_4$). The wavelengths (nm) of the maximal absorption are indicated with arrows. **(D)** Fluorescence spectra of 100 μ M NBDHEX (excitation at 430 nm) before (solid line) and after $\text{Na}_2\text{S}_2\text{O}_4$ (dashed line). The slight change in color of the two conditions is shown in the insert. Spectra and images from **(A–D)** are

(Continued)

FIGURE 7 | Continued

representative of three independent experiments. (E) SDS-PAGE (4–12%) of 2 µg of HIS-gG3PD after 80 min of incubation at 25°C with NBDHEX (+NBDHEX) in the presence or not of g3p, or with ethanol (no NBDHEX). Gel was photographed under UV light (UV, right) before staining with Coomassie blue (Coomassie, left). Molecular size markers are reported in the left. Images are representative of three independent experiments. (F) Comparison of the UV-visible spectra of NBDHEX (green and orange line) or MTZ (solid and dashed line) incubated with HIS-gG3PD and g3p (G3PD) at time 0 min and after 80 min of incubation at 25°C (T0 and T80, respectively). Arrows indicate the wavelengths (nm) of the maximal absorption. Spectra are representative of three independent experiments.

ETC (Han and Collins, 2012), the encystation-dependent localization of gG3PD to mitosomes could be a reminiscence of mitochondrial function of mG3PDs, where they participate in the g3p shuttle and supply electrons to the mitochondria ETC. A homolog of FAD-dependent mG3PD has been identified also in the mitosomes of the microsporidia *Antonospora locustae*, a group of spore-forming fungus-related intracellular parasites (Dolgikh et al., 2011). The protein is expressed in the spore and localizes in the mitosomes, where it channels reducing equivalent to the so called alternative oxidase (Dolgikh et al., 2011). Similarly, the presence of alternative ETCs in *G. duodenalis*, as in the anaerobic bacteria respiration, cannot be excluded (Unden and Bongaerts, 1997; Han and Collins, 2012). GiOR-1, a di-flavoprotein able to reduce the gCYTb5-IV and having ferredoxin-independent and NADPH-dependent reductase activity, has been localized to the *G. duodenalis* mitosome, suggesting that a NAD(P)-dependent ETC exists in this organelle (Jedelský et al., 2011; Pyrih et al., 2014). Similarly, the presence of a pyridine nucleotide-disulphide oxidoreductase domain and of a putative metal binding domain in gG3PD, both present in the flavoprotein reductase family (Argyrou and Blanchard, 2004), may imply that the protein possesses a combined dehydrogenase and reductase activity, although the final acceptor, if any, is still to be identified. Our results disclose a new perspective on the role of mitosome in *G. duodenalis* suggesting that mitosomal components and functions can change during the parasite life cycle. Indeed, gG3PD was not detected in the proteome of mitosomes isolated from trophozoites (Jedelský et al., 2011).

Looking for compounds affecting the gG3PD activity, we demonstrate that the 7-NBD derivative NBDHEX, a patented anti-tumor drug (Ricci et al., 2005; Turella et al., 2005), exerts cytotoxic activity toward *G. duodenalis* trophozoites and, when administered *in vivo*, hampers the g3p dehydrogenase activity of gG3PD. The IC₅₀ of NBDHEX is twofold to fivefold lower than MTZ, proving that the compound is more effective in killing *G. duodenalis* than the reference drug, even in microaerobic conditions. This indicates that the presence of O₂ does not produce opposite effects on NBDHEX, as on the contrary occurs for re-oxidation of MTZ nitroradical anions. *G. duodenalis* is a microaerophilic parasite that lives in the fairly aerobic (up to 60 µM O₂) environment of the upper intestine, so that a drug potentially effective also in presence of O₂ is

more attractive for therapeutic use. We show that NBDHEX binds to gG3PD, when administered both *in vivo* and *in vitro*. NBDHEX is an excellent electrophile that can easily form σ-complexes, as occurs between glutathione and the C-4 position of the drug in the G-site of GST, leading to the inhibition of the detoxifying and anti-apoptotic activity of human GSTP1-1 (Ricci et al., 2005; Federici et al., 2009). Since no gene coding for GST is present in *G. duodenalis* (Morrison et al., 2007), we can *bona fide* exclude that antigiardial activity of NBDHEX may be due to any GST inhibition, although a low level of GSH has been detected (Krauth-Siegel and Leroux, 2012). The formation of σ-complexes likely occurs between NBDHEX and gG3PD, as suggested by in gel fluorescence of gG3PD after NBDHEX treatment, but, unfortunately, our attempts to identify these complexes by mass spectrometry were unsuccessful. Furthermore, we demonstrate the occurrence of NBDHEX covalent adducts at several gG3PD cysteine residues, with the 7-nitro group of the drug being reduced either completely to amine or partially to hydroxylamine. Different NBDHEX modified cysteine residues of His-gG3PD were found in different experimental conditions, i.e., NBDHEX treatment *in E. coli* or *in vitro*, likely as the result of a differential accessibility of the drug to such residues. Our *in vitro* assays and MS data indicate that the nitro reduced NBDHEX adducts derive from the gG3PD-mediated electrochemical reduction of the drug, possibly via the formation of highly reactive intermediates, such as nitroso or hydroxylamine radicals. It is well known that during the FAD-mG3PD-mediated oxidation of the 2-hydroxy group of g3p, to form DHAP, two electrons are transferred to FAD and then to the quinone pool (Mráček et al., 2013). Similarly, gG3PD activity can generate two electrons able to reduce the nitro group to a hydroxylamine intermediate. Enzymatic reduction has also been proposed as a mechanism for the activation of nitrocompounds, i.e., MTZ, leading to protein covalent adducts formation and cytotoxicity in several microaerophilic protozoan parasites. In particular, the flavoprotein TRxR can nitroreduce MTZ, by a process involving its flavin cofactor, thus forming covalent adducts with the drug (Leitsch et al., 2007, 2009, 2011). Remarkably, although gG3PD displays nitroreductase activity toward NBDHEX, no nitroreduction of MTZ could be observed in our experimental conditions. Nitroimidazoles and other nitrocompounds seem to be metabolized in *G. duodenalis* in a different manner, also in comparison to *E. histolytica* and *T. vaginalis*, and protein adducts can be formed only with some of these drugs (Leitsch et al., 2012). Indeed, gG3PD was not identified among the proteins forming adducts with MTZ or tinidazole neither in *G. duodenalis* nor in *E. histolytica* (Leitsch et al., 2007, 2012). In particular, these differences in nitrocompound metabolism have been related to the adaptation of *G. duodenalis* to rather high concentrations of O₂ in the upper small intestine. We can speculate that gG3PD-mediated NBDHEX nitroreduction may be influenced by a redox-cycling property of 7-NBD derivative in presence of O₂. NBF-SPh, a compound related to NBDHEX, has a redox-cycling activity with nitro group cycling to nitroso and hydroxylamine intermediates by reversible electron transfer to

O_2 before becoming exhausted and finally reduced to amine (Partridge et al., 2012). During redox-cycling, NBF-SPh rapidly converts O_2 to ROS at a higher rate than that of the most toxic redox-cycling quinones and the nitrocompound MTZ. Bio-reduction of the redox cycling naphthoquinone menadione by flavoprotein/iron-sulphur-mediated electron transfer in both *G. duodenalis* trophozoites and cysts has been proven to be a potent generator of ROS, even in the presence of low levels of oxygen, thus leading to parasite killing (Paget et al., 2004). Therefore, we propose that the cytotoxicity exerted by NBDHEX against *G. duodenalis* could be due to its nitroreduction and to ROS generation during the reductive process, likely involving gG3PD. Finally, it should be considered that nitroreduction of NBDHEX, at least in part mediated by gG3PD, could subtract electrons from their physiological acceptor(s) thus altering the *G. duodenalis* intracellular redox metabolism.

Although further studies are necessary to fully understand the metabolic pathways involving the gG3PD, as well as the mechanisms of the enzyme regulation in *G. duodenalis*, we have clearly proven, for the first time, that a functional FAD-dependent gG3PD works in *G. duodenalis* and could be a valuable potential candidate for the design of novel antigiardial drugs having NBDHEX, a representative of novel class of antitumoral molecules, as leading compound.

References

- Adam, R. D. (2001). Biology of *Giardia lamblia*. *Clin. Microbiol. Rev.* 14, 447–475. doi: 10.1128/CMR.14.3.447-475.2001
- Albertyn, J., Hohmann, S., Thevelein, J. M., and Prior, B. A. (1994). GPD1, which encodes glycerol-3-phosphate dehydrogenase, is essential for growth under osmotic stress in *Saccharomyces cerevisiae*, and its expression is regulated by the high-osmolarity glycerol response pathway. *Mol. Cell. Biol.* 14, 4135–4144.
- Alsmark, U. C., Sicheritz-Ponten, T., Foster, P. G., Hirt, R. P., and Embley, T. M. (2009). Horizontal gene transfer in eukaryotic parasites: a case study of *Entamoeba histolytica* and *Trichomonas vaginalis*. *Methods Mol. Biol.* 532, 489–500. doi: 10.1007/978-1-60327-853-9_28
- Andersson, J. O., Sjögren, A. M., Horner, D. S., Murphy, C. A., Dyal, P. L., Svärd, S. G., et al. (2007). A genomic survey of the fish parasite *Spironucleus salmonicida* indicates genomic plasticity among diplomonads and significant lateral gene transfer in eukaryote genome evolution. *BMC Genomics* 8:51. doi: 10.1186/1471-2164-8-51
- Argüello-García, R., Bazán-Tejeda, M. L., and Ortega-Pierres, G. (2009). Encystation commitment in *Giardia duodenalis*: a long and winding road. *Parasite* 16, 247–258. doi: 10.1051/parasite/2009164247
- Argyrou, A., and Blanchard, J. S. (2004). Flavoprotein disulfide reductases: advances in chemistry and function. *Prog. Nucleic Acid Res. Mol. Biol.* 78, 89–142. doi: 10.1016/S0079-6603(04)78003-4
- Bell, R. M., and Coleman, R. A. (1980). Enzymes of glycerolipid synthesis in eukaryotes. *Annu. Rev. Biochem.* 49, 459–487. doi: 10.1146/annurev.bi.49.070180.002331
- Bénéré, E., Inocencio da Luz, R. A., Vermeesch, M., Cos, P., and Maes, L. (2007). A new quantitative in vitro microculture method. *J. Microbiol. Methods* 71, 101–106. doi: 10.1016/j.mimet.2007.07.014
- Bragg, P. D., and Hou, C. (1999). Effect of NBD chloride (4-chloro-7-nitrobenzo-2-oxa-1,3-diazole) on the pyridine nucleotide transhydrogenase of *Escherichia coli*. *Biochim. Biophys. Acta* 1413, 159–171. doi: 10.1016/S0005-2728(99)00090-0
- Chen, H., Lu, Y., and Jiang, J. G. (2012). Comparative analysis on the key enzymes of the glycerol cycle metabolic pathway in *Dunaliella salina* under osmotic stresses. *PLoS ONE* 7:e37578. doi: 10.1371/journal.pone.0037578
- Chowdhury, S. K., Raha, S., Tarnopolsky, M. A., and Singh, G. (2007). Increased expression of mitochondrial glycerophosphate dehydrogenase and antioxidant enzymes in prostate cancer cell lines/cancer. *Free Radic. Res.* 41, 1116–1124. doi: 10.1080/10715760701579314
- Cole, S. T., Eigmeyer, K., Ahmed, S., Honore, N., Elmes, L., Anderson, W. F., et al. (1988). Nucleotide sequence and gene-polypeptide relationships of the glpABC operon encoding the anaerobic sn-glycerol-3-phosphate dehydrogenase of *Escherichia coli* K-12. *J. Bacteriol.* 170, 2448–2456.
- Dagley, M. J., Dolezal, P., Likic, V. A., Smid, O., Purcell, A. W., Buchanan, S. K., et al. (2009). The protein import channel in the outer mitosomal membrane of *Giardia intestinalis*. *Mol. Biol. Evol.* 26, 1941–1947. doi: 10.1093/molbev/msp117
- Dinkel, H., Van Roey, K., Michael, S., Davey, N. E., Weatheritt, R. J., Born, D., et al. (2014). The eukaryotic linear motif resource ELM: 10 years and counting. *Nucleic Acids Res.* 42, D259–D266. doi: 10.1093/nar/gkt1047
- Dolezal, P., Smid, O., Rada, P., Zubáková, Z., Bursák, D., Suták, R., et al. (2005). *Giardia* mitosomes and trichomonad hydrogenosomes share a common mode of protein targeting. *Proc. Natl. Acad. Sci. U.S.A.* 102, 10924–10929. doi: 10.1073/pnas.0500349102
- Dolgikh, V. V., Senderskiy, I. V., Pavlova, O. A., Naumov, A. M., and Beznoussenko, G. V. (2011). Immunolocalization of an alternative respiratory chain in Antonospora (Paranosema) locustae spores: mitosomes retain their role in microsporidial energy metabolism. *Eukaryot. Cell* 10, 588–593. doi: 10.1128/EC.00283-10
- Federici, L., Lo Sterzo, C., Pezzola, S., Di Matteo, A., Scaloni, F., Federici, G., et al. (2009). Structural basis for the binding of the anticancer compound 6-(7-nitro-2,1,3-benzoxadiazol-4-ylthio)hexanol to human glutathione s-transferases. *Cancer Res.* 69, 8025–8034. doi: 10.1158/0008-5472.CAN-09-1314
- Gardino, A. K., and Yaffe, M. B. (2011). 14-3-3 proteins as signaling integration points for cell cycle control and apoptosis. *Semin. Cell Dev. Biol.* 22, 688–695. doi: 10.1016/j.semcdb.2011.09.008
- Gault, M. J., Gillin, F. D., and Zenian, A. J. (1987). *Giardia lamblia*: stimulation of growth by human intestinal mucus and epithelial cells in serumfree medium. *Exp. Parasitol.* 64, 29–37. doi: 10.1016/0014-4894(87)90005-1
- Gillin, F. D., Gault, M. J., Hofmann, A. F., Gurantz, D., and Sauch, J. F. (1986). Biliary lipids support serum-free growth of *Giardia lamblia*. *Infect. Immun.* 53, 641–645.

Acknowledgments

We are grateful to Dr. Marialuisa Casella, Istituto Superiore di Sanità, Rome (IT), for the priceless technical assistance with mass spectrometry analyses; to Dr. Pavel Dolezal, Charles University, Prague (CZ), for the gift of the anti-Tom40 antibody; to Dr. Ed Jarroll, Lehman College, NY (USA); and Dr. Harry van Keulen, Cleveland State University (USA) for providing us with anti-gPGM antibody. We thanks Professor Norbert Müller, University of Bern (CH), for the help in drug testing and critical reading of the manuscript and Dr. Donatella Pietraforte, Istituto Superiore di Sanità, Rome (IT), for the fruitful criticism. We also acknowledge Dr. Raffaele Fabrini and Dr. Alessio Bocedi, University of Rome “Tor Vergata” for NBDHEX supply. This study has been partially supported by Istituto Superiore di Sanità (project 14A1/678/2014 and Onco-Technology Program project 13ONC/5).

Supplementary Material

The Supplementary Material for this article can be found online at: <http://journal.frontiersin.org/article/10.3389/fmib.2015.00544/abstract>

- Großhennig, S., Schmidl, S. R., Schmeisky, G., Busse, J., and Stölke, J. (2013). Implication of glycerol and phospholipid transporters in *Mycoplasma pneumoniae* growth and virulence. *Infect. Immun.* 81, 896–904. doi: 10.1128/IAI.01212-12
- Hall, T. A. (1999). BioEdit: a user-friendly biological sequence alignment editor and analysis. *Nucleic Acids Symp. Ser.* 41, 95–98.
- Halliez, M. C., and Buret, A. G. (2013). Extra-intestinal and long term consequences of *Giardia duodenalis* infections. *World J. Gastroenterol.* 19, 8974–8985. doi: 10.3748/wjg.v19.i47.8974
- Han, J., and Collins, L. J. (2012). Reconstruction of sugar metabolic pathways of *Giardia lamblia*. *Int. J. Proteomics* 2012:980829. doi: 10.1155/2012/980829
- Hounkong, K., Sawangjaroen, N., and Phongpaichit, S. (2011). A colorimetric method for the evaluation of anti-giardial drugs in vitro. *Exp. Parasitol.* 127, 600–603. doi: 10.1016/j.exppara.2010.09.006
- Husain, A., Sato, D., Jeelani, G., Soga, T., and Nozaki, T. (2012). Dramatic increase in glycerol biosynthesis upon oxidative stress in the anaerobic protozoan parasite *Entamoeba histolytica*. *PLoS Negl. Trop. Dis.* 6:e1831. doi: 10.1371/journal.pntd.0001831
- Janssen, M. J., van Voorst, F., Ploeger, G. E., Larsen, P. M., Larsen, M. R., de Kroon, A. I., et al. (2002). Photolabeling identifies an interaction between phosphatidylcholine and glycerol-3-phosphate dehydrogenase (Gut2p) in yeast mitochondria. *Biochemistry* 41, 5702–5711. doi: 10.1021/bi025550j
- Jarroll, E. L., Muller, P. J., Meyer, E. A., and Morse, S. A. (1981). Lipid and carbohydrate metabolism of *Giardia lamblia*. *Mol. Biochem. Parasitol.* 2, 187–196. doi: 10.1016/0166-6851(81)90099-2
- Jedelsky, P. L., Dolezal, P., Rada, P., Pyrih, J., Smíd, O., Hrdý, I., et al. (2011). The minimal proteome in the reduced mitochondrion of the parasitic protist *Giardia intestinalis*. *PLoS ONE* 6:e17285. doi: 10.1371/journal.pone.0017285
- Kistler, W. S., and Lin, E. C. (1972). Purification and properties of the flavine-stimulated anaerobic L-glycerophosphate dehydrogenase of *Escherichia coli*. *J. Bacteriol.* 112, 539–547.
- Kleppe, R., Martinez, A., Døskeland, S. O., and Haavik, J. (2011). The 14-3-3 proteins in regulation of cellular metabolism. *Semin. Cell Dev. Biol.* 22, 713–719. doi: 10.1016/j.semcdb.2011.08.008
- Krauth-Siegel, R. L., and Leroux, A. E. (2012). Low-molecular-mass antioxidants in parasites. *Antioxid. Redox Signal.* 17, 583–607. doi: 10.1089/ars.2011.4392
- Lalle, M. (2010). Giardiasis in the post genomic era: treatment, drug resistance and novel therapeutic perspectives. *Infect. Disord. Drug Targets* 10, 283–294. doi: 10.2174/187152610791591610
- Lalle, M., Camerini, S., Cecchetti, S., Sayadi, A., Crescenzi, M., and Pozio, E. (2012). Interaction network of the 14-3-3 protein in the ancient protozoan parasite *Giardia duodenalis*. *J. Proteome Res.* 11, 2666–2683. doi: 10.1021/pr300199
- Lalle, M., Salzano, A. M., Crescenzi, M., and Pozio, E. (2006). The *Giardia duodenalis* 14-3-3 protein is post-translationally modified by phosphorylation and polyglycation of the C-terminal tail. *J. Biol. Chem.* 281, 5137–5148. doi: 10.1074/jbc.M509673200
- Leitsch, D., Burgess, A. G., Dunn, L. A., Krauer, K. G., Tan, K., Duchêne, M., et al. (2011). Pyruvate:ferredoxin oxidoreductase and thioredoxin reductase are involved in 5-nitroimidazole activation while flavin metabolism is linked to 5-nitroimidazole resistance in *Giardia lamblia*. *J. Antimicrob. Chemother.* 66, 1756–1765. doi: 10.1093/jac/dkr192
- Leitsch, D., Kolarich, D., Binder, M., Stadlmann, J., Altmann, F., and Duchêne, M. (2009). *Trichomonas vaginalis*: metronidazole and other nitroimidazole drugs are reduced by the flavin enzyme thioredoxin reductase and disrupt the cellular redox system. Implications for nitroimidazole toxicity and resistance. *Mol. Microbiol.* 72, 518–536. doi: 10.1111/j.1365-2958.2009.06675.x
- Leitsch, D., Kolarich, D., Wilson, I. B., Altmann, F., and Duchêne, M. (2007). Nitroimidazole action in *Entamoeba histolytica*: a central role for thioredoxin reductase. *PLoS Biol.* 5:e211. doi: 10.1371/journal.pbio.0050211
- Leitsch, D., Schlosser, S., Burgess, A., and Duchêne, M. (2012). Nitroimidazole drugs vary in their mode of action in the human parasite *Giardia lamblia*. *Int. J. Parasitol. Drugs Drug Resist.* 2, 166–170. doi: 10.1016/j.ijpdrr.2012.04.002
- Lopez, A. B., Sener, K., Jarroll, E. L., and van Keulen, H. (2003). Transcription regulation is demonstrated for five key enzymes in *Giardia intestinalis* cyst wall polysaccharide biosynthesis. *Mol. Biochem. Parasitol.* 128, 51–57. doi: 10.1016/S0166-6851(03)00049-5
- Miki, K., and Wilson, T. H. (1978). Proton translocation associated with anaerobic transhydrogenation from glycerol 3-phosphate to fumarate in *Escherichia coli*. *Biochem. Biophys. Res. Commun.* 83, 1570–1575. doi: 10.1016/0006-291X(78)91400-6
- Morrison, H. G., McArthur, A. G., Gillin, F. D., Aley, S. B., Adam, R. D., Olsen, G. J., et al. (2007). Genomic minimalism in the early diverging intestinal parasite *Giardia lamblia*. *Science* 317, 1921–1926. doi: 10.1126/science.1143837
- Mráček, T., Drahota, Z., and Houštěk, J. (2013). The function and the role of the mitochondrial glycerol-3-phosphate dehydrogenase in mammalian tissues. *Biochim. Biophys. Acta* 1827, 401–410. doi: 10.1016/j.bbabiobio.2012.11.014
- Müller, J., and Hemphill, A. (2013). New approaches for the identification of drug targets in protozoan parasites. *Int. Rev. Cell Mol. Biol.* 301, 359–401. doi: 10.1016/B978-0-12-407704-1.00007-5
- Paget, T. A., Maceckho, P. T., and Jarroll, E. L. (1998). Metabolic changes in *Giardia intestinalis* during differentiation. *J. Parasitol.* 84, 222–226. doi: 10.2307/3284474
- Paget, T., Maroulis, S., Mitchell, A., Edwards, M. R., Jarroll, E. L., and Lloyd, D. (2004). Menadione kills trophozoites and cysts of *Giardia intestinalis*. *Microbiology* 150, 1231–1236. doi: 10.1099/mic.0.26836-0
- Partridge, E. V., Eriksson, E. S., Penketh, P. G., Baumann, R. P., Zhu, R., Shyam, K., et al. (2012). 7-Nitro-4-(phenylthio)benzofuran is a potent generator of superoxide and hydrogen peroxide. *Arch. Toxicol.* 86, 1613–1625. doi: 10.1007/s00204-012-0872-9
- Pearson, W. R., and Lipman, D. J. (1988). Improved tools for biological sequence comparison. *Proc. Natl. Acad. Sci. U.S.A.* 85, 2444–2448. doi: 10.1073/pnas.85.8.2444
- Pellizzari Tregnó, F., Sau, A., Pezzola, S., Geroni, C., Lapenta, C., Spada, M., et al. (2009). In vitro and in vivo efficacy of 6-(7-nitro-2,1,3-benzoxadiazol-4-ylthio)hexanol (NBDHEX) on human melanoma. *Eur. J. Cancer* 45, 2606–2617. doi: 10.1016/j.ejca.2009.06.033
- Powell, S., Szklarczyk, D., Trachana, K., Roth, A., Kuhn, M., Müller, J., et al. (2012). eggNOG v3.0: orthologous groups covering 1133 organisms at 41 different taxonomic ranges. *Nucleic Acids Res.* 40, D284–D289. doi: 10.1093/nar/gk11060
- Pyrih, J., Harant, K., Martincová, E., Sutak, R., Lesuisse, E., Hrdý, I., et al. (2014). *Giardia intestinalis* incorporates heme into cytosolic cytochrome b5. *Eukaryot. Cell* 13, 231–239. doi: 10.1128/EC.00200-13
- Ricci, G., De Maria, F., Antonini, G., Turella, P., Bullo, A., Stella, L., et al. (2005). 7-Nitro-2,1,3-benzoxadiazole derivatives, a new class of suicide, inhibitors for glutathione S-transferases. Mechanism of action of potential anticancer drugs. *J. Biol. Chem.* 280, 26397–16405. doi: 10.1074/jbc.M503295200
- Ryan, U., and Cacciò, S. M. (2013). Zoonotic potential of *Giardia*. *Int. J. Parasitol.* 43, 943–956. doi: 10.1016/j.ijpara.2013.06.001
- Schofield, P. J., Edwards, M. R., and Kranz, P. (1991). “Glucose metabolism in *Giardia intestinalis*.” *Mol. Biochem. Parasitol.* 45, 39–47. doi: 10.1016/0166-6851(91)90025-2
- Schupp, D. G., Januschka, M. M., Sherlock, L. A., Stibbs, H. H., Meyer, E. A., Bemrick, W. J., et al. (1988). Production of viable *Giardia* cysts in vitro: determination by fluorogenic dye staining, excystation, and animal infectivity in the mouse and Mongolian gerbil. *Gastroenterology* 95, 1–10.
- Shevchenko, A., Wilm, M., Vorm, O., and Mann, M. (1996). Mass spectrometric sequencing of proteins silver-stained polyacrylamide gels. *Anal. Chem.* 68, 850–858.
- Singh, G. (2014). Mitochondrial FAD-linked glycerol-3-phosphate dehydrogenase: a target for cancer therapeutics. *Pharmaceuticals (Basel)* 7, 192–206. doi: 10.3390/ph7020192
- Sousa, M. C., Gonçalves, C. A., Baires, V. A., and Poiares-da-Silva, J. (2001). Adherence of *Giardia lamblia* trophozoites to Int-407 human intestinal cells. *Clin. Diagn. Lab. Immunol.* 8, 258–265. doi: 10.1128/cdli.8.2.258-265.2001
- Stevens, T. L., Gibson, G. R., Adam, R., Maier, J., Allison-Ennis, M., and Das, S. (1997). Uptake and cellular localization of exogenous lipids by *Giardia lamblia*, a primitive eukaryote. *Exp. Parasitol.* 86, 133–143. doi: 10.1006/expa.1997.4162
- Suescún-Bolívar, L. P., and Thomé, P. E. (2015). Osmosensing and osmoregulation in unicellular eukaryotes. *World J. Microbiol. Biotechnol.* 31, 435–443. doi: 10.1007/s11274-015-1811-8

- Tamura, K., Stecher, G., Peterson, D., Filipski, A., and Kumar, S. (2013). MEGA5: molecular evolutionary genetics analysis using maximum likelihood, evolutionary distance, and maximum parsimony methods. *Mol. Biol. Evol.* 28, 2731–2739. doi: 10.1093/molbev/msr121
- Tentori, L., Dorio, A. S., Mazzon, E., Muzi, A., Sau, A., Cuzzocrea, S., et al. (2011). The glutathione transferase inhibitor 6-(7-nitro-2,1,3-benzoxadiazol-4-ylthio)hexanol (NBDHEX) increases temozolomide efficacy against malignant melanoma. *Eur. J. Cancer* 47, 1219–1230. doi: 10.1016/j.ejca.2010.12.008
- Tovar, J., León-Avila, G., Sánchez, L. B., Sutak, R., Tachezy, J., van der Giezen, M., et al. (2003). Mitochondrial remnant organelles of *Giardia* function in iron-sulphur protein maturation. *Nature* 426, 172–176. doi: 10.1038/nature01945
- Turella, P., Cerella, C., Filomeni, G., Bullo, A., De Maria, F., Ghibelli, L., et al. (2005). Proapoptotic activity of new glutathione S-transferase inhibitors. *Cancer Res.* 65, 3751–3761. doi: 10.1158/0008-5472.CAN-04-3903
- Unden, G., and Bongaerts, J. (1997). Alternative respiratory pathways of *Escherichia coli*: energetics and transcriptional regulation in response to electron acceptors. *Biochim. Biophys. Acta* 1320, 217–234. doi: 10.1016/S0005-2728(97)00034-0
- Varga, M. E., and Weiner, J. H. (1995). Physiological role of GlpB of anaerobic glycerol-3-phosphate dehydrogenase of *Escherichia coli*. *Biochem. Cell Biol.* 73, 147–153. doi: 10.1139/o95-018
- Walz, A.-C., Demel, R. A., de Kruijff, B., and Mutzel, R. (2002). Aerobic sn-glycerol-3-phosphate dehydrogenase from *Escherichia coli* binds to the cytoplasmic membrane through an amphipathic alpha-helix. *Biochem. J.* 365, 471–479. doi: 10.1042/BJ20011853
- Waterhouse, A. M., Procter, J. B., Martin, D. M., Clamp, M., and Barton, G. J. (2009). Jalview Version 2—a multiple sequence alignment editor and analysis workbench. *Bioinformatics* 25, 1189–1191. doi: 10.1093/bioinformatics/btp033
- Watkins, R. R., and Eckmann, L. (2014). Treatment of giardiasis: current status and future directions. *Curr. Infect. Dis. Rep.* 16:396. doi: 10.1007/s11908-014-0396-y
- Yang, W., Cao, Y., Sun, X., Huang, F., He, Q., Qiao, D., et al. (2007). Isolation of a FAD-GPDH gene encoding a mitochondrial FAD-dependent glycerol-3-phosphate dehydrogenase from *Dunaliella salina*. *J. Basic Microbiol.* 47, 266–274. doi: 10.1002/jobm.200610263
- Yeh, J. I., Chinte, U., and Du, S. (2008). Structure of glycerol-3-phosphate dehydrogenase, an essential monotopic membrane enzyme involved in respiration and metabolism. *Proc. Natl. Acad. Sci. U.S.A.* 105, 3280–3285. doi: 10.1073/pnas.0712331105
- Yichoy, M., Duarte, T. T., De Chatterjee, A., Mendez, T. L., Aguilera, K. Y., Roy, D., et al. (2011). Lipid metabolism in *Giardia*: a post-genomic perspective. *Parasitology* 138, 267–278. doi: 10.1017/S0031182010001277

Conflict of Interest Statement: The authors declare that the research was conducted in the absence of any commercial or financial relationships that could be construed as a potential conflict of interest.

Copyright © 2015 Lalle, Camerini, Cecchetti, Finelli, Sferra, Müller, Ricci and Pozio. This is an open-access article distributed under the terms of the Creative Commons Attribution License (CC BY). The use, distribution or reproduction in other forums is permitted, provided the original author(s) or licensor are credited and that the original publication in this journal is cited, in accordance with accepted academic practice. No use, distribution or reproduction is permitted which does not comply with these terms.

Giardia fatty acyl-CoA synthetases as potential drug targets

Fengguang Guo¹, Guadalupe Ortega-Pierres^{2*}, Raúl Argüello-García², Haili Zhang¹ and Guan Zhu^{1*}

OPEN ACCESS

Edited by:

Anjan Debnath,
University of California, San Diego,
USA

Reviewed by:

Dinesh Sriramulu,
Shres Consultancy, India
Larissa M. Podust,
University of California, San Diego,
USA

*Correspondence:

Guadalupe Ortega-Pierres,
Department of Genetics
and Molecular Biology, Center
for Research and Advanced Studies
of the National Polytechnic Institute,
Avenue Instituto Politécnico
Nacional 2508, San Pedro Zacatenco,
07360 Mexico City, Mexico
gortega@cinvestav.mx;
Guan Zhu,
Department of Veterinary
Pathobiology, College of Veterinary
Medicine and Biomedical Sciences,
Texas A&M University, College
Station, Texas 77843-4467, USA
gzhu@cvm.tamu.edu

Specialty section:

This article was submitted to
Antimicrobials, Resistance
and Chemotherapy,
a section of the journal
Frontiers in Microbiology

Received: 22 March 2015

Accepted: 08 July 2015

Published: 22 July 2015

Citation:

Guo F, Ortega-Pierres G,
Argüello-García R, Zhang H
and Zhu G (2015) Giardia fatty
acyl-CoA synthetases as potential
drug targets.
Front. Microbiol. 6:753.
doi: 10.3389/fmicb.2015.00753

¹ Department of Veterinary Pathobiology, College of Veterinary Medicine and Biomedical Sciences, Texas A&M University, College Station, Texas, USA, ² Department of Genetics and Molecular Biology, Center for Research and Advanced Studies of the National Polytechnic Institute, Mexico City, Mexico

Giardiasis caused by *Giardia intestinalis* (syn. *G. lamblia*, *G. duodenalis*) is one of the leading causes of diarrheal parasitic diseases worldwide. Although limited drugs to treat giardiasis are available, there are concerns regarding toxicity in some patients and the emerging drug resistance. By data-mining genome sequences, we observed that *G. intestinalis* is incapable of synthesizing fatty acids (FA) *de novo*. However, this parasite has five long-chain fatty acyl-CoA synthetases (GiACS1 to GiACS5) to activate FA scavenged from the host. ACS is an essential enzyme because FA need to be activated to form acyl-CoA thioesters before they can enter subsequent metabolism. In the present study, we performed experiments to explore whether some GiACS enzymes could serve as drug targets in *Giardia*. Based on the high-throughput datasets and protein modeling analyses, we initially studied the GiACS1 and GiACS2, because genes encoding these two enzymes were found to be more consistently expressed in varied parasite life cycle stages and when interacting with host cells based on previously reported transcriptome data. These two proteins were cloned and expressed as recombinant proteins. Biochemical analysis revealed that both had apparent substrate preference toward palmitic acid (C16:0) and myristic acid (C14:0), and allosteric or Michaelis–Menten kinetics on palmitic acid or ATP. The ACS inhibitor triacsin C inhibited the activity of both enzymes ($IC_{50} = 1.56 \mu\text{M}$, $K_i = 0.18 \mu\text{M}$ for GiACS1, and $IC_{50} = 2.28 \mu\text{M}$, $K_i = 0.23 \mu\text{M}$ for GiACS2, respectively) and the growth of *G. intestinalis* *in vitro* ($IC_{50} = 0.8 \mu\text{M}$). As expected from giardial evolutionary characteristics, both GiACSs displayed differences in overall folding structure as compared with their human counterparts. These observations support the notion that some of the GiACS enzymes may be explored as drug targets in this parasite.

Keywords: *Giardia intestinalis*, fatty acyl-CoA synthetases, drug target, protein modeling, triacsin-C

Introduction

Giardia intestinalis (syn. *G. lamblia*, *G. duodenalis*) is one of the major causative agents of diarrheal diseases in humans around the world. In the U.S. alone, there are estimated 1.2–2 million (but up to 8 million) cases per year, resulting in annual costs of >\$30 million USD (Hlavsa et al., 2005; Yoder et al., 2007, 2010, 2012). The recently reported infection rates range from 0.4–7.6% in developed countries, and 0.9–40% in developing countries (Plutzer et al., 2010; Feng and Xiao, 2011). Because *Giardia* cysts exhibit moderate resistance to the chlorine used in treating water for drinking and

recreational purposes, it is also one of the most common water-borne pathogens and is listed as a Category B priority pathogen in the NIH/CDC Biodefense program¹. In addition to water-borne and food-borne transmissions, *G. intestinalis* is also a zoonotic pathogen capable of transmitting infections between animals and humans. Drugs to treat giardiasis are available, but the choices are limited (e.g., metronidazole, tinidazole, albendazole, and nitazoxanide) (Busatti et al., 2009; Tian et al., 2010; Tejman-Yarden and Eckmann, 2011; Granados et al., 2012). These drugs are also not 100% effective and may be unsuitable for some patients due to toxicity. Drug resistance is also an emerging problem (Ali and Nozaki, 2007; Lalle, 2010; Tian et al., 2010). Therefore, new or alternative drugs are needed, particularly if massive infection occurs under natural or man-made conditions.

Giardia species are anaerobic protozoa evolutionarily branched early at the base of eukaryotes (Morrison et al., 2007). The genome of *G. intestinalis* has been sequenced and reported in 2007, which revealed that this parasite has none or limited ability to synthesize most nutrients *de novo*, such as amino acids, nucleosides, and fatty acids (FA) (Morrison et al., 2007). In FA metabolism, *Giardia* lacks both types I and II synthetic pathways, and thus relies on scavenging FAs from hosts. This notion is also supported by earlier biochemical analysis on this parasite (Jarroll et al., 1981; Beach et al., 1990; Das et al., 2002; Lee et al., 2007). This anaerobic protozoan retains limited fatty acyl extension ability by possessing one or more elongating (ELO) genes. Congruent with its anaerobic life style, *Giardia* also lacks enzymes for FA degradation and β-oxidation. FA scavenged from hosts are first activated by acyl-CoA synthetase (ACS, aka. FA-CoA ligase, ACL) to form fatty acyl-CoA (FA-CoA) thioesters before they can enter to subsequent metabolic pathways, such as FA elongation and synthesis of lipids and biomembranes (**Figures 1A,B**). Therefore, targeting ACS may block the entire FA metabolism, thus killing the parasite.

In this study, we cloned and expressed two of the five ACSs from *G. intestinalis* (named as GiACS1 and GiACS2) as maltose-binding protein (MBP)-fusion proteins, and characterized their

¹<http://www.niaid.nih.gov/topics/BiodefenseRelated/Biodefense/Pages/CatA.aspx>

substrate preference and enzyme kinetic features. We also showed that the ACS inhibitor triacsin C could not only inhibit the activity of GiACS1 and GiACS2, but also display efficacy against the growth of *G. intestinalis* *in vitro* at micromolar levels.

Materials and Methods

Data-mining the *G. intestinalis* ACS Genes and their Expression Profiles

To ensure the full recovery of ACS genes from the *G. intestinalis* genomes, we searched the *GiardiaDB*² and the *Giardia* reference genomes at the National Center for Biotechnology Information³ (NCBI) with relevant keywords and by BLAST searches using known long-chain fatty acyl (LCFA)-CoA protein sequences as queries. The identities of GiACS proteins were further confirmed by BLAST searches for their orthologs and signature domains at the NCBI Conserved Domain Database⁴ (CDD). This strategy identified five *G. intestinalis* ACS (GiACS) orthologs and three related genes that are summarized in **Table 1**.

By taking advantage of already published and publically available transcriptome datasets at the *GiardiaDB*, we also data-mined the expression levels and fold changes of the five GiACS genes to evaluate their importance and potential differential roles in various parasite stages. These included their transcript levels in trophozoites and cysts, as well as during the encystation, excystation, and interactions with host cells that were determined by serial analysis of gene expression (SAGE), microarray analysis, and RNA-seq using the Illumina HiSeq2000 platform (Palm et al., 2005; Morf et al., 2010; Ringqvist et al., 2011; Franzen et al., 2013). Expression data of individual GiACS genes were extracted from corresponding datasets in *GiardiaDB* and values were plotted for comparison.

Protein Modeling

Structure homology modeling was performed on GiACS1 and GiACS2 (853 and 693 aa, respectively) using the I-Tasser

²<http://www.giardiadb.org>

³<http://www.ncbi.nlm.nih.gov/>

⁴<http://www.ncbi.nlm.nih.gov/cdd>

TABLE 1 | Fatty acyl-CoA (FA-CoA) synthetase (ACS) orthologs and related genes identified from the *Giardia intestinalis* genome and their top hits at the NCBI conserved domain (CDD) database.

Gene Name	GenBank Accession No.	GiardiaDB Gene ID	GiardiaDB description	Protein size	CDD top hit	CDD accession	E-value to CDD top hit
GiACS1	XP_001705891	GL50803_9062	Long-chain fatty acid (FA) CoA ligase 5	853 aa	LC-FACS_euk	cd05927	8.73E-120
GiACS2	XP_001706424	GL50803_15063	Long-chain FA CoA ligase 5	693 aa	LC-FACS_euk	cd05927	1.92E-157
GiACS3	XP_001705009	GL50803_21118	Long-chain FA CoA ligase 5	765 aa	LC-FACS_euk	cd05927	2.72E-117
GiACS4	XP_001708520	GL50803_30476	Long-chain FA CoA ligase 4	804 aa	LC-FACS_euk	cd05927	8.47E-163
GiACS5	XP_001709411	GL50803_113892	Long-chain FA CoA ligase, putative	758 aa	LC-FACS_euk	cd05927	5.37E-117
Unnamed	XP_001707853	GL50803_17170	Long-chain FA CoA ligase 5	1,523 aa	VL_LC_FACS_like	cd05907	6.85E-19
Unnamed	XP_001710279	GL50803_86511	Acyl-CoA synthetase (ACS)	970 aa	ATP-grasp_5	pfam13549	4.05E-38
Unnamed	XP_001709605	GL50803_16667	ACS	905 aa	ATP-grasp_5	pfam13549	1.16E-38

(Iterative Threading ASSEmbly Refinement) webserver at <http://zhanglab.ccmb.med.umich.edu/I-TASSER/> (Zhang, 2008; Roy et al., 2010). This platform is the most widely used system to build structural protein models from query sequences using the solved crystal structures contained at the RCSB Protein Data Bank (PDB) as templates. The quality of the model is given by a C-score (range -5 to 2), which is an index that considers TM and RMSD scores and allows for the ranking of the degrees of similarity between query and template protein structures. The C-score is used in combination with the TM score (range 0–1) to obtain the best model (Yang et al., 2015). The root-mean-square-deviation (RMSD) score indicates a measure of the differences (in Å) between values predicted by retrieved models and the values actually observed in PDB templates. The quality of protein models obtained was further visualized and tested by Ramachandran plots in the Discovery Studio v4.1 client (AccelrysTM) software. To compare the overall folding of two given protein models, the PDB files generated by I-Tasser platform were submitted to the TM-Align platform⁵ that retrieves the RMSD and TM scores for the structural alignment of the proteins studied. According to PDB statistics, TM-scores below 0.2 corresponds to randomly chosen unrelated proteins, whereas a score higher than 0.5 match generally the same fold.

Expression of Recombinant GiACS Proteins

From identified *GiACS* genes, we chose to first clone and express two genes for potential functional analysis (i.e., *GiACS1* and *GiACS2*, corresponding to the *G. intestinalis* WB strain Gene ID numbers GL50803_9062 and GL50803_15063, or GenBank accession numbers XP_001705891 and XP_001706424, respectively) (Table 1). Genomic DNA was isolated from the WB strain of *G. intestinalis* (ATCC # 30957) using Qiagen DNeasy Blood & Tissue Kit using protocol recommended for cultured cells. For biochemical analysis, the entire intron less open reading frames (ORFs) of *GiACS1* and *GiACS2* genes were amplified from the genome DNA by PCR using high-fidelity *Pfu* Turbo HotStart DNA polymerase (Agilent Technologies, Los Angeles, CA, USA). Linker sequences containing *Bam*HI and *Hind*III restriction sites were added to the sense and antisense primers, respectively (Table 2). The PCR products were digested by *Bam*HI and *Hind*III, and ligated into the linearized pMAL-c2E vector. The ligated plasmids were transferred into the Rosetta 2 strain of *Escherichia coli* competent cells (Novagen) and cultured

⁵<http://zhanglab.ccmb.med.umich.edu/TM-align/>

TABLE 2 | Primers used in the cloning of *GiACS1* and *GiACS2* genes.

Gene Name	Orientation	Linker	Sequence (5'-3') ¹
<i>GiACS1</i>	Forward	<i>Bam</i> HI	ctggatccATGATCTTCCATTCTAAAC
<i>GiACS1</i>	Reverse	<i>Hind</i> III	gcaagcttCTCTCCTTATCAACCATGGCTTC
<i>GiACS2</i>	Forward	<i>Bam</i> HI	ctggatccATGTCGGATTCATCTGCC
<i>GiACS2</i>	Reverse	<i>Sall</i>	ggctcgacCTTACTAGATGGCTAGA

¹Lower cases indicate added linker sequences.

in LB agar plates containing 100 µg/mL ampicillin, from which plasmids were isolated from individual colonies by E.Z.N.A. plasmid DNA miniprep kit (Omega Bio-Tek, Atlanta, GA, USA) and sequenced by Sanger sequencing technique at the Texas A&M University Gene Technologies Laboratory⁶ to confirm their identity and sequence accuracy.

The expression of MBP-fusion proteins was carried out as described (Guo and Zhu, 2012; Guo et al., 2014; Yu et al., 2014). Briefly, engineered plasmids were transferred into the Rosetta 2 strain of *E. coli* to grow colonies in LB agar plates containing 100 µg/mL ampicillin and 34 µg/mL chloramphenicol, from which bacterial colonies (less than 1 week old) were individually transferred into 25 mL LB broth containing 0.2% glucose and allowed to grow at 37°C overnight. The next day, bacterial broths were diluted by 1:100 with fresh medium and incubated at 37°C for 2 h or until OD₄₉₅ reached to ~0.5, followed by the induction of expression by isopropyl β-D-1-thiogalactopyranoside (IPTG) (0.3 mM) at 16°C overnight. Bacteria were collected by centrifugation (6000 × g, 10 min) and lysed by sonication in Tris-HCl buffer (pH 7.5), from which the recombinant proteins were purified by amylose resin-based affinity chromatography according to the manufacturer's instructions (New England Biolabs). The quality and quantity of purified proteins were analyzed by SDS-PAGE and Bradford assay using BSA as the protein standard. Proteins were used immediately after the purification or stored at -20°C.

Biochemical Assays

The ACS activity was determined by a five, 5'-dithio-bis-(2-nitrobenzoate) (DTNB) colorimetric assay for both *GiACS1* and *GiACS2*. In the assay, free CoA in reduced form (CoA-SH) reacted with DTNB to form 5-thionitrobenzoic acid that was measured at OD₄₁₂ (Bernson, 1976; Zhuravleva et al., 2012; Guo et al., 2014). Reactions were carried out in 200 µL Tris-HCl buffer (0.1 mM, pH 8.0) containing 10 mM KCl, 50 µM CoA, 500 µM ATP, 10 mM MgCl₂, and 100 µM FA. The concentrations of substrates and cofactors might be varied for determining their dose-response curves and FA with carbon chains ranging from C2:0 to C30:0 were used for determining substrate preference. Reactions were started by the addition of 1 µg of recombinant MBP-GiACS proteins, followed by incubation at 32°C for 10 min, and then stopped by heating samples at 80°C for 5 min. Following sample cooling to room temperature, 4 µL of DTNB (5 mM) was added into each reaction that was allowed for color development for 5 min, followed by the measurement of OD₄₁₂ values with a Multiskan Spectrum spectrophotometer (Thermo Scientific). Serial concentrations of CoA in the same reaction buffer were assayed and used as standard curves for calculating the amounts of CoA reduced in experimental samples. Enzyme kinetic parameters were determined using varied concentrations of palmitic acid (10–600 µM) and ATP (10–3000 µM), respectively.

To confirm the formation of palmitoyl-CoA catalyzed by *GiACS1* and *GiACS2*, we performed a radioactive assay in which reactions were carried out with the use of ³H-palmitic acid (25 µM) and other reagents as described above. Negative

⁶<http://www.idmb.tamu.edu/gtl/>

controls consisted of an MBP-tag to replace MBP-GiACS proteins for background subtraction. After the reaction, samples were subjected to a heptane extraction procedure to remove free palmitic acid, and the radioactivity of ^3H -palmitoyl-CoA in the aqueous phase was counted in a Beckman Coulter LS 6000SE counter as described (Fritzler and Zhu, 2007; Fritzler et al., 2007). We also evaluated the effects of an ACS inhibitor, triacsin C (2,4,7-undecatrienyl nitrosohydrazone; CAS 76896-80-5) on the GiACS activity, in which 1–32 μM of triacsin C was used to determine the IC_{50} value. In each experiment, there was a set of reactions under the same conditions, but without enzyme for use as controls for background subtractions.

Efficacy of Triacsin C on the Growth of *G. intestinalis* In Vitro

The effect of triacsin C on the growth of *G. intestinalis* (WB strain) *in vitro* was assessed by subculture in liquid medium as described (Arguello-Garcia et al., 2004). In this assay, 1×10^6 *Giardia* trophozoites were cultured in 4.5-mL screw-capped vials containing fresh TYI-S-33 medium (less than 1 week old) containing varied concentrations of Triacsin C (0.13–16 μM) for 24 h at 37°C. Then 1×10^5 drug-exposed trophozoites were transferred to new 4.5-mL vials containing drug-free medium and incubated for additional 48 h at 37°C. Parasites were then counted and the parasite growth was expressed as the percent of surviving trophozoites in comparison to those in the negative controls that did not receive an inhibitor.

Results

The Genome of *G. intestinalis* Encodes Five Long Chain FA-CoA Synthetases that are Differentially Expressed the Parasite

By data-mining the genome sequences of *G. intestinalis* (WB), we identified eight candidate genes encoding proteins that either exhibited high degree of identities with other known ACS proteins or annotated as long-chain FA CoA ligases or ACSs by the *GiardiaDB* (Table 1). Among them, five genes (designated as *GiACSI* to *GiACSS5*) appear to encode for ACS enzymes based on their identities to other ACS proteins and by the presence of AMP-binding domain, ACS signature motifs, and other active sites in their protein sequences (Figure 1C; Supplementary Figure S1). The top hit at the NCBI CDD for all five *GiACCS* proteins is LC_FACS_euk (CDD No. cd05927) with expectation values (*E*-values) ranging from 1.92E-157 to 5.37E-117 (Table 1). Among the other three genes, GL50803_17170 (GenBank: XP_001707853) was annotated as “LCFA CoA ligase 5,” and several short regions within the sequence could be mapped to the “VL_LC_FACS_like” domain at CDD (cd05907) with a much less significant E-value at 6.85E-19 (Table 1). The sequence also lacked most of the active sites in ACS, but only contained limited conserved amino acids at the two signature motifs, suggesting that GL50803_17170 was derived from an ancient very-long LC-FACS, but probably lost its ACS function. The remaining two genes were annotated as ACSs (GL50803_86511, GenBank: XP_001710279; and GL50803_16667, GenBank: XP_001709605)

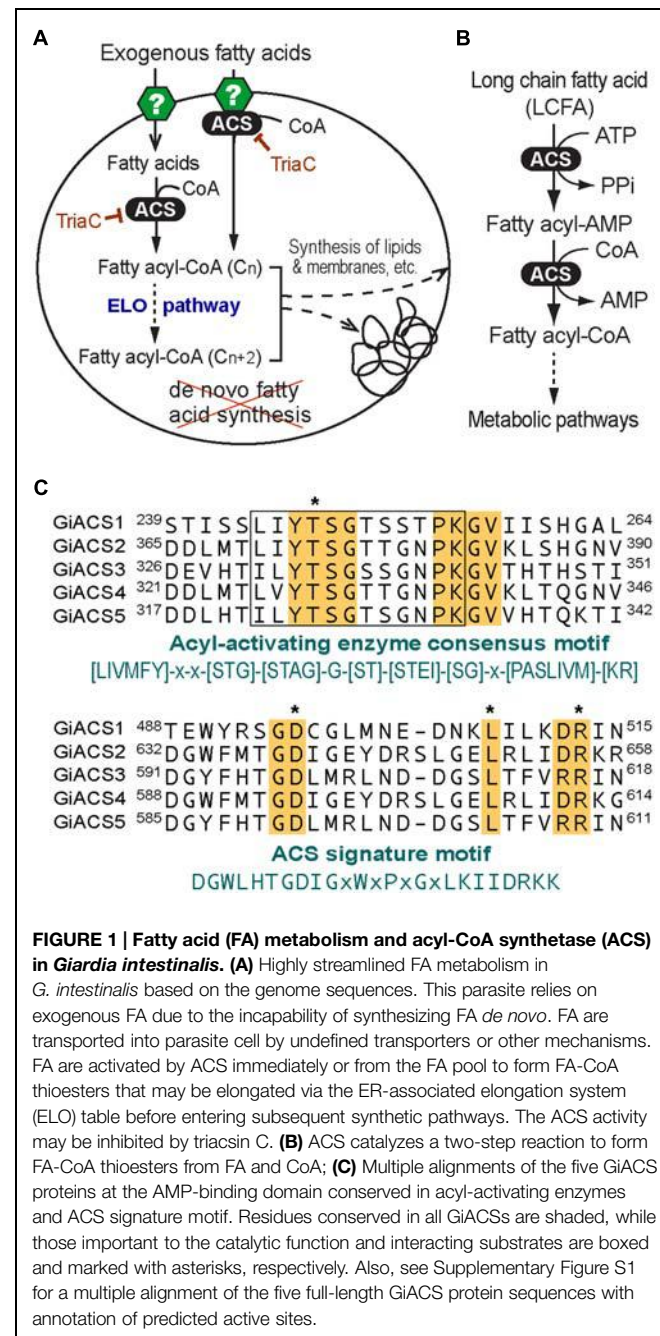


FIGURE 1 | Fatty acid (FA) metabolism and acyl-CoA synthetase (ACS) in *Giardia intestinalis*. **(A)** Highly streamlined FA metabolism in *G. intestinalis* based on the genome sequences. This parasite relies on exogenous FA due to the incapability of synthesizing FA *de novo*. FA are transported into parasite cell by undefined transporters or other mechanisms. FA are activated by ACS immediately or from the FA pool to form FA-CoA thioesters that may be elongated via the ER-associated elongation system (ELO) table before entering subsequent synthetic pathways. The ACS activity may be inhibited by triacsin C. **(B)** ACS catalyzes a two-step reaction to form FA-CoA thioesters from FA and CoA; **(C)** Multiple alignments of the five *GiACCS* proteins at the AMP-binding domain conserved in acyl-activating enzymes and ACS signature motif. Residues conserved in all *GiACCS*s are shaded, while those important to the catalytic function and interacting substrates are boxed and marked with asterisks, respectively. Also, see Supplementary Figure S1 for a multiple alignment of the five full-length *GiACCS* protein sequences with annotation of predicted active sites.

(Table 1). They both contained an ATP_grasp-5 domain (CDD: pfam549) with less significant *E*-values at 4.05E-38 and 1.16E-38, respectively. Interestingly, proteins encoded by these two genes were ortholog of CoA-binding proteins from prokaryotes, suggesting they were derived from prokaryotic genes by lateral gene transfer and might more likely function as CoA-binding proteins than as ACS. Based on these observations, we concluded that the *G. intestinalis* genome encoded five ACSs and three ACS-related proteins.

Further transcriptome analysis by data-mining previously published transcriptome data generated using various platforms

(i.e., SAGE, RNA-seq, and microarray) and available at *GiardiaDB* (Palm et al., 2005; Morf et al., 2010; Ringqvist et al., 2011; Franzen et al., 2013), we noticed that the five *GiACS* genes were differentially expressed in different parasite stages (**Figure 2**). In trophozoites, an earlier SAGE analysis detected the transcripts of four *GiACS* genes (with the exception of only *GiACS4*) (**Figure 2A**), whereas a more recent RNA-seq analysis was able to detect the transcripts of all five *GiACS* genes (**Figure 2B**). However, the general expression profiles in these two datasets were similar (i.e., the highest for *GiACS3* and *GiACS5*, moderate for *GiACS1* and *GiACS2*, and the lowest for *GiACS4*). In other stages including cysts and parasites during encystation and excystation, *GiACS1* was the most highly expressed among all *GiACS* genes in all stages in the SAGE dataset (**Figure 2A**). *GiACS1* also maintained the highest levels of expression during excystation process, but mid-level expressions during the encystation process (**Figure 2A**). *GiACS2* was consistently expressed at moderate levels in all parasite stages, while *GiACS3* had relatively high transcript levels in trophozoites and during encystation, but generally lower levels in cysts and excystation. *GiACS4* was consistently the lowest or

undetectable in all stages, whereas *GiACS5* was highly expressed in trophozoites and during encystation, but slightly expressed during excystation (**Figure 2A**). In agreement with the SAGE analysis, a microarray analysis also detected apparent down-regulation of *GiACS3* and up-regulation of *GiACS5* during the encystation process (**Figure 2C**). Although *GiACS4* gene displays the lowest or even undetectable expression levels in all parasite life cycle stages, this gene significantly elevated its expression during the interaction with host cells or when culture medium is changed from DMEM to TYDK medium (**Figure 2D**). Although further functional studies are needed to delineate the biological roles played by the five *Giardia* ACS genes, their differential expressions in various biological processes and conditions clearly imply that they might play differential roles in the parasite life cycle.

Insights from *GiACS1* and *GiACS2* Protein Models

Considering the aforementioned data and the fact that chemotherapy in giardiasis is mostly directed against the trophozoite stage, the *GiACS1*, and *GiACS2* proteins were

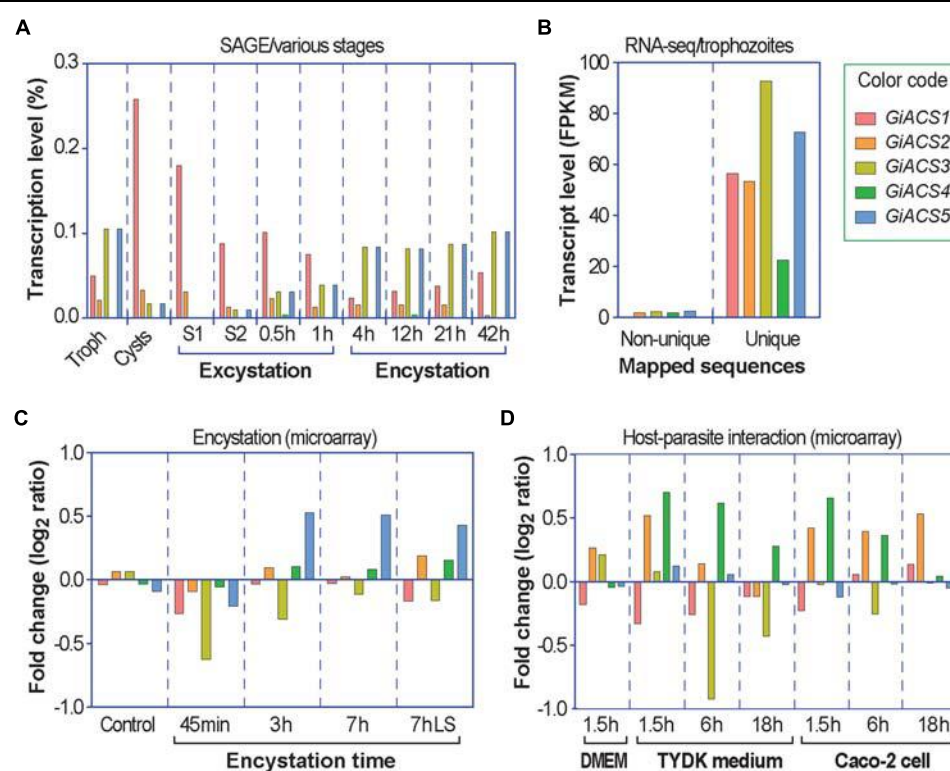


FIGURE 2 | Differential expressions of the five *GiACS* genes as determined by data-mining previously published transcriptome data available at *GiardiaDB*. All data were derived from *G. intestinalis* assemblage A WB strain. **(A)** Expression profiles based on serial analysis of gene expression (SAGE) in trophozoites (Troph), cysts, and during excystation and encystation (Palm et al., 2005). S1 (stage 1) = under acidic condition to mimic the stomach. S2 (stage 2) = trypsin and slight alkaline conditions to mimic the small intestines. **(B)** Transcriptional levels in trophozoites based on strand-specific RNA-seq using the Illumina HiSeq2000 platform (Franzen et al., 2013). FPKM = fragments per kilobase of exon model per million mapped reads; **(C)** Transcriptional changes in response to encystation stimuli based on a dual-color hybridization of a full-genome microarray analysis, in which encystation was induced *in vitro* for 45 min, 3 h, and 7 h by standard 2-step protocol or for 7 h by lipid starvation (7hLS) (Morf et al., 2010). **(D)** Transcriptional changes in trophozoites during interacting with host cells as determined by a full-genome microarray analysis, in which trophozoites were used to infect Caco-2 cells in DMEM medium or cultured in cell-free TYDK medium for varied times (Ringqvist et al., 2011).

et al., 2013). FPKM = fragments per kilobase of exon model per million mapped reads; **(C)** Transcriptional changes in response to encystation stimuli based on a dual-color hybridization of a full-genome microarray analysis, in which encystation was induced *in vitro* for 45 min, 3 h, and 7 h by standard 2-step protocol or for 7 h by lipid starvation (7hLS) (Morf et al., 2010).

(D) Transcriptional changes in trophozoites during interacting with host cells as determined by a full-genome microarray analysis, in which trophozoites were used to infect Caco-2 cells in DMEM medium or cultured in cell-free TYDK medium for varied times (Ringqvist et al., 2011).

considered as potential drug targets due to their stable and comparable transcription levels in trophozoites (**Figure 2B**), even though expression of both proteins differ upon trophozoite–epithelial cell interactions. GiACS2 was up regulated while GiACS1 was down regulated at ≤ 6 h of interacting with host cells (**Figure 2D**). In addition, GiACS1 is a much larger protein (853 aa) than the other GiACSS and their human counterparts (generally <700 aa); hence, the GiACS1 represents a divergent ACS.

In an initial mining of ACS crystals in PDB, protozoan templates were absent. When the GiACS1 and GACS2 sequences were submitted to preliminary modeling, the retrieved models shared the highest scores with members of the CoA synthetase family as firefly luciferase, ACS of *Saccharomyces cerevisiae* and acetoacetyl-CoA synthetase of *Streptomyces lividans* (PDB IDs: 2D1S, 1RY2, and 4WD1, respectively). From these, the

yeast homolog (1RY2) was chosen as template for refinement of protein models due to its ACS nature that closely matches with the proposed GiACS functions. In this way, a template-directed modeling was performed and the two GiACS models (**Figures 3A,D**) had satisfactory scores: C-score: -2.57, TM-score = 0.636, and RMSD = 0.95 for GiACS1; C-score: -1.04, TM-score = 0.773, and RMSD = 1.65 for GiACS2. These data reflect that GiACS models share 63.6% (GiACS1) and 77.3% (GiACS2) homology (average deviation $<2\text{\AA}$) with respect to the yeast ACS template. Also, the identity in sequence may be indicated with the available PDB structures resolved since I-Tasser is good for modeling protein targets in the “twilight zone” (20–30% identity), which have no or weakly homologous templates (Roy et al., 2010).

In a further assessment of the quality for GiACS1/2 protein models, the Ramachandran plots were constructed. This tool

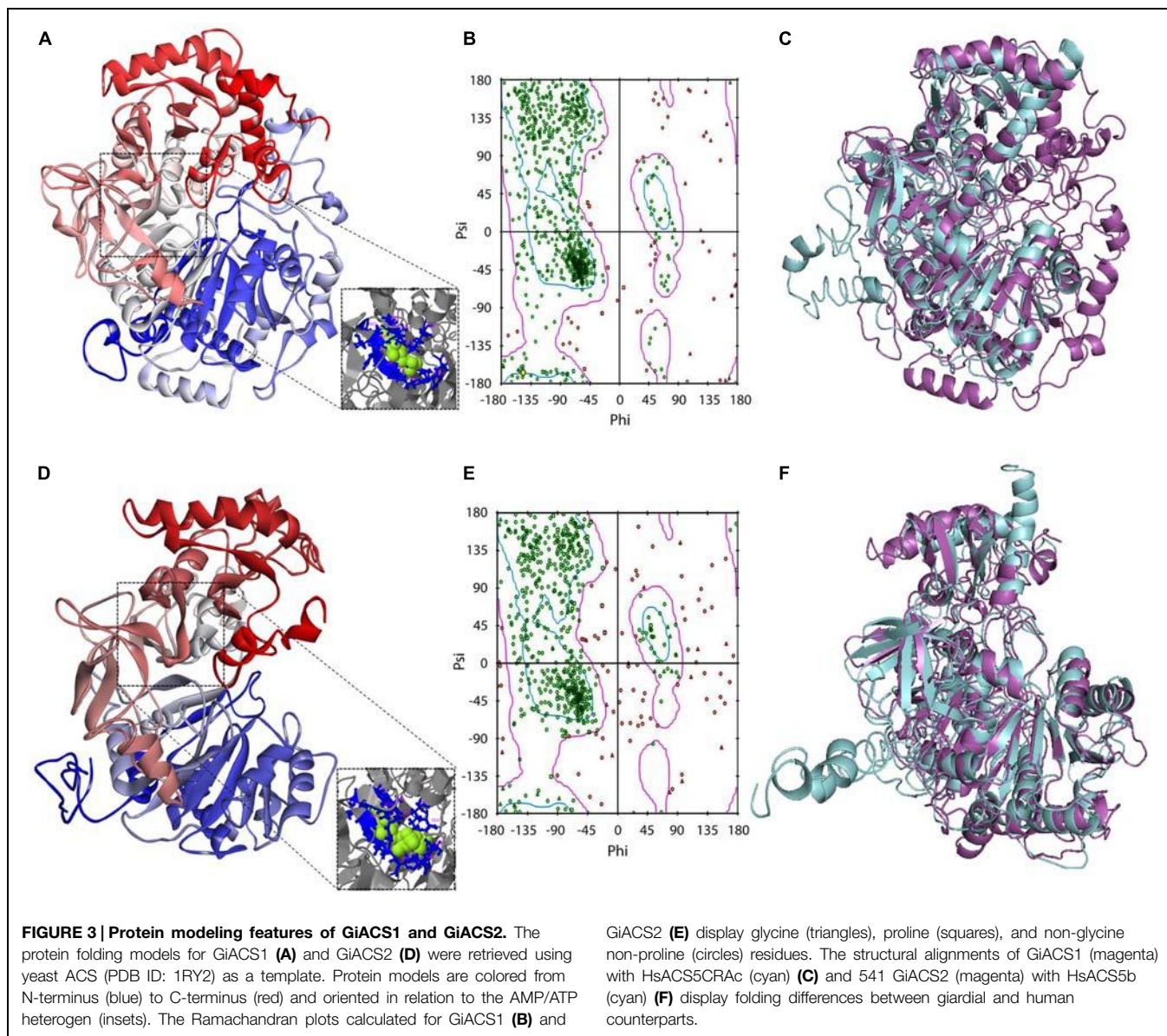


TABLE 3 | Ramachandran plots statistics of GiACS1 and GiACS2.

Residues in Ramachandran plot	GiACS1 (853 aa)	GiACS2 (693 aa)
In most favored regions	581 (78.30%)	443 (72.63%)
In additionally allowed regions	125 (16.85%)	104 (17.04%)
In generously allowed or disallowed regions	36 (4.85%)	63 (10.33%)
Non-Gly and non-Pro residues	742 (100%)	610 (100%)
# Gly (triangles)	66	43
# Pro (squares)	45	40

not only predicts secondary structures from dihedral angles of individual amino acids (ϕ and ψ), but also provides distributions of residues in “favored regions” (contoured in blue line), “additionally allowed regions” (contoured in pink line), and the external “generously allowed” and “not allowed” regions as stated by the ProCheck platform (**Figures 3B,E**). The special cases of glycine and proline are ruled out as recommended and only residues contained in the two former regions were considered of satisfactory conformation. These distributions for GiACS1 and GiACS2 are listed in **Table 3**. In this, more than 75% of residues fall within favored regions, more than 15% fall within allowed regions and <10% are in external regions. In summary, up to 95.15% of residues in GiACS1 and 89.67% of residues in GiACS2 have a satisfactory conformation within the protein structure predicted for these molecules; hence, the protein models obtained have an acceptable quality.

Further analyses to evaluate GiACS1 and GiACS2 as likely druggable targets were performed to determine the structural alignment of GiACSS with their most resembling human counterparts. In these, two isoforms of the human long chain fatty acyl CoA synthetases had the closest similarity to these GiACSS: the 5CRAC isoform (HsACS5CRAC, Acc. No. gb| EAW49534.1, 663 aa) displaying the highest expectation value (8e-76) and 37% of sequence identity with GiACS1 over a 64.1% coverage and the 5b isoform (HsACS5b, Acc. No. NP_976313.1, 683 aa) that displayed the highest expectation value (5e-60) and 26% of sequence identity with GiACS2 over a 79.4% coverage. Despite the high *E*-values, the structural comparison of giardial and human counterparts revealed striking differences: GiACS1 and HsACS5CRAC had 31.0% of structure identity over a span of 561 aa (RMSD: 3.20; TM-score: 0.769 normalized with HsACS5CRAC) while GiACS2 and HsACS5b shared 23.9% of structure identity over a span of 594 aa (RMSD: 3.90; TM-score: 0.775 normalized with HsACS5b). In general, there were obvious folding differences between the *Giardia* and human ACS

counterparts (**Figures 3C,F**), particularly in the case of GiACS1 as a consequence of the multiple insertions contained in this unusually large (853 aa) molecule. Based on these observations, it was tempting to compare purified GiACS in terms of catalytic abilities and susceptibility to specific inhibitors.

Functional Confirmation of GiACS1 and GiACS2 as a Long Chain FA-CoA Synthetase

After we determined that *G. intestinalis* possessed five ACSs, we decided to first investigate the biochemical features for two of them. We selected GiACS1 and GiACS2 in our initial study because both genes were relatively highly and consistently expressed in different life cycle stages, and GiACS2 appeared to be important in host–parasite interaction. Their whole ORFs were successfully cloned into the pMAL-c2E expression vector, and their products were expressed as MBP-fusion proteins (**Figure 4A**, inset). GiACS1 protein was purified into high purity, while the majority of GiACS2 was expressed at expected size, but some lower bands were present, suggesting some incomplete translation of GiACS2 probably due to the differences in codon usage between *G. intestinalis* and *E. coli*.

Using DTNB assay, we were able to individually evaluate the activity of GiACS1 and GiACS2 toward various saturated FA with chain lengths ranging from C2:0 to C30:0. Both GiACS1 and GiACS2 displayed the highest activity over palmitic acid (C16:0) and myristic acid (C14:0) (**Figure 4A**). Their activity on other FA was much lower, mostly ranging from ~5% to ~25%. These observations confirmed that both GiACS1 and GiACS2 are long-chain FACS with a relatively restricted substrate preference toward C14:0 and C16:0 FA. This feature makes these two GiACS proteins differ from the two *Cryptosporidium* ACSs that could use C12:0–C18:0 FA with comparable levels of activity (Guo et al., 2014). In kinetic studies, these two enzymes exhibited allosteric and Michaelis–Menten kinetics toward palmitic acid and ATP, respectively (**Figures 4B,C**). Their kinetics parameters are listed in **Table 4**. We also validated the function of GiACS1 and GiACS2 by directly detecting the formation of palmitoyl-CoA using a radioactive assay, in which both enzymes exhibited specific activities comparable to those obtained using DTNB assay (**Figure 4E**).

Triacsin C Inhibits GiACS1 and GiACS2 Enzyme Activity as Well as the *In Vitro* Growth of *G. intestinalis*

We further tested whether GiACS1 and GiACS2 were amendable to the inhibition by an ACS inhibitor triacsin C, and observed

TABLE 4 | Kinetic parameters for GiACS1 and GiACS2¹.

Enzyme	Substrate	K' or K _m (μM)	V _{max} (μmol/mg/min)	² h	K _i of triacsin C (μM)
GiACS1	Palmitic acid	13.09 ± 2.42	1.25 ± 0.12	1.36	0.18
	ATP	279 ± 18.46	2.19 ± 0.04		
GiACS2	Palmitic acid	11.15 ± 0.54	2.64 ± 0.06	2.19	0.23
	ATP	175 ± 18.68	3.55 ± 0.08		

¹Values for K', K_m, and V_{max} are expressed as mean ± SD; ²h = Hill coefficient.

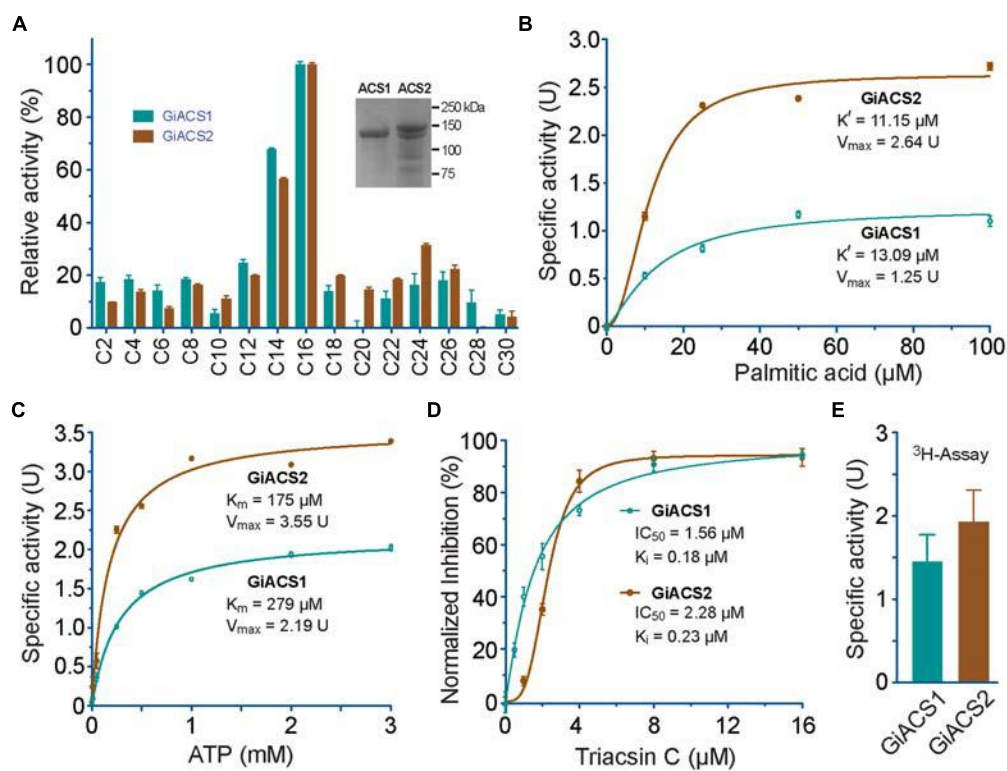


FIGURE 4 | Enzyme kinetic features of recombinant GiACS1 and GiACS2 as determined by a 5, 5'-dithio-bis-(2-nitrobenzoate) (DTNB) colorimetric assay. (A) Substrate preference of GiACS1 and GiACS2 toward FA with varied carbon chain lengths. Relative activities were shown in comparison with that on the C16:0 palmitic acid. Inset showed SDS-PAGE analysis of purified recombinant GiACS1 and GiACS2 as maltose-binding protein (MBP)-fusion proteins; **(B)** Allosteric kinetics of

GiACS proteins on palmitic acid; **(C)** Michaelis-Menten kinetics of GiACS on ATP; **(D)** Inhibition of triacsin C on the GiACS enzyme activity; and **(E)** Enzyme activity by detecting the formation of ^3H -palmitoyl-CoA using a heptane extraction-based radioactive assay. Bars represent SEM derived from three or more reactions. At least two independent assays were performed for each experiment, and the data from one representative assay were shown here. $U = \mu\text{mol}/\text{mg}/\text{min}$.

that this compound could inhibit their enzyme activity with IC_{50} values at 1.56 and 2.28 μM on GiACS1 and GiACS2, respectively (Figure 4D). Their corresponding K_i values were at 0.18 and 0.23 μM , respectively, based on a competitive inhibition model (Cheng and Prusoff, 1973) (Figure 4D). The efficacy data were comparable to those observed for the two ACSs from the apicomplexan parasite *Cryptosporidium parvum* (i.e., IC_{50} values at 3.70 and 2.32 μM for CpACS1 and CpACS2, respectively) (Guo et al., 2014).

Since the major goal of this study is to explore the potential of GiACSSs to serve as drug targets, we further investigated the *in vitro* efficacy of triacsin C against the growth of *G. intestinalis* in axenic culture. We observed that triacsin C indeed effectively inhibited the parasite growth in a dose-dependent manner with an estimated IC_{50} value at 0.8 μM (Figure 5). At other tested doses, 2.2 μM and $\geq 10 \mu\text{M}$ triacsin C achieved 90 and 100% inhibitions, respectively.

Discussion

FA are essential to all organisms as one of the major components of biomembranes. In most organisms, FA also serves as an

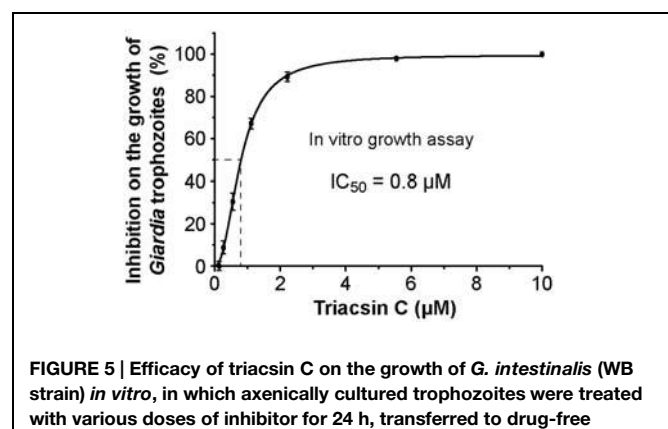


FIGURE 5 | Efficacy of triacsin C on the growth of *G. intestinalis* (WB strain) *in vitro*, in which axenically cultured trophozoites were treated with various doses of inhibitor for 24 h, transferred to drug-free medium, and allowed to grow for additional 48 h before being counted for calculating the parasite growth.

energy source. Because FA needs to be activated to form FA-CoA before they can enter subsequent metabolic pathways, enzymes catalyzing the formation of FA-CoA are essential and considered as potential drug targets. We have recently reported that ACS enzymes could serve as effective drug targets in *Cryptosporidium*

(Guo et al., 2014), which prompted us to explore whether ACSs could also be targeted for developing novel anti-*Giardia* drugs. Indeed, in the present study, we have confirmed that the ACS inhibitor could inhibit not only the reactions catalyzed by GiACS2, but also the *in vitro* growth of *G. intestinalis* at sub-micromolar levels (Figure 5). The possibility to consider GiACS1 and GiACS2 as likely drug targets was further supported by bioinformatics data in which protein modeling analyses showed structural differences between giardial and human counterparts (Figure 3F). This fact could be the result of evolutionary processes in which the giardial ACSs are likely ancestors of other ACSs counterparts. In this context, it is conceivable that GiACS1 (853 aa) could have had a reductive process during evolution. In spite of the predicted satisfactory quality of the protein models in this study, further crystallographic studies in purified GiACS1/2 will offer additional insights not only for site-targeted drug design, but also to assess if a differential adaptation in the catalytic pocket of GiACS2, as compared to GiACS1, exists. Moreover, the possibility to recover enzyme activities from recombinant GiACS1/2 will allow refining crystallographic analyses at distinct enzyme conformations and under interaction with Triacsin C or other specific inhibitors. This renders an advantage over the failure to detect enzyme activities in other parasitic recombinant ACSs (Matesanz et al., 1999; Guo et al., 2014).

Triacsin C is an analog of polyunsaturated FA that was first isolated from the fungal *Streptomyces aureofaciens* (Omura et al., 1986). It is known as a long-chain ACS-specific inhibitor with little effect on short-chain or mitochondrial-type ACSs in mammals (Omura et al., 1986; Tomoda et al., 1987; Hartman et al., 1989; Van Horn et al., 2005). Mammals possess six genes encoding long-chain ACS enzymes that are designated as ACSL1–6 including some variants produced by alternative intron-splicing with varied spectra of substrate preferences (Soupene and Kuypers, 2008; Watkins and Ellis, 2012). Among them, triacsin

C is an effective inhibitor for ACSL1, ACSL3, and ACSL4 (IC_{50} values between 4 and 7.5 μ M), but not for ACSL5, ACS6_v1, and ACS6_v2 (Van Horn et al., 2005). The abundance of ACSLs and their varied sensitivities to triacsin C might explain its ineffectiveness on the recycling of FA into phospholipids in mammalian cells (Igal et al., 1997) and its selective inhibition on *Cryptosporidium* both *in vitro* and *in vivo* (Guo et al., 2014). Collectively, the present study not only supports the notion that ACS enzymes can be explored as drug targets in *Giardia*, but also provides strong proof-of-concept data for the further identification of triacsin C analogs and other classes of small molecules for developing more selective inhibitors against the parasite.

Acknowledgments

This research was supported in part by grants funded by the Texas A&M University-CONACYT Collaborative Research Program (Proposal No. 2010-012 to GZ and GO-P), and by the National Institute of Allergy and Infectious Diseases, National Institutes of Health (grant R21 AI119710 and R01 AI44594 to GZ). We also thank *GiardiaDB* (<http://www.giardiadb.org/>) and investigators who made their genome and transcriptome data available at *GiardiaDB*. We are grateful to Arturo Pérez Taylor for informatics assistance and Alejandro Sosa for his useful comments on protein modeling.

Supplementary Material

The Supplementary Material for this article can be found online at: <http://journal.frontiersin.org/article/10.3389/fmib.2015.00753>

References

- Ali, V., and Nozaki, T. (2007). Current therapeutics, their problems, and sulfur-containing-amino-acid metabolism as a novel target against infections by "mitochondrion" protozoan parasites. *Clin. Microbiol. Rev.* 20, 164–187. doi: 10.1128/CMR.00019-06
- Arguello-Garcia, R., Cruz-Soto, M., Romero-Montoya, L., and Ortega-Pierres, G. (2004). Variability and variation in drug susceptibility among *Giardia duodenalis* isolates and clones exposed to 5-nitroimidazoles and benzimidazoles *in vitro*. *J. Antimicrob. Chemother.* 54, 711–721. doi: 10.1093/jac/dkh388
- Beach, D. H., Holz, G. G. Jr., Singh, B. N., and Lindmark, D. G. (1990). Fatty acid and sterol metabolism of cultured *Trichomonas vaginalis* and *Tritrichomonas foetus*. *Mol. Biochem. Parasitol.* 38, 175–190. doi: 10.1016/0166-6851(90)90021-D
- Bernson, V. S. M. (1976). Acetyl-CoA hydrolase; activity, regulation and physiological significance of the enzyme in brown adipose tissue from hamster. *Eur. J. Biochem.* 67, 403–410. doi: 10.1111/j.1432-1033.1976.tb0705.x
- Busatti, H. G., Santos, J. F., and Gomes, M. A. (2009). The old and new therapeutic approaches to the treatment of giardiasis: where are we? *Biologics* 3, 273–287.
- Cheng, Y., and Prusoff, W. H. (1973). Relationship between the inhibition constant (K_1) and the concentration of inhibitor which causes 50 per cent inhibition (I_{50}) of an enzymatic reaction. *Biochem. Pharmacol.* 22, 3099–3108. doi: 10.1016/0006-2952(73)90196-2
- Das, S., Stevens, T., Castillo, C., Villasenor, A., Arredondo, H., and Reddy, K. (2002). Lipid metabolism in mucous-dwelling amitochondriate protozoa. *Int. J. Parasitol.* 32, 655–675. doi: 10.1016/S0020-7519(02)00006-1
- Feng, Y., and Xiao, L. (2011). Zoonotic potential and molecular epidemiology of *Giardia* species and giardiasis. *Clin. Microbiol. Rev.* 24, 110–140. doi: 10.1128/CMR.00033-10
- Franzen, O., Jerlstrom-Hultqvist, J., Einarsson, E., Ankarklev, J., Ferella, M., Andersson, B., et al. (2013). Transcriptome profiling of *Giardia intestinalis* using strand-specific RNA-seq. *PLoS Comput. Biol.* 9:e1003000. doi: 10.1371/journal.pcbi.1003000
- Fritzler, J. M., Millership, J. J., and Zhu, G. (2007). *Cryptosporidium parvum* long-chain fatty acid elongase. *Eukaryot. Cell* 6, 2018–2028. doi: 10.1128/ec00210-07
- Fritzler, J. M., and Zhu, G. (2007). Functional characterization of the acyl-[acyl carrier protein] ligase in the *Cryptosporidium parvum* giant polyketide synthase. *Int. J. Parasitol.* 37, 307–316. doi: 10.1016/j.ijpara.2006.10.014
- Granados, C. E., Reveiz, L., Uribe, L. G., and Criollo, C. P. (2012). Drugs for treating giardiasis. *Cochrane Database Syst. Rev.* 12, CD007787. doi: 10.1002/14651858.CD007787.pub2
- Guo, F., Zhang, H., Fritzler, J. M., Rider, S. D. Jr., Xiang, L., McNair, N. N., et al. (2014). Amelioration of *Cryptosporidium parvum* infection *in vitro* and *in vivo* by targeting parasite fatty acyl-coenzyme A synthetases. *J. Infect. Dis.* 209, 1279–1287. doi: 10.1093/infdis/jit645
- Guo, F., and Zhu, G. (2012). Presence and removal of a contaminating NADH oxidation activity in recombinant maltose-binding protein fusion

- proteins expressed in *Escherichia coli*. *Biotechniques* 52, 247–253. doi: 10.2144/0000113822
- Hartman, E. J., Omura, S., and Laposata, M. (1989). Triacsin C: a differential inhibitor of arachidonoyl-CoA synthetase and nonspecific long chain acyl-CoA synthetase. *Prostaglandins* 37, 655–671. doi: 10.1016/0090-6980(89)90103-2
- Hlavsa, M. C., Watson, J. C., and Beach, M. J. (2005). Giardiasis surveillance—United States, 1998–2002. *MMWR Surveill. Summ.* 54, 9–16.
- Igal, R. A., Wang, P., and Coleman, R. A. (1997). Triacsin C blocks de novo synthesis of glycerolipids and cholesterol esters but not recycling of fatty acid into phospholipid: evidence for functionally separate pools of acyl-CoA. *Biochem. J.* 324 (Pt 2), 529–534.
- Jarroll, E. L., Muller, P. J., Meyer, E. A., and Morse, S. A. (1981). Lipid and carbohydrate metabolism of *Giardia lamblia*. *Mol. Biochem. Parasitol.* 2, 187–196. doi: 10.1016/0166-6851(81)90099-2
- Lalle, M. (2010). Giardiasis in the post genomic era: treatment, drug resistance and novel therapeutic perspectives. *Infect. Disord. Drug Targets* 10, 283–294. doi: 10.2174/187152610791591610
- Lee, S. H., Stephens, J. L., and Englund, P. T. (2007). A fatty-acid synthesis mechanism specialized for parasitism. *Nat. Rev. Microbiol.* 5, 287–297. doi: 10.1038/nrmicro1617
- Matesanz, F., Duran-Chica, I., and Alcina, A. (1999). The cloning and expression of Pfacs1, a *Plasmodium falciparum* fatty acyl coenzyme A synthetase-1 targeted to the host erythrocyte cytoplasm. *J. Mol. Biol.* 291, 59–70. doi: 10.1006/jmbi.1999.2964
- Morf, L., Spycher, C., Rehrauer, H., Fournier, C. A., Morrison, H. G., and Hehl, A. B. (2010). The transcriptional response to encystation stimuli in *Giardia lamblia* is restricted to a small set of genes. *Eukaryot. Cell* 9, 1566–1576. doi: 10.1128/EC.00100-10
- Morrison, H. G., McArthur, A. G., Gillin, F. D., Aley, S. B., Adam, R. D., Olsen, G. J., et al. (2007). Genomic minimalism in the early diverging intestinal parasite *Giardia lamblia*. *Science* 317, 1921–1926. doi: 10.1126/science.1143837
- Omura, S., Tomoda, H., Xu, Q. M., Takahashi, Y., and Iwai, Y. (1986). Triacsin, new inhibitors of acyl-CoA synthetase produced by *Streptomyces* sp. *J. Antibiot.* 39, 1211–1218. doi: 10.7164/antibiotics.39.1211
- Palm, D., Weiland, M., McArthur, A. G., Winiecka-Krusnell, J., Cipriano, M. J., Birkeland, S. R., et al. (2005). Developmental changes in the adhesive disk during *Giardia* differentiation. *Mol. Biochem. Parasitol.* 141, 199–207. doi: 10.1016/j.molbiopara.2005.03.005
- Plutzer, J., Ongerth, J., and Karanis, P. (2010). Giardia taxonomy, phylogeny and epidemiology: facts and open questions. *Int. J. Hyg. Environ. Health* 213, 321–333. doi: 10.1016/j.ijheh.2010.06.005
- Ringqvist, E., Avesson, L., Soderbom, F., and Svard, S. G. (2011). Transcriptional changes in *Giardia* during host-parasite interactions. *Int. J. Parasitol.* 41, 277–285. doi: 10.1016/j.ijpara.2010.09.011
- Roy, A., Kucukural, A., and Zhang, Y. (2010). I-TASSER: a unified platform for automated protein structure and function prediction. *Nat. Protoc.* 5, 725–738. doi: 10.1038/nprot.2010.5
- Soupene, E., and Kuypers, F. A. (2008). Mammalian long-chain acyl-CoA synthetases. *Exp. Biol. Med.* 233, 507–521. doi: 10.3181/0710-MR-287
- Tejman-Yarden, N., and Eckmann, L. (2011). New approaches to the treatment of giardiasis. *Curr. Opin. Infect. Dis.* 24, 451–456. doi: 10.1097/QCO.0b013e32834ad401
- Tian, H. F., Chen, B., and Wen, J. F. (2010). Giardiasis, drug resistance, and new target discovery. *Infect. Disord. Drug Targets* 10, 295–302. doi: 10.2174/187152610791591629
- Tomoda, H., Igarashi, K., and Omura, S. (1987). Inhibition of acyl-CoA synthetase by triacsin. *Biochim. Biophys. Acta* 921, 595–598. doi: 10.1016/0005-2760(87)90088-9
- Van Horn, C. G., Caviglia, J. M., Li, L. O., Wang, S., Granger, D. A., and Coleman, R. A. (2005). Characterization of recombinant long-chain rat acyl-CoA synthetase isoforms 3 and 6: identification of a novel variant of isoform 6. *Biochemistry* 44, 1635–1642. doi: 10.1021/bi0477211
- Watkins, P. A., and Ellis, J. M. (2012). Peroxisomal acyl-CoA synthetases. *Biochim. Biophys. Acta* 1822, 1411–1420. doi: 10.1016/j.bbadi.2012.02.010
- Yang, J., Yan, R., Roy, A., Xu, D., Poisson, J., and Zhang, Y. (2015). The I-TASSER Suite: protein structure and function prediction. *Nat. Methods* 12, 7–8. doi: 10.1038/nmeth.3213
- Yoder, J. S., Beach, M. J., and Centers for Disease Control and Prevention. (2007). Giardiasis surveillance—United States, 2003–2005. *MMWR Surveill. Summ.* 56, 11–18.
- Yoder, J. S., Gargano, J. W., Wallace, R. M., Beach, M. J., and Centers for Disease Control and Prevention. (2012). Giardiasis surveillance—United States, 2009–2010. *MMWR Surveill. Summ.* 61, 13–23.
- Yoder, J. S., Harral, C., Beach, M. J., and Centers for Disease Control and Prevention. (2010). Giardiasis surveillance - United States, 2006–2008. *MMWR Surveill. Summ.* 59, 15–25.
- Yu, Y., Zhang, H., Guo, F., Sun, M., and Zhu, G. (2014). A unique hexokinase in *Cryptosporidium parvum*, an apicomplexan pathogen lacking the Krebs cycle and oxidative phosphorylation. *Protist* 165, 701–714. doi: 10.1016/j.protis.2014.08.002
- Zhang, Y. (2008). I-TASSER server for protein 3D structure prediction. *BMC Bioinformatics* 9:40. doi: 10.1186/1471-2105-9-40
- Zhuravleva, E., Gut, H., Hynx, D., Marcellin, D., Bleck, C. K., Genoud, C., et al. (2012). Acyl coenzyme A thioesterase Them5/Acot15 is involved in cardiolipin remodeling and fatty liver development. *Mol. Cell. Biol.* 32, 2685–2697. doi: 10.1128/MCB.00312-12

Conflict of Interest Statement: The authors declare that the research was conducted in the absence of any commercial or financial relationships that could be construed as a potential conflict of interest.

Copyright © 2015 Guo, Ortega-Pierres, Argüello-García, Zhang and Zhu. This is an open-access article distributed under the terms of the Creative Commons Attribution License (CC BY). The use, distribution or reproduction in other forums is permitted, provided the original author(s) or licensor are credited and that the original publication in this journal is cited, in accordance with accepted academic practice. No use, distribution or reproduction is permitted which does not comply with these terms.



Identification of natural inhibitors of *Entamoeba histolytica* cysteine synthase from microbial secondary metabolites

OPEN ACCESS

Edited by:

Anjan Debnath,
University of California, San Diego,
USA

Reviewed by:

Paul F. Moundjpa,
University of Yaounde I, Cameroon
Mark S. Butler,
University of Queensland, Australia

*Correspondence:

Tomoyoshi Nozaki,
Department of Parasitology, National
Institute of Infectious Diseases,
1-23-1 Toyama, Shinjuku-ku,
Tokyo 162-8640, Japan
nozaki@nih.go.jp;
Kazuro Shiomi,
Kitasato Institute for Life Sciences,
Kitasato University, 5-9-1 Shirokane,
Minato-ku, Tokyo 108-8641, Japan
shiomi@lisci.kitasato-u.ac.jp

Specialty section:

This article was submitted to
Antimicrobials, Resistance
and Chemotherapy,
a section of the journal
Frontiers in Microbiology

Received: 12 May 2015

Accepted: 31 August 2015

Published: 14 September 2015

Citation:

Mori M, Jeelani G, Masuda Y, Sakai K, Tsukui K, Waluyo D, Tarwadi, Watanabe Y, Nonaka K, Matsumoto A, Ômura S, Nozaki T and Shiomi K (2015) Identification of natural inhibitors of *Entamoeba histolytica* cysteine synthase from microbial secondary metabolites. *Front. Microbiol.* 6:962.
doi: 10.3389/fmicb.2015.00962

Mihoko Mori^{1,2}, Ghulam Jeelani³, Yui Masuda², Kazunari Sakai², Kumiko Tsukui³, Danang Waluyo⁴, Tarwadi⁴, Yoshio Watanabe⁵, Kenichi Nonaka^{1,2}, Atsuko Matsumoto^{1,2}, Satoshi Ômura¹, Tomoyoshi Nozaki^{3,6*} and Kazuro Shiomi^{1,2*}

¹ Kitasato Institute for Life Sciences, Kitasato University, Tokyo, Japan, ² Graduate School of Infection Control Sciences, Kitasato University, Tokyo, Japan, ³ Department of Parasitology, National Institute of Infectious Diseases, Tokyo, Japan,

⁴ Biotech Center, Badan Pengkajian Dan Penerapan Teknologi, Banten, Indonesia, ⁵ Research and Development Division, MicroBiopharm Japan Co. Ltd, Iwata, Japan, ⁶ Graduate School of Life and Environmental Sciences, University of Tsukuba, Tsukuba, Japan

Amebiasis is a common worldwide diarrheal disease, caused by the protozoan parasite, *Entamoeba histolytica*. Metronidazole has been a drug of choice against amebiasis for decades despite its known side effects and low efficacy against asymptomatic cyst carriers. *E. histolytica* is also capable of surviving sub-therapeutic levels of metronidazole *in vitro*. Novel drugs with different mode of action are therefore urgently needed. The sulfur assimilatory *de novo* L-cysteine biosynthetic pathway is essential for various cellular activities, including the proliferation and anti-oxidative defense of *E. histolytica*. Since the pathway, consisting of two reactions catalyzed by serine acetyltransferase (SAT) and cysteine synthase (CS, O-acetylserine sulfhydrylase), does not exist in humans, it is a rational drug target against amebiasis. To discover inhibitors against the CS of *E. histolytica* (EhCS), the compounds of Kitasato Natural Products Library were screened against two recombinant CS isozymes: EhCS1 and EhCS3. Nine compounds inhibited EhCS1 and EhCS3 with IC₅₀ values of 0.31–490 µM. Of those, seven compounds share a naphthoquinone moiety, indicating the structural importance of the moiety for binding to the active site of EhCS1 and EhCS3. We further screened >9,000 microbial broths for CS inhibition and purified two compounds, xanthofulvin and exophillic acid from fungal broths. Xanthofulvin inhibited EhCS1 and EhCS3. Exophillic acid showed high selectivity against EhCS1, but exhibited no inhibition against EhCS3. *In vitro* anti-amebic activity of the 11 EhCS inhibitors was also examined. Deacetylkinamycin C and nanaomycin A showed more potent amebicidal activity with IC₅₀ values of 18 and 0.8 µM, respectively, in the cysteine deprived conditions. The differential sensitivity of trophozoites against deacetylkinamycin C in the presence or absence of L-cysteine in the medium and the IC₅₀ values against EhCS suggest the amebicidal effect of deacetylkinamycin C is due to CS inhibition.

Keywords: amebiasis, compound library screening, cysteine synthase, *Entamoeba histolytica*, secondary metabolites

Introduction

Amebiasis is a common diarrheal disease in humans, arising from infection with the parasitic protozoan *Entamoeba histolytica*. WHO estimates 50 million people are infected worldwide, resulting in 40,000–100,000 deaths annually (Harque et al., 2003; Stanley, 2003; Ximénez et al., 2009). Transmission occurs via the fecal–oral route, either directly by person to person contact or indirectly through consumption of contaminated food or water. In developed countries, including Japan, domestic cases of amebiasis are increasing among men who have sex with men, particularly those infected with HIV (Watanabe et al., 2011; Hung et al., 2012).

Metronidazole has been a drug of choice against amebiasis for decades despite its low efficacy against asymptomatic cyst carriers (Ali and Nozaki, 2007). Moreover, metronidazole is teratogenic and causes several adverse side effects, such as nausea, vomiting, and a metallic taste (Ohnishi et al., 2014). It has been shown that *E. histolytica* is capable of surviving sub-therapeutic levels of metronidazole *in vitro* (Samarawickrema et al., 1997; Wassmann et al., 1999). Therefore, new drugs with targets and modes of action different from those of metronidazole are urgently needed.

The *de novo* biosynthetic pathway of L-cysteine, is essential for various cellular activities, including the attachment, motility, proliferation, and anti-oxidative defense of *E. histolytica* (Gillin and Diamond, 1981; Fahey et al., 1984; Jeelani et al., 2010, 2014; Hussain et al., 2011). Since the homologous pathway does not exist in humans, it could be a rational drug target for anti-amebic agents. This pathway consists of two reactions catalyzed by serine acetyltransferase (SAT, EC 2.3.1.30) and cysteine synthase (CS, O-acetylserine sulfhydrylase, EC 2.5.1.47) (Figure 1; Nozaki et al., 1998, 1999, 2005). In the first reaction, L-serine is acetylated with acetyl-CoA by SAT, and in the second reaction, the alanyl moiety of O-acetylserine is transferred to sulfide by CS to produce L-cysteine. This sulfur-assimilatory cysteine biosynthetic pathway exists in bacteria, plants, and some parasitic protozoa, including *Leishmania major*, *Trichomonas vaginalis*, and *Trypanosoma cruzi*. The *E. histolytica* genome encodes three isotypes of SAT (EhSAT1-3) and CS (EhCS1-3) (Nozaki et al., 2005; Ali and Nozaki, 2007; Hussain et al., 2009). The SAT and CS enzymes of *E. histolytica* have unique features. Three isotypes of SAT and CS are all present in the cytosol, whereas in plants three isotypes are compartmentalized, i.e., the cytosol, mitochondria, and plastids. EhCS1 and EhSAT1 do not form a heteromeric complex (Nozaki et al., 1999; Kumar et al., 2011), which is in stark contrast to bacteria and plants, in which SAT and CS form such a complex (Kredich et al., 1969; Feldman-Salit et al., 2009). In addition, EhSAT1-3 are both sequence-wise and biochemically divergent; EhSAT1-3 show remarkably different sensitivity against allosteric feedback by L-cysteine (Ali and Nozaki, 2007; Hussain et al., 2009). Thus, amebic SATs and EHCSs are a rational target to develop anti-amebic drugs.

The sulfur-assimilatory cysteine biosynthetic pathway in plants and bacteria have been exploited for drug development (Salsi et al., 2010; Amori et al., 2012; Spyros et al., 2013). Nagpal et al. (2012) recently performed *in silico* screening of ZINC database studies based on the crystal structure of

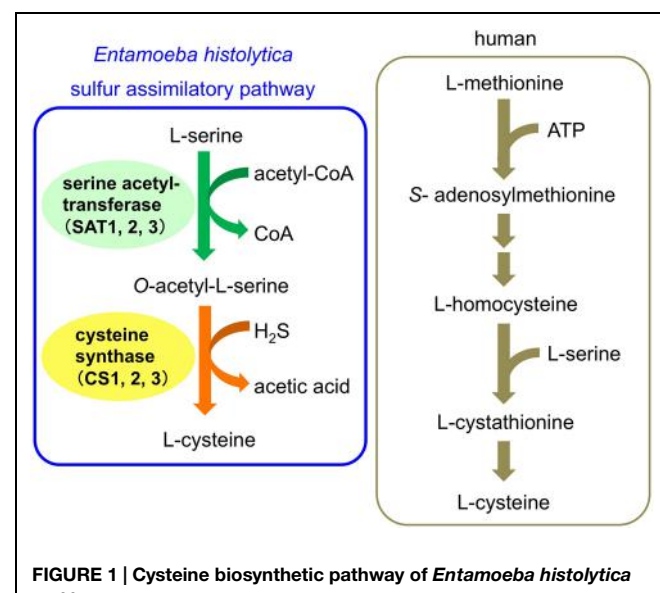


FIGURE 1 | Cysteine biosynthetic pathway of *Entamoeba histolytica* and human.

EhCS1. One compound was discovered and showed moderate inhibitory activity against EhCS1 (74% inhibition at 100 μ M) *in vitro*. A similar virtual screening was also carried out against *Trichomonas* CS, which yielded some potential inhibitors (Singh et al., 2013).

Structure-based drug discovery can identify potential ligand compounds fit for predicted active sites of target proteins. Alternatively, screening of natural product libraries or microbial extracts by directly evaluating inhibitory activity against target enzymes can also identify existent and novel inhibitors. Consequently, we developed an enzymatic assay system using recombinant CSs to identify inhibitors with potentially novel and diverse structures.

Natural products have been playing a very important role in drug discovery and development for over a century. In particular, microbial secondary metabolites have provided many kinds of compounds, and it is widely considered that a plethora of unique chemical compounds must still exist undiscovered in the microbial environment (Newman and Cragg, 2012).

Several anti-amebic compounds have been found from natural sources, particularly from plants. However, microbial metabolite sources have not been vigorously exploited (Singh et al., 2009) as plants or herbs used for traditional remedies have been historically utilized to isolate active anti-amebic components.

In this study, we utilized two libraries of microbial secondary metabolites, a chemically defined natural product library and microbial culture broths as a source of novel lead compounds for anti-amebic drugs. We first screened 316 compounds from the Kitasato Natural Products Library against the recombinant enzymes of two representative CSs: EhCS1 and EhCS3. We also screened extracts from more than 9,000 fungal and actinomycete culture broths against EhCS1 and EhCS3. We obtained two compounds, xanthofulvin and exophillic acid, as EhCS1 inhibitors from the broths of two fungi, *Penicillium* sp. and *Exophiala* sp., respectively.

Xanthofulvin, which contains a xanthone moiety in its structure, inhibited both EhCS1 and EhCS3. The other inhibitor, exophillic acid, showed high selectivity against EhCS1. *In vitro* antiamebic activity of the 11 EhCS inhibitors found were also evaluated.

Materials and Methods

Expression and Purification of Recombinant

E. histolytica CSs

The *E. coli* BL21 (DE3) cell introduced pET-EhCS (CS1, CS3) construct was used for protein expression. Each EhCSs protein was expressed by 1 mM isopropyl β -D-thiogalactopyranoside induction for 12 h at 30°C. After induction, the *E. coli* cell was harvested and re-suspended in the lysis buffer (50 mM Tris-HCl, pH 8.0, and 300 mM NaCl) containing 0.5 mM phenylmethylsulfonyl fluoride. The suspension was sonicated and centrifuged at 24,000 $\times g$ for 30 min at 4°C. The histidine-tagged rEhCS proteins were purified from the supernatant fraction using a Ni²⁺-NTA column and tagged proteins were eluted with 100–200 mM imidazole in 50 mM Tris-HCl, pH 8.0, and 300 mM NaCl. The purity of the eluted rEhCS proteins was confirmed by SDS-PAGE and then dialyzed in 50 mM Tris-HCl, and 150 mM NaCl, pH 8.0 containing 10% glycerol (v/v) for 24 h at 4°C. The dialyzed proteins were stored at -80°C with glycerol in small aliquots until use, purified proteins retaining activity for more than three months when stored at this temperature.

Evaluation of Enzymatic Activities

For measurement of CS inhibitory activity, 10 μ l of sample solution [dimethylsulfoxide (DMSO)/H₂O = 1/1 solution] and 30 μ l of reaction mixture, composed of 2 μ l of 50 mM O-acetyl-L-serine, 2 μ l of 50 mM Na₂S, 12.5 μ l of 200 mM Tris-HCl (pH 7.5), and 13.5 μ l of water, was poured into each well of a flat-bottom 96-well plate. After 10 μ l of enzyme solution (containing 0.1 μ g of rEhCS1 or rEhCS3 in H₂O) was added to each well, plates were incubated for 15 min at 37°C. The final concentrations of reagents in each well are; 2 mM O-acetyl-L-serine, 2 mM Na₂S, and 50 mM Tris-HCl. The enzymatic reaction was stopped by adding 50 μ l of acetic acid (>99.9%), and subsequently the reaction for cysteine detection was started by adding 50 μ l of acid-ninhydrin reagent (Gaitonde, 1967). The mixture in each well was transferred to a 96-well PCR plate and heated at 95°C for 10 min. After the plate was cooled on ice, the mixture was transferred into a flat-bottom 96-well plate filled with 100 μ l of ethanol (EtOH). Absorbance at 560 nm was measured by spectrophotometer (SH-9000Lab, Corona Electric, Ibaraki, Japan). A standard inhibitor of this assay system does not exist, therefore we defined that the values without samples are 0% inhibition, and the values without both samples and enzyme are 100% inhibition. To determine whether the sample interferes the acid-ninhydrin reagent reaction, 10 μ l of sample solution, 10 μ l of water, and 30 μ l of 1 mM cysteine solution (cysteine hydrochloric acid salt in water) were mixed in a well of 96-well microtiter plate, and then 50 μ l of acetic acid (>99.9%) and 50 μ l of acid-ninhydrin reagent were added. The mixture was treated

and measured the absorbance at 560 nm as above mentioned to check the effect of the sample to the color reaction.

Evaluation of Cytotoxicity against MRC-5 Cells

Human fibroblast cells, MRC-5, were plated on 96-well flat bottom plates at a density of 1.5 \times 10⁴ cells/well with 100 μ l of MEM medium (Life Technologies, Grand Islands, NY, USA) containing 10% fetal bovine serum (Hana-nesco Bio, Tokyo, Japan) and 1% penicillin-streptomycin (Life Technologies) and incubated at 37°C with 5% CO₂ for 2 days. Test compounds in 5 μ l of 50% DMSO-H₂O and 100 μ l of MEM medium were mixed and added to each well. After 2 days cultivation at 37°C with 5% CO₂, cell density and morphological changes were observed under a microscope. After observation, 10 μ l of WST-8 solution (Dojindo, Kumamoto, Japan) was added to the cells and the plate was incubated at 37°C with 5% CO₂ for 2 h. Then, absorbance at 450 nm was measured by spectrophotometer (SH-9000Lab, Corona Electric). Cytotoxicity was measured in duplicate. Staurosporine (our product, in Kitasato Natural Products Library) was used as a positive (cytotoxic) compound. The concentration range of test compounds are: 1.6 to 50 μ g/ml (final concentration) for kerriamycin B, kerriamycin C, and aggreticin; 0.075 to 10 μ g/ml for deacetylkinamycin C, deoxyfrenolicin, nanaomycin A, and naphthacemycin A₉; 3.1 to 200 μ g/ml for tetracycline and patulin; 9.4 to 75 μ g/ml for exophillic acid. IC₅₀ values were calculated by the equation described in the reference (Arita-Morioka et al., 2015).

Screening Sources

The Kitasato Natural Products Library comprises 316 compounds. Each compound was dissolved in DMSO at 1.0 mg/ml. The source microbes for screening were collected in Japan and Indonesia. Fungal strains originating in Japan were isolated from soil samples collected near plants. Actinomycetes originating in Japan were isolated from plants as well as from soil samples attached to plant roots. The Indonesian fungi and actinomycetes were isolated from soils, plants and insects. In total, 9,173 broth extract samples (4,800 fungal plus 4,373 from actinomycete) were prepared. After cultivation, the same amount of EtOH was added to each broth, which were then centrifuged. Obtained supernatants were used for screening as broth extract samples.

Screening of CS Inhibitors from Natural Compounds and Microbial Broths

Each 5 μ l of DMSO solution (1 mg/ml, final concentration 100 μ g/ml) of 316 library compounds and 5 μ l of water (total 10 μ l of DMSO/H₂O = 1/1 solution per well) were poured into each well of a 96-well microtiter plate to screen for CS inhibitors. For screening microbial broths, 10 μ l of the individual broth extract samples (50% EtOH solution) were poured into each well of a 96-well microtiter plate and dried up *in vacuo*. After drying, 10 μ l of DMSO/H₂O = 1/1 solution was added and dissolved. Samples showing more than 50% inhibitory activity and having no inhibitory activities against acid ninhydrin reaction were selected for further evaluation. The inhibition values were measured in duplicate or triplicate.

The concentration range of test compounds are: 0.15 to 20 µg/ml (final concentration) for kerriamycin B, kerriamycin C, and aggreticin; 2.0 to 250 µg/ml for deacetylkinamycin C, deoxyfrenolicin, nanaomycin A, tetracycline and patulin; 1.5 to 200 µg/ml for naphthacemycin A₉; 3.1 to 400 µg/ml for xanthofulvin, terreinol and citromycetin; 0.06 to 200 µg/ml for exophillic acid. IC₅₀ values were calculated as shown in Section "Evaluation of Cytotoxicity against MRC-5 Cells" with each concentration range.

Isolation of CS Inhibitors from Culture Broths of Microorganisms

Isolation of Xanthofulvin from a Culture Broth of *Penicillium* sp. if08054

Producing strain and cultivation

The fungal strain *Penicillium* sp. if08054 was isolated from a soil sample collected at Jember, Java Island, Indonesia. The sequence of the 28S rDNA D1/D2 region of this strain had 100% similarity with *Penicillium lagena*. However, the results of morphological and sequencing analyses confirmed that the producing strain, if08054, was an unidentified species of the genus *Penicillium*. The medium used to culture this organism consisted of 2% rice starch, 1% glucose, 2% soybean meal, 1% KH₂PO₄, 0.5% MgSO₄·7H₂O (pH was not adjusted). Frozen broth of this strain (0.2 ml) was inoculated into a 250-ml Erlenmeyer flask containing 20 ml of medium and incubated in a rotary shaker (220 rpm) at 25°C for 3 days. This seed culture (0.5 ml) was inoculated into a 500-ml Erlenmeyer flask containing 50 ml of medium and the production culture was incubated in a rotary shaker (220 rpm) at 25°C for 4 days.

Isolation of xanthofulvin from the culture broth

The culture broth (50 ml) was extracted with 50 ml of *n*-BuOH, and the extract was evaporated and dried *in vacuo*. The dried extract (0.23 g) was dissolved in 50 ml of 50% EtOH-H₂O, and after removing EtOH, then applied to an ODS column (30φ × 300 mm, YMC, Kyoto, Japan). The column was eluted with H₂O-acetonitrile (MeCN) system to give six fractions (0, 20, 40, 60, 80, and 100% MeCN, each 0.6 l). The 40% MeCN fraction (50 mg) was purified by Sephadex LH-20 column chromatography (10φ × 300 mm, GE Healthcare Bio-Sciences, Piscataway, NJ, USA; solvent, MeOH). The eluate was fractionated every 1 ml. Fractions 46–50 were collected and concentrated *in vacuo* to dryness to afford xanthofulvin (1.9 mg). Fractions 41–43 contained terreinol (2.1 mg). The 20% MeCN fraction (25 mg) of ODS column chromatography was purified by preparative HPLC (column, Pegasil ODS SP100, 20φ × 250 mm, Senshu Scientific, Tokyo, Japan; solvent, 20% MeCN-H₂O; flow rate, 7.0 mL/min; detection, UV at 254 nm). The peak eluted at 24–26 min was collected and concentrated *in vacuo* to dryness to afford citromycetin (7.8 mg).

Xanthofulvin. Yellowish-brown amorphous. ¹H NMR (500 MHz, DMSO-*d*₆) δ 7.69 (1H, s), 6.85 (1H, s), 6.49 (1H, s), 4.78 (2H, s), 2.66 (3H, s), 2.19 (3H, s). ESI-MS calcd. for C₂₈H₁₇O₁₄ [M-H]⁻: 577.0624, found 577.0628 [M-H]⁻.

Terreinol. Yellowish-brown amorphous. ¹H NMR (400 MHz, CD₃OD) δ 6.97 (1H, s), 4.92 (1H, d, 16 Hz), 4.75 (1H, d, 16 Hz),

4.06 (1H, m), 3.97 (1H, dd, 15 and 7.5 Hz), 2.66 (1H, m), 2.13 (3H, s), 2.13 (1H, m, overlapped), 2.04 (1H, m), 1.89 (1H, m). ESI-MS calcd. for C₁₃H₁₄O₅Na [M+Na]⁺: 273.0739, found 273.0730 [M+Na]⁺.

Citromycetin. Yellow amorphous. ¹H NMR (400 MHz, CD₃OD) δ 6.51 (1H, s), 6.20 (1H, s), 5.01 (2H, s), 2.33 (3H, s). ESI-MS calcd. for C₂₈H₂₁O₁₄ [2M+H]⁺: 581.0931, found 581.0923 [2M+H]⁺.

Isolation of Exophillic Acid from a Culture Broth of *Exophiala* sp. FKI-7082

Producing strain and cultivation

The fungal strain *Exophiala* sp. FKI-7082 was isolated from a soil sample collected in Kouzu-shima Island, Japan. The producing strain FKI-7082 was classified in the genus *Exophiala* according to its morphology. This fungal strain was maintained on an LcA slant consisting of 0.1% glycerol, 0.08% KH₂PO₄, 0.02% K₂HPO₄, 0.02% MgSO₄·7H₂O, 0.02% KCl, 0.2% NaNO₃, 0.02% yeast extract, and 1.5% agar (adjusted to pH 6.0 before sterilization). A loopful of spores was inoculated into two test tubes, each containing 10 ml of a seed medium consisting of 2% glucose, 0.5% Polypeptone (Nihon Pharmaceutical, Tokyo, Japan), 0.2% yeast extract, 0.2% KH₂PO₄, 0.05% MgSO₄·7H₂O, and 0.1% agar (adjusted to pH 6.0 before sterilization) and incubated on a shaker at 27°C for 3 days. One milliliter of the seed culture was inoculated into each of ten 500-ml Erlenmeyer flasks, each containing 100 ml of a production medium consisting of 3% soluble starch, 1% glycerol, 2% soy bean meal, 0.3% dry yeast, 0.3% KCl, 0.05% KH₂PO₄, and 0.05% MgSO₄·7H₂O (adjusted to pH 6.5 before sterilization) and incubated on a rotary shaker at 27°C for 6 days.

Isolation of exophillic acid from the culture broth

The obtained culture broth (1 l) was extracted with 1 l of EtOH and mycelia were then removed by centrifugation and filtration. After evaporation, the residue was extracted three times with 1 l of ethyl acetate, and the organic layer was dried *in vacuo*. The dried extract (1.2 g) was dissolved in a small amount of chloroform and then applied to a silica gel column (30φ × 140 mm, particle size: 0.063–0.200 mm, Merck, Darmstadt, Germany). The column was eluted with chloroform-MeOH system to give five fractions (100:0, 99:1, 98:2, 95:5, 90:10, 50:50, and 0:100, each 200 ml). The two active fractions, 90:10 fraction (27 mg) and 50:50 fraction (442 mg), were combined and applied to an ODS column (30φ × 70 mm, YMC). An H₂O-MeCN system (0, 20, 40, 50, 60, 80, and 100% MeCN, each 100 ml) was used as eluent. The active component was eluted in 40–100% MeCN fractions. One of the fractions, 60% MeCN fraction (151 mg), was purified by preparative HPLC (column, Pegasil ODS SP100, 20φ × 250 mm, Senshu Scientific; solvent, 100% MeOH; flow rate, 9.0 mL/min; detection, UV at 210 nm). The main peak was collected and concentrated *in vacuo* to dryness to afford exophillic acid (103.4 mg).

Exophillic acid. White amorphous. ¹H NMR (400 MHz, pyridine-*d*₅) δ 7.36 (1H, d, 2.0 Hz), 7.30 (1H, d, 2.0 Hz), 7.10 (1H, d, 2.0 Hz), 6.90 (1H, d, 2.0 Hz), 5.62 (1H, d, 7.5), 4.39 (1H, dd, 12.0, 2.5 Hz), 4.37 (1H, t, 7.5 Hz), 4.33 (1H, dd, 12.0, 5.0 Hz), 4.32

(1H, m), 4.30 (1H, m), 3.94 (1H, ddd, 7.5, 5.0, 2.5 Hz), 3.39 (1H, dt, 13.0, 7.5 Hz), 3.34 (1H, dt, 13.0, 7.5 Hz), 2.97 (2H, t, 7.5 Hz), 1.85 (2H, m), 1.76 (2H, m), 1.42 (2H, m), 1.39 (2H, m), 1.31 (4H, m), 1.23 (16H, br.s, overlapped), 0.87 (3H, t, 7.0 Hz), 0.85 (3H, t, 7.0 Hz). ESI-MS calcd. for $C_{38}H_{55}O_{12}$ [M-H]⁻: 703.3694, found 703.3683 [M-H]⁻.

Measurement of Anti-Amebic Activity

Trophozoites of *E. histolytica* clonal strain HM-1:IMSS cl6 were cultured axenically in Diamond's BI-S-33 medium at 35.5°C (Clark and Diamond, 2002). Trophozoites were harvested in 3–4 days after inoculation of 1/30 to 1/12 of the total culture volume. After the cultures were chilled on ice for 5 min, trophozoites were collected by centrifugation at 500 × g for 10 min at 4°C and washed twice with BI-S-33 medium. The obtained trophozoites were suspended in BI-S-33 medium and approximately 1 × 10⁴ trophozoites in 200 µl of BI-S-33 medium were poured into each well of a 96-well plate and incubated for 2 h. Subsequently, the medium was removed and 200 µl of BI-S-33 medium or cysteine-deprived BI-S-33 medium containing 1% (v/v) penicillin/streptomycin (Life Technologies) together with test compounds (final concentrations; 0.1, 1, 10, 100 µg/ml for kerriamycin B, kerriamycin C, aggreticin, and xanthofulvin; 0.1, 1, 10, 50, 100 µg/ml for the other compounds) was added to each well and incubated under anaerobic conditions for 48 h. After incubation, the medium was removed and 90 µl of pre-warmed Opti-MEM I (Life Technologies) and 10 µl of WST-1 solution (Dojindo) were added to each well. Viability of trophozoites was detected with absorbance at 450 nm (SH-9000Lab, Corona Electric). Cytotoxicity was measured in triplicate. IC₅₀ values were calculated as shown in Section "Evaluation of Cytotoxicity against MRC-5 Cells" with the concentration range showed above. Metronidazole (Sigma-Aldrich, MO, USA) was used as positive control.

Results and Discussion

Screening of the Kitasato Natural Products Library for CS Inhibitors

Entamoeba histolytica has two classes of CS isotypes: EhCS1/EhCS2 and EhCS3. While EhCS1 and EhCS2 are identical except for two amino acid changes (Nozaki et al., 1998), whereas EhCS3 is most divergent from EhCS1 and EhCS2, with 83% amino acid identity (Ali and Nozaki, 2007). Therefore, we selected EhCS1 and EhCS3 as representative CSs in this study.

The Kitasato Natural Products Library consists of >300 natural or semisynthetic compounds. We initially evaluated the EhCS1/EhCS3 inhibitory activity of all compounds at 100 µg/ml. Nine compounds, kerriamycins B and C, aggreticin, tetracycline, patulin, nanaomycin A, deacetylkinamycin C, deoxyfrenolicin, and naphthacemycin A₉, exhibited inhibition of EhCS1 and/or EhCS3, and their IC₅₀ values were subsequently determined (Table 1). The structures of these inhibitors are shown in Figure 2. Only naphthacemycin A₉ inhibited EhCS1 selectively, whereas the other compounds showed inhibitory activity against both EhCS1 and EhCS3. Three compounds, kerriamycins B

TABLE 1 | Inhibitory activities of EhCS inhibitors from the Kitasato Natural Products Library.

Compound	IC ₅₀ (µM)	
	CS1	CS3
Kerriamycin B	0.63 ± 0.07	0.31 ± 0.01
Kerriamycin C	1.2 ± 0.04	0.56 ± 0.04
Aggreticin	0.98 ± 0.05	0.64 ± 0.10
Deacetylkinamycin C	21 ± 2.4	22 ± 3.7
Deoxyfrenolicin	57 ± 2.0	53 ± 1.1
Nanaomycin A	53 ± 3.9	65 ± 4.4
Naphthacemycin A ₉	75 ± 1.8	>490
Tetracycline	170 ± 16	190 ± 9.5
Patulin	490 ± 81	470 ± 37

and C, and aggreticin, showed the most potent inhibition (IC₅₀ = 0.31–1.2 µM). The IC₅₀ values against human fibroblast cells MRC-5 of the nine compounds were also evaluated, as shown in Table 2.

The naphthoquinone substructure is found in most of the inhibitors shown in Figure 2. The most potent EhCS1 and EhCS3 inhibitors, kerriamycins B and C (Hayakawa et al., 1985a,b) and aggreticin (Ōmura et al., 1988) have the same chromophore containing the naphthoquinone substructure. The structural difference among the three compounds is the number of sugar moieties (Figure 2). Despite these structural differences, they inhibited EhCSs at similar concentrations, suggesting that the chromophore structure is essential for inhibitory activity but the sugar moieties may not be important. These compounds are known to have biological activities such as anti-Gram-positive bacteria (Hayakawa et al., 1987), anti-cancer properties (Hayakawa et al., 1987), stimulation of platelet aggregation (Ōmura et al., 1988), and inhibition of protein SUMOylation (Fukuda et al., 2009).

Deacetylkinamycin C (kinamycin F) is the perdeacetylated compound of kinamycin C, and has the naphthoquinone substructure in its chromophore (Figure 2; Ōmura et al., 1973; Gould et al., 1994; Mithani et al., 1994). Its inhibition potency against EhCS ranked next to the kerriamycins, with the IC₅₀ values of 21 µM (EhCS1) and 22 µM (EhCS3), respectively. Kinamycin C displays anti-Gram-positive bacterial activity and anti-tumor activity (Ōmura et al., 1973; Hasinoff et al., 2006). Kinamycins can bind to DNA weakly and produce DNA- and protein-damaging effects (Hasinoff et al., 2006; O'Hara et al., 2007).

Nanaomycin A, a naphthoquinone antibiotic, has anti-malarial activity (Tanaka et al., 1999) along with anti-fungal, anti-bacterial, and anti-mycoplasma activities (Tanaka et al., 1975). Both nanaomycin A and its structural-related compound, deoxyfrenolicin (Ellestad et al., 1966; Iwai et al., 1978), showed modest inhibitory activity against EhCS1 and EhCS3 (IC₅₀ = 53–65 µM). The structural difference between the two compounds is the length of alkyl chain attached to a chromophore. Therefore, the chromophore containing the naphthoquinone substructure must be important for the

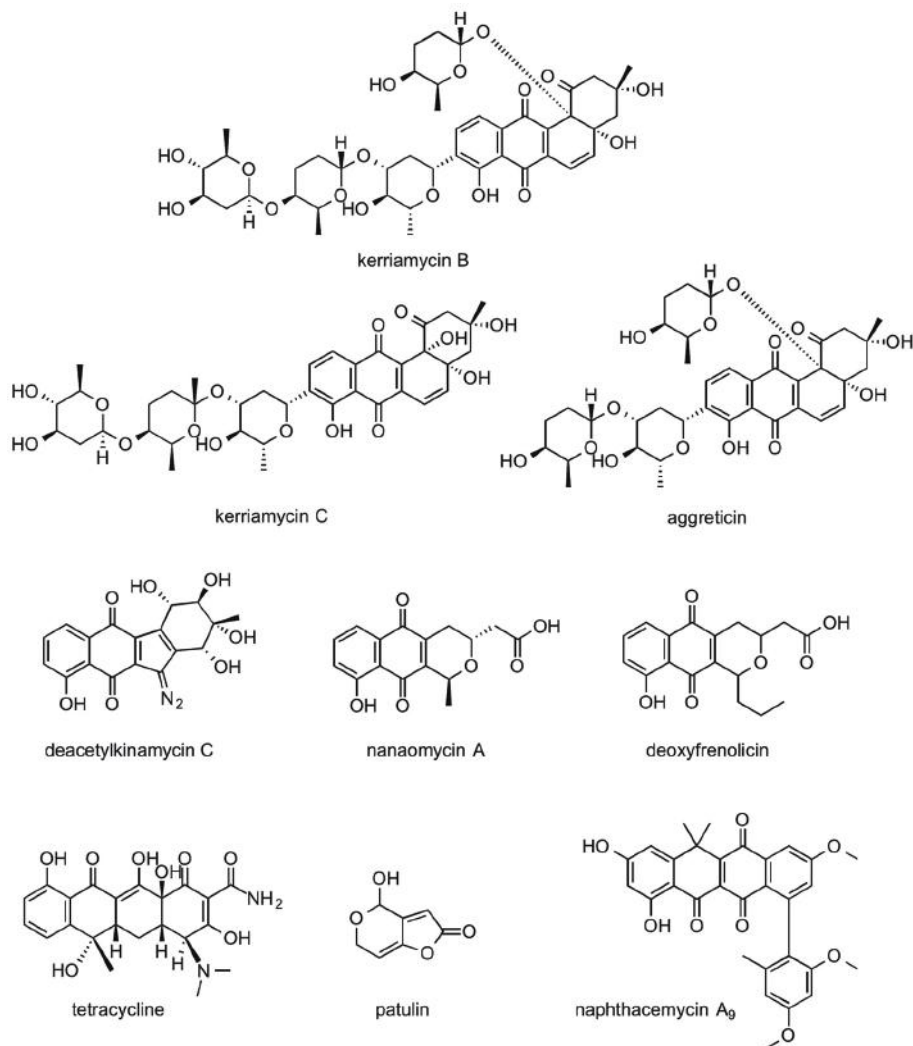


FIGURE 2 | Structures of EhCS inhibitors from the Kitasato Natural Products Library.

inhibition of EhCSs. Unfortunately, cytotoxicities against MRC-5 cells of nanaomycin A and deoxyfrenolicin were also more potent than CS inhibitory activities, as in the case of deacetylkinamycin C.

Tetracycline also has a naphthoquinone-like substructure in its chromophore. However, inhibition of EhCS1 and EhCS3 by tetracycline was weak, with IC₅₀ values of 170 and 190 μM , respectively. One of the mycotoxins, patulin, is the smallest inhibitor found in this screening. Inhibition of both EhCS1 and EhCS3 by patulin was also weak.

Naphthacemycin A₉, isolated from a broth of *Streptomyces* sp. KB3346-5 was found to be a novel potentiator of imipenem activity against methicillin-resistant *Staphylococcus aureus* (Omura et al., 2009). Naphthacemycins have naphthacene structures with an aryl group attached via biaryl bond. This compound showed selective inhibitory activity against EhCS1; the IC₅₀ value was 75 μM . However, it displayed no inhibition of EhCS3.

Taken together from the results of screening of the Kitasato Natural Products Library, the naphthoquinone moiety appears to be a common important structure for the inhibition of EhCSs.

Screening of the Microbial Broths for CS Inhibitors

Extracts of 9,173 fungal and actinomycete broths were screened for inhibition of CS activity of recombinant EhCS1 and EhCS3. Screening results are shown in Table 3. Many microbial broth extracts selectively inhibited one isoenzyme, but not the other. We found that 104 extracts solely inhibited EhCS1, while 167 extracts solely inhibited EhCS3. Seventy extracts inhibited both EhCS1 and EhCS3. We found a comparable number of active extracts from broths of fungi and actinomycetes. This is in good contrast to the CS inhibitors found from the Kitasato Natural Products Library; most of them inhibited both EhCS1 and EhCS3.

TABLE 2 | *In vitro* anti-amebic activity and cytotoxicity against MRC-5 cells of EhCS inhibitors.

Compound	Cytotoxicity	
	Against <i>Entamoeba histolytica</i> IC ₅₀ (μM)	
	Cys (+)	Cys (-)
Kerriamycin B	26 ± 1.5	23 ± 0.3
Kerriamycin C	6.9 ± 0.4	3.0 ± 0.6
Aggregatin	54 ± 4.8	18 ± 0.7
Deacetylkinamycin C	140 ± 13	18 ± 10
Deoxyfrenolicin	1.3 ± 0.04	0.5 ± 0.1
Nanaomycin A	12 ± 0.4	0.8 ± 0.04
Naphthacemycin A ₉	>390	>390
Tetracycline	>230	>230
Patulin	>650	110 ± 12
Xanthofulvin	>170	>170
Exophillic acid	>140	>140
NT, Not tested. Cys (+), normal BI-S-33 medium (8 mM L-cysteine); Cys (-), cysteine deprived BI-S-33 medium.		

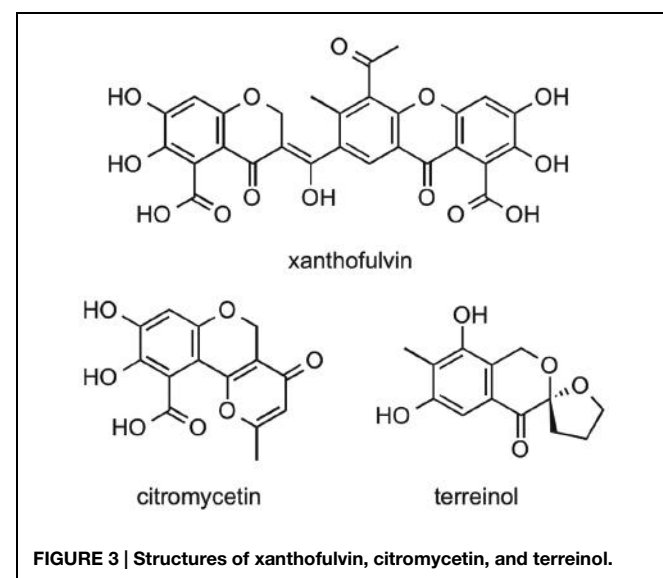
TABLE 3 | EhCS inhibitors found in microbial broth extracts.

Origin	Number of samples	CS1	CS3	CS1 and CS3
Fungi	4,800	64	87	47
Actinomycetes	4,373	40	80	23
Total	9,173	104	167	70
		(1.1%)	(1.8%)	(0.8%)

We tested the above-mentioned active broth extracts showing CS inhibitory activity for cytotoxicity using human fibroblast cells (MRC-5), and selected two fungal broth extracts with no or low cytotoxicity. One extract was obtained from *Penicillium* sp. if08054, which showed inhibitory activity against both isotypes. The other extract was from *Exophiala* sp. FKI-7082, which showed inhibitory activity specifically against EhCS1. We isolated xanthofulvin and exophillic acid as the active components from the broths of these two fungal strains, respectively.

Xanthofulvin, an EhCS1 and EhCS3 Inhibitor from a Broth of *Penicillium* sp. if08054

Xanthofulvin was isolated from the *n*-BuOH extract of a broth of *Penicillium* sp. if08054 using an ODS column. CS inhibitory activity was found in the 40% acetonitrile (MeCN) fraction. Subsequently, about 2 mg of xanthofulvin (Figure 3; Kumagai et al., 2003) was purified by preparative HPLC from 50 ml of the cultured broth. Two structurally related compounds, citromycetin (Robertson et al., 1951; Capon et al., 2007) and terreinol (Macedo et al., 2004) were also isolated from the 20% MeCN fraction and 40% MeCN fraction, respectively. The structures of the compounds were confirmed by 1D and 2D NMR spectra and MS spectra. Xanthofulvin was originally isolated as a semaphorin inhibitor with the IC₅₀ value of 0.09 μg/mL (Kumagai et al., 2003). We compared

**FIGURE 3 |** Structures of xanthofulvin, citromycetin, and terreinol.

CS inhibitory activity of xanthofulvin, citromycetin, and terreinol. The IC₅₀ values of these compounds against two EhCS isotypes are shown in Table 4. Among these three compounds, only xanthofulvin inhibited EhCSs, whereas citromycetin and terreinol showed no inhibitory activities against EhCSs at 1,400 or 1,600 μM. Xanthofulvin inhibited EhCS1 more potently than EhCS3: the IC₅₀ values against EhCS1 and EhCS3 are 7.9 and 110 μM, respectively. Xanthofulvin has a naphthoquinone-like substructure similar to EhCS inhibitors identified from the Kitasato Natural Products Library. Although citromycetin and terreinol also have xanthofulvin-related structures, no/weak inhibitory activities against EhCSs were detected. Therefore, the three-dimensional conformation provided by the dimeric-like structure of xanthofulvin seems to be important for producing inhibition of EhCSs.

Exophillic Acid, a CS1 Inhibitor from a Broth of *Exophiala* sp. FKI-7082

Exophillic acid was isolated from the ethyl acetate extract of the broth of *Exophiala* sp. FKI-7082 by silica gel and ODS column chromatography (Figure 4; Ondeyka et al., 2003). The structure was clarified by measurement of MS and NMR spectra. Exophillic acid was originally isolated from a broth of *Exophiala pisciphila*, and its main biological activity includes inhibition of the strand transfer reaction

TABLE 4 | Inhibitory activities of xanthofulvin, citromycetin, and terreinol against EhCS1 and EhCS3.

Compound	IC ₅₀ (μM)	
	CS1	CS3
Xanthofulvin	7.9 ± 1.3	110 ± 8.2
Terreinol	>1,600	>1,600
Citromycetin	>1,400	>1,400

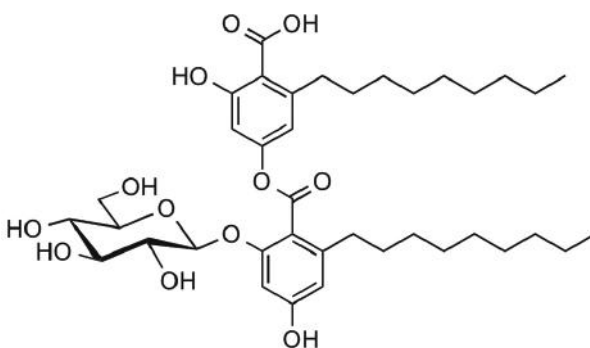


FIGURE 4 | Structure of exophillic acid.

of HIV-1 integrase (Ondeyka et al., 2003). Exophillic acid inhibited EhCS1 with the IC_{50} value of $24 \pm 2.9 \mu\text{M}$, whereas it showed no inhibition against EhCS3 even at a concentration of 2.5 mM . Exophillic acid is a dimeric alkylbenzoate glucoside and does not contain naphthoquinone. Exophillic acid likely recognizes the structural differences between the two enzymes. Further structure elucidation is needed to understand EhCS1-specific inhibition by exophillic acid.

Anti-*Entamoeba histolytica* Activity of CS Inhibitors

We next examined whether the CS inhibitors show an amebicidal activity against *E. histolytica* trophozoites *in vitro*. To verify whether an amebicidal activity is due to inhibition of CS, we estimated the IC_{50} values of inhibitors against *E. histolytica* trophozoites in the cysteine-supplemented and cysteine-deprived BI-S-33 medium. In theory, the amebicidal activity and the growth inhibitory effects should be more pronounced in the absence of cysteine than in the presence of cysteine if these effects are due to the inhibition of CS. The amebicidal activities of CS inhibitors are shown in **Table 4**, together with the cytotoxicity of the compounds against MRC-5 cells.

Deacetylkinamycin C, nanaomycin A, and patulin showed cysteine-dependent amebicidal activity. The IC_{50} of deacetylkinamycin C against EhCSs (21 and $22 \mu\text{M}$) and the IC_{50} value in the cysteine-deprived medium ($18 \mu\text{M}$) were comparable, which suggests the amebicidal effect of deacetylkinamycin C is likely due to CS inhibition. Nanaomycin A exhibited amebicidal activity 15-fold more potent in cysteine-deprived medium, however, the IC_{50} values against EhCSs were less potent than the amebicidal activity. Though patulin also showed selective amebicidal activity, inhibition of EhCSs was less potent than its antiamebic activity. Xanthofulvin and exophillic acid did not show amebicidal activities at 170 and $140 \mu\text{M}$, respectively. It was reported that xanthofulvin was not likely incorporated into cells (Kaneko et al., 2006; Kikuchi et al., 2009). In an *E. histolytica* case, it may be difficult to incorporate this compound into cells. The reason

why exophillic acid did not exhibit amebicidal activity was unknown.

Deacetylkinamycin C, which has DNA- and protein-damaging effects (Colis et al., 2014), showed potent cytotoxicity against MRC-5 cells; the IC_{50} value against MRC-5 cells was lower than those of the IC_{50} values against *E. histolytica* cells and against EhCS. Nanaomycin A and deoxyfrenolicin also showed cytotoxicity against MRC-5 cells, at the lower concentrations showing CS inhibition, as in the case of deacetylkinamycin C. Although most compounds that inhibited EhCS in this study were toxic against a human-derived cell line, MRC-5, it is possible to design and produce by organic synthesis their derivatives that possess EhCS-dependent anti-amebic activity but lack cytotoxicity to humans. To design such derivatives, structural studies are needed to determine the moieties required for binding to EhCS.

In this study, we identified nine general EhCS inhibitors and two isotype-specific EhCS inhibitors, naphthacemycin A₉ and exophillic acid, from microbial secondary metabolite sources. A naphthoquinone structure seemed to contribute significantly to EhCS inhibition. One EhCS1-selective inhibitor, naphthacemycin A₉, has a naphthacene structure with an aryl group attached via biaryl bond. The other EhCS1-selective inhibitor, exophillic acid, has a depside structure which two aryl groups attach to via an ester bond. For EhCS1-selective inhibition, the substituted small aryl group is likely important. Further structural studies using EhCS inhibitors found in this study are needed for developing anti-amebic drugs. We also found EhCS3-selective inhibitors from both fungal and actinomycete broths. These EhCS3-selective inhibitors will be purified and identified in future studies. Since CS is also present in other protozoa, such as *Trichomonas vaginalis*, *Leishmania major*, and *Trypanosoma cruzi*, the newly identified CS inhibitors in this study can also be exploited to develop drugs against other neglected parasitic diseases.

Acknowledgments

We thank Dr. Kenichiro Nagai and Ms. Noriko Sato, School of Pharmacy, Kitasato University for the measurement of mass and NMR spectra. We also thank Mr. Satoshi Tsuge and Mr. Wataru Fukasawa for the measurement of EhCS inhibitory activity and amebicidal activity. This work was supported by JSPS Grant-in-Aid for Scientific Research (C) (26460129) and Kitasato University Research Grant for Young Researchers (to MM), a grant for research on emerging and re-emerging infectious diseases from the Ministry of Health, Labor and Welfare of Japan (H26-Shinkosaiko-ippan-009), a grant for research to promote the development of anti-AIDS pharmaceuticals from the Japan Health Sciences Foundation (KHA1101) (to TN), a grant for Science and Technology Research Partnership for Sustainable Development (SATREPS) from Japan Science and Technology Agency and Japan International Cooperation Agency (to MM, KT, DW, T, KS, and TN).

References

- Ali, V., and Nozaki, T. (2007). Current therapeutics, their problems, and sulfur-containing-amino-acid metabolism as a novel target against infections by "mitochondrion" protozoan parasites. *Clin. Microbiol. Rev.* 20, 164–187. doi: 10.1128/CMR.00019-06
- Amori, L., Katkevica, S., Bruno, A., Campanini, B., Felici, P., Mozzarelli, A., et al. (2012). Design and synthesis of *trans*-2-substituted-cyclopropane-1-carboxylic acids as the first non-natural small molecule inhibitors of O-acetylserine sulfhydrylase. *Med. Chem. Commun.* 3, 1111–1116. doi: 10.1039/c2md20100c
- Arita-Morioka, K., Yamanaka, K., Mizunoe, Y., Ogura, T., and Sugimoto, S. (2015). Novel strategy for biofilm inhibition by using small molecules targeting molecular chaperone DnaK. *Antimicrob. Agents Chemother.* 59, 633–641. doi: 10.1128/AAC.04465-14
- Capon, R. J., Stewart, M., Ratnayake, R., Lacey, E., and Gill, J. H. (2007). Citromycetins and bilains A-C: new aromatic polyketides and diketopiperazines from Australian marine-derived and terrestrial *Penicillium* spp. *J. Nat. Prod.* 70, 1746–1752. doi: 10.1021/np0702483
- Clark, C. G., and Diamond L. S. (2002). Methods for cultivation of luminal parasitic protists of clinical importance. *Clin. Microbiol. Rev.* 15, 329–341. doi: 10.1128/CMR.15.3.329-341.2002
- Colis, L. C., Woo, C. M., Hegan, D. C., Li, Z., Glazer, P. M., and Herzon, S. B. (2014). The cytotoxicity of (-)-lomaiviticin A arises from induction of double-strand breaks in DNA. *Nat. Chem.* 6, 504–510. doi: 10.1038/nchem.1944
- Ellestad, G. A., Whaley, H. A., and Patterson, E. L. (1966). The structure of frenolicin. *J. Am. Chem. Soc.* 88, 4109–4110. doi: 10.1021/ja00969a050
- Fahey, R. C., Newton, G. L., Arrick, B., Overdank-Bogart, T., Aley, S. B., and S. B. (1984). *Entamoeba histolytica*: a eukaryote without glutathione metabolism. *Science* 224, 70–72. doi: 10.1126/science.6322306
- Feldman-Salit, A., Wirtz, M., Hell, R., and Wade, R. C. (2009). A mechanistic model of the cysteine synthase complex. *J. Mol. Biol.* 386, 37–59. doi: 10.1016/j.jmb.2008.08.075
- Fukuda, I., Ito, A., Uramoto, M., Saitoh, H., Kawasaki, H., Osada, H., et al. (2009). Kerriamycin B inhibits protein SUMOylation. *J. Antibiot.* 62, 221–224. doi: 10.1038/ja.2009.10
- Gaitonde, M. K. (1967). A spectrophotometric method for the direct determination of cysteine in the presence of other naturally occurring amino acids. *Biochem. J.* 104, 627–633. doi: 10.1042/bj1040627
- Gillin, F. D., and Diamond, L. S. (1981). *Entamoeba histolytica* and *Giardia lamblia*: effects of cysteine and oxygen tension on trophozoite attachment to glass and survival in culture media. *Exp. Parasitol.* 52, 9–17. doi: 10.1016/0014-4894(81)90055-2
- Gould, S. J., Tamayo, N., Melville, C. R., and Cone M. C. (1994). Revised structures for the kinamycin antibiotics: 5-diazobenzo[b]fluorenes rather than benzo[b]carbazole cyanamides. *J. Am. Chem. Soc.* 116, 2207–2208. doi: 10.1021/ja00084a096
- Harque, R., Huston, C. D., Hughes, M., Houpt, E., Petri, W. A. Jr. (2003). Amebiasis. *N. Engl. J. Med.* 348, 1565–1573. doi: 10.1056/NEJMra022710
- Hasinoff, B. B., Wu, X., Yalowich, J. C., Goodfellow, V., Laufer, R. S., Adedayo, O., et al. (2006). Kinamycins A and C, bacterial metabolites that contain an unusual diazo group, as potential new anticancer agents: antiproliferative and cell cycle effects. *Anticancer Drugs* 17, 825–837. doi: 10.1097/01.cad.0000224442.78211.27
- Hayakawa, Y., Adachi, K., Iwakiri, T., Imamura, K., Furihata, K., Seto, H., et al. (1987). Kerriamycins A, B and C, new isotetracenone antibiotics. *Agric. Biol. Chem.* 51, 1397–1405. doi: 10.1271/bbb1961.51.1397
- Hayakawa, Y., Furihata, K., Seto, H., and Ōtake, N. (1985a). The structures of new isotetracenone antibiotics, kerriamycins A, B and C. *Tetrahedron Lett.* 26, 3475–3478. doi: 10.1016/S0040-4039(00)98668-4
- Hayakawa, Y., Iwakiri, T., Imamura, K., Seto, H., and Ōtake, N. (1985b). Studies on the isotetracenone antibiotics II. Kerriamycins A, B and C, new antitumor antibiotics. *J. Antibiot.* 38, 960–963. doi: 10.7164/antibiotics.38.960
- Hung, C.-C., Chang, S.-Y., and Ji, D.-D. (2012). *Entamoeba histolytica* infection in men who have sex with men. *Lancet* 12, 729–736. doi: 10.1016/S1473-3099(12)70147-0
- Hussain, S., Ali, V., Jeelani, G., and Nozaki, T. (2009). Isoform-dependent feedback regulation of serine O-acetyltransferase isoenzymes involved in L-cysteine biosynthesis of *Entamoeba histolytica*. *Mol. Biochem. Parasitol.* 163, 39–47. doi: 10.1016/j.molbiopara.2008.09.006
- Hussain, A., Jeelani, G., Sato, D., and Nozaki, T. (2011). Global analysis of gene expression in response to L-cysteine deprivation in the anaerobic protozoan parasite *Entamoeba histolytica*. *BMC Genomics* 12, 275. doi: 10.1186/1471-2164-12-275
- Iwai, Y., Kora, A., Takahashi, Y., Hayashi, T., Awaya, J., Masuma, R., et al. (1978). Production of deoxyfrenolicin and a new antibiotic, frenolicin B by *Streptomyces roseofulvus* strain AM-3867. *J. Antibiot.* 31, 959–965. doi: 10.7164/antibiotics.31.959
- Jeelani, G., Husain, A., Sato, D., Ali, V., Suematsu, M., Soga, T., et al. (2010). Two atypical L-cysteine-regulated NADPH-dependent oxidoreductases involved in redox maintenance, L-cystine and iron reduction, and metronidazole activation in the enteric protozoan *Entamoeba histolytica*. *J. Biol. Chem.* 285, 26889–26899. doi: 10.1074/jbc.M110.106310
- Jeelani, G., Sato, D., Soga, T., Watanabe, H., and Nozaki, T. (2014). Mass spectrometric analysis of L-cysteine metabolism: physiological role and fate of L-cysteine in the enteric protozoan parasite *Entamoeba histolytica*. *MBio* 5:e01995-14. doi: 10.1128/mBio.01995-14
- Kaneko, S., Iwanami, A., Nakamura, M., Kishino, A., Kikuchi, K., Shibata, S., et al. (2006). A selective Sema 3A inhibitor enhances regenerative responses and functional recovery of the injured spinal cord. *Nat. Med.* 12, 1380–1389. doi: 10.1038/nm1505
- Kikuchi, K., Kumagai, K., and Kimura, T. (2009). Semaphorin 3A inhibitor. *Jikken Igaku* 27, 686–691.
- Kredich, N. M., Becker, M. A., and Tomkins, G. M. (1969). Purification and characterization of cysteine synthase, a bifunctional protein complex, from *Salmonella typhimurium*. *J. Biol. Chem.* 244, 2428–2439.
- Kumagai, K., Hosotani, N., Kikuchi, K., Kimura, T., and Saji, I. (2003). Xanthofulvin, a novel semaphorin inhibitor produced by a strain of *Penicillium*. *J. Antibiot.* 56, 610–616. doi: 10.7164/antibiotics.56.610
- Kumar, S., Raj, I., Nagpal, I., Subbarao, N., and Gourinath, S. (2011). Structural and biochemical studies of serine acetyltransferase reveal why the parasite *Entamoeba histolytica* cannot form a cysteine synthase complex. *J. Biol. Chem.* 286, 12533–12541. doi: 10.1074/jbc.M110.197376
- Macedo, F. C., Porto, A. L. M., and Marsaioli, A. J. (2004). Terreinol – a novel metabolite from *Aspergillus terreus*: structure and 13C labeling. *Tetrahedron Lett.* 45, 53–55. doi: 10.1016/j.tetlet.2003.10.128
- Mithani, S., Weeratunga, G., Taylor, N. J., and Dmitrienko, G. I. (1994). The kinamycins are diazofluorenes and not cyanocarbazoles. *J. Am. Chem. Soc.* 116, 2209–2210. doi: 10.1021/ja00084a097
- Nagpal, I., Raj, I., Subbarao, N., and Gourinath, S. (2012). Virtual screening, identification and in vitro testing of novel inhibitors of O-acetyl-L-serine sulfhydrylase of *Entamoeba histolytica*. *PLoS ONE* 7:e30305. doi: 10.1371/journal.pone.0030305
- Newman, D. J., and Cragg, G. M. (2012). Natural products as sources of new drugs over the 30 years from 1981 to 2010. *J. Nat. Prod.* 75, 311–335. doi: 10.1021/np200906s
- Nozaki, T., Ali, V., and Tokoro, M. (2005). Sulfur-containing amino acid metabolism in parasitic protozoa. *Adv. Parasitol.* 60C, 1–99. doi: 10.1016/S0065-308X(05)60001-2
- Nozaki, T., Asai, T., Kobayashi, S., Ikegami, F., Noji, M., Saito, K., et al. (1998). Molecular cloning and characterization of the genes encoding two isoforms of cysteine synthase in the enteric protozoan parasite *Entamoeba histolytica*. *Mol. Biochem. Parasitol.* 97, 33–44. doi: 10.1016/S0166-6851(98)00127-7
- Nozaki, T., Asai, T., Sanchez, L. B., Kobayashi, S., Nakazawa, M., and Takeuchi, T. (1999). Characterization of the gene encoding serine acetyltransferase, a regulated enzyme of cysteine biosynthesis from the protist parasites *Entamoeba histolytica* and *Entamoeba dispar*. Regulation and possible function of the cysteine biosynthetic pathway in *Entamoeba*. *J. Biol. Chem.* 274, 32445–32452. doi: 10.1074/jbc.274.45.32445
- O'Hara, K. A., Wu, X., Patel, D., Liang, H., Yalowich, J. C., Chen, N., et al. (2007). Mechanism of the cytotoxicity of the diazoparaquinone antitumor antibiotic kinamycin F. *Free Rad. Biol. Med.* 43, 1132–1144. doi: 10.1016/j.freeradbiomed.2007.07.005
- Ohnishi, K., Sakamoto, N., Kobayashi, K., Iwabuchi, S., Nakamura-Uchiyama, F., Ajisawa, A., et al. (2014). Subjective adverse reactions to

- metronidazole in patients with amebiasis. *Parasitol. Int.* 63, 698–700. doi: 10.1016/j.parint.2014.05.006
- Ōmura, S., Nakagawa, A., Fukamachi, N., Miura, S., Takahashi, Y., Komiya, K., et al. (1988). OM-4842, a new platelet aggregation inhibitor from *Streptomyces*. *J. Antibiot.* 41, 812–813. doi: 10.7164/antibiotics.41.812
- Ōmura, S., Nakagawa, A., Yamada, H., Hata, T., Furusaki, A., and Watanabe, T. (1973). Structures and biological properties of kinamycin A, B, C, and D. *Chem. Pharm. Bull.* 21, 931–940. doi: 10.1248/cpb.21.931
- Ōmura, S., Takahashi, Y., Kim, J.-P., Hanaki, H., Tomoda, H., Suzuki, M., et al. (2009). KB-3345-5 substances, their fermentative manufacture, and antibacterial agents containing them. *Jpn. Kokai Tokkyo Koho JP2009046404.*
- Ondeyka, J. G., Deborah, L. Z., Dombrowski, A. W., Polishook, J. D., Felock, P. J., Hazuda, D. J., et al. (2003). Isolation, structure and HIV-1 integrase inhibitory activity of exophilic acid, a novel fungal metabolite from *Exophiala pisciphila*. *J. Antibiot.* 56, 1018–1023. doi: 10.7164/antibiotics.56.1018
- Robertson, A., Whalley, W. B., and Yates, J. (1951). Chemistry of fungi. XV. Degradation of methyl O-dimethylcitromycetin. *J. Chem. Soc.* 2013–2018. doi: 10.1039/jr9510002013
- Salsi, E., Bayden, A. S., Spyros, F., Amadas, A., Campanini, B., Bettati, S., et al. (2010). Design of O-acetylserine sulfhydrylase inhibitors by mimicking nature. *J. Med. Chem.* 53, 345–356. doi: 10.1021/jm901325e
- Samarawickrema, N. A., Brown, D. M., Upcroft, J. A., Thammalerd, N., and Upcroft, P. (1997). Involvement of superoxide dismutase and pyruvate: ferredoxin oxidoreductase in mechanisms of metronidazole resistance in *Entamoeba histolytica*. *J. Antimicrob. Chemother.* 40, 833–840. doi: 10.1093/jac/40.6.833
- Singh, S., Bharti, N., and Mohapatra, P. P. (2009). Chemistry and biology of synthetic and naturally occurring antiamoebic agents. *Chem. Rev.* 109, 1900–1947. doi: 10.1021/cr068217k
- Singh, S., Sablok, G., Farmer, R., Singh, A. K., Gautam, B., and Kumar, S. (2013). Molecular dynamic simulation and inhibitor prediction of cysteine synthase structured model as a potential drug target for Trichomoniasis. *BioMed Res. Int.* 390920, 15. doi: 10.1155/2013/390920
- Spyros, F., Singh, R., Cozzani, P., Campanini, B., Salsi, E., Felici, P., et al. (2013). Isozyme-specific ligands for O-acetylserine sulfhydrylase, a novel antibiotic target. *PLoS ONE* 8:e77558. doi: 10.1371/journal.pone.0077558
- Stanley, S. L. Jr. (2003). Amoebiasis. *Lancet* 361, 1025–1034. doi: 10.1016/S0140-6736(03)12830-9
- Tanaka, Y., Kamei, K., Otoguro, K., and Ōmura, S. (1999). Heme-dependent radical generation: possible involvement in antimarial action of non-peroxide microbial metabolites, nanaomycin A and radicicol. *J. Antibiot.* 52, 880–888. doi: 10.7164/antibiotics.52.880
- Tanaka, H., Koyama, Y., Nagai, T., Marumo, H., and Ōmura, S. (1975). Nanaomycins, new antibiotics produced by a strain of *Streptomyces*. *J. Antibiot.* 28, 868–875. doi: 10.7164/antibiotics.28.868
- Wassmann, C., Hellberg, A., Tannich, E., and Bruchhaus, I. (1999). Metronidazole resistance in the protozoan parasite *Entamoeba histolytica* is associated with increased expression of iron-containing superoxide dismutase and peroxiredoxin and decreased expression of ferredoxin 1 and flavin reductase. *J. Biol. Chem.* 274, 26051–26056. doi: 10.1074/jbc.274.37.26051
- Watanabe, K., Gatanaga, H., Escueta-de Cadiz, A., Tanuma, J., Nozaki, T., and Oka, S. (2011). Amebiasis in HIV-1-infected Japanese men: clinical features and response to therapy. *PLoS Negl. Trop. Dis.* 5:e1318. doi: 10.1371/journal.pntd.0001318
- Ximénez, C., Morán, P., Rojas, L., Valadaz, A., and Gomez, A. (2009). Reassessment of the epidemiology of amebiasis: state of the art. *Infect. Gen. Evol.* 9, 1023–1032. doi: 10.1016/j.meegid.2009.06.008

Conflict of Interest Statement: The authors declare that the research was conducted in the absence of any commercial or financial relationships that could be construed as a potential conflict of interest.

Copyright © 2015 Mori, Jeelani, Masuda, Sakai, Tsukui, Waluyo, Tarwadi, Watanabe, Nonaka, Matsumoto, Ōmura, Nozaki and Shiomi. This is an open-access article distributed under the terms of the Creative Commons Attribution License (CC BY). The use, distribution or reproduction in other forums is permitted, provided the original author(s) or licensor are credited and that the original publication in this journal is cited, in accordance with accepted academic practice. No use, distribution or reproduction is permitted which does not comply with these terms.



Heat Shock Protein 90 regulates encystation in *Entamoeba*

Meetali Singh¹, Shalini Sharma², Alok Bhattacharya² and Utpal Tat^{1*}

¹ Department of Biochemistry, Indian Institute of Science, Bangalore, India, ² School of Life Sciences, Jawaharlal Nehru University, New Delhi, India

OPEN ACCESS

Edited by:

Anjan Debnath,
University of California, San Diego,
USA

Reviewed by:

Sergio Oscar Angel,
Instituto de Investigaciones
Biotecnológicas (IIB-INTECH),
Argentina

Sudip K. Ghosh,
Indian Institute of Technology
Kharagpur, India

*Correspondence:

Utpal Tat¹
tatu@biochem.iisc.ernet.in

Specialty section:

This article was submitted to
Antimicrobials, Resistance
and Chemotherapy,
a section of the journal
Frontiers in Microbiology

Received: 03 June 2015

Accepted: 28 September 2015

Published: 13 October 2015

Citation:

Singh M, Sharma S, Bhattacharya A
and Tat¹ U (2015) Heat Shock Protein
90 regulates encystation
in *Entamoeba*.
Front. Microbiol. 6:1125.
doi: 10.3389/fmicb.2015.01125

Enteric protozoan *Entamoeba histolytica* is a major cause of debilitating diarrheal infection worldwide with high morbidity and mortality. Even though the clinical burden of this parasite is very high, this infection is categorized as a neglected disease. Parasite is transmitted through feco-oral route and exhibit two distinct stages namely – trophozoites and cysts. Mechanism and regulation of encystation is not clearly understood. Previous studies have established the role of Heat shock protein 90 (Hsp90) in regulating stage transition in various protozoan parasites like *Giardia*, *Plasmodium*, *Leishmania*, and *Toxoplasma*. Our study for the first time reports that Hsp90 plays a crucial role in life cycle of *Entamoeba* as well. We identify Hsp90 to be a negative regulator of encystation in *Entamoeba*. We also show that Hsp90 inhibition interferes with the process of phagocytosis in *Entamoeba*. Overall, we show that Hsp90 plays an important role in virulence and transmission of *Entamoeba*.

Keywords: *Entamoeba*, Hsp90, phagocytosis, encystation, 17-AAG, Cyst

INTRODUCTION

Entamoeba histolytica is a primitive protozoan and causative organism of amoebiasis. It is estimated that around 50 million people are infected with *E. histolytica* in tropical and developing nations. *Entamoeba* infection could either be asymptomatic or present itself as invasive intestinal amoebiasis with symptoms including colitis, dysentery, and toxic megacolon. If not checked in time, the disease could manifest as invasive extra-intestinal amoebiasis including amoebic liver abscess. Fatality rate for amoebiasis is higher compared to giardiasis caused by a related enteric parasite *Giardia*. The frontline drug for treatment of amoebiasis is metronidazole. However, there are many dose-related side effects associated with the drug and there is emergence of drug resistance as well (Freeman et al., 1997).

Entamoeba has a biphasic life cycle. The two stages of its life cycle are trophozoite and cyst. Human is the only known host of *E. histolytica*. Infection of the host happens upon ingestion of food contaminated by *Entamoeba* cysts. Cysts are environmentally resistant infective stage of *Entamoeba*. Ingested cysts undergo excystation to form trophozoites in small intestine. Trophozoites are the pathological stage of the life cycle and colonize large intestine, where they rapidly proliferate (Aguilar-Diaz et al., 2011). Virulence of trophozoites is characterized by their ability of phagocytosis. Phagocytosis is a well-studied process in mammalian host defense system. But our understanding of phagocytosis process in *Entamoeba* is still in its nascence. Many studies have identified signaling pathways regulating phagocytosis and proteome of phagosomes has been recently elucidated (Huston et al., 2003; Marion et al., 2005; Okada et al., 2005; Okada and Nozaki, 2006; Tovy et al., 2011; Mansuri et al., 2014).

For development of new therapeutics against *Entamoeba*, it is essential to understand the regulation of its virulence and life cycle. There have been few efforts by different groups to understand the regulation and mechanism of stage transition in *Entamoeba* (Ehrenkaufer et al., 2007, 2013; De Cádiz et al., 2013; Mi-Ichi et al., 2015). However, questions like: what are the cues for stage transition, how stage transition is regulated and what is the mechanism of stage transition; are largely unanswered.

Heat shock protein 90 (Hsp90), a key molecular chaperone, has been implicated to play a crucial role in growth and life cycle of protozoa like *Giardia*, *Plasmodium*, *Leishmania*, *Toxoplasma*, and *Trypanosoma* (Wiesgl and Clos, 2001; Graefe et al., 2002; Banumathy et al., 2003; Echeverria et al., 2005; Nageshan et al., 2014; Rochani et al., 2014). In *Giardia*, Hsp90 has been shown to regulate encystation and inhibition of Hsp90 promotes encystation (Nageshan et al., 2014). In *Plasmodium falciparum* Hsp90 regulates ring to trophozoites transition (Banumathy et al., 2003). Hsp90 is an abundant protein and regulates various biological pathways. Its clients include transcription factors, kinases and other non-signaling proteins like telomerase etc. (Taipale et al., 2010). Hsp90 is a dimeric protein with three domains. The N-terminal domain is the ATP binding domain and links to the middle domain via a flexible linker. Middle domain interacts with various clients and co-chaperones and also harbors the critical catalytic Arg. C-terminal is responsible for dimer formation (Pearl and Prodromou, 2006; Taipale et al., 2010). Hsp90 function is regulated by many co-chaperones, which are well conserved in higher eukaryotes (Johnson and Brown, 2009).

Many of the signaling proteins identified in phagosome proteome like Rab11, PAK6, TOR, and Rac1 are known interactors of Hsp90 in mammalian cells (Ohji et al., 2006; Keestra et al., 2013; Bozza et al., 2014). Hsp90 has also been shown to regulate phagocytosis in murine macrophage cell lines (Yan et al., 2004).

In our previous study, we had shown that *Entamoeba* Hsp90 is an active ATPase and its activity was inhibited by pharmacological inhibitor of Hsp90 – 17-allylamino-17-demethoxygeldanamycin (17-AAG; Singh et al., 2014). Others and we have also shown that Hsp90 is crucial for survival and growth of *E. histolytica* (Debnath et al., 2014; Singh et al., 2014). Inhibition of Hsp90 by 17-AAG results in death of *Entamoeba* trophozoites. *Entamoeba* also has a minimal co-chaperone repertoire and lacks many conserved co-chaperones (Singh et al., 2014).

In the current study, we have examined specific roles of Hsp90 in *Entamoeba* life cycle. We found Hsp90 to regulate the process of phagocytosis and encystation. We show that pharmacological inhibition of Hsp90 in trophozoites of *E. histolytica* interferes with the process of phagocytosis. Further, we have used *E. invadens* as a model for encystation to examine the role of Hsp90 in stage transition. We have analyzed the transcriptome data available at amoebadb.org and observed that Hsp90 expression levels along with few of its co-chaperones decrease in cysts followed by an increase during excystation. We now provide an experimental evidence for the role of Hsp90 in encystation process using pharmacological approach. We observe an increase

in encystation upon Hsp90 inhibition. Together our results provide evidence for the role of Hsp90 in essential processes such as phagocytosis in actively proliferating trophozoites. Inhibition of Hsp90 function with sub lethal doses of Hsp90 inhibitors disrupts growth of trophozoites and promotes encystation.

MATERIALS AND METHODS

Culture

Entamoeba histolytica strain HM-1: IMSS was maintained in TYI-S-33 medium at 33.5°C containing 15% heat inactivated adult bovine serum (Himedia), and 2.5% Diamond vitamin mix (Sigma; Diamond et al., 1978). *E. invadens* was maintained in TYI-S-33 medium at 25°C.

Phagocytosis Assay

To quantify phagocytosis rate of *E. histolytica*, 5×10^4 *Entamoeba* cells were incubated with 10^7 washed RBCs in TYI-S-33 medium at 37°C for 1 h in 1 mL culture medium. Cells were centrifuged and non-phagocytized RBCs were lysed with cold distilled water and *Entamoeba* cells were harvested by centrifugation at 1000g for 2 min. Cells were washed with PBS. Cells containing engulfed RBCs were lysed in 1 mL formic acid and absorbance was recorded at 397 nm (Somlata et al., 2012). Cells were also observed under microscope to ascertain phagocytosis. To test the effect of Hsp90 inhibition on phagocytosis, cells were pre treated with 600 nM 17-AAG for 24 h. 0.2% DMSO was used to treat control cells.

Immunofluorescence Assay

Entamoeba histolytica cells were resuspended in incomplete TYI-S-33 medium and transferred onto acetone-cleaned coverslips placed in a petridish and allowed to adhere for 5 min at 37°C. Cells were fixed with 3.7% paraformaldehyde (PFA) in PBS at 37°C for 30 min after taking out the culture medium. Fixed cells were permeabilized with 0.1% Triton-X-100 in PBS for 3 min and washed with PBS followed by quenching with 50 mM NH₄Cl in PBS for 30 min. The coverslips were then blocked with 1% BSA in PBS for 1 h and then incubated with primary antibody for 1 h at 37°C. After that, cells were washed with 1% BSA in PBS and labeled with secondary antibody at 37°C for 30 min. Antibody dilutions used are as follows: α-EhHsp90 was used at 1:100, TRITC-phalloidin (Sigma; 1 mg/ml) at 1:200 and anti-rabbit Alexa-488 (Molecular probes) at 1:200. The stained cells were washed with PBS followed by mounting on a glass slide using DABCO {1,4-diazbicyclo (2,2,2) octane} (sigma) as antifade. The edges of coverslips were sealed to avoid drying. Confocal images were taken using an Olympus Fluoview FV1000 laser-scanning microscope.

Cell Viability Assay

Cell viability assay was carried out as described previously (Singh et al., 2014). Briefly, 15,000 *E. invadens* trophozoites grown to log phase were seeded per well in TYI-S-33 medium or LG medium in a 96-well plate. Cells were treated for 24 h with 17-AAG (concentration varying from 10 nM to 100 μM). DMSO (0.2%)

was used as control. Cell viability was assessed by trypan blue dye exclusion. 50% Growth inhibitory concentration (GI_{50}) was calculated by plotting percent survival against \log_{10} 17-AAG concentration.

Encystation

Entamoeba invadens trophozoites grown to log phase were chilled on ice for 5 min and harvested by centrifugation at 600g for 5 min. Trophozoites were induced for encystation in LG medium (TYI medium without glucose diluted to 47% with 5% adult bovine serum and 2.5% Diamond vitamin mix) at a concentration of 5×10^5 cells/mL (Singh et al., 2011). Induction was carried out for 72 h. Cysts were identified under microscope by their spherical refractile morphology and staining of chitin cell wall by caulfloor white. Number of cysts formed, was scored by counting cysts resistant to detergent (0.05% SDS). For effect of Hsp90 inhibition on encystations, trophozoites were treated with 600 nM 17-AAG for 24 h. 0.2% DMSO was used as control. Treated cells were then induced for encystation in LG medium. Cells were also treated with 200 μ M DTT for 5 h to induce ER stress and treated cells were then induced for encystation.

Immunoblot

Equal number of trophozoites and cyst were harvested and lysed in laemmli buffer. Lysate was resolved on 10% polyacrylamide SDS gel under reducing conditions and immunoblot for EiHsp90 was carried out as described previously (Singh et al., 2014). Ponceau profile was used as a representative of equal loading.

RNA Extraction and RT PCR

RNA extraction was carried out using TriZol reagent (Thermo Fisher Scientific) according to manufacturer's instructions. The concentration and purity of the RNA extracted were evaluated using the Nanodrop spectrophotometer (Thermo Scientific). 2 μ g RNA of all samples was used to synthesize cDNA using Verso cDNA Synthesis kit (Thermo Fisher Scientific) according to manufacturer's instructions.

Primers for Aha1c, Sgt1, and HOP were designed as follows: Aha1c Fwd: 5'-CCGAGAGATTGACTGCCGTG-3', Aha1c Rev: 5'-GGCCATGTGTTAACCTCCA-3' (product size: 154 bp), Sgt1 Fwd: 5'-CGCAGTGAGTTCAACGAGA-3', Sgt1 rev: 5'-TGTAAACAGCGTCCCAGTCT-3' (product size: 242 bp), and HOP fwd: 5'-TAGAGCCGGACAATGAAGCA-3', HOP Rev: 5'-ACGCCATCAAAGCTTCAGTG-3' (Product size: 237 bp). rRNA primers were used as described before (Makioka et al., 2009). Amplification was performed in Mastercycler (Eppendorf) for 25 cycles. RT-PCR products were analyzed on a 2% agarose gel with ethidium bromide and rRNA amplicon was used as loading control for comparing trophozoites and cysts samples.

RESULTS

Hsp90 Inhibition by 17-AAG Interferes with Erythrophagocytosis in *Entamoeba*

Erythrophagocytosis is a well-accepted method to quantitate phagocytosis rate by *Entamoeba*. *E. histolytica* cells were treated

with 600 nM 17-AAG for 24 h. DMSO was used as control. Treated cells were then incubated with washed RBCs for 1 h. Microscopic observation was carried to ensure phagocytosis was optimum in control cells at end of 1 h (Figure 1A). Phagocytosis of control and treated cells was compared by absorbance of hemoglobin released from engulfed RBCs. It was observed that upon inhibition of Hsp90 by 17-AAG, there was a 60% decrease in phagocytosis by *Entamoeba* compared to DMSO treated cells (Figure 1B). This suggests Hsp90 plays a crucial role in regulation of phagocytosis.

In order to understand the role of Hsp90 in erythrophagocytosis, immuno-fluorescence staining was carried out. Hsp90 is found at the phagocytic cups along with actin during erythrophagocytosis (Figure 1C). Quantitation of the staining in images during erythrophagocytosis showed that fluorescence intensity of Hsp90 is higher in phagocytic cups compared to the rest of the cell and that there is a high degree of co-localization between Hsp90 and actin (Pearson correlation coefficient 0.8) implicating that Hsp90 is enriched in the cups along with actin. We also observed that Hsp90 did not get localized in mature phagosomes (Figure 1D).

Cell motility is required for host cell invasion and survival of *E. histolytica*. *Entamoeba* cells extend finger like projections called pseudopodia during cell movement that is driven by actin polymerization underneath the plasma membrane (Voigt and Guillen, 1999). It is observed that Hsp90 also gets accumulated at the leading edge of the cell during pseudopod extension and cell motility (Figure 1E). The enrichment of Hsp90 at the advancing pseudopods and phagocytic cups suggests that it may play a role in cell motility and initiation of phagocytosis.

Hsp90 Expression Levels are Modulated during Encystation Process

Hsp90 is known to regulate stage transition in various parasites and its levels get modulated in different stages of parasite life cycle. Hsp90 as a chaperone modulates both activation and inactivation of various client proteins. Some of the Hsp90 clients including transcription factors are activated upon a depletion of free Hsp90 pool and on the other hand many clients which are dependent on Hsp90 for their activation are degraded upon Hsp90 inhibition. In *Entamoeba*, very little is known about Hsp90 biology or the clients. Therefore, it is of interest to understand how Hsp90 levels are modulated in the entire life cycle. Hsp90 and its co-chaperone homologs were identified in *E. invadens* by homology search. Hsp90 (EIN_134370) co-chaperones identified included Aha1c (EIN_036190), Sgt1 (EIN_038830), Hop (EIN_109220), PP5 (EIN_054040), and Cns1 (EIN_168820). Transcript data for expression of these genes was retrieved from amoebadb.org (De Cádiz et al., 2013; Ehrenkaufer et al., 2013). It was observed that Hsp90 transcript levels decrease by 150-folds in cysts compared to trophozoites during encystation. On the other hand, during excystation Hsp90 levels were observed to increase again by 270-folds in excysting parasites compared to cysts (Figure 2). Hsp90 co-chaperones are known to regulate Hsp90 function by either activating or suppressing ATPase activity or by facilitating Hsp90-client interaction or aid in chaperone function.

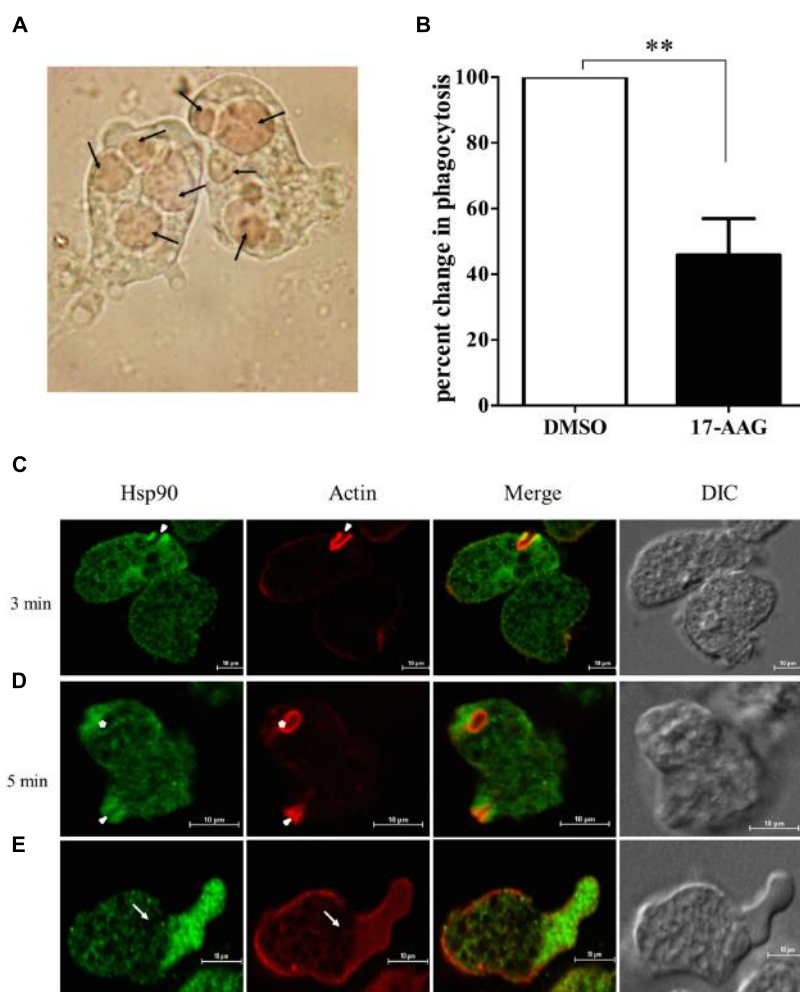


FIGURE 1 | Hsp90 regulates phagocytosis in *Entamoeba histolytica*. **(A)** Microscopic image of *Entamoeba* showing engulfed RBCs. Arrows show engulfed RBCs. **(B)** Hsp90 inhibition by 600 nM 17-AAG decreases phagocytosis by 60% in comparison to DMSO treated cells ($P < 0.01$). Graph is representative of three experiments. **(C)** Localization of Hsp90 during erythrophagocytosis: *E. histolytica* cells were incubated with RBCs for different time points at 37°C. The cells were then fixed, stained with rabbit anti-Hsp90 and followed by secondary labeling with Alexa 488 (EhHsp90) and TRITC-Phalloidin (Actin) and Solid arrow represents phagocytic cups and asterisk indicates mature phagosome **(D)**. **(E)** Arrow represents pseudopod extension and enrichment of Hsp90. Differential interference contrast (DIC).

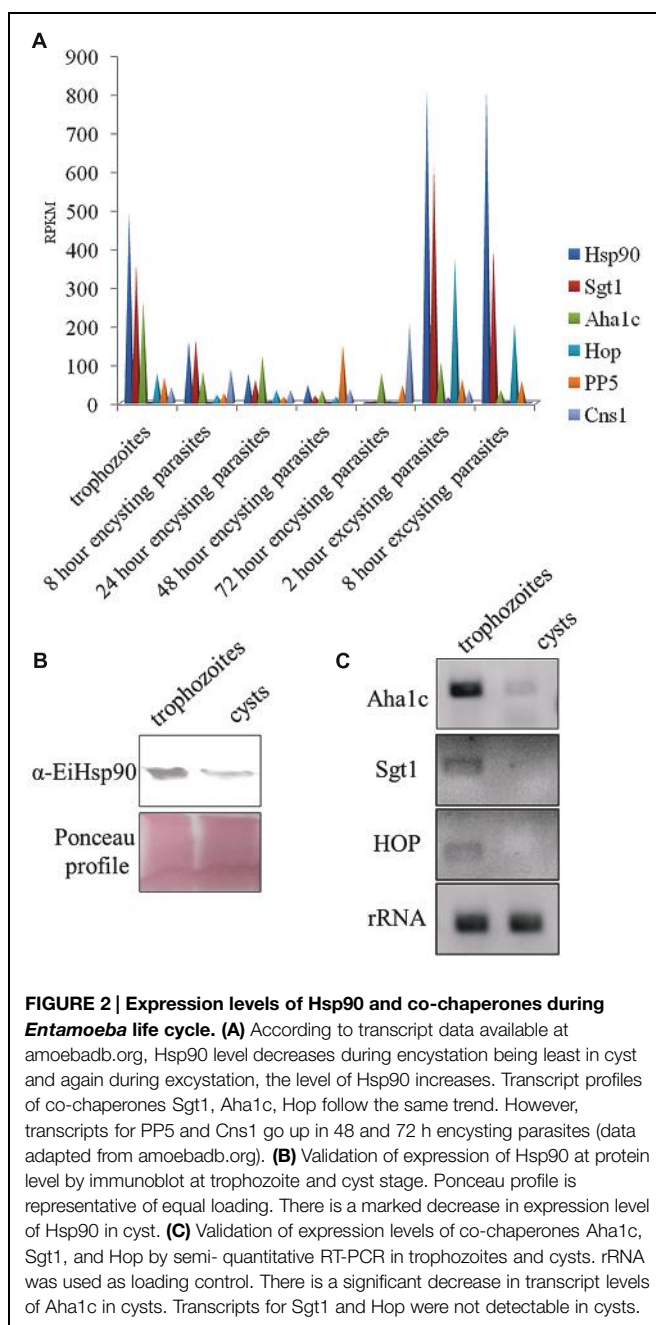
Therefore, expression levels of various Hsp90 co-chaperones were also analyzed. It was observed that with the exception of PP5 and Cns1, other three identified co-chaperones of Hsp90 in *Entamoeba* show expression profiles similar to Hsp90 (Figure 2A). Aha1c, an activator of Hsp90 ATPase activity, also shows a threefold decrease in transcript levels in cysts compared to trophozoites followed by an increase of 1.3-folds in excysting parasites.

Transcript data available at amoebadb.org was further validated by immunoblot of Hsp90 in trophozoites and cysts. A marked decrease in the expression of Hsp90 protein was observed in cysts (Figure 2B). Further, transcript levels of Hsp90 co-chaperones were also validated by semi-quantitative RT PCR. A significant down-regulation of Aha1c was observed in cysts and no transcript for Sgt1 and Hop was detected in cysts by RT PCR (Figure 2C). rRNA was used as control for equal loading. These

observations altogether suggest that a functional Hsp90 multi-chaperone complex is involved in maintaining the trophozoite stage of parasite and a decrease in Hsp90 and co-chaperone levels co-relates with encystation.

Hsp90 is a Negative Regulator of Encystation

Hsp90 is known to regulate stage differentiation in various other protozoa including *Giardia*, *Plasmodium*, *Leishmania*, and *Toxoplasma* (Wiesigl and Clos, 2001; Graefe et al., 2002; Banumathy et al., 2003; Nageshan et al., 2014). Therefore, in light of the expression profile of Hsp90 in *Entamoeba* life cycle, its involvement in stage transition was examined. Firstly, we determined the GI_{50} value of Hsp90 inhibition for *E. invadens* by 17-AAG in both the growth medium TYI-S-33 and encystation LG medium. The GI_{50} in TYI-S-33 and LG medium are 711 and



935 nM, respectively, (Figure 3A). A sub lethal concentration of 600 nM was chosen for all further inhibition studies. *E. invadens* encystation was established *in vitro* and cyst formation was scored by either cauloform white staining of chitin (Figure 3B) or by counting detergent resistant cysts.

Trophozoites were treated for 24 h with 600 nM 17-AAG and DMSO was used as vehicle control. Post 24 h, 17-AAG and DMSO treated trophozoites were transferred to LG medium to induce encystation. Cyst formation was scored after 72 h. A twofold increase in cyst formation was observed in 17-AAG treated parasites compared to DMSO treated parasites (Figures 3C,D). We observed this increase is specific to Hsp90

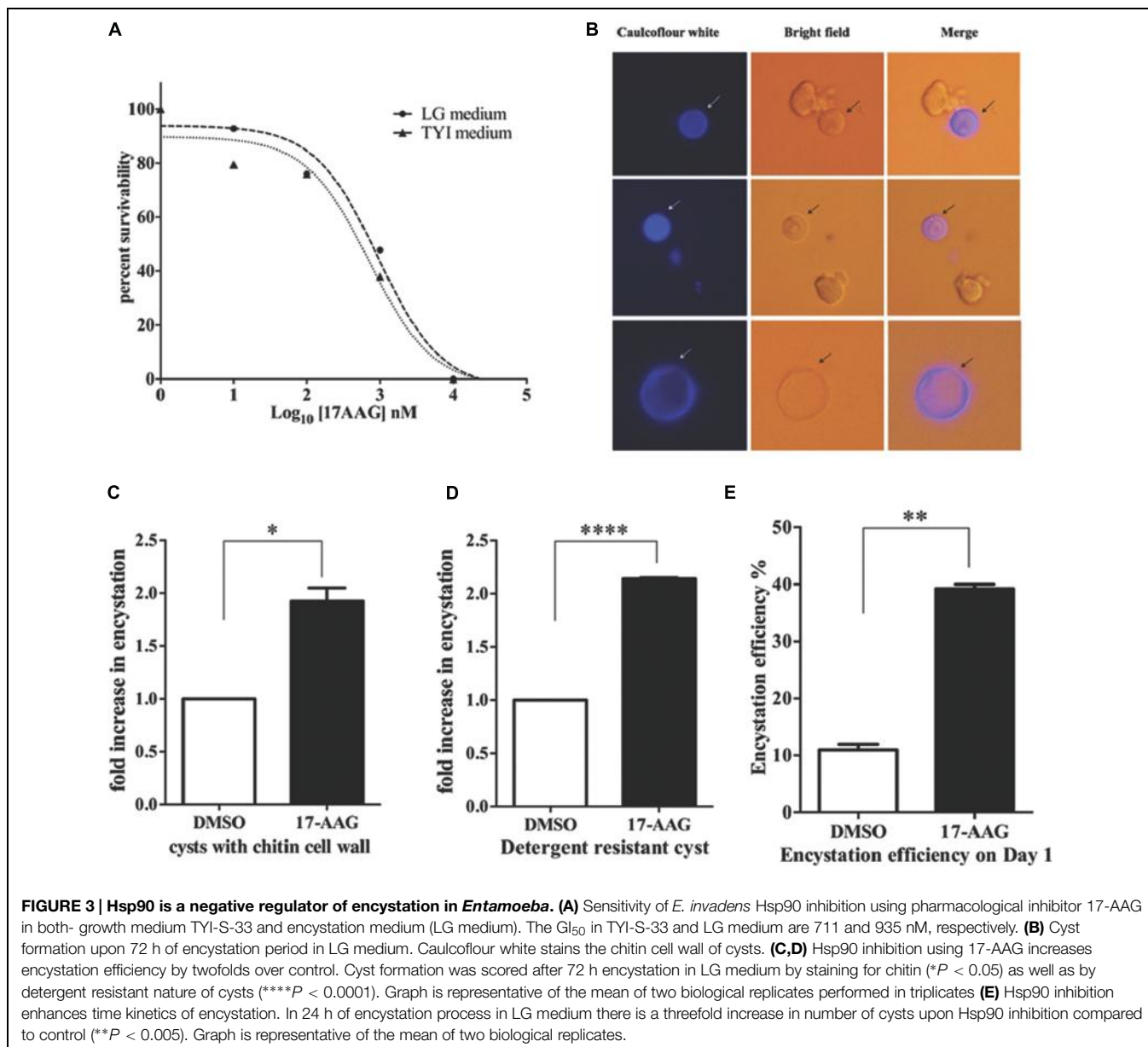
inhibition and not a general stress by treating *E. invadens* with DTT to induce ER stress and score for encystation rate. No significant change was observed in encystation efficiency upon ER stress (Supplementary Figure S1). Further, it was observed that the conversion of 17-AAG treated trophozoites to cysts on day 1 of encystation itself was threefolds higher than DMSO treated cells (Figure 3E). This suggests that Hsp90 acts as a negative regulator of encystation process. Inhibition of Hsp90 promotes encystation.

DISCUSSION

Phagocytosis is a key hallmark of *Entamoeba* virulence. During invasion of intestine and extra-intestinal tissue, parasite has to phagocytize host epithelial cells and erythrocytes. Phagocytosis is an important bioprocess for virulence, growth and survival of *Entamoeba* (Bracha and Mirelman, 1984). There are extensive studies on signaling involved in phagocytosis (Sahoo et al., 2004; Aslam et al., 2012; Mansuri et al., 2014). Hsp90 has been also implicated in regulating cell motility and actin polymerization in cancer cells (Taiyab and Rao Ch, 2011). We demonstrate that inhibition of Hsp90 interferes with phagocytosis of RBCs by the parasite, which is important for parasite virulence and survival. We see specific localization of Hsp90 at the phagocytic cup and not in mature phagosome suggesting Hsp90 may play an important role for initiation of phagocytosis. We also see enhanced localization of Hsp90 in pseudopodia suggesting involvement of Hsp90 in cell motility.

We also studied the role of Hsp90 in *Entamoeba* life cycle during stage transition from trophozoites to cysts. As mentioned before, Hsp90 is known to regulate life cycle in many related protozoa like *Plasmodium*, *Giardia*, *Leishmania*, *Toxoplasma* etc. (Wiesigl and Clos, 2001; Graefe et al., 2002; Banumathy et al., 2003; Echeverria et al., 2005; Nageshan et al., 2014; Rochani et al., 2014). Hsp90 is also known to regulate morphogenesis to filamentous form in *Candida albicans* (Shapiro et al., 2009).

In *Entamoeba*, encystation and excystation are complex biological processes. High throughput studies have determined the transcriptional and metabolite level changes during encystation and excystation (Jeehani et al., 2012; De Cádiz et al., 2013; Ehrenkaufer et al., 2013). There is an up-regulation of transporters, cytoskeletal proteins, proteins involved in vesicular trafficking, cysteine proteases, components of the proteasome, and enzymes for chitin biosynthesis and a down-regulation of metabolic genes. In this study, we have demonstrated for the first time involvement of Hsp90 in regulation of encystation process in *Entamoeba*. We show that upon Hsp90 inhibition there is a twofold increase in conversion of trophozoites to cysts. In a closely related parasite *Giardia lamblia*, Hsp90 has been shown to be a negative regulator of encystation (Nageshan et al., 2014). Hsp90 is traditionally well known to regulate various signaling and stress response pathways in higher eukaryotes. Cues for encystation are unknown but it is believed that environmental factors, like nutritional stress, change in gut micro-flora and host response are perceived by the parasite (Bailey and Rengyapian, 1980; Vázquezdelara-Cisneros and Arroyo-Begovich, 1984; Byers



et al., 2005). These cues act as a trigger for encystation. Hsp90 could possibly act as a transducer of these environmental cues leading to the initiation of encystation. Our study shows that inhibition of Hsp90 results in accelerated initiation of encystation process with a substantial increase in cysts observed on 24 h of encystation. We also examined if increased encystation is specific to Hsp90 inhibition or a general stress response. In *Plasmodium falciparum*, ER stress is known to induce stage transition to gametocyte (Chaubey et al., 2014). We induced ER stress at trophozoite stage by DTT treatment followed by induction of encystation. However, no significant change in encystation rate was observed upon ER stress, thus suggesting increased encystation is not a general stress response.

Transcriptome data suggests, that the level of Hsp90 transcript during excystation goes up by 270-folds compared to cysts

(De Cádiz et al., 2013; Ehrenkaufer et al., 2013). Therefore, it will not be far-fetched to hypothesize that inhibition of Hsp90 during excystation can inhibit the excystation process. Further studies are required to understand the involvement of Hsp90 in excystation process. Hsp90 clients include many kinases, transcription factors and cytoskeletal proteins to name a few. Identification of Hsp90 clients in *Entamoeba* and their modulation in the encystation and excystation process will help in understanding the molecular details of Hsp90's role in *Entamoeba* life cycle.

Our previous observation that Hsp90 is essential for survival of *Entamoeba* (Singh et al., 2014) and its involvement in regulation of phagocytosis, encystation and possibly in excystation indicates Hsp90 to be an excellent therapeutic target. Hsp90 is also known to regulate drug resistance in many fungal

species (Rutherford and Lindquist, 1998; Cowen et al., 2009). Therefore, it will also be worth exploring a combination therapy with Hsp90 inhibitors in the cases of drug resistant amoebiasis.

ACKNOWLEDGMENTS

We thank Dr. Sudha Bhattacharya for providing *Entamoeba invadens* culture. We thank Dr. Manish Grover for critical reading of manuscript and Dr. Rishi Kumar for extensive discussions on experimental strategy. We would like to thank IISc microscope facility, Ashok Kumar Sahoo from 'Advanced

Instrument Research Facility' JNU and Tripti Panwar from SLS, JNU for confocal imaging. Funding from DBT-IISc partnership grant is acknowledged. Funding for MS and SS from Council of Scientific & Industrial Research (India) is acknowledged. MS acknowledges funding from Bristol Myers Squibb fellowship.

SUPPLEMENTARY MATERIAL

The Supplementary Material for this article can be found online at: <http://journal.frontiersin.org/article/10.3389/fmich.2015.01125>

REFERENCES

- Aguilar-Diaz, H., Carrero, J. C., Arguello-Garcia, R., Laclette, J. P., and Morales-Montor, J. (2011). Cyst and encystment in protozoan parasites: optimal targets for new life-cycle interrupting strategies? *Trends Parasitol.* 27, 450–458. doi: 10.1016/j.pt.2011.06.003
- Aslam, S., Bhattacharya, S., and Bhattacharya, A. (2012). The Calmodulin-like calcium binding protein EhCaBP3 of *Entamoeba histolytica* regulates phagocytosis and is involved in actin dynamics. *PLoS Pathog.* 8:e1003055. doi: 10.1371/journal.ppat.1003055
- Bailey, G. B., and Rengyopian, S. (1980). Osmotic stress as a factor controlling encystation of *Entamoeba invadens*. *Arch. Invest. Med. (Mex.)* 11, 11–16.
- Banumathy, G., Singh, V., Pavithra, S. R., and Tatu, U. (2003). Heat shock protein 90 function is essential for *Plasmodium falciparum* growth in human erythrocytes. *J. Biol. Chem.* 278, 18336–18345. doi: 10.1074/jbc.M211309200
- Bozza, G., Capitani, M., Montanari, P., Benucci, B., Biancucci, M., Nardi-Dei, V., et al. (2014). Role of ARF6, Rab11 and external Hsp90 in the trafficking and recycling of recombinant-soluble *Neisseria meningitidis* adhesin A (rNadA) in human epithelial cells. *PLoS ONE* 9:e110047. doi: 10.1371/journal.pone.0110047
- Bracha, R., and Mirelman, D. (1984). Virulence of *Entamoeba histolytica* trophozoites. Effects of bacteria, microaerobic conditions, and metronidazole. *J. Exp. Med.* 160, 353–368.
- Byers, J., Faigle, W., and Eichinger, D. (2005). Colonic short-chain fatty acids inhibit encystation of *Entamoeba invadens*. *Cell Microbiol.* 7, 269–279. doi: 10.1111/j.1462-5822.2004.00457.x
- Chaubey, S., Grover, M., and Tatu, U. (2014). Endoplasmic reticulum stress triggers gametocytogenesis in the malaria parasite. *J. Biol. Chem.* 289, 16662–16674. doi: 10.1074/jbc.M114.551549
- Cowen, L. E., Singh, S. D., Kohler, J. R., Collins, C., Zaas, A. K., Schell, W. A., et al. (2009). Harnessing Hsp90 function as a powerful, broadly effective therapeutic strategy for fungal infectious disease. *Proc. Natl. Acad. Sci. U.S.A.* 106, 2818–2823. doi: 10.1073/pnas.0813394106
- Debnath, A., Shahinas, D., Bryant, C., Hirata, K., Miyamoto, Y., Hwang, G., et al. (2014). Hsp90 inhibitors as new leads to target parasitic diarrheal diseases. *Antimicrob. Agents Chemother.* 58, 4138–4144. doi: 10.1128/AAC.02576-14
- De Cádiz, A. E., Jeelani, G., Nakada-Tsukui, K., Caler, E., and Nozaki, T. (2013). Transcriptome analysis of encystation in *Entamoeba invadens*. *PLoS ONE* 8:e74840. doi: 10.1371/journal.pone.0074840
- Diamond, L. S., Harlow, D. R., and Cunnick, C. C. (1978). A new medium for the axenic cultivation of *Entamoeba histolytica* and other *Entamoeba*. *Trans. R. Soc. Trop. Med. Hyg.* 72, 431–432. doi: 10.1016/0035-9203(78)90144-X
- Echeverria, P. C., Matrajt, M., Harb, O. S., Zappia, M. P., Costas, M. A., Roos, D. S., et al. (2005). Toxoplasma gondii Hsp90 is a potential drug target whose expression and subcellular localization are developmentally regulated. *J. Mol. Biol.* 350, 723–734. doi: 10.1016/j.jmb.2005.05.031
- Ehrenkaufer, G. M., Haque, R., Hackney, J. A., Eichinger, D. J., and Singh, U. (2007). Identification of developmentally regulated genes in *Entamoeba histolytica*: insights into mechanisms of stage conversion in a protozoan parasite. *Cell Microbiol.* 9, 1426–1444. doi: 10.1111/j.1462-5822.2006.00882.x
- Ehrenkaufer, G. M., Weedall, G. D., Williams, D., Lorenzi, H. A., Caler, E., Hall, N., et al. (2013). The genome and transcriptome of the enteric parasite *Entamoeba invadens*, a model for encystation. *Genome Biol.* 14:R77. doi: 10.1186/gb-2013-14-7-r77
- Freeman, C. D., Klutman, N. E., and Lamp, K. C. (1997). Metronidazole. A therapeutic review and update. *Drugs* 54, 679–708.
- Graef, S. E., Wiesigil, M., Gaworski, I., Macdonald, A., and Clos, J. (2002). Inhibition of HSP90 in *Trypanosoma cruzi* induces a stress response but no stage differentiation. *Eukaryot. Cell* 1, 936–943. doi: 10.1128/EC.1.6.936-943.2002
- Huston, C. D., Boettner, D. R., Miller-Sims, V., and Petri, W. A. (2003). Apoptotic killing and phagocytosis of host cells by the parasite *Entamoeba histolytica*. *Infect. Immun.* 71, 964–972. doi: 10.1128/IAI.71.2.964-972.2003
- Jeelani, G., Sato, D., Husain, A., Escueta-De Cadiz, A., Sugimoto, M., Soga, T., et al. (2012). Metabolic profiling of the protozoan parasite *Entamoeba invadens* revealed activation of unpredicted pathway during encystation. *PLoS ONE* 7:e37740. doi: 10.1371/journal.pone.0037740
- Johnson, J. L., and Brown, C. (2009). Plasticity of the Hsp90 chaperone machine in divergent eukaryotic organisms. *Cell Stress Chaperones* 14, 83–94. doi: 10.1007/s12192-008-0058-9
- Keestra, A. M., Winter, M. G., Auburger, J. J., Frassle, S. P., Xavier, M. N., Winter, S. E., et al. (2013). Manipulation of small Rho GTPases is a pathogen-induced process detected by NOD1. *Nature* 496, 233–237. doi: 10.1038/nature12025
- Makioka, A., Kumagai, M., Kobayashi, S., and Takeuchi, T. (2009). Involvement of serine proteases in the excystation and metacystic development of *Entamoeba invadens*. *Parasitol. Res.* 105, 977–987. doi: 10.1007/s00436-009-1478-x
- Mansuri, M. S., Bhattacharya, S., and Bhattacharya, A. (2014). A novel alpha kinase EhAK1 phosphorylates actin and regulates phagocytosis in *Entamoeba histolytica*. *PLoS Pathog.* 10:e1004411. doi: 10.1371/journal.ppat.1004411
- Marion, S., Laurent, C., and Guillen, N. (2005). Signalization and cytoskeleton activity through myosin IB during the early steps of phagocytosis in *Entamoeba histolytica*: a proteomic approach. *Cell Microbiol.* 7, 1504–1518. doi: 10.1111/j.1462-5822.2005.00573.x
- Mi-Ichi, F., Miyamoto, T., Takao, S., Jeelani, G., Hashimoto, T., Hara, H., et al. (2015). Entamoeba mitosomes play an important role in encystation by association with cholesterol sulfate synthesis. *Proc. Natl. Acad. Sci. U.S.A.* 112, E28884–E28890. doi: 10.1073/pnas.1423718112
- Nageshan, R. K., Roy, N., Ranade, S., and Tatu, U. (2014). Trans-spliced heat shock protein 90 modulates encystation in *Giardia lamblia*. *PLoS Negl. Trop. Dis.* 8:e2829. doi: 10.1371/journal.pntd.0002829
- Ohji, G., Hidayat, S., Nakashima, A., Tokunaga, C., Oshiro, N., Yoshino, K., et al. (2006). Suppression of the mTOR-raptor signaling pathway by the inhibitor of heat shock protein 90 geldanamycin. *J. Biochem.* 139, 129–135. doi: 10.1093/jb/mvj008
- Okada, M., Huston, C. D., Mann, B. J., Petri, W. A. Jr., Kita, K., and Nozaki, T. (2005). Proteomic analysis of phagocytosis in the enteric protozoan parasite *Entamoeba histolytica*. *Eukaryot. Cell* 4, 827–831. doi: 10.1128/EC.4.4.827-831.2005
- Okada, M., and Nozaki, T. (2006). New insights into molecular mechanisms of phagocytosis in *Entamoeba histolytica* by proteomic analysis. *Arch. Med. Res.* 37, 244–252. doi: 10.1016/j.arcmed.2005.10.003
- Pearl, L. H., and Prodromou, C. (2006). Structure and mechanism of the Hsp90 molecular chaperone machinery. *Annu. Rev. Biochem.* 75, 271–294. doi: 10.1146/annurev.biochem.75.103004.142738

- Rochani, A. K., Mithra, C., Singh, M., and Tatu, U. (2014). Heat shock protein 90 as a potential drug target against surra. *Parasitology* 141, 1148–1155. doi: 10.1017/S0031182014000845
- Rutherford, S. L., and Lindquist, S. (1998). Hsp90 as a capacitor for morphological evolution. *Nature* 396, 336–342. doi: 10.1038/24550
- Sahoo, N., Labruyere, E., Bhattacharya, S., Sen, P., Guillen, N., and Bhattacharya, A. (2004). Calcium binding protein 1 of the protozoan parasite *Entamoeba histolytica* interacts with actin and is involved in cytoskeleton dynamics. *J. Cell Sci.* 117, 3625–3634. doi: 10.1242/jcs.01198
- Shapiro, R. S., Uppuluri, P., Zaas, A. K., Collins, C., Senn, H., Perfect, J. R., et al. (2009). Hsp90 orchestrates temperature-dependent *Candida albicans* morphogenesis via Ras1-PKA signaling. *Curr. Biol.* 19, 621–629. doi: 10.1016/j.cub.2009.03.017
- Singh, M., Shah, V., and Tatu, U. (2014). A novel C-terminal homologue of Aha1 co-chaperone binds to heat shock protein 90 and stimulates its ATPase activity in *Entamoeba histolytica*. *J. Mol. Biol.* 426, 1786–1798. doi: 10.1016/j.jmb.2014.01.008
- Singh, N., Bhattacharya, S., and Paul, J. (2011). *Entamoeba invadens*: dynamics of DNA synthesis during differentiation from trophozoite to cyst. *Exp. Parasitol.* 127, 329–333. doi: 10.1016/j.exppara.2010.08.013
- Somlata, Kamanna, S., Agrahari, M., Babuta, M., Bhattacharya, S., and Bhattacharya, A. (2012). Autophosphorylation of Ser428 of EhC2PK plays a critical role in regulating erythrophagocytosis in the parasite *Entamoeba histolytica*. *J. Biol. Chem.* 287, 10844–10852. doi: 10.1074/jbc.M111.308874
- Taipale, M., Jarosz, D. F., and Lindquist, S. (2010). HSP90 at the hub of protein homeostasis: emerging mechanistic insights. *Nat. Rev. Mol. Cell Biol.* 11, 515–528. doi: 10.1038/nrm2918
- Taiyab, A., and Rao Ch, M. (2011). HSP90 modulates actin dynamics: inhibition of HSP90 leads to decreased cell motility and impairs invasion. *Biochim. Biophys. Acta* 1813, 213–221. doi: 10.1016/j.bbamcr.2010.09.012
- Tovy, A., Hertz, R., Siman-Tov, R., Syan, S., Faust, D., Guillen, N., et al. (2011). Glucose starvation boosts *Entamoeba histolytica* virulence. *PLoS Negl. Trop. Dis.* 5:e1247. doi: 10.1371/journal.pntd.0001247
- Vázquezdelara-Cisneros, L. G., and Arroyo-Begovich, A. (1984). Induction of encystation of *Entamoeba invadens* by removal of glucose from the culture medium. *J. Parasitol.* 70, 629–633. doi: 10.2307/3281741
- Voigt, H., and Guillen, N. (1999). New insights into the role of the cytoskeleton in phagocytosis of *Entamoeba histolytica*. *Cell Microbiol.* 1, 195–203. doi: 10.1046/j.1462-5822.1999.00021.x
- Wiesigl, M., and Clos, J. (2001). Heat shock protein 90 homeostasis controls stage differentiation in *Leishmania donovani*. *Mol. Biol. Cell* 12, 3307–3316. doi: 10.1091/mbc.12.11.3307
- Yan, L., Cerny, R. L., and Cirillo, J. D. (2004). Evidence that hsp90 is involved in the altered interactions of *Acanthamoeba castellanii* variants with bacteria. *Eukaryot. Cell* 3, 567–578. doi: 10.1128/EC.3.3.567-578.2004

Conflict of Interest Statement: The authors declare that the research was conducted in the absence of any commercial or financial relationships that could be construed as a potential conflict of interest.

Copyright © 2015 Singh, Sharma, Bhattacharya and Tatu. This is an open-access article distributed under the terms of the Creative Commons Attribution License (CC BY). The use, distribution or reproduction in other forums is permitted, provided the original author(s) or licensor are credited and that the original publication in this journal is cited, in accordance with accepted academic practice. No use, distribution or reproduction is permitted which does not comply with these terms.

Heat shock protein 90 inhibitors repurposed against *Entamoeba histolytica*

Dea Shahinas^{1*}, Anjan Debnath², Christian Benedict¹, James H. McKerrow² and Dylan R. Pillai³

¹ Department of Laboratory Medicine and Pathobiology, University of Toronto, Toronto, ON, Canada, ² Skaggs School of Pharmacy and Pharmaceutical Sciences, University of California, San Diego, La Jolla, CA, USA, ³ Department of Pathology and Laboratory Medicine, University of Calgary, Calgary, AB, Canada

OPEN ACCESS

Edited by:

Tzi Bun Ng,

The Chinese University of Hong Kong,
China

Reviewed by:

Yuji Morita,

Aichi Gakuin University, Japan
Giovanna Riccardi,
University of Pavia, Italy

***Correspondence:**

Dea Shahinas,

Department of Laboratory Medicine
and Pathobiology, University of
Toronto, Toronto, ON, M5S 1A1
Canada

dea.shahinas@alum.utoronto.ca

Specialty section:

This article was submitted to
Antimicrobials, Resistance and
Chemotherapy,
a section of the journal
Frontiers in Microbiology

Received: 30 January 2015

Accepted: 11 April 2015

Published: 28 April 2015

Citation:

Shahinas D, Debnath A, Benedict C,
McKerrow JH and Pillai DR (2015)
Heat shock protein 90 inhibitors
repurposed against *Entamoeba*
histolytica. *Front. Microbiol.* 6:368.
doi: 10.3389/fmicb.2015.00368

Hsp90 is an essential chaperone responsible for trafficking a vast array of client proteins, which are substrates that Hsp90 regulates in eukaryotic cells under stress conditions. The ATP-binding N-terminal domain of Hsp90 (also known as a GHKL type ATPase domain) can serve as a specific drug target, because sufficient structural diversity in the ATP-binding pocket of Hsp90 allows for ortholog selectivity of Hsp90 inhibitors. The primary objective of this study is to identify inhibitors specific for the ATP-binding domain of *Entamoeba histolytica* Hsp90 (EhHsp90). An additional aim, using a combination of site-directed mutagenesis and a protein *in vitro* assay, is to show that the antiparasitic activity of Hsp90 inhibitors is dependent on specific residues within the ATP-binding domain. Here, we tested the activity of 43 inhibitors of Hsp90 that we previously identified using a high-throughput screen. Of the 43 compounds tested, 19 competed for binding of the EhHsp90 ATP-binding domain. Five out of the 19 EhHsp90 protein hits demonstrated activity against *E. histolytica* *in vitro* culture: rifabutin, rutilantin, cetylpyridinium chloride, pararosaniline pamoate and gentian violet. These five top *E. histolytica* Hsp90 inhibitors showed 30–100% inhibition of *E. histolytica* in culture in the micromolar range. These data suggest that *E. histolytica*-specific Hsp90 inhibitors are possible to identify and provide important lead compounds for the development of novel antiamebic drugs.

Keywords: EhHsp90 inhibitors, rifabutin, rutilantin, cetylpyridinium chloride, pararosaniline pamoate, gentian violet

Introduction

Entamoeba histolytica is a protozoan intestinal parasite that causes amebiasis worldwide (Walsh, 1986), Amebiasis presents as diarrhea in humans causing 50 million cases of invasive disease and 70–100 thousand deaths worldwide (Stanley, 2003; Ralston and Petri, 2011b). Current therapy relies solely on metronidazole and is complicated by resistance and adverse neurotoxic, mutagenic and carcinogenic effects (Freeman et al., 1997; Kapoor et al., 1999; Bendesky et al., 2002). Considering the prevalence of amebiasis and the lack of other therapeutic options, it is of paramount importance to search for other effective, better-tolerated antiamebic drugs. To this end, we propose the discovery of new antiamebic drugs by targeting heat shock protein 90 (Hsp90), one of the best-studied members of the heat shock protein (HSP) family.

Stress inducible cytosolic Hsp90 exists in the form of a multi-chaperone complex and is essential for helping client proteins to fold (Li and Buchner, 2013). As such, it is essential for normal eukaryotic growth and development (Li and Buchner, 2013). The existing model suggests that the stress inducible isoform of cytosolic Hsp90 serves as a buffer of phenotypic variation and potentiator of drug resistance by preventing cellular toxicity caused by misfolded and aggregated proteins in response to heat shock or pharmacological stress (Cowen and Lindquist, 2005; Cowen et al., 2009; Marubayashi et al., 2010). Many Hsp90 clients are essential cellular proteins with pathogenic functions that render the inhibition of the Hsp90 pathway lethal in cells undergoing pathogenic, pharmacological or heat-shock stress, but not in normal cells (Cowen and Lindquist, 2005; Chiosis et al., 2006; Cerchietti et al., 2009, 2010; Cowen et al., 2009; Taldone et al., 2010). Pharmacologic inhibition of Hsp90 effectively results in lethality in abnormal cells such as infected or transformed cells by disruption of the broad spectrum of Hsp90 interactions and signaling pathways (Jhaveri et al., 2011; Usmani and Chiosis, 2011). As such, this inhibition provides specific anti-disease effects and a decreased likelihood for developing resistance.

In particular, inhibition of this ATPase activity at the N-terminal ATP-binding domain is an effective approach for blocking its function and interaction with client proteins (Jhaveri et al., 2011; Usmani and Chiosis, 2011). Significant similarity exists at the ATP-binding domain between other eukaryotic stress-inducible Hsp90s and parasite Hsp90s such as *Plasmodium falciparum* Hsp90 (PfHsp90) and *E. histolytica* Hsp90 (EhHsp90) (Banumathy et al., 2003; Pavithra et al., 2004, 2007; Acharya et al., 2007; Kumar et al., 2007; Pallavi et al., 2010). In addition, the pocket architecture of the orthologous ATP binding domains of stress inducible Hsp90 also contains unique residues that can be selectively targeted by inhibitors (Wider et al., 2009; Corbett and Berger, 2010; Pallavi et al., 2010). Such unique residues may be involved in ligand binding, but do not participate in the catalytic function of this domain, because residues involved in catalysis are essential for the ATPase function of this domain and are therefore conserved (Wider et al., 2009; Corbett and Berger, 2010; Pallavi et al., 2010). For example, crystal structures of human and *P. falciparum* Hsp90 N-terminal domains (PDB ID: 2FWZ and 3K60, respectively) reveal that PfHsp90 Met84 adopts a different side-chain rotamer than human Met98, altering the shape of the “ceiling” of the binding pocket (Corbett and Berger, 2010). Ser52, Lys112 and Val186 of human (Hs) Hsp90 are replaced by Ala38, Arg98 and Ile173 in PfHsp90 (Corbett and Berger, 2010). Even though these residues are not involved in ATP hydrolysis (Corbett and Berger, 2010), in general, these differences in pocket architecture suggest that the PfHsp90 ATP-binding domain is slightly more hydrophobic, constricted, and basic relative to the human ortholog (Corbett and Berger, 2010).

We hypothesize that targeting of cytosolic-inducible Hsp90 is a viable strategy for drug discovery as this protein is essential in most eukaryotes studied to date e.g., *Drosophila melanogaster* (Bandura et al., 2013), *Caenorhabditis elegans* (Inoue et al., 2003), *P. falciparum* (Banumathy et al., 2003). In addition, conservation of the N-terminus ATP binding domain suggests that this domain

is under selection pressure to be conserved so that it may provide the energy needed to fold client proteins. Due to both this conservation, and presence of unique residues that may confer selectivity, repurposing of previously identified Hsp90 inhibitors is an attractive strategy and opportunity to capitalize on existing safety and pharmacokinetic data. Therefore, we tested the effect of 43 previously identified HsHsp90 and *P. falciparum* (PfHsp90) (Shahinas et al., 2010) inhibitors for their ability to inhibit EhHsp90. The objectives of this study were: (1) to biochemically characterize and identify the unique residues in the ATP binding pocket of HsHsp90 vs. EhHsp90; (2) to explore the selectivity of binding of these inhibitors to EhHsp90, PfHsp90 and HsHsp90 as well as to the site-directed mutants of each of these domains (3) to assess the effect of selective inhibitors on *E. histolytica* in cell culture.

Materials and Methods

Cloning and Protein Purification

A *P. falciparum* Hsp90 ATP-binding domain construct was amplified from genomic DNA harvested from the intra-erythrocytic life cycle of *P. falciparum* strain 3D7 obtained from the MR4 Malaria Research and Reference Resource Center (Forward primer: 5' CGCCGGCGCCATATGAGTTTCCAAG 3' Reverse primer 5' CGCCGGCGGGATCCTAAATTCTAAACT 3') and was cloned into the pET28b vector (Novagen). The *E. histolytica* Hsp90 ATP-binding domain was also amplified from genomic DNA extracted from a frozen *E. histolytica* (strain HM1:IMSS) culture obtained from the American Type Culture Collection (ATCC) (Forward primer: 5' CCGGGATCCATGGGA AATAGAAAAA 3') (Reverse primer: 5' GCGCGGTTTCGAAATA TTGAATAAATTTC 3') and was cloned into the pET28a vector (Novagen).

The clones were expressed in *E. coli* Bl21 (DE3) Codon Plus cells (Agilent Technologies) grown in terrific broth (12 g tryptone, 24 g yeast extract, 17 mM KH₂PO₄, 72 mM K₂HPO₄ and 4 mL glycerol per liter broth), and induced with 0.4 mM Isopropyl β-D-1-thiogalactopyranoside (IPTG) overnight at 24°C. These *E. coli* cells were harvested by centrifugation (5000 rpm for 10 min), resuspended in lysis buffer (20 mM 4-(2-hydroxyethyl)-1-piperazineethanesulfonic acid (HEPES), pH 7.5, 10% glycerol, 20 mM imidazole, 500 mM NaCl, 0.5% nonyl phenoxypolyethoxylethanol NP-40 surfactant) and supplemented with 100× bacterial protease inhibitor cocktail (Sigma). Cells were lysed by 5 times 45 s rounds (separated by a pause of 45 s) of sonication. The cell debris was removed by centrifugation (14,000 rpm for 30 min), and the protein was purified using nickel-nitrotriacetic acid (Ni-NTA) resin (QIAGEN). Tobacco etch virus (TEV) protease was added at a ratio of 1:50 TEV protease in dialysis buffer [20 mM HEPES, pH 7.5, 100 mM NaCl, 5 mM MgCl₂, and 0.01 mM 4,40-dianilino-1,10-binaphthyl-5,50-disulfonic acid dipotassium salt (bis-ANS)] and incubated overnight at 4°C. This mixture was washed over a Ni-NTA column to remove the TEV protease and cleaved polyhistidine tags from the purified protein. The proteins were concentrated to ~10 mg/mL using Amicon® Ultra centrifugal filters for protein concentration (Millipore) and centrifugation

at 2800 rpm. The same conditions were used for the expression and purification of all the proteins used in this study. The HsHsp90 ATP binding domain pET15b (Novagen) clone was kindly provided by Dr. Daniel Gewirth (Hauptman-Woodward Medical Research Institute).

Site-Directed Mutagenesis

Site-directed mutants were generated using site-specific primers (**Supplementary File 2**) that target unique residues in the ATP binding pockets of HsHsp90, PfHsp90, and EhHsp90 proteins. The site directed mutagenesis procedure was followed as per instructions of the QuickChange site-directed mutagenesis kit (Agilent Technologies, Santa Clara, CA) with some modifications. Briefly, the mutant plasmid was amplified using the proofreading enzyme *Pfx* (Invitrogen, Carlsbad, CA). Denaturation of the initial template was allowed to take place for 3 min at 95°C. After the initial denaturation, 14 cycles of denaturation (95°C), annealing (58°C) and elongation (68°C) took place. The nascent template was digested by the *DpnI* enzyme (37°C for 1 h), which digests methylated DNA that has been replicated inside *E. coli* Dh5-alpha bacteria (Invitrogen), which were used for the plasmid purification in this case. The undigested (amplified) plasmids were transformed in ultracompetent *E. coli* XL-Gold 10 cells (Agilent Technologies, Santa Clara, CA). The plasmids were purified using the Qiagen Miniprep kit (Qiagen, Germantown, MD). These plasmids were screened for the presence of the mutation using Sanger sequencing (Applied Biosystems 3130xl, Carlsbad, CA) after amplification of the Hsp90 ATP binding domain gene using standard T7 primers and annealing conditions (Novagen, Madison, WI).

4,40-dianalino-1,10-binaphthyl-5,50-disulfonic acid dipotassium salt (bis-ANS) Binding Assay with the PfHsp90 ATP-Binding Domain

By optimization of a previously established technique (Wassenberg et al., 2000), the fluorescent probe 4,40-dianalino-1,10-binaphthyl-5,50-disulfonicacid dipotassium salt (bis-ANS, Sigma-Aldrich) was used to demonstrate nucleotide binding to the ATP-binding domain of PfHsp90 (Shahinas et al., 2010). Recombinant purified protein (final protein concentration 1 μM) was pre-incubated for 45 min at 37°C with no drug or in the presence of 200 nL of drug to a final concentration of 100 nM (Spectrum and Lopac libraries) and 50 nM (Prestwick library). bis-ANS was then added to a final concentration of 5 μM in binding buffer [20 mM tris(hydroxymethyl) aminomethane(Tris) pH 7.5, 10 mM MgCl₂, 50 mM KCl] in a final volume of 20 μL and incubated at 37°C for 30 min. In order to facilitate the high throughput screening of 4000 compounds, all these volumes were optimized for robotic handling. Drug distribution was carried out using a pintool that can accurately dispense 200 nL volumes. Fluorescence emission data were collected on an EnVision fluorescent monochromator spectrophotometer (Perkin-Elmer Life Sciences). Excitation wavelength for bis-ANS was set at 372 nm, and emission was captured at 490 nm. All chemical compounds had 99% purity by high performance liquid chromatography (HPLC).

Entamoeba histolytica Culture Experiments

E. histolytica trophozoites (HM1:IMSS strain from ATCC) were maintained in TYI-S-33 medium (20 g casein digest, 10 g yeast extract, 10 g glucose, 2 g sodium chloride, 1 g L-cysteine HCl, 0.2 g ascorbic acid, 1 g K₂HPO₄, 0.6 g KH₂PO₄, 28.75 mg ferric nitrate per liter) that was supplemented with penicillin (100 U/mL), streptomycin (100 μg/mL), and 10% adult bovine serum, under axenic conditions according to the methods of Diamond (Diamond et al., 1978; Debnath et al., 2004, 2005). All of the experiments were conducted with trophozoites that had been harvested during the logarithmic phase of growth. The logarithmic phase of growth was determined by counting the cells using the particle counter (Beckman Coulter) and the cells were maintained in this growth phase by routine passage every 2 days. Compounds were tested for antiparasitic activity using an ATP-bioluminescence based screen for cell growth and survival (Debnath et al., 2012). Assay plates were inoculated with trophozoites (5 × 10³ parasites/well) and incubated in the GasPak™ EZ Anaerobe Gas Generating Pouch Systems (VWR, West Chester, PA) to maintain anaerobic conditions throughout the incubation period. The assays were performed in triplicate using the CellTiter-Glo Luminescent Cell Viability Assay (Promega). Metronidazole was used as a positive control because it is the current treatment for *E. histolytica* infection.

Results

Homology Modeling Reveals Ortholog-specific Residues in the N-terminal ATP-binding Domain of Hsp90

Homology modeling studies using the crystal structures of PfHsp90 (PDB accession no. 3K60) and HsHsp90 (PDB accession no. 2FWZ) and the homology model of EhHsp90 ATP-binding domain suggest that although the pocket is overall very well conserved, there are three corresponding positions that contain unique residues in the three structures (**Figure 1**). Ser52, Asn106, and Lys112 in HsHsp90 correspond to Ala38, Asn92, and Arg98 in PfHsp90 and Cys49, Cys103 and Arg109 in EhHsp90. This finding suggests that the ATP-binding pocket of EhHsp90 may not be as constricted as that of PfHsp90 but it is more hydrophobic than that of PfHsp90 and HsHsp90.

Biochemical Screen with Recombinant EhHsp90 ATP-binding Domain

We have previously reported the results of an initial screen vs. HsHsp90 and PfHsp90 based on competitive inhibition of bis-ANS binding with 4000 compounds consisting of natural compounds [Spectrum], FDA approved drugs [Prestwick], and pharmacologically active compounds [Lopac] (Shahinas et al., 2010). Forty-three compounds were identified that caused a reduction of >70% in fluorescence against HsHsp90 and PfHsp90 ATP binding domains, suggesting competitive inhibition of ATP-binding (Shahinas et al., 2010). This threshold of >70% fluorescence inhibition was set based on Hsp90 inhibition by radicicol, a well-known cross-species Hsp90 inhibitor (Schulte et al., 1998, 1999). Screening of these 43 inhibitors against

the EhHsp90 ATP-binding domain showed that 19 of them competitively inhibit this domain by >70% (**Figure 2**).

Site-directed Mutagenesis of Unique Residues in Orthologous Hsp90 ATP-binding Domains Affects Inhibitor Selectivity

To determine the importance of the three unique positions tabulated in **Figure 1D**, site directed mutants were generated

at each of those sites in the corresponding vectors. The proteins were expressed and the affinity of each mutant for any of the 43 compounds was determined based on competitive inhibition of bis-ANS binding using the same conditions as for the wild-type proteins. Even though, the expression level and yield varied among the different mutants, equal concentration of each protein was used to test competitive inhibition with bis-ANS. The top 10 inhibitors for the

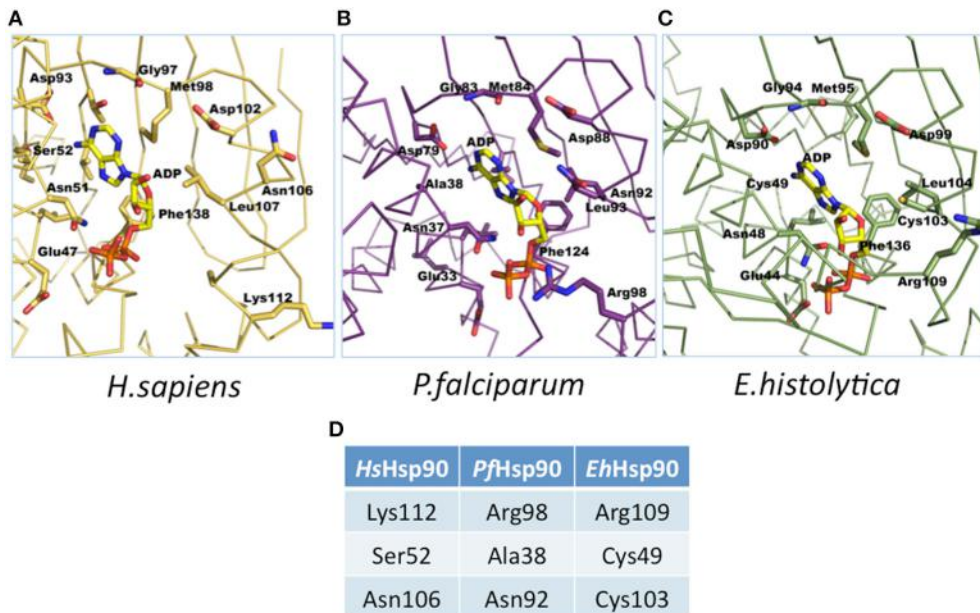


FIGURE 1 | Illustration of ATP binding pocket differences. (A)

Molecular model of adenosine diphosphate (ADP) in the adenosine triphosphate (ATP) binding pocket of human (2FWZ) Hsp90 (HsHsp90). **(B)** Molecular model of ADP in the ATP binding pocket of *P. falciparum* (3K60) Hsp90 (PfHsp90). **(C)** Molecular model of ADP in the ATP binding pocket of *E. histolytica* Hsp90 (EhHsp90) (based on PfHsp90 template: 3K60). **(D)** Summary of the unique residues in the ATP binding pockets of HsHsp90, PfHsp90 and EhHsp90. Please note that these residues are at conserved positions in the 3D model. These residues were mutated by site-directed mutagenesis to examine alterations in binding specificity.

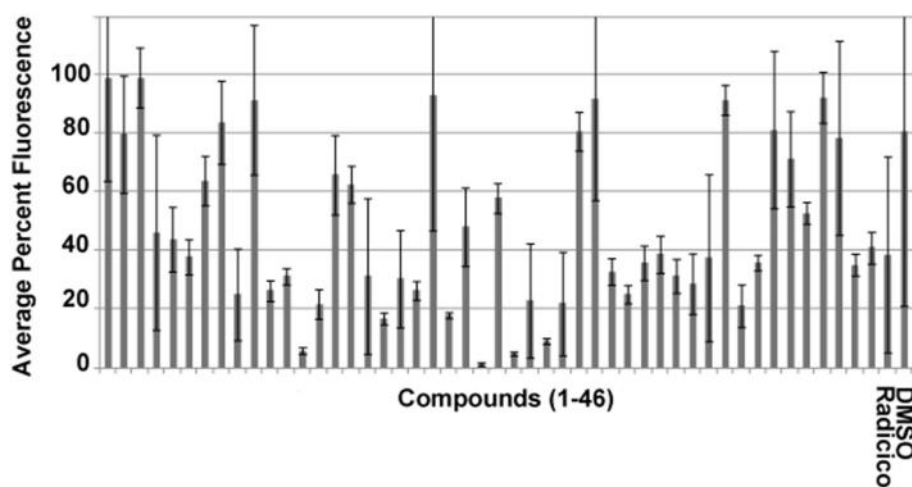


FIGURE 2 | Competitive binding assay using the fluorescent probe bis-ANS for the identification of EhHsp90 inhibitors at a final concentration of 2.5 μ M. The error bars represent standard deviation of duplicate readings. Inhibition is defined as >70% reduction of fluorescence in

this assay. Compounds 1–43 are listed in **Supplementary File 1**. Please note that 48 compounds are shown, of which five could not be obtained any longer from the manufacturer. Therefore, the manuscript focuses on the rest 43 compounds, which were used for downstream assays.

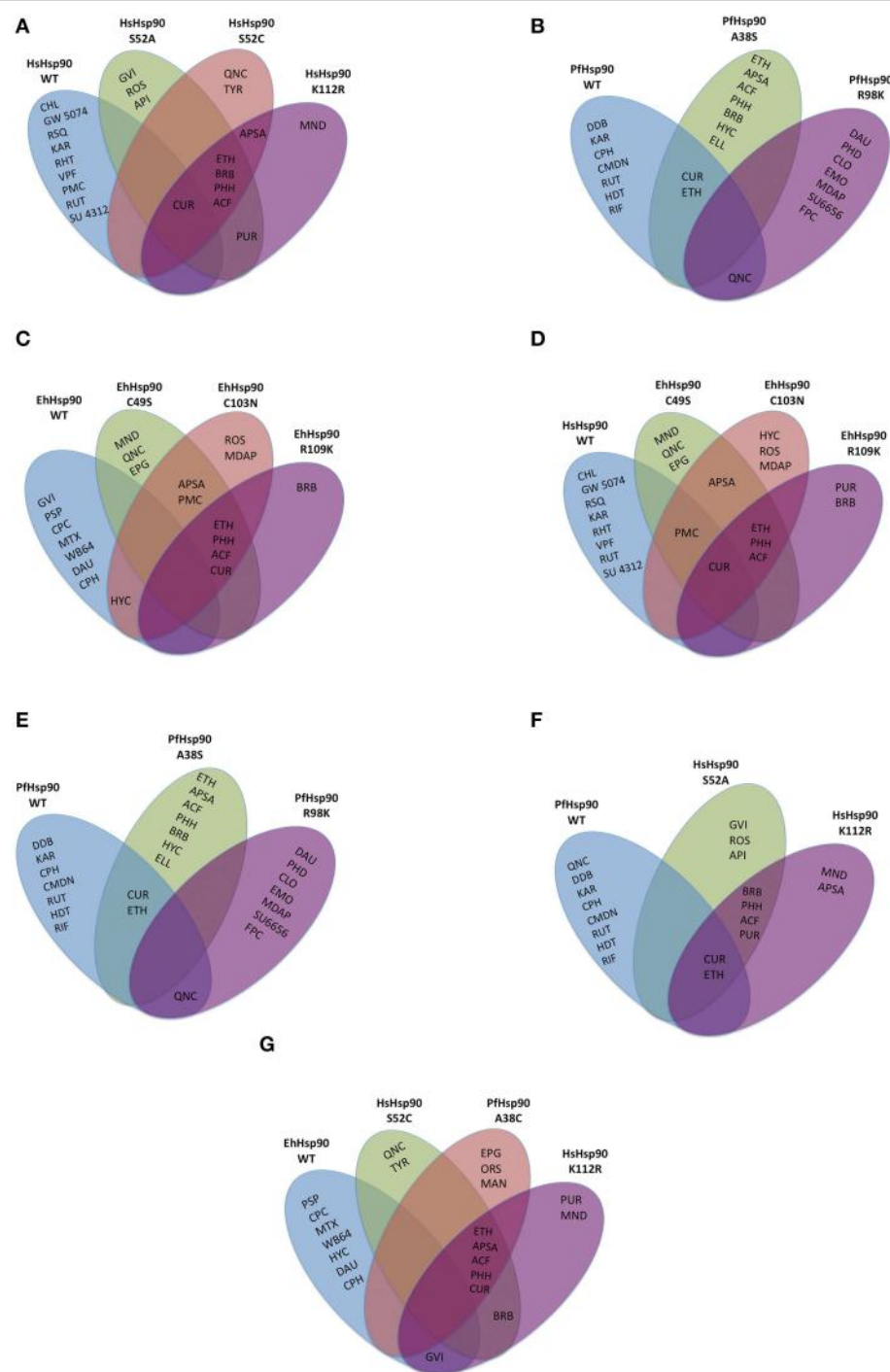


FIGURE 3 | Drug binding specificity of the Hsp90 ATP binding domains and their mutants. Top 10 inhibitors are shown for each of the wild-type (WT) or site-directed mutant ATP binding domains. Any inhibitors in overlapping ovals are not selective. Inhibition was evaluated by competition for bis-ANS binding. Top 10 inhibitors of the HsHsp90 (**A**), PfHsp90 (**B**), EhHsp90 (**C**) ATP binding domains and the mutants generated in each domain, respectively. (**D**) Top 10 inhibitors of HsHsp90 and mutants that

mimic HsHsp90 residues at the corresponding positions (1). (**E**) Top 10 inhibitors of HsHsp90 and mutants that mimic HsHsp90 residues at the corresponding positions (2). (**F**) Top 10 inhibitors of PfHsp90 and mutants that mimic PfHsp90 residues at the corresponding positions. (**G**) Top 10 inhibitors of EhHsp90 and mutants that mimic EhHsp90 residues at the corresponding positions. The abbreviations for the drugs displayed in this figure are listed in **Supplementary File 1**.

wild-type (WT) protein and each mutant are shown relative to each other in the Venn diagrams of **Figure 3**. Venn diagrams show common inhibitors that compete for binding

TABLE 1 | Summary of inhibition results for the EhHsp90 protein screen and the effect of the inhibitors on *E. histolytica* culture.

Compound	Percent inhibition of fluorescence in protein screen at 2.5 μ M (%)	Percent inhibition of <i>E. histolytica</i> growth at 25 μ M (%)
GW5074	70.5	–
Sanguinarine sulfate	71.3	–
Rifabutin	73.7	30
Bilirubin	73.7	–
Clofazimine	73.7	–
Purpurin	75.0	–
Tyrphostin AG 538	75.0	–
Rutilantin	77.1	100
Rifaximin	78.2	–
Berberine chloride	78.3	–
Chlorophyllide	78.9	–
Amodiaquindihydrochloride dihydrate	82.1	–
Daunorubicin hydrochloride	83.2	–
WB 64 (Malachite Green)	84.9	–
Hycanthone	90.9	–
Mitoxantronedihydrochloride	95.3	–
Cetylpyridinium chloride	95.9	42
Pararosanilinepamoate	99.0	81
Gentian Violet	99.3	35

(overlapping ellipses) and unique inhibitors that compete for binding of this ATP binding domain (where no overlap is observed). It is important to note that most of these residues confer selectivity of binding for the 43 inhibitors tested. There are three inhibitors among the 43 tested that show consistent non-selective high inhibition: quinacrine (QNC), curcumin (CUR), and ethaverine hydrochloride (ETH). The abbreviations used for the drugs shown in **Figure 3** are listed in **Supplementary File 1**.

EhHsp90 Inhibitor Effect on Cell Culture

The hits of the protein screen were next tested against a standard lab strain of *E. histolytica* HM1:IMSS *in vitro*. Five out of the 19 EhHsp90 protein hits inhibited *E. histolytica* growth (replication of trophozoites) in the range of 30–100% at the concentration of 25 μ M (**Table 1**). These five compounds were: rifabutin, rutilantin, cetylpyridinium chloride, pararosaniline pamoate, and gentian violet. Based on the site directed mutagenesis experiment outlined above, rifabutin showed the highest inhibition against PfHsp90 and displayed amino acid preferences for A38, N92, and R98. Rutilantin was present in the top 10 inhibitors of the HsHsp90 and PfHsp90 constructs and displayed preference for N106 in HsHsp90 and N92 in the corresponding position of PfHsp90. Pararosaniline pamoate and gentian violet showed highest inhibition for the EhHsp90 construct and displayed preference of binding as assessed by competitive inhibition for C49, C103, and R109. These results are summarized in **Table 2**. From these five compounds, it was possible to obtain titration curves for pararosaniline pamoate and rutilantin with IC50s of 1.1 μ M and 2 μ M, respectively (**Figure 4**).

TABLE 2 | Summary of biochemical specificity results for inhibitors of *E. histolytica* in culture.

Drug	Chemical structure	Highest % inhibition	Amino acid preference
Rifabutin (RIF)		PfHsp90	PfHsp90: A38 + N92 + R98
Rutilantin (RUT)		HsHsp90 & PfHsp90	HsHsp90: N106 PfHsp90: N92
Cetylpyridinium chloride (CPC)		EhHsp90	EhHsp90: C49 + C103 + R109
Pararosaniline pamoate (PSP)		EhHsp90	EhHsp90: C49 + C103 + R109
Gentian Violet (GVI)		EhHsp90	EhHsp90: C49 + C103 + R109 HsHsp90: S52A or K112R

The chemical structures shown here have been adapted from ChemDB (Pavithra et al., 2007; Corbett and Berger, 2010).

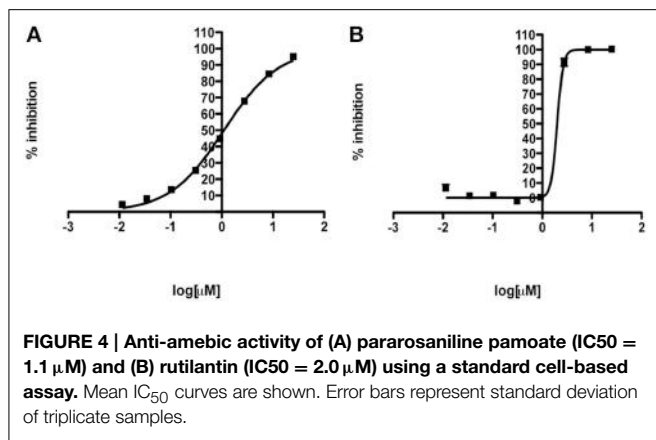


FIGURE 4 | Anti-amebic activity of (A) pararosaniline pamoate ($IC_{50} = 1.1 \mu M$) and (B) rutilantin ($IC_{50} = 2.0 \mu M$) using a standard cell-based assay. Mean IC_{50} curves are shown. Error bars represent standard deviation of triplicate samples.

Discussion

The discovery of five compounds that target HSP90 and inhibit *E. histolytica* growth has significant implications for antiparasitic drug development. Amebiasis caused by *E. histolytica* is responsible for 35–50 million cases of symptomatic disease and about 100,000 deaths per year (Ralston and Petri, 2011b). Parasite cysts are transmitted through contaminated food and water (Stanley, 2003). Currently, nitroimidazoles (metronidazole) are prescribed for treatment, but despite toxic side effects, cure is not reached in 40–60% of the patients (Ralston and Petri, 2011b). In addition, novel drugs for *E. histolytica* are urgently needed as the approved therapy (metronidazole) may result in clinical treatment failure due to resistance.

Infection occurs after ingestion of cysts and may lead to liver abscess (Ralston and Petri, 2011a,b). Parasite excystation in the small intestine produces eight trophozoites per cyst, which colonize the large intestine, existing both in the lumen and attached to mucus and epithelial cells (Petri et al., 2002). Not all strains have the same virulence and are capable of causing liver abscess (Ralston and Petri, 2011b). Chaperoning of virulence factors by stress-inducible Hsp90 is likely to be important. Therefore, inhibition of Hsp90 ATP binding is a compelling strategy for antiparasitic drug design.

Our recombinant Hsp90 ATP-binding domain assay relies on competitive inhibition of bis-ANS competes with ATP for the ATPase domain and emits fluorescence upon binding at the hydrophobic pocket (Wassenberg et al., 2000). This suggests that the hit compounds identified here compete for the ATP-binding domain. While the full binding mode has not been fully elucidated for these hits, the Hsp90 ATP-binding domain contains several basic and hydrophobic residues that are characteristic of protein binding pockets that bind structurally diverse compounds (Dutta and Inouye, 2000).

Only 19 out of the 43 compounds inhibited bis-ANS binding of the EhHsp90 ATP binding domain and 43 of the 43 compounds inhibited the HsHsp90 ATP binding domain. This result suggests that there is sufficient biochemical diversity in this pocket to allow for ortholog selectivity of some of these compounds. This hypothesis was further tested by the site

directed mutagenesis study which showed selective binding of most of the 43 drugs tested upon switch of one of the three unique residues in each of the binding pockets of EhHsp90, PfHsp90, and HsHsp90. This experiment showed that sufficient structural diversity in the ATP-binding pocket of Hsp90 allows for ortholog selectivity of Hsp90 through manipulation of the architecture of EhHsp90, malaria and human Hsp90 by mutagenesis.

The 19 EhHsp90 hits were further tested against live *E. histolytica* trophozoites. Five of the 19 compounds exhibited inhibitory activity *in vitro*. The other 14 compounds may not have been able to penetrate the plasma membrane of the trophozoites *in vitro* or otherwise access EhHsp90. The five inhibitors of EhHsp90 with promising activity against the parasite were rifabutin, rutilantin, cetylpyridinium chloride, pararosaniline pamoate, and gentian violet. Rifabutin is a rifamycin-class antibiotic with an ansamycin moiety (O'Brien et al., 1987, 1990). Ansamycin inhibitors such as geldanamycin are well characterized inhibitors of the chaperone activity of Hsp90 (Bohen, 1998; Onuoha et al., 2007; Porter et al., 2009). Both rifamycin and rifabutin have been used widely against mycobacteria (O'Brien et al., 1987, 1990), but there is no report of their use against amebiasis. Other studies have suggested that rifabutin is effective against cryptosporidiosis, another intestinal parasitic infectious disease (Holmberg et al., 1998; Fichtenbaum et al., 2000). The antibiotic rutilantin has antiphage and antiviral activity (Asheshov and Gordon, 1961; Hume et al., 1965). Cetylpyridinium chloride is an antiseptic compound that is used in mouthwash and other mouth/throat care products (Sheen et al., 2003; Herrera et al., 2005; Gunsolley, 2008; Herrera, 2009; Rioboo et al., 2011). Potent activity has also been reported against a fungal pathogen: *Candida albicans* (Jones et al., 1995). Pararosaniline pamoate has already been used as an antiparasitic drug against schistosomiasis in the Philippines (Pesigan et al., 1967). This compound has shown anti-Hsp90 activity in another high throughput screen as well (United States Patent Application 20110263693). Gentian violet is also known as crystal violet and is one of the constituents of the Gram stain used to visualize bacteria (Berberovic, 1953; Saji et al., 1994). 1% solution of gentian violet is reported as a treatment for *C. albicans* infections (Traboulisi et al., 2011). Gentian violet and pararosaniline pamoate are structurally related molecules (triarylmethanes group). Considering this previous literature and actual usage, these drugs come with known pharmacokinetic, pharmacodynamics, and safety profiles that allow bypassing of the initial evaluation of bioavailability, metabolic stability, adsorption, and excretion.

Conclusion

ATP is required for client protein and co-chaperone binding with Hsp90 (Prodromou et al., 1997). Therefore, inhibition of the Hsp90 ATP binding is lethal in all higher organisms studied to date and may prove effective in the treatment of amebiasis. The efficacy and safety of these candidate drugs needs to be reassessed

in animal models. Even if the repurposed drug candidates reported here do not turn out to be optimal antiamebic agents, they provide a starting point for further structure-based drug design. Novel drugs for amebiasis as well as other neglected tropical diseases are urgently needed and Hsp90 provides a radically new target whereby resistance can be circumvented. The long term goal of these preliminary studies is co-formulation of drug combinations including Hsp90 inhibitors.

References

- Acharya, P., Kumar, R., and Tatu, U. (2007). Chaperoning a cellular upheaval in malaria: heat shock proteins in *Plasmodium falciparum*. *Mol. Biochem. Parasitol.* 153, 85–94. doi: 10.1016/j.molbiopara.2007.01.009
- Asheshov, I. N., and Gordon, J. J. (1961). Rutilantin: an antibiotic substance with antiphage activity. *Biochem. J.* 81, 101–104.
- Bandura, J. L., Jiang, H., Nickerson, D. W., and Edgar, B. A. (2013). The molecular chaperone Hsp90 is required for cell cycle exit in *Drosophila melanogaster*. *PLoS Genet.* 9:e1003835. doi: 10.1371/journal.pgen.1003835
- Banumathy, G., Singh, V., Pavithra, S. R., and Tatu, U. (2003). Heat shock protein 90 function is essential for *Plasmodium falciparum* growth in human erythrocytes. *J. Biol. Chem.* 278, 18336–18345. doi: 10.1074/jbc.M211309200
- Bendesky, A., Menendez, D., and Ostrosky-Wegman, P. (2002). Is metronidazole carcinogenic? *Mutat. Res.* 511, 133–144. doi: 10.1016/S1383-5742(02)00007-8
- Berberovic, M. (1953). [Triphenyl methane dyes (brilliant green and crystal violet) as substitution for gentian violet in bacterial staining according to Gram]. *Hig. Cas. Hig. Mikrobiol. Epidemiol. Sanit. Teh.* 5, 415–418.
- Bohen, S. P. (1998). Genetic and biochemical analysis of p23 and ansamycin antibiotics in the function of Hsp90-dependent signaling proteins. *Mol. Cell. Biol.* 18, 3330–3339.
- Cerchiotti, L. C., Hatzi, K., Caldas-Lopes, E., Yang, S. N., Figueroa, M. E., Morin, R. D., et al. (2010). BCL6 repression of EP300 in human diffuse large B cell lymphoma cells provides a basis for rational combinatorial therapy. *J. Clin. Invest.* 120, 4569–4582. doi: 10.1172/JCI42869
- Cerchiotti, L. C., Lopes, E. C., Yang, S. N., Hatzi, K., Bunting, K. L., Tsikitas, L. A., et al. (2009). A purine scaffold Hsp90 inhibitor destabilizes BCL-6 and has specific antitumor activity in BCL-6-dependent B cell lymphomas. *Nat. Med.* 15, 1369–1376. doi: 10.1038/nm.2059
- Chiosis, G., Caldas Lopes, E., and Solit, D. (2006). Heat shock protein-90 inhibitors: a chronicle from geldanamycin to today's agents. *Curr. Opin. Investig. Drugs* 7, 534–541.
- Corbett, K. D., and Berger, J. M. (2010). Structure of the ATP-binding domain of *Plasmodium falciparum* Hsp90. *Proteins* 78, 2738–2744. doi: 10.1002/prot.22799
- Cowen, L. E., and Lindquist, S. (2005). Hsp90 potentiates the rapid evolution of new traits: drug resistance in diverse fungi. *Science* 309, 2185–2189. doi: 10.1126/science.1118370
- Cowen, L. E., Singh, S. D., Kohler, J. R., Collins, C., Zaas, A. K., Schell, W. A., et al. (2009). Harnessing Hsp90 function as a powerful, broadly effective therapeutic strategy for fungal infectious disease. *Proc. Natl. Acad. Sci. U.S.A.* 106, 2818–2823. doi: 10.1073/pnas.0813394106
- Debnath, A., Akbar, M. A., Mazumder, A., Kumar, S., and Das, P. (2005). *Entamoeba histolytica*: characterization of human collagen type I and Ca²⁺-activated differentially expressed genes. *Exp. Parasitol.* 110, 214–219. doi: 10.1016/j.exppara.2005.03.007
- Debnath, A., Das, P., Sajid, M., and McKerrow, J. H. (2004). Identification of genomic responses to collagen binding by trophozoites of *Entamoeba histolytica*. *J. Infect. Dis.* 190, 448–457. doi: 10.1086/422323
- Debnath, A., Parsonage, D., Andrade, R. M., He, C., Cobo, E. R., Hirata, K., et al. (2012). A high-throughput drug screen for *Entamoeba histolytica* identifies a new lead and target. *Nat. Med.* 18, 956–960. doi: 10.1038/nm.2758
- Diamond, L. S., Harlow, D. R., and Cunnick, C. C. (1978). A new medium for the axenic cultivation of *Entamoeba histolytica* and other *Entamoeba*. *Trans. R. Soc. Trop. Med. Hyg.* 72, 431–432. doi: 10.1016/0035-9203(78)90144-X
- Dutta, R., and Inouye, M. (2000). GHKL, an emergent ATPase/kinase superfamily. *Trends Biochem. Sci.* 25, 24–28. doi: 10.1016/S0968-0004(99)01503-0
- Fichtenbaum, C. J., Zackin, R., Feinberg, J., Benson, C., and Griffiths, J. K. (2000). Rifabutin but not clarithromycin prevents cryptosporidiosis in persons with advanced HIV infection. *AIDS* 14, 2889–2893. doi: 10.1097/00002030-20001220-00010
- Freeman, C. D., Klutman, N. E., and Lamp, K. C. (1997). Metronidazole. A therapeutic review and update. *Drugs* 54, 679–708. doi: 10.2165/00003495-199754050-00003
- Gunsolley, J. C. (2008). Uncontrolled randomized clinical trial demonstrates similar long-term (6 months) antigingivitis and antiplaque efficacy for 2 mouth rinses: one that uses cetylpyridinium chloride (CPC) as an active agent and the other that uses essential oils (EO) as an active agent. *J. Evid. Based Dent. Pract.* 8, 85–86. doi: 10.1016/j.jebdp.2008.03.004
- Herrera, D. (2009). Cetylpyridinium chloride-containing mouth rinses and plaque control. *Evid. Based Dent.* 10, 44. doi: 10.1038/sj.ebd.6400647
- Herrera, D., Santos, S., Ferrus, J., Barbieri, G., Trombelli, L., and Sanz, M. (2005). Efficacy of a 0.15% benzoylamine hydrochloride and 0.05% cetylpyridinium chloride mouth rinse on 4-day de novo plaque formation. *J. Clin. Periodontol.* 32, 595–603. doi: 10.1111/j.1600-051X.2005.00718.x
- Holmberg, S. D., Moorman, A. C., Von Bargen, J. C., Palella, F. J., Loveless, M. O., Ward, D. J., et al. (1998). Possible effectiveness of clarithromycin and rifabutin for cryptosporidiosis chemoprophylaxis in HIV disease. HIV Outpatient Study (HOPS) Investigators. *JAMA* 279, 384–386. doi: 10.1001/jama.279.5.384
- Hume, V., Westwood, J. C., and Appleyard, G. (1965). The anti-viral action of rutilantin. *A. J. Gen. Microbiol.* 38, 143–151. doi: 10.1099/00221287-38-1-143
- Inoue, T., Takamura, K., Yamae, H., Ise, N., Kawakami, M., Tabuse, Y., et al. (2003). *Caenorhabditis elegans* DAF-21 (HSP90) is characteristically and predominantly expressed in germline cells: spatial and temporal analysis. *Dev. Growth Differ.* 45, 369–376. doi: 10.1046/j.1440-169X.2003.00706.x
- Jhaveri, K., Taldone, T., Modi, S., and Chiosis, G. (2011). Advances in the clinical development of heat shock protein 90 (Hsp90) inhibitors in cancers. *Biochim. Biophys. Acta.* 1823, 742–755. doi: 10.1016/j.bbamcr.2011.10.008
- Jones, D. S., Schep, L. J., and Shepherd, M. G. (1995). The effect of cetylpyridinium chloride (CPC) on the cell surface hydrophobicity and adherence of *Candida albicans* to human buccal epithelial cells *in vitro*. *Pharm. Res.* 12, 1896–1900. doi: 10.1023/A:1016231620470
- Kapoor, K., Chandra, M., Nag, D., Paliwal, J. K., Gupta, R. C., and Saxena, R. C. (1999). Evaluation of metronidazole toxicity: a prospective study. *Int. J. Clin. Pharmacol. Res.* 19, 83–88.
- Kumar, R., Pavithra, S. R., and Tatu, U. (2007). Three-dimensional structure of heat shock protein 90 from *Plasmodium falciparum*: molecular modelling approach to rational drug design against malaria. *J. Biosci.* 32, 531–536. doi: 10.1007/s12038-007-0052-x
- Li, J., and Buchner, J. (2013). Structure, function and regulation of the hsp90 machinery. *Biomed. J.* 36, 106–117. doi: 10.4103/2319-4170.113230
- Marubayashi, S., Koppikar, P., Taldone, T., Abdel-Wahab, O., West, N., Bhagwat, N., et al. (2010). HSP90 is a therapeutic target in JAK2-dependent myeloproliferative neoplasms in mice and humans. *J. Clin. Invest.* 120, 3578–3593. doi: 10.1172/JCI42442
- O'Brien, R. J., Geiter, L. J., and Lyle, M. A. (1990). Rifabutin (ansamycin LM427) for the treatment of pulmonary Mycobacterium avium complex. *Am. Rev. Respir. Dis.* 141(4 Pt 1), 821–826. doi: 10.1164/ajrccm/141.4_Pt_1.821
- O'Brien, R. J., Lyle, M. A., and Snider, D. E. Jr. (1987). Rifabutin (ansamycin LM 427): a new rifamycin-S derivative for the treatment of mycobacterial diseases. *Rev. Infect. Dis.* 9, 519–530. doi: 10.1093/clinids/9.3.519

Supplementary Material

The Supplementary Material for this article can be found online at: <http://journal.frontiersin.org/article/10.3389/fmicb.2015.00368/abstract>

Supplementary File 1 | The list of chemical name abbreviations used throughout the manuscript.

Supplementary File 2 | List of primers used for site-directed mutagenesis.

- Onuoha, S. C., Mukund, S. R., Coulstock, E. T., Sengerova, B., Shaw, J., McLaughlin, S. H., et al. (2007). Mechanistic studies on Hsp90 inhibition by ansamycin derivatives. *J. Mol. Biol.* 372, 287–297. doi: 10.1016/j.jmb.2007.06.065
- Pallavi, R., Roy, N., Nageshan, R. K., Talukdar, P., Pavithra, S. R., Reddy, R., et al. (2010). Heat shock protein 90 as a drug target against protozoan infections: biochemical characterization of HSP90 from *Plasmodium falciparum* and *Trypanosoma evansi* and evaluation of its inhibitor as a candidate drug. *J. Biol. Chem.* 285, 37964–37975. doi: 10.1074/jbc.M110.155317
- Pavithra, S. R., Banumathy, G., Joy, O., Singh, V., and Tatu, U. (2004). Recurrent fever promotes *Plasmodium falciparum* development in human erythrocytes. *J. Biol. Chem.* 279, 46692–46699. doi: 10.1074/jbc.M409165200
- Pavithra, S. R., Kumar, R., and Tatu, U. (2007). Systems analysis of chaperone networks in the malarial parasite *Plasmodium falciparum*. *PLoS Comput. Biol.* 3, 1701–1715. doi: 10.1371/journal.pcbi.0030168
- Pesigan, T. P., Banzon, T. C., Santos, A. T., Nosenas, J., and Zabala, R. G. (1967). Pararosaniline pamoate (CI-403-A) in the treatment of Schistosoma japonicum infection in the Philippines. *Bull. World Health Organ.* 36, 263–274.
- Petri, W. A. Jr., Haque, R., and Mann, B. J. (2002). The bittersweet interface of parasite and host: lectin-carbohydrate interactions during human invasion by the parasite *Entamoeba histolytica*. *Annu. Rev. Microbiol.* 56, 39–64. doi: 10.1146/annurev.micro.56.012302.160959
- Porter, J. R., Ge, J., Lee, J., Normant, E., and West, K. (2009). Ansamycin inhibitors of Hsp90: nature's prototype for anti-chaperone therapy. *Curr. Top. Med. Chem.* 9, 1386–1418. doi: 10.2174/15680260978995719
- Prodromou, C., Roe, S. M., O'Brien, R., Ladbury, J. E., Piper, P. W., and Pearl, L. H. (1997). Identification and structural characterization of the ATP/ADP-binding site in the Hsp90 molecular chaperone. *Cell* 90, 65–75. doi: 10.1016/S0092-8674(00)80314-1
- Ralston, K. S., and Petri, W. A. (2011a). The ways of a killer: how does *Entamoeba histolytica* elicit host cell death? *Essays Biochem.* 51, 193–210. doi: 10.1042/bse0510193
- Ralston, K. S., and Petri, W. A. Jr. (2011b). Tissue destruction and invasion by *Entamoeba histolytica*. *Trends Parasitol.* 27, 254–263. doi: 10.1016/j.pt.2011.02.006
- Rioboo, M., Garcia, V., Serrano, J., O'Connor, A., Herrera, D., and Sanz, M. (2011). Clinical and microbiological efficacy of an antimicrobial mouth rinse containing 0.05% cetylpyridinium chloride in patients with gingivitis. *Int. J. Dent. Hyg.* 10, 98–106. doi: 10.1111/j.1601-5037.2011.00523.x
- Saji, M., Taguchi, S., Shikida, R., and Ohkuni, H. (1994). [Bactericidal effects of gentian violet (Gv) and acrinol (Ac) against methicillin-resistant *Staphylococcus aureus* (MRSA) and gram-negative bacteria isolated from clinical materials]. *Kansenshogaku Zasshi* 68, 1287–1289. doi: 10.11150/kansenshogakuzasshi1970.68.1287
- Schulte, T. W., Akinaga, S., Murakata, T., Agatsuma, T., Sugimoto, S., Nakano, H., et al. (1999). Interaction of radicicol with members of the heat shock protein 90 family of molecular chaperones. *Mol. Endocrinol.* 13, 1435–1448. doi: 10.1210/mend.13.9.0339
- Schulte, T. W., Akinaga, S., Soga, S., Sullivan, W., Stensgard, B., Toft, D., et al. (1998). Antibiotic radicicol binds to the N-terminal domain of Hsp90 and shares important biologic activities with geldanamycin. *Cell Stress Chaperones* 3, 100–108.
- Shahinas, D., Liang, M., Datti, A., and Pillai, D. R. (2010). A repurposing strategy identifies novel synergistic inhibitors of *Plasmodium falciparum* heat shock protein 90. *J. Med. Chem.* 53, 3552–3557. doi: 10.1021/jm901796s
- Sheen, S., Eisenburger, M., and Addy, M. (2003). Effect of toothpaste on the plaque inhibitory properties of a cetylpyridinium chloride mouth rinse. *J. Clin. Periodontol.* 30, 255–260. doi: 10.1034/j.1600-051X.2003.300312.x
- Stanley, S. L. Jr. (2003). Amoebiasis. *Lancet* 361, 1025–1034. doi: 10.1016/S0140-6736(03)12830-9
- Taldone, T., Gillan, V., Sun, W., Rodina, A., Patel, P., Maitland, K., et al. (2010). Assay strategies for the discovery and validation of therapeutics targeting *Brugia pahangi* Hsp90. *PLoS Negl. Trop. Dis.* 4:e714. doi: 10.1371/journal.pntd.0000714
- Traboulisi, R. S., Mukherjee, P. K., Chandra, J., Salata, R. A., Jurevic, R., and Ghannoum, M. A. (2011). Gentian violet exhibits activity against biofilms formed by oral *Candida* isolates obtained from HIV-infected patients. *Antimicrob. Agents. Chemother.* 55, 3043–3045. doi: 10.1128/AAC.01601-10
- Usmani, S. Z., and Chiosis, G. (2011). HSP90 inhibitors as therapy for multiple myeloma. *Clin. Lymphoma Myeloma Leuk.* 11(Suppl. 1), S77–S81. doi: 10.1016/j.clml.2011.03.027
- Walsh, J. A. (1986). Problems in recognition and diagnosis of amebiasis: estimation of the global magnitude of morbidity and mortality. *Rev. Infect. Dis.* 8, 228–238. doi: 10.1093/clinids/8.2.228
- Wassenberg, J. J., Reed, R. C., and Nicchitta, C. V. (2000). Ligand interactions in the adenosine nucleotide-binding domain of the Hsp90 chaperone, GRP94. II. Ligand-mediated activation of GRP94 molecular chaperone and peptide binding activity. *J. Biol. Chem.* 275, 22806–22814. doi: 10.1074/jbc.M001476200
- Wider, D., Peli-Gulli, M. P., Briand, P. A., Tatu, U., and Picard, D. (2009). The complementation of yeast with human or *Plasmodium falciparum* Hsp90 confers differential inhibitor sensitivities. *Mol. Biochem. Parasitol.* 164, 147–152. doi: 10.1016/j.molbiopara.2008.12.011

Conflict of Interest Statement: The authors declare that the research was conducted in the absence of any commercial or financial relationships that could be construed as a potential conflict of interest.

Copyright © 2015 Shahinas, Debnath, Benedict, McKerrow and Pillai. This is an open-access article distributed under the terms of the Creative Commons Attribution License (CC BY). The use, distribution or reproduction in other forums is permitted, provided the original author(s) or licensor are credited and that the original publication in this journal is cited, in accordance with accepted academic practice. No use, distribution or reproduction is permitted which does not comply with these terms.

Phenotypic and transcriptional profiling in *Entamoeba histolytica* reveal costs to fitness and adaptive responses associated with metronidazole resistance

OPEN ACCESS

Edited by:

Arjan Debnath,
University of California, San Diego,
USA

Reviewed by:

Yuji Morita,
Aichi Gakuin University, Japan
Upinder Singh,
Stanford University, USA

*Correspondence:

Tomoyoshi Nozaki,
Department of Parasitology, National
Institute of Infectious Diseases,
Toyama 1-23-1, Shinjuku-ku, Tokyo
162-8640, Japan
nozaki@nih.go.jp

†Present Address:

Gil M. Penuliar,
Institute of Biology, College of
Science, University of the Philippines,
Quezon City, Philippines

Specialty section:

This article was submitted to
Antimicrobials, Resistance and
Chemotherapy,
a section of the journal
Frontiers in Microbiology

Received: 13 February 2015

Accepted: 08 April 2015

Published: 05 May 2015

Citation:

Penuliar GM, Nakada-Tsukui K and
Nozaki T (2015) Phenotypic and
transcriptional profiling in *Entamoeba histolytica* reveal costs to fitness and
adaptive responses associated with
metronidazole resistance.
Front. Microbiol. 6:354.
doi: 10.3389/fmicb.2015.00354

Gil M. Penuliar^{1,2†}, Kumiko Nakada-Tsukui¹ and Tomoyoshi Nozaki^{1,3*}

¹ Department of Parasitology, National Institute of Infectious Diseases, Tokyo, Japan, ² Department of Parasitology, Gunma University Graduate School of Medicine, Maebashi, Japan, ³ Graduate School of Life and Environmental Sciences, University of Tsukuba, Tsukuba, Japan

Antimicrobial chemotherapy is critical in the fight against infectious diseases caused by *Entamoeba histolytica*. Among the drugs available for the treatment of amebiasis, metronidazole (MTZ) is considered the drug of choice. Recently, *in vitro* studies have described MTZ resistance and the potential mechanisms involved. Costs to fitness and adaptive responses associated with resistance, however, have not been investigated. In this study we generated an HM-1 derived strain resistant to 12 μM MTZ (MTZR). We examined its phenotypic and transcriptional profile to determine the consequences and mRNA level changes associated with MTZ resistance. Our results indicated increased cell size and granularity, and decreased rates in cell division, adhesion, phagocytosis, cytopathogenicity, and glucose consumption. Transcriptome analysis revealed 142 differentially expressed genes in MTZR. In contrast to other MTZ resistant parasites, MTZR did not down-regulate pyruvate:ferredoxin oxidoreductase, but showed increased expression of genes for a hypothetical protein (HP1) and several iron-sulfur flavoproteins, and downregulation of genes for leucine-rich proteins. Fisher's exact test showed 24 significantly enriched GO terms in MTZR, and a 3-way comparison of modulated genes in MTZR against those of MTZR cultured without MTZ and HM-1 cultured with MTZ, showed that 88 genes were specific to MTZR. Overall, our findings suggested that MTZ resistance is associated with specific transcriptional changes and decreased parasite virulence.

Keywords: *Entamoeba histolytica*, metronidazole, drug resistance, transcriptome

Introduction

Currently, 500 million cases of amebiasis are reported each year (World Health Organization Amoebiasis, 1997). Most of these cases are children from developing nations, who are particularly vulnerable to infectious diseases (Marie and Petri, 2014). Among the drugs available for the treatment of amebic dysentery and amebic liver abscess, metronidazole (MTZ) is one of the most widely used, and is often considered the drug of choice (Löfmark et al., 2010). Treatment with MTZ is usually very effective, i.e., no clinical isolates with high levels of resistance have been observed.

However, reports of patients refractory to the drug are documented (Koutsaimanis et al., 1979; Dooley and O'Morain, 1988). In addition, *in vitro* studies on the induction of MTZ resistance in *Entamoeba histolytica* are described (Samarawickrema et al., 1997; Wassmann et al., 1999). Coincidentally, clinical and *in vitro* resistance to the drug in *Trichomonas vaginalis* (Müller et al., 1980; Wright et al., 2010), *Giardia lamblia* (Müller et al., 2007; Tejman-Yarden et al., 2011), *Blastocystis* spp. (Mirza et al., 2011a,b), *Neisseria gonorrhoeae* (Yoshikawa et al., 1974), and several anaerobic bacteria (Pumbwe et al., 2007; Peláez et al., 2008; Tanih et al., 2011) have also been reported since the drug was introduced in 1960 (Figure S1) (Durel et al., 1960). Based on these findings, it is reasonable to assume that clinical resistance to MTZ might soon be reported in *E. histolytica*.

Unlike aerobic cells, anaerobic organisms are sensitive to MTZ because their electron transport proteins have sufficient negative redox potential that can activate MTZ (Samuelson, 1999). After entering the cell, the drug is reduced to a cytotoxic nitro radical anion by electron donors like thioredoxin reductase and ferredoxin (Fdx), which in turn serve as electron acceptors for pyruvate:ferredoxin oxidoreductase (PFOR) (Samuelson, 1999; Leitsch et al., 2007). The nitro radical anion is reduced further to a nitrosoimidazole, and further reduction leads to the formation of hydroxylamine and eventually to an amine (West et al., 1982; Moreno and Docampo, 1985; Ludlum et al., 1988). In *E. histolytica*, the actual mechanism of action is not fully understood, but evidences from other organisms suggest inhibition of DNA synthesis, and damage to DNA, protein, and other cell components by oxidation and adduct formation (Ludlum et al., 1988; Sisson et al., 2000; Leitsch et al., 2007).

A few mechanisms have been proposed to explain how pathogens survive MTZ treatment. The process varies among organisms, but the general principle includes at least one of the following: altered reduction efficiency (Leiros et al., 2004), drug inactivation (Ralph and Clarke, 1978), reduced drug uptake (Lacey et al., 1993), active efflux (Pumbwe et al., 2007), and increased DNA damage repair (Land and Johnson, 1999). In *E. histolytica*, Samarawickrema et al. (1997) reported the increased expression of iron-containing superoxide dismutase (Fe-SOD) in a strain resistant to 10 μ M MTZ, while Wassmann et al. (1999) showed that in addition to Fe-SOD upregulation, resistance to 40 μ M MTZ was associated with increased peroxiredoxin (Prx) expression and decreased expression of Fdx. On the contrary, Tazreiter et al. (2008) showed no substantial increase in Fe-SOD expression and less than 3-fold upregulation of Fdx and Prx in cells exposed to 50 μ M MTZ. In addition, all three studies did not find any significant changes in PFOR expression, indicating that its downregulation may not be mandatory for low to modest drug resistance in this parasite. Studies on MTZ resistance in *T. vaginalis* and *G. lamblia* also showed variable results regarding the role of PFOR (Quon et al., 1992; Rasoloson et al., 2002; Müller et al., 2008; Leitsch et al., 2011). Strains of *T. vaginalis* deficient in PFOR activity, for example, showed only low levels of anaerobic resistance to MTZ (Rasoloson et al., 2002). In addition, some clinical strains exhibited resistance only under aerobic conditions, and were completely sensitive to MTZ in the

absence of oxygen (Rasoloson et al., 2002). These strains also showed no decrease in PFOR activity (Rasoloson et al., 2002). Other reports, however, have shown decreased Fdx levels in MTZ resistant trichomonads (Ralph et al., 1974; Yarlett et al., 1986) and anaerobic resistance that was correlated with decreased PFOR activity (Kulda et al., 1989). From these results, it is conceivable that different pathways are involved in drug activation, and that various mechanisms for MTZ resistance exist in protozoa.

Currently, most of the work done in *E. histolytica* focused either on pathways known to activate, i.e., chemically reduce, MTZ (Leitsch et al., 2007) or antioxidants that counteract oxidative stress, such as pyruvate:ferredoxin oxidoreductase, superoxide dismutase, and peroxiredoxin (Samarawickrema et al., 1997; Wassmann et al., 1999). Fitness costs and adaptive responses have not yet been examined. In this study we generated an *E. histolytica* HM-1-derived isogenic strain resistant to 12 μ M MTZ (MTZR). By comparing its phenotype and transcriptional profile against the parental strain, our goal was to identify phenotypic and transcriptional changes related to or involved in MTZ resistance. We compared the transcriptome of a single MTZR line cultured with MTZ [MTZR (+)] against MTZR cultured without the drug [MTZR (-)], and HM-1 exposed to MTZ [HM-1 (+)] to determine the significance of the genes we identified. Finally, to verify their involvement in resistance, some genes were overexpressed by episomal transfection, followed by drug challenge.

Materials and Methods

Chemicals and Reagents

MTZ, ornidazole, emetine, chloroquine, paromomycin, L-cysteine, and N-(trans-Epoxysuccinyl)-L-leucine 4-guanidinobutyramide (E-64) were purchased from Sigma-Aldrich (St. Louis, MO, USA), while tinidazole was acquired from LTK Laboratories (St. Paul, MN, USA). DNazol reagent, TRIzol reagent, PLUS reagent, Lipofectamine, and genetin (G418) were secured from Invitrogen (Carlsbad, CA, USA). All other chemicals were obtained from Wako Pure Chemical Industries (Osaka, Japan) unless otherwise stated. Drugs were dissolved either in distilled water or dimethyl sulfoxide (DMSO) to a stock concentration of 100 mM and stored at -30°C .

Cultivation and Induction of MTZ Resistance

E. histolytica strain HM-1:IMSS cl6 (HM-1) (Diamond et al., 1972) was cultured under axenic conditions in 6 mL BI-S-33 medium (BIS) at 35.5°C in 13 \times 100 mm Pyrex screw cap culture tubes (Corning, Corning, NY) (Diamond et al., 1978). Induction of MTZ resistance was initiated when cells in mid-logarithmic phase of growth were exposed to 1 μ M of the drug until late logarithmic phase. In this study, cultures with cell concentrations between 4×10^4 and 2×10^5 /mL were considered to be in mid-logarithmic phase, and corresponds to cell densities after 1 and 2 days, respectively, after the cultures were initiated with at $2-5 \times 10^4$ trophozoites per mL. The drug concentration was increased by 1 μ M until it reached 4 μ M. Cells were maintained with the same dose for 4 weeks before further increase in drug concentration was made. A strain growing at 12 μ M MTZ

[MTZR (+)] was obtained approximately after 28 weeks, and was used in all experiments. MTZR was also cultured without the drug [MTZR (-)] for 24 h up to 1 week when we tested for reversibility of resistance and when samples were prepared for microarray.

Cultivation of Chinese Hamster Ovary (CHO) Cells

CHO cells, a gift from Dr. Kentaro Hanada, were cultured in Ham's F-12 medium (GIBCO, Invitrogen Co., Auckland, New Zealand) with 10% fetal calf serum (Medical Biological Laboratory International, Woburn, MA, USA) in 25 cm² canted neck culture flasks (IWAKI, Tokyo, Japan) at 37°C with humidified air and 5% CO₂.

Growth Kinetics

After trophozoite cultures in mid-log phase of HM-1 and MTZR were placed on ice for 5 min to detach cells from the glass surface, cells were collected by centrifugation 500 × g for 5 min at room temperature. After centrifugation, spent medium was discarded and the pellet was resuspended in 1–2 mL of BIS medium. The cell number was estimated on a haemocytometer. Approximately 6 × 10⁴ trophozoites were inoculated in 6 mL BIS medium with or without 12 µM MTZ, and the cultures were examined every 24 h for 5 days. Trypan blue exclusion assay was used to determine the number of viable cells in duplicate cultures (Penuliar et al., 2011).

Half Maximal Inhibitory Concentration (IC₅₀) and Cross-Resistance

Trophozoites in mid-log phase of HM-1 and MTZR were harvested, resuspended in BIS medium as described above, and the concentration was adjusted to 1 × 10⁵ cells/mL. About 1 × 10⁴ cells in 100 µL BIS were seeded per well of a 96-well microtiter plate (Iwaki, Tokyo, Japan) and incubated at 35.5°C for 1 h under anaerobic conditions using Anaerocult A (Merck, Darmstadt, Germany). One hundred microliters of BIS containing 2-fold increases in concentration of the drugs listed in Table 1 was added, and the plates incubated for 24 and 48 h. The medium was removed and replaced with 200 µL 10% WST-1 reagent (Roche, Indianapolis, IN, USA) in phosphate-buffered saline (PBS) and the plates incubated for 20–40 min. Optical density at 450 nm was measured using a DTX 880 Multimode Detector (Beckman Coulter, Fullerton, CA, USA). The percentage of viable cells was calculated after subtraction of background absorbance as % viability = (absorbance of treated cells/absorbance of untreated cells) × 100%. IC₅₀ values were calculated using the sigmoidal dose-response equation in GraphPad Prism 5.0 (GraphPad Software, La Jolla, CA, USA). All experiments were repeated three times with two replicates per experiment. To assay the hydrogen peroxide sensitivity of the transformants harboring one of the following plasmids: HP1-HA, ISF1-HA, ISF2-HA, ISF4-HA, and pEhEx-HA, about 1 × 10⁴ cells were seeded per well of a 96-well microtiter plate and incubated at 35.5°C for 12–16 h under anaerobic conditions. The cells were then exposed to 25–1600 µM of hydrogen peroxide for 4 h. Then the cell viability was measured by using WST-1 reagent as described above.

TABLE 1 | IC₅₀ of drugs used to treat amebiasis and hydrogen peroxide in HM-1 and MTZR.

Compound	Description	HM-1	MTZR	RI ^a
Chloroquine	Amebicide	1562.7 ± 0.3	3125.3 ± 0.4	2.0
Emetine	Amebicide	12.8 ± 0.3	50.3 ± 0.3	3.9
Metronidazole	Amebicide	6.5 ± 0.3	12.9 ± 0.3	2.0
Ornidazole	Amebicide	6.5 ± 0.3	12.3 ± 0.3	1.9
Paromomycin	Amebicide	12.6 ± 0.4	25.1 ± 0.3	2.0
Tinidazole	Amebicide	12.6 ± 0.2	24.9 ± 0.3	2.0
Hydrogen peroxide	Stress inducer	244.2 ± 0.4	488.1 ± 0.3	2.0

^aResistance index values are determined by dividing the IC₅₀ of drug in MTZR by that in HM-1.

CHO Monolayer Destruction Assay

Rate of CHO monolayer destruction was measured as described previously with minor modifications (Penuliar et al., 2011). Briefly, CHO cells in logarithmic phase of growth were prepared as follows. After spent medium was discarded, CHO cells were incubated with trypsin-EDTA at 37°C for 5 min to detach cells. Cells were transferred to a 50 mL tube containing 5 mL of Ham's F-12 medium and cell density was estimated on a haemocytometer. Cells were collected by centrifugation at 500 × g for 10 min at room temperature. After the supernatant was discarded, the cell pellet was re-suspended in Ham's F-12 medium at 1 × 10⁵ CHO cells per mL. Approximately 100 µL of the CHO suspension was dispensed into each well on a 96-well plate and the plate was incubated at 37°C as described (Penuliar et al., 2011) for 24–48 h until CHO cells form a monolayer. The medium was removed and the plates washed twice with warm PBS. Approximately 1 × 10⁴ cells of HM-1 and MTZR were resuspended in 200 µL Opti-MEM medium (GIBCO, Invitrogen Co., Auckland, New Zealand) and added to each well. The plates were incubated under anaerobic conditions at 35.5°C for 15 min intervals up to 2 h. The plates were placed on ice for 15 min to release adhered trophozoites and washed twice with cold PBS. The percentage of CHO monolayer destroyed was determined relative to wells without the ameba using 10% WST-1.

Substrate Gel Electrophoresis

Proteinase activity was detected by substrate gel electrophoresis as described previously (Hellberg et al., 2000). Briefly, 20 µg of cell lysate from HM-1 and MTZR strains were separated in a 12% [w/v] sodium dodecyl sulfate (SDS)-polyacrylamide gel copolymerized with 0.1% [w/v] gelatin. The gel was incubated in 2.5% [v/v] Triton X-100 for 1 h and then in 100 mM sodium acetate, pH 4.5, 1% [v/v] Triton X-100, and 20 mM dithiothreitol for 3 h at 37°C. Bands were visualized after staining with 0.5% [w/v] Coomassie Brilliant Blue R-250.

Phagocytosis Assay

Trophozoites of HM-1 and MTZR in mid-logarithmic phase of growth were harvested, resuspended in BIS medium as described above, and the concentration was adjusted to 1 × 10⁶ cells/mL. Approximately 1.0 × 10⁶ of HM-1 and MTZR trophozoites

were seeded on each well of 12-well plates. Spent medium was removed and replaced with 500 µL warmed BIS with 1.5×10^7 FluoSpheres carboxylate-modified (2.0 µm) Nile Red fluorescent beads (Invitrogen, Eugene, OR, USA). The plates were sealed and incubated at 35.5°C for up to 80 min. After incubation, 500 µL of PBS containing 2% galactose was added and the plates incubated on ice for at least 20 min. Formaldehyde was added to a final concentration of 4% and plates incubated on ice for 1 h. The cells were collected, washed three times with cold PBS and analyzed by flow cytometry as previously described (Nakada-Tsukui et al., 2005). Cells that ingested the beads were gated based on increased fluorescence compared to control non-phagocytic cells.

Glucose Consumption

Trophozoites of HM-1 and MTZR in mid-logarithmic phase of growth were harvested, resuspended in BIS medium as described above, and the concentration was adjusted to 1×10^7 cells/mL. Approximately 1×10^7 cells were seeded in 6-well dishes and incubated for 12 and 24 h. Spent medium was decanted and centrifuged at $500 \times g$ for 5 min. Glucose consumption was determined from the clarified medium using a Glucose (GO) Assay kit (Sigma Aldrich, Saint Louis, MO, USA) according to manufacturer's protocol.

Estimation of Total Protein Amount in a Single Cell

Trophozoites of HM-1 and MTZR in mid-logarithmic phase of growth were harvested as described above. Cell pellet was re-suspended in PBS at 1×10^6 /mL. Approximately 500 µL of the cell suspension were dispensed to a 1.5 mL tube and the cells were collected by centrifugation at $500 \times g$ for 3 min at 4°C. After the supernatant was carefully removed, the cell pellet was lysed with 50 µL of lysis buffer [50 mM Tris-HCl, pH 7.5, 150 mM NaCl, 1% Triton-X 100, complete mini EDTA-free protease inhibitor cocktail (Roche Molecular Biochemicals, Mannheim, Germany) and 200 mM E-64]. Protein amount of the lysate were quantified by DC protein assay kit (Bio-Rad Laboratories, Inc., Hercules, CA, USA).

RNA Isolation

HM-1 and MTZR were cultured with and without 12 µM MTZ in 25 cm² tissue culture flasks. HM-1 cultured with the drug was incubated for 5 h [(HM-1 (+)], while MTZR without MTZ was maintained for 1 week [(MTZR (-)]. Except for HM-1 (+), the spent medium for all other cultures were removed and replaced with fresh BIS with and without the drug and the flasks incubated at 35.5°C for 5 h. Total RNA was extracted with TRIzol Reagent according to the manufacturer's instructions for cells grown in monolayers; cleaned with RNeasy kit (Qiagen, Hilden, Germany), and assessed for quality with the Experion automated electrophoresis system and Experion RNA StdSens analysis kit (Bio-Rad Laboratories, Inc., Hercules, CA, USA). RNA quantity was determined by measuring the absorbance at 260 nm with NanoDrop ND-1000 UV-Vis spectrophotometer (NanoDrop Technologies, Wilmington, DE, USA).

Microarray Hybridization

Samples from two independent RNA extractions were processed using Ambion MessageAmpTM Premier RNA Amplification Kit (Applied Biosystems, Foster City, CA, USA) according to manufacturer's instructions. Fragmented cRNA was then hybridized onto a probe array chip (Eh_Eia520620F) that was custom-made by Affymetrix (Santa Clara, CA, USA) (Husain et al., 2011; Penuliar et al., 2012) using kits and protocols specified in the Affymetrix GeneChip Expression Analysis Technical Manual (Affymetrix, Santa Clara, CA, USA). Following hybridization, arrays were washed, stained with streptavidin-phycoerythrin (Molecular Probes, Eugene, OR, USA) using Affymetrix GeneChip Fluidics Station 450, and scanned with an Affymetrix GeneChip Scanner 3000 at 570 nm. Each array image was visually screened to check for scratches, signal artifacts, and debris.

The microarray used in this study was made based on *E. histolytica* and *E. invadens* sequences stored at TIGR and Pathema databases (Loftus et al., 2005; <http://amoebadb.org/amoeba/>). It contained 9230 probe sets for *E. histolytica* and an additional 25 and 81 control probe sets for *Entamoeba* and Affymetrix, respectively (Eh_Eia520620F_Eh). Nomenclature for the IDs was based on whether the probe set is unique to either Pathema (e.g., EHI_123456) or TIGR (e.g., 12.m00345), or is found in both databases (e.g., 98.m00765_234567). Probe sets labeled with “_at” represent a single gene, while those labeled with “_s_at” represent probe sets that share all probes identically with at least two sequences. The “_s_at” probe sets represent highly similar transcripts, shorter forms of alternatively polyadenylated transcripts, or common regions in the 3' ends of multiple alternative splice forms. Probe sets labeled with “_x_at,” on the other hand, represent probe sets where it was not possible to select either a unique probe set or a probe set with identical probes among multiple transcripts. These probe sets could cross-hybridize with other genes in an unpredictable manner (Affymetrix, Santa Clara, CA, USA).

Data Normalization, Analysis, and Deposition

Raw probe intensities were generated by the GeneChip Operating Software (GCOS) and GeneTitan Instrument from Affymetrix. Resulting expression values were analyzed by R/BioConductor and GeneSpring GX Ver.11.5 to identify differentially expressed genes. Reproducibility of the experiments was determined by Pearson's correlation coefficient and confirmed by principal component analysis (Pearson, 1901; Stigler, 1989). Only genes that were considered “present” by GCOS in both arrays were used in further analysis. Gene probe sets were considered differentially expressed between samples if they had at least a 3-fold change and a *P*-value < 0.05 , calculated using Welch's *t*-test (Welch, 1947), after multiple test correction by the Benjamini–Hochberg method (Benjamini and Hochberg, 1995). A *post-hoc* test using Tukey's Honestly Significant Difference test was conducted to determine significant differences between samples (Tukey, 1949). Probe sets ending with “_x_at” were removed together with redundant genes identified by sequence alignment using ClustalW2.48 Finally, RefSeq's annotated pseudogenes were omitted from

the final list (ClustalW2; <http://www.ebi.ac.uk/Tools/msa/clustalw2/>).

Nucleotide sequences of differentially expressed genes were searched against GenBank (<http://www.ncbi.nlm.nih.gov/genbank/>) and Amoeba DB (<http://amoebadb.org/amoeba/>) by using Basic Local Alignment Search Tool (BLAST; <http://blast.ncbi.nlm.nih.gov/Blast.cgi>). Matches against hypothetical proteins (HP) with E -value $< e^{-50}$ and maximal scoring pair alignment that covered at least 40% were considered as putative orthologs (McLysaght et al., 2003). Hierarchical clustering of modulated genes in MTZR, MTZR (−), and HM-1 (+) was performed with Cluster 3.0 (<http://bonsai.hgc.jp/~mdehoon/software/cluster/software.htm>) using average linkage, while dendograms and heatmaps were generated with Java TreeView version 1.1.6r2. (<http://jtreeview.sourceforge.net>) Gene Ontology (GO) annotations were mined from the Gene Ontology Annotation Database (<http://www.ebi.ac.uk>), and Amoeba DB. GO term enrichment was computed using Fisher's exact test (Agresti, 1992), against a background consisting of all GO IDs for genes symbols beginning with EHI, which were downloaded from the QuickGO database of European Molecular Biology Laboratory - European Bioinformatics Institute (EMBL-EBI) (Taxon ID: 5759) (<http://www.ebi.ac.uk/QuickGO/>). Genomic location of each gene was obtained from Pathema-Entamoeba (<http://pathema.jcvi.org>) while transmembrane domain prediction was performed using the following online servers: HMMTOP (<http://www.enzim.hu>), SOSUI (<http://bp.nuap.nagoya-u.ac.jp>), TMHMM (<http://www.cbs.dtu.dk>), TopPred (<http://mobyle.pasteur.fr>), TMpred (<http://www.ch.embnet.org>), and Phobius (<http://phobius.sbc.su.se>). Signal peptide sequences were predicted using SignalP (<http://www.cbs.dtu.dk>), SOSUSignal (<http://bp.nuap.nagoya-u.ac.jp>), and Phobius. Putative transmembrane domains and signal peptides were considered present only if positive hits were found in all programs used. Venn diagrams were constructed using Venn Diagram Generator (<http://www.pangloss.com/seidel/Protocols/venn.cgi>).

The microarray data reported in this paper has been deposited in the Gene Expression Omnibus (GEO) database (<http://www.ncbi.nlm.nih.gov/geo/>) with accession number GSE35990.

Generation of Transgenic Ameba Overexpressing HP1 and ISFs

Full-length gene sequences were amplified from MTZR cDNA with sense- and anti-sense primers containing appropriate restriction sites (Table S2). PCR primers were designed as follows: sense primers contained 26~30 nucleotides corresponding to a region of each gene encoding the amino-terminal portion of each target proteins, fused at the 5' end with three additional nucleotides and SmaI restriction enzyme recognition site (tccCCCGGG); reverse primers contained 22~33 nucleotides corresponding to a region of each gene encoding the carboxyl-terminal portion of each target proteins, fused at the 5' end with three additional nucleotides and Xhol restriction enzyme recognition site (ccgCTCGAG). PCR was performed with the cDNA as a template using a DNA Engine Peltier Thermal Cycler (Bio-Rad, Hercules, CA, USA). The PCR cycling conditions

consisted of an initial step of denaturation at 94°C for 1 min, followed by 30 cycles of denaturation at 98°C for 10 s, annealing at 55°C for 30 s, and extension at 72°C for 60 s with Phusion DNA polymerase (New England BioLabs, Tokyo, Japan). Resultant PCR fragments were precipitated with ethanol, digested with appropriate restriction enzymes, and then purified from an exised piece of agarose gel by using GENECLEAN kit (Funakoshi, Tokyo, Japan). After purification, the gene was inserted into an expression plasmid, pEhEx, as previously described (Penuliar et al., 2012). The plasmid was introduced into *E. histolytica* G3 strain by lipofection, with minor modifications as previously described (Penuliar et al., 2012). Briefly, *E. histolytica* G3 trophozoites in the mid-logarithmic growth phase were harvested as described above, and re-suspended with Opti-MEM medium supplemented with 5 mg/mL L-cysteine and 1 mg/mL ascorbic acid at 1×10^5 cells/mL. Approximately 5 mL of the suspension was dispensed into each well on a 12-well plate and the plate was incubated under anaerobic condition at 35.5°C for 30 min. Following incubation, 4.5 mL medium from each well was removed and 500 μL liposome–plasmid–mixture (5 μg plasmid, 10 μL PLUS reagent, 20 μL Lipofectamine in Opti-MEM medium) was added. After 5 h of transfection, cells were harvested by placing the plate on ice for 15 min, then added to culture tubes with 5.5 mL cold BIS, and incubated at 35.5°C for 24 h. Transformants were initially selected in the presence of 1 μg/mL of G418, and drug concentration was gradually increased to 10 μg/mL during the following 6 weeks before the transformants were analyzed.

Reverse Transcriptase (RT)-PCR and Quantitative Real-Time (qRT)-PCR

Total RNA from semi-confluent cultures, about 2×10^5 cells/mL, of HM-1, MTZR, and transformants harboring one of the following plasmids: pEhEx-HA (mock plasmid), HP1-HA, ISF1-HA, ISF2-HA, and ISF4-HA, cultured in 25 cm² flasks, was extracted and quantified as described previously (Penuliar et al., 2012). cDNA was reverse transcribed from 5 μg RNA with the SuperScript III First-Strand Synthesis System, and RT-PCR was performed with the resulting cDNA as template and primers listed in Table S2 on a DNA Engine Peltier Thermal Cycle (Bio-Rad Laboratories, Inc., Hercules, CA, USA). The PCR parameters used were: an initial denaturation step at 95°C for 2 min followed by 30 cycles of denaturation at 94°C for 15 s, annealing at 55°C for 30 s, and extension at 72°C for 30 or 60 s. The products were resolved on 1.5% [w/v] agarose gel with 0.5 μg/mL ethidium bromide, visualized, and photographed under ultraviolet illumination.

The Fast SYBR Green Master Mix (Applied Biosystems, Foster City, CA, USA) was used for qRT-PCR in accordance with the manufacturer's instructions. The list of primers for genes whose expression was quantified by qRT-PCR can be found in Table S1, and includes a housekeeping gene, RNA polymerase II gene (*rpoII*), as control. Each PCR reaction contained 5 μL (1:50 dilution) of cDNA and 15 μL primer mix, composed of 10 μL 2X Fast SYBR Green Master Mix, sense and antisense primers, and nuclease-free water, to bring the volume to 20 μL. qRT-PCR was performed using StepOne Plus Real-Time PCR System (Applied

Biosystems, Foster City, CA, USA) with the following cycling conditions: enzyme activation at 95°C for 20 s, followed by 40 cycles of denaturation at 95°C for 3 s and annealing/extension at 60°C for 30 s. All test samples were run in triplicate including an RT-negative control for each sample set along with a blank control consisting of nuclease-free water in place of cDNA. Quantification for each target gene was determined by the $\Delta\Delta Ct$ method with *rpoII* as reference gene (Livak and Schmittgen, 2001).

Statistical Analysis

Correlation coefficients were calculated using the Student's *t*-test function of Microsoft Excel statistical package (Microsoft Corp., Redmond, WA, USA). Probability levels (*P*) < 0.05 were considered significant.

Results

Generation and Phenotypic Characterization of MTZR

Exposure of HM-1 to MTZ concentrations up to 3 μ M for 24 h did not result in any significant changes in cell morphology. Cells continued to grow and cultures formed confluent lawns after 72 h. Starting at 6 μ M MTZ, however, cells became rounder than usual and were slightly bigger in size. Cells also took longer to attach to surfaces and for cultures to form confluent lawns. Cell viability, however, was verified by cell adhesion and trypan blue exclusion assay. After 29 weeks, cells growing at 12 μ M MTZ (MTZR) were obtained. We tried to increase the concentration of MTZ further, but this resulted in further increase in doubling time.

The population doubling time of MTZR was significantly longer compared to HM-1 (26.8 ± 0.9 and 18.2 ± 0.5 h, respectively; *P*-value < 0.001, Figure 1). MTZR also appeared rounder, bigger, and more granular than HM-1. In contrast, parental cells exposed to 12 μ M MTZ showed signs of morphological changes as early as 2 h, rounding in 5 h, cell shrinkage, and detachment within 24 h. The slight enlargement of MTZR (+) compared to HM-1 was suggested when we measured the total protein content of MTZR and HM-1, 4.81 ± 0.04 and 4.24 ± 0.03 pg/cell, respectively. Flow cytometric analysis also confirmed that MTZR was slightly larger than HM-1 (data not shown).

The IC₅₀ of MTZ in MTZR and HM-1 was 12.9 ± 0.3 and 6.5 ± 0.3 μ M, respectively, and its resistance index was 2.0 (Table 1). When MTZR was cultured without the drug for 1 week followed by MTZ challenge for 24 h, percent survival was only 28%, indicating that resistance to the drug was reversible (data not shown). To determine if MTZR was cross-resistant with other amebicides, the IC₅₀ of the drugs listed in Table 1, against MTZR and HM-1 was determined. Results showed that MTZR had reduced sensitivity to the drugs.

MTZR had a slower rate of CHO monolayer destruction, especially at early time points, indicating a slight decrease in virulence (*P*-value < 0.05 for 30, 45, 60, and 75 min; Figure 2A). This was consistent with the observed decrease in intensity of bands corresponding to cysteine protease 1 and 2 (CP1 and

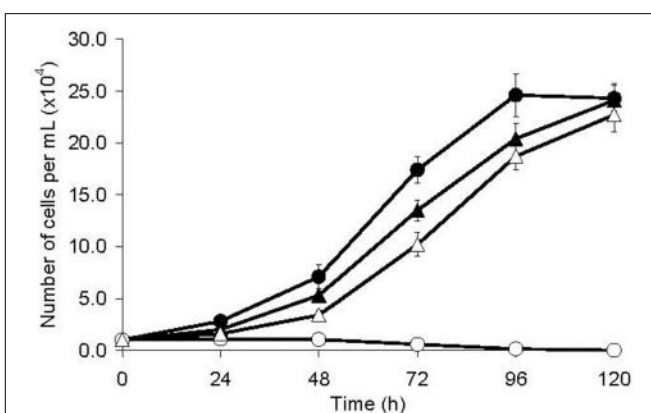


FIGURE 1 | Growth kinetics of HM-1 (circles) and MTZR (triangles) cultured with (open symbols) or without (filled symbols) 12 μ M MTZ.

CP2, synonymous to EhCP-A1 and EhCP-A2, respectively) in the zymogram (Figure 2B), and by an ImageJ (<http://rsbweb.nih.gov/ij/>) analysis of the same bands that indicated an approximately 33% decrease in band areas. The band for CP5 (EhCP-A5) and control bands (arrow head) were comparable between HM-1 and MTZR. The decrease in cytopathy in MTZR was also indicated by the lower number of engulfed beads (Figure 2C) and percentage of cells with engulfed beads in the phagocytosis assay (Figure 2D). MTZR also consumed glucose at a reduced rate compared to HM-1 (*P*-value < 0.05, Figure 2E). In addition, MTZR adhered to plastic surfaces, and to fibronectin- and collagen-coated plates at relatively comparable levels, but not as efficiently as HM-1 (Supplementary Figure S2).

Transcriptomic Analysis of MTZR

Our expression data showed variations in the number of differentially expressed genes between MTZR and HM-1 cultured with and without MTZ (GEO ID: GSE35990). To identify genes whose expression was most highly affected, a general filtering of the expression data, as indicated in Materials and Methods, was used. This resulted in the identification of 142 probe sets for MTZR, 58 probe sets for MTZR (-), and 37 probe sets for HM-1 (+) that showed at least 3-fold changes compared to HM-1 (-) (Figure 3A, Table S3). In MTZR, 95 (66.9%) of the genes were upregulated, while 47 (33.1%) genes were downregulated (Tables 2, 3). Only 55 (38.7%) genes were annotated after conducting BLAST search, while 87 (61.3%) genes encoded for proteins of unknown function, i.e., hypothetical proteins (Table S4). The most upregulated gene was a hypothetical protein (HP) (EHI_006850) with some similarity to a zinc finger protein in *E. histolytica* (*E*-value = $1.0e^{-46}$), designated as HP1 in this study. Its expression in MTZR was increased by 36.9 folds. Genes for DNA polymerase (EHI_164190), iron-sulfur flavoprotein (ISF) (EHI_025710), AIG1 family protein [XP_648192 (522.m00018)], and four other HPs were also upregulated by more than 10 folds. The most downregulated genes were three leucine-rich proteins [EHI_033560, EHI_077280, EHI_124070 (371.m00031)] which had fold changes of more than 160, and two AIG family

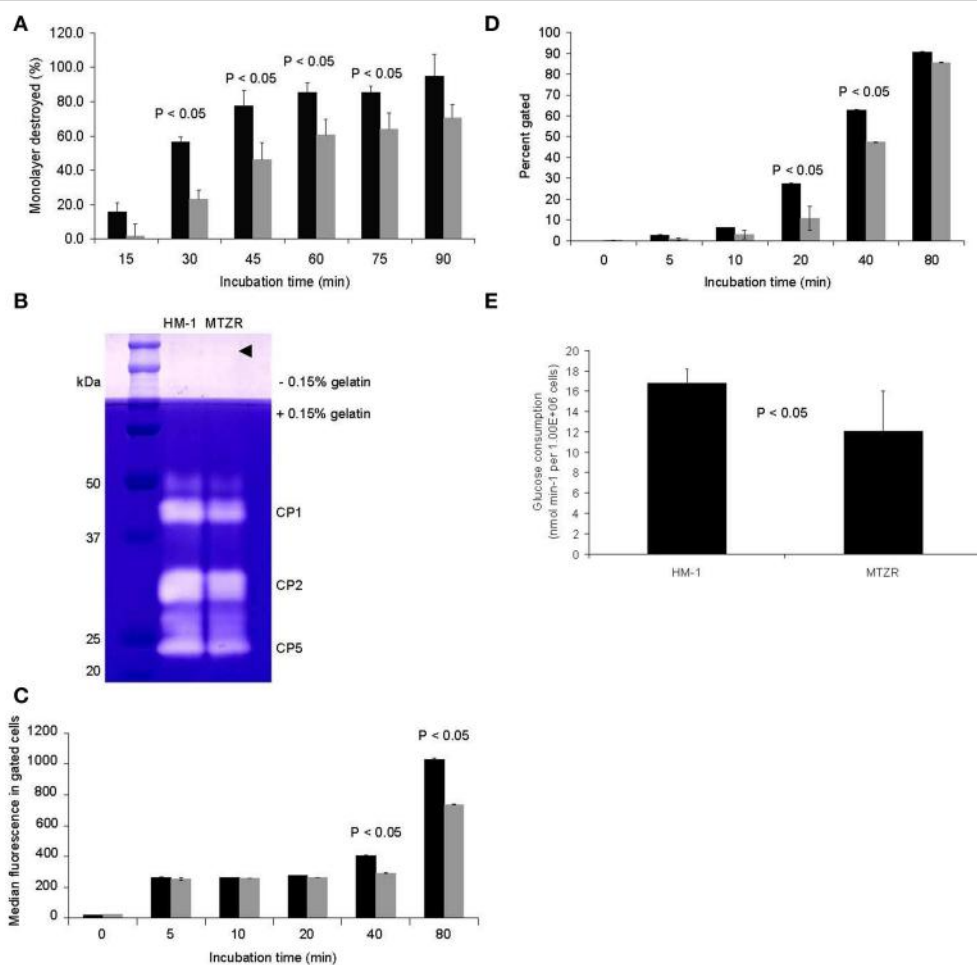


FIGURE 2 | Phenotypic changes observed in MTZR. Statistical significance is indicated (P -value < 0.05). **(A)** CHO monolayer destruction assay of HM-1 (black bars) and MTZR (gray bars). **(B)** Zymography of whole cell lysates of HM-1 and MTZR. An arrowhead indicates comparable protein loading per lane as estimated by CBB

staining of irrelevant proteins. **(C,D)** Phagocytosis assay with carboxylated beads in HM-1 (black bars) and MTZR (gray bars). The number of beads phagocytosed **(C)** and the percentage of cells with engulfed beads **(D)** at indicated time points are compared between HM-1 and MTZR. **(E)** Glucose consumption assay.

proteins [XP_648014 (628.m00011), EHI_180390] and two CPs (EHI_160330, EHI_121160) genes that were downregulated by at least 5 folds. The two CPs identified had high similarity to CP7 (synonymous to EhCP-B1) (81%) based on amino acid sequence (Tillack et al., 2007). The differential expression of 16 genes was validated by qRT-PCR, using rpoII as an endogenous control (Table 4). Pearson's correlation coefficient (0.81) between microarray and qRT-PCR results indicated a reasonable degree of concordance between the fold-changes of the genes selected for this comparison.

To determine whether the genes we identified were important in MTZ resistance or resulted from a general stress response, a 3-way comparison of differentially expressed genes in MTZR, MTZR (-) and HM-1 (+) was performed. Figures 3A,B, and Table S3 show that out of 142 genes modulated in MTZR, 48 genes (33.8%) were also modulated in MTZR (-), while only 8 genes (5.6%) were differentially transcribed in HM-1 (+). Among the genes specifically modulated

in MTZR were DNA polymerase (EHI_164190), 4 AIG1 family proteins [EHI_026000, EHI_126550, EHI_126560, XP_648127 (554.m00020)], four iron-sulfur flavoproteins (EHI_022270, EHI_022600, EHI_181710, EHI_067720, EHI_103260), metal-dependent hydrolase (EHI_054690), dUTP nucleotidohydrolase domain-containing protein (EHI_072960), three serine-rich 25 kDa antigen protein [EHI_073980, EHI_072000, EHI_072000 (82.m00164)], two Ras family protein (EHI_074750, EHI_045600), Rho guanine nucleotide exchange factor (EHI_006140), and a competence/damage-inducible protein (EHI_090260). In MTZR (-), AP-2 complex protein (EHI_014390), serine acetyltransferase (EHI_021570), zinc finger protein (EHI_091050), cysteine protease (EHI_117650), and a cell division control protein (EHI_154270) were specifically modulated. In HM-1 (+), on the other hand, genes for heat shock proteins [EHI_005657 (181.m00064), EHI_156560 (482.m00014), EHI_034710] were specifically upregulated together with genes putatively involved in drug resistance

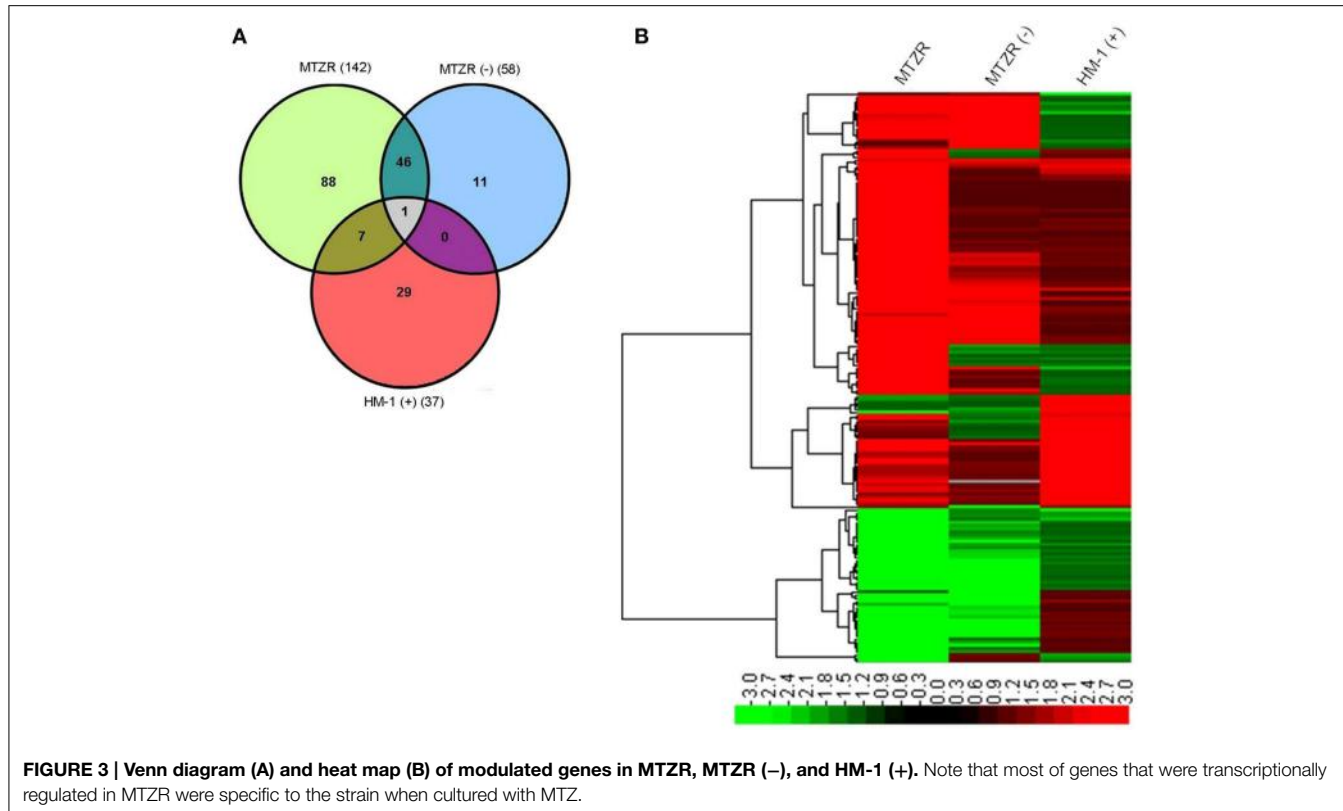


FIGURE 3 | Venn diagram (A) and heat map (B) of modulated genes in MTZR, MTZR (-), and HM-1 (+). Note that most of genes that were transcriptionally regulated in MTZR were specific to the strain when cultured with MTZ.

like P-glycoprotein 5 (EHI_075410, EHI_125030) and ATP-binding cassette protein (EHI_134470, EHI_178580). Two iron-sulfur flavoproteins (EHI_025710, EHI_138480) and an ABC transporter [EHI_084730 (36.m00218)] were upregulated in both MTZR and HM-1 (+), although their expression in HM1 (+) was 2 to 3 folds higher. It is also interesting to note that in all three strains, induction of gene transcription clearly prevailed over inhibition. This was particularly true for HM-1 (+) where almost 95% of the modulated genes were upregulated.

Go Classification, Features, and Clustering on the Genome

To have a general view of the cellular functions regulated as a result of MTZ resistance, we performed a GO enrichment analysis. A total of 132 GO terms were mined from Amoeba DB representing 63 unique GO IDs (Table S5). However, based on Fisher's exact test, only 24 terms were significantly enriched in MTZR (Table 5). Genes involved in GTP binding and proteolysis were the most highly enriched, followed by genes associated with cysteine-type peptidase activity, small GTPase-mediated signal transduction, oxidoreductase activity, protein kinase activity, and electron carrier activity. Roughly, the enriched terms could be classified into four functional categories, namely (1) nucleotide binding, (2) metabolism, (3) oxidative stress response, and (4) signal transduction.

Only a fraction of the differentially expressed genes in MTZR (about 5%) encoded for membrane proteins, based on positive results for transmembrane and signal peptide predictions

(Table S6). Only 21 genes (14.8%) contained at least one transmembrane domain. Eleven of these were upregulated, while 10 were downregulated. Proteins encoded by 25 genes (17.6%) also had predicted signal peptides. Only seven genes have both transmembrane domains and signal peptides. Only one, however, was annotated as tyrosine kinase (EHI_118410), while the rest were all genes for HPs.

Most of the modulated genes were encoded on different scaffolds. Thirty-four genes (30.6% of EHI-probe sets), however, formed 15 sets of dyads or triads that occupied the same contig (Table S7). Included were genes for four AIG1 family proteins (EHI_126550, EHI_126560, EHI_176700, EHI_176580) and two Ras family proteins (EHI_045450, EHI_045600). In four sets of genes, the members were found to be located on opposite strands, but the regulation of their expression was the same and their fold-changes were comparable. For some genes found on the same strand, the distance between the genes was less than 1 kb. It was therefore possible for these genes to be co-regulated by the same transcription factor.

Functional Analysis

To study further the relationship between the expression of some of the modulated genes in MTZR with drug resistance, generation of stable transformants overexpressing HA-tagged HP1, ISF1, ISF2, and ISF4 was performed (Figure 4A). The mRNA level of these proteins was estimated by qRT-PCR. The levels of mRNA of HP1 and ISFs were about 5.5 or 2.5 to 3 fold, respectively, higher in MTZR compared to their expression in HM-1 transfected

TABLE 2 | List of annotated genes that were upregulated in MTZR by >3 fold compared to HM-1.

Probe Set ID	NCBI RefSeq	Gene name	P-value	Fold-change
EHI_164190_at	XM_001913665.1	DNA polymerase, putative	2.80E-03	12.9
EHI_025710_at	XM_644279.1	Iron-sulfur flavoprotein, putative	4.50E-05	11.6
522.m00018_at	XM_643100.1	AIG1 family protein	6.50E-04	11.5
EHI_189960_at	XM_647238.1	ADP-ribosylation factor 1, putative	9.20E-04	7.2
EHI_026000_s_at	XM_643099.1	AIG1 family protein, putative	2.60E-03	6.5
EHI_138480_at	XM_650038.1	Iron-sulfur flavoprotein, putative	6.50E-04	6.3
EHI_073980_s_at	XM_648468.1	Serine-rich 25 kDa antigen protein	1.10E-02	6.2
EHI_022270_s_at	XM_644761.1	Iron-sulfur flavoprotein	1.60E-02	5.5
EHI_129890_at	XM_646723.1	Type A flavoprotein, putative	1.00E-02	5.4
EHI_022600_s_at	XM_643169.1	Iron-sulfur flavoprotein	1.40E-02	5.4
EHI_181710_s_at	XM_001914510.1	Iron-sulfur flavoprotein, putative	1.30E-02	5.3
82.m00157_s_at	XM_648374.1	Surface antigen ariel1	6.80E-03	5.3
EHI_096770_at	XM_650580.1	Acetyltransferase, putative	1.30E-02	4.9
EHI_072960_s_at	XM_001914217.1	dUTP nucleotidohydrolase domain protein	3.20E-02	4.9
EHI_067720_s_at	XM_643101.1	Iron-sulfur flavoprotein, putative	5.30E-04	4.8
EHI_072000_s_at	XM_001913846.1	Serine-rich 25 kDa antigen protein, putative	9.40E-03	4.8
EHI_103260_s_at	XM_001913434.1	Iron-sulfur flavoprotein	2.30E-02	4.5
82.m00164_s_at	XM_648353.1	Serine-rich 25 kDa antigen protein	4.10E-02	4.1
EHI_074750_at	XM_644490.1	Ras family GTPase	3.80E-04	3.9
EHI_148550_at	XM_652392.1	Protein tyrosine kinase domain-containing protein	4.10E-02	3.8
432.m00028_at	XM_643464.1	AIG1 family protein	2.70E-04	3.7
EHI_075660_at	XM_643678.1	CAAX prenyl protease, putative	1.70E-04	3.6
EHI_075150_at	XM_643772.2	NAD-specific glutamate dehydrogenase, putative	6.10E-03	3.6
EHI_126550_at	XM_643463.2	AIG1 family protein, putative	2.00E-03	3.5
EHI_082060_at	XM_646822.1	Leucine rich repeat protein, BspA family	1.00E-02	3.4
36.m00218_s_at	XM_649994.1	Truncated ABC transporter, putative	4.80E-02	3.3
EHI_147020_at	XM_644619.1	Ser/thr protein phosphatase family protein	9.30E-04	3.3
EHI_092100_at	XM_649470.1	Chitinase, putative	4.10E-02	3.2
EHI_045450_at	XM_652204.1	Ras family GTPase	8.70E-04	3.1
EHI_029620_s_at	XM_642949.1	Aldose reductase, putative	1.20E-03	3.1
EHI_118410_at	XM_644811.1	Tyrosine kinase, putative	7.20E-03	3.1
EHI_075640_at	XM_001914030.1	Protein phosphatase domain-containing protein	2.10E-02	3.1
EHI_045600_at	XM_648507.1	Ras family protein	2.30E-02	3.1
EHI_126560_at	XM_001914189.1	AIG1 family protein, putative	1.40E-02	3.1
EHI_091450_at	XM_645308.2	Cysteine protease, putative	9.00E-04	3.0

with mock vector (pEhEx-HA). Transformants cultured with 10 μ M G418 were challenged with MTZ for 48 h (**Figure 4B**). The highest concentration shown was based on the IC₅₀ of MTZ against HM-1, performed under the same conditions (6.5 μ M). No significant difference in percent survival was observed at all concentrations tested between the overexpressors and control (**Figure 4B**). Neither was significant difference in survival against hydrogen peroxide, observed, among the transformants (**Figure 4C**).

Discussion

Differences in MTZR Generation in This Study and Previous Works

Currently, only 4 studies have been published regarding *E. histolytica* and its response to or resistance to MTZ (Samarawickrema et al., 1997; Wassmann et al., 1999; Leitsch

et al., 2007; Tazreiter et al., 2008). These studies either exposed wild-type cells to serum level concentrations of the drug (70–100 μ M) or generated drug resistant trophozoites, similar to what we did in this study. However, the MTZ concentrations used in these studies and ours differ, which might explain some of the differences observed. The concentration used here is slightly higher compared to those used by Samarawickrema et al. 10 μ M (Samarawickrema et al., 1997), but significantly lower than those used by Wassmann et al. 40 μ M (Wassmann et al., 1999), Tazreiter et al. 50 μ M (Tazreiter et al., 2008), and Leitsch et al. 50 μ M (Leitsch et al., 2007). Our strain adapted more quickly to 1 μ M MTZ compared to the strain used by Samarawickrema (7 vs. 38 days) but overall the length of time used to generate MTZR was comparable.

For reasons we do not understand, our attempts to further increase the level of resistance failed, and no resistance above the concentration used here could be established. We could

TABLE 3 | List of annotated genes that were downregulated in MTZR by > 3 fold.

Probe Set ID	NCBI RefSeq	Gene name	P-value	Fold-change
EHI_033560_s_at	XM_001913757.1	Leucine rich repeat protein 1	2.20E-04	171.4
EHI_077280_s_at	XM_649853.2	Leucine rich repeat protein, BspA family	1.70E-04	163.1
371.m00031_s_at	XM_643815.1	BspA-like leucine rich repeat protein, putative	3.50E-04	163
628.m00011_at	XM_642922.1	AIG1 family protein	4.10E-04	8.4
EHI_160330_s_at	XM_001914054.1	Cysteine protease, putative	3.90E-03	7.3
EHI_121160_s_at	XM_001914417.1	Cysteine protease, putative	2.20E-03	7.3
EHI_054690_at	XM_646973.2	Metal dependent hydrolase, putative	4.90E-04	5.8
EHI_180390_at	XM_648725.1	AIG1 family protein, putative	2.40E-03	5.0
EHI_174230_s_at	XM_647412.2	S-adenosylmethionine synthetase	5.40E-03	4.1
EHI_176700_at	XM_001914268.1	AIG1 family protein, putative	1.00E-02	4.1
EHI_179060_at	XM_651187.2	Glycosyltransferase	9.10E-03	3.6
EHI_176580_at	XM_643164.1	AIG1 family protein, putative	5.90E-04	3.5
EHI_090260_at	XM_645039.1	Competence/damage-inducible protein, putative	6.80E-04	3.4
EHI_020250_at	XM_643256.1	Lecithin:cholesterol acyltransferase protein	7.30E-03	3.3
2.m00624_s_at	XM_652243.1	Protein kinase, putative	3.20E-02	3.3
EHI_006140_at	XM_648345.1	Rho guanine nucleotide exchange factor, putative	3.00E-02	3.2
EHI_026360_s_at	XM_650291.1	Phosphoserine aminotransferase, putative	6.30E-03	3.2
554.m00020_s_at	XM_643035.1	AIG1 family protein, putative	3.00E-03	3.0
EHI_067220_at	XM_647568.1	Rho family GTPase	1.90E-03	3.0
EHI_061760_at	XM_643432.1	Protein folding regulator	2.00E-02	3.0

TABLE 4 | qRT-PCR validation of selected genes from our microarray data.

Probe set ID	Gene name	Fold change by Microarray	Fold change by qRT-PCR	Regulation
EHI_096770_at	Acetyltransferase, putative	4.9	4.6	Upregulated
EHI_176700_at	AIG1 family protein, putative	4.1	5.1	Downregulated
EHI_126550_at	AIG1 family protein, putative	3.5	5.1	Upregulated
EHI_164190_at	DNA polymerase, putative	12.9	2.5	Upregulated
EHI_006850_at	Hypothetical protein 1	36.9	57.8	Upregulated
EHI_165190_at	Hypothetical protein 2	27.1	16.3	Upregulated
EHI_127670_at	Hypothetical protein 3	17	25.2	Downregulated
EHI_087210_at	Hypothetical protein 4	8.9	22.5	Upregulated
EHI_054690_at	Metal dependent hydrolase, putative	5.8	15.4	Downregulated
EHI_138480_at	Iron-sulfur flavoprotein, putative (ISF1)	6.3	5.8	Upregulated
EHI_025710_at	Iron-sulfur flavoprotein, putative (ISF2)	11.6	15.8	Upregulated
EHI_129890_at	Type A flavoprotein, putative	5.4	3.8	Upregulated
EHI_022600_s_at	Iron-sulfur flavoprotein (ISF4)	5.4	8.1	Upregulated
EHI_075150_at	NAD-specific glutamate dehydrogenase, putative	3.6	16.8	Upregulated
EHI_147020_at	Ser/thr protein phosphatase family protein	3.3	1.9	Upregulated
EHI_118410_at	Tyrosine kinase, putative	3.1	2.3	Upregulated

not culture MTZR consistently at drug concentrations higher than 12 μ M. In contrast, strains of *Trichomonas* and *Giardia* can be readily adapted to grow at 584 μ M and 115 μ M MTZ, respectively (Kulda et al., 1984; Townson et al., 1992). Our results are therefore consistent with previous reports indicating that MTZ resistant strains are more difficult to generate in *E. histolytica* (Samarawickrema et al., 1997). While the concentration we used is several times lower than serum levels after MTZ treatment (Van Oosten et al., 1986), the changes we observed may still provide insights as to what occurs in the

parasite *in vivo*. It was previously reported that in an abscess, parasites encounter significantly lower levels of drug than those found in the serum as drug penetration is limited by poor perfusion and mechanical barriers such as fibrin clots and the abscess wall (Sirinek, 2000).

Decrease in Growth and Reversibility of Resistance in MTZR

Formation of drug resistance is often accompanied by fitness costs (Andersson and Hughes, 2010). One particular cost,

TABLE 5 | List of GO terms that were significantly enriched in MTZR.

GO ID	GO Name	Aspect	Count	p-value
GO:0005525	GTP binding	Function	14	3.95E-06
GO:0005622	Intracellular	Component	11	8.89E-03
GO:0006508	Proteolysis	Process	10	2.78E-08
GO:0007264	Small GTPase mediated signal transduction	Process	8	4.58E-05
GO:0008234	Cysteine-type peptidase activity	Function	8	5.09E-09
GO:0016491	Oxidoreductase activity	Function	7	2.06E-05
GO:0008152	Metabolic process	Process	6	5.52E-03
GO:0004713	Protein tyrosine kinase activity	Function	5	5.20E-10
GO:0006508	Proteolysis	Process	4	1.34E-02
GO:0009055	Electron carrier activity	Function	4	9.26E-05
GO:0015031	Protein transport	Process	3	3.99E-03
GO:0003887	DNA-directed DNA polymerase activity	Function	2	2.06E-02
GO:0004222	Metalloendopeptidase activity	Function	2	1.54E-03
GO:0005089	Rho guanyl-nucleotide exchange factor activity	Function	2	4.95E-02
GO:0005886	Plasma membrane	Component	2	5.95E-04
GO:0006260	DNA replication	Process	2	2.66E-02
GO:0006520	Cellular amino acid metabolic process	Process	2	1.84E-03
GO:0008408	3'-5' exonuclease activity	Function	2	7.91E-04
GO:0010181	FMN binding	Function	2	3.29E-03
GO:0035023	Regulation of Rho protein signal transduction	Process	2	4.95E-02
GO:0004648	O-Phospho-L-serine:2-oxoglutarate aminotransferase activity	Function	1	5.39E-03
GO:0006564	L-Serine biosynthetic process	Process	1	5.39E-03
GO:0006913	Nucleocytoplasmic transport	Process	1	5.39E-03
GO:0008483	Transaminase activity	Function	1	3.71E-02
GO:0050662	Coenzyme binding	Function	1	4.23E-02

reduction in growth rate, is the main parameter that determines the rate by which resistance develops and level of resistance reached. Similar to resistant strains previously generated (Samarawickrema et al., 1997; Wassmann et al., 1999), the doubling time of MTZR was longer compared to HM-1. Fitness cost in growth associated with drug resistance are well documented in mammalian cells, e.g., lymphoma and cancer cells (Lee, 1993; Bishop et al., 2001). It should be noted, however, that the growth kinetics of MTZR in the absence of drug pressure improved over time. This indicates that some of the drug-selection-induced changes developed by MTZR were temporal and reversible. This also indicates that cells in the culture may have varying degrees of resistance. In addition, MTZR (–) that was re-exposed to MTZ showed significantly lower growth compared to MTZR, but slightly higher compared to HM-1, which may indicate that some drug-selection-induced changes in MTZR were still operative even after the removal of drug pressure.

Cross-Resistance in MTZR

The resistance level displayed by MTZR is significantly lower compared to previous reports: the IC₅₀ value of 12 μM in this study compared to 40 μM in the previous study (Samuelson, 1999; Wassmann et al., 1999). However, its survival in otherwise lethal concentration of MTZ for long periods of incubation, does indicate reduced sensitivity and resistance. The cross-resistance

of MTZR to ornidazole and tinidazole is not surprising, because both are 5-nitroimidazoles like MTZ. It is therefore likely that their mode of action and mechanism of resistance were similar (Pasupuleti et al., 2014). *T. vaginalis* isolates that were characterized as having very high resistance to MTZ were similarly insensitive to tinidazole (Narcisi and Secor, 1996). In the case of paromomycin, emetine, chloroquine, and hydrogen peroxide, it is possible that the reduced sensitivity was nonspecific and could be due to an increased capacity of MTZR to deal with stress. Studies have shown that cell lines resistant to one drug are often cross-resistant to closely related drugs or to unrelated compounds when their mode of action is the same or when they carry membrane alterations (Upcroft and Upcroft, 1993).

Decreased Adhesion, Phagocytosis, Cytolysis, and Virulence in MTZR

In *E. histolytica*, establishment and outcome of infection depend heavily on adhesive and invasive capacity (Flores-Romo et al., 1997). Recently, drug resistance has been shown to modulate these factors and vice versa (Giha et al., 2006). The decreased rate of adhesion observed in MTZR indicated that MTZ selection negatively affected the synthesis or expression of surface adhesion molecules. While other studies have shown that cell adhesion is a key determinant in drug resistance (Shain and Dalton, 2001), this apparently was not the case in MTZ resistance. Inhibition of adherence in this parasite has previously been

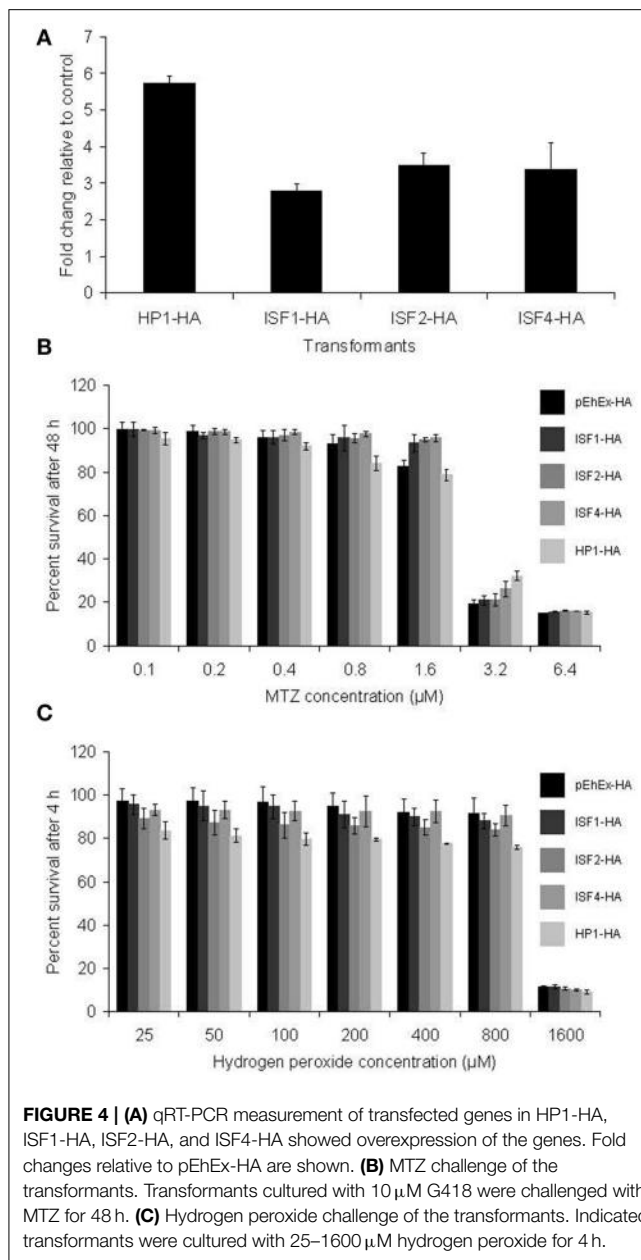


FIGURE 4 | (A) qRT-PCR measurement of transfected genes in HP1-HA, ISF1-HA, ISF2-HA, and ISF4-HA showed overexpression of the genes. Fold changes relative to pEhEx-HA are shown. **(B)** MTZ challenge of the transformants. Transformants cultured with 10 μM G418 were challenged with MTZ for 48 h. **(C)** Hydrogen peroxide challenge of the transformants. Indicated transformants were cultured with 25–1600 μM hydrogen peroxide for 4 h.

shown to decrease host cell cytotoxicity (Ravdin et al., 1985) and experimental evidence strongly suggests the involvement of surface adhesins in phagocytosis (Heron et al., 2011). As shown in the results, MTZR also had decreased cytopathy and phagocytosis (Figures 2A,C). The decreased band intensity for CP1 and CP2 in the zymogram may partially explain this phenotype. CP1 has been shown to be upregulated in a mouse model of amebic colitis following invasion (Gilchrist et al., 2006), while CP2 has been reported to contribute to intestinal damage and liver abscess formation (Hellberg et al., 2001). Our microarray data, however, did not show any significant repression of these genes, except for two uncharacterized CPs that were repressed by more than 7 folds. These CPs had high similarity (81%) to CP7 (also called EhCP-B1) based on amino acid sequence (Tillack et al.,

2007). No significant change was observed in the expression of the genes known to be involved in the inactivation and intracellular trafficking of CPs such as intrinsic inhibitors of CPs (Sato et al., 2006) and cysteine protease binding protein family 1 (Nakada-Tsukui et al., 2012) and other lysosomal hydrolase carriers (Furukawa et al., 2012, 2013; Marumo et al., 2014). It is also possible, however, that resistance to MTZ may not necessarily result to decreased virulence *in vivo*.

Implications from Transcriptomic Profiling of MTZR

Our transcriptomic profiling suggests that the transcriptomic changes we observed in MTZR strain cultured with MTZ were a combination of the changes responsible for MTZ resistance and those associated with the adaptation to stresses caused by the exposure to MTZ. However, we believe that among the observed changes, the changes that were specific to MTZR strain with MTZ and absent in HM-1 with MTZ were responsible, at least in part, for resistance, rather than adaptation. This is based on the following observations: the transcriptomic profile of *E. histolytica* HM-1 cultured with MTZ was remarkably different from that of MTZR strain cultured with MTZ, while MTZR strain cultured with or without MTZ showed similar transcriptomic profiles. In other words, a larger number of common changes in gene expression were identified between MTZR strain cultured with MTZ and those without MTZ when compared between MTZR strain cultured with MTZ and HM-1 cultured with MTZ.

GO enrichment of MTZR-associated transcriptomic changes revealed regulation of genes encoding for proteins potentially involved in nucleotide binding, metabolism, oxidative stress response, and signal transduction. These are apparently the processes most influenced by MTZ resistance. However, since most of the genes are without GO annotations, it is likely that additional processes are involved. When we examined the genomic locations of these genes, we found that 30% of them formed dyads or triads that occupied the same contig. While some genes forming dyads and triads are apart by more than 10 kb, the distance between some of the adjacent genes in dyads and triads was less than 1 kb. Thus, co-expression of some genes in dyads and triads in MTZR could be attributed to a shared regulatory system.

Consistent with previous findings, no significant difference in PFOR mRNA levels was observed between MTZR and HM-1 (Samarawickrema et al., 1997; Wassmann et al., 1999; Tazreiter et al., 2008). This observation could mean 3 things. First, it's likely that the level of resistance achieved in this study was not sufficient to downregulate PFOR, although a similar finding was reported in strains resistant to 40 μM MTZ (Wassmann et al., 1999). Second, since *E. histolytica* lacks pyruvate dehydrogenase (Clark et al., 2007; Tazreiter et al., 2008) or pyruvate decarboxylase (Lo and Reeves, 1978), the significance of PFOR cannot be overstated. The lack of an alternative enzyme to compensate for its downregulation makes this enzyme difficult to repress without severe consequences to the ameba. Third, in contrast to *Giardia* and *Trichomonas*, lack of PFOR downregulation may indicate the existence of an alternative mechanism for MTZ resistance in this parasite. It should be noted, however, that clinically resistant

isolates of *Trichomonas* have been reported with no decrease in PFOR activity (Müller and Gorrell, 1983).

Two previous studies have reported the upregulation of Fe-SOD and downregulation of Fdx in the MTZ resistant ameba (Samarawickrema et al., 1997; Wassmann et al., 1999). In the previous work, fold changes were determined based on enzyme activity assay or northern blot (Samarawickrema et al., 1997; Wassmann et al., 1999). Disparity, however, between changes in mRNA abundance and enzyme activity have been reported, and in some cases, increases in enzyme activity can exceed those of mRNA abundance (Glanemann et al., 2003). Interestingly, the lack of Fe-SOD modulation in cells exposed to MTZ was also reported by Tazreiter et al. (2008). On the contrary, in this work, neither gene was modulated significantly. It is possible that similar to PFOR, differences in resistance levels could explain the lack of modulation in the levels of Fe-SOD and Fdx. Other studies also indicated that Fe-SOD and Fdx are not tightly associated with MTZ resistance. It was shown that parasites in which Fdx was repressed did not display full resistance to MTZ (Rasoloson et al., 2002) and in bacteria, increased SOD activity was not always associated with MTZ resistance (Smith and Edwards, 1995).

In this study, genes involved in nucleic acid synthesis and binding, stress response, metabolism, and vesicular trafficking were mostly affected in MTZR. The significance of these genes relative to phenotypic changes and drug resistance will be discussed here through their known roles in *E. histolytica* or in other organisms, in regulating key cell functions. One should also note that since only a single MTZ resistant line was analyzed in this study, it is possible that MTZ resistance can be also conferred by the mechanisms that are independent of those described in this study.

Nucleic Acid Synthesis and Binding

In prokaryotes, upregulation of DNA polymerases imparts plasticity to their genome, allowing them to adapt in unfavorable environmental conditions (Joseph et al., 2006). It has been suggested that pathogenic bacteria utilize this adaptation to develop resistance against therapeutic agents (Karpinets et al., 2006). Since it has been shown that primary effect of MTZ is rapid inhibition of DNA replication (Ludlum et al., 1988; Sisson et al., 2000; Leitsch et al., 2007), the upregulation of a DNA polymerase (EHI_164190) in this study may indicate that this mode of action is operative in MTZ resistance. One hypothetical protein identified in this study (HP1, EHI_006850) has some similarity to zinc finger proteins, which are known to be involved in DNA recognition, RNA packaging, and transcriptional activation (Laity et al., 2001). It has an NAD⁺-binding pocket and a tetrachlorodibenzo-p-dioxin (TCDD)-inducible poly(ADP-ribose) polymerase (PARP)-like domain that is involved in the attachment of ADP-ribose units to DNA-binding proteins (Ma et al., 2001). It's also known to be a regulatory component induced by DNA damage and an enzyme involved in DNA repair (Nguewa et al., 2006; Marchler-Bauer et al., 2011). The dUTP nucleotidohydrolase (EHI_072960) upregulated in MTZR may be involved in the removal of dUTP from the dNTP pool, *de novo* biosynthesis of dTTP, and DNA

replication as reported (Richards et al., 1984; Gadsden et al., 1993). In cancer cells, high level of dUTPase is implicated as a mechanism of resistance to chemotherapy (Ladner et al., 2000).

Stress Response

ISFs that were modulated in MTZR are part of family of redox-active proteins mainly found in anaerobic prokaryotes (Andrade et al., 2005). In NCBI, 18 ISF genes are annotated in the *E. histolytica* genome, although 50% of these are identical proteins (<http://www.ncbi.nlm.nih.gov/>). In this study 7 ISF probe sets were upregulated by at least 4 folds in MTZR. The overexpression of ISF1 (EHI_138480) was also observed in HM-1 (+), while ISF2 was upregulated in both MTZR (-) and HM-1 (+). These 2 ISFs were upregulated in HM-1 (+) by least 20 folds, compared to 6 to 11 folds in MTZR, hinting that these genes are involved in stress response. These two genes were also induced in *E. histolytica* cultured under L-cysteine deprived and oxidative stress conditions (Vicente et al., 2009; Husain et al., 2011), but were downregulated in a mouse model of intestinal amebiasis (Gilchrist et al., 2006). Our findings together with these reports suggest that induction of these ISFs, particularly ISF1, is an adaptation that may enhance survival when cells experience environmental stress.

Metabolism

Several metabolic genes were upregulated in MTZR. NAD-specific glutamate dehydrogenase (EHI_075150) catalyzes the oxidative deamination of glutamate to α -ketoglutarate using NAD as cofactor (Plaitakis and Zaganas, 2001; Girinathan et al., 2014). Most likely, its upregulation is a part of stress response. In humans, its activity is regulated through ADP-ribosylation, and interestingly, Arf1 (EHI_189960) was also upregulated in this study (Herrero-Yraola et al., 2001). Chitinase (EHI_092100) (Escueta- De Cadiz et al., 2013) was also upregulated in MTZR and MTZR (-) by at least 3 folds, although its precise role in drug resistance is not known. In plants, its upregulation plays a defensive role against toxins and antibiotics (Gooday, 1999). Aldose reductase (EHI_029620), on the other hand, can reduce a broad spectrum of substrates including cytotoxic aldehydes (Ramana, 2011). Its upregulation in human liver cancer cells was associated with resistance to daunorubicin and was confirmed by sensitizing cells to the drug by the addition of aldose reductase inhibitors (Lee et al., 2001).

The decrease in cell growth observed in MTZR may be partially explained by the repression of phosphoserine aminotransferase (EHI_026360) (Ali and Nozaki, 2006; Mishra et al., 2010), which catalyzes the conversion of 3-phosphohydroxypyruvate to L-phosphoserine, the second step of phosphorylated serine biosynthetic pathway (Ali and Nozaki, 2006). L-serine has a well-recognized role in cell proliferation, providing precursors for amino acids, protein synthesis, and nucleotide synthesis (Nozaki et al., 2005; Tabatabaie et al., 2010). The downregulation of this enzyme, therefore, may contribute to the decreased growth rate. The repression of lecithin: cholesterol acyltransferase (EHI_020250) may also be associated with decreased growth rate, because the

enzyme is crucial in the maturation, remodeling, and metabolism of high density lipoprotein, HDL (Calabresi et al., 2011).

BspA1 Gene Family

Several genes encoding for leucine-rich repeat (LRR) proteins of the BspA family were also modulated in MTZR, and were the most downregulated genes with fold changes of more than 150. LRR is known to provide a structural framework for the formation of protein-protein interactions and serve as recognition motifs for surface proteins (Kobe and Kajava, 2001). BspA family protein was originally identified in *Bacteroides forsythus* and the LRR motifs of the BspA protein have been linked to cell binding to components of the extracellular matrix (Sharma et al., 1998). It is therefore possible that their downregulation may partially explain the reduced adhesion seen in MTZR. It was previously shown that an LRR BspA family protein in *E. histolytica* was located primarily on the plasma membrane, although it did not show whether the protein was involved in surface interactions (Davis et al., 2006).

AIG1 Gene Family

The *E. histolytica* AIG1 gene family consists of 47 members (Biller et al., 2010), and in this study 10 genes were found to be differentially expressed by 3 to 11 folds. Members of this protein family contain a domain found in *Arabidopsis* protein AIG1, which is likely involved in plant recognition and resistance to bacterial pathogens (Reuber and Ausubel, 1996). In *E. histolytica*, however, some AIG proteins appear to be linked with virulence. Comparative genomic analysis of Japanese clinical isolates indicated that an AIG family protein (EHI_176590) and the region around it were uniquely present in KU50, a strain isolated from a diarrheic patient, but absent in a non-pathogenic isolate called KU27 (Nakada-Tsukui et al., unpublished data). Interestingly, the same gene was downregulated by 2.7 folds in MTZR, and two adjacent genes encoding for AIG family proteins (EHI_176580 and EHI_176700) were also repressed by 3 to 4 folds. A previous study also reported the upregulation of an AIG family protein (EHI_180390) in a pathogenic strain of *E. histolytica* (Biller et al., 2010), although here the same gene was downregulated by 5 folds. It is therefore possible that the downregulation of these AIG family proteins might be related to the decrease in MTZR's cytopathogenicity.

Overall, we believe that these transcriptional changes participate in a global regulatory response resulting to the fitness costs and adaptive responses we observed in MTZR. The fact that more genes were upregulated than downregulated also suggests that increasing the amount of cellular components that play roles in stress response, DNA repair and others, is more important in developing low levels of resistance to MTZ than repression of proteins involved in activating the drug. Indeed, the most profound difference we observed between MTZR and HM-1 was the upregulation of genes for several ISF proteins. It should be noted, however, that more than half of the genes reported in this study are hypothetical. It is also likely that the effects of the

repressed genes, although fewer in number, are more important in explaining the growth defect.

Functional Analysis of Potential Resistance Genes

In this study, we examined possible role of genes encoding HP1 and several ISF proteins in MTZ resistance. However, their episomal transfection and overexpression did not confer MTZ resistance to the extent observed in MTZR. Thus, at present, direct causal connection between HP1 and ISF overexpression and MTZ resistance has not been demonstrated. It is likely that in *E. histolytica*, resistance to the drug is multi-factorial in nature and requires the global regulation of genes involved in several key cell processes and not just DNA repair and stress response.

In conclusion, here we described the biological state of *E. histolytica* that was selected for MTZ resistance *in vitro*. Phenotypic and transcriptional profiling revealed fitness costs and adaptive responses that we could associate with drug resistance. Some of the consequences of resistance included decreased cell growth and virulence, which have significant implications on host-pathogen interaction and infection outcome. Comparative transcriptional analysis, on the other hand, revealed genes not previously associated with MTZ resistance in this parasite. The list of differentially transcribed genes also did not indicate in MTZR a reduced capacity to activate MTZ, but hinted on adaptations to tolerate the lethal effects of MTZ. Identifying the signaling mediators for the proteins that these genes encode, however, requires further investigation. Finally, while our data showed that high levels of MTZ resistance cannot be readily induced *in vitro*, the data presented here may still help researchers in better understanding the mechanisms involved should clinical cases of high levels of resistance are reported in the future.

Acknowledgments

We thank Takashi Makiuchi, Ghulam Jeelani, Yumiko Saito-Nakano, and Joseph Marzo for valuable discussions. We thank Dr. Kentaro Hanada, Department of Biochemistry and Cell Biology, National Institute of Infectious Diseases for providing CHO cells. This work was supported by a Grant-in-Aid for Scientific Research from the Ministry of Education, Culture, Sports, Science and Technology (MEXT) of Japan (23117001, 23117005, 23390099, 14506236), a grant for research on emerging and re-emerging infectious diseases from the Ministry of Health, Labour and Welfare of Japan (H23-Shinkosaiko-ippan-014, H26-Shinkosaiko-ippan-009), a grant for research to promote the development of anti-AIDS pharmaceuticals from the Japan Health Sciences Foundation (KHA1101).

Supplementary Material

The Supplementary Material for this article can be found online at: <http://journal.frontiersin.org/article/10.3389/fmicb.2015.00354/abstract>

References

- Agresti, A. (1992). A survey of exact inference for contingency tables. *Stat. Sci.* 7, 131–153. doi: 10.1214/ss/1177011454
- Ali, V., and Nozaki, T. (2006). Biochemical and functional characterization of phosphoserine aminotransferase from *Entameba histolytica*, which possesses both phosphorylated and non-phosphorylated serine metabolic pathways. *Mol. Biochem. Parasitol.* 145, 71–83. doi: 10.1016/j.molbiopara.2005.09.008
- Andersson, D. I., and Hughes, D. (2010). Antibiotic resistance and its cost: is it possible to reverse resistance? *Nat. Rev. Microbiol.* 8, 260–271. doi: 10.1038/nrmicro2319
- Andrade, S. L., Cruz, F., Drennan, C. L., Ramakrishnan, V., Rees, D. C., Ferry, J. G., et al. (2005). Structures of the iron-sulfur flavoproteins from Methanosaerina thermophila and *Archaeoglobus fulgidus*. *J. Bacteriol.* 187, 3848–3854. doi: 10.1128/JB.187.11.3848-3854.2005
- Benjamini, Y., and Hochberg, Y. (1995). Controlling the false discovery rate: a practical and powerful approach to multiple testing. *J. R. Stat. Soc. Ser. B Stat. Methodol.* 57, 289–300.
- Biller, L., Davis, P. H., Tillack, M., Matthiesen, J., Lotter, H., Stanley, S. L. Jr., et al. (2010). Differences in the transcriptome signatures of two genetically related *Entamoeba histolytica* cell lines derived from the same isolate with different pathogenic properties. *BMC Genomics* 11:63. doi: 10.1186/1471-2164-11-63
- Bishop, A. J., Kosaras, B., Carls, N., Sidman, R. L., and Schiestl, R. H. (2001). Susceptibility of proliferating cells to benzo[a]pyrene-induced homologous recombination in mice. *Carcinogenesis* 22, 641–649. doi: 10.1093/carcin/22.4.641
- Calabresi, L., Baldassarre, D., Simonelli, S., Gomaraschi, M., Amato, M., Castelnuovo, S., et al. (2011). Plasma lecithin:cholesterol acyltransferase and carotid intima-media thickness in European individuals at high cardiovascular risk. *J. Lipid Res.* 52, 1569–1574. doi: 10.1194/jlr.P014977
- Clark, C. G., Cecilia, U., Alsmark, M., Hofer, M., Saito-Nakano, Y., Ali, V., et al. (2007). Structure and content of the *Entamoeba histolytica* genome. *Adv. Parasitol.* 65, 51–190. doi: 10.1016/S0065-308X(07)65002-7
- Davis, P. H., Zhang, Z., Chen, M., Zhang, X., Chakraborty, S., Stanley, S. L., et al. (2006). Identification of a family of BspA like surface proteins of *Entamoeba histolytica* with novel leucine-rich repeats. *Mol. Biochem. Parasitol.* 145, 111–116. doi: 10.1016/j.molbiopara.2005.08.017
- Diamond, L. S., Harlow, D. R., and Cunnick, C. C. (1978). A new medium for the axenic cultivation of *Entamoeba histolytica* and other *Entamoeba*. *Trans. R. Soc. Trop. Med. Hyg.* 72, 431–432. doi: 10.1016/0035-9203(78)90144-X
- Diamond, L. S., Mattern, C. F., and Bartgis, I. L. (1972). Viruses of *Entamoeba histolytica*. I. Identification of transmissible virus-like agents. *J. Virol.* 9, 326–341.
- Dooley, C. P., and O'Morain, C. A. (1988). Recurrence of hepatic amebiasis after successful treatment with metronidazole. *J. Clin. Gastroenterol.* 10, 339–342. doi: 10.1097/00004836-198806000-00022
- Durel, P., Couture, J., Collart, P., and Girot, C. (1960). Flagyl (metronidazole). *Br. J. Vener. Dis.* 36, 154–162. doi: 10.1136/sti.36.3.154
- Escueta- De Cadiz, A., Jeelani, G., Nakada-Tsukui, K., Caler, E., and Nozaki, T. (2013). Transcriptome analysis of encystation in *Entamoeba invadens*. *PLoS ONE* 8:e74840. doi: 10.1371/journal.pone.0074840
- Flores-Romo, L., Estrada-García, T., Shibayama-Salas, M., Campos-Rodríguez, R., Bacon, K., Martínez-Palomo, A., et al. (1997). *In vitro* *Entamoeba histolytica* adhesion to human endothelium: a comparison using two strains of different virulence. *Parasitol. Res.* 83, 397–400. doi: 10.1007/s004360050271
- Furukawa, A., Nakada-Tsukui, K., and Nozaki, T. (2012). Novel transmembrane receptor involved in phagosome transport of lysozymes and β -hexosaminidase in the enteric protozoan *Entamoeba histolytica*. *PLoS Pathog.* 8:e1002539. doi: 10.1371/journal.ppat.1002539
- Furukawa, A., Nakada-Tsukui, K., and Nozaki, T. (2013). Cysteine protease-binding protein family 6 mediates the trafficking of amylases to phagosomes in the enteric protozoan *Entamoeba histolytica*. *Inf. Immun.* 81, 1820–1829. doi: 10.1128/IAI.00915-12
- Gadsden, M. H., McIntosh, E. M., Game, J. C., Wilson, P. J., and Haynes, R. H. (1993). dUTP pyrophosphatase is an essential enzyme in *Saccharomyces cerevisiae*. *EMBO J.* 12, 4425–4431.
- Giha, H. A., Elbashir, M. I., A-Elbasit, I. E., A-Elgadir, T. M., ElGhazali, G. E., Mackinnon, M. J., et al. (2006). Drug resistance-virulence relationship in *Plasmodium falciparum* causing severe malaria in an area of seasonal and unstable transmission. *Acta Trop.* 97, 181–187. doi: 10.1016/j.actatropica.2005.10.004
- Gilchrist, C. A., Houpt, E., Trapaidze, N., Fei, Z., Crasta, O., Asgharpour, A., et al. (2006). Impact of intestinal colonization and invasion on the *Entamoeba histolytica* transcriptome. *Mol. Biochem. Parasitol.* 147, 163–176. doi: 10.1016/j.molbiopara.2006.02.007
- Girinathan, B. P., Braun, S. E., and Govind, R. (2014). *Clostridium difficile* glutamate dehydrogenase is a secreted enzyme that confers resistance to H₂O₂. *Microbiology* 160, 47–55. doi: 10.1099/mic.0.071365-0
- Glanemann, C., Loos, A., Gorret, N., Willis, L. B., O'Brien, X. M., Lessard, P. A., et al. (2003). Disparity between changes in mRNA abundance and enzyme activity in *Corynebacterium glutamicum*: implications for DNA microarray analysis. *Appl. Microbiol. Biotechnol.* 61, 61–68. doi: 10.1007/s00253-002-1191-5
- Gooday, G. W. (1999). Aggressive and defensive roles for chitinases. *EXS* 87, 157–169. doi: 10.1007/978-3-0348-8757-1_11
- Hellberg, A., Leippe, M., and Bruchhaus, I. (2000). Two major 'higher molecular mass proteinases' of *Entamoeba histolytica* are identified as cysteine proteinases 1 and 2. *Mol. Biochem. Parasitol.* 105, 305–309. doi: 10.1016/S0166-6851(99)00194-2
- Hellberg, A., Nickel, R., Lotter, H., Tannich, E., and Bruchhaus, I. (2001). Overexpression of cysteine proteinase 2 in *Entamoeba histolytica* or *Entamoeba dispar* increases amoeba-induced monolayer destruction *in vitro* but does not augment amoebic liver abscess formation in gerbils. *Cell. Microbiol.* 3, 13–20. doi: 10.1046/j.1462-5822.2001.00086.x
- Heron, B. T., Sateriale, A., Teixeira, J. E., and Huston, C. D. (2011). Evidence for a novel *Entamoeba histolytica* lectin activity that recognises carbohydrates present on ovalbumin. *Int. J. Parasitol.* 41, 137–144. doi: 10.1016/j.ijpara.2010.07.011
- Herrero-Yraola, A., Bakhit, S. M., Franke, P., Weise, C., Schweiger, M., Jorcke, D., et al. (2001). Regulation of glutamate dehydrogenase by reversible ADP-ribosylation in mitochondria. *EMBO J.* 20, 2404–2412. doi: 10.1093/emboj/20.10.2404
- Husain, A., Jeelani, G., Sato, D., and Nozaki, T. (2011). Global analysis of gene expression in response to L-cysteine deprivation in the anaerobic protozoan parasite *Entamoeba histolytica*. *BMC Genomics* 12:275. doi: 10.1186/1471-2164-12-275
- Joseph, N., Duppatala, V., and Rao, D. N. (2006). Prokaryotic DNA mismatch repair. *Prog. Nucleic Acid Res. Mol. Biol.* 81, 1–49. doi: 10.1016/S0079-6603(06)81001-9
- Karpinets, T., Greenwood, D., Pogribny, I., and Samatova, N. (2006). Bacterial stationary-state mutagenesis and Mammalian tumorigenesis as stress-induced cellular adaptations and the role of epigenetics. *Curr. Genomics* 7, 481–496. doi: 10.2174/138920206779315764
- Kobe, B., and Kajava, A. V. (2001). The leucine-rich repeat as a protein recognition motif. *Curr. Opin. Struct. Biol.* 11, 725–732. doi: 10.1016/S0959-440X(01)00266-4
- Koutsaimanis, K. G., Timms, P. W., and Rée, G. H. (1979). Failure of metronidazole in a patient with hepatic amebic abscess. *Am. J. Trop. Med. Hyg.* 28, 768–769.
- Kulda, J., Cerkasov, J., Demes, P., and Cerkasovová, A. (1984). *Tritrichomonas foetus*: stable anaerobic resistance to metronidazole *in vitro*. *Exp. Parasitol.* 57, 93–103. doi: 10.1016/0014-4894(84)90068-7
- Kulda, J., Kabíčková, H., Tachezy, J., Čerkasovová, A., and Čerkasov, J. (1989). "Metronidazole resistant trichomonads: mechanisms of *in vitro* developed anaerobic resistance," in *Biochemistry and Molecular Biology of 'Anaerobic' Protozoa*, eds D. Lloyd, G. H. Coombs and T. A. P. Paget (Chur: Harwood Academic Publishers), 137–160.
- Lacey, S. L., Moss, S. F., and Taylor, G. W. (1993). Metronidazole uptake by sensitive and resistant isolates of *Helicobacter pylori*. *J. Antimicrob. Chemother.* 32, 393–400.
- Ladner, R. D., Lynch, F. J., Groshen, S., Xiong, Y. P., Sherrod, A., Caradonna, S. J., et al. (2000). dUTP nucleotidohydrolase isoform expression in normal and neoplastic tissues: association with survival and response to 5-fluorouracil in colorectal cancer. *Cancer Res.* 60, 3493–3503.
- Laity, J. H., Lee, B. M., and Wright, P. E. (2001). Zinc finger proteins: new insights into structural and functional diversity. *Curr. Opin. Struct. Biol.* 11, 39–46. doi: 10.1016/S0959-440X(00)00167-6

- Land, K. M., and Johnson, P. J. (1999). Molecular basis of metronidazole resistance in pathogenic bacteria and protozoa. *Drug Resist. Updat.* 2, 289–294. doi: 10.1054/drup.1999.0104
- Lee, K. W., Ko, B. C., Jiang, Z., Cao, D., and Chung, S. S. (2001). Overexpression of aldose reductase in liver cancers may contribute to drug resistance. *Anticancer Drugs* 12, 129–132. doi: 10.1097/00001813-200102000-00005
- Lee, W. P. (1993). The role of reduced growth rate in the development of drug resistance of HOB1 lymphoma cells to vincristine. *Cancer Lett.* 73, 105–111. doi: 10.1016/0304-3835(93)90251-4
- Leiros, H. K., Kozielski-Stuhrmann, S., Kapp, U., Terradot, L., Leonard, G. A., and McSweeney, S. M. (2004). Structural basis of 5-nitroimidazole antibiotic resistance: the crystal structure of NimA from *Deinococcus radiodurans*. *J. Biol. Chem.* 279, 55840–55849. doi: 10.1074/jbc.M408044200
- Leitsch, D., Burgess, A. G., Dunn, L. A., Krauer, K. G., Tan, K., Duchêne, M., et al. (2011). Pyruvate:ferredoxin oxidoreductase and thioredoxin reductase are involved in 5-nitroimidazole activation while flavin metabolism is linked to 5-nitroimidazole resistance in *Giardia lamblia*. *J. Antimicrob. Chemother.* 66, 1756–1765. doi: 10.1093/jac/dkr192
- Leitsch, D., Kolarich, D., Wilson, I. B., Altmann, F., and Duchêne, M. (2007). Nitroimidazole action in *Entamoeba histolytica*: a central role for thioredoxin reductase. *PLoS Biol.* 5:e211. doi: 10.1371/journal.pbio.0050211
- Livak, K. J., and Schmittgen, T. D. (2001). Analysis of relative gene expression data using real-time quantitative PCR and the 2-(Delta Delta C(T)) Method. *Methods* 25, 402–408. doi: 10.1006/meth.2001.1262
- Lo, H. S., and Reeves, R. E. (1978). Pyruvate-to-ethanol pathway in *Entamoeba histolytica*. *Biochem. J.* 171, 225–230.
- Löfmark, S., Edlund, C., and Nord, C. E. (2010). Metronidazole is still the drug of choice for treatment of anaerobic infections. *Clin. Infect. Dis.* 50, S16–S23. doi: 10.1086/647939
- Loftus, B., Anderson, I., Davies, R., Alsmark, U. C., Samuelson, J., Amedeo, P., et al. (2005). The genome of the protist parasite *Entamoeba histolytica*. *Nature* 433, 865–868. doi: 10.1038/nature03291
- Ludlum, D. B., Colinas, R. J., Kirk, M. C., and Mehta, J. R. (1988). Reaction of reduced metronidazole with guanosine to form an unstable adduct. *Carcinogenesis* 9, 593–596. doi: 10.1093/carcin/9.4.593
- Ma, Q., Baldwin, K. T., Renzelli, A. J., McDaniel, A., and Dong, L. (2001). TCDD-inducible poly(ADP-ribose) polymerase: a novel response to 2,3,7,8-tetrachlorodibenzo-p-dioxin. *Biochem. Biophys. Res. Commun.* 289, 499–506. doi: 10.1006/bbrc.2001.5987
- Marchler-Bauer, A., Lu, S., Anderson, J. B., Chitsaz, F., Derbyshire, M. K., DeWeese-Scott, C., et al. (2011). CDD: a Conserved Domain Database for the functional annotation of proteins. *Nucleic Acids Res.* 39, D225–D229. doi: 10.1093/nar/gkq1189
- Marie, C., and Petri, W. A. Jr. (2014). Regulation of virulence of *Entamoeba histolytica*. *Annu. Rev. Microbiol.* 68, 493–520. doi: 10.1146/annurev-micro-091310-130550
- Marumo, K., Nakada-Tsukui, K., Tomii, K., and Nozaki, T. (2014). Ligand heterogeneity of the cysteine protease binding protein family in the parasitic protist *Entamoeba histolytica*. *Int. J. Parasitol.* 44, 625–635. doi: 10.1016/j.ijpara.2014.04.008
- McLysaght, A., Baldi, P. F., and Gaut, B. S. (2003). Extensive gene gain associated with adaptive evolution of poxviruses. *Proc. Natl. Acad. Sci. U.S.A.* 100, 15655–15660. doi: 10.1073/pnas.2136653100
- Mirza, H., Teo, J. D., Upcroft, J., and Tan, K. S. (2011a). A rapid, high-throughput viability assay for *Blastocystis* spp. reveals metronidazole resistance and extensive subtype-dependent variations in drug susceptibilities. *Antimicrob. Agents Chemother.* 55, 637–648. doi: 10.1128/AAC.00900-10
- Mirza, H., Wu, Z., Kidwai, F., and Tan, K. S. (2011b). A metronidazole-resistant isolate of *Blastocystis* spp. is susceptible to nitric oxide and downregulates intestinal epithelial inducible nitric oxide synthase by a novel parasite survival mechanism. *Infect. Immun.* 79, 5019–5026. doi: 10.1128/IAI.05632-11
- Mishra, V., Ali, V., Nozaki, T., and Bhakuni, V. (2010). *Entamoeba histolytica* Phosphoserine aminotransferase (EhPSAT): insights into the structure-function relationship. *BMC Res. Notes* 3:52. doi: 10.1186/1756-0500-3-52
- Moreno, S. N., and Docampo, R. (1985). Mechanism of toxicity of nitro compounds used in the chemotherapy of trichomoniasis. *Environ. Health Perspect.* 64, 199–208. doi: 10.1289/ehp.8564199
- Müller, J., Ley, S., Felger, I., Hemphill, A., and Müller, N. (2008). Identification of differentially expressed genes in a *Giardia lamblia* WB C6 clone resistant to nitazoxanide and metronidazole. *J. Antimicrob. Chemother.* 62, 72–82. doi: 10.1093/jac/dkn142
- Müller, J., Sterk, M., Hemphill, A., and Müller, N. (2007). Characterization of *Giardia lamblia* WB C6 clones resistant to nitazoxanide and to metronidazole. *J. Antimicrob. Chemother.* 60, 280–287. doi: 10.1093/jac/dkm205
- Müller, M., and Gorrell, T. E. (1983). Metabolism and metronidazole uptake in *Trichomonas vaginalis* isolates with different metronidazole susceptibilities. *Antimicrob. Agents Chemother.* 24, 667–673. doi: 10.1128/AAC.24.5.667
- Müller, M., Meingassner, J. G., Miller, W. A., and Ledger, W. J. (1980). Three metronidazole-resistant strains of *Trichomonas vaginalis* from the United States. *Am. J. Obstet. Gynecol.* 138, 808–812.
- Nakada-Tsukui, K., Tsuboi, K., Furukawa, A., Yamada, Y., and Nozaki, T. (2012). A novel class of cysteine protease receptors that mediate lysosomal transport. *Cell. Microbiol.* 14, 1299–1317. doi: 10.1111/j.1462-5822.2012.01800.x
- Nakada-Tsukui, K., Saito-Nakano, Y., Ali, V., and Nozaki, T. (2005). A retromerlike complex is a novel Rab7 effector that is involved in the transport of the virulence factor cysteine protease in the enteric protozoan parasite *Entamoeba histolytica*. *Mol. Biol. Cell* 16, 5294–5303. doi: 10.1091/mbc.E05-04-0283
- Narcisi, E. M., and Secor, W. E. (1996). In vitro effect of tinidazole and furazolidone on metronidazole-resistant *Trichomonas vaginalis*. *Antimicrob. Agents Chemother.* 40, 1121–1125.
- Nguewa, P. A., Fuertes, M. A., Cepeda, V., Alonso, C., Quevedo, C., Soto, M., et al. (2006). Poly(ADP-ribose) polymerase-1 inhibitor 3-aminobenzamide enhances apoptosis induction by platinum complexes in cisplatin-resistant tumor cells. *Med. Chem.* 2, 47–53. doi: 10.2174/157340606775197697
- Nozaki, T., Ali, V., and Tokoro, M. (2005). Sulfur-containing amino acid metabolism in parasitic protozoa. *Adv. Parasitol.* 60, 1–99. doi: 10.1016/S0065-308X(05)60001-2
- Pasupuleti, V., Escobedo, A. A., Deshpande, A., Thota, P., Roman, Y., and Hernandez, A. V. (2014). Efficacy of 5-nitroimidazoles for the treatment of giardiasis: a systematic review of randomized controlled trials. *PLoS Negl. Trop. Dis.* 8:e2733. doi: 10.1371/journal.pntd.0002733
- Pearson, K. (1901). On lines and planes of closest fit to systems of points in space. *Philos. Mag.* 2, 559–572. doi: 10.1080/14786440109462720
- Peláez, T., Cercenado, E., Alcalá, L., Marín, M., Martín-López, A., Martínez-Alarcón, J., et al. (2008). Metronidazole resistance in *Clostridium difficile* is heterogeneous. *J. Clin. Microbiol.* 46, 3028–3032. doi: 10.1128/JCM.00524-08
- Penuliar, G. M., Furukawa, A., Nakada-Tsukui, K., Husain, A., Sato, D., and Nozaki, T. (2012). Transcriptional and functional analysis of trifluoromethionine resistance in *Entamoeba histolytica*. *J. Antimicrob. Chemother.* 67, 375–386. doi: 10.1093/jac/dkr484
- Penuliar, G. M., Furukawa, A., Sato, D., and Nozaki, T. (2011). Mechanism of trifluoromethionine resistance in *Entamoeba histolytica*. *J. Antimicrob. Chemother.* 66, 2045–2052. doi: 10.1093/jac/dkr238
- Plaitakis, A., and Zaganas, I. (2001). Regulation of human glutamate dehydrogenases: implications for glutamate, ammonia and energy metabolism in brain. *J. Neurosci. Res.* 66, 899–908. doi: 10.1002/jnr.10054
- Pumbwe, L., Chang, A., Smith, R. L., and Wexler, H. M. (2007). BmeRABC5 is a multidrug efflux system that can confer metronidazole resistance in *Bacteroides fragilis*. *Microb. Drug Resist.* 13, 96–101. doi: 10.1089/mdr.2007.719
- Quon, D. V., d’Oliveira, C. E., and Johnson, P. J. (1992). Reduced transcription of the ferredoxin gene in metronidazole-resistant *Trichomonas vaginalis*. *Proc. Natl. Acad. Sci. U.S.A.* 89, 4402–4406. doi: 10.1073/pnas.89.10.4402
- Ralph, E. D., and Clarke, D. A. (1978). Inactivation of metronidazole by anaerobic and aerobic bacteria. *Antimicrob. Agents Chemother.* 14, 377–383. doi: 10.1128/AAC.14.3.377
- Ralph, E. D., Clarke, J. T., Libke, R. D., Luthy, R. P., and Kirby, W. M. (1974). Pharmacokinetics of metronidazole as determined by bioassay. *Antimicrob. Agents Chemother.* 6, 691–696.
- Ramana, K. V. (2011). Aldose reductase: new insights for an old enzyme. *Biomol. Concepts* 2, 103–114. doi: 10.1515/bmc.2011.002
- Rasoloson, D., Vanáková, S., Tomková, E., Rázga, J., Hrdy, I., Tachezý, J., et al. (2002). Mechanisms of in vitro development of resistance to metronidazole in *Trichomonas vaginalis*. *Microbiology* 148, 2467–2477.

- Ravdin, J. I., Murphy, C. F., Salata, R. A., Guerrant, R. L., and Hewlett, E. L. (1985). N-Acetyl-D-galactosamine-inhibitable adherence lectin of *Entamoeba histolytica*. I. Partial purification and relation to amoebic virulence *in vitro*. *J. Infect. Dis.* 151, 804–815.
- Reuber, T. L., and Ausubel, F. M. (1996). Isolation of Arabidopsis genes that differentiate between resistance responses mediated by the RPS2 and RPM1 disease resistance genes. *Plant Cell* 8, 241–249.
- Richards, R. G., Sowers, L. C., Laszlo, J., and Sedwick, W. D. (1984). The occurrence and consequences of deoxyuridine in DNA. *Adv. Enzyme Regul.* 22, 157–185. doi: 10.1016/0065-2571(84)90013-X
- Samarawickrema, N. A., Brown, D. M., Upcroft, J. A., Thammapalerd, N., and Upcroft, P. (1997). Involvement of superoxide dismutase and pyruvate:ferredoxin oxidoreductase in mechanisms of metronidazole resistance in *Entamoeba histolytica*. *J. Antimicrob. Chemother.* 40, 833–840.
- Samuelson, J. (1999). Why metronidazole is active against both bacteria and parasites. *Antimicrob. Agents Chemother.* 43, 1533–1541.
- Sato, D., Nakada-Tsukui, K., Okada, M., and Nozaki, T. (2006). Two cysteine protease inhibitors, EhICP1 and 2, localized in distinct compartments, negatively regulate secretion in *Entamoeba histolytica*. *FEBS Lett.* 580, 5306–5312. doi: 10.1016/j.febslet.2006.08.081
- Shain, K. H., and Dalton, W. S. (2001). Cell adhesion is a key determinant in *de novo* multidrug resistance (MDR): new targets for the prevention of acquired MDR. *Mol. Cancer Ther.* 1, 69–78.
- Sharma, A., Sojar, H. T., Glurich, I., Honma, K., Kuramitsu, H. K., and Genco, R. J. (1998). Cloning, expression, and sequencing of a cell surface antigen containing a leucine-rich repeat motif from *Bacteroides forsythus* ATCC 43037. *Infect. Immun.* 66, 5703–5710.
- Sirinek, K. R. (2000). Diagnosis and treatment of intra-abdominal abscesses. *Surg. Infect. (Larchmt)* 1, 31–38. doi: 10.1089/109629600321272
- Sisson, G., Jeong, J. Y., Goodwin, A., Bryden, L., Rossler, N., Lim-Morrison, S., et al. (2000). Metronidazole activation is mutagenic and causes DNA fragmentation in *Helicobacter pylori* and in *Escherichia coli* containing a cloned *H. pylori* RdxA(+) (Nitroreductase) gene. *J. Bacteriol.* 182, 5091–5096. doi: 10.1128/JB.182.18.5091-5096.2000
- Smith, M. A., and Edwards, D. I. (1995). Redox potential and oxygen concentration as factors in the susceptibility of *Helicobacter pylori* to nitroheterocyclic drugs. *J. Antimicrob. Chemother.* 35, 751–764. doi: 10.1093/jac/35.6.751
- Stigler, S. M. (1989). Francis galton's account of the invention of correlation. *Stat. Sci.* 4, 73–79 doi: 10.1214/ss/1177012580
- Tabatabaie, L., Klomp, L. W., Berger, R., and de Koning, T. J. (2010). L-serine synthesis in the central nervous system: a review on serine deficiency disorders. *Mol. Genet. Metab.* 99, 256–262. doi: 10.1016/j.ymgme.2009.10.012
- Tanih, N. F., Ndip, L. M., and Ndip, R. N. (2011). Characterisation of the genes encoding resistance to metronidazole (rdxA and frxA) and clarithromycin (the 23S-rRNA genes) in South African isolates of *Helicobacter pylori*. *Ann. Trop. Med. Parasitol.* 105, 251–259. doi: 10.1179/136485911X1289983 8683485
- Tazreiter, M., Leitsch, D., Hatzenbichler, E., Mair-Scorpio, G. E., Steinborn, R., Schreiber, M., et al. (2008). *Entamoeba histolytica*: response of the parasite to metronidazole challenge on the levels of mRNA and protein expression. *Exp. Parasitol.* 120, 403–410. doi: 10.1016/j.exppara.2008.09.011
- Tejman-Yarden, N., Millman, M., Lauwaet, T., Davids, B. J., Gillin, F. D., Dunn, L., et al. (2011). Impaired parasite attachment as fitness cost of metronidazole resistance in *Giardia lamblia*. *Antimicrob. Agents Chemother.* 55, 4643–4651. doi: 10.1128/AAC.00384-11
- Tillack, M., Biller, L., Irmer, H., Freitas, M., Gomes, M. A., Tannich, E., et al. (2007). The *Entamoeba histolytica* genome: primary structure and expression of proteolytic enzymes. *BMC Genomics* 8:170. doi: 10.1186/1471-2164-8-170
- Townson, S. M., Laqua, H., Upcroft, P., Boreham, P. F., and Upcroft, J. A. (1992). Induction of metronidazole and furazolidone resistance in *Giardia*. *Trans. R. Soc. Trop. Med. Hyg.* 86, 521–522. doi: 10.1016/0035-9203(92)90095-T
- Tukey, J. W. (1949). Comparing individual means in the analysis of variance. *Biometrics* 5, 99–114. doi: 10.2307/3001913
- Upcroft, J. A., and Upcroft, P. (1993). Drug resistance and *Giardia*. *Parasitol. Today* 9, 187–190. doi: 10.1016/0169-4758(93)90144-5
- Van Oosten, M. A., Notten, F. J., and Mikx, F. H. (1986). Metronidazole concentrations in human plasma, saliva, and gingival crevice fluid after a single dose. *J. Dent. Res.* 65, 1420–1423. doi: 10.1177/00220345860650120801
- Vicente, J. B., Ehrenkaufer, G. M., Saraiva, L. M., Teixeira, M., and Singh, U. (2009). *Entamoeba histolytica* modulates a complex repertoire of novel genes in response to oxidative and nitrosative stresses: implications for amebic pathogenesis. *Cell Microbiol.* 11, 51–69. doi: 10.1111/j.1462-5822.2008.01236.x
- Wassmann, C., Hellberg, A., Tannich, E., and Bruchhaus, I. (1999). Metronidazole resistance in the protozoan parasite *Entamoeba histolytica* is associated with increased expression of iron-containing superoxide dismutase and peroxiredoxin and decreased expression of ferredoxin 1 and flavin reductase. *J. Biol. Chem.* 274, 26051–26056. doi: 10.1074/jbc.274.37.26051
- Welch, B. L. (1947). The generalization of "Student's" problem when several different population variances are involved. *Biometrika* 34, 28–35. doi: 10.1093/biomet/34.1-2.28
- West, S. B., Wislocki, P. G., Fiorentini, K. M., Alvaro, R., Wolf, F. J., and Lu, A. Y. (1982). Drug residue formation from ronidazole, a 5-nitroimidazole. I. Characterization of *in vitro* protein alkylation. *Chem. Biol. Interact.* 41, 265–279. doi: 10.1016/0009-2797(82)90105-3
- World Health Organization Amoebiasis. (1997). WHO/PAHO/UNESCO report. A consultation with experts on amoebiasis. Mexico City, Mexico 28–29 January, 1997. *Epidemiol. Bull.* 18, 13–4.
- Wright, J. M., Webb, R. I., O'Donoghue, P., Upcroft, P., and Upcroft, J. A. (2010). Hydrogenosomes of laboratory-induced metronidazole-resistant *Trichomonas vaginalis* lines are downsized while those from clinically metronidazole-resistant isolates are not. *J. Eukaryot. Microbiol.* 57, 171–176. doi: 10.1111/j.1550-7408.2009.00455.x
- Yarlett, N., Yarlett, N. C., and Lloyd, D. (1986). Ferredoxin-dependent reduction of nitroimidazole derivatives in drug-resistant and susceptible strains of *Trichomonas vaginalis*. *Biochem. Pharmacol.* 35, 1703–1708. doi: 10.1016/0006-2952(86)90327-8
- Yoshikawa, T. T., Miyamoto, S., Chow, A. W., and Guze, L. B. (1974). *In vitro* resistance of *Neisseria gonorrhoeae* to metronidazole. *Antimicrob. Agents Chemother.* 6, 327–329. doi: 10.1128/AAC.6.3.327

Conflict of Interest Statement: The authors declare that the research was conducted in the absence of any commercial or financial relationships that could be construed as a potential conflict of interest.

Copyright © 2015 Penuliar, Nakada-Tsukui and Nozaki. This is an open-access article distributed under the terms of the Creative Commons Attribution License (CC BY). The use, distribution or reproduction in other forums is permitted, provided the original author(s) or licensor are credited and that the original publication in this journal is cited, in accordance with accepted academic practice. No use, distribution or reproduction is permitted which does not comply with these terms.



Quantitative RT-PCR assay for high-throughput screening (HTS) of drugs against the growth of *Cryptosporidium parvum* *in vitro*

Haili Zhang and Guan Zhu *

Department of Veterinary Pathobiology, College of Veterinary Medicine & Biomedical Sciences, Texas A&M University, College Station, TX, USA

OPEN ACCESS

Edited by:

Anjan Debnath,
University of California, San Diego,
USA

Reviewed by:

Xiamming Chen,
Creighton University, USA
Nigel Yarlett,
Pace University, USA
Momar Ndao,
McGill University, Canada

*Correspondence:

Guan Zhu,
Department of Veterinary
Pathobiology, College of Veterinary
Medicine & Biomedical Sciences,
Texas A&M University, 4467 TAMU,
College Station, TX 77843-4467, USA
gzhu@cvm.tamu.edu

Specialty section:

This article was submitted to
Antimicrobials, Resistance and
Chemotherapy,
a section of the journal
Frontiers in Microbiology

Received: 09 May 2015

Accepted: 04 September 2015

Published: 22 September 2015

Citation:

Zhang H and Zhu G (2015)
Quantitative RT-PCR assay for
high-throughput screening (HTS) of
drugs against the growth of
Cryptosporidium parvum *in vitro*.
Front. Microbiol. 6:991.
doi: 10.3389/fmicb.2015.00991

Our laboratory has previously developed a qRT-PCR assay to assess drug efficacy on the growth of *Cryptosporidium parvum* *in vitro* by detecting the levels of parasite 18S rRNA. This approach displayed up to four orders of magnitude of linear dynamic range and was much less labor-intensive than the traditional microscopic methods. However, conventional qRT-PCR protocol is not very amendable to high-throughput analysis when total RNA needs to be purified by lengthy, multi-step procedures. Recently, several commercial reagents are available for preparing cell lysates that could be directly used in downstream qRT-PCR analysis (e.g., Ambion Cell-to-cDNA kit and Bio-Rad iScript sample preparation reagent). Using these reagents, we are able to adapt the qRT-PCR assay into high-throughput screening of drugs *in vitro* (i.e., 96-well and 384-well formats for the cultivation of parasites and qRT-PCR detection, respectively). This qRT-PCR protocol is able to give a >150-fold linear dynamic range using samples isolated from cells infected with various numbers of parasites. The new assay is also validated by the NIH-recommended intra-plate, inter-plate, and inter-day uniformity tests. The robustness and effectiveness of the assay are also confirmed by evaluating the anti-cryptosporidial efficacy of paromomycin and by a small scale screening of compounds.

Keywords: *Cryptosporidium parvum*, *in vitro*, qRT-PCR, high-throughput screening, assay development, paromomycin

Introduction

Cryptosporidium is a genus of protozoan pathogens belonging to the Phylum Apicomplexa that infect humans and/or animals. Among them, *C. parvum* and *C. hominis* are the two major species causing water-borne and food-borne diarrheal illness in humans (Baldursson and Karanis, 2011; Budu-Amoako et al., 2011). These two and some other species, including *C. meleagridis*, *C. muris*, *C. canis*, and *C. felis*, also cause opportunistic infections in AIDS patients (AIDS-OIs) that can be chronic and fatal (Thompson et al., 2005; Feasey et al., 2011; O'connor et al., 2011; Shirley et al., 2012). A more recent multi-country study also revealed that *Cryptosporidium* is one of the top five diarrheal-causing pathogens in children in developing countries, in which the infection increased death rate and negatively affected the growth of children (Kotloff et al., 2013). However, options to treat cryptosporidiosis are limited. In fact, only a single drug, nitazoxanide (NTZ) is approved by the U.S. Food and Drug Administration (FDA) to treat

human cryptosporidial infection in immunocompetent patients. Moreover, NTZ is ineffective in treating cryptosporidiosis in AIDS patients, and its efficacy in immunocompetent patients is also debatable (Cabada and White, 2010; Feasey et al., 2011; O'Connor et al., 2011; Checkley et al., 2015).

Two approaches are commonly employed in early stages of drug discovery against infectious diseases. Hits and leads may be identified from new chemical entities by directly testing their efficacies against an *in vitro* or *in vivo* model of disease (traditional methods), or by screening compounds against drug targets from a pathogen such as essential enzymes or receptors (target-based methods). In the later case, identified hits/leads will still be evaluated on their *in vitro* efficacy before being advanced to *in vivo* drug testing. Therefore, the availability of a good *in vitro* disease model is critical in drug discovery against diseases including cryptosporidiosis. *In vitro* models of cryptosporidial infection are available, including the cultivation of *C. parvum* in HCT-8 or Caco-2 cells (Arrowood, 2002; Cai et al., 2005; Karanis and Aldeybari, 2011). However, there is a need for developing new methods that can efficiently evaluate the parasite growth in response to drug treatment in high-throughput or high-volume format. Conventional microscopic examination to count the numbers of parasites stained chemically or by immunofluorescence labeled antibodies is highly labor-intensive and sometimes subjective, making it unsuitable for testing a large number of drugs. ELISA and chemiluminescence immunoassay methods were reported, but they appeared to have relatively narrow linear dynamic ranges of detection (i.e., the ratio between the largest and smallest signal values of detection is proportional to the difference between the two samples, such as the relationship between the OD values and concentrations of an antigen in an ELISA assay) and heavily relying on the quality and availability of specific antibodies.

More recent approaches include quantitating parasite loads by quantitative PCR (qPCR), qRT-PCR and automated fluorescence imaging analysis that are generally more advantageous than the earlier methods. Among them, the qRT-PCR method originally developed in our laboratory evaluates drug efficacy by detecting the relative levels of parasite 18S rRNA transcripts, which displays up to four orders of magnitude of linear dynamic range between the cycle threshold (C_T) value and the logarithm of the number of oocyst inoculum (Cai et al., 2005; Ctrnáctá et al., 2010; Zhang et al., 2012). However, classic qRT-PCR protocol is not very amendable to the high-throughput or high-volume analysis when total RNA needs to be purified by lengthy, multi-step procedures.

Here we report an improved and simplified qRT-PCR protocol for evaluating of drug efficacies against the growth of *C. parvum* *in vitro*. This new protocol takes advantage of the commercially available lysis buffers to prepare cell lysates that could be directly used in downstream qRT-PCR analysis. We also re-optimized the primers and procedures, and adapted the *in vitro* cultivation of parasite in 96-well plates and real-time RT-PCR detection in 384-well plates, making the protocol suitable for high-throughput or high-volume evaluation of drug efficacy against the growth of *C. parvum* *in vitro*.

Materials and Methods

Cultivation of Parasite *In Vitro*

Fresh oocysts of *C. parvum* (Iowa strain) were purchased from Bunch Grass Farm (Deary, ID). Oocysts were further purified by a Percoll-based gradient centrifugation method and surface sterilized with 10% bleach for 7 min on ice, followed by washes with phosphate-buffered saline (PBS). Only *C. parvum* oocysts less than 3 months old were used in all experiments. An ileocecal colorectal adenocarcinoma cell line (HCT-8, ATCC # CCL-244) was used to host the growth of *C. parvum* *in vitro*. One day before the inoculation, HCT-8 cells were seeded in 96-well plates (2.5×10^4 cells/well) containing RPMI 1640 medium supplied with 10% fetal bovine serum (200 μ L medium/well in all experiments) and allowed to grow overnight at 37°C under 5% CO₂ atmosphere until they reached ~90% confluence. The infection and growth of *C. parvum* *in vitro* in 96-well plates were examined by differential interference contrast (DIC) microscopy and immunofluorescence (IF) labeling using a rabbit polyclonal antiserum raised against *C. parvum* sporozoite total membrane proteins (Zeng and Zhu, 2006; Zeng et al., 2006; Fritzler et al., 2007), and by qRT-PCR (as described below).

For generating standard curves, host cells were inoculated with five-fold serial dilutions of parasite oocysts (i.e., 4×10^4 – 64 oocysts/well), responding to the ratios between parasite and host cells ranging from ~1:1 to 1:625. For drug testing, host cells were infected with 2×10^4 oocysts per well (i.e., ratio 1:2). After inoculation, parasite oocysts were allowed to undergo excystation and invasion into host cells for 3 h at 37°C. Free parasites and oocyst walls in the medium were removed from the plates by an exchange of the culture medium. Drugs at specified concentrations were added into the culture at this time point (i.e., immediately after the medium exchange). Parasite-infected cells were then incubated at 37°C for additional 41 h (i.e., total 44 h infection time). For dose response of paromomycin (PRM), 3 × serial diluted PRM from 30 to 800 μ g/mL (i.e., 42–1120 μ M) was added to infected cells after 3 h post-infection (hpi) and the treatment lasted for 41 h. At least two independent experiments were conducted for every experimental condition, each including two replicates drugs and three replicates for negative and positive controls.

Preparation of Cell Lysates

Plates containing HCT-8 cells infected with *C. parvum* for 44 h and uninfected cells grown under the same condition were first centrifuged in a Sigma 2–5 plate centrifuge (Sigma Laborzentrifugen GmbH, Germany) for 10 min at 1000 × g to ensure that free merozoites in the medium were firmly settled on the bottom of the wells. Medium was removed by gentle flicking the plate over a container placed in the biosafety cabinet, followed by two gentle washes with PBS. After removal of PBS and blotting plates on paper towels to remove remaining drops, plates were placed on ice in a rectangle bucket. An eight-channel electronic pipette (Rainin Instrument, Oakland, CA) was used to add PBS and lysis buffer in subsequent procedures.

For extracting total RNA used in high-throughput screening (HTS), 200 μ L of ice-cold Bio-Rad iScript qRT-PCR sample

preparation reagent (lysis buffer) (Bio-Rad Laboratories, Hercules, CA) was added into each well. Plates were sealed with adhesive and heat sealing films and the bucket containing racked plates on ice was secured in a multi-tube vortexer (VX-2500, VWR International, Radnor, PA) and subjected to vortex for 20 min at the speed set at 7. Plates were then incubated at 75°C for 15 min, followed by centrifugation (5 min, 2000 × g) to settle down cell debris. Supernatants were used immediately in subsequent qRT-PCR reactions or the plates were stored at -80°C until use.

Real-time qRT-PCR Assay

The levels of 18S rRNA transcripts from *C. parvum* and host cells (referred to as Cp18S and Hs18S) were detected by real-time qRT-PCR method using qScript™ one-step SYBR green qRT-PCR kit (Quanta Biosciences, Gaithersburg, MD). Cell lysates prepared as described above were diluted by 100 and 2000 folds for detecting Cp18S and Hs18S transcripts, respectively. Reactions were performed in hard-shell 384-well skirted PCR plates (Bio-Rad Laboratories, Hercules, CA) (10 μL/well) containing 3 μL diluted cell lysate, 5 μL one-step SYBR green master mix, 0.2 μL RT master mix and the following primers: Cp18S-1011F (5'-TTG TTC CTT ACT CCT TCA GCA C-3') and Cp18S-1185R (5'-TCC TTC CTA TGT CTG GAC CTG-3') primer pair for Cp18S rRNA (GenBank accession number: NC_006986.1), and Hs18S-1F (5'-GGC GCC CCC TCG ATG CTC TTA-3') and Hs18S-1R (5'-CCC CCG GCC GTC CCT CTT A-3') primer pair for Hs18S rRNA (GenBank accession number: NR_003286). Among them, Cp18S-1011F and Cp18S-1185R were described in our earlier studies reporting the original qRT-PCR assay and the efficacy of S-adenosylhomocysteine hydrolase inhibitors against the growth of *C. parvum* *in vitro* (Cai et al., 2005; Ctrnáctá et al., 2010), whereas Hs18S-1F and Hs18S-1R represented our newly optimized primers (that were also described in one of our more recent publications (Zhang et al., 2012). Hs18S levels were used as controls and for normalization. All reagents for the qRT-PCR were loaded using an epMotion 5070 automated pipetting system (Eppendorf, Hauppauge, NY).

Real-time qRT-PCR reactions were performed by a Bio-Rad CFX384 Touch Real-Time PCR Detection System. The reactions started with synthesizing cDNA at 50°C for 20 min, followed by 5 min at 95°C to denature RNA-cDNA hybrids and deactivate reverse transcriptase, and 40 two-temperature thermal cycles of PCR amplification at 95°C, 10 s and 58°C, 30 s. At the end of PCR amplification, melting curve analysis was performed between 65 and 95°C. At least two technical replicates were included in qRT-PCR reactions for each sample.

After qRT-PCR reactions were completed, amplification curves and melting peaks were examined to assess the quality and specificity of the reactions, followed by the computation of relative parasite loads based on the cycle threshold (C_T) values of Cp18S and Hs18S transcripts as previously described. Briefly, the means of C_T values from technical replicates were first obtained for individual biological replicates, which were used to compute ΔC_T values between Cp18S and Hs18S (i.e., $\Delta C_T = C_{T[Cp18S]} - C_{T[Hs18S]}$), and $\Delta\Delta C_T$ values between each experimental sample and control (i.e., $\Delta\Delta C_T = \Delta C_{T[sample]} - \Delta C_{T[control]}$).

Standard curves were generated by plotting ΔC_T values against the logarithm of the oocyst numbers used to inoculate cells, followed by linear regression to obtain the slope value (parameter A in Equation below) to calculate the detection efficiency and parasite loads using the following equation as described (Cai et al., 2005):

$$\text{Inhibition (\%)} = (1 - 10^{A \cdot \Delta\Delta C_T}) \cdot (100)$$

Because all samples contained much lower levels of Cp18S rRNA than those of Hs18S rRNA, we used two different dilution factors (i.e., 100- and 2000-fold dilutions of lysates for detecting Cp18S and Hs18S, respectively) as described above to maintain the linearity of detections. These dilution factors needed to be considered in calculating the relative level between Cp18S and Hs18S in a specified sample:

$$\text{Relative } [Cp18S] = \frac{[Cp18S]}{[Hs18S]} = \left(\frac{100}{2000} \right) \cdot 10^{A \cdot \Delta C_{T[Cp18S-Hs18S]}}$$

However, the effect of the dilution factors was eliminated in subsequent computation of the relative growth of *C. parvum* (Cp) between a sample (s) and control (c) based on $\Delta\Delta C$ values:

$$\text{Relative Cp growth} = \frac{\left(\frac{[Cp18S]_s}{[Hs18S]_s} \right)}{\left(\frac{[Cp18S]_c}{[Hs18S]_c} \right)} = \frac{\left(\frac{100}{2000} \right) \cdot 10^{A \cdot \Delta C_{T[s]}}}{\left(\frac{100}{2000} \right) \cdot 10^{A \cdot \Delta C_{T[c]}}} = 10^{A \cdot \Delta\Delta C_{T[s-c]}}$$

Evaluation of the Growth of Host Cells and Parasite in 96-well Plates

We also evaluated the growth of *C. parvum* in 96-well plates by qRT-PCR and microscopy, in which HCT-8 cells were cultured and infected with *C. parvum* as described above. For qRT-PCR analysis, total RNA was isolated from cells using an RNeasy RNA isolation kit (Qiagen), rather than directly using cell lysates, to ensure more precise measurements of the levels of Cp18S and Hs18S transcripts. RNA samples included those from cells infected with *C. parvum* for 3 and 44 h, respectively, and from uninfected cells cultured under the same condition and for the same time periods. For microscopic examination, sterilized glass coverslips were gently broken into pieces and placed into selected wells before seeding host cells. Cells infected with parasites for 3 and 44 h were fixed in 3.7% paraformaldehyde and stained with a rabbit polyclonal antibody against total *C. parvum* membrane proteins following standard protocols (Chen et al., 2003; Zeng et al., 2006). Samples were then mounted onto glass microscopic slides with a Anti-Fade mounting medium containing 4',6-diamidino-2-phenylindole (DAPI) for counter-staining nuclei (Molecular Probes, Invitrogen), and examined under Olympus BX51 Research Microscope.

Assay Quality Assessment

In addition to determining the linear dynamic range from standard curve derived from samples infected with varied numbers parasites, the uniformity and signal variability of the assay were also validated according to the "Assay Guidance

Manual" (see chapter "HTS Assay Validation" at <http://www.ncbi.nlm.nih.gov/books/NBK53196/>) (Iversen et al., 2012). This method is recommended by the National Center for Advancing Translational Sciences (NCATS), National Institutes of Health (NIH) (see "Pre-Clinical Research Toolbox" at <http://www.ncats.nih.gov/expertise/preclinical>). In this study, inter-day tests were performed by three independent experiments. Each experiment used three 96-well plates to assess inter-plate variations, and each plate contained three experimental groups, which included uninfected HCT-8 cells ("Min" background signal), cells infected with parasites but untreated ("Max" signal), and cells that were infected with parasites and treated with 120 µg/mL (168 µM) of PRM ("Mid" signal). These groups (32 wells each) were arranged in an interleaved-signal format according to the Assay Guidance Manual.

The cultivation of host cells and *C. parvum* *in vitro*, preparation of cell lysates, and qRT-PCR assay were performed as described above. PRM was added into specified wells after the invasion and the removal of uninfected parasites. At the same time, DMSO at 0.5% final concentration was added into all wells. Based on the qRT-PCR data, mean (AVG), standard deviation (SD), and coefficient of variation (CV) were calculated for each group in each plate. Signal window (SW) and Z' factor for each plate were calculated based on the Assay Guidance Manual as follows (Iversen et al., 2012):

$$SW = \frac{(AVG_{max} - 3SD_{max}/\sqrt{n}) - (AVG_{min} + 3SD_{min}/\sqrt{n})}{SD_{max}/\sqrt{n}}$$

$$Z' = \frac{(AVG_{max} - 3SD_{max}/\sqrt{n}) - (AVG_{min} + 3SD_{min}/\sqrt{n})}{AVG_{max} - AVG_{min}}$$

Small-scale Drug Screening

The assay is currently used in our laboratory to test drug efficacy and screen compound libraries against *C. parvum* *in vitro*. Here we report the data on 48 small molecules designated as C001–C048 to provide a snapshot on the assay performance. HCT-8 cells were cultured in 96-well plates and infected with *C. parvum* using procedures described above. In primary screening, drugs dissolved in DMSO were added into the culture immediately after the medium exchange at 3 h post-infection (hpi) time (10 µM final concentration). Each plate contained five negative controls without receiving drug treatment and three positive controls treated by 100 µg/mL (140 µM) of PRM. Each well, including negative and positive controls, contained 0.5% DMSO. At 44 hpi time, cell lysates were prepared using Bio-Rad iScript lysis buffer and the anti-cryptosporidial efficacies of drugs were evaluated by qRT-PCR as described above. Compounds that inhibited >65% of the parasite growth were re-tested. Two of the most effective drugs were then selected to generate dose-response curves to determine IC₅₀ values.

Results and Discussions

Growth of Host Cells and Parasites in 96-well Format in the 44-h Infection Assay

Similar to other apicomplexans, *Cryptosporidium* sporozoites invade host cells and undergo at least two generation of asexual

cell cycles (merogony) before entering sexual development (gametogenesis and fertilization between macro- and micro-gametes) to form oocysts. We have observed that most *C. parvum* cultured in 24- or 48-well plates may complete the second generation of merogony and a large number of free merozoites may be released into the culture medium at 48 hpi. This complicates the quantification of parasite loads because free merozoites in the medium may be easily washed off during the sample preparation. To minimize this problem, our laboratory uses the 44 h infection assay, in which the majority of the intracellular parasites are in the late stage of meronts and only a minimal number of merozoites are present in the medium. To confirm that *C. parvum* cultured in 96-well plates followed similar invasion and intracellular developmental timeline, we compared the parasite growth at 3 and 44 hpi by qRT-PCR and fluorescence microscopy. We also evaluate the host cell growth at the time points correlated to the 3 and 44 hpi by qRT-PCR.

Using qRT-PCR, we have observed rapid intracellular parasite growth (i.e., 34-fold increase of Cp18S rRNA from 3 to 44 hpi) (**Figure 1A**), which gave us a good dynamic range to quantify the relative parasite growth. For comparison, there was only ~1.6-fold increase of uninfected Hs18S cultured for the same time period (**Figure 1B**), indicating that parasite grew >20 times faster than the HCT-8 cells in this cultivation system. We also observed that parasite infection slightly reduced the HCT-8 cell growth (i.e., ~10% decrease based on Hs18S rRNA levels) (**Figure 1B**), which might be attributed by the arrest of host cell growth upon infection and cell death upon the completion of merogony development and the release of parasite merozoites as reported by other investigators (Dobbelaere and Küenzi, 2004; Brunet et al., 2008).

DIC microscopy and IF labeling revealed the successful invasion of *C. parvum* sporozoites into the host cells after 3-h initial incubation of oocysts with host cells, in which the elongated sporozoites were transformed to small round trophozoites (**Figure 1C**, 3 hpi panel). However, it was possible that some sporozoites might have attached to, but failed to invade into host cells or undergo further development at the 3 hpi time point. The growth of parasite into late stage of meronts as evidenced by the presence of multiple nuclei in many meronts by DAPI staining (**Figure 1C**, 44 hpi panel). Intracellular parasites in these stages were also clearly visualized by IF staining using a rabbit antiserum against *C. parvum* sporozoite membrane proteins (**Figure 1C**, TRITC staining). These observations indicated that parasite cultured in 96-well plates exhibited an intracellular development timeline similar to those cultured in 24- and 48-well plates. Because majority of the parasites still remained intracellular at 44 hpi, they could be lysed together with host cell monolayers for RNA extraction. However, we still included a plate centrifugation step before washing cell monolayers and preparing cell lysates to ensure any free merozoites released into the medium were not excluded from subsequent analysis.

Optimization the Sample Preparation used for Simplified qRT-PCR

Several commercial lysis buffers are currently available for preparing cell lysates suitable for qRT-PCR without further

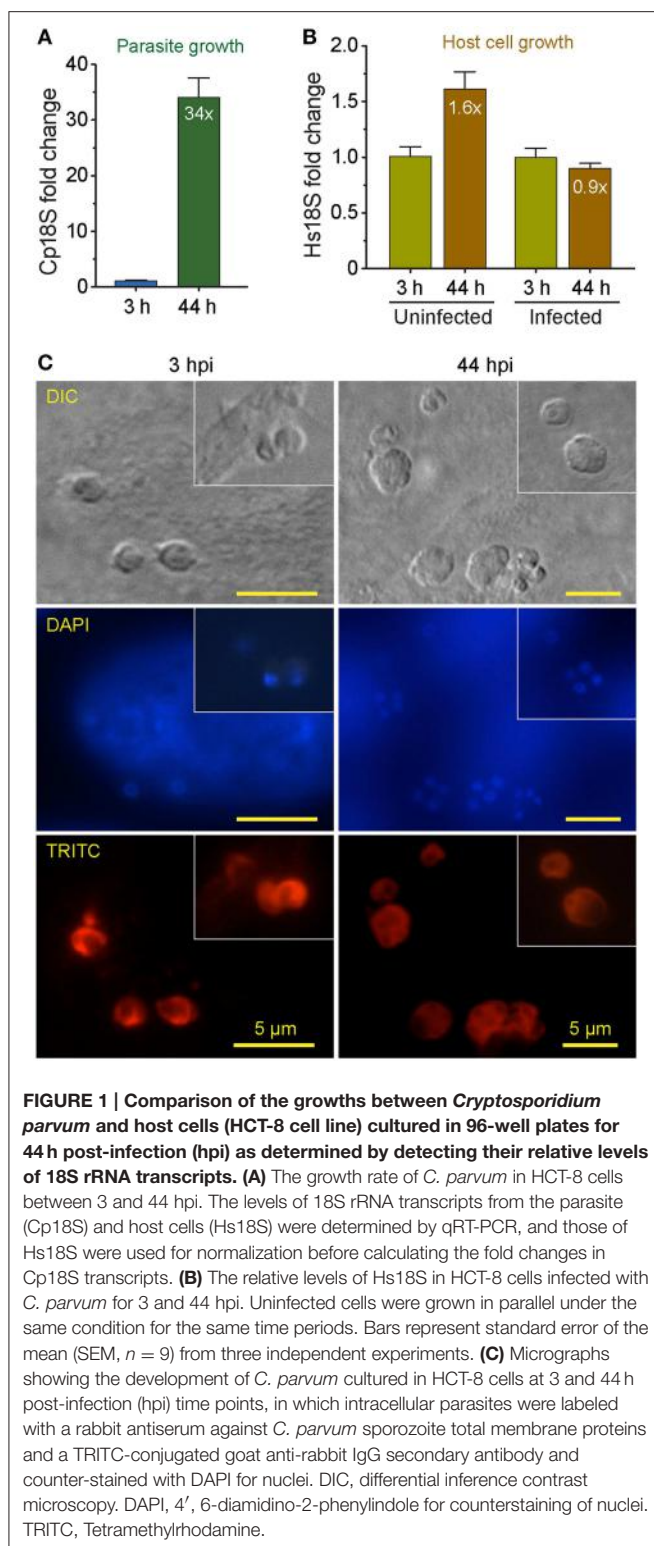


FIGURE 1 | Comparison of the growths between *Cryptosporidium parvum* and host cells (HCT-8 cell line) cultured in 96-well plates for 44 h post-infection (hpi) as determined by detecting their relative levels of 18S rRNA transcripts. (A) The growth rate of *C. parvum* in HCT-8 cells between 3 and 44 hpi. The levels of 18S rRNA transcripts from the parasite (Cp18S) and host cells (Hs18S) were determined by qRT-PCR, and those of Hs18S were used for normalization before calculating the fold changes in Cp18S transcripts. **(B)** The relative levels of Hs18S in HCT-8 cells infected with *C. parvum* for 3 and 44 hpi. Uninfected cells were grown in parallel under the same condition for the same time periods. Bars represent standard error of the mean (SEM, $n = 9$) from three independent experiments. **(C)** Micrographs showing the development of *C. parvum* cultured in HCT-8 cells at 3 and 44 h post-infection (hpi) time points, in which intracellular parasites were labeled with a rabbit antiserum against *C. parvum* sporozoite total membrane proteins and a TRITC-conjugated goat anti-rabbit IgG secondary antibody and counter-stained with DAPI for nuclei. DIC, differential interference contrast microscopy. DAPI, 4', 6-diamidino-2-phenylindole for counterstaining of nuclei. TRITC, Tetramethylrhodamine.

purification of RNA (Ho et al., 2013). At the early of the project, we briefly evaluated Ambion Cells-to-cDNA™ II kit (Life Technologies) and iScript™ RT-qPCR Sample Preparation Reagent (Bio-Rad), and observed slight better performance in releasing intracellular parasite RNA by the Bio-Rad's reagent

(data not shown) that was then used in our subsequent assay development. We also observed that standard sample preparation procedures recommended by the manufacturer was insufficient to release parasite RNA, largely because intracellular parasites were contained in parasitophorous vacuoles and protected by extra layers of membranes. We hence performed experiments to determine the optimal conditions including the amounts of lysis buffer and the addition of vortex and heating steps.

We observed that heat treatment of cell lysates at 75°C for 10–30 min significantly improved the release of parasite RNA. When samples were lysed in 100, 150, or 200 μ L/well lysis buffer, heat treatment for 10, 20, or 30 min reduced the C_T [Cp18S] values from 24.4, 24.0, and 23.9 to 22.4, 22.3, and 22.2 in the 100 μ L/well group, from 25.3, 24.9, and 24.5 to 23.6, 23.4, and 23.3 in the 150 μ L/well group, or from 25.6, 25.5, and 25.2 to 23.9, 23.6, and 23.6 in the 200 μ L/well group, respectively ($p < 0.005$ by Student *t*-test in all samples in comparison to the unheated counterparts) (Figure 2). However, we also observed certain levels of heat-induced host cell RNA degradation (i.e., C_T [Hs18S] values in heated samples were increased by ~0.2–1.0) (Figure 2). One possible explanation was that the host cell membranes could be rapidly lysed to release RNA with ice-cold lysis buffer (as heating was not included in the manufacturer's protocol), and there was a small window of time at the beginning of the heating process for the host cell RNases to become active before being deactivated by heat. On the other hand, more parasite RNA was released after the temperature reached to 75°C and RNases were deactivated. However, the final host cell RNA concentrations appeared to be consistent within each experimental group (i.e., CV values at 0.75–3.04% for all groups), indicating that the RNA degradation would not result in inconsistency in subsequent determination of relative Hs18S levels. Finally, based on the observation that heating between 10 and 20 min in wells containing 200 μ L lysis buffer resulted in the least degradation of host cell RNA (ΔC_T at 0.20–0.25), but the most improvement in releasing parasite RNA (ΔC_T at –1.8 to –2.0), we determined that the optimal condition was the use of 200 μ L iScript™ RT-qPCR Sample Preparation Reagent and heating for 15 min.

The subsequent qRT-PCR amplification protocol in 384-well format using cell lysates was effective and specific based on agarose gel analysis of amplicons (data not shown) and post-run analysis of amplification and melting curves (Figure 3). In the melting curves, Cp18S and Hs18S displayed two strong and distinguishable peaks, although there was a small minor peak in the Cp18S curves (Figure 3B).

Assay Validation on Plate Uniformity, Linear Dynamic Range, and Drug Testing

Three experimental cell culture groups were used in assay validation (i.e., a total of 864 uninfected, infected/untreated, and infected/PRM-treated samples in nine plates). For uninfected cell samples containing that should not contain any Cp18S transcripts, the determined Cp18S C_T values were resulted from low level non-specific amplification due to the lack of specific templates and/or self-amplification of primers, which was similar to the background signals produced in negative controls without

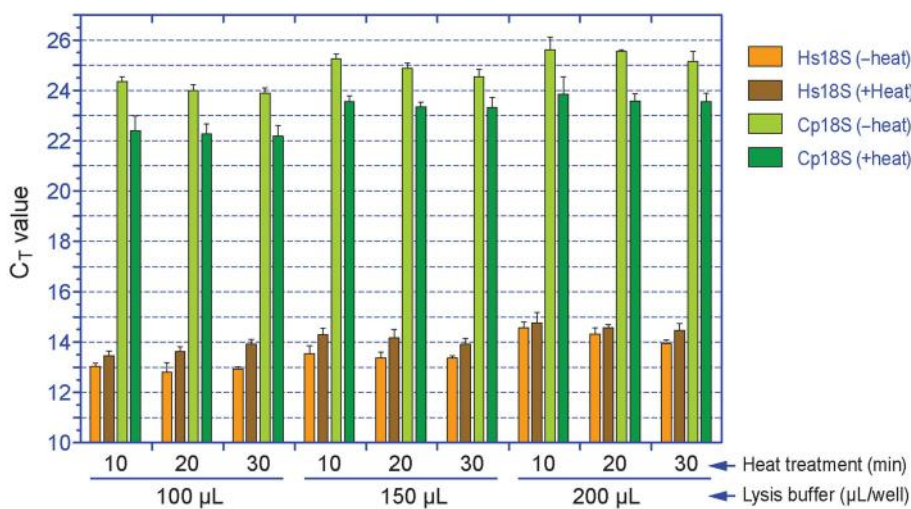


FIGURE 2 | Effects of the amount of lysis buffer and heat treatment on the release of RNA from *Cryptosporidium parvum* and HCT-8 cells. Cell lysates were first diluted by 100 and 2000 times with nuclease-free water prior to qRT-PCR detection for Cp18S and Hs18S rRNA transcripts, respectively. The plotted C_T values were not calibrated to equal volume of lysis buffer. Bars represent standard error of the mean (SEM, $n = 6$). Heat treatment vs. un-treatment control, $p < 0.005$ by Student's t -test in all samples.

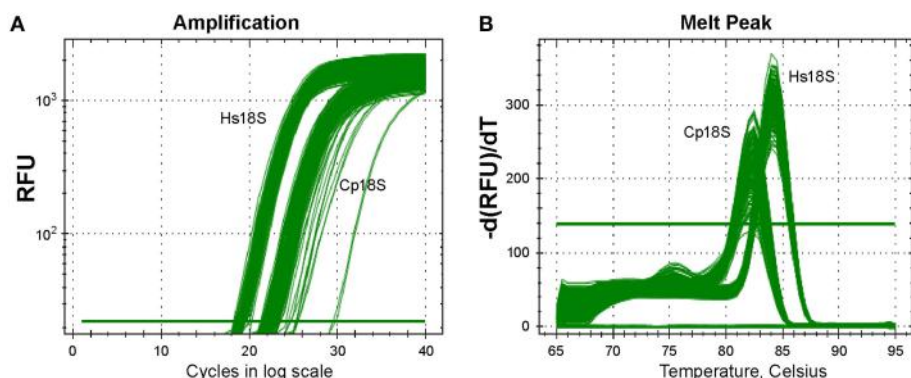


FIGURE 3 | Specific detection of Cp18S and Hs18S rRNA transcripts as demonstrated by amplification curve (A) and melting curve (B) analyses of a representative plate. Lysates of HCT-8 cells grown in 96-well plates and infected with *Cryptosporidium parvum* for 44 h were used in qRT-PCR reactions in 384-well format.

enzyme in a biochemical assay. Under the conditions used in the assay, the overall mean of C_T values for Cp18S from uninfected cells in all plates was 30.14 (between 29.34 and 31.07). These C_T values were much higher than those derived from cells infected with *C. parvum* (mean = 22.15, between 21.40 and 22.90) (Table 1). Because of the negative correlation (inversely proportional) relationship between C_T values and template concentrations, the higher C_T values in uninfected cells indicated that the noise signals in this assay (i.e., background signals in negative controls in the absence of parasites) were roughly >250-fold lower than the signals from the infected cells (i.e., noise levels equivalent to 0.4% of the signals). For Hs18S transcripts, the overall mean of C_T values from all groups was 13.46 (between 12.92 and 14.06). In the infected/untreated groups, the average ΔC_T value difference between those of Hs18S

and Cp18S was 8.6 (Table 1). After considering the dilution factors (i.e., cell lysates used for detecting Hs18S and Cp18S transcripts were diluted by 100 and 2000 folds, respectively), these C_T values suggested the presence of 7000–8000-fold more Hs18S than Cp18S in a typical sample.

Using the validation protocols recommended by NIH/NCATS, we observed high intra-plate, inter-plate, and inter-day uniformity for the assay (Table 2). All CV values were <5%, much better than the 20% threshold recommended by the Assay Guidance Manual. No significant inter-plate and inter-day data shifts were observed. The SW and Z' values in the nine plates were ranging from 17.35 to 44.14 and 0.73 to 0.87, respectively. Both values were much higher than the recommended acceptance criterions (i.e., SW ≥ 2 and Z' ≥ 0.4). The excellence of the assay is largely due to high specificity in the

TABLE 1 | Summary of the C_T values in the uniformity assay using the simplified qRT-PCR assay^a.

Exp	Plate	Infected, untreated				Infected, PRM-treated				Uninfected, untreated			
		Cp18S		Hs18S		Cp18S		Hs18S		Cp18S		Hs18S	
		Mean	SD	Mean	SD	Mean	SD	Mean	SD	Mean	SD	Mean	SD
1	1	22.24	0.17	13.93	0.17	23.32	4.31	13.55	2.55	30.70	0.25	13.58	0.31
1	2	22.57	0.20	13.77	0.19	23.85	0.30	13.88	0.18	31.07	0.26	12.92	0.30
1	3	22.90	0.53	14.06	0.23	24.47	0.41	13.88	0.25	30.68	0.19	13.69	0.19
2	1	21.67	0.25	13.49	0.25	23.29	0.33	13.51	0.22	30.15	0.29	13.51	0.20
2	2	21.40	0.25	13.32	0.18	23.17	0.27	13.25	0.22	29.68	0.27	13.36	0.29
2	3	21.94	0.52	13.45	0.34	23.65	0.43	13.42	0.34	30.08	0.26	13.42	0.36
3	1	21.93	0.36	13.02	0.38	23.59	0.31	12.99	0.28	29.78	0.26	13.09	0.38
3	2	22.25	0.27	13.33	0.29	23.83	0.31	13.27	0.27	29.34	0.24	13.30	0.25
3	3	22.49	0.41	13.57	0.34	24.09	0.26	13.45	0.30	29.79	0.40	13.44	0.28

^aAll mean values are C_T values derived from each plate in three independent cell cultivation experiments (Exp) performed in different dates. PRM, paromomycin at 120 μ g/mL (168 μ M).

TABLE 2 | Assay validation on the uniformity of the simplified qRT-PCR assay based on normalized ΔC_T values^a.

Exp	Plate	Infected, untreated			Infected, PRM-treated			Uninfected, untreated			SW	Z'	Efficacy of PRM	
		Mean	SD	CV (%)	Mean	SD	CV (%)	Mean	SD	CV (%)			% Inh	SD
1	1	8.31	0.23	2.00	10.08	0.40	2.00	17.12	0.35	1.45	30.40	0.86	69.54	7.84
1	2	8.79	0.20	1.61	9.97	0.32	1.61	18.15	0.36	1.42	31.74	0.87	54.90	10.49
1	3	8.84	0.49	3.94	10.60	0.39	3.94	16.99	0.21	0.89	44.14	0.82	69.34	7.81
2	1	8.18	0.36	3.13	9.78	0.36	3.13	16.64	0.40	1.72	23.94	0.81	66.07	8.30
2	2	8.08	0.36	3.16	9.93	0.33	3.16	16.32	0.38	1.65	24.80	0.81	71.46	6.35
2	3	8.49	0.47	3.95	10.24	0.64	3.95	16.67	0.48	2.02	18.26	0.75	67.30	13.58
3	1	8.91	0.53	4.24	10.59	0.46	4.24	16.68	0.45	1.89	18.06	0.73	67.20	11.32
3	2	8.92	0.31	2.47	10.57	0.44	2.47	16.04	0.33	1.45	24.79	0.81	66.67	10.19
3	3	8.92	0.47	3.77	10.65	0.39	3.77	16.37	0.45	1.94	17.35	0.74	68.82	8.70

^aAll mean values are ΔC_T values between Cp18S and Hs18S derived from each plate in three independent cell cultivation experiments (Exp) performed in different dates. % Inh, % inhibition; PRM, paromomycin at 120 μ g/mL (168 μ M); SW, signal window; Z', Z' score.

RT-PCR amplification, resulting in a ~256-fold signal difference between infected and uninfected samples as described above. In the PRM-treated groups, the classic anti-cryptosporidial drug inhibited the parasite growth by 66.07–71.46% in all plates except for the plate 2 in experiment 1 that was at a slightly lower level of 54.90% (Table 2). These values were consistent with our *in vitro* drug efficacy tests using total RNA samples isolated by traditional column-based isolation kits from cells cultured in 24- and 48-well plates (Cai et al., 2005; Zhang et al., 2012; Yu et al., 2014).

We also generated standard curves from cells infected with various numbers of parasites. We considered that this approach was better than the traditional method using serially diluted RNA templates, because standard curves derived from various numbers of infected parasites would correct systematic errors from infection, sample preparation to qRT-PCR procedures, rather than to only correct the errors introduced at the qRT-PCR step. In this assay, linear relationship was observed between the ΔC_T values and the samples isolated from cells infected with $64\text{--}4 \times 10^4$ oocysts per well (Figure 4A). The ΔC_T values

from samples infected with more or less parasites frequently fell outside of the linear range (data not shown). The linear dynamic range for this new assay (~156-fold) was smaller than our previously reported assay using conventional protocols (Cai et al., 2005). There were two possible explanations. Firstly, the 96-well format had lower limits on the number of parasites that could be cultured in 96-well without density effect. Secondly, in comparison to conventional RNA isolation methods, cell lysates contained much less RNA due to the less efficiency in releasing RNA by the lysis buffer and higher dilutions needed to minimize the inhibition of RT-PCR reactions caused by substances present in the lysis buffer. However, the 156-fold linear dynamic range was sufficient for testing drug efficacy *in vitro*, as it could theoretically resolve <1% changes of parasite loads in the assay system.

We further evaluated the assay by testing the dose-response of PRM on the parasite growth, in which the drug at concentrations from 30 to 800 μ g/mL reduced the growth of *C. parvum* by 19–97%. Using a non-linear curve fit with a sigmoidal model, the IC₅₀ value was determined at 88.1 μ g/mL (123 μ M) (Figure 4B).

These inhibition values were comparable to those obtained in our previous report at 89.7 $\mu\text{g}/\text{ml}$ (Cai et al., 2005), suggesting that the assay was suitable for determining the inhibitory kinetics and IC_{50} values of anti-cryptosporidial compounds identified by HTS.

Testing the Assay by a Small Scale Drug Screening

In the primary screening of 48 small molecules (10 μM each), two compounds (C012 and C020) displayed cytotoxicity on HCT-8 cells, while others displayed a wide range of effects on the *C. parvum* growth *in vitro* (i.e., from -86.6 to 98.8% inhibition) (Figure 5). The negative inhibition values suggested that a few compounds might actually promote the parasite growth and/or affected more on host cells than on parasites, which could be evaluated by looking at the Hs18S and Cp18S C_T values. For example, for C023 with -86.6% inhibition, the mean C_T values for Hs18S and Cp18S were 13.38 and 18.08 (vs. 13.63 and 19.17 in the DMSO control), suggesting that this compound likely promoted the parasite growth more than reducing the host cell growth. Because we were interested only

in identifying anti-cryptosporidial inhibitors in this study, we repeated the primary testing on the seven most efficacious compounds, in which six compounds exhibited similar efficacies (Figure 5A, red circles). We also performed dose-response experiments on C004 and C028, in which both compounds at 10 μM displayed the same efficacy as observed in the two primary testing experiments (Figure 5B). Their IC_{50} values were at 0.98 and 1.33 μM , respectively, suggesting that these two compounds might be further explored for drug development or serve as leads. Experiments to further characterize these two compounds and other top hits from the 48 compounds are still ongoing as part of our larger effort in discovering new anti-cryptosporidial drugs, which will be reported separately. Nonetheless, these observations conformed the robustness and suitability of the assay in high-throughput screening of drugs by directly evaluating their anti-cryptosporidial efficacy *in vitro*.

Conclusions

We have developed a simplified real-time qRT-PCR assay suitable for high-throughput or high-volume screening of drugs against

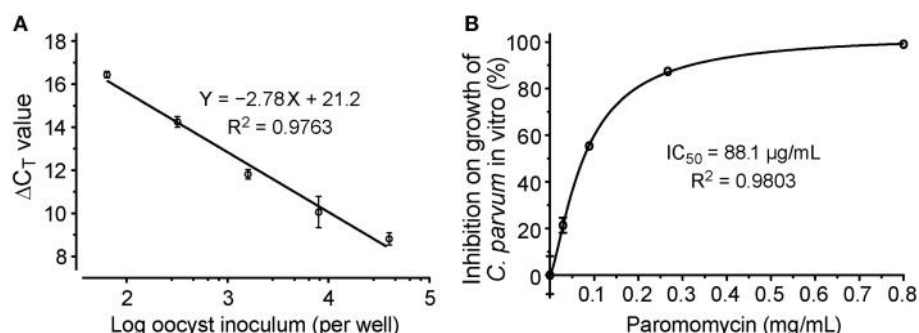


FIGURE 4 | Evaluation of drug efficacy using the new qRT-PCR assay. (A) Standard curves showing the relationship between the number of inoculated oocysts and $\Delta C_T(C_{p18S}-Hs18S)$ values; **(B)** Dose-response curve on the *in vitro* anti-cryptosporidial activity of paromomycin. Bars represent standard errors of the mean (SEM) derived from at least two biological replicates.

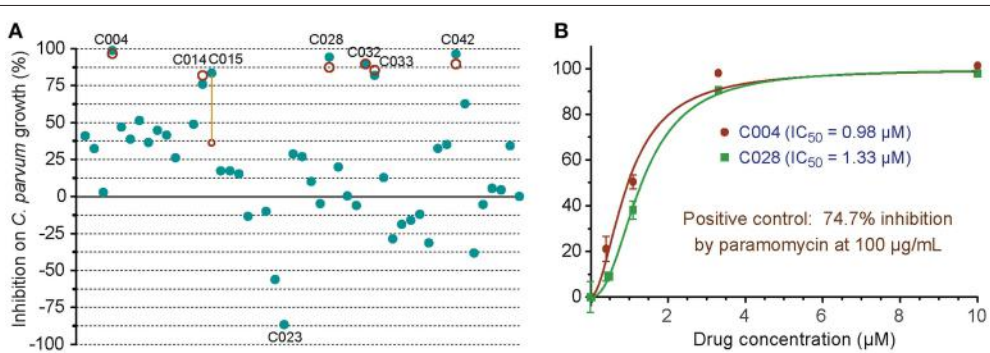


FIGURE 5 | In vitro anti-cryptosporidial activities of 48 small molecules (C001–C048). (A) Efficacies of all 48 compounds (10 μM each) obtained from primary screening (solid teal round dots). A second test was performed on seven top hits (red circles), in which six compounds displayed similar levels of efficacy between the two tests as shown by overlaps or near distances of their corresponding teal dots and red circles. Only one compound showed significantly different efficacies between the two tests (highlighted by a yellow line to link the corresponding teal dot and red circle). Compound codes are given on the seven top hits and one of the potential parasite growth enhancer as discussed in the text. **(B)** Dose-response curves on the anti-cryptosporidial activities of C004 and C028 compounds. Paromomycin at 100 $\mu\text{g}/\text{ml}$ (140 μM) was used as a positive control in this assay. Bars represent standard errors of the mean (SEM) derived from at least two biological replicates.

the growth of *C. parvum* *in vitro*. This was achieved by directly using cell lysates in qRT-PCR amplification. The assay was adapted and optimized in 96-well format for culturing parasite and 384-well format for SYBR-green based one-step real-time RT-PCR amplification and detection. Intra-plate, inter-plate, and inter-day uniformities were validated by NIH/NCATS recommended tests (i.e., SW and Z' values = 17.35–44.14 and 0.73–0.87, respectively). The assay exhibited >150-fold linear dynamic range using samples isolated from cells infected with serially diluted parasites. The robustness and effectiveness of the assay were also confirmed by evaluating the anti-cryptosporidial

efficacy of paromomycin, and by a small scale screening of 48 compounds.

Acknowledgments

Research reported in this study was supported by the National Institute of Allergy and Infectious Diseases of the National Institutes of Health under award number R21AI099850 (to GZ). The content is solely the responsibility of the authors and does not necessarily represent the official views of the National Institutes of Health.

References

- Arrowood, M. J. (2002). *In vitro* cultivation of cryptosporidium species. *Clin. Microbiol. Rev.* 15, 390–400. doi: 10.1128/CMR.15.3.390-400.2002
- Baldursson, S., and Karanis, P. (2011). Waterborne transmission of protozoan parasites: review of worldwide outbreaks - an update 2004–2010. *Water Res.* 45, 6603–6614. doi: 10.1016/j.watres.2011.10.013
- Brunet, J., Pfaff, A. W., Abidi, A., Unoki, M., Nakamura, Y., Guinard, M., et al. (2008). *Toxoplasma gondii* exploits UHFR1 and induces host cell cycle arrest at G2 to enable its proliferation. *Cell. Microbiol.* 10, 908–920. doi: 10.1111/j.1462-5822.2007.01093.x
- Budu-Amoako, E., Greenwood, S. J., Dixon, B. R., Barkema, H. W., and McClure, J. T. (2011). Foodborne illness associated with *Cryptosporidium* and *Giardia* from livestock. *J. Food Prot.* 74, 1944–1955. doi: 10.4315/0362-028X.JFP-11-107
- Cabada, M. M., and White, A. C. Jr. (2010). Treatment of cryptosporidiosis: do we know what we think we know? *Curr. Opin. Infect. Dis.* 23, 494–499. doi: 10.1097/QCO.0b013e32833d0e52
- Cai, X., Woods, K. M., Upton, S. J., and Zhu, G. (2005). Application of quantitative real-time reverse transcription-PCR in assessing drug efficacy against the intracellular pathogen *Cryptosporidium parvum* *in vitro*. *Antimicrob. Agents Chemother.* 49, 4437–4442. doi: 10.1128/AAC.49.11.4437-4442.2005
- Checkley, W., White, A. C. Jr., Jaganath, D., Arrowood, M. J., Chalmers, R. M., Chen, X. M., et al. (2015). A review of the global burden, novel diagnostics, therapeutics, and vaccine targets for cryptosporidium. *Lancet Infect. Dis.* 15, 85–94. doi: 10.1016/S1473-3099(14)70772-8
- Chen, X. M., Huang, B. Q., Splinter, P. L., Cao, H., Zhu, G., McNiven, M. A., et al. (2003). *Cryptosporidium parvum* invasion of biliary epithelia requires host cell tyrosine phosphorylation of cortactin via c-Src. *Gastroenterology* 125, 216–228. doi: 10.1016/S0016-5085(03)00662-0
- Ctrnáctá, V., Fritzler, J. M., Surinová, M., Hrdý, I., Zhu, G., and Stejskal, F. (2010). Efficacy of S-adenosylhomocysteine hydrolase inhibitors, D-eritadenine and (S)-DHPA, against the growth of *Cryptosporidium parvum* *in vitro*. *Exp. Parasitol.* 126, 113–116. doi: 10.1016/j.exppara.2010.04.007
- Dobbelaere, D. A., and Künen, P. (2004). The strategies of the *Theileria* parasite: a new twist in host-pathogen interactions. *Curr. Opin. Immunol.* 16, 524–530. doi: 10.1016/j.coim.2004.05.009
- Feesey, N. A., Healey, P., and Gordon, M. A. (2011). Review article: the aetiology, investigation and management of diarrhoea in the HIV-positive patient. *Aliment. Pharmacol. Ther.* 34, 587–603. doi: 10.1111/j.1365-2036.2011.04781.x
- Fritzler, J. M., Millership, J. J., and Zhu, G. (2007). *Cryptosporidium parvum* long-chain fatty acid elongase. *Eukaryotic Cell* 6, 2018–2028. doi: 10.1128/EC.00210-07
- Ho, Y. K., Xu, W. T., and Too, H. P. (2013). Direct quantification of mRNA and miRNA from cell lysates using reverse transcription real time PCR: a multidimensional analysis of the performance of reagents and workflows. *PLoS ONE* 8:e72463. doi: 10.1371/journal.pone.0072463
- Iversen, P. W., Benoit Beck, B., Yun-Fei Chen, Y., Dere, W., Devanarayan, V., Eastwood, B. J., et al. (2012). *Validation [Online]*. Eli Lilly & Company and the National Center for Advancing Translational Sciences. Available online at: <http://www.ncbi.nlm.nih.gov/books/NBK53196/> (Accessed on September 09, 2015).
- Karanis, P., and Aldeyari, H. M. (2011). Evolution of *Cryptosporidium* *in vitro* culture. *Int. J. Parasitol.* 41, 1231–1242. doi: 10.1016/j.ijpara.2011.08.001
- Kotloff, K. L., Nataro, J. P., Blackwelder, W. C., Nasrin, D., Farag, T. H., Panchalingam, S., et al. (2013). Burden and aetiology of diarrhoeal disease in infants and young children in developing countries (the Global Enteric Multicenter Study, GEMS): a prospective, case-control study. *Lancet* 382, 209–222. doi: 10.1016/S0140-6736(13)60844-2
- O'Connor, R. M., Shaffie, R., Kang, G., and Ward, H. D. (2011). Cryptosporidiosis in patients with HIV/AIDS. *AIDS* 25, 549–560. doi: 10.1097/QAD.0b013e3283437e88
- Shirley, D. A., Moonah, S. N., and Kotloff, K. L. (2012). Burden of disease from cryptosporidiosis. *Curr. Opin. Infect. Dis.* 25, 555–563. doi: 10.1097/QCO.0b013e328357e569
- Thompson, R. C., Olson, M. E., Zhu, G., Enomoto, S., Abrahamsen, M. S., and Hijjawi, N. S. (2005). *Cryptosporidium* and cryptosporidiosis. *Adv. Parasitol.* 59, 77–158. doi: 10.1016/S0065-308X(05)59002-X
- Yu, Y., Zhang, H., Guo, F., Sun, M., and Zhu, G. (2014). A unique hexokinase in *Cryptosporidium parvum*, an apicomplexan pathogen lacking the Krebs cycle and oxidative phosphorylation. *Protist* 165, 701–714. doi: 10.1016/j.protis.2014.08.002
- Zeng, B., Cai, X., and Zhu, G. (2006). Functional characterization of a fatty acyl-CoA-binding protein (ACBP) from the apicomplexan *Cryptosporidium parvum*. *Microbiology* 152, 2355–2363. doi: 10.1099/mic.0.28944-0
- Zeng, B., and Zhu, G. (2006). Two distinct oxysterol binding protein-related proteins in the parasitic protist *Cryptosporidium parvum* (Apicomplexa). *Biochem. Biophys. Res. Commun.* 346, 591–599. doi: 10.1016/j.bbrc.2006.05.165
- Zhang, H., Guo, F., and Zhu, G. (2012). Involvement of host cell integrin alpha2 in *Cryptosporidium parvum* infection. *Infect. Immun.* 80, 1753–1758. doi: 10.1128/IAI.05862-11
- Conflict of Interest Statement:** The authors declare that the research was conducted in the absence of any commercial or financial relationships that could be construed as a potential conflict of interest.
- Copyright © 2015 Zhang and Zhu. This is an open-access article distributed under the terms of the Creative Commons Attribution License (CC BY). The use, distribution or reproduction in other forums is permitted, provided the original author(s) or licensor are credited and that the original publication in this journal is cited, in accordance with accepted academic practice. No use, distribution or reproduction is permitted which does not comply with these terms.**



Oleylphosphocholine (OIPC) arrests *Cryptosporidium parvum* growth *in vitro* and prevents lethal infection in interferon gamma receptor knock-out mice

OPEN ACCESS

Edited by:

Anjan Debnath,

University of California, San Diego,
USA

Reviewed by:

Dmitri Debabov,

NovaBay Pharmaceuticals, USA
Kayode K. Ojo,
University of Washington, USA

*Correspondence:

Momar Ndao,

National Reference Centre
for Parasitology, Research Institute
of the McGill University Health Centre,
1001 Decarie Boulevard, Room EM3
3244, Montreal, QC H4A 3J1,
Canada

momar.ndao@mcgill.ca

[†]These authors have contributed
equally to this work.

Specialty section:

This article was submitted to
Antimicrobials, Resistance
and Chemotherapy,
a section of the journal
Frontiers in Microbiology

Received: 12 May 2015

Accepted: 01 September 2015

Published: 23 September 2015

Citation:

Sonzogni-Desautels K, Renteria AE,
Camargo FV, Di Lenardo TZ,
Mikhail A, Arrowood MJ, Fortin A
and Ndao M (2015)

Oleylphosphocholine (OIPC) arrests
Cryptosporidium parvum growth
in vitro and prevents lethal infection
in interferon gamma receptor
knock-out mice.

Front. Microbiol. 6:973.
doi: 10.3389/fmicb.2015.00973

Karine Sonzogni-Desautels^{1,2†}, Axel E. Renteria^{1,3†}, Fabio V. Camargo¹,
Thomas Z. Di Lenardo³, Alexandre Mikhail¹, Michael J. Arrowood⁴, Anny Fortin^{5,6} and
Momar Ndao^{1,2,3*}

¹ National Reference Centre for Parasitology, Research Institute of the McGill University Health Centre, Montreal, QC, Canada

² Institute of Parasitology, Macdonald Campus, McGill University, Montreal, QC, Canada, ³ Department of Experimental Medicine, McGill University, Montreal, QC, Canada, ⁴ Division of Foodborne, Waterborne, and Environmental Diseases, Center for Disease Control and Prevention, Atlanta, GA, USA, ⁵ Department of Biochemistry, McGill University, Montreal, QC, Canada, ⁶ Dafra Pharma R&D, Turnhout, Belgium

Cryptosporidium parvum is a species of protozoa that causes cryptosporidiosis, an intestinal disease affecting many mammals including humans. Typically, in healthy individuals, cryptosporidiosis is a self-limiting disease. However, *C. parvum* can cause a severe and persistent infection that can be life-threatening for immunocompromised individuals, such as AIDS patients. As there are no available treatments for these patients that can cure the disease, there is an urgent need to identify treatment options. We tested the anti-parasitic activity of the alkylphosphocholine oleylphosphocholine (OIPC), an analog of miltefosine, against *C. parvum* in *in vitro* and *in vivo* studies. *In vitro* experiments using *C. parvum* infected human ileocecal adenocarcinoma cells (HCT-8 cells) showed that OIPC has an EC₅₀ of 18.84 nM. Moreover, no cell toxicity has been seen at concentrations \leq 50 μ M. C57BL/6 interferon gamma receptor knock-out mice, were infected by gavage with 4000 *C. parvum* oocysts on Day 0. Oral treatments, with OIPC, miltefosine, paromomycin or PBS, began on Day 3 post-infection for 10 days. Treatment with OIPC, at 40 mg/kg/day resulted in 100% survival, complete clearance of parasite in stools and a 99.9% parasite burden reduction in the intestines at Day 30. Doses of 30 and 20 mg/kg/day also demonstrated an increased survival rate and a dose-dependent parasite burden reduction. Mice treated with 10 mg/kg/day of miltefosine resulted in 50% survival at Day 30. In contrast, control mice, treated with PBS or 100 mg/kg/day of paromomycin, died or had to be euthanized between Days 6 and 13 due to severe illness. Results of parasite burden were obtained by qPCR and cross-validated by both flow cytometry of stool oocysts and histological sections of the ileum. Together, our results strongly support that OIPC represents a potential candidate for the treatment of *C. parvum* infections in immunocompromised patients.

Keywords: *Cryptosporidium parvum*, cryptosporidiosis, oleylphosphocholine, OIPC, miltefosine, interferon gamma receptor knockout mice, oocysts, parasite burden

Introduction

Cryptosporidium parvum is an obligate parasite of the phylum Apicomplexa that infects the microvilli of the small intestine of many mammalian hosts including humans (Ryan and Xiao, 2014). Considered as a major waterborne pathogen (drinking and recreational water) that can also be transmitted through contaminated foods (Fayer et al., 2000; Cacciò and Putignani, 2014), *C. parvum* outbreaks have been widely reported in numerous countries from all continents (Cacciò et al., 2005; Putignani and Menichella, 2010; Cacciò and Putignani, 2014). This parasite can remain infectious for months in a humid environment (Robertson et al., 1992; King et al., 2005; Cacciò and Putignani, 2014). As a result, *C. parvum* has been categorized as a class B bioterrorist pathogen by the Center for Disease Control and Prevention (CDC; Feldmann et al., 2002; Rotz et al., 2002).

As one of the major causative agents of cryptosporidiosis in humans, along with *Cryptosporidium hominis* (Cacciò et al., 2005), *C. parvum* causes self-limiting watery diarrhea or persistent and severe diarrhea depending on the age and the immune status of the patient (Chalmers and Davies, 2010; Putignani and Menichella, 2010; Shikani and Weiss, 2014). Indeed, *C. parvum* infection has been reported to be life-threatening in AIDS patients, among which the prevalence of cryptosporidiosis was determined to be 14% in developed countries and 24% in developing countries (Collinet-Adler and Ward, 2010; Putignani and Menichella, 2010). *Cryptosporidium* spp., along with *Giardia* spp., has also been identified as the leading cause of chronic or persistent diarrhea in children in a context of malnutrition or immunodeficiency (Thapar and Sanderson, 2004; Putignani and Menichella, 2010). The Global Enteric Multicenter Study identified Cryptosporidium as one of the top five pathogens causing mild to severe diarrhea in children under the age of 2 in developing countries (Kotloff et al., 2013). Studies have shown that *Cryptosporidium* infections in young children have often resulted in stunting and lead to poor cognitive functions later in childhood (Berkman et al., 2002). However, currently available treatments have demonstrated limited effect in these vulnerable populations (Mead and Arrowood, 2014).

Nitazoxanide, the only American Food and Drug Association (FDA) approved drug to treat cryptosporidiosis in immunocompetent patients, has shown little activity to fight against *C. parvum* infections in AIDS patients (Cabada and White, 2010; Rossignol, 2010; Mead and Arrowood, 2014). Similarly, paromomycin, the currently used drug to treat *C. parvum* infections in AIDS patients, has shown modest activity and limited results in different case studies (Hewitt et al., 2000; Rossignol, 2010). With no efficient way to treat immunocompromised patients, many drugs have been tested over the years, but very few have shown consistent activity (Mead and Arrowood, 2014).

Oleylphosphocholine (OlPC, C₂₃H₄₈NO₄P) belongs to the family of alkylphosphocholines (Hernandez et al., 2014) and is structurally related to miltefosine (van Blitterswijk and Verheij, 2008), with the chemical formula C₂₁H₄₆NO₄P · xH₂O. Both compounds have shown *in vitro* and *in vivo* anti-leishmanial activity (Fortin et al., 2014), and *in vitro* activity of miltefosine

against *C. parvum* has also been reported (Shahiduzzaman et al., 2009). This study reports the strong activity of OlPC, both *in vitro* and *in vivo* in an immunocompromised C57BL/6 IFN γ R-KO mouse model of *C. parvum* infection.

Materials and Methods

Parasites

Cryptosporidium parvum (Iowa strain) oocysts, generously provided by Dr. Michael J. Arrowood (CDC, Atlanta, GA, USA), were maintained through a C57BL/6 IFN γ R-KO mouse infection model previously described by our laboratory (von Oettingen et al., 2008). Oocysts were purified following the reported technique (von Oettingen et al., 2008) and were stored in 2.5% (w/v) aqueous potassium dichromate (K₂Cr₂O₇, Sigma-Aldrich, Oakville, ON, Canada) at 4°C.

Test Compound

Oleylphosphocholine was generously provided by Dafra Pharma Research and Development (Turnhout, Belgium) and stored at 4°C, away from light. For *in vitro* studies, OlPC was diluted to a stock solution of 11.5 mM in ddH₂O. Miltefosine (Sigma-Aldrich, Oakville, ON, Canada) was used as a control in the *in vitro* assays because of its previously reported activity against *C. parvum* (Shahiduzzaman et al., 2009). Paromomycin (Sigma-Aldrich) was also used as a control in the *in vitro* assays. The drugs were prepared fresh daily in phosphate-buffered saline (PBS) for animal studies.

Host Cells

For *in vitro* studies, human colonic tumor cells (ileocecal adenocarcinoma; HCT-8: ATCC CCL-244) were used. Cells were maintained in T225 flasks (BD Bioscience, Mississauga, ON, Canada) using DMEM media (Wisent, St-Bruno, QC, Canada). For OlPC *in vitro* studies, media was supplemented with 10 µg/ml gentamycin, 10 µg/ml streptomycin, 100 U/ml penicillin, 10% heat-inactivated fetal bovine serum (FBS), and non-essential amino acids (NEAA; Wisent). For the cytotoxicity assays, cells were grown in supplemented DMEM without phenol red and further supplemented with 4.5 g/L D-glucose (Sigma-Aldrich, Oakville, ON, Canada) and 110 mg/L sodium pyruvate (Sigma-Aldrich). For miltefosine and paromomycin *in vitro* studies, media was supplemented with 10 µg/ml gentamicin, 50 µg/ml streptomycin, 50 U/ml penicillin, and 10% heat-inactivated FBS.

Cytotoxicity of OlPC in HCT-8 Cells

XTT assay (Sigma-Aldrich) was used (Roehm et al., 1991), which relies on the ability of live cells to cleave XTT causing a colorimetric change, to quantify the possible cytotoxicity of OlPC in HCT-8 cells. For this assay, DMEM without phenol red was used. Initially, 5 × 10⁴ HCT-8 cells in 200 µL of supplemented DMEM were seeded in a 96-well flat-bottom plates (BD Falcon, Franklin Lakes, NJ, USA) and incubated overnight (or until they reached ~80% confluence) at 37°C with 5% CO₂. Freshly prepared serial dilutions of OlPC diluted in

supplemented DMEM were used and 50 μ L of these solutions were added to the wells to obtain final OlPC concentrations ranging from 10 to 1000 μ M (4.33 to 433 μ g/mL). Samples were run in quadruplicate and plates were incubated at 37°C with 5% CO₂ for 48 h. Then, 50 μ L of XTT (dissolved in DMEM) was added to each well and plates were re-incubated for 4 h. Absorbance was measured at 450 nm using a plate reader (EL800 BioTek; Fisher, Nepean, ON, Canada).

C. parvum Infection Model in HCT-8 Cells

We tested the effect of OlPC on *C. parvum* sporozoites in HCT-8 cells. Briefly, 24-well flat-bottom plates (BD Falcon) were seeded with 3×10^5 cells in 1.4 mL of supplemented DMEM and incubated overnight (or until they reached ~80% confluence) at 37°C with 5% CO₂. Stock oocysts in 2.5% K₂Cr₂O₇ were washed three times with 0.1 M acetate-NaCl buffer, pH 5.5, and subsequently incubated in 10 mM sodium periodate on ice for 20 min. Oocysts were then washed three times with PBS containing 0.1% bovine serum albumin (BSA; Sigma-Aldrich). To release the sporozoites from the oocysts (excystation), parasites were incubated in DMEM containing 0.75% sodium taurocholate (Sigma-Aldrich) at 37°C for 30 min or until 50% excystation was determined by microscopy. Then, sporozoites from 1×10^5 oocysts were inoculated in each well. Non-infected cells incubated with supplemented DMEM served as negative controls as well as infected cells incubated with supplemented DMEM, as positive controls. OlPC was serially diluted in supplemented DMEM and was subsequently added to each well at concentrations ranging from 10 pM to 100 μ M (4.33 pg/mL to 43.3 μ g/mL). Miltefosine and paromomycin, diluted in supplemented DMEM, were also tested at concentrations ranging from 10 pM to 10 μ M (4.08 pg/mL to 4.08 μ g/mL) and 10 pM to 100 μ M (7.14 pg/mL to 71.4 μ g/mL) respectively, to serve as controls. Plates were further incubated for 48 h at 37°C with 5% CO₂. *In vitro* assays were run two independent times and each condition was run in triplicate for the miltefosine assay and in duplicate for the OlPC and the paromomycin assays. At the completion of the incubation, supernatants were removed and cells were lifted using 0.25% trypsin in EDTA (Wisent). To assess parasite burden in each well and determine the efficacy of OlPC, miltefosine or paromomycin against *C. parvum*, DNA was extracted from samples using QIAamp DNA Mini Kit (Qiagen, Toronto, ON, Canada). Purified DNA was stored at -20°C until use.

Quantitative Polymerase Chain Reaction Primers, Probe, and Standard Curve

Parasite burden from DNA samples from *in vitro* assays as well as from mouse fecal and intestinal samples were assessed by quantitative polymerase chain reaction (qPCR) targeting the hsp70 gene of *C. parvum* (GenBank: U69698.2) using the LightCycler 2.0 system (Roche, Laval, QC, Canada). Primers and probe sequences (TaqMan) were used according to previously published sequences (Shahiduzzaman et al., 2009). Briefly, a master mix per sample was prepared by adding 5 μ L of PCR-grade water (Roche), 2 μ L of 10 μ M of forward primer (CP_hsp70_fwd: 5'-AACTTTAgCTCCAgTTgAgAAA

gTACTC-3'; Tib MolBiol, Adelphia, NJ, USA), 2 μ L of 10 μ M reverse primer (CP_hsp70_rvs: 5'-CATggCTCTTACGgTTA AAgATTCC-3'; MolBiol), 2 μ L of 2 μ M 5' 6-carboxy fluorescein reporter dye (FAM) probe with a 3' tetramethylrhodamine quencher dye (TMR; hsp-taq: 5'-AATACGgTgTAgAAC CACCAACCAATAACATC-3'; MolBiol), and 4 μ L of buffer mix containing dNTP, MgCl₂, and Taq-polymerase (Roche). Prior to the polymerase chain reaction, 5 μ L of sample and 15 μ L of master mix were added to LightCycler capillaries (Roche). The initial denaturation step was conducted at 95°C for 15 min followed by 45 cycles of denaturation at 94°C for 15 s and annealing at 60°C for 1 min (Shahiduzzaman et al., 2009).

In order to quantify parasite burden, a standard curve was necessary. First, *C. parvum* oocysts were diluted to concentrations of 1×10^1 to 1×10^6 in 200 μ L and then, they were disrupted by five freeze-thaw cycles of 2 min incubation in liquid nitrogen followed by 2 min incubation in a 56°C water bath. Second, DNA from the oocyst extracts was purified using QIAamp DNA Blood Mini Kit (Qiagen) and these samples were run (qPCR) in the LightCycler 2.0; qPCR was used to correlate threshold cycle values (C_t values) to parasite burden ($R^2 = 0.9989$). This standard curve was used to extrapolate parasite burden from DNA samples from *in vitro* assays as well as from mouse stool and intestine samples.

Immunocompromised Mouse Model of *C. parvum* Infection

Cryptosporidium parvum oocysts in 2.5% K₂Cr₂O₇ were washed three times with PBS; parasites were then counted using a hemocytometer and diluted in PBS to a concentration of 4×10^4 /mL. Six to eight week old C57BL/6 IFN γ R-KO female and male mice (Jackson Laboratories, Bar Harbor, ME, USA) were infected with a lethal dose of 4000 oocysts in 100 μ L of PBS on Day 0 using a 22-gage gavage needle (CDVM, St-Hyacinthe, QC, Canada). Mice were separated in eight groups (13 mice/group for treated groups and 4–8 mice/group for control groups). Groups 1 and 2 were non-infected controls, treated per os (oral gavage) with PBS or with 40 mg/kg/day of OlPC, respectively. Group 3 was infected and treated with PBS (positive controls). Groups 4–6 were infected and treated per os with 40, 30, and 20 mg/kg/day of OlPC, respectively. Groups 7 and 8 were infected controls treated per os with 10 mg/kg/day of miltefosine and 100 mg/kg/day of paromomycin, respectively. Treatment started at Day 3 and continued for 10 days. OlPC and control drugs were prepared fresh on a daily basis for the length of the treatment. Mice were weighted daily. Starting on Day 4, individual stool samples were collected every 3–4 days until study termination.

Five mice from each group were sacrificed at Day 10 (before daily treatment) to assess and compare disease progression. Other mice were maintained until study termination (Day 30) unless they were found dead or had to be sacrificed due to severe illness. Because of the lethality of this model (von Oettingen et al., 2008; Ndao et al., 2013) an objective mouse rating system based on symptom severity and behavioral changes was developed in accordance with the Animal Care Committee and the Canadian Council on Animal Care (CCAC) guidelines to

determine when mice should be sacrificed due to illness. Upon death or euthanasia, the mouse ileum was preserved in formalin for histological purposes and the rest of the intestine (duodenum to rectum) was collected individually and chopped into 0.5 cm pieces into a 60 mL specimen container (ThermoFisher Scientific, Ottawa, ON, Canada) with 10 mL of 0.02% (v/v) Tween20 in PBS (one container per mouse). During necropsy, stool was also collected for oocyst purification.

After completion of the *in vivo* study, a constant volume of purified oocysts from intestinal samples of mice from each treatment groups was inoculated to naïve C57BL/6 IFN γ R-KO mice to determine if the concentration of oocysts remaining in the intestines of treated mice was able to induce clinical signs of cryptosporidiosis in naïve mice.

All mouse studies were conducted at the Montreal General Hospital rodent animal facility site of the Research Institute of McGill University Health Center. All studies performed were approved and in accordance with the MGH Facility Animal Care Committee and also in accordance with the CCAC guidelines.

Oocyst Purification from Intestinal Samples and Oocyst Burden Analysis by qPCR

For each mouse intestine sample in 0.02% (v/v) Tween20 in PBS, 0.05 g of sputasol (dry mixture of 10% DTT, 76% NaCl, 2% KCl, 10% Na₂HPO₄, and 2% KHPO₄) was added. Oocyst purification was performed using a previously described method reported in literature and by our lab (Meloni, 1996; von Oettingen et al., 2008). Briefly, each sample was homogenized for 2 min at 7000 rpm with the Polytron PT3000D homogenizer (Kinematica, Lucerne, Switzerland). Between each sample, the homogenizer was cleaned with bleach and ethanol to avoid cross-contamination. Samples were placed on a rotary mixer at low speeds for 90 min at room temperature. Samples were then transferred to 50 mL Falcon tubes (BD Falcon, Franklin Lakes, NJ, USA) and centrifuged at 2000 × g for 10 min at 4°C. The supernatant was removed and the pellet was resuspended in 8 mL of 0.02% (v/v) Tween20 in ddH₂O and 2 mL of diethyl ether (Sigma-Aldrich, Oakville, ON, Canada). Samples were thoroughly vortexed and centrifuged at 2000 × g for 10 min at 4°C. The layers containing fatty cells and tissues as well as the supernatants were removed. The pellets were washed with 20 mL of cold ddH₂O and centrifuged at 2000 × g for 10 min at 4°C. Supernatants were discarded and the pellets resuspended in 20 mL of saturated NaCl. Samples were vortexed thoroughly, carefully overlayed with 5 mL of cold ddH₂O and centrifuged at 2000 × g for 10 min at 4°C. Five milliliters of the interphase were collected and centrifuged at 2000 × g for 10 min at 4°C; supernatants were discarded and oocyst-containing pellets were resuspended in 1 mL PBS containing 10 µg/ml streptomycin and 100 U/ml penicillin. Purified oocyst samples were stored at 4°C. For qPCR analysis, 200 µL were taken from each purified oocyst sample and five freeze/thaw cycles of 2 min incubation in liquid nitrogen followed by 2 min incubation in a 56°C water bath were performed. DNA was then extracted using the QIAamp DNA Blood Mini Kit (Qiagen) and samples was used for qPCR analysis.

Oocyst Purification from Stool Samples and Oocyst Shedding Analysis by qPCR

Individual stool samples were collected in 500 µL of distilled and deionized (18.2 MΩ cm) water (ddH₂O) and stored in microcentrifuge tubes at 4°C until used. Samples were thoroughly vortexed until stools were homogenized to smaller particles, then centrifuged at 14000 × g and washed with cold ddH₂O. Supernatants were discarded and the pellets resuspended in 1 mL of saturated NaCl. Samples were vortexed thoroughly, carefully overlayed with 250 µL of cold ddH₂O and centrifuged at 1600 × g for 10 min at 4°C. All of the supernatant was collected and the sample was exposed to another NaCl-ddH₂O overlay. The supernatants collected from both overlays were centrifuged at 14000 × g for 3 min at 4°C, combined into one tube and resuspended in 200 µL of ddH₂O. Purified oocysts were exposed to five freeze/thaw cycles as described above. DNA was extracted using the QIAamp DNA Blood Mini Kit and stored at -20°C until oocyst shedding was quantified by qPCR. Values were normalized by gram of stool.

Oocyst Burden Analysis by Flow Cytometry

All oocyst samples purified from mouse intestine were incubated in a final concentration of 1% paraformaldehyde for 15–30 min prior to analysis. Briefly, 40 µL of sample and 50 µL of CountBright™ absolute counting beads (Invitrogen, Burlington, ON, Canada) were added to a paraformaldehyde solution for a final volume of 500 µL. Oocysts within each sample were quantified by morphology (FSC-A and SSC-A) using BD LSRFortessa™ cell analyser (BD, Franklin Lakes, NJ, USA). Oocysts were initially identified with a FITC-labeled mouse IgG3 monoclonal antibody targeting a surface antigen (AbD Serotec, Raleigh, NC, USA). Results demonstrated that 98% of the FITC positive events occupied a distinct population by size and complexity in the FSC-A and SSC-A channels. Results generated by flow cytometry are based on unstained samples gating on this distinct oocyst population. Oocyst concentration per sample was calculated by determining the quantity of sample collected based on the number of CountBright™ bead events collected. Final oocyst numbers were normalized by gram of mouse intestines.

Histopathology

Cryptosporidium parvum is known to preferentially infect the jejunum and ileum (Fayer and Xiao, 2008), thus the ileum was collected for histopathology. Liver and spleen were also fixed in formalin, paraffin-embedded and cut to 4 µm thick sections. Sections were stained with hematoxylin and eosin to further assess disease progression by light microscopy.

Data Analysis

All *in vitro* studies and qPCR data were analyzed using Microsoft Excel (Microsoft Corporation, Redmond, WA, USA). Graphs and P-values were obtained using GraphPad Prism® version 6.0 (GraphPad Software, Inc., La Jolla, CA, USA). Results represent mean ± standard error mean (SEM). For OlPC and miltefosine EC₅₀ calculations, the same software, GraphPad Prism® version 6.0, the non-linear fit of EC₅₀ shift and the “shared value for

all data sets" constraint for Bottom and Top were used. Flow cytometry data was analyzed using FlowJo v10 analytical software (Treestar, Inc., San Carlos, CA, USA).

Results

OIPC and Miltefosine Inhibit *C. parvum* Infection in HCT-8 Cells *In Vitro*

To test the efficacy of OIPC to inhibit *C. parvum* infection *in vitro*, we used HCT-8 cells which allowed the parasite to replicate (Widmer et al., 2000). Miltefosine was used as a control as its efficiency to inhibit *C. parvum* infection *in vitro* has already been described (Shahiduzzaman et al., 2009). However, the dose of 100 μM was not tested for miltefosine as cell toxicity has been reported at a concentration of 24.5 μM when cells are incubated for 45 h (Shahiduzzaman et al., 2009). For the OIPC and the miltefosine assays, DNA was extracted after 48 h of incubation with the compound. A standard curve was used to correlate threshold cycle values (C_t values) obtained by qPCR to parasite burden. Then, for each well, the percentage of parasite burden reduction was assessed according to this formula:

$$= [1 - (\text{parasite burden from tested well/parasite burden of positive control})] * 100$$

Positive controls were infected cells incubated with supplemented media (no compound). **Figure 1** represents the mean of the parasite burden reduction of tested wells for each concentration of OIPC (A) and miltefosine (B) \pm SEM.

HCT-8 cells treated with 100, 10, and 1 μM of OIPC showed the highest *C. parvum* inhibition with 87, 84, and 85% reduction in parasite burden, respectively (**Figure 1A**). Therefore, these concentrations of OIPC are not statistically different than uninfected controls showing the clear potency of these treatments to inhibit *C. parvum* infection *in vitro*. There is a statistical difference ($P < 0.0001$) between OIPC treatment and uninfected controls starting at the concentration of 100 nM due to the lack of efficiency of these doses to inhibit *C. parvum* infection. Results demonstrated a dose-dependent reduction of *C. parvum* burden when treated with increasing concentrations of OIPC and a calculated EC₅₀ of 18.84 nM. Cell toxicity of OIPC was not observed at concentrations of $\leq 50 \mu\text{M}$ using an XTT assay (data not shown).

Miltefosine at concentrations of 10 and 1 μM showed the highest inhibitory effect with 85 and 69% reduction in parasite burden, respectively (**Figure 1B**). Similarly to the OIPC treatment, at these concentrations, there is no statistical difference between the miltefosine treatment and uninfected cells. So, OIPC is as potent as miltefosine at inhibiting *C. parvum* infection *in vitro* at a concentration of 10 μM (84 vs. 85%), but OIPC better inhibits infection at a concentration of 1 μM (85 vs. 69%). The calculated EC₅₀ for miltefosine is 0.81 μM , which is slightly lower than the previously published value of 1.87 μM for this compound and this parasite (Shahiduzzaman et al., 2009), but within the same range. Batch differences in oocyst virulence due primarily to freshness are normal and can explain this type of variation. Concentrations of paromomycin ranging from 10 pM to 100 μM were tested to determine the ability of this compound

to inhibit *C. parvum* infection *in vitro*. However, no significant effect was observed (data not shown), which is in agreement with what has been published previously (Ndao et al., 2013).

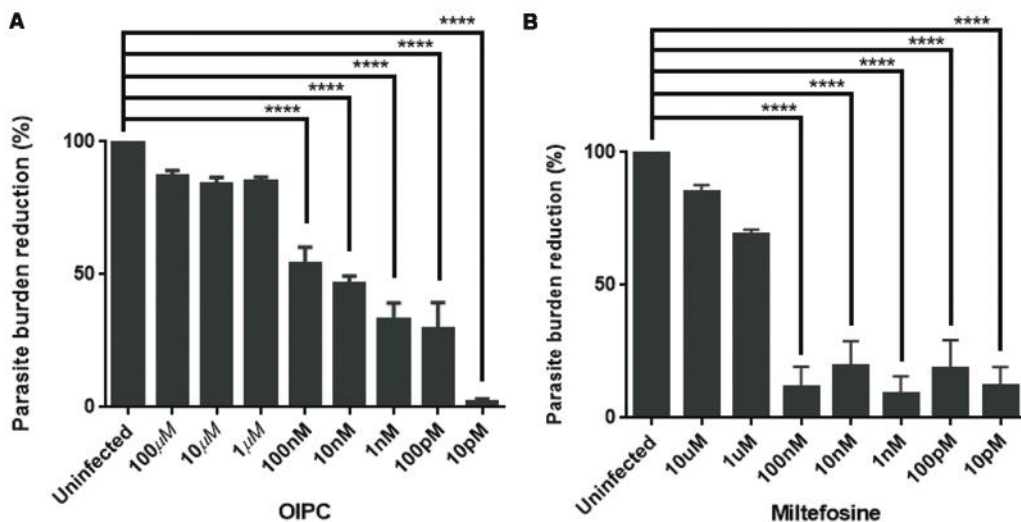
OIPC shows a Dose-Dependent Effect on *C. parvum*-Induced Mortality in an Immunodeficient Mouse Model

The C57BL/6 IFN γ R-KO mouse model is an excellent model to assess the efficacy of compounds to treat acute *C. parvum* infection because of the high susceptibility of these knockout mice to this parasite (von Oettingen et al., 2008; Ndao et al., 2013). According to previous reports, mice infected with as low as 1500 oocysts had a mortality rate of 80% by Day 14 (Ndao et al., 2013). Therefore, in this study, mice were infected with 4000 oocysts, and survival, as well as parasite burden reduction, was used to differentiate an effective treatment from an inefficient treatment. To ensure the objectivity of the study, an external blinded examiner scored the mice reaching pre-defined critical clinical end-points according to a pre-established rating system.

As expected, infected controls started showing symptoms of illness as early as Day 5 and had a very high mortality rate at Day 14. For the PBS treated group, mice started showing signs of illness (such as hunched back, weight loss, dehydration, lethargy, and watery stools) at Day 5 and all mice from this group died or were euthanized between Days 6 and 10 (**Figure 2**). Mice treated with 100 mg/kg/day of paromomycin for 10 days displayed clinical symptoms of cryptosporidiosis at Day 7 and a 60% mortality rate was observed at Day 9. Some paromomycin-treated mice did survive until Day 13 but, the Mantel-Cox or the Gehan-Breslow-Wilcoxon tests used to compare survival curves showed no significant difference with the PBS-treated group (**Figure 2**).

Mice treated with 10 mg/kg/day of miltefosine, the analog of OIPC, also showed signs of illness as early as Day 7 and a 50% mortality rate at Day 13 but, survivors remained alive until the end of the study (Day 30; **Figure 2**). This clear difference in survival rates with the PBS-treated group ($P < 0.001$) determined that a 10 mg/kg/day miltefosine treatment for 10 days significantly decreased mortality. Nevertheless, at Day 30, clinical signs of cryptosporidiosis were still visible in these mice such as 15% weight loss, hunched backs, dehydration, and soft stools.

Mice treated with 40 mg/kg/day of OIPC displayed a 100% survival rate by the experimental endpoint (Day 30; $P < 0.001$; **Figure 2**). Additionally, the onset of symptoms began later (Day 9) than the PBS-treated controls; clinical signs were less severe and did not last as long in comparison with other groups. Furthermore, at Day 10, which is the peak of infection (von Oettingen et al., 2008), weight loss (about 10% reduction from initial weight for the 40 mg/kg/day OIPC-treated group) was already significantly lower compared to any of the infected control groups ($> 15\%$ of initial weight, $P < 0.05$, data not shown). By Day 30, 40 mg/kg/day OIPC-treated mice looked healthy as they displayed no visible signs of illness. Moreover, unlike the miltefosine-treated group, 40 mg/kg/day OIPC-treated mice had exceeded, by Day 30, their initial weights ($P < 0.0001$, data not shown). Mice treated with 30 mg/kg/day of OIPC for 10 days, had less severe clinical signs of cryptosporidiosis. For



these latter mice, on one hand, treatment was not able to rescue all mice which showed a severe weight loss of up to 15% of initial weight; on the other hand, the onset of symptoms was delayed to Days 8 or 9. Their survival rate was of 87.5% at Day 11, 75% at Day 30 (Figure 2) and, by Day 30, the survivors displayed no visible signs of illness and had returned to their initial weights (data not shown). Finally, the lowest dose of OIPC (20 mg/kg/day) was still able to rescue 75% of mice at Day 30 even if there were still visible signs of illness and mice had a 5% weight loss in comparison with initial weights. Non-infected mice treated with 40 mg/kg/day of OIPC presented a constant weight through the length of the study and no clinical sign were noted in this group (data not shown).

OIPC Eliminates Oocyst Shedding in a Dose-Dependent Manner

All infected mice began shedding oocysts between Days 5 and 7. Stool samples were collected from individual mice, processed and analyzed by qPCR. At Day 10, infected mice treated with PBS and with 100 mg/kg/day of paromomycin were shedding 8.52×10^7 and 1.84×10^8 oocysts per gram of stool (oo/g of stool) respectively (data not shown). Similarly, mice treated with 10 mg/kg/day of miltefosine were shedding 1.94×10^8 oo/g of stool at Day 10 (Figure 3). At Days 14 and 30, surviving mice of this group continued to shed considerable levels of oocysts; 1.49×10^7 and 1.5×10^7 oo/g of stool respectively (Figure 3).

In mice treated with 40 mg/kg/day of OIPC, oocyst shedding reduction occurred as early as Day 10 with only 7.59×10^6 oo/g of stool which is a significant reduction in comparison with the 10 mg/kg miltefosine group ($P < 0.01$; Figure 3). At Day 14, after 10 days of OIPC-treatment, oocyst shedding in this group was even lower with 5.14×10^3 oo/g, representing a 99.96% reduction (4-log reduction) in oocyst shedding. At Day

14, the 40 mg/kg/day OIPC-treated group is also statistically different when compared with the 10 mg/kg miltefosine-treated mice ($P < 0.05$; Figure 3). Finally, at Day 30, there was a 100% elimination of oocyst shedding (>7-log reduction) in all mice of the 40 mg/kg/day OIPC-treated group ($P < 0.0001$; Figure 3). Light microscopy was used to confirm qPCR results. Indeed, all the samples of 40 mg/kg/day OIPC-treated mice at Day 30 were negative as no oocysts could be visualized under the microscope.

Mice treated with 30 mg/kg/day of OIPC showed a similar tendency in oocyst shedding as the 40 mg/kg/day OIPC-treated group. Effectively, all average oocyst counts were significantly

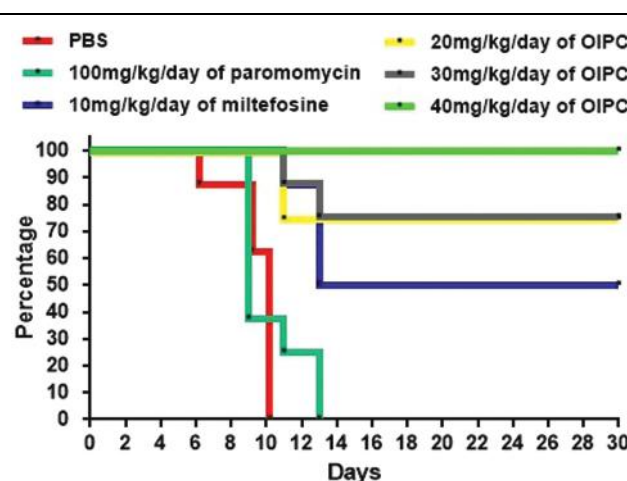


FIGURE 2 | Survival curves in C57BL/6 IFN γ R-KO mice infected with *C. parvum*. Results are shown in a survival curve. Results do not include mice sacrificed at Day 10 for disease progression analysis. On Day 30 remaining mice were sacrificed along with uninfected controls.

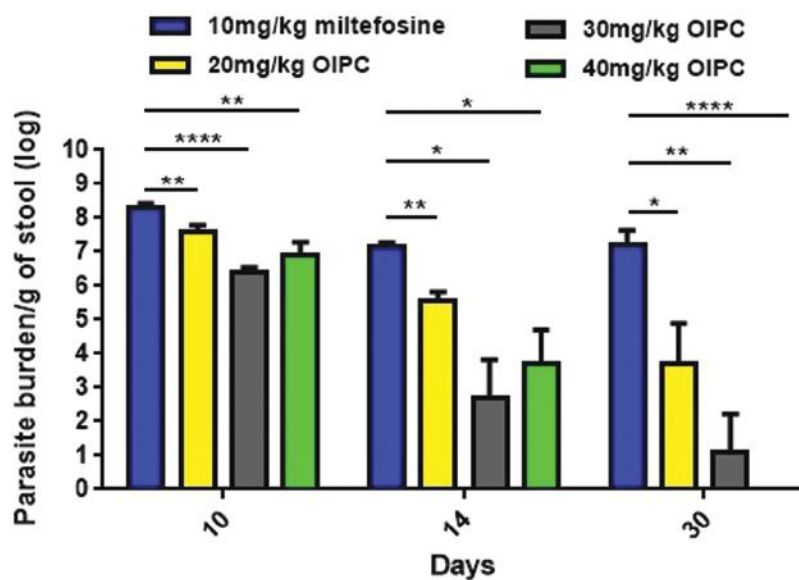


FIGURE 3 | Oocyst shedding in C57BL/6 IFN γ R-KO mice infected with *C. parvum*. All stool samples were collected from individual mice within each group, processed and analyzed by qPCR. Results were normalized to shed oocysts per grams of stool. Error bars were calculated as \pm SEM (* $P < 0.05$, ** $P < 0.01$, and **** $P < 0.0001$).

lower when compared with the 10 mg/kg/day miltefosine-treated group (Figure 3); at Day 10, the average oocyst shedding was 2.45×10^6 oo/g of stool ($P < 0.0001$), at Day 14, 4.9×10^2 oo/g of stool ($P < 0.05$) and, at Day 30, 13 oo/g of stool ($P < 0.01$). Mice treated with 20 mg/kg/day of OIPC had the least important reduction in oocyst shedding but remained significantly lower than the 10 mg/kg miltefosine-treated mice. In fact, 4.04×10^7 , 3.68×10^5 , and 5.95×10^3 oo/g of stool, was evaluated in these 20 mg/kg/day OIPC-treated mice at Day 10 ($P < 0.01$), Day 14 ($P < 0.01$), and Day 30 ($P < 0.05$) respectively (Figure 3).

Oocyst shedding was not statistically different between mice treated with 30 mg/kg/day and 40 mg/kg/day at Days 10 and 14. The fact that the numerical value of the mean for parasite burden/g of stool for the 40 mg/kg/day treated mice was slightly higher at Days 10 and 14 than the one for 30 mg/kg/day treated mice is most probably due to inter-individual variations in this mouse model.

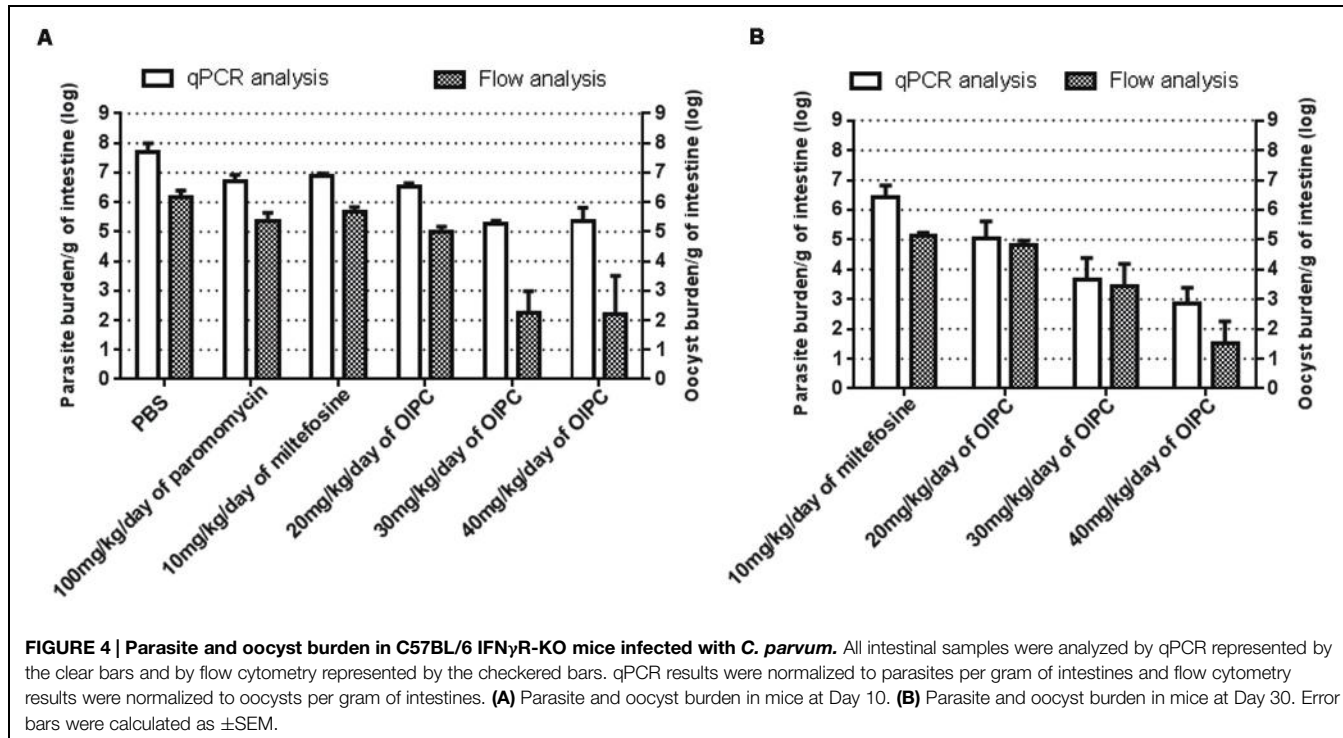
OIPC Significantly Reduces Parasite Burden in the Intestines of C57BL/6 IFN γ R-KO Mice Infected with *C. parvum*

To quantitate parasite and oocyst burden in the intestines and assess disease progression of infected mice during and after their respective treatments, mice were euthanized and intestines were collected at two time points: Days 10 or 30. Intestinal samples from every mouse were processed individually to purify *C. parvum* parasites, analyzed using qPCR and normalized to parasites per gram of intestines (p/g of intestines). On Day 10, infected control groups revealed massive levels of *C. parvum* in the gut. Mice treated with PBS had the highest parasite burden with 4.77×10^7 p/g of intestines followed by mice treated with 100 mg/kg/day of paromomycin with 5.01×10^6 p/g of intestines

(Figure 4A). Mice treated with 10 mg/kg/day of miltefosine also had very high parasite burden with 7.94×10^6 p/g of intestines (Figure 4A). In mice treated with OIPC, parasite burden was significantly lower compared to the infected PBS control group. After 7 days of treatment (Day 10), 20 mg/kg/day OIPC-treated mice showed a parasite burden of 3.44×10^6 p/g of intestines ($P < 0.01$; Figure 4A). In mice treated with 30 mg/kg/day of OIPC the parasite burden was even lower with 1.81×10^5 p/g of intestines ($P < 0.001$) corresponding to a 99.6% (2-log reduction) parasite burden reduction in comparison with the PBS control group (Figure 4A). Similarly, mice treated with 40 mg/kg/day of OIPC also revealed a 99.6% reduction in parasite burden with 2.25×10^5 p/g of intestines ($P < 0.001$) when compared to the infected PBS control mice (Figure 4A).

By Day 30, 17 days after the completion of the treatments, surviving mice treated with 10 mg/kg miltefosine exhibited a high parasite burden with 2.65×10^6 p/g of intestines (Figure 4B). Parasite burden decreased in mice treated with OIPC when compared to the 10 mg/kg miltefosine-treated mice following a dose-dependent response. Indeed, in mice treated with 20 mg/kg/day of OIPC, parasite burden obtained was 1.09×10^5 p/g of intestines (not significant, $P > 0.05$), whereas in mice treated with 30 mg/kg/day and 40 mg/kg/day, parasite burden was 4.66×10^3 p/g of intestines (99.8% parasite burden reduction, $P < 0.05$) and 692 p/g of intestines (99.97% parasite burden reduction, $P < 0.01$) respectively (Figure 4B). Additionally, by Day 30 there was an overall reduction in parasite burden in each group compared to their burden at Day 10.

To cross-validate results obtained by qPCR and to confirm the presence of *C. parvum* oocysts in the intestines, flow cytometry was used to quantify the number of oocysts per gram of intestines (oo/g of intestines). Flow cytometry data analysis allowed to



identify oocysts by their size and morphology (FSC-A and SSC-A) and to count them for each intestinal sample. In general, total parasite burdens calculated by flow cytometry were lower than those obtained by qPCR suggesting the presence of other stages of the parasite in the intestines that flow cytometry cannot distinguish. However, the results were supportive of those of the qPCR. Mice treated with PBS, 100 mg/kg paromomycin and 10 mg/kg miltefosine showed an oocyst burden of 1.46×10^6 oo/g of intestines, 2.3×10^5 oo/g of intestines and 4.53×10^5 oo/g of intestines respectively (Figure 4A). In mice treated with 20 mg/kg/day of OIPC, 9.4×10^4 oo/g of intestines was detected which consisted in a 93.5% decrease in oocyst burden compared to the PBS treated group ($P < 0.01$). The reductions in oocyst burden increase in mice treated with 30 or 40 mg/kg/day of OIPC were only 180 oo/g of intestines (99.98% reduction, $P < 0.01$) and 167 oo/g of intestines (99.98% reduction, $P < 0.01$) respectively (Figure 4A). In both cases an average 4-log reduction in oocyst burden was observed when compared to PBS treated mice. In surviving mice treated with 10 mg/kg miltefosine, oocyst burden at Day 30 was 1.4×10^5 oo/g of intestines which is comparable to their oocyst burden at Day 10 (Figures 4A,B). At Day 30, at 20 mg/kg/day of OIPC, oocyst levels were slightly lower (6.63×10^4 oo/g of intestines) than mice treated with 10 mg/kg/day of miltefosine, but this difference remained statistically non-significant (52.6% oocyst burden reduction, Figure 4B). At 30 mg/kg/day of OIPC, oocyst burden (2.81×10^3 oo/g of intestines) increased compared to the oocyst burden at Day 10 but still represented a 98% oocyst burden reduction compared to the oocyst burden at Day 30 for 10 mg/kg miltefosine-treated mice (Figure 4B). Finally, at 40 mg/kg/day of OIPC, mice showed the lowest oocyst burden in their intestines

with 34 oo/g of intestine representing a 99.98% oocyst burden reduction when compared to the 10 mg/kg miltefosine-treated mice ($P < 0.01$, Figure 4B).

OIPC Eliminates the Presence of Oocysts in Histological Sections of the Ileum of C57BL/6 IFN γ R-KO Mice Infected with *C. parvum*

To visually validate the presence of *C. parvum* life cycle stages in the intestines of infected mice, the ileum was collected from all mice at time of death. Sections from the ileum were prepared and stained (H&E) for histopathology purposes. Ileum sections from mice treated with PBS and 100 mg/kg/day of paromomycin at Day 10 revealed an overwhelming presence of *C. parvum* life cycle stages and severe damage to the epithelium of the intestine (Figures 5A,B). Damage to intestinal mucosa includes blunting of the villi, acute inflammation and formation of fibrin (fibrinous hemorrhagic enteritis) resulting from local hemorrhage and clotting (Figures 5A,B). The ileum of mice treated with 10 mg/kg/day of miltefosine was as severely damaged and infected as the other controls (Figure 5C). At Day 10, *C. parvum* oocysts were also abundantly present in mice treated with 20 mg/kg/day of OIPC and intestinal damage was also present but to a lesser extent than in the infected controls (Figure 6A). At the dose of 30 mg/kg/day of OIPC, mild intestinal damage and inflammation were noticeable and *C. parvum* oocysts were scarcely visible (Figure 6B). Finally, at 40 mg/kg/day, mice displayed practically no signs of intestinal damage or inflammation and a rare presence of *C. parvum* oocysts at Day 10 (Figure 6C). Slides from the ileum of non-infected controls were also prepared to provide a negative reference for comparison (data not shown).

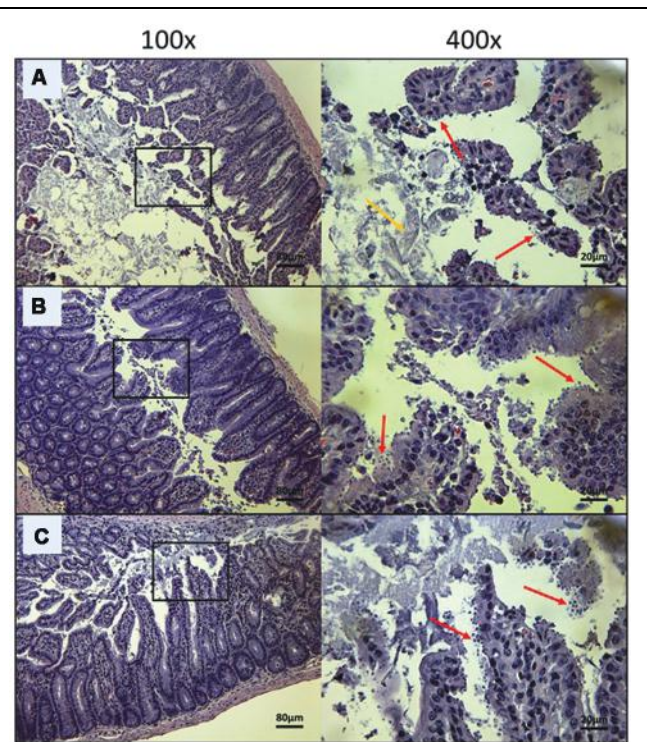


FIGURE 5 | Day 10 histological sections of the ileum of control C57BL/6 IFN γ R-KO mice infected with *C. parvum*. Representative transverse sections of the ileum stained with H&E showing disease progression. **(A)** Ileum of mice treated with PBS. Formation of fibrin is noticeable (yellow arrow). **(B)** Ileum of mice treated with 100 mg/kg/day of paromomycin. **(C)** Ileum of mice treated with 10 mg/kg/day of miltefosine. **(A–C)** Shows severe epithelial damage and abundance of oocysts. Each group is represented at 100 and 400x magnifications. Red arrows indicate *C. parvum* oocysts.

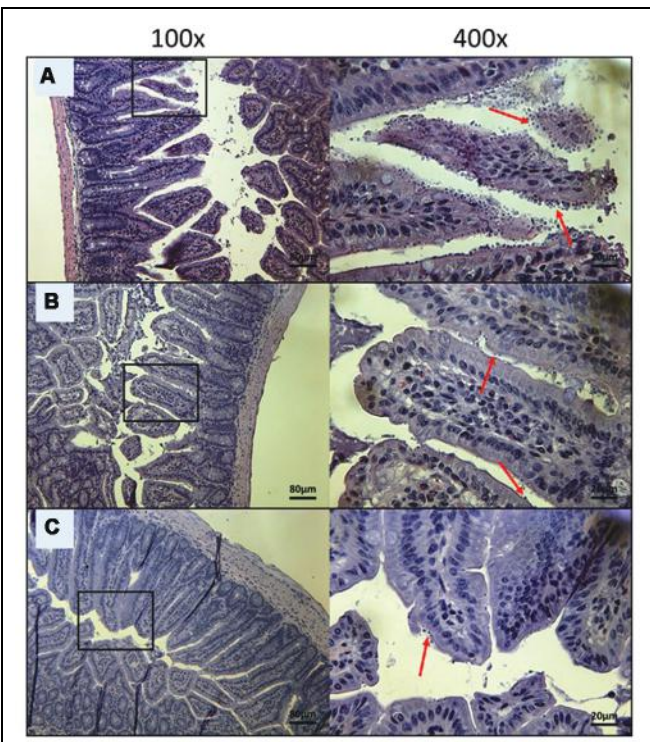


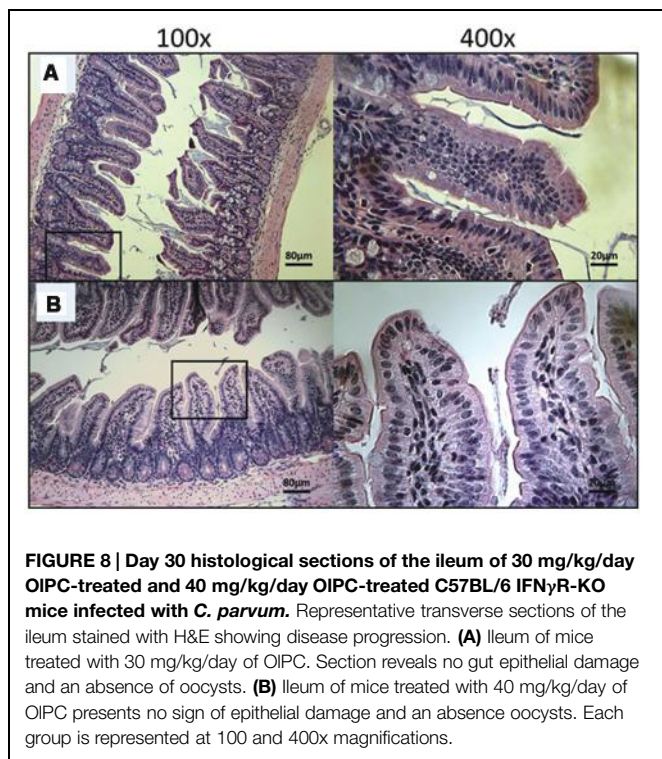
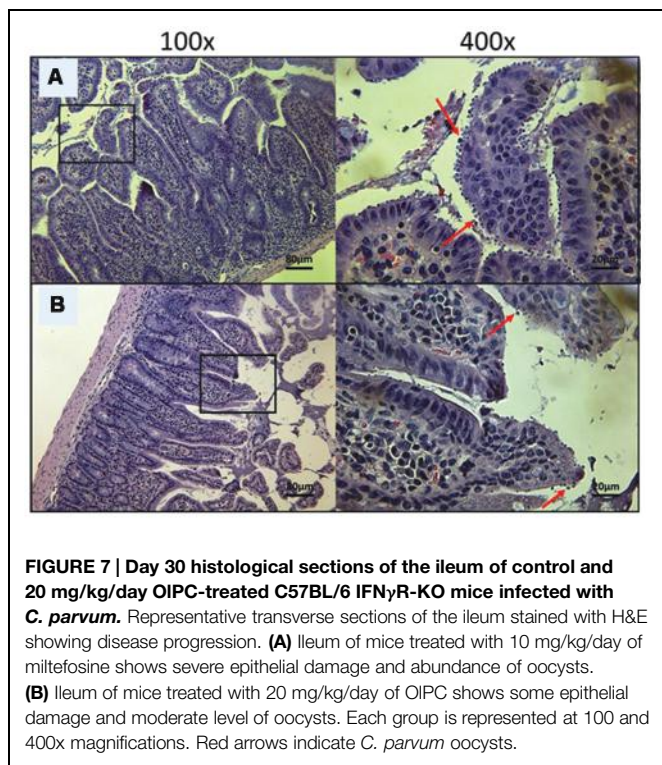
FIGURE 6 | Day 10 histological sections of the ileum of OIPC-treated C57BL/6 IFN γ R-KO mice infected with *C. parvum*. Representative transverse sections of the ileum stained with H&E showing disease progression. **(A)** Ileum of mice treated with 20 mg/kg/day of OIPC shows significant epithelial damage and abundance of oocysts. **(B)** Ileum of mice treated with 30 mg/kg/day of OIPC. **(C)** Ileum of mice treated with 40 mg/kg/day of OIPC. Sections from **(B,C)** reveal mild gut epithelial damage and rare presence of oocysts. Each group is represented at 100 and 400x magnifications. Red arrows indicate *C. parvum* oocysts.

At Day 30, the surviving mice treated with 10 mg/kg/day of miltefosine revealed an abundant presence of *C. parvum* oocysts and severe damage to the gut epithelium (Figure 7A). At the lowest concentration of OIPC, mice displayed a moderate presence of *C. parvum* oocysts and only mild damage to the intestinal epithelium (Figure 7B). At 30 and 40 mg/kg/day of OIPC, mice showed a complete absence of *C. parvum* oocysts and a healthy ileum in comparison with controls (Figures 8A,B). Sections of ileum, liver and spleen (data not shown) were also processed in uninfected (control) mice treated with 40 mg/kg/day for 10 days and no inflammation or toxicity was noticeable.

Residual Infectious Oocyst Concentration from Mice Exposed to OIPC is not Sufficient to Cause a New Infection in Naïve C57BL/6 IFN γ R-KO Mice

Another experiment was conducted to determine whether there was a sufficient number of infectious oocysts (more than the minimal infectious dose) remaining in the intestines of surviving mice at Days 10 or 30 to transmit the parasite and cause a new infection. To do so, naïve C57BL/6 IFN γ R-KO mice were

infected with a constant volume of the purified oocysts from mouse intestinal samples coming from the different treatment groups from both Days 10 and 30. In order to determine if naïve mice were infected, stool samples were taken once a week, processed and analyzed by qPCR and light microscopy (Table 1). Presence of *C. parvum* oocysts or DNA in the stool of these naïve mice suggests that a fully complete life cycle was achieved by the parasite. Therefore, the concentration of infectious oocysts in the purified intestinal samples of mice from the *in vivo* study would be considered to cause a new infection. Results demonstrated that only the purified intestinal samples from 40 mg/kg/day OIPC-treated mice at Day 30 were not able to successfully transmit a *C. parvum* infection in naïve C57BL/6 IFN γ R-KO mice. For these inoculated naïve mice, no oocysts could be seen by light microscopy and no DNA could be detected by qPCR in the stool even by Day 35 (Table 1). Additionally, no sign of illness were observed and the histological sections of the ileum revealed a complete absence of oocysts (data not shown). This observation corroborates previous results as 40 mg/kg/day OIPC-treated mice have been shown to have practically cleared the infection at D30. However, naïve C57BL/6 IFN γ R-KO mice infected with purified intestinal samples from other treatment groups developed signs



of cryptosporidiosis. By Day 17, these inoculated naïve mice exhibited signs of illness (hunched back, weight loss, dehydration, lethargy, and watery stools). Moreover, oocysts could be seen by light microscopy and detected by qPCR (Table 1). Histological

sections revealed a heavy presence of *C. parvum* oocysts and severe damage to the microvilli (data not shown). These results suggested that the oocysts in the purified intestinal samples of the other groups were sufficient to transmit *C. parvum* to a new host and cause acute cryptosporidiosis.

Discussion

Cryptosporidium parvum is a recognized threat to public health (Guerrant, 1997; Feldmann et al., 2002) and has been reported in more than 40 countries in all five continents (Putignani and Menichella, 2010). Many waterborne outbreaks reported in the past decade do not limit *C. parvum* infection to developing countries, but have been reported in Canada, USA, Sweden, and France as a result of tap water contamination (Putignani and Menichella, 2010). On one hand, *Cryptosporidium* causes persistent diarrhea and stunting in young children (Putignani and Menichella, 2010; Bouzid et al., 2013; Richard et al., 2014; Shikani and Weiss, 2014) and, on the other hand, AIDS patients can develop a chronic infection that can be fatal (Chen et al., 2002; Chalmers and Davies, 2010; Bouzid et al., 2013; Mead and Arrowood, 2014). The major issue comes from the lack of efficacious treatment options for cryptosporidial infections (Mead and Arrowood, 2014).

In this present study, we addressed the need for a new efficacious treatment against cryptosporidiosis by testing the compound OIPC, an alkylphosphocholine drug, already in clinical development against leishmaniasis. As a close analog of miltefosine, a drug recently approved by the FDA to treat cutaneous, mucosal and visceral leishmaniasis (FDA, 2014) and to treat primary amebic meningoencephalitis (CDC, 2013), OIPC is suspected to share a similar mode of action by interfering with parasitic lipid biosynthesis and cellular membrane integrity while inducing apoptosis of the parasite (Dorlo et al., 2012). Repurposing OIPC as an anti-cryptosporidiosis drug would have several advantages as the safety of this compound is already reported and pharmacological as well as pharmacokinetics studies are already ongoing (Fortin et al., 2012).

Initial *in vitro* results demonstrated that OIPC efficiently inhibits *C. parvum* infection of HCT-8 cells after 48 h exposure to the drug. OIPC reduced parasite burden by 84% at $\geq 10 \mu\text{M}$ and exhibited significant activity down to 10 nM with an EC₅₀ of 18.84 nM. We report here that the concentrations used for OIPC and miltefosine to achieve a significant reduction in *C. parvum* infectivity were far lower than the one published in the literature for paromomycin (EC₅₀ of 711 μM), the currently used drug against cryptosporidiosis in AIDS patients (Armson et al., 1999; Downey et al., 2008). The toxicity profile displayed by OIPC was also very low with a 40% reduction in host cell viability only at 100 μM and higher. Conversely, it was reported that HCT-8 cells presented signs of toxicity when exposed to miltefosine for 48 h at concentrations as low as 24.5 μM (Shahiduzzaman et al., 2009). Therefore, OIPC surpasses miltefosine in regards to its safety in host cells. Even though many drugs have been shown to successfully inhibit *C. parvum* infection *in vitro*, many of them have failed to inhibit cryptosporidiosis in an animal model (Mead

TABLE 1 | Infectivity of purified intestinal samples from the *in vivo* study in naïve C57BL/6 IFN γ R-KO mice.

Treatment ^a		Day 10 ^b		Day 17 ^b		Day 35 ^b	
		Microscopy	qPCR	Microscopy	qPCR	Microscopy	qPCR
PBS	Day 10	Yes	Yes	-	-	-	-
	Day 30	-	-	-	-	-	-
100 mg/kg of paromomycin	Day 10	Yes	Yes	-	-	-	-
	Day 30	-	-	-	-	-	-
10 mg/kg of miltefosine	Day 10	Yes	Yes	-	-	-	-
	Day 30	No	No	Yes	Yes	-	-
20 mg/kg of OlPC	Day 10	Yes	Yes	-	-	-	-
	Day 30	No	No	Yes	Yes	-	-
30 mg/kg of OlPC	Day 10	Yes	Yes	-	-	-	-
	Day 30	No	No	Yes	Yes	-	-
40 mg/kg of OlPC	Day 10	No	No	No	Yes	-	-
	Day 30	No	No	No	No	No	No

^aTreatment given to mice during the *in vivo* study. Purified intestinal samples from these mice at Days 10 or 30 were used to infect naïve C57BL/6 IFN γ R-KO mice.

^bRepresents the day post-inoculation that the stool from naïve mice was collected. The presence of *C. parvum* oocysts or its DNA in the stool of naïve mice is scored qualitatively. Dashes represent no available data due to mouse mortality during study: either there was no purified intestinal sample available to inoculate naïve mice (i.e., no PBS-treated mice in the *in vivo* study survived until Day 30) or naïve mice died during rechallenge study (no naïve mice inoculated with purified intestinal samples from mice treated with miltefosine survived until stool collection on Day 35).

and Arrowood, 2014). Such is the case for monensin (Blagburn et al., 1991) and paromomycin which only started to show efficacy in dexamethasone immunosuppressed mice at very high doses of 1 g/kg/day (Healey et al., 1995). Because the action of the drugs on *C. parvum* parasites is more direct when tested *in vitro* than in an animal model, it is possible that the results from the former does not translate to the latter (Mead and Arrowood, 2014). In fact, many factors influence the effect of drugs *in vivo* on pathogens such as its bioavailability, pharmacodynamics and pharmacokinetics as well as food and drug interactions. Thus, it is important to understand the limitations of the *C. parvum* *in vitro* model to mimic an *in vivo* model of infection and we must acknowledge *in vitro* results only as informative precursors to further investigations in animal models.

Therefore, to determine whether the *in vitro* activity of OlPC on *C. parvum* could be translated *in vivo*, we decided to use C57BL/6 IFN γ R-KO mice, an animal model highly susceptible to *C. parvum* infection (You and Mead, 1998; von Oettingen et al., 2008). Unlike other immunocompromised animal models where a very large *C. parvum* inoculum must be given (such as the dexamethasone (Yang and Healey, 1993; Healey et al., 1995), the SCID (Mead et al., 1995; Tzipori et al., 1995), the neonatal (Downey et al., 2008) or the malnourished models (Costa et al., 2012), C57BL/6 IFN γ R-KO mice can consistently develop severe illness with an infectious dose of only 10 oocysts (Yang et al., 2000; von Oettingen et al., 2008). It has also been demonstrated that doses as low as 1000 oocysts were lethal by Days 9–14 (Mead and You, 1998; You and Mead, 1998) and 1500 oocysts lead to 80% death in these mice (Ndao et al., 2013). In our study, mice received 4000 oocysts by oral gavage and began receiving treatment at Day 3 for a period of 10 consecutive days. By increasing the inoculum in these mice, we were able to achieve 100% mortality in PBS treated mice by Day 10 which allowed us to clearly identify the efficacy of the treatment. As early as

Day 10, major differences between mice treated with the highest doses of OlPC (30 and 40 mg/kg/day) with other groups could already be seen. Not only did 40 mg/kg/day of OlPC reduce parasite and oocyst burden in the intestinal tract by 99.6 and 99.98% respectively after only 7 days of daily treatment (Day 10), it also allowed 100% of these mice to survive until the experimental endpoint (Day 30; $P < 0.001$). At Day 30, parasite and oocyst burden in the intestines of the 40 mg/kg/day OlPC-treated group reached a 99.97 and 99.98% reduction respectively ($P < 0.001$) in comparison with the 10 mg/kg miltefosine group. These data firmly support that, even after the completion of the treatment with OlPC, mice did not show any sign of relapse in parasite burden or recurrence in clinical symptoms. In addition, a complete elimination of oocyst shedding in the stools was observed and no parasite was noticed by light microscopy of histology section of ileum of 40 mg/kg/day OlPC-treated mice at Day 30. In consequence, it is not surprising that purified intestinal samples from 40 mg/kg/day OlPC-treated mice at D30 were incapable of further transmitting the infection to naïve C57BL/6 IFN γ R-KO mice. Together, this validates the hypothesis that OlPC rescued/cured immunocompromised mice from a lethal infection with *C. parvum* and, even if the 40 mg/kg/day OlPC treatment did not completely clear infection at Day 30 (Figure 4B), it is not likely that the surviving parasites can cause a recrudescence of infection if mice were not sacrificed at Day 30.

In short, we used a stringent animal model that clearly discriminated if a drug was sufficiently potent to rescue mice from a lethal infection. In this model, paromomycin, given at 100 mg/kg/day for 10 days, failed to rescue mice, whereas in a neonatal model, where the same dosage of paromomycin was given for 6 days, it was able to reduce oocyst burden in the distal colon by 97% and oocyst shedding by 96% (Downey et al., 2008). However, these numbers are not corroborated by clinical cases, where paromomycin treatments are associated with a high

probability of relapse in AIDS patients (Hewitt et al., 2000; Cabada and White, 2010). At lower doses, 30 and 20 mg/kg/day of OlPC, treatments were still able to keep 75% of infected mice alive at Day 30, but were not able to eliminate oocyst shedding. Moreover, purified intestinal samples from these mice were capable of transmitting the infection to other naïve C57BL/6 IFN γ R-KO mice. This suggests that the dose of these OlPC treatment regimens were not sufficient to eliminate *C. parvum* parasites or to prevent a recurrent infection after the end of the treatment (even though there was a 98% oocyst burden reduction in the intestines by Day 30). Finally, miltefosine was also tested at 10 mg/kg/day for 10 days as a control because of the similar properties and structure it shares with OlPC. Results demonstrated that it had modest, but significant level of activity against *C. parvum* infection since it was able to rescue 50% of infected mice at Day 30. However, the surviving mice were still heavily infected and presented severe signs of illness.

No sign of discomfort or behavioral changes were noted in infected and uninfected mice treated with 40 mg/kg/day of OlPC for 10 days, which is supportive of data previously obtained in a mouse model of leishmaniasis (Fortin et al., 2014). Additionally, sections of the ileum, liver and spleen from these mice showed no signs of toxicity or inflammation associated to OlPC (data not shown).

The present study did not compare miltefosine and OlPC at the same dosages across the entire range. While this may be perceived as a limitation, it was reflective of concerns regarding miltefosine toxicity at higher doses (FDA, 2014).

In summary, the strong activity of OlPC on *C. parvum* parasites *in vitro* was thoroughly supported by the outcome of the animals in our *in vivo* study as OlPC rescues C57BL/6 IFN γ R-KO mice from a lethal infection of *C. parvum*. Data obtained by qPCR from the *in vivo* study was not only cross-validated by flow cytometry and light microscopy, but was also confirmed visually by histological sections from mice ileums. Furthermore, OlPC demonstrated, at its highest dose, a lasting effect and mice showed no sign of relapse of infection even 17 days after the end of the treatment. As an analog of miltefosine, we hypothesize that OlPC will have the same mechanism of action on the parasite, that is by causing an irreversible inhibition of the phospholipid biosynthesis pathway leading to the apoptosis in the parasite; further studies will be needed to confirm this hypothesis (Anthony et al., 1999; Dorlo et al., 2012). Together, this

establishes OlPC as novel, consistent, sustainable, safe, and potent anti-cryptosporidial treatment option for immunocompromised patients.

Disclosure

AF works as a consultant for Dafra Pharma R&D.

Author Contributions

KSD and AER performed *in vitro* experiments, data analysis and manuscript preparation. AER and FVC performed *in vivo* studies in mice. TZDL and AER performed flow cytometry data acquiring and analysis. AM processed stool and intestinal samples from mice. MJA provided *C. parvum* oocysts for experiments. AF provided the OlPC compound and advice on experiment design. MN designed and supervised all experiments. KSD, MJA, AF, and MN improved manuscript to final approved version. All authors reviewed final version of the manuscript and agreed on accuracy.

Acknowledgments

The National Reference Centre for Parasitology is supported by Public Health Agency of Canada/National Microbiology Laboratory grant MOA 4500299739, the Foundation of the Montreal General Hospital and the Research Institute of the McGill University Health Centre. This study would not have been possible without the valuable help of Nathalie Martel for mouse colony management and the technical help of Annie Beauchamp for mouse procedures. Part of the *in vitro* testing of OlPC was funded by Dafra Pharma R&D through grant #110402 from IWT, Flanders, Belgium (Innovatie door Wetenschap en Technologie) to AF.

The use of trade names and names of commercial sources is for identification only and does not imply endorsement by the Centers for Disease Control and Prevention or the U.S. Department of Health and Human Services. The findings and conclusions in this report are those of the authors and do not necessarily represent the views of the Centers for Disease Control and Prevention.

References

- Anthony, M. L., Zhao, M., and Brindle, K. M. (1999). Inhibition of phosphatidylcholine biosynthesis following induction of apoptosis in HL-60 cells. *J. Biol. Chem.* 274, 19686–19692. doi: 10.1074/jbc.274.28.19686
- Armson, A., Meloni, B. P., Reynoldson, J. A., and Thompson, R. C. (1999). Assessment of drugs against *Cryptosporidium parvum* using a simple *in vitro* screening method. *FEMS Microbiol. Lett.* 178, 227–233. doi: 10.1111/j.1574-6968.1999.tb08681.x
- Berkman, D. S., Lescano, A. G., Gilman, R. H., Lopez, S. L., and Black, M. M. (2002). Effects of stunting, diarrhoeal disease, and parasitic infection during infancy on cognition in late childhood: a follow-up study. *Lancet* 359, 564–571. doi: 10.1016/S0140-6736(02)07744-9
- Blagburn, B. L., Sundermann, C. A., Lindsay, D. S., Hall, J. E., and Tidwell, R. R. (1991). Inhibition of *Cryptosporidium parvum* in neonatal Hsd:(ICR)BR Swiss mice by polyether ionophores and aromatic amidines. *Antimicrob. Agents Chemother.* 35, 1520–1523. doi: 10.1128/AAC.35.7.1520
- Bouzid, M., Hunter, P., Chalmers, R., and Tyler, K. (2013). *Cryptosporidium* pathogenicity and virulence. *Clin. Microbiol. Rev.* 26, 115–134. doi: 10.1128/CMR.00076-12
- Cabada, M., and White, A. C. (2010). Treatment of cryptosporidiosis: do we know what we think we know? *Curr. Opin. Infect. Dis.* 23, 494–499. doi: 10.1097/QCO.0b013e32833de052
- Cacciò, S. M., and Putignani, L. (2014). “Epidemiology of human cryptosporidiosis,” in *Cryptosporidium: Parasite and Disease*, eds S. M. Caccio and G. Widmer (Vienna: Springer), 43–79.

- Cacciò, S. M., Thompson, R. C., McLauchlin, J., and Smith, H. V. (2005). Unravelling *Cryptosporidium* and *Giardia* epidemiology. *Trends Parasitol.* 21, 430–437. doi: 10.1016/j.pt.2005.06.013
- CDC. (2013). Investigational drug available directly from CDC for the treatment of infections with free-living amebae. *MMWR* 62:666.
- Chalmers, R. M., and Davies, A. P. (2010). Minireview: clinical cryptosporidiosis. *Exp. Parasitol.* 124, 138–146. doi: 10.1016/j.exppara.2009.02.003
- Chen, X.-M., Keithly, J. S., Paya, C. V., and Larusso, N. F. (2002). Cryptosporidiosis. *N. Engl. J. Med.* 346, 1723–1731. doi: 10.1056/NEJMra013170
- Collinet-Adler, H. D., and Ward, H. D. (2010). Cryptosporidiosis: environmental, therapeutic, and preventive challenges. *Euro. J. Clin. Microbiol. Infect. Dis.* 29, 927–935. doi: 10.1007/s10096-010-0960-9
- Costa, L., Noronha, F., Roche, J., Sevilleja, J., Warren, C., Oriña, R., et al. (2012). Novel in vitro and in vivo models and potential new therapeutics to break the vicious cycle of *Cryptosporidium* infection and malnutrition. *J. Infect. Dis.* 205, 1464–1471. doi: 10.1093/infdis/jis216
- Dorlo, T. P. C., Balasegaram, M., Beijnen, J., and De Vries, P. (2012). Miltefosine: a review of its pharmacology and therapeutic efficacy in the treatment of leishmaniasis. *J. Antimicrob. Chemother.* 67, 2576–2597. doi: 10.1093/jac/dks275
- Downey, A. S., Chong, C. R., Graczyk, T. K., and Sullivan, D. J. (2008). Efficacy of pyrvium pamoate against *Cryptosporidium parvum* infection in vitro and in a neonatal mouse model. *Antimicrob. Agents Chemother.* 52, 3106–3112. doi: 10.1128/AAC.00207-08
- Fayer, R., Morgan, U., and Upton, S. J. (2000). Epidemiology of *Cryptosporidium*: transmission, detection and identification. *Int. J. Parasitol.* 30, 1305–1322. doi: 10.1016/S0020-7519(00)00135-1
- Fayer, R., and Xiao, L. (2008). *Cryptosporidium and Cryptosporidiosis*. Boca Raton: CRC Press.
- FDA. (2014). *Fda Approves Impavido to Treat Tropical Disease Leishmaniasis*. Available at: <http://www.fda.gov/newsevents/newsroom/pressannouncements/ucm389671.htm> [accessed 17 April 2014].
- Feldmann, H., Czub, M., Jones, S., Dick, D., Garbutt, M., Grolla, A., et al. (2002). Emerging and re-emerging infectious diseases. *Med. Microbiol. Immunol.* 191, 63–74. doi: 10.1007/s00430-002-0122-5
- Fortin, A., Caridha, D. P., Leed, S., Ngundam, F., Sena, J., Bosschaerts, T., et al. (2014). Direct comparison of the efficacy and safety of oral treatments with oleylphosphocholine (OlPC) and miltefosine in a mouse model of *L. major* cutaneous leishmaniasis. *PLoS Negl. Trop. Dis.* 8:e3144. doi: 10.1371/journal.pntd.0003144
- Fortin, A., Hendrickx, S., Yardley, V., Cos, P., Jansen, H., and Maes, L. (2012). Efficacy and tolerability of oleylphosphocholine (OlPC) in a laboratory model of visceral leishmaniasis. *J. Antimicrob. Chemother.* 67, 2707–2712. doi: 10.1093/jac/dks273
- Guerrant, R. L. (1997). Cryptosporidiosis: an emerging, highly infectious threat. *Emerg. Infect. Dis.* 3, 51–57. doi: 10.3201/eid0301.970106
- Healey, M. C., Yang, S., Rasmussen, K. R., Jackson, M. K., and Du, C. (1995). Therapeutic efficacy of paromomycin in immunosuppressed adult mice infected with *Cryptosporidium parvum*. *J. Parasitol.* 81, 114–116. doi: 10.2307/3284020
- Hernandez, L., Galvez, R., Montoya, A., Checa, R., Bello, A., Bosschaerts, T., et al. (2014). First study on efficacy and tolerability of a new alkylphosphocholine molecule (oleylphosphocholine-OlPC) in the treatment of canine leishmaniasis due to *Leishmania infantum*. *Parasitol. Res.* 113, 157–164. doi: 10.1007/s00436-013-3638-2
- Hewitt, R. G., Yiannoutsos, C. T., Higgs, E. S., Carey, J. T., Geiseler, P. J., Soave, R., et al. (2000). Paromomycin: no more effective than placebo for treatment of cryptosporidiosis in patients with advanced human immunodeficiency virus infection. AIDS Clinical Trial Group. *Clin. Infect. Dis.* 31, 1084–1092. doi: 10.1086/318155
- King, B., Keegan, A., Monis, P., and Saint, C. (2005). Environmental temperature controls *Cryptosporidium* oocyst metabolic rate and associated retention of infectivity. *Appl. Environ. Microbiol.* 71, 3848–3857. doi: 10.1128/AEM.71.7.3848-3857.2005
- Kotloff, K. L., Nataro, J. P., Blackwelder, W. C., Nasrin, D., Farag, T. H., Panchalingam, S., et al. (2013). Burden and aetiology of diarrhoeal disease in infants and young children in developing countries (the Global Enteric Multicenter Study, GEMS): a prospective, case-control study. *Lancet* 382, 209–222. doi: 10.1016/S0140-6736(13)60844-2
- Mead, J. R., and Arrowood, M. J. (2014). “Treatment of cryptosporidiosis,” in *Cryptosporidium: Parasite and Disease*, eds S. M. Caccio and G. Widmer (Vienna: Springer), 455–486.
- Mead, J. R., and You, X. (1998). Susceptibility differences to *Cryptosporidium parvum* infection in two strains of gamma interferon knockout mice. *J. Parasitol.* 84, 1045–1048. doi: 10.2307/3284643
- Mead, J. R., You, X., Pharr, J. E., Belenkaya, Y., Arrowood, M. J., Fallon, M. T., et al. (1995). Evaluation of maduramicin and alborelixin in a SCID mouse model of chronic cryptosporidiosis. *Antimicrob. Agents Chemother.* 39, 854–858. doi: 10.1128/AAC.39.4.854
- Meloni, B. P. (1996). Simplified methods for obtaining purified oocysts from mice and for growing *Cryptosporidium parvum* in vitro. *J. Parasitol.* 82, 757–762. doi: 10.2307/3283888
- Nda, M., Nath Chowdhury, M., Sajid, M., Marcus, V., Mashiyama, S., Sakanari, J., et al. (2013). A cysteine protease inhibitor rescues mice from a lethal *Cryptosporidium parvum* infection. *Antimicrob. Agents Chemother.* 57, 6063–6073. doi: 10.1128/AAC.00734-13
- Putignani, L., and Menichella, D. (2010). Global distribution, public health and clinical impact of the protozoan pathogen *Cryptosporidium*. *Interdiscip. Perspect. Infect. Dis.* 2010, 753512.
- Richard, S., Black, R., Gilman, R., Guerrant, R., Kang, G., Lanata, C., et al. (2014). Catch-up growth occurs after diarrhea in early childhood. *J. Nutr.* 144, 965–971. doi: 10.3945/jn.113.187161
- Robertson, L. J., Campbell, A. T., and Smith, H. V. (1992). Survival of *Cryptosporidium parvum* oocysts under various environmental pressures. *Appl. Environ. Microbiol.* 58, 3494–3500.
- Roehm, N. W., Rodgers, G. H., Hatfield, S. M., and Glasebrook, A. L. (1991). An improved colorimetric assay for cell proliferation and viability utilizing the tetrazolium salt XTT. *J. Immunol. Methods* 142, 257–265. doi: 10.1016/0022-1759(91)90114-U
- Rossignol, J.-F. (2010). *Cryptosporidium* and *Giardia*: treatment options and prospects for new drugs. *Exp. Parasitol.* 124, 45–53. doi: 10.1016/j.exppara.2009.07.005
- Rotz, L. D., Khan, A. S., Lillibridge, S. R., Ostroff, S. M., and Hughes, J. M. (2002). Public health assessment of potential biological terrorism agents. *Emerg. Infect. Dis.* 8, 225–230. doi: 10.3201/eid0802.010164
- Ryan, U., and Xiao, L. (2014). “Taxonomy and molecular taxonomy,” in *Cryptosporidium: Parasite and Disease*, eds S. M. Caccio and G. Widmer (Vienna: Springer), 3–41.
- Shahiduzzaman, M., Dyachenko, V., Obwaller, A., Unglaube, S., and Daugschies, A. (2009). Combination of cell culture and quantitative PCR for screening of drugs against *Cryptosporidium parvum*. *Vet. Parasitol.* 162, 271–277. doi: 10.1016/j.vetpar.2009.03.009
- Shikani, H., and Weiss, L. M. (2014). “Human cryptosporidiosis: a clinical perspective,” in *Cryptosporidium: Parasite and Disease*, eds S. M. Caccio and G. Widmer (Vienna: Springer), 383–421.
- Thapar, N., and Sanderson, I. R. (2004). Diarrhoea in children: an interface between developing and developed countries. *Lancet* 363, 641–653. doi: 10.1016/S0140-6736(04)15599-2
- Tzipori, S., Rand, W., and Theodos, C. (1995). Evaluation of a two-phase scid mouse model preconditioned with anti-interferon-gamma monoclonal antibody for drug testing against *Cryptosporidium parvum*. *J. Infect. Dis.* 172, 1160–1164. doi: 10.1093/infdis/172.4.1160
- van Blitterswijk, W. J., and Verheij, M. (2008). Anticancer alkylphospholipids: mechanisms of action, cellular sensitivity and resistance, and clinical prospects. *Curr. Pharm. Des.* 14, 2061–2074. doi: 10.2174/138161208785294636
- von Oettingen, J., Nath-Chowdhury, M., Ward, B. J., Rodloff, A. C., Arrowood, M. J., and Nda, M. (2008). High-yield amplification of *Cryptosporidium parvum* in interferon γ receptor knockout mice. *Parasitology* 135, 1151–1156. doi: 10.1017/S0031182008004757
- Widmer, G., Corey, E. A., Stein, B., Griffiths, J. K., and Tzipori, S. (2000). Host cell apoptosis impairs *Cryptosporidium parvum* development in vitro. *J. Parasitol.* 86, 922–928.

- Yang, S., Benson, S. K., Du, C., and Healey, M. C. (2000). Infection of immunosuppressed C57BL/6N adult mice with a single oocyst of *Cryptosporidium parvum*. *J. Parasitol.* 86, 884–887. doi: 10.2307/3284990
- Yang, S., and Healey, M. C. (1993). The immunosuppressive effects of dexamethasone administered in drinking water to C57BL/6N mice infected with *Cryptosporidium parvum*. *J. Parasitol.* 79, 626–630. doi: 10.2307/3283395
- You, X., and Mead, J. R. (1998). Characterization of experimental *Cryptosporidium parvum* infection in IFN-gamma knockout mice. *Parasitology* 117(Pt 6), 525–531. doi: 10.1017/S0031182098003424

Conflict of Interest Statement: The authors declare that the research was conducted in the absence of any commercial or financial relationships that could be construed as a potential conflict of interest.

Copyright © 2015 Sonzogni-Desautels, Renteria, Camargo, Di Lenardo, Mikhail, Arrowood, Fortin and Ndao. This is an open-access article distributed under the terms of the Creative Commons Attribution License (CC BY). The use, distribution or reproduction in other forums is permitted, provided the original author(s) or licensor are credited and that the original publication in this journal is cited, in accordance with accepted academic practice. No use, distribution or reproduction is permitted which does not comply with these terms.

